frontiers | Research Topics

Neuromuscular disorders and peripheral neuropathies – case report collection

2022

Edited by
Giovanni Meola

Published in
Frontiers in Neurology

FRONTIERS EBOOK COPYRIGHT STATEMENT

The copyright in the text of individual articles in this ebook is the property of their respective authors or their respective institutions or funders. The copyright in graphics and images within each article may be subject to copyright of other parties. In both cases this is subject to a license granted to Frontiers.

The compilation of articles constituting this ebook is the property of Frontiers.

Each article within this ebook, and the ebook itself, are published under the most recent version of the Creative Commons CC-BY licence. The version current at the date of publication of this ebook is CC-BY 4.0. If the CC-BY licence is updated, the licence granted by Frontiers is automatically updated to the new version.

When exercising any right under the CC-BY licence, Frontiers must be attributed as the original publisher of the article or ebook, as applicable.

Authors have the responsibility of ensuring that any graphics or other materials which are the property of others may be included in the CC-BY licence, but this should be checked before relying on the CC-BY licence to reproduce those materials. Any copyright notices relating to those materials must be complied with.

Copyright and source acknowledgement notices may not be removed and must be displayed in any copy, derivative work or partial copy which includes the elements in question.

All copyright, and all rights therein, are protected by national and international copyright laws. The above represents a summary only. For further information please read Frontiers' Conditions for Website Use and Copyright Statement, and the applicable CC-BY licence.

ISSN 1664-8714
ISBN 978-2-8325-3071-9
DOI 10.3389/978-2-8325-3071-9

About Frontiers

Frontiers is more than just an open access publisher of scholarly articles: it is a pioneering approach to the world of academia, radically improving the way scholarly research is managed. The grand vision of Frontiers is a world where all people have an equal opportunity to seek, share and generate knowledge. Frontiers provides immediate and permanent online open access to all its publications, but this alone is not enough to realize our grand goals.

Frontiers journal series

The Frontiers journal series is a multi-tier and interdisciplinary set of open-access, online journals, promising a paradigm shift from the current review, selection and dissemination processes in academic publishing. All Frontiers journals are driven by researchers for researchers; therefore, they constitute a service to the scholarly community. At the same time, the *Frontiers journal series* operates on a revolutionary invention, the tiered publishing system, initially addressing specific communities of scholars, and gradually climbing up to broader public understanding, thus serving the interests of the lay society, too.

Dedication to quality

Each Frontiers article is a landmark of the highest quality, thanks to genuinely collaborative interactions between authors and review editors, who include some of the world's best academicians. Research must be certified by peers before entering a stream of knowledge that may eventually reach the public - and shape society; therefore, Frontiers only applies the most rigorous and unbiased reviews. Frontiers revolutionizes research publishing by freely delivering the most outstanding research, evaluated with no bias from both the academic and social point of view. By applying the most advanced information technologies, Frontiers is catapulting scholarly publishing into a new generation.

What are Frontiers Research Topics?

Frontiers Research Topics are very popular trademarks of the *Frontiers journals series*: they are collections of at least ten articles, all centered on a particular subject. With their unique mix of varied contributions from Original Research to Review Articles, Frontiers Research Topics unify the most influential researchers, the latest key findings and historical advances in a hot research area.

Find out more on how to host your own Frontiers Research Topic or contribute to one as an author by contacting the Frontiers editorial office: frontiersin.org/about/contact

Neuromuscular disorders and peripheral neuropathies – case report collection 2022

Topic editor
Giovanni Meola — University of Milan, Italy

Citation
Meola, G., ed. (2023). *Neuromuscular disorders and peripheral neuropathies – case report collection 2022*. Lausanne: Frontiers Media SA. doi: 10.3389/978-2-8325-3071-9

Table of contents

07 Novel Variants of *ANO5* in Two Patients With Limb Girdle Muscular Dystrophy: Case Report
Matthew Katz, Fleur C. Garton, Mark Davis, Robert D. Henderson and Pamela A. McCombe

12 Scoliosis Orthopedic Surgery Combined With Nusinersen Intrathecal Injection Significantly Improved the Outcome of Spinal Muscular Atrophy Patient: A Case Report
Beiyu Xu, Cuijie Wei, Xiao Hu, Wenzhu Li, Zhen Huang, Chengli Que, Jianxing Qiu, Chunde Li and Hui Xiong

19 Nodopathies in the Early Diagnosis of Axonal Forms of Guillain-Barré Syndrome
Sara Urdiales-Sánchez, José-Ramiro González-Montaña, Ricardo Diaz-Pérez, Pablo Calvo-Calleja, María-Antonia Gutiérrez-Trueba and Javier Urdiales-Urdiales

28 Case Report: A Novel AChR Epsilon Variant Causing a Clinically Discordant Salbutamol Responsive Congenital Myasthenic Syndrome in Two Egyptian Siblings
Marta Gómez-García de la Banda, Emmanuel Simental-Aldaba, Nagia Fahmy, Damien Sternberg, Patricia Blondy, Susana Quijano-Roy and Edoardo Malfatti

35 Analysis of Clinical Symptoms of Guillain–Barré Syndrome Induced by Heat Stroke: Three Case Reports and Literature Review
Xiao-xiao Ni, Cong-lin Wang, Ye-qun Guo and Zhi-feng Liu

43 The Combined Efficacy of a Two-Year Period of Cybernic Treatment With a Wearable Cyborg Hybrid-Assistive Limb and Leuprorelin Therapy in a Patient With Spinal and Bulbar Muscular Atrophy: A Case Report
Hideaki Nakatsuji, Tetsuhiko Ikeda, Atsushi Hashizume, Masahisa Katsuno, Gen Sobue and Takashi Nakajima

50 A Remarkable Case of Acute Motor-Sensory Axonal Polyneuropathy (AMSAN) Variant of Guillain Barré Syndrome, in a Diabetic Patient Infected With COVID-19: A Case Report and Review of the Literature
Sajjad Ali, Alvina Karam, Aarish Lalani, Sadia Jawed, Musfirah Moin, Zain Douba and Murtaza Ali

56 Case Report: A 72-Year-Old Woman With Progressive Motor Weakness, Dry Eyes and High Levels of Serum Neurofilament Light Chain
Maria Janina Wendebourg, Jens Kuhle and Martin Hardmeier

62 Case Reports: Novel Missense Variants in the Filamin C Actin Binding Domain Cause Variable Phenotypes
Daniele Velardo, Maria Grazia D'Angelo, Andrea Citterio, Elena Panzeri, Laura Napoli, Claudia Cinnante, Maurizio Moggio, Giacomo Pietro Comi, Dario Ronchi and Maria Teresa Bassi

69 Case report: Coexistence of myotonia congenita and Brugada syndrome in one family
Ann Cordenier, Anja Flamez, Thomy de Ravel, Alexander Gheldof, Luigi Pannone, Carlo De Asmundis, Gudrun Pappaert and Véronique Bissay

76 Case report: Thirty-year progression of an EMPF1 encephalopathy due to defective mitochondrial and peroxisomal fission caused by a novel *de novo* heterozygous *DNM1L* variant
Charlène Lhuissier, Bart E. Wagner, Amy Vincent, Gaëtan Garraux, Olivier Hougrand, Rudy Van Coster, Valerie Benoit, Deniz Karadurmus, Guy Lenaers, Naïg Gueguen, Arnaud Chevrollier and Isabelle Maystadt

85 Case report: Wallerian degeneration: The innate-immune response to adult-onset Still's disease peripheral nerve injury
Hao Cheng, He Lv, Yan Wang and Gui-Qiang Wang

91 Autosomal dominant GDAP1 mutation with severe phenotype and respiratory involvement: A case report
Adrian Rodriguez-Hernandez, Meagan Mayo, Lilibeth Jauregui and Pooja Patel

97 Case report: Recreational nitrous oxide abuse triggered peripheral neuropathy possibly through the immune-mediated pathogenesis
Mei-Xue Dong, Qing Wang, Jun-Feng Xu, Ling Hu, Ying Yu and Tao Li

103 Elderly onset of MELAS in a male: A case report
Sheng-Peng Diao, Song-Fa Chen, Ai-Qun Liu, Zhi-Hua Zhou, Zhong-Xing Peng and Ming-Fan Hong

110 Case report: A novel variant in *SLC25A46* causing sensorimotor polyneuropathy and optic atrophy
Louise Sloth Kodal, Sophia Hammer-Hansen, Sonja Holm-Yildiz, Karen Grønskov, Helena Gásdal Karstensen and Tina Dysgaard

116 Lipid storage myopathy due to late-onset multiple Acyl-CoA dehydrogenase deficiency with novel mutations in ETFDH: A case report
Huihong Tian, Yi Zhong, Zhihua Liu, Liping Wei, Yanbo Yuan, Yuhu Zhang and Limin Wang

121 Case report: Brachial plexopathy caused by malignant peripheral nerve sheath tumor and review of the literature
Mengjie Chen, Xiuli Li and Xinhong Feng

127 Phenotypic variability within the desminopathies: A case series of three patients
Dennis Yeow, Matthew Katz, Robert Henderson, Sandhir Prasad, Russell Denman, Stefan Blum, Mark Davis, Thomas Robertson and Pamela McCombe

133 Case report: SCN4A p.R1135H gene variant in combination with thyrotoxicosis causing hypokalemic periodic paralysis
Zhi Zhang and Banghui Xiao

137 Case report: Adult-onset limb girdle muscular dystrophy in sibling pair due to novel homozygous *LAMA2* missense variant
Matthew Katz, Leigh B. Waddell, Michaela Yuen, Samantha J. Bryen, Emily Oates, Fleur C. Garton, Thomas Robertson, Robert David Henderson, Sandra T. Cooper and Pamela A. McCombe

144 Case report: Novel *ETFDH* compound heterozygous mutations identified in a patient with late-onset glutaric aciduria type II
Sijia Zhu, Dongxue Ding, Jianhua Jiang, Meirong Liu, Liqiang Yu and Qi Fang

151 Efficacy of vamorolone in treatment of Duchene muscle dystrophy. A meta-analysis
Rowan H. Elhalag, Karam R. Motawea, Nesreen Elsayed Talat, Samah S. Rouzan and Jaffer Shah

160 Ultrasound-guided glenohumeral joint injections for shoulder pain in ALS: A case series
Katherine M. Burke, Amy S. Ellrodt, Benjamin C. Joslin, Pia P. Sanpitak, Claire MacAdam, Prabhav Deo, Kevin Ozment, Cristina Shea, Stephen A. Johnson, Doreen Ho, Samuel K. Chu, Ashwin N. Babu, Colin K. Franz and Sabrina Paganoni

166 Novel compound heterozygous mutations of LAMA2-limb–girdle muscular dystrophy: A case report and literature review
Duo-Zi Wang, Bing-Hu Li, Qiong Ma, Zhou Yu, Kai Chen, Ying He and Song Tan

171 Case report: Anti-CNTN1 antibody-associated nodopathies disease with asymmetric onset
Qian Li, Qing Chen, Ting Zhang, Ying Xu, Yanmin Kan and Jing Zhang

178 Case report: Flail leg syndrome in familial amyotrophic lateral sclerosis with L144S *SOD1* mutation
Ewa Zapalska, Dominika Wrzesień and Adam Stępień

185 Beneficial effects and safety of traditional Chinese medicine for chronic inflammatory demyelinating polyradiculoneuropathy: A case report and literature review
Yao Xie, Lesang Li, Le Xie, Junlin Jiang, Ting Yao, Guo Mao, Shiliang Wang, Anchao Lin, Jinwen Ge and Dahua Wu

194 Increased expression of cell adhesion molecules in myofasciitis
Xue Ma, Huajie Gao, Li Xu, Zhuajin Bi, Suqiong Ji and Bitao Bu

204 Disability evaluation in patients with Guillain-Barre syndrome and SARS-CoV-2 infection
Sofía S. Sanchez-Boluarte, Wilfor Aguirre-Quispe, Jhon Tacunan-Cuellar, Arantxa N. Sanchez-Boluarte and Darwin Segura-Chavez

213 A case report of Andersen-Tawil syndrome misdiagnosed with myodystrophy
Xiuqin Zhao, Hengbing Zu and Kai Yao

219 Case report: MELAS and T3271C mitochondrial mutation in an adult woman
Dong-hua Chen, Wei Li, Hai-shan Jiang and Chao Yuan

frontiers | Frontiers in Neurology

CASE REPORT
published: 08 April 2022
doi: 10.3389/fneur.2022.868655

Novel Variants of *ANO5* in Two Patients With Limb Girdle Muscular Dystrophy: Case Report

Matthew Katz[1]*, *Fleur C. Garton*[2], *Mark Davis*[3], *Robert D. Henderson*[1] and *Pamela A. McCombe*[1,4]

[1] Department of Neurology, Royal Brisbane and Women's Hospital, Brisbane, QLD, Australia, [2] Institute for Molecular Bioscience, The University of Queensland, Brisbane, QLD, Australia, [3] Department of Diagnostic Genomics, Pathwest Laboratory Medicine, Perth, WA, Australia, [4] Centre for Clinical Research, The University of Queensland, Brisbane, QLD, Australia

Here we report on two unrelated adult patients presenting with Limb girdle muscular dystrophy who were found to have novel variants in *ANO5.* Both patients had prominent weakness of their proximal lower limbs with mild weakness of elbow flexion and markedly elevated creatine kinase. Next generation sequencing using a custom-designed neuromuscular panel was performed in both patients. In one patient, 336 genes were targeted for casual variants and in the other patient (using a later panel design), 464 genes were targeted. One patient was homozygous for a novel splice variant [c.294+5G>A; p.(Ala98Ins4*)] in *ANO5.* Another patient was compound heterozygous for two variants in *ANO5*; a common frameshift variant [c.191dupA; p.(Asn64fs)] and a novel missense variant [c.952G>C; p.(Ala318Pro)]. These findings support the utility of next generation sequencing in the diagnosis of patients presenting with a Limb girdle muscular dystrophy phenotype and extends the genotypic spectrum of *ANO5* disease.

Keywords: case report, limb girdle muscular dystrophy, ANO5, novel variant, next generation sequencing

OPEN ACCESS

Edited by:
Giovanni Meola,
University of Milan, Italy

Reviewed by:
Matthew Wicklund,
University of Colorado, United States
Gabriella Silvestri,
Catholic University of the Sacred Heart, Italy

***Correspondence:**
Matthew Katz
matthew.katz@health.qld.gov.au

Specialty section:
This article was submitted to Neuromuscular Disorders and Peripheral Neuropathies, a section of the journal Frontiers in Neurology

Received: *03 February 2022*
Accepted: *11 March 2022*
Published: *08 April 2022*

Citation:
Katz M, Garton FC, Davis M, Henderson RD and McCombe PA (2022) Novel Variants of ANO5 in Two Patients With Limb Girdle Muscular Dystrophy: Case Report. Front. Neurol. 13:868655. doi: 10.3389/fneur.2022.868655

INTRODUCTION

Anoctamin 5 (ANO5) is a protein that belongs to a family of calcium-activated chloride channels and phospholipid scramblases (1). The exact function of the ANO5 protein is not completely understood although it has been shown to play a role in sarcolemma repair (1). Recessive variants of *ANO5* have been associated with a range of muscle diseases including limb girdle muscular dystrophy (LGMD R12), (2, 3) distal myopathy (Miyoshi-like muscular dystrophy type 3), (4) exercise induced myalgia, (5) recurrent rhabdomyolysis, (6) axial myopathy (7) and asymptomatic hyperCKemia (5).

Patients with LGMD R12 typically present in adulthood with slowly progressive proximal lower limb and bicep weakness that is often asymmetric. This is associated with markedly elevated creatine kinase (CK) levels (2, 3). For unknown reasons females homozygous for *ANO5* variants tend to have a less severe phenotype than males (5). Dilated cardiomyopathy and cardiac conduction disease have been reported but are rare (8). Magnetic resonance imaging (MRI) of the lower limbs often shows selective atrophy and fatty infiltration of the posterior calf and thigh muscles (9).

Here we report the clinical, pathologic, and genetic findings of two unrelated patients presenting with LGMD who were found to have novel variants in *ANO5.*

CASE REPORT

Patient 1

This 35-year-old Iranian man presented with slowly progressive upper and lower limb weakness from the age of 20 years. At the time of presentation, the patient had difficulty standing from the seated position and washing his hair. There were no sensory symptoms. There was no significant medical history. The patient was borne to non-consanguineous parents. His brother had similar symptoms, but four other siblings were unaffected.

On examination he had a waddling gait. There was no muscle wasting. Tone was normal. There was MRC 4/5 weakness of hip flexion and extension, hip adduction and knee flexion and extension. There was MRC 4+/5 weakness of elbow flexion bilaterally. Distal upper and lower limb strength was normal (MRC 5/5). Facial, ocular and neck strength was normal (MRC 5/5). Reflexes were normal. The sensory examination was normal. The CK was 1990. An MRI of the upper limbs performed 3 years earlier showed increased T2 signal of teres major and long head of triceps bilaterally without atrophy or fatty infiltration (**Figure 1**). A muscle biopsy showed end-stage muscle disease consistent with a chronic muscular dystrophy.

Previous genetic testing for Becker muscular dystrophy and facioscapulohumeral muscular dystrophy (FSHD) was negative. The patient had also undergone targeted sequencing of the fukutin related protein (*FKRP*) gene, which was normal. Next generation sequencing (NGS) using a custom-designed 336 gene neuromuscular panel (PathWest Laboratory, Australia) (10) revealed homozygosity for a novel splice variant [c.294+5G>A; p.(Ala98Ins4*)] in intron 5 of the *ANO5* gene (ClinVar https://www.ncbi.nlm.nih.gov/clinvar/variation/1326848/?new_evidence=true).

While *in silico* analysis was not indicative of a likely splice effect, complementary DNA studies demonstrated intron inclusion and a complete absence of normal product (**Figure 2**). His brother was also found to be homozygous for the same variant on targeted sequencing of *ANO5*.

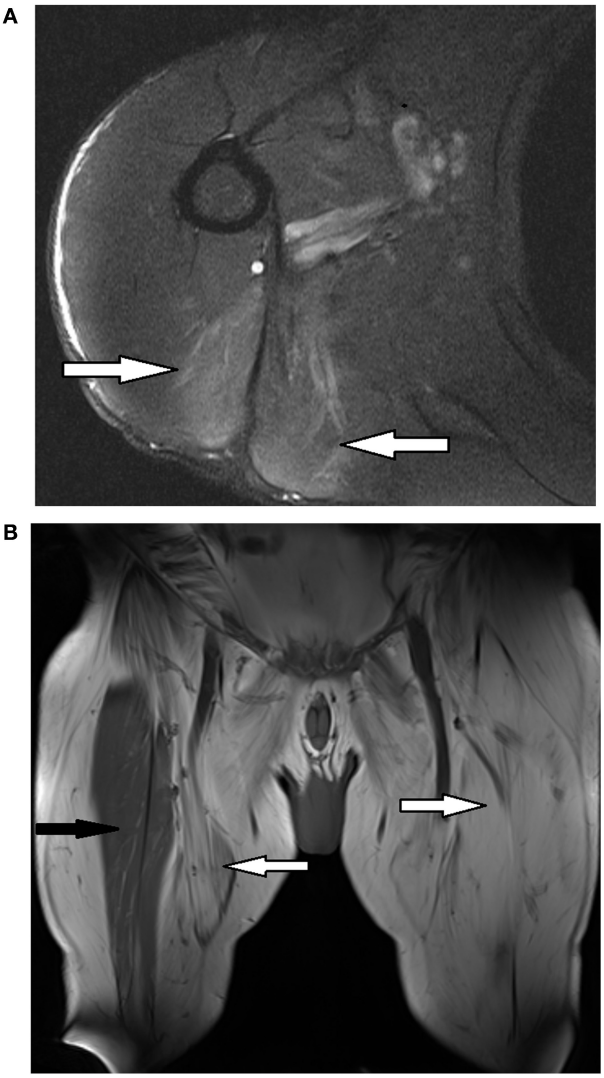

FIGURE 1 | Magnetic resonance imaging (MRI) of selected muscles from patients 1 and 2. **(A)** Left shoulder of patient 1 - axial T2* weighted sequence showing increased T2 signal of teres major and long head triceps (white arrows). **(B)** Bilateral thighs of patient 2 - coronal T1^ weighted sequence showing extensive fatty replacement of anterior and medial thigh muscles (white arrows) with relative preservation of the right rectus femoris (black arrow). *T2, transverse relaxation time; ^T1, longitudinal relaxation time.

Patient 2

This 55 year-old man presented with slowly progressive lower and upper limb weakness from the age of 35 years. At the time of presentation, he had difficulty rising from the seated position and walking up stairs. There was no significant medical history. There was no family history of muscle weakness.

On examination he had a waddling gait. There was wasting of the calf muscles bilaterally. The other limb muscles were of normal bulk. Tone was normal. There was MRC 4/5 weakness of hip flexion, hip extension, hip adduction, hip abduction, knee flexion and right knee extension. There was MRC 3/5 weakness of left knee extension. There was MRC 4+/5 weakness of elbow flexion and extension bilaterally. Distal upper and lower limb strength was normal (MRC 5/5). Facial, ocular and neck strength was normal (MRC 5/5). Reflexes were reduced in the upper and lower limbs. The sensory examination was normal. The CK was 4,910.

An EMG showed myopathic motor units without abnormal spontaneous activity in the right vastus medialis, vastus lateralis, biceps femoris and medial gastrocnemius. There were fibrillations with reduced recruitment of large motor units in the right tibialis anterior. MRI of the upper and lower limbs showed fatty infiltration and mild atrophy of the posterior calf and thigh muscles along with fatty infiltration and atrophy of the pectoral, latissimus dorsi and teres muscles (**Figure 1**). An echocardiogram did not show evidence of cardiomyopathy. The patient declined to undergo a muscle biopsy.

Next generation sequencing using a custom-designed 464 gene neuromuscular panel (PathWest Laboratory, Australia) (10) revealed compound heterozygosity for two variants in the *ANO5* gene; a previously reported pathogenic frameshift

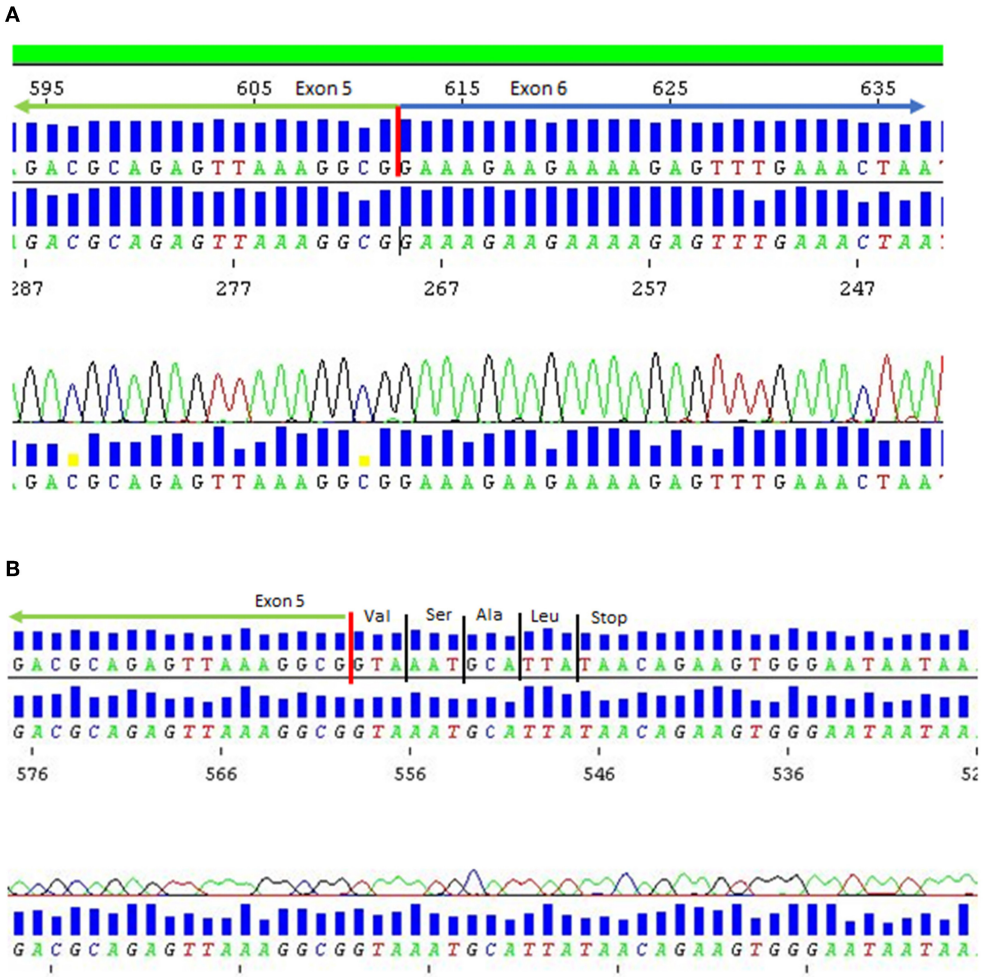

FIGURE 2 | DNA sequence chromatogram for patient 1. **(A)** Normal control mRNA. **(B)** Patient 1 mRNA showing loss of exon 5 donor splice site resulting in intron inclusion and premature termination of protein due to presence of stop codon in variant mRNA.

variant [c.191dupA; p.(Asn64fs)] in exon 5 that results in a premature stop signal and a novel missense variant [c.952G>C; p.(Ala318Pro)] in exon 10 (ClinVar https://www.ncbi.nlm.nih.gov/clinvar/variation/1327991/?new_evidence=false#id_first). Segregation studies were not possible as the patient's first-degree relatives were not available for genetic testing.

DISCUSSION

We describe two patients presenting with LGMD who were found to have novel *ANO5* variants after NGS using a custom-designed neuromuscular genetic panel. The use of multigene panels is especially helpful for the diagnosis of LGMD R12 as its phenotype can overlap with other types of LGMD (11) and muscle biopsies in these patients are often non-diagnostic and show non-specific myopathic or dystrophic changes (7, 12) although skeletal muscle amyloid deposits have been identified in some cases (13). The identification of disease causing variants with NGS also helps with genetic counseling in those with LGMD by allowing for targeted genetic testing in family members that could be carriers or at risk of inheriting the disease.

Patient 1 was a 35-year-old Iranian man who was homozygous for a novel splice variant [c.294+5G>A; p (Ala98Ins4*)]. This variant leads to intron inclusion resulting in premature truncation of the protein, is absent from controls (14–17) and segregates with disease in the affected sibling (13, 18) (**Figure 2** and **Table 1**). Patient 1 has Iranian ancestry. Most reported cases of LGMD R12 have been in European patients (3). However, LGMD R12 has been reported in patients from the Middle East, including Saudi Arabia (18), Jordan (19) and Afghanistan (20).

Patient 2 was a 55-year-old Caucasian man who was compound heterozygous for the frameshift variant [c.191dupA; p.(Asn64fs)] and a novel missense variant [c.952G>C; p.(Ala318Pro)]. Through a founder effect, the frameshift variant [c.191dupA; p.(Asn64fs)] is the most common pathogenic *ANO5* variant identified in European patients with LGMD R12 (3). The missense variant [c.952G>C; p.(Ala318Pro)] in patient 2 is

TABLE 1 | Genetic summary for *ANO5* variants.

Patient	Transcript reference	hg38	Codon variant	Amino acid change	POPmax	*In silico* prediction*	ACMG-AMP classification
Patient 1	NM_213599.3	11:22221215	c.294+5G>A	p.Ala98Ins4*	NR	–	Pathogenic (PVS1, PM2, PP1)
Patient 2	NM_213599.3	11:22250310	c.952G>C	p.Ala318Pro	NR	DDD	Variant of uncertain significance (PM2, PM3, PP3)
	NM_213599.3	11:22221107	c.191dupA	p.Asn64fs	0.0021	–	Pathogenic (PVS1, PS4, PP5)

ACMG-AMP = American College of Medical Genetics and Genomics - Association for Molecular Pathology (version: 8.4.7 from Varsome), hg38 = human reference genome, NR = allele not previously reported, POPmax = maximum allele frequency in each reference population from 1000GP, ExAC, gnomAD, and ESP.
** = Meta SVM, Meta LR, and M-CAP in silico prediction ("D" = deleterious, "T" = tolerated).*

absent from controls, is strongly conserved (21) and predicted to be damaging *in silico* (22, 23) (**Table 1**). Currently considered a variant of uncertain significance as per the American College of Medical Genetics and Genomics—Association for Molecular Pathology (ACMG-AMP) guidelines (24) additional functional evidence could help elucidate its impact. Detailed, mutation-specific assessments across *ANO5* are lacking in the literature but loss of *ANO5* has been shown to cause defective membrane repair (1). The novel missense variant we report in patient 2 is located within the first transmembrane domain of the protein (25) and could influence the effectiveness of membrane transport for repair (ie. coordination of annexins), particularly in muscle where it is highly expressed (26). The clinical presentation of patient 2 with adult onset, slowly progressive proximal lower limb and biceps weakness and significantly elevated CK is typical of other cases of LGMD R12 reported in the literature (2, 3).

CONCLUSION

ANO5 variants are not uncommon in LGMD but occur with a spectrum of LGMD severity. Our findings extend the genotypic spectrum of *ANO5* disease and supports the utility of next generation sequencing in the diagnostic process. Further work on understanding disease mechanisms underlying *ANO5* associated LGMD is needed to address relevant therapeutic avenues.

DATA AVAILABILITY STATEMENT

The datasets presented in this article are not readily available because of ethical and privacy restrictions. Requests to access the datasets should be directed to the corresponding author/s.

ETHICS STATEMENT

Ethical review and approval was not required for the study on human participants in accordance with the local legislation and institutional requirements. The patients/participants provided their written informed consent to participate in this study. Written informed consent was obtained from the individual(s) for the publication of any potentially identifiable images or data included in this article.

AUTHOR CONTRIBUTIONS

FG and MD assisted with the genetic data and review of paper. RH and PM assisted with overall review of the paper. All authors contributed to the article and approved the submitted version.

ACKNOWLEDGMENTS

The authors thank Jonas Bjorkman (Pathology Queensland) for his contribution of genetic data to **Figure 2**.

REFERENCES

1. Foltz SJ, Cui YY, Choo HJ, Hartzell HC. ANO5 ensures trafficking of annexins in wounded myofibers. *J Cell Biol*. (2021) 220:1–19. doi: 10.1083/jcb.202007059
2. Bolduc V, Marlow G, Boycott KM, Saleki K, Inoue H, Kroon J, et al. Recessive mutations in the putative calcium-activated chloride channel anoctamin 5 cause proximal LGMD2L and distal MMD3 muscular dystrophies. *Am J Hum Genet*. (2010) 86:213–21. doi: 10.1016/j.ajhg.2009.12.013
3. Hicks P, Sarkozy A, Muelas N, Koehler K, Huebner A, Hudson G, et al. P63 a founder mutation in Anoctamin 5 is a major cause of limb girdle muscular dystrophy. *Neuromuscul Disord*. (2011) 21:S24–5. doi: 10.1016/S0960-8966(11)70082-7
4. Mahjneh I, Jaiswal J, Lamminen A, Somer M, Marlow G, Kiuru-Enari S, et al. A new distal myopathy with mutation in anoctamin 5. *Neuromuscul Disord*. (2010) 20:791–5. doi: 10.1016/j.nmd.2010.07.270
5. Penttilä S, Palmio J, Suominen T, Raheem O, Evilä A, Gomez NM, et al. Eight new mutations and the expanding phenotype variability in muscular dystrophy caused by ANO5. *Neurology*. (2012) 78:897–903. doi: 10.1212/WNL.0b013e31824c4682
6. Milone M, Liewluck T, Winder TL, Pianosi PT. Amyloidosis and exercise intolerance in ANO5 muscular dystrophy. *Neuromuscul Disord*. (2012) 22:13–5. doi: 10.1016/j.nmd.2011.07.005
7. Silva AMS, Coimbra-Neto AR, Souza PVS, Winckler PB, Gonçalves MVM, Cavalcanti EBU, et al. Clinical and molecular findings in a cohort of ANO5-related myopathy. *Ann Clin Transl Neurol*. (2019) 6:1225–38. doi: 10.1002/acn3.50801
8. Wahbi K, Béhin A, Bécane HM, Leturcq F, Cossée M, Laforêt P, et al. Dilated cardiomyopathy in patients with mutations in anoctamin 5. *Int J Cardiol*. (2013) 168:76–9. doi: 10.1016/j.ijcard.2012.09.070
9. Sarkozy A, Deschauer M, Carlier RY, Schrank B, Seeger J, Walter MC, et al. Muscle MRI findings in limb girdle muscular dystrophy type 2L. *Neuromuscul Disord*. (2012) 22(Suppl. 2):122–9. doi: 10.1016/j.nmd.2012.05.012

10. Beecroft SJ, Yau KS, Allcock RJN, Mina K, Gooding R, Faiz F, et al. Targeted gene panel use in 2249 neuromuscular patients: the Australasian referral center experience. *Ann Clin Transl Neurol.* (2020) 7:353–62. doi: 10.1002/acn3.51002
11. Savarese M, Di Fruscio G, Tasca G, Ruggiero L, Janssens S, De Bleecker J, et al. Next generation sequencing on patients with LGMD and nonspecific myopathies: findings associated with ANO5 mutations. *Neuromuscul Disord.* (2015) 25:533–41. doi: 10.1016/j.nmd.2015.03.011
12. Seguí F, Gonzalez-Quereda L, Sanchez A, Matas-García A, Garrabou G, Rodriguez MJ, et al. Anoctamin 5 (ANO5) muscular dystrophy—three different phenotypes and a new histological pattern. *Neurol Sci.* (2020) 41:2967–71. doi: 10.1007/s10072-020-04453-y
13. Liewluck T, Winder TL, Dimberg EL, Crum BA, Heppelmann CJ, Wang Y, et al. ANO5-muscular dystrophy: clinical, pathological and molecular findings. *Eur J Neurol.* (2013) 20:1383–9. doi: 10.1111/ene.12191
14. Auton A, Abecasis GR, Altshuler DM, Durbin RM, Bentley DR, Chakravarti A, et al. A global reference for human genetic variation. *Nature.* (2015) 526:68–74. doi: 10.1038/nature15393
15. Lek M, Karczewski KJ, Minikel E V, Samocha KE, Banks E, Fennell T, et al. Analysis of protein-coding genetic variation in 60,706 humans. *Nature.* (2016) 536:285–91. doi: 10.1038/nature19057
16. Karczewski KJ, Francioli LC, Tiao G, Cummings BB, Alföldi J, Wang Q, et al. Variation across 141,456 human exomes and genomes reveals the spectrum of loss-of-function intolerance across human protein-coding genes. *bioRxiv[Preprint].* (2019). bioRxiv: 531210. doi: 10.1101/531210
17. *Exome Variant Server, NHLBI GO Exome Sequencing Project (ESP), Seattle, WA*. Available online at: https://evs.gs.washington.edu/EVS/
18. Bohlega S, Monies DM, Abulaban AA, Murad HN, Alhindi HN, Meyer BF. Clinical and genetic features of anoctaminopathy in Saudi Arabia. *Neurosciences.* (2015) 20:173–7. doi: 10.17712/nsj.2015.2.20140547
19. Little AA, Mckeever PE, Gruis KL. Novel mutations in the anoctamin 5 gene (ANO5) associated with limb-girdle muscular dystrophy 2L. *Muscle and Nerve.* (2013) 47:287–91. doi: 10.1002/mus.23542
20. Schessl J, Kress W, Schoser B. Novel ANO5 mutations causing hyper-CK-emia, limb girdle muscular weakness and miyoshi type of muscular dystrophy. *Muscle and Nerve.* (2012) 45:740–2. doi: 10.1002/mus.23281
21. Ramani R, Krumholz K, Huang YF, Siepel A. Phastweb: a web interface for evolutionary conservation scoring of multiple sequence alignments using phastCons and phyloP. *Bioinformatics.* (2019) 35:2320–2. doi: 10.1093/bioinformatics/bty966
22. Dong C, Wei P, Jian X, Gibbs R, Boerwinkle E, Wang K, et al. Comparison and integration of deleteriousness prediction methods for nonsynonymous SNVs in whole exome sequencing studies. *Hum Mol Genet.* (2015) 24:2125–37. doi: 10.1093/hmg/ddu733
23. Jagadeesh KA, Wenger AM, Berger MJ, Guturu H, Stenson PD, Cooper DN, et al. M-CAP eliminates a majority of variants of uncertain significance in clinical exomes at high sensitivity. *Nat Genet.* (2016) 48:1581–6. doi: 10.1038/ng.3703
24. Richards S, Aziz N, Bale S, Bick D, Das S, Gastier-Foster J, et al. Standards and guidelines for the interpretation of sequence variants: a joint consensus recommendation of the American college of medical genetics and genomics and the association for molecular pathology sue. *Genet Med.* (2015) 17:405–24. doi: 10.1038/gim.2015.30
25. Bateman A, Martin MJ, Orchard S, Magrane M, Agivetova R, Ahmad S, et al. UniProt: the universal protein knowledgebase in 2021. *Nucleic Acids Res.* (2021) 49:D480–9.
26. Lonsdale J, Thomas J, Salvatore M, Phillips R, Lo E, Shad S, et al. The Genotype-Tissue Expression (GTEx) project. *Nat Genet.* (2013) 45:580–5. doi: 10.1038/ng.2653

Conflict of Interest: The authors declare that the research was conducted in the absence of any commercial or financial relationships that could be construed as a potential conflict of interest.

Publisher's Note: All claims expressed in this article are solely those of the authors and do not necessarily represent those of their affiliated organizations, or those of the publisher, the editors and the reviewers. Any product that may be evaluated in this article, or claim that may be made by its manufacturer, is not guaranteed or endorsed by the publisher.

Copyright © 2022 Katz, Garton, Davis, Henderson and McCombe. This is an open-access article distributed under the terms of the Creative Commons Attribution License (CC BY). The use, distribution or reproduction in other forums is permitted, provided the original author(s) and the copyright owner(s) are credited and that the original publication in this journal is cited, in accordance with accepted academic practice. No use, distribution or reproduction is permitted which does not comply with these terms.

frontiers | Frontiers in Neurology

CASE REPORT
published: 25 April 2022
doi: 10.3389/fneur.2022.869230

Scoliosis Orthopedic Surgery Combined With Nusinersen Intrathecal Injection Significantly Improved the Outcome of Spinal Muscular Atrophy Patient: A Case Report

Beiyu Xu[1†], Cuijie Wei[2†], Xiao Hu[3], Wenzhu Li[4], Zhen Huang[4], Chengli Que[5], Jianxing Qiu[6], Chunde Li[1] and Hui Xiong[2*]*

[1] Department of Orthopedic/Spine Surgery, Peking University First Hospital, Beijing, China, [2] Department of Pediatrics, Peking University First Hospital, Beijing, China, [3] Department of Anesthesiology, Peking University First Hospital, Beijing, China, [4] Department of Rehabilitation Medicine, Peking University First Hospital, Beijing, China, [5] Department of Respiratory and Critical Care Medicine, Peking University First Hospital, Beijing, China, [6] Department of Radiology, Peking University First Hospital, Beijing, China

OPEN ACCESS

Edited by:
Giovanni Meola,
University of Milan, Italy

Reviewed by:
Stefania Corti,
University of Milan, Italy
Liliana Vercelli,
Centro Sclerosi Multipla, Ospedale San Luigi Gonzaga, Italy

***Correspondence:**
Chunde Li
lichunde@vip.sina.com
Hui Xiong
xh_bjbj@163.com

[†]These authors have contributed equally to this work

Specialty section:
This article was submitted to Neuromuscular Disorders and Peripheral Neuropathies, a section of the journal Frontiers in Neurology

Received: 04 February 2022
Accepted: 14 March 2022
Published: 25 April 2022

Citation:
Xu B, Wei C, Hu X, Li W, Huang Z, Que C, Qiu J, Li C and Xiong H (2022) Scoliosis Orthopedic Surgery Combined With Nusinersen Intrathecal Injection Significantly Improved the Outcome of Spinal Muscular Atrophy Patient: A Case Report. Front. Neurol. 13:869230. doi: 10.3389/fneur.2022.869230

Background: Spinal muscular atrophy (SMA) is an autosomal recessive disorder caused by pathogenic variation of the survival motor neuron (SMN) 1 gene. Symptoms of SMA include progressive limb muscle weakness, atrophy, and severe scoliosis. Nusinersen is an antisense oligonucleotide that can enhance the production of the SMN protein. Here, we report a case with scoliosis who received orthopedic surgery combined with Nusinersen intrathecal injections.

Case Presentation: Scoliosis orthopedic surgery followed by Nusinersen intrathecal injections was given to a 16-year-old girl who had thoracic and lumbar scoliosis and type 3 SMA. Surgery was performed for T3-S2 posterolateral fusion (PLF), with a channel left on the vertebral laminae of L3-L4. The balance of the spine and pelvis was significantly improved and the height increased by 9 cm. Lumbar puncture was conducted with local anesthesia under ultrasound and CT guidance through the laminae channel and Nusinersen was successfully injected. Comparing the two approaches, real-time ultrasound guidance for intrathecal Nusinersen injections after spinal surgery is preferred, however, CT guidance is an alternative if the initial puncture procedure is difficult. After the aforementioned multidisciplinary treatment, a good outcome was achieved, as demonstrated by a 2-point increase in RULM and MFM32 scores 2 months later.

Conclusion: Scoliosis orthopedic surgery combined with Nusinersen intrathecal injection is an effective treatment for SMA patients with scoliosis.

Keywords: SMA, scoliosis orthopedic surgery, Nusinersen intrathecal injection, real-time ultrasound guidance, CT guidance, case report

INTRODUCTION

Spinal muscular atrophy (SMA) is an autosomal recessive disorder that leads to the degeneration and even loss of the motor neurons in the spinal cord. Usually, it is caused by the deletion of exon 7 of the SMN1 gene. It has been noted that its incidence is ∼10 in 100,000 at birth and later prevalence of individuals with classic forms of the disease is ∼1–2 per 100,000 persons (1). According to the age of onset and maximum exercise capacity, there are three different types of SMA, namely, type 1, type 2, and type 3, in children, and type 4 in adulthood. Among those, type 1 SMA is the most severe and also the most common fatal neuromuscular disorder in infants (2). SMN2 gene undergoes alternative splicing and produces a truncated mRNA isoform missing exon seven. A C-to-T nucleotide transition at position six of exon seven of the SMN2 gene is responsible for the alternative splicing. The resulted truncated SMN protein is non-functional and thought to be degraded rapidly. About 10% of SMN2 pre-mRNA is properly spliced and subsequently translated into full-length SMN protein. Therefore, the quantity of the functional SMN protein produced and the clinical severity of SMA is dependent on the number of the SMN2 gene copies retained in the SMA patients.

Nusinersen is an anti-sense oligonucleotide, which was designed to modify the splicing behavior of the SMN2 gene and thus increase the inclusion of exon7 and the expression of the full-length SMN protein (3, 4). It was approved by the US Food and Drug Administration (FDA) in late December 2016, the European Medicines Agency in June 2017 (5), and the Chinese national medical product administration (NMPA) in 2019. Due to its inability to pass through the blood–brain barrier, Nusinersen can only be administered intrathecally through lumbar puncture (6).

Respiratory dysfunction is the most common complication and primary cause of death in SMA. Patients may have difficulty in clearing lower respiratory secretions due to cough weakness, and some with severe scoliosis may develop restrictive ventilatory dysfunction due to their severe chest wall deformity. Scoliosis and hip subluxation or dislocation are the two most common orthopedic problems encountered by patients with SMA (3). The collapsing long C-shaped scoliosis (7), typically seen in children with SMA, is caused by the weakness of the trunk muscles and their inability to keep the spine in the upright position (4). Such curvature may involve a large segment of the spine with its apex often located in the thoraco-lumbar junction, extending into the pelvis and leading to the development of a significant imbalance between trunk and pelvis (8). The age of onset, severity, and progression of scoliosis are related to the type of SMA and the extent of muscle weakness (9). The more severely the child is affected, the higher the probability of developing scoliosis at an earlier age and also the greater anticipated curve progression (1). Spinal fusion is recommended in the presence of documented scoliosis progression and curves between 40° and 60° in children, ideally at 10 years of age or older (10), especially, if there is a recorded deterioration in their motor function or pulmonary capacities. However, intrathecal injection treatment is very difficult for the patients who have received orthopedic surgery because of the lack of anatomical landmarks on the vertebral laminae and deficient flexion of the lumbar spine after scoliosis orthopedic surgery and there were few experiences in China up to date.

Here, we report an SMA case with scoliosis who underwent orthopedic surgery followed by Nusinersen intrathecal injections, and technical essentials of the procedure. It perfectly reflects the multidisciplinary cooperation.

CASE REPORT

Clinical Data

The case is a 16-year-old girl who achieved independent walking at one year old. She was found to have progressive muscle weakness with waddled gait and difficulty walking up and down stairs and squatting at 3 years old. She developed tremor in both the hands at the age of 5 years. At the age of 12, the patient was unable to squat or walk up and down stairs. She lost her ability to walk at 13 years old and ability to stand at 15 years old. Currently, she is wheelchair bound. The muscle strength of the patient's upper limbs is relatively preserved compared to her lower limbs and she can write in a prone position, but cannot lift heavy objects. Her intelligence is normal. There is no consanguinity in the parents and no history of any neurological disorders, genetic conditions, or early deaths in either parents' family.

On examination, the patient had atrophic muscles in her proximal lower limbs and relatively pseudohypertrophy of the gastrocnemius. Her upper extremity strength was Grade 4 and lower extremity strength was Grades 2-3, based on Medical Research Council (MRC) scale. She was observed exhibiting tongue fasciculations. She has tongue fasciculation and atrophy, areflexia, joint contractures, ankylosis of both feet, and severe scoliosis.

Her EMG showed neurogenic injury with abnormal insertional activity and reduced recruitment pattern. The muscle MRI showed fatty infiltration, amyotrophy, and edema.

Diagnostic Tests

Her genetic testing showed homozygous deletion (exon7 and exon8) of the SMN1 gene, and there were 3 copies of the SMN2 gene. Then, the systemic functions were assessed in detail after diagnosis.

Orthopedic Complications

Scoliosis and pelvis obliquity developed after the patient lost her independent walking. She was diagnosed to have long C-shaped thoracolumbar scoliosis with cobb angel of 63° at present. Inclination of the pelvis was 9.5°. Because of the inclination of pelvis and scoliosis, she needs to use both hands to maintain balance while sitting, therefore, making it impossible for her to study or work with her upper limbs.

Respiratory Involvement

Pulmonary function test showed a decrease vital capacity and an increased residual volume. Her diffusing lung capacity for carbon

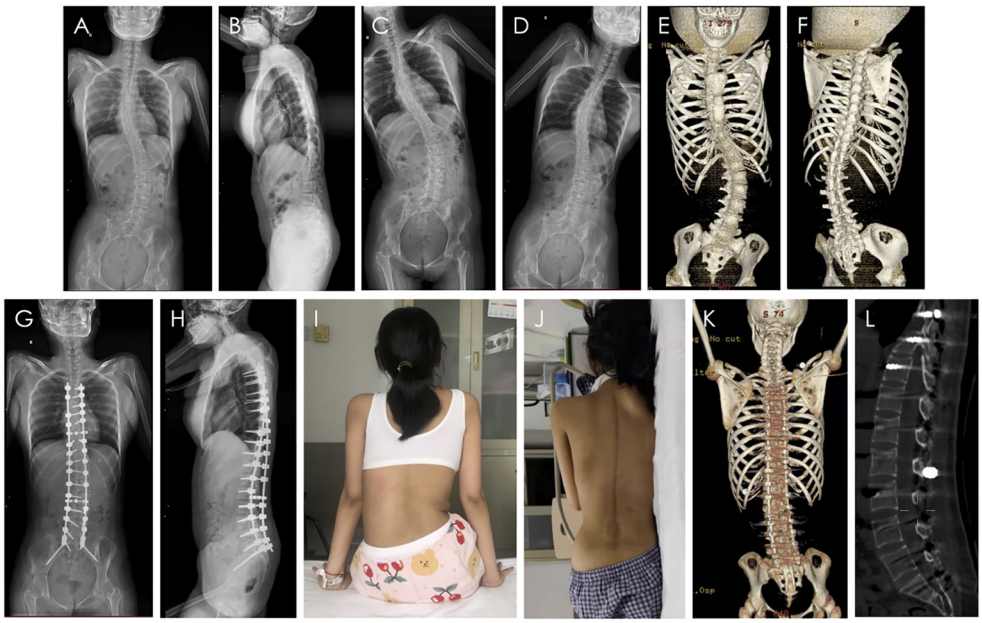

FIGURE 1 | Scoliosis orthopedic surgery. X-ray, CT images and appearance of the SMA patient with scoliosis. **(A)** The anteroposterior view of spinal X-ray before surgery. **(B)** The lateral view of spinal X-ray before surgery. **(C,D)** The left and right bending view of spinal X-ray before surgery. **(E,F)** The three-dimensional CT images before surgery. **(G)** The anteroposterior view of spinal X-ray after surgery. **(H)** The lateral view of spinal X-ray after surgery. **(I)** The appearance of the back before surgery. **(J)** The appearance of the back after surgery. **(K)** The three-dimensional CT images after surgery. **(L)** The sagittal CT images after surgery and the osseous channel are circled in the figure.

monoxide (DLCO) was 79.45% predicted. The patient's lung function damage was presented as restrictive ventilatory defect.

SCOLIOSIS ORTHOPEDIC SURGERY

Rapid progression of scoliosis and decompensation of the trunk can lead to cardiorespiratory functional impairment in an unexpectedly short period of time. In order to free up the upper limbs for daily activities and to prevent cardiorespiratory functional deterioration, spinal fusion is recommended for her. In consideration of the pelvis obliquity and the flexibility of scoliosis, an isolated posterior spinal arthrodesis should be sufficient to achieve satisfactory correction of her deformity, without the need for additional anterior surgery or preoperative spinal traction. Scoliosis orthopedic surgery with sequential Nusinersen intrathecal injection was decided with fully consent from both the patient and her parents. She received the T3-S2 PLF surgery with 30 pedicle screws implanted in September 2021.

Because of the severe pelvic tilt, orthopedic fusion surgery was fixed to the S2 segment, and S2 sacral alar–iliac screws were planted for spinal–pelvic fixation. The surgical procedure was technically successful and well-tolerated. No severe postoperative complications were noted. The scoliosis correction rate was up to 71.4% and her height had increased by 9 cm. Pelvic inclination angle improved from 9.5° (preoperative) to 0.5° (postoperative) and pelvic tilt was well-corrected (**Figure 1**).

Clinical outcomes of the orthopedic surgery are summarized in **Table 1**.

Nusinersen Intrathecal Injection

The intrathecal injection was completed at the 30th day after the orthopedic surgery. In a novel procedure, the osseous channel was left on the vertebral laminae of L3-L4 to facilitate subsequent intrathecal injection in this case. This included partial removal of the superior half of the lamina, the spinous process of L4 and the inferior half of the lamina and the spinous process of L3 with complete excision of the intervening ligamentum flavum.

Lumbar punctures were successfully performed with local anesthesia under real-time ultrasound guidance through the laminae channel for the first and second Nusinersen injections (**Figures 2A,B**), although it was time-consuming to find the anatomical structure in which echo signal was affected by the postoperative local anatomical changes and implants. Considering the comfort and minimization of tissue injury to the patient, lumbar puncture was guided with the help of CT for the third and fourth dosage of Nusinersen (**Figures 2C–E**). Location, direction, and depth of puncture was quickly and clearly determined by CT, with a much higher resolution. In the CT guidance process, low-dose parameters were set, and the final radiation amount of a single operation was presumably in the very low range of 0.1 (mSv), which was equivalent to the radiation amount of 1 chest CT (0.05–0.24 mSv). Clinical data from the Nusinersen intrathecal injection are shown in **Table 2**.

Postoperative Recovery

During the perioperative period, the patient received individualized rehabilitation intervention as soon as possible

TABLE 1 | The clinical data and outcome about the orthopedic surgery.

	Preoperative	Intraoperative records	Postoperative
Scoliosis angle (°)	63		18
Height (cm)	140		149
Inclination of pelvis (°)	9.5		0.5
Height difference of shoulders (cm)	2.3		0.5
Height difference of crista iliaca (cm)	1.5		0
Perpendicular distance of S1 and convex point (cm)	3.8		1.9
Weight (kg)	35.3		38
BMI (kg/m^2)	18.01		17.1
Operation time (min)		437	
Antihepatic time (min)		565	
Operative position		Prone position	
Fusion level		T3-S2 (S2 alar-iliac)	
Intraoperative blood loss (ml)		750	
Heterogenous blood transfusion (ml)		400 (RBC) / 200 (Plasma)	
Autologous blood transfusion (ml)		668	
Number of pedicle screws		30	

according to the results of different means of assessment, including: (1) manual active-assistive stretching of lower extremity joints; (2) thoraco-lumbar sacral or those for posture and to promote function; (3) muscle strength training and functional activity exercise; (4) bicycle training with resistance; and (5) respiratory muscle training.

In this study, the MFM 32, RULM, and HFMSE scales were used to evaluate the changes in motor function of the patient (**Table 2**). After the surgery and three doses of Nusinersen, both MFM32 and RULM scores improved by 2 points, due to improvements in muscle strength and motor function of upper extremities. However, HFMSE scores decreased temporally after surgery, because the surgery damaged the trunk muscles, which affected some activities, such as rolling over. It will probably take some time to recover.

Above all, spinal orthopedic surgery not only increased the thoracic volume of the patient, but also facilitated the rehabilitation exercise process. The motor functions of patients improved significantly after the surgery, four doses of Nusinersen and rehabilitation training.

DISCUSSION

Spinal muscular atrophy affects motor neurons of the spinal cord and the lower bulbar nuclei (11). It manifests clinically with progressive limb and trunk weakness affecting the proximal trunk muscles more than the distal muscles and the lower limbs more than the upper ones according to the natural history (12). According to the patient's manifestation and gene test result, she was diagnosed SMA, type 3. She received further multidisciplinary treatment in our neuromuscular disorder center.

The spinal deformity develops as a consequence of the generalized weakness and poor ambulatory function (11). Patients with SMA and mild scoliosis who lose ambulatory capacity and became wheelchair-bound show rapid deterioration of their scoliosis and pelvis obliquity (13). Orthopedic surgery is the primary treatment for the patients with neuromuscular scoliosis and pelvic tilt, and is also an important part of the standard care for SMA patients. If the orthopedic corrective surgery is not performed in time, the spinal deformity will significantly be aggravated and the costal arch will gradually impact the iliac crest, resulting in severe lumbar and costal pain. Furthermore, the cardiopulmonary function and gastrointestinal function will deteriorate gradually with the aggravation of chest and abdominal compression, and eventually become life-threatening. The objective of the orthopedic surgery is to correct the tilt and balance of the pelvis, restore the coronal and sagittal balance of the spine, promote potential for upper limb rehabilitation exercise and consequently improve the quality of life of the patient (11). The correction rate for scoliosis depends on the flexibility of the spine. Greater flexibility results in a better correction rate (14). Spinal development usually become mature between the ages of 13–16 accompanied by acceptable curve flexibility, however, spinal flexibility decreases with age (15). Therefore, the optimal age for scoliosis surgery is between 13 and 16 years of age (16). In this case, the balance of the spine and pelvis was improved significantly and the height increased by 9 cm, and the patient was able to sit alone without the assistance of hands after surgery, thus, facilitating the rehabilitation exercises. The trend of improvement of the patient's motor function can be seen in the short term and the further long term follow-up is required.

Nusinersen is an effective, life-changing treatment in children of all ages with SMA (5, 17). It can be administered intrathecally even in children with severe scoliosis or following spine surgery (18, 19). The spinous processes are removed and the vertebra is fixed with the posterior screw rod system during scoliosis correction surgery (20). Due to the lack of anatomical landmarks on the vertebral laminae and deficient flexion of the lumbar spine after orthopedic fusion surgery (21), the space for needle insertion between the adjacent spinous processes is limited. Therefore, the intrathecal injection treatment is very difficult for the patients who have received orthopedic surgery. Cervical puncture can be used for Nusinersen administration. However, this approach was not necessarily due to the high technical success rate of lumbar punctures given that even the slightest error during a cervical puncture operation may cause cervical spinal cord injury, paralysis, and apnea. Transforaminal approach has been used frequently for intrathecal injections after spinal surgery, however, there is a risk of injuries to nerve roots and vessels, which pass through the foramen. In order to preserve

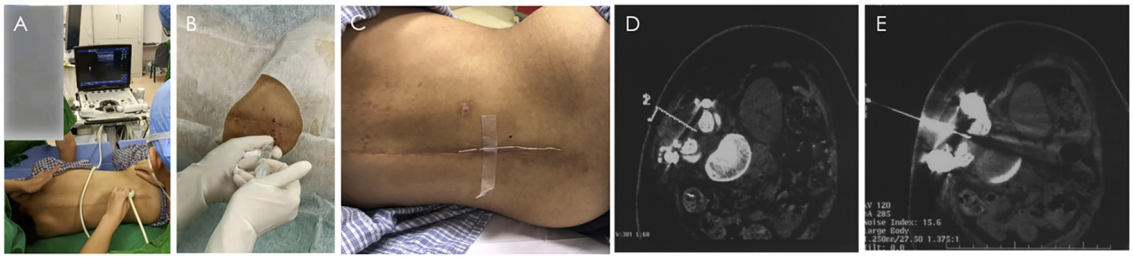

FIGURE 2 | Nusinersen intrathecal injection process under the guidance of B-ultrasound and CT. **(A,B)** Real-time ultrasound-guided lumbar puncture. **(A)** Ultrasound probe position of paramedian sagittal oblique scan at the level of lamina. **(B)** Local anesthesia before intrathecal injection. C-E CT-guided lumbar puncture. **(C)** Place a metal positioning wire at the posterior midline around the lumbar spine. **(D)** Determine the needle insertion route through CT scan, and calculate the needle insertion point on the body surface and needle insertion angle. **(E)** The puncture needle successfully entered the subarachnoid space).

TABLE 2 | Clinical and motor function evaluation with Nusinersen intrathecal injection.

Nusinersen intrathecal injection and assessment scale	Preoperative	1st injection	2nd injection	3rd injection	4th injection
Guidance mode		Ultrasound-guided	Ultrasound-guided	CT-guided	CT-guided
Operation time (min)		65	49	15	15
Time of puncture (min)		30	40	3	3
VAS score after injection		3	5	1	1
Intraoperative lidocaine dose (ml)		10	10	1	1
MFM32	57	58	58	59	
RULM	34	36	36	36	
HFMSE	33	31	31	31	

the channel for intrathecal injection, an L3-L4 laminectomy can be performed at the same time as spinal correction and fusion surgery in this patient.

The first two lumbar punctures were performed with local anesthesia under real-time ultrasound guidance while the third and fourth ones were administered with CT guidance through the laminae channel.

Compared with the CT guidance, ultrasound guidance is available readily at the bedside and radiation-free, but it is important for a clinically experienced physician to perform the procedure because metal artifacts such as implants can interfere with the ultrasound. It always takes a period of time to find the vertebral space using ultrasound, and the longer operation time brings more discomfort to the patient (22). CT-guided intrathecal injection is a feasible method of Nusinersen administration for patients with difficult lumbar puncture because of the severe scoliosis or spinal stabilization with a high technical success rate (23). In this case, CT-guided puncture required less operative time, a lower local anesthetic dose, and lower VAS score after the procedure compared with ultrasound guidance. Considering the advantages and disadvantages of both guidance approaches, we recommend real-time ultrasound guidance for the first intrathecal injection of Nusinersen for SMA patients after spinal surgery, which can be replaced by CT guidance if the first puncture process is difficult.

In summary, scoliosis orthopedic surgery combined with Nusinersen intrathecal injection is an effective and efficient procedure for SMA patients with scoliosis. The patient benefited from the osseous channel left during orthopedic surgery. Not only were the scoliosis and pelvic tilt significantly corrected, but the intrathecal injection was performed safely. As with all the single case studies, further studies with larger sample sizes are needed.

DATA AVAILABILITY STATEMENT

The original contributions presented in the study are included in the article/supplementary material, further inquiries can be directed to the corresponding authors.

ETHICS STATEMENT

The studies involving human participants were reviewed and approved by the Ethics Committee of Peking University First Hospital (No. 2015[916], Beijing, China). Written informed consent to participate in this study was provided by the participants' legal guardian/next of kin. Written informed consent was obtained from the individual(s), and minor(s)' legal guardian/next of kin, for the publication of any potentially identifiable images or data included in this article.

AUTHOR CONTRIBUTIONS

BX was a major contributor in writing the manuscript and completed the orthopedic surgery. CW designed the study, performed the lumbar punctures, and revised the manuscript. BX and CW both contributed equally to this work. XH facilitated the lumbar punctures. WL, ZH, and CQ all revised the manuscript. CL revised the manuscript, supervised the lumbar punctures, and completed the orthopedic surgery. HX designed the study and also revised the manuscript. All these authors critically revised and approved the final manuscript.

FUNDING

This work was supported by the grants from the National Natural Science Foundation of China (No. 82171393); the National Key Research and Development Program of China (No. 2016YFC0901505), and Beijing Key Laboratory of Molecular Diagnosis and Study on Pediatric Genetic Diseases (No. BZ0317).

ACKNOWLEDGMENTS

The authors are grateful to our research participant and her family.

REFERENCES

1. Verhaart IEC, Robertson A, Wilson IJ, Aartsma-Rus A, Cameron S, Jones CC, et al. Prevalence, incidence and carrier frequency of 5q-linked spinal muscular atrophy - a literature review. *Orphanet J Rare Dis.* (2017) 12:124. doi: 10.1186/s13023-017-0671-8
2. Lamb C, Peden A. Understanding the experience of living with spinal muscular atrophy: a qualitative description. *J Neurosci Nurs.* (2008) 40:250–6. doi: 10.1097/01376517-200808000-00009
3. Rigo F, Chun SJ, Norris DA, Hung G, Lee S, Matson J, et al. Pharmacology of a central nervous system delivered 2′-O-methoxyethyl-modified survival of motor neuron splicing oligonucleotide in mice and nonhuman primates. *J Pharmacol Exp Ther.* (2014) 350:46–55. doi: 10.1124/jpet.113.212407
4. Talbot K, Tizzano EF. The clinical landscape for SMA in a new therapeutic era. *Gene Ther.* (2017) 24:529–33. doi: 10.1038/gt.2017.52
5. Gidaro T, Servais L. Nusinersen treatment of spinal muscular atrophy: current knowledge and existing gaps. *Dev Med Child Neurol.* (2019) 61:19–24. doi: 10.1111/dmcn.14027
6. Szabó L, Gergely A, Jakus R, Fogarasi A, Grosz Z, Molnár MJ, et al. Efficacy of nusinersen in type 1, 2 and 3 spinal muscular atrophy: Real world data from Hungarian patients. *Eur J Paediatr Neurol.* (2020) 27:37–42. doi: 10.1016/j.ejpn.2020.05.002
7. Glascock J, Sampson J, Haidet-Phillips A, Connolly A, Darras B, Day J, et al. Treatment algorithm for infants diagnosed with spinal muscular atrophy through newborn screening. *J Neuromuscul Diseases.* (2018) 5:145–58. doi: 10.3233/JND-180304
8. Swarup I, MacAlpine EM, Mayer OH, Lark RK, Smith JT, Vitale MG, et al. Impact of growth friendly interventions on spine and pulmonary outcomes of patients with spinal muscular atrophy. *Eur Spine J.* (2021) 30:768–74. doi: 10.1007/s00586-020-06564-8
9. Wijngaarde CA, Brink RC, de Kort FAS, Stam M, Otto LAM, Asselman FL, et al. Natural course of scoliosis and lifetime risk of scoliosis surgery in spinal muscular atrophy. *Neurology.* (2019) 93:e149–e158. doi: 10.1212/WNL.0000000000007742
10. Shen PC, Lu CC, Liang WC, Tien YC, Jong YJ, Lu YM, et al. Predictors for deformity progression in a spinal muscular atrophy cohort after scoliosis correction surgery. *Clin Spine Surg.* (2020) 33:E407–E414. doi: 10.1097/BSD.0000000000000989
11. Finkel RS, Mercuri E, Meyer OH, Simonds AK, Schroth MK, Graham RJ, et al. Diagnosis and management of spinal muscular atrophy: Part 2: pulmonary and acute care; medications, supplements and immunizations; other organ systems; and ethics. *Neuromuscul Disord.* (2018) 28:197–207. doi: 10.1016/j.nmd.2017.11.004
12. Modi HN, Suh SW, Hong JY, Cho JW, Park JH, Yang JH. Treatment and complications in flaccid neuromuscular scoliosis (Duchenne muscular dystrophy and spinal muscular atrophy) with posterior-only pedicle screw instrumentation. *Eur Spine J.* (2010) 19:384–93. doi: 10.1007/s00586-009-1198-z
13. Farber HJ, Phillips WA, Kocab KL, Hanson DS, Heydemann JA, Dahl BT, et al. Impact of scoliosis surgery on pulmonary function in patients with muscular dystrophies and spinal muscular atrophy. *Pediatr Pulmonol.* (2020) 55:1037–42. doi: 10.1002/ppul.24664
14. Weaver JJ, Natarajan N, Shaw DWW, Apkon SD, Koo KSH, Shivaram GM, et al. Transforaminal intrathecal delivery of nusinersen using cone-beam computed tomography for children with spinal muscular atrophy and extensive surgical instrumentation: early results of technical success and safety. *Pediatr Radiol.* (2018) 48:392–7. doi: 10.1007/s00247-017-4031-6
15. Geraci AP, Black K, Jin M, Rimler S, Evans A. Transforaminal lumbar puncture for intrathecal nusinersen administration. *Muscle Nerve.* (2018). doi: 10.1002/mus.26082. [Epub ahead of print].
16. Nascene DR, Ozutemiz C, Estby H, McKinney AM, Rykken JB. Transforaminal lumbar puncture: an alternative technique in patients with challenging access. *AJNR Am J Neuroradiol.* (2018) 39:986–91. doi: 10.3174/ajnr.A5596
17. Michelson D, Ciafaloni E, Ashwal S, Lewis E, Narayanaswami P, Oskoui M, et al. Evidence in focus: Nusinersen use in spinal muscular atrophy: Report of the Guideline Development, Dissemination, and Implementation Subcommittee of the American Academy of Neurology. *Neurology.* (2018) 91:923–33. doi: 10.1212/WNL.0000000000006502
18. Zhang J, Cui X, Chen S, Dai Y, Huang Y, Zhang S. Ultrasound-guided nusinersen administration for spinal muscular atrophy patients with severe scoliosis: an observational study. *Orphanet J Rare Dis.* (2021) 16:274. doi: 10.1186/s13023-021-01903-4
19. Bortolani S, Stura G, Ventilii G, Vercelli L, Rolle E, Ricci F, et al. Intrathecal administration of nusinersen in adult and adolescent patients with spinal muscular atrophy and scoliosis: transforaminal versus conventional approach. *Neuromuscul Disord.* (2019) 29:742–6. doi: 10.1016/j.nmd.2019.08.007
20. Long WD, Smith BG. A Review: The Use of Growing Rods to Treat Scoliosis in Patients with Spinal Muscular Atrophy. *Seminars in Spine Surgery.* (2012) 24:164–168. doi: 10.1053/j.semss.2012.04.006
21. McElroy MJ, Shaner AC, Crawford TO, Thompson GH, Kadakia RV, Akbarnia BA, et al. Growing rods for scoliosis in spinal muscular atrophy: structural effects, complications, hospital stays. *Spine.* (2011) 36:1305–11. doi: 10.1097/BRS.0b013e3182194937
22. Elsharkawy H, Maheshwari A, Babazade R, Perlas A, Zaky S, Mounir-Soliman L. Real-time ultrasound-guided spinal anesthesia in patients with predicted difficult anatomy. *Minerva Anestesiol.* (2017) 83:465–73. doi: 10.23736/S0375-9393.16.11610-4
23. Rosiak G, Lusakowska A, Milczarek K, Konecki D, Fraczek A, Rowinski O, et al. Ultra-low radiation dose protocol for CT-guided intrathecal nusinersen

injections for patients with spinal muscular atrophy and severe scoliosis. *Neuroradiology*. (2021) 63:539–45. doi: 10.1007/s00234-021-02643-9

Conflict of Interest: The authors declare that the research was conducted in the absence of any commercial or financial relationships that could be construed as a potential conflict of interest.

Publisher's Note: All claims expressed in this article are solely those of the authors and do not necessarily represent those of their affiliated organizations, or those of the publisher, the editors and the reviewers. Any product that may be evaluated in this article, or claim that may be made by its manufacturer, is not guaranteed or endorsed by the publisher.

Copyright © 2022 Xu, Wei, Hu, Li, Huang, Que, Qiu, Li and Xiong. This is an open-access article distributed under the terms of the Creative Commons Attribution License (CC BY). The use, distribution or reproduction in other forums is permitted, provided the original author(s) and the copyright owner(s) are credited and that the original publication in this journal is cited, in accordance with accepted academic practice. No use, distribution or reproduction is permitted which does not comply with these terms.

frontiers | Frontiers in Neurology

ORIGINAL RESEARCH
published: 25 May 2022
doi: 10.3389/fneur.2022.902172

Nodopathies in the Early Diagnosis of Axonal Forms of Guillain-Barré Syndrome

Sara Urdiales-Sánchez[1], José-Ramiro González-Montaña[2], Ricardo Diaz-Pérez[1], Pablo Calvo-Calleja[1], María-Antonia Gutiérrez-Trueba[1] and Javier Urdiales-Urdiales[3]*

[1] Section of Clinical Neurophysiology, Universitary Hospital of Cabueñes, Gijón, Spain, [2] Department of Medicine, Surgery and Anatomy Veterinary, University of León, León, Spain, [3] Service of Clinical Neurophysiology, Universitary Hospital of León, León, Spain

OPEN ACCESS

Edited by:
Giovanni Meola,
University of Milan, Italy

Reviewed by:
Satish Vasant Khadilkar,
Bombay Hospital, India
Antonino Uncini,
University of Studies G. d'Annunzio Chieti and Pescara, Italy

****Correspondence:***
José-Ramiro González-Montaña
jramirogonzalez@unileon.es

Specialty section:
This article was submitted to Neuromuscular Disorders and Peripheral Neuropathies, a section of the journal Frontiers in Neurology

Received: *22 March 2022*
Accepted: *22 April 2022*
Published: *25 May 2022*

Citation:
Urdiales-Sánchez S, González-Montaña J-R, Diaz-Pérez R, Calvo-Calleja P, Gutiérrez-Trueba M-A and Urdiales-Urdiales J (2022) Nodopathies in the Early Diagnosis of Axonal Forms of Guillain-Barré Syndrome. Front. Neurol. 13:902172. doi: 10.3389/fneur.2022.902172

Introduction: Guillain-Barré syndrome (GBS) has been classified into demyelinating and axonal subtypes or forms, such as acute motor axonal neuropathy (AMAN) and regional pharyngeal-cervical-brachial variant (PCBv).

Objective: To study the relationship between motor nerve conduction blocks (CBs) and prognosis in AMAN and PCBv.

Patients and Methods: We retrospectively analyzed six cases of AMAN and PCBv with serial nerve conduction studies (NCS) and electromyography (EMG).

Results: The serial NCS (1st−2nd and 3rd week) showed, as the most constant data, a decreased amplitude of the compound muscle action potential (CMAP) in 100% of cases. CBs were present in 66.6% of cases. EMG (3rd week) showed signs of severe denervation in 33.3%. All patients were treated from the 1st−2nd week of evolution with intravenous immunoglobulins (IVIGs). Patients with CBs (1st−2nd and 3rd week), showed reversible CBs or reversible conduction failure (RCF) and complete recovery at 1 month. Patients without CBs, with persistent reduced distal CMAP amplitude (dCMAP), showed severe acute denervation due to axonal degeneration (3rd week and 1st−3rd month) and a slow recovery of several months.

Conclusions: Not all axonal forms of GBS have a poor prognosis. This study of AMAN and PCBv shows that patients with CBs can have reversible CBs or RCF, and good prognosis. Patients without CBs, with persistent reduction of dCMAP amplitude decrement, have severe acute denervation, and a worse prognosis. AMAN and PCBv have a continuous spectrum ranging from CBs due to dysfunction/disruption of Nodes of Ranvier, called nodopathies, with reversible CBs or RCF and good prognosis, to axonal degeneration with worse prognosis.

Keywords: acute motor axonal neuropathy, nerve conduction blocks, nodopathies, nodo-paranodopathies, regional variants, Guillain-Barré syndrome

INTRODUCTION

Traditionally and currently, Guillain-Barre Syndrome (GBS) applies to a broad spectrum of acute acquired and immune-mediated inflammatory polyradiculoneuropathies, with classification generally into two major groups or forms, demyelinating forms, such as acute demyelinating polyneuropathy (AIDP) and axonal forms, such as acute motor axonal neuropathy (AMAN) and the more frequent regional pharyngeal-cervical-brachial variant (PCBv) with axonal pattern (1).

The frequency of AMAN ranges from 6–7% in the United Kingdom and Spain to 30–65% in Asia and Central and South America (1).

Acute motor axonal neuropathy is a post-infectious autoimmune process against peripheral nerve antigens, associated with the presence of antiganglioside antibodies anti-GM1, GD1a, GM1b, and GalNAc-GD1a (1–3). PCBv is associated with a heterogeneous immunological profile of anti-ganglioside, anti-GT1a, anti-GT1b, GQ1b, GD1a, and GT1b antibodies (4–6). Gangliosides contribute to the stability of proteins that maintain the binding of axon and myelin at the paranodes and of sodium channels at the nodes of Ranvier. Antibodies bind to gangliosides at nodes of Ranvier, resulting in inactivation of voltage-dependent sodium channels or may produce primary axonal degeneration (3, 7).

The diagnosis is clinical, supported by electrodiagnostic, cerebrospinal fluid (CSF), and antiganglioside antibodies. AMAN presents with acute progressive weakness, with relative symmetry in upper and lower limbs, without sensory symptoms and osteotendinous reflexes usually being preserved (1). PCBv appears with progressive oropharyngeal, facial, and cervicobrachial weakness (sometimes affecting the arms) (1, 8, 9).

Based on electrodiagnosis, AMAN was previously characterized by axonal degeneration with decreased CMAP amplitude without signs of demyelination (10, 11). Currently, motor conduction blocks (CBs) without signs of demyelination (temporal dispersion of the CMAP) are described as being, in some cases, reversible CBs or reversible conduction failure (RCF) (12). A similar finding restricted to the upper extremities is observed in the PCBv (9, 13, 14).

MATERIALS AND METHODS

We retrospectively analyzed six cases of patients with AMAN and regional axonal variant PCBv, aged 18–73 years, from the Universitary Hospital of León. The research protocol and informed consent were requested and approved by the corresponding Medical Research Ethics Committee (CEIm).

Patients began with progressive loss of strength in their extremities (4 cases), dysphagia and neck and upper limb muscles weakness (1 case), and dysarthria followed by dysphagia and bilateral facial paralysis (1 case). No sensory symptoms were detected in any of the patients. The clinical features and neurophysiological studies (serial NCS and needle EMG) findings were evaluated. Laboratory test, such as antiganglioside antibodies serologies and cerebrospinal fluid (CSF) test were analyzed.

Electrophysiological studies were carried out using a Keypoint Medtronic EMG system. Recordings were performed by standard methods using surface stimulating and recording electrodes. The MCV measurement of the median and ulnar nerves was carried out by stimulation at the wrist, elbow, axilla, and Erb's point while recording over abductor pollicis brevis (APB) and abductor digiti minimi (ADM), respectively. MCV of peroneal nerve was assessed by stimulation at the ankle and knee while recording over the extensor digitorum brevis muscle (EDB). Minimal F-wave latencies were recorded from APB and abductor hallucis muscles after stimulation at the wrist and ankle, respectively. An H-reflex was recorded over soleus muscle after tibial nerve stimulation at the popliteal fossa. The axillary nerve was stimulated at the Erb's point while recording from the deltoid muscle. The spinal accessory nerve was stimulated at the posterior triangle of the neck while recording from the trapezius muscle. The phrenic nerve conduction study was stimulated on posterior border of the sternocleidomastoid muscle and recorded 5 cm from the xiphoid process (G1) with reference electrode (G2) 16 cm away from the ipsilateral costal margin. Sensory conduction velocity (SCV) of the median and ulnar nerves was determined from digit III and V to the wrist, respectively. An antidromic SCV of the sural nerves was obtained after stimulating the midcalf. Electromyography (EMG) was recorded with concentric needle electrodes from the right deltoid, APB, tibialis anterior (TA), and facial muscles. We analyzed the duration and morphology of the motor units, the presence of spontaneous activity, and the EMG pattern at maximum voluntary effort.

Accuracy was optimized using the Rajabally et al. (15) and Uncini et al. (16) electrodiagnostic criteria for axonal forms of GBS. In summary, the first and second studies must not show AIDP features and at least one of the following in two nerves: distal compound muscle action potential (dCMAP) amplitude <80% lower limit of normal (LLN) with persistent reduction in the following studies; proximal/distal CMAP (pCMAP/dCMAP) amplitude ratio <0.7 (excluding tibial nerve) on the first test, which can be recovered without increased temporal dispersion (dCMAP duration ≤120% ULN or pCMAP/dCMAP duration ratio ≤130%); absence of isolated F waves (or persistence <20%). The term RCF is used when at least in two nerves, there is evidence of a >150% increase dCMAP amplitude without increased dCMAP duration (≤120% ULN) or pCMAP/dCMAP amplitude ratio <0.7 in the first test that improves more than 0.2 in the following tests without increase in temporal dispersion

Abbreviations: AIDP, acute inflammatory demyelinating polyneuropathy; AMAN, acute motor axonal neuropathy; CBs, nerve conduction blocks; CMAP, compound muscle action potential; CMAP-A p/d, compound muscle action amplitude; proximal/distal (mV = millivolts); CMAP-D, CMAP duration (ms = milliseconds); CSF, cerebrospinal fluid; CV, conduction velocities; dCMAP, distal compound muscle action potential; DML, distal motor latency (ms = milliseg); EMG, electromyography; CMAP-D, compound muscle action potential duration (ms = milliseconds); GBS, Guillain-Barre syndrome; IVIG, intravenous immunoglobulins; LLN, lower limit of normal; MCV, motor conduction velocities; MRA, magnetic resonance angiography; NCS, nerve conduction studies; PCBv, pharyngeal-cervical-brachial variant; pCMAP, proximal compound muscle action potential; RCF, reversible conduction failure; and ULN, upper limit of normal.

(16). According to this, the term RCF applies to CBs that recover without showing temporal dispersion, a correlate of de-remyelination.

RESULTS

All 6 cases had a history of previous upper respiratory tract infection or self-limited diarrhea, with an acute progressive course of weakness, without sensory symptoms (**Table 1**). Serial NCS showed a decreased CMAP amplitude >80% LLN in all cases, as well as at least two nerves with normal conduction velocities (CVs) and normal sensory conduction parameters. The CBs were established according to the criteria described by the American Association of Neuromuscular and Electrodiagnostic Medicine (AANEM) (17) and criteria described by Rajabally et al. (15) and Uncini et al. (16): a definite partial CB was defined as a decrease in amplitude or area >50%, with a temporal dispersion <30%. Probable partial CB was defined as an amplitude or area decrease of 30–49%, with a temporal dispersion <30%. RCF was defined according to criteria described from Uncini et al. (16).

Four cases with CBs (1st−2nd and 3rd week), one of them (PCBv) with an absence of F waves in upper limbs (2nd and 3rd week), and absent or mild signs of acute denervation (3rd week) showed reversible CBs or RCF and complete recovery in 1 month. Two cases without CBs (1st−2nd and 3rd week), with persistent reduction in dCMAP amplitude and severe signs of acute denervation due to axonal degeneration (3rd week and 1st−3rd month) showed slow recovery up to several months (**Figures 1**, **2** and **Tables 2**, **3**).

All patients were treated from the 1st to 2nd week of evolution with intravenous immunoglobulins (IVIGs), and their disabilities were assessed with the Hughes functional rating scale before treatment, 1 month and 6 months after onset. Rapid recovery was defined as an improvement of two or more points in the Hughes grade scoring system within 1 month from the beginning, and slow recovery defined as inability to walk independently (grade 3 or more) 1 month after.

DISCUSSION

Usefulness of Anti-ganglioside Antibodies

Anti-GM1 and anti-GD1a antibodies are markers of axonal damage in axonal forms (AMAN), not seeing in demyelinating forms (AIDP) (18, 19). They are time-dependent, being more useful in early stages with progression to severe forms and they decrease over time (1, 2, 4–6, 20). Positive antiganglioside antibodies are considered a useful but not required aid in the diagnosis of axonal forms of GBS because they interfere with the albumin-cytological dissociation of CSF, which is also dependent on the time being requested (1, 9); this may explain the negative results in cases 1, 2, 5, and 6 (milder cases in which antiganglioside antibodies were requested at a later stage); and the positivity in cases 3 and 4 (severe cases, in which antiganglioside antibodies were requested earlier).

The CBs and the Term RCF

When we talk about CBs, we mean CBs along the axon, having their marker in the reduction of the pCMAP amplitude and in the pCMAP/dCMAP ratio (distal CBs are described by reduced dCMAP amplitude). It had been observed that in some patients diagnosed with AMAN, the decrease in CMAP amplitude with CBs persisted over time, while others showed rapid recovery with normalization of previous abnormalities, indicating that some axonal forms may be characterized by reversible CBs or RCF (12, 21–24).

Uncini et al. (16) defined the term RCF when a pCMAP/dCMAP amplitude ratio <0.7 at the first test which improves more than 0.2 in the following trials, without temporal dispersion (pCMAP/dCMAP duration ratio ≤130%). The failure to distinguish between reversible CBs or RCF and demyelinating conduction block (decreased CMAP

TABLE 1 | Clinical features, CSF, antiganglioside antibodies and evolution.

Case	Clinical features	CSF and other test	Antiganglioside antibodies	Evolution Recovery
1	Acute and progressive weakness of upper and lower limbs	Normal CSF	Negative (made on day 20th after the onset)	Good evolution. Rapid recovery. Hospital discharge after a month.
2	Acute and progressive weakness of upper and lower limbs	CSF with increased protein level	Negative (made on day 15th after the onset)	Good evolution. Rapid recovery. Hospital discharge after a month.
3	Acute and progressive weakness of upper and lower limbs	CSF with increased protein level	Anti-GM1 positive (made on day 10th after the onset)	Slow recovery lasting several months.
4	Acute and progressive weakness of upper and lower limbs	CSF with increased protein level	Anti-GM1 positive (made on day 11th after the onset)	Slow recovery lasting several months.
5	Acute dysphagia, followed by weakness of neck muscles and upper limb	Normal CSF. Cranial and medullary MRI normal	Negative (made on day 20th after the onset)	Good evolution. Rapid recovery. Hospital discharge after a month.
6	Acute dysarthria followed by dysphagia, bilateral facial paralysis, velopharyngeal and lingual paralysis and dyspnea.	Normal CSF. Cranial MRI and MRA normal	Negative (made on day 20th after the onset)	Good evolution. Rapid recovery. Hospital discharge after a month

CSF, cerebrospinal fluid; MRI, magnetic resonance imaging; MRA, magnetic resonance angiography.

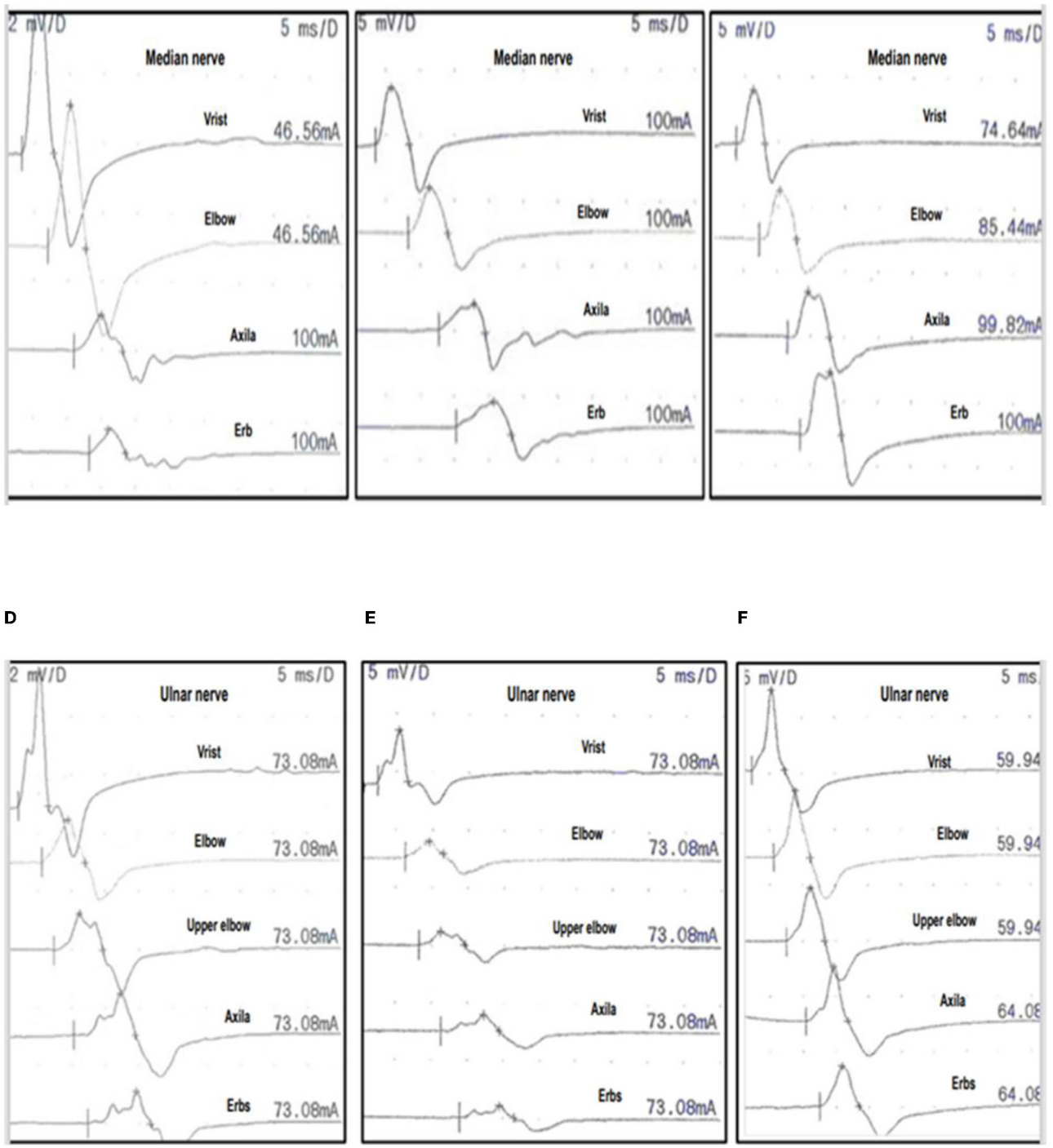

FIGURE 1 | Serial nerve conduction studies (NCS) of case 1. Three serial NCS of the median nerve **(A–C)** and ulnar nerve **(D–F)** in case 1, performed at 1 week, 3 weeks, and 1 month after onset (see **Tables 2**, **3** for nerve conduction values). Median nerve: 1st week **(A)**, 3rd week **(B)**, 4th at 1 month **(C)** with CMAP recorded after stimulation from distal to proximal, with stimulation at wrist elbow, axilla and Erb's point, to APB muscle. Ulnar nerve: 1st week **(D)**, 3rd week **(E)**, 4th at 1 month **(F)** with CMAP recorded after distal to proximal stimulation at wrist, below elbow, above elbow, axilla and Erb's point, to ADM muscle. In the 1st and 3rd week the median and ulnar nerves show CBs or amplitude ratio pCMAP/dCMAP <0.7, and duration ratio pCMAP/dCMAP <130%. DML and MCV are preserved (**Table 3**). At 1 month, RCF (amplitude ratio pCMAP/dCMAP <0.7 on the first test) improves more than 0.2 in the median and ulnar nerve. Consequently, these changes are indicative of RCF. APB, abductor pollicis brevis; ADM, abductor digiti minimi; BCs: motor conduction blocks; CMAP, compound motor action potential; pCMAP, proximal CMAP; dCMAP, distal CMAP; DML, distal motor latency; VCM, motor conduction velocity.

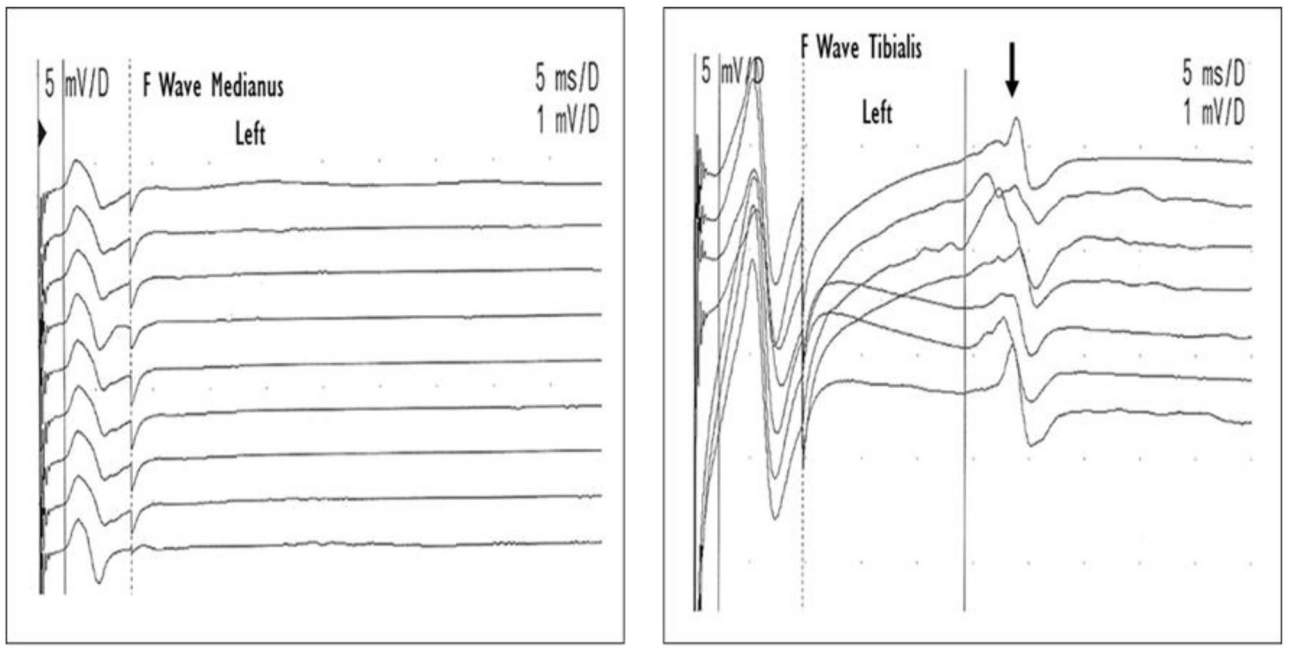

FIGURE 2 | Case 5. Pharyngo-cervical-brachial variant (PCBv). F wave performed in the 2nd week. Low amplitude CMAP and absence of F waves of the left median nerve **(A)**, and normal F waves (arrow) in the left tibial nerve **(B)**.

amplitude with pCMAP/dCMAP duration >130%) leads to the misclassification of AMAN patients with RCF as AIDP (12, 16).

The Emerging Concept of Nodopathies and Nodo-Paranodopathies

It is based on the discovery of nodal and paranodal antigenic targets. Anti-ganglioside antibody-mediated neuropathies share a common pathogenic mechanism of node of Ranvier dysfunction/disruption, which can follow two different pathways: a rapid recovery of the affected node for AMAN with RCF or a progression of AMAN with axonal degeneration with slow recovery (7, 22, 25, 26). GBS has traditionally been classified into demyelinating or axonal subtype or form according to whether the myelin or axon is primarily affected. This dichotomous classification generated confusion in the electroneurophysiological diagnosis of axonal neuropathy with antiganglioside antibodies (AMAN and PCBv). To clarify this confusion, Unicini and Kuwabara (26) categorize neuropathies with antiganglioside antibodies, characterized by a common pathogenic mechanism of dysfunction/disruption at the nodes of Ranvier, called nodopathies. The AMAN axonal subtype of GBS is a prototype of nodopathy in the first phase of AMAN with CBs without signs of demyelination (temporal dispersion) and resolving rapidly (days or weeks). The advantages of the term nodopathies are that they points out directly to the site of nerve injury; resolve the paradox that an axonal form may be reversible with a good prognosis; and emphasizes the potential reversibility in neuropathies, which traditionally were thought to be characterized only by axonal degeneration, opening a therapeutic window for timely targeted treatments (26).

The CBs and Prognosis

Not all axonal forms (AMAN and PCBv) of GBS have a poor prognosis, as was thought a few years ago. Animal models and clinical studies in AMAN show antibodies and complement deposits in the nodes, an immune process causing node elongation, deanchoring of the paranode non-compacted myelin, and conduction failure with CBs (7). In the initial stages of the immune process, the dysfunction of the nodal region is reversible; but if the immunological reaction progresses, the Ca+ influx into the axon causes axonal degeneration (25). The different forms of AMAN form a continuous pathophysiological spectrum ranging from RCF to axonal degeneration (23). CBs, especially reversible CBs, are a good prognostic factor in patients with AMAN (27). In EMG, severe acute denervation indicates axonal degeneration and a worse prognosis, whose recovery requires longer time (28).

Early Diagnosis and Treatment of GBS

Alterations of the proximal nerve trunk with CBs in NCS are a very relevant feature in the early stages of the disease (29, 30). Since the pathophysiology of GBS is dynamic, serial NCS is necessary for the accurate classification of GBS subtypes at an early stage (12, 16, 30). Early diagnosis of GBS in the first week of evolution is difficult, but it is important to start treatment early, since 25% of patients need ventilatory support and 20% are unable to walk after 6 months (1).

TABLE 2 | Nerve conduction studies (NCS) and electromyography (EMG).

Case	1st NCS: 1st-2nd week	2nd NCS and EMG: 3rd week	3rd NCS and EMG: 1nd-3rd month	Diagnosis
1	Decreased CMAP amplitude. Normal MCV. CBs. Preserved F-wave latencies.	Decreased CMAP amplitude. Normal MCV. CBs. Preserved F-wave latencies EMG: mild acute denervation in lower limbs.	Normal NCS. Normal F-waves. Reversible CBs or RCF. EMG: normal	Nodopathies AMAN
2	Decreased CMAP amplitude. Normal MCV. CBs. Preserved F-wave latencies.	Decreased CMAP amplitude. Normal MCV. CBs. Preserved F-wave latencies. EMG: absent acute denervation.	Normal NCS. Normal F-waves. Reversible CBs or RCF. EMG: normal	Nodopathies AMAN
3	Decreased CMAP amplitude. Normal MCV. Low F-wave persistence (<20%) with preserved latencies.	Decreased CMAP amplitude. Normal MCV. Low F-wave persistence (<20%), with preserved latencies. EMG: severe acute denervation in upper and lower limb muscles.	Persistent decreased CMAP amplitude. Normal MCV. EMG: severe acute denervation in upper and lower limb muscles.	Classic AMAN
4	Decreased CMAP amplitude. Normal MCV. Low F-wave persistence (<20%) with preserved latencies.	Decreased CMAP amplitude. Normal MCV. Low F-wave persistence (<20%), with preserved latencies. EMG: severe acute denervation of severe in upper and lower limb muscles.	Absence or persistent decrease of CMAP amplitude. Normal MCV. EMG: severe acute denervation in upper and lower limb muscles.	Classic AMAN
5	Decreased CMAP amplitude in upper limbs and Spinal accessory nerve. Normal MCV. CBs upper limb. Low F-wave persistence (<20%) with preserved latencies in the 1st week in upper limbs. Absence of F- waves in the 2nd week in upper limbs. Normal repetitive nerve stimulation.	Decreased CMAP amplitude in upper limbs and Spinal accessory nerve. Normal MCV. CBs in upper limb. Absence of F-waves in upper limbs. EMG: mild acute denervation in upper limbs muscles.	Normal NCS. Normal F-waves. Reversible CBs or RCF. EMG: normal	Nodopathies Regional AMAN (PCBv).
6	Decreased CMAP amplitude in upper limbs, both facial nerves, and right phrenic nerve. CBs in upper limb. Normal MCV. Preserved F-wave latencies.	Decreased CMAP amplitude in upper limbs, both facial nerves, and right phrenic nerve. CBs in upper limb. Normal MCV. Preserved F-wave latencies. EMG: mild acute denervation in orbicularis oris bilateral and upper limbs muscle	Normal NCS. Normal F-waves. Reversible CBs or RCF. EMG: normal.	Nodopathies Regional AMAN (PCBv).

NCS, nerve conduction studies; CMAP, compound muscle action potential; MCV, motor conduction velocities; CBs, conduction blocks; RCF, reversible conduction failure. To summarize table content, only motor NCS are indicated (sensory NCS were normal).

RCF and Potential Therapeutic Implications

The presence of RCF indicates, in antibody-mediated disorders, a temporary therapeutic potential. Treatments targeting conduction failure before axonal degeneration occurs may be beneficial. The presence of potentially reversible conduction failure has implications for diagnosis and prognosis and stimulates the search for targeted immunological treatments that may halt progression to axonal degeneration (31).

Therefore, We Make a Protocol Proposal for Early Diagnosis and Treatment

Perform the first NCS of the nerve trunks, such as proximal segments, and F waves during the 1st week of evolution; if there are data of possible GBS, start treatment with IVIG; if there are no conclusive data, the NCS should be repeated during the 2nd week. Perform the following NCS and EMG in the 3rd week and at 1 month of evolution to determine the subtype or form of GBS and the presence of reversible CBs or RCF for possible nodopathies, indicating a good prognosis, and to determine the degree of acute denervation, which if severe, would indicate a worse prognosis. Early diagnosis and treatment could be essential to avoid, as far as possible, an evolution to axonal degeneration. It should be recalled that in an early stage, the GBS diagnosis can be essentially clinical supported by electrophysiological studies. Thus, treatment should be initiated as early as possible, if necessary, without the confirmatory data from electrophysiological studies.

We propose the use of the following terminology: nodo-paranodopathies in the initial phases of GBS, when CBs are observed, nodopathies if the CBs are reversible or RCF and paranodopathies if CBs with temporal dispersion of the CMAP is observed; and to continue to use the classical diagnosis AMAN in the more advanced axonal forms with axonal degeneration, and AIDP in the demyelinating forms; thus respecting the traditional and the new emerging term of nodo-paranodopathies. In our opinion, today the term nodopathy is not a diagnosis but a pathophysiological category.

The term nodopathy with RCF does apply to an early phase as it takes at least two serial NCS and few weeks from onset. In

TABLE 3 | Nerve conduction studies (NCS) in all patients.

AMAN (Acute Motor Axonal Neuropathy)

		Median nerve					Ulnar nerve					Peroneal nerve				
Case	Day	CMAP-A (p/d ratio)	LDM	CMAP-D	VCM	Wave F	CMAP-A (p/d ratio)	DML	CMAP-D	VCM	Wave F	CMAP-A (p/d ratio)	LDM	CMAP-D	VCM	Wave F
1	5	**0.7/4.7**[a] **(0.1)**[b]	3.5	4.9	48	26	**1.1/4.4**[a] **(0.2)**[b]	2.5	4.1	51	30	**1.4/4.1**[a] **(0.3)**[b]	3.5	4.7	43	48
	21	**0.9/2.9**[a] **(0.3)**[b]	3.1	4,6	53	22	**0.9/3.9**[a] **(0.2)**[b]	2.2	4.5	51	31	**2.3/**6.2 **(0.1)**[b]	4.2	4.9	44	46
	31	4.8/4.1 (1.1)[c]	3.8	4.3	51	22	3.6/4.2 (0.8)[c]	2.4	5.0	60	30	6.1/11,1 (0.5)[c]	4.1	4.6	42	48
2	5	**0.5/2**[a] **(0.2)**[b]	4.8	6.7	51	27	**0.2/2.1**[a] **(0.09)**[b]	3.8	4.8	51	32	**2.1/3.9**[a] **(0.5)**[b]	4.2	4.9	41	49
	21	**2.5/**6.1 **(0.4)**[b]	3.8	4.8	50	28	**0.4/0.8**[a] **(0.5**[b]**)**	3.9	4.6	56	32	**2.3/3.5**[a] **(0.6)**[b]	4.9	5.9	40	48
	32	5.5/6.1 (0.9)[c]	3.7	4.9	51	27	**2.3/2.8**[a] (0.8)[c]	3.7	4.5	54	31	**3.4/2.9**[a] (1.0)[c]	4.2	4.9	41	49
3	6	**1/1.4**[a] (0.7**)**	3.8	4.6	47	26	**0.5/0.7**[a] (0.7)	3.5	4.9	55	27	**1.1/1.4**[a] (0.7)	5.4	4.3	47	47
	22	**1.3/1.6**[a](0.8)	3.3	4.6	48	27	**0.6/0.7**[a] (0.8)	3	5.9	55	28	**0.5/0.7**[a] (0.7)	4.8	4.9	47	48
	48	**0.9/1.4**[a] (0.6)	3.4	4.7	48	29	**0.5/0.7**[a](0.7**)**	3.2	5.8	49	30	**0.7/0.8** [a]**(**0.8)	6.5	4.8	47	48
4	7	**0.9/1.2**[a](0.7)	3.1	4.2	49	29	**0.7/0.9**[a] **(**0.7)	3.1	4.2	50	29	**0.9/1.2**[a] **(**0.7)	3.2	4.3	45	48
	21	**0.5/0.7**[a] (0.7)	4.8	4,4	49	30	**0.5/0.7**[a] (0.7)	3.9	4.3	49	31	**0.1/0.1**[a] (1.0)	4	7.2	45	49
	49	**0.1/0.2**[a] (0.5)	4.9	4.9	48	31	**A**	**A**	**A**	**A**	**A**	**A**	**A**	**A**	**A**	**A**

Pharyngeal-cervical-brachial variant (vPCBv)

		Median nerve					Axillar nerve			Spinal accessory nerve			Facial nerve		Phrenic nerve	
Case	Day	CMAP-A (p/d ratio)	DML	CMAP-D	MCV	FW	CMAP-A	DML	CMAP-D	CMAP-A	DML	CMAP-D	CMAP-A	DML	CMAP-A	DML
5	5	**1.9/3.9**[a](**0.4**)[b]	2.0	4.2	59	29	**2.2**[a]	2.6	3.9	**0.3**[a]	4.1	3.6	ND	ND	0.9	4.6
	21	**1.8/3.8**[a] **(0.4)**[b]	2.1	4.1	50	**A**	**0.7**[a]	2.7	3.8	**0.3**[a]	4.2	3.7	ND	ND	0.8	4.7
	32	4.6/4.7 (0.9)[c]	2.9	4.7	54	29	4.7	2.6	3.7	4.6	4.1	3.6	ND	ND	0.9	4.6
6	6	**0.7/1.5** [a] **(0.4)**[b]	2.6	4.3	52	27	4.5	3.2	3.1	3.9	2.1	3.2	**0.5**[a]	1.2	**0.1**[a]	3.7
	22	**0.9/1.9**[a] **(0.4)**[b]	2.7	4.2	51	28	4.8	3.1	3.0	3.9	2.0	3.1	**0.7**[a]	1.3	**0.1**[a]	3.7
	39	4.5/4.8 (0.9)[c]	2.6	4.1	52	27	5.2	3.1	3.1	4.2	2.1	3.1	1.1	1.2	0.8	3.7

A, absent; CMAP-A p/d, amplitude of compound muscle action potential, proximal/distal (mV); LDM, distal motor latency (ms); CMAP-D, CMAP duration (ms); F-wave, F-wave latency (ms); MCV, motor conduction velocity (m/s); ND, not done.

Abnormal motor nerve conduction parameters: [a]dCMAP-A <80% LLN. [b]BCs or amplitude ratio pCMAP/dCMAP <0.7 in first or second test. [c]That improves more than 0.2 in the last test (RCF). CMAP-D (nerves, median >7.6 ms; ulnar >8.0 ms; and peroneal >8.5 ms).

Bold indicates abnormal values that meet (16, 17, 30). To shorten the content of the table, only motor nerve conduction studies are indicated (sensory conduction values were normal). Reference values adapted from Chen et al. (33), Gutierrez- Rivas et al. (34), and Preston and Shapiro (35).

the early GBS phase, CBs without abnormal temporal dispersion in the first phase can be found also in classical AIDP, which is a demyelinating paranoid-internodopathy (32).

CONCLUSION

Not all axonal forms of GBS have axonal degeneration with a poor prognosis. AMAN and PCBv have a continuous pathophysiological spectrum ranging from CBs due to dysfunction/disruption of the nodes of Ranvier, called nodopathies, with reversible CBs or RCF and good prognosis, to axonal degeneration, with a worse prognosis. According to the findings of the AMAN and PCBv studies, patients with CBs can have reversible CBs or RCF, absent or mild acute denervation and better prognosis. Patients without CBs and with persistent reduction in dCMAP amplitude have severe acute denervation due to axonal degeneration and a worse prognosis. NCS can support the early diagnosis of GBS, if we observe alteration of F waves, or CBs, which are a very relevant feature in the initial phase, sometimes necessary for serial NCS and also for the classification of GBS subtypes. The term nodopathies points directly to the site of the lesion and highlights the possible reversibility of these neuropathies that were traditionally characterized only by axonal degeneration, and stimulates research into immunological treatments with specific monoclonal antibodies.

DATA AVAILABILITY STATEMENT

The raw data supporting the conclusions of this article will be made available by the authors, without undue reservation.

ETHICS STATEMENT

The studies involving human participants were reviewed and approved by Medical Research Ethics Committee (MREC), date 25-06-2019; number 1996.- Acute polyradiculoneuropathy. Guillain-Barré Syndrome. The importance of electromyography in the early diagnosis. Main Research: JUU from Clinical Neurophysiology. The patients/participants provided their written informed consent to participate in this study.

AUTHOR CONTRIBUTIONS

SU-S and JU-U: study concept and design, drafting of the initial manuscript, nerve conduction studies (NCS), electromyography (EMG), and acquisition of data. SU-S, RD-P, PC-C, and M-AG-T: literature review. SU-S, JU-U, and J-RG-M: data review, interpretation and discussion of results, and revision of the final manuscript. All authors approved the final version of the manuscript.

REFERENCES

1. Van den Berg B, Walgaard C, Drenthen J, Fokke C, Jacobs BC, Van Doorn PA. Guillain–Barré syndrome: pathogenesis, diagnosis, treatment and prognosis. *Nat Rev Neurol.* (2014) 10:469–82. doi: 10.1038/nrneurol.2014.121
2. Odaka M, Koga M, Yuki N, Susuki K, Hirata K. Longitudinal changes of anti-ganglioside antibodies before and after Guillain–Barré syndrome onset subsequent to *Campylobacter jejuni* enteritis. *J Neurol Sci.* (2003) 210:99–103. doi: 10.1016/S0022-510X(03)00029-7
3. Yuki N, Hartung H-P. Guillain–Barré syndrome. *N Engl J Med.* (2012) 366:2294–304. doi: 10.1056/NEJMra1114525
4. Más-Lázaro C, García-Pastor A, Díaz-Insa S, Moltó-Jordà JM, Lacruz-Ballester L. Variante faringocervicobraquial del síndrome de Guillain-Barré: una entidad clínica bien definida con un perfil inmunológico heterogéneo. *Rev Neurol.* (2008) 47:579–81. doi: 10.33588/rn.4711.2008074
5. Nagashima T, Koga M, Odaka M, Hirata K, Yuki N. Continuous spectrum of pharyngeal-cervical-brachial variant of Guillain-Barré syndrome. *Arch Neurol.* (2007) 64:1519–23. doi: 10.1001/archneur.64.10.1519
6. Nagashima T, Koga M, Odaka M, Hirata K, Yuki N. Clinical correlates of serum anti-GT1a IgG antibodies. *J Neurol Sci.* (2004) 219:139–45. doi: 10.1016/j.jns.2004.01.005
7. Gross S, Fischer A, Rosati M, Matiasek L, Corlazzoli D, Cappello R, et al. Nodo-paranodopathy, internodopathy and cleftopathy: target-based reclassification of Guillain–Barré-like immune-mediated polyradiculoneuropathies in dogs and cats. *Neuromuscul Disord.* (2016) 26:825–36. doi: 10.1016/j.nmd.2016.08.015
8. Ropper AH. Further regional variants of acute immune polyneuropathy: bifacial weakness or sixth nerve paresis with paresthesias, lumbar polyradiculopathy, and ataxia with pharyngeal-cervical-brachial weakness. *Arch Neurol.* (1994) 51:671–5. doi: 10.1001/archneur.1994.00540190051014
9. Wakerley BR, Yuki N. Pharyngeal-cervical-brachial variant of Guillain–Barré syndrome. *J Neurol Neurosurg Psychiatry.* (2014) 85:339–44. doi: 10.1136/jnnp-2013-305397
10. Feasby TE, Gilbert JJ, Brown WF, Bolton CF, Hahn AF, Koopman WF, et al. An acute axonal form of Guillain-Barré polyneuropathy. *Brain.* (1986) 109:1115–26. doi: 10.1093/brain/109.6.1115
11. Hadden RDM, Cornblath DR, Hughes RAC, Zielasek J, Hartung H-P, Toyka KV, et al. Electrophysiological classification of Guillain-Barré syndrome: clinical associations and outcome. *Ann Neurol.* (1998) 44:780–8. doi: 10.1002/ana.410440512
12. Uncini A, Kuwabara S. Electrodiagnostic criteria for Guillain–Barré syndrome: a critical revision and the need for an update. *Clin Neurophysiol.* (2012) 123:1487–95. doi: 10.1016/j.clinph.2012.01.025
13. Arai M, Susuki K, Koga M. Axonal pharyngeal-cervical-brachial variant of Guillain-Barré syndrome without anti-GT1a IgG antibody. *Muscle Nerve.* (2003) 28:246–50. doi: 10.1002/mus.10424
14. Taieb G, Grapperon AM, Duclos Y, Franques J, Labauge P, Renard D, et al. Proximal conduction block in the pharyngeal-cervical-brachial variant of Guillain-Barre syndrome. *Muscle Nerve.* (2015) 52:1102–6. doi: 10.1002/mus.24729
15. Rajabally YA, Durand M-C, Mitchell J, Orlikowski D, Nicolas G. Electrophysiological diagnosis of Guillain–Barré syndrome subtype: could a single study suffice? *J Neurol Neurosurg Psychiatry.* (2015) 86:115–9. doi: 10.1136/jnnp-2014-307815
16. Uncini A, Ippoliti L, Shahrizaila N, Sekiguchi Y, Kuwabara S. Optimizing the electrodiagnostic accuracy in Guillain-Barré syndrome subtypes: criteria sets and sparse linear discriminant analysis. *Clin Neurophysiol.* (2017) 128:1176–83. doi: 10.1016/j.clinph.2017.03.048
17. Olney RK. Consensus criteria for the diagnosis of partial conduction block. *Muscle Nerve.* (1999) 22:S225–S229.

18. Kim JK, Bae JS, Kim D-S, Kusunoki S, Kim JE, Kim JS, et al. Prevalence of anti-ganglioside antibodies and their clinical correlates with Guillain-Barré syndrome in Korea: a nationwide multicenter study. *J Clin Neurol.* (2014) 10:94–100. doi: 10.3988/jcn.2014.10.2.94
19. Sekiguchi Y, Uncini A, Yuki N, Misawa S, Notturno F, Nasu S, et al. Antiganglioside antibodies are associated with axonal Guillain–Barré syndrome: a Japanese–Italian collaborative study. *J Neurol Neurosurg Psychiatry.* (2012) 83:23–8. doi: 10.1136/jnnp-2011-300309
20. Delmont E, Willison H. Diagnostic utility of auto antibodies in inflammatory nerve disorders. *J Neuromuscul Dis.* (2015) 2:107–12. doi: 10.3233/JND-150078
21. Capasso M, Notturno F, Manzoli C, Yuki N, Uncini A. Reversible conduction failure in pharyngeal-cervical-brachial variant of Guillain-Barre syndrome. *Muscle Nerve.* (2010) 42:608–12. doi: 10.1002/mus.21801
22. Gürsoy AE, Kolukisa M, Babacan-Yildiz G, Altintaş Ö, Yaman A, Asil T. Reversible conduction failure in overlap of Miller Fisher syndrome and pharyngeal-cervical-brachial variant of Guillain-Barré syndrome in the spectrum of nodo-paranodopathies. *J Clin Neurosci.* (2014) 21:1269–71. doi: 10.1016/j.jocn.2013.10.022
23. Kokubun N, Nishibayashi M, Uncini A, Odaka M, Hirata K, Yuki N. Conduction block in acute motor axonal neuropathy. *Brain.* (2010) 133:2897–908. doi: 10.1093/brain/awq260
24. Kuwabara S, Yuki N, Koga M, Hattori T, Matsuura D, Miyake M, et al. IgG anti-GM1 antibody is associated with reversible conduction failure and axonal degeneration in Guillain-Barré syndrome. *Ann Neurol.* (1998) 44:202–8. doi: 10.1002/ana.410440210
25. Uncini A, Susuki K, Yuki N. Nodo-paranodopathy: beyond the demyelinating and axonal classification in anti-ganglioside antibody-mediated neuropathies. *Clin Neurophysiol.* (2013) 124:1928–34. doi: 10.1016/j.clinph.2013.03.025
26. Uncini A, Kuwabara S. Nodopathies of the peripheral nerve: an emerging concept. *J Neurol Neurosurg Psychiatry.* (2015) 86:1186–95. doi: 10.1136/jnnp-2014-310097
27. Niu J, Liu M, Sun Q, Li Y, Wu S, Ding Q, et al. Motor nerve conduction block predicting outcome of Guillain-Barre syndrome. *Front Neurol.* (2018) 9:399. doi: 10.3389/fneur.2018.00399
28. López-Esteban P, Gallego I, Gil-Ferrer V. Criterios neurofisiológicos en el síndrome de Guillain-Barré infantil. *Ocho años de experiencia [Electrodiagnostic criteria for childhood Guillain-Barré syndrome. Eight years' experience. Rev Neurol.* (2013) 56:275–82. doi: 10.33588/rn.5605.2012615
29. Albertí MA, Alentorn A, Martínez-Yelamos S, Martínez-Matos JA, Povedano M, Montero J, et al. Very early electrodiagnostic findings in Guillain-Barré syndrome. *J Peripher Nerv Syst.* (2011) 16:136–42. doi: 10.1111/j.1529-8027.2011.00338.x
30. Berciano J, Orizaola P, Gallardo E, Pelayo-Negro AL, Sánchez-Juan P, Infante J, et al. Very early Guillain-Barré syndrome: a clinical-electrophysiological and ultrasonographic study. *Clin Neurophysiol Pract.* (2020) 5:1–9. doi: 10.1016/j.cnp.2019.11.003
31. Uncini A, Santoro L. The electrophysiology of axonal neuropathies: more than just evidence of axonal loss. *Clin Neurophysiol.* (2020) 131:2367–74. doi: 10.1016/j.clinph.2020.07.014
32. Uncini A, Mathis S, Wallat JM. New classification of autoimmune neuropathies based on target antigens and involved domains of myelinated fibres. *J Neurol Neurosurg Psychiatry.* (2022) 93:57–67. doi: 10.1136/jnnp-2021-326889
33. Chen R, Collins S, Remtulla H, Parkes A, Bolton CF. Phrenic nerve conduction study in normal subjects. *Muscle Nerve.* (1995) 18:330–5. doi: 10.1002/mus.880180311
34. Gutiérrez-Rivas E, Jímenez Hernández MD, Pardo Fernández J, Romero-Acebal M. *Manual de electromiografía clínica*. 3ª. Madrid, España: Ergon (2021). 432 p. Available online at: https://ergon.es/producto/manual_electromiografia_clinica/ (accessed May 3, 2021).
35. Preston DC, Shapiro BE. *Electromyography and Neuromuscular Disorders. Clinical-Electrophysiologic Correlations. 2rd Edn*. Philadelphia: Elsevier Health Sciences (2005).

Conflict of Interest: The authors declare that the research was conducted in the absence of any commercial or financial relationships that could be construed as a potential conflict of interest.

Publisher's Note: All claims expressed in this article are solely those of the authors and do not necessarily represent those of their affiliated organizations, or those of the publisher, the editors and the reviewers. Any product that may be evaluated in this article, or claim that may be made by its manufacturer, is not guaranteed or endorsed by the publisher.

Copyright © 2022 Urdiales-Sánchez, González-Montaña, Diaz-Pérez, Calvo-Calleja, Gutiérrez-Trueba and Urdiales-Urdiales. This is an open-access article distributed under the terms of the Creative Commons Attribution License (CC BY). The use, distribution or reproduction in other forums is permitted, provided the original author(s) and the copyright owner(s) are credited and that the original publication in this journal is cited, in accordance with accepted academic practice. No use, distribution or reproduction is permitted which does not comply with these terms.

frontiers | Frontiers in Neurology

CASE REPORT
published: 02 June 2022
doi: 10.3389/fneur.2022.909715

Case Report: A Novel AChR Epsilon Variant Causing a Clinically Discordant Salbutamol Responsive Congenital Myasthenic Syndrome in Two Egyptian Siblings

Marta Gómez-García de la Banda[1,2,3†], *Emmanuel Simental-Aldaba*[4,5†], *Nagia Fahmy*[6], *Damien Sternberg*[3,7], *Patricia Blondy*[3], *Susana Quijano-Roy*[1,2,3,8] *and Edoardo Malfatti*[2,4,9,10*]

[1] Pediatric Neurology and ICU Department, AP-HP Université Paris Saclay, Hôpital Raymond Poincaré, Garches, France, [2] Reference Center for Neuromuscular Diseases Centre "Nord- Est- Ile de France", FILNEMUS, Creteil, France, [3] European Reference Center Network (Euro-NMD ERN), Paris, France, [4] APHP, Centre de Référence de Pathologie Neuromusculaire Nord-Est-Ile-de-France, Henri Mondor University Hospital, Créteil, France, [5] Department of Neurorehabilitation, Instituto Nacional de Rehabilitación "LGII", Mexico City, Mexico, [6] Neuromuscular Unit, Faculty of Medicine, Ain Shams University, Cairo, Egypt, [7] Service de Biochimie Métabolique, Centre de Génétique, Groupe Hospitalier Pitié-Salpêtrière, APHP Sorbonne Université, Paris, France, [8] Centre de Recherche en Myologie, UMRS974, Paris, France, [9] Univ Paris Est Créteil, INSERM, IMRB, Créteil, France, [10] AP-HP, Hôpital Mondor, Service d'histologie, Créteil, France

Congenital myasthenic syndromes (CMS) are inherited disorders that lead to abnormal neuromuscular transmission. Post-synaptic mutations are the main cause of CMS, particularly mutations in *CHRNE*. We report a novel homozygous *CHRNE* pathogenic variant in two Egyptian siblings showing a CMS. Interestingly, they showed different degrees of extraocular and skeletal muscle involvement; both presented only a partial response to cholinesterase inhibitors, and rapidly and substantially ameliorated after the addition of oral β2 adrenergic agonists. Here, we enlarge the genetic spectrum of *CHRNE*-related congenital myasthenic syndromes and highlight the importance of a β2 adrenergic agonists treatment.

Keywords: congenital myasthenic syndrome, *CHRNE*, neuromuscular junction, β2 adrenergic agonists, salbutamol

OPEN ACCESS

Edited by:
Giovanni Meola, University of Milan, Italy

Reviewed by:
Elena Maria Pennisi, Ospedale San Filippo Neri, Italy
Carmelo Rodolico, University of Messina, Italy

***Correspondence:**
Edoardo Malfatti
edoardo.malfatti@aphp.fr

†These authors have contributed equally to this work and share first authorship

Specialty section:
This article was submitted to Neuromuscular Disorders and Peripheral Neuropathies, a section of the journal Frontiers in Neurology

Received: *31 March 2022*
Accepted: *02 May 2022*
Published: *02 June 2022*

Citation:
Gómez-García de la Banda M, Simental-Aldaba E, Fahmy N, Sternberg D, Blondy P, Quijano-Roy S and Malfatti E (2022) Case Report: A Novel AChR Epsilon Variant Causing a Clinically Discordant Salbutamol Responsive Congenital Myasthenic Syndrome in Two Egyptian Siblings. Front. Neurol. 13:909715. doi: 10.3389/fneur.2022.909715

INTRODUCTION

Congenital myasthenic syndromes (CMS) are a heterogeneous group of rare inherited neuromuscular transmission disorders characterized by fluctuant muscle weakness and fatigability, classically described as non-progressive disorder with a low impact on the walking ability (1). Their estimated prevalence is 1 in 500,000 in Europe (2), with higher frequency in some geographic areas with high consanguinity rates, such as North Africa (3). To date, mutations in more than 30 genes are known to be associated with CMS, which can be classified into pre-synaptic, synaptic, and post-synaptic, according to the location of the molecular defect (4, 5).

Post-synaptic defects have been reported to be the most frequent cause in more than half of CMS, particularly those due to mutations in the gene encoding the ε subunit of the acetylcholine receptor (*CHRNE*) (5, 6).

Mutations of *CHRNE* gene are associated with two types of mechanisms: a low expression of functional ACh receptors (AChR) at the cell surface, causing a primary acetylcholine receptor deficiency, also called "low expressor" CMS, or a kinetic defect in the acetylcholine receptor, where the amount of AChR is normal, but there is an alteration in the channel opening time after acetylcholine binding, leading either to slow channel syndrome, if the opening time is excessively prolonged, or to fast channel syndrome, if the closure is too fast (7).

The typical CMS presentation occurs in infancy with marked fatigability, ophthalmoparesis, bilateral ptosis, mildly progressive facial, bulbar, axial, and limb weakness with respiratory involvement related to myasthenic crisis (8, 9).

Clinical manifestations of AChR ε subunit deficiency may vary considerably between affected families (10), and the same family members. This results in a heterogeneous phenotype between siblings with different clinical courses and prognoses (11, 12).

The primary therapeutic intervention in low expressor *CHRNE*-associated CMS is the cholinesterase inhibitor pyridostigmine. Reported treatment experience with low expression *CHRNE* mutations shows that cholinesterase inhibitors cause a favorable but incomplete response, improving muscular strength, particularly in ocular muscles. In poorly or incompletely responsive patients, other therapies have been considered, such as beta2 adrenergic receptor agonists (albuterol, salbutamol) or the 3,4- diaminopyridine (21).

The use of 3,4- diaminopyridine results in further improvement when the response to initial therapy is not sufficient or incomplete (13). The addition of beta2 adrenergic receptor agonists stabilizes the neuromuscular junction structure and reduces the acetylcholine dispersion, thus producing a dramatic improvement in some cases (14). This is different from other CMS, as, for instance, slow channel CMS or *DOK7* CMS, where the addition of pyridostigmine potentially worsens symptoms (15).

Here, we report on two siblings with a clinically heterogeneous CMS linked to a novel *CHRNE* variant and describe their variable therapeutic response to pyridostigmine, and oral β2 adrenergic agonists.

CASE REPORT

Patient 1 (P1), an 11-year-old boy, and Patient 2 (P2), an 8-year-old girl, are the third and fourth born of a sibship of four, born to healthy consanguineous Egyptian parents. The first-born deceased at 5 years, following a respiratory infection, suggesting a probable neuromuscular involvement.

P1 presented at 8 months with ptosis, ophthalmoplegia, poor cry, and nasal regurgitations. His psychomotor development was normal, but he developed fatigable generalized muscle weakness with frequent respiratory infections. Detection of antibodies against AChR and MuSK was negative; electrophysiologic studies showed a decremental response in the compound muscle action potential in response to repetitive stimulation in the median nerve. Serum lactate and CK levels were normal. On the base of clinical suspicion of a seronegative myasthenia gravis, a treatment with pyridostigmine was started at 6 months. The latter only showed a slight amelioration of the weakness and fatigability. P1 successively underwent plasma exchanges, repeated intravenous immunoglobulin therapy, and a thymectomy. The course was progressive and led to gait loss at 6 years.

Referred to our center at 8 years, he showed bilateral ptosis and ophthalmoplegia, nasal voice, facial weakness with open mouth, and diffuse muscle weakness, particularly in triceps and hamstrings (3 MRC), but also in deltoid, quadriceps, and psoas muscles (4 MRC). The *Garches* myasthenic score was 60/100, and he had a very restricted indoor ambulation, necessitating a wheelchair for the exteriors (**Figure 1**). Spirometry revealed respiratory involvement with a forced vital capacity (FVC) of 1,640 ml (89%) when sitting and 1,060 ml (59%) in supine position, highly suggesting a diaphragmatic weakness. EKG and cardiac ultrasonography were normal.

Patient 2 was born at term after an uneventful pregnancy and reached the normal milestones at expected age. She presented ptosis and frequent respiratory infections at 2 years old. ENMG showed a significant decremental response in repetitive nerve stimulation. There were no anti-AChR and anti-MUSK antibodies in serum. A therapy with Pyridostigmine 60 mg two times a day was started, and the response was partial, with fluctuating muscle weakness and fatigability despite adequate dosing (7 mg/ kg/day).

On referral to our clinic at 5 years old, neurological examination revealed symmetrical axial and proximal muscular weakness, bilateral ptosis, and facial weakness with open mouth (**Figure 2**). She had fluctuant fatigability, being able to walk with mild restrictions for 500 meters. 6MWT corresponded to 448 meters, and she scored 70/100 at *Garches*' myasthenic score. There was no bulbar involvement, including dysphagia and dysphonia. Respiratory test revealed an FCV of 133 ml (84%) in sitting positions and 1,900 ml (70%) in supine position. Cardiac workup was normal.

Based on the familial clinical story and the ancillary tests, a diagnosis of CMS was suspected in both children.

Molecular Studies

Next-Generation-Sequencing (NGS)-based screening of 54 genes involved in muscular excitability (a list on request), among which 30 CMS causing genes, including *CHRNE,* was performed in the proband P1 using a SeqCapEZ capture design (Nimblegen), and a MiSeq sequencer (Illumina). A total of 1,101 coding sequences and flanking regions were sequenced. Variants were identified through a bioinformatics pipeline (Genodiag, Paris, France). Copy number variations (CNVs) in targeted regions were searched for by a dedicated algorithm based on comparison of normalized number of reads of each region among the 12 samples of the sequence run. Variants were filtered according to their frequency in the general population (GnomAD) and in the patient's samples. It revealed the presence of a homozygousc.632_633dupCGp. (Gly212Argfs*3) variant in the exon 7 of *CHRNE*gene. The same variant was detected by Sanger sequencing of *CHRNE* exon 7 in a homozygous state in Patient P2, and in a heterozygous state in both healthy parents.

FIGURE 1 | Clinical features, P1. P1, an 11-year-old boy with before treatment with salbutamol, showing severe bilateral ptosis and facial weakness **(A)**; note the improvement after salbutamol treatment; he showed only mild ptosis **(B)** and less fatigability, being able to walk without aid **(C)**.

This variant predicts a shift in a translation reading frame, a change of glycine 212 to arginine, and a premature stop codon at Codon 214 (**Figure 3**). This premature termination codon may trigger nonsense-mediated decay of *CHRNE* mRNAs. Such a homozygous frame shift in the *CHRNE* gene results in low expressor-type CMS.

FIGURE 2 | Clinical features, P2. P2, an 8-year-old girl presenting with sever bilateral ptosis before treatment with salbutamol **(A)**; amelioration of the eyelid ptosis **(B)**; amelioration of strength in neck extensor muscles **(C)**.

FIGURE 3 | Genetics. A 2-bp shift of a reading frame from Codon 212 and premature stop codon at codon 214 of *CHRNE* gene (an image of this part of mRNA was taken from Alamut Visual software, Interactive Biosoftware Sophia Genetics).

Response to Treatment

The clinical status before and after the introduction of Salbutamol is listed in **Table 1**. Both patients were initially treated with pyridostigmine from ages 6 months (P1) and 10 months (P2), with a favorable but incomplete response, despite adequate dosing (at least 1 mg/Kg/dose for at least 4 doses per day). We introduced a concomitant treatment with salbutamol, which was well tolerated without side effects, with a progressive dose until 6 mg/day in both children, (P1 at.17 mg/Kg/day; P2 at.2 mg/kg/day), taken in three divided doses. An important improvement of the weakness was observed in both P1 and P2 from the first 2 weeks of treatment, particularly in P1. At the 6-month visit, P1 was able to walk and run, using the wheelchair only for long distances, with a 6MWT of 390 mts. Ptosis and ophthalmoplegia were also partially ameliorated, with a 71/100 in the Garches Myasthenic score, corresponding to a 10-point amelioration. Importantly, the spirometry showed an FVC of 2,530 ml (94%) in sitting position, and 2,560 ml (95%) in supine position, highlighting a spectacular amelioration compared to the first assessment, 1,060 ml, 59% in supine position (**Table 1**).

On the long term, P1 showed mild fluctuating symptoms, including increased fatigability and restricted ambulation some months after starting the treatment, and he showed a myasthenic crisis with extreme fatigue, loss of ambulation, swallowing difficulties, and diaphragmatic involvement (FVC of 36%) needing hospitalization. The fatigability and respiratory involvement disappeared in 1 day.

TABLE 1 | Response to treatment, adding oral β2 adrenergic agonists (salbutamol).

	Before treatment with salbutamol		After treatment with salbutamol	
	P1	P2	P1	P2
Facial involvement	Severe bilateral ptosis and ophthalmoplegia.	Bilateral ptosis and ophthalmoplegia.	Mild bilateral ptosis.	Mild ophthalmoplegia.
Muscle weakness	Global muscle weakness.	Proximal and axial muscular weakness.	Mild muscle weakness.	Normal
Walking ability	Very restricted ambulation.	Able to walk with mild restrictions.	Able to walk.	No restrictions to walk.
Myasthenic score (pts)	60/100	70/100	71/100	85/100
6MWT (mts)	Not able to walk more than 6 steps.	448	390	486
Diaphragm involvement	Present.	Absent.	Absent.	Absent.
FVC Sitting (ml)	1,640 (89%)	1,330 (84%)	2,530 (94%)	1,640 (103%)
FVC Supine (ml)	1,060 (59%)	1,900 (70%)	2,560 ml (95%)	1,460 (92%)

Yo, years old; mo, months old; FVC, forced vital capacity.

P2 with a milder clinical phenotype at the baseline significantly improved her axial strength and her ptosis after treatment, showing an amelioration of 15 points in the myasthenic score. 6MWT was 486, consisting of a gain of 38 meters. CV remained stable and without respiratory infections.

In these times, both patients follow treatment without any respiratory involvement, and mild-to-moderate motors symptoms with occasional fluctuations in time.

DISCUSSION

CMS are a heterogeneous group of inherited disorders caused by mutations in genes that lead to impaired neuromuscular transmission (15). Most CMS are caused by molecular defects in the acetylcholine nicotinic receptor of the muscle, in particular *CHRNE*, which accounts almost 80% of all CMS (5, 16, 17), leading to AChR deficiency (15).

Based on a similar clinical phenotype, consisting with poorly responding myasthenia and their family history, we suspected a congenital myasthenic syndrome in both P1 and P2. Genetic studies disclosed a novel never-reported variant mutation in *CHRNE,* confirmed by segregation studies. Frame shift mutations of *CHRNE* gene are associated with a low expression of the ACh receptors at the cell surface, termed as a "low expressor" CMS mechanism, which is the most common type of CMS.

Clinically, *CHRNE* have been described as mild and non-progressive disorders, but some authors have recently reported loss of ambulation in several patients (10, 11, 18–20). A wide spectrum symptom, even among individuals within the same family, has been reported, spanning from severe cases with premature and fatal respiratory failure and milder cases presenting only with ptosis (8, 11). P1 and P2 manifested a typical phenotype with early-onset bilateral ptosis, ophtalmoparesis, facial, neck muscle and proximal limb weakness, with fluctuant fatigability, discordant severity, but also a marked respiratory dysfunction and symptoms, generating a risk of life-threatening complications. Of note, the genetically unconfirmed first born of the sibship died of respiratory infection during infancy.

The precise mechanisms of this clinical variability discordance in severity are not well understood; they might be associated with epigenetic, varying-phenotype mutations, sex variation, and environmental factors (11). In any case, we stress the importance to monitor tightly the respiratory function in patients with ACHRε deficiency.

From a therapeutic standpoint, we only observed a partial response to esterase inhibitors as reported previously (13). The introduction of salbutamol resulted in more consistent response (**Table 1**), without side effects in both children.

The mechanism of action β2 adrenergic receptors agonist on the neuromuscular junction has remained unknown until today, but some studies revealed that they increase quantal release and reduce the conductance of the AChR channel (9) and increase the number of briefs intraburst closures, causing an open-channel blockade of AChR (21).

Treatment with salbutamol led to a clear respiratory benefit in both children, suggesting an improvement of diaphragmatic weakness. The association of the acetylcholinesterase inhibitors may lead to a significant impact, not just on their strength and fatigability, but also on their autonomy for daily life, without significant side effects, thus reinforcing that β2-adrenergic receptor agonist therapy could be the first choice of pharmacological strategy for treating CMS with *CHRNE* mutations, as previously reported (22).

Our observations and the review of the literature suggest that mutations in the genes coding for subunits of the acetylcholine receptor, and, in particular, the epsilon subunit, should be the first researched in patients presenting with symptoms of myasthenia and decremental response on repetitive stimulation in absence of anti-AchR and anti-musk antibodies. Mutations in the *CHRNE* with a low expressor profile may be identified in severe infantile cases and may have a mild response on acetylcholinesterase inhibitors. In these cases, adding β2 adrenergic agonists could, as in our cases, result in an important gain of motor and respiratory function (9, 23–25).

CONCLUSION

In conclusion, these cases broaden the genetic spectrum of *CHRNE*-related myasthenic syndromes. Further studies are

needed to confirm the relationship between this mutation, the progressive course, and the response to treatment.

DATA AVAILABILITY STATEMENT

The datasets presented in this article are not readily available because of ethical and privacy restrictions. Requests to access the datasets should be directed to the corresponding author.

ETHICS STATEMENT

The studies involving human participants were reviewed and approved by Comité de Protection des Personnes Est IV DC-2012-1693. Written informed consent to participate in this study was provided by the participants' legal guardian/next of kin. Written informed consent was obtained from the individual(s), and minor(s)' legal guardian/next of kin, for the publication of any potentially identifiable images or data included in this article.

AUTHOR CONTRIBUTIONS

MG-G, NF, SQ-R, and EM: study conception, design, and supervision of the course of the project. MG-G, ES-A, NF, and PB: data collection, taking responsibility of patient follow-up, data management, and reporting. MG-G, ES-A, PB, DS, SQ-R, and EM: analysis and interpretation of results, taking responsibility of logical interpretation based on a literature review, and presentation of the results. MG-G, ES-A, DS, SQ-R, and EM: draft manuscript preparation and taking responsibility of the construction of the whole or body of the manuscript. All the authors reviewed the results, provided critical feedback, and approved the final version of the manuscript.

ACKNOWLEDGMENTS

We are grateful to our little patients and their family. We would also like to thank the health care providers involved in the care of the patients. The authors had full editorial control of the manuscript and provided their final approval of all content.

REFERENCES

1. Engel AG. Current status of the congenital myasthenic syndromes. *Neuromuscul Disord.* (2012) 22:99–111. doi: 10.1016/j.nmd.2011.10.009
2. Hantaï D, Nicole S, Eymard B. Congenital myasthenic syndromes: an update. *Curr Opin Neurol.* (2013) 26:561–8. doi: 10.1097/WCO.0b013e328364dc0f
3. Richard P, Gaudon K, Haddad H, Ammar AB, Genin E, Bauché S, et al. The *CHRNE* 1293insG founder mutation is a frequent cause of congenital myasthenia in North Africa. *Neurology.* (2008) 71:1967–72. doi: 10.1212/01.wnl.0000336921.51639.0b
4. Engel AG. Congenital myasthenic syndromes in 2012. *Curr Neurol Neurosci Rep.* (2012) 12:92–101. doi: 10.1007/s11910-011-0234-7
5. Abicht A, Dusl M, Gallenmüller C, Guergueltcheva V, Schara U, Della Marina A, et al. Congenital myasthenic syndromes: achievements and limitations of phenotype-guided gene-after-gene sequencing in diagnostic practice: a study of 680 patients. *Hum Mutat.* (2012) 33:1474–84. doi: 10.1002/humu.22130
6. Rodríguez Cruz PM, Palace J, Beeson D. Congenital myasthenic syndromes and the neuromuscular junction. *Curr Opin Neurol October.* (2014) 27:566–75. doi: 10.1097/WCO.0000000000000134
7. Engel AG. Genetic basis and phenotypic features of congenital myasthenic syndromes. *Handb Clin Neurol.* (2018) 148:565–89. doi: 10.1016/B978-0-444-64076-5.00037-5
8. Finsterer J. Congenital myasthenic syndromes. *Orphanet J Rare Dis.* (2019) 14:57. doi: 10.1186/s13023-019-1025-5
9. Vanhaesebrouck AE, Beeson D. The congenital myasthenic syndromes: expanding genetic and phenotypic spectrums and refining treatment strategies. *Curr Opin Neurol.* (2019) 32:696–703. doi: 10.1097/WCO.0000000000000736
10. Faber CG, Molenaar PC, Vles JSH, Bonifati DM, Verschuuren JJGM, van Doorn PA, et al. AChR deficiency due to epsilon-subunit mutations: two common mutations in the Netherlands. *J Neurol.* (2009) 256:1719–23. doi: 10.1007/s00415-009-5190-7
11. Natera-de Benito D, Domínguez-Carral J, Muelas N, Nascimento A, Ortez C, Jaijo T, et al. Phenotypic heterogeneity in two large Roma families with a congenital myasthenic syndrome due to *CHRNE* 1267delG mutation. A long-term follow-up. *Neuromuscul Disord.* (2016) 26:789–95. doi: 10.1016/j.nmd.2016.08.005
12. Ardissone A, Moroni I, Bernasconi P, Brugnoni R. Congenital myasthenic syndrome: phenotypic variability in patients harbouring p. T159P mutation in CHRNE gene. *Acta Myol.* (2017) 36:28–32.
13. Lee M, Beeson D, Palace J. Therapeutic strategies for congenital myasthenic syndromes. *Ann N Y Acad Sci.* (2018) 1412:129–36. doi: 10.1111/nyas.13538
14. Fromageot C, Lofaso F, Annane D, Falaize L, Lejaille M, Clair B, et al. Supine fall in lung volumes in the assessment of diaphragmatic weakness in neuromuscular disorders. *Arch Phys Med Rehabil.* (2001) 82:123–8. doi: 10.1053/apmr.2001.18053
15. Engel AG, Shen X-M, Selcen D, Sine SM. Congenital myasthenic syndromes: pathogenesis, diagnosis, and treatment. *Lancet Neurol.* (2015) 14:420–34. doi: 10.1016/S1474-4422(14)70201-7
16. Ohno K, Milone M, Shen X-M, Engel AG, A. frameshifting mutation in *CHRNE* unmasks skipping of the preceding exon. *Hum Mol Genet.* (2003) 12:3055–66. doi: 10.1093/hmg/ddg334
17. Richard P, Gaudon K, Fournier E, Jackson C, Bauché S, Haddad H, et al. A synonymous CHRNE mutation responsible for an aberrant splicing leading to congenital myasthenic syndrome. *Neuromuscul Disord.* (2007) 17:409–14. doi: 10.1016/j.nmd.2007.01.018
18. Abicht A, Stucka R, Karcagi V, Herczegfalvi A, Horváth R, Mortier W, et al. A common mutation (epsilon1267delG) in congenital myasthenic patients of Gypsy ethnic origin. *Neurology.* (1999) 53:1564–9. doi: 10.1212/WNL.53.7.1564
19. Mihaylova V, Scola RH, Gervini B, Lorenzoni PJ, Kay CK, Werneck LC. Et al. Molecular characterisation of congenital myasthenic syndromes in Southern Brazil. *J Neurol Neurosurg Psychiatry.* (2010) 81:973–7. doi: 10.1136/jnnp.2009.177816
20. Ohno K, Anlar B, Ozdirim E, Brengman JM, DeBleecker JL, Engel AG. Myasthenic syndromes in Turkish kinships due to mutations in the acetylcholine receptor. *Ann Neurol.* (1998) 44:234–41. doi: 10.1002/ana.410440214
21. Farmakidis C, Pasnoor M, Barohn RJ, Dimachkie MM. Congenital myasthenic syndromes: a clinical and treatment approach. *Curr Treat Options Neurol.* (2018) 20:36. doi: 10.1007/s11940-018-0520-7
22. Sadeh M, Shen X-M, Engel AG. Beneficial effect of albuterol in congenital myasthenic syndrome with epsilon-subunit mutations. *Muscle Nerve August.* (2011) 44:289–91. doi: 10.1002/mus.22153
23. Beeson D. Congenital myasthenic syndromes: recent advances. *Curr Opin Neurol.* (2016) 29:565–71. doi: 10.1097/WCO.0000000000000370
24. Padmanabha H, Saini AG, Sankhyan N, Singhi P. COLQ-related congenital myasthenic syndrome and response to salbutamol therapy. *J Clin*

Neuromuscul Dis. (2017) 18:162–3. doi: 10.1097/CND.0000000000000160

25. McMacken GM, Spendiff S, Whittaker RG, O'Connor E, Howarth RM, Boczonadi V, et al. Salbutamol modifies the neuromuscular junction in a mouse model of ColQ myasthenic syndrome. *Hum Mol Genet.* (2019) 28:2339–51. doi: 10.1093/hmg/ddz059

Conflict of Interest: The authors declare that the research was conducted in the absence of any commercial or financial relationships that could be construed as a potential conflict of interest.

Publisher's Note: All claims expressed in this article are solely those of the authors and do not necessarily represent those of their affiliated organizations, or those of the publisher, the editors and the reviewers. Any product that may be evaluated in this article, or claim that may be made by its manufacturer, is not guaranteed or endorsed by the publisher.

Copyright © 2022 Gómez-García de la Banda, Simental-Aldaba, Fahmy, Sternberg, Blondy, Quijano-Roy and Malfatti. This is an open-access article distributed under the terms of the Creative Commons Attribution License (CC BY). The use, distribution or reproduction in other forums is permitted, provided the original author(s) and the copyright owner(s) are credited and that the original publication in this journal is cited, in accordance with accepted academic practice. No use, distribution or reproduction is permitted which does not comply with these terms.

frontiers | Frontiers in Neurology

CASE REPORT
published: 17 June 2022
doi: 10.3389/fneur.2022.910596

Analysis of Clinical Symptoms of Guillain–Barré Syndrome Induced by Heat Stroke: Three Case Reports and Literature Review

Xiao-xiao Ni[1†], *Cong-lin Wang*[2], *Ye-qun Guo*[1] *and Zhi-feng Liu*[2*]

[1] Department of Hyperbaric Oxygen Medicine and Rehabilitation, General Hospital of Southern Theater Command of PLA, Guangzhou, China, [2] Department of Critical Care Medicine, General Hospital of Southern Theater Command of PLA, Guangzhou, China

Background: Heat stroke is a potentially fatal condition that is caused by elevated core temperature. Guillain–Barré syndrome (GBS) induced by heat stroke is extremely rare and has only been reported in few case reports. The purpose of this case study was to evaluate the clinical symptoms, neuroelectrophysiological and imageological features of GBS after heat stroke.

Methods: We reviewed our hospital records and previously published reports to find the cases of GBS after heat stroke. The clinical, imageological, and electrophysiological profiles, treatment and prognosis were presented and analyzed.

Results: We retrieved three cases of GBS induced by heat stroke from our hospital, which presented as lesions on multiple cranial and peripheral nerves and albuminocytologic dissociation in the cerebrospinal fluid. All of these patients had disorders of consciousness at the early stage of heat stroke and a "pseudo-recovery period" after they recovered from coma after heat stroke. After immunoglobulin administration and immunoregulation therapy, these patients' neurological deficiencies were relieved significantly. But there are still disabilities and almost totally reliant on others.

Conclusions: The number of the cases of GBS induced by HS reported in this study has been the most in the recent 5 years. Clinicians should pay attention to patients with heat stroke with sustained coma and the sudden quadriplegia. Early, exact and timely diagnosis and treatment of GBS need to be performed, to accelerate recovery and improve prognosis.

Keywords: heat stroke, nervous injury, Guillain-Barré syndrome, peripheral neuropathy, nervous system

OPEN ACCESS

Edited by:
Helmar C. Lehmann,
University of Cologne, Germany

Reviewed by:
Christian Zammit,
University of Malta, Malta
Meghana Srinivas,
Emory University, United States

****Correspondence:***
Zhi-feng Liu
Zhifengliu7797@163.com

†Present address:
Xiao-xiao Ni,
Department of Hyperbaric Oxygen Medicine and Rehabilitation, General Hospital of Southern Theater Command of PLA, Guangzhou, China

Specialty section:
This article was submitted to Neuromuscular Disorders and Peripheral Neuropathies, a section of the journal Frontiers in Neurology

Received: *13 April 2022*
Accepted: *23 May 2022*
Published: *17 June 2022*

Citation:
Ni X-x, Wang C-l, Guo Y-q and Liu Z-f (2022) Analysis of Clinical Symptoms of Guillain–Barré Syndrome Induced by Heat Stroke: Three Case Reports and Literature Review. Front. Neurol. 13:910596. doi: 10.3389/fneur.2022.910596

INTRODUCTION

Heat stroke (HS) is a life-threatening disease and the most severe condition of heat-related illness, characterized by core body temperature >104°F (40°C) and neurological dysfunction such as confusion, seizures, or loss of consciousness (1). HS is divided into nonexertional HS and environmental heat stroke (EHS). The central nervous system is highly sensitive to hyperthermia, leading to neurological complications due to the involvement of the cerebellum, basal ganglia, and peripheral nerves. There are various manifestations of nervous system injuries after HS, including

cerebellar injury, subarachnoid hemorrhage, peripheral nerve injury, and so on (2). However, what is the relationship of HS and Guillain–Barré syndrome (GBS)? Relevant reports are few and GBS after HS was sometimes thought to be unrelated to HS. The exact relationship between GBS and HS remains to be studied.

Guillain–Barré syndrome is considered to be the most common cause of acute flaccid paralysis that affects all age groups worldwide and can lead to disability and high risk of mortality (3). Most patients present with an antecedent illness, most commonly upper respiratory tract infection, before the onset of progressive motor weakness (4). Heat stroke as an inducement of GBS was observed in the recent years. GBS is a group of acute immune-mediated paralytic neuropathies characterized by rapidly progressive bilateral weakness of the extremities with hyporeflexia or areflexia (5). Subtypes are mainly categorized into demyelinating and axonal forms according to the clinical course, nerve conduction velocities, and immunologic findings. The typical form of GBS is acute inflammatory demyelinating polyradiculoneuropathy (AIDP), whereas the main axonal forms are subdivided into acute motor axonal neuropathy (AMAN) and acute motor and sensory axonal neuropathy (AMSAN) (3). The pathological changes are lymphocyte infiltration and macrophage infiltration around small and medium blood vessels of peripheral nerve tissue and nerve fiber demyelination. The development of GBS is associated with the phenomenon of molecular mimicry and with cross-reactivity. At present, it is believed that GBS is an autoimmune disease, in which the body's immune system produces immune responses against peripheral nerves, resulting in peripheral nerve demyelination (3). GBS after HS is very easily misidentified with peripheral nerve injury. How to distinguish GBS from peripheral nerve injury after HS is a clinical problem?

In the past 5 years, we have retrieved 3 cases of acute GBS induced by HS in our hospital. In general, GBS after heat stroke has only been reported in case reports, and there are few reports describing the findings on clinical features of GBS after HS. Therefore, this study aims to observe the clinical progress of GBS after HS, changes in immunological indicators and the efficacy of immunoregulatory therapy.

MATERIALS AND METHODS

This study was conducted in accordance with the Declaration of Helsinki. We reviewed the electronic medical records for patients who had HS from 1 January 2016 to 1 March 2022 in our hospital. For all cases from our hospital records, we recorded the patient's gender, age, blood pressure, core temperature (immediately after admission), Glasgow coma scale (GCS) on arrival, DIC score, liver and kidney function, blood coagulation function, blood routine, cardiac indicators, analysis of cerebrospinal fluid (CSF), results of neuroelectrophysiological examination, brain magnetic resonance imaging (MRI), and the clinical prognosis. The same variables were collected from the previously reported cases if available (clinical background, patient characteristics, results of neuroelectrophysiological and laboratory examination, MRI findings, and prognosis). The Barthel index was evaluated to assess daily living ability at 90 days after HS.

For literature research, we reviewed published scientific reports by searching the PubMed database and China National Knowledge Infrastructure (CNKI). Search strategies were developed to find publications containing subject headings and key words (text words) including heat stroke, heat or sun disorder, injury, illness, stress, related, shock, exhaustion; heat stroke; neurology; nervous system; Guillain–Barré syndrome; peripheral neuropathy; and case, cases. Papers included were limited to human subjects and publication types (case reports, case series). Publications of cases that had an exertional component or nonexertional HS (e.g., confined spaces, Bikram Yoga, and electric blankets) were both included in this study. Papers excluded from review were those unrelated to Guillain–Barré syndrome or peripheral neuropathy or where individual patient data were not available.

RESULTS

A total of 6,286 publications (3,379 from PubMed, 2,907 from CNKI) between 1990 and 2021 were identified using the structured online search strategy. A total of 48 articles were screened in full-text review and 6,238 publications were excluded. A total of three articles were unable to obtain and 37 articles were not clinically relevant. A total of four articles including 4 cases were included following review (6–9). We extracted 3 cases from our hospital (searching between January 2016 and March 2022). The detailed clinical data of these seven cases are shown in **Table 1**. The average age was 40.4 ± 4.73 years (range, 25–57 years), and most of the patients were men (85.7%). About 71.43% (5/7) of the patients had multiple organ damage (MOD). The average GCS score was 5.33 points (range, 3–10 points) and the duration of coma was 5.5 ± 0.71 days. The average duration from HS to extremity weakness was 13.2 ±1.31 days (range, 8–15 days). There was a period from the patient recovering from coma to developing quadriplegia, which was called "pseudo-recovery period" by us. The average duration of "pseudo-recovery period" was 7.6 ± 1.67 days (range, 1–12 days). Albuminocytologic dissociation (protein cell separation) was shown in the cerebrospinal fluid (CSF) collected by lumbar puncture of all these patients. Electromyography of these patients revealed impairment of sensorimotor fibers in bilateral median, ulnar, tibial, and common peroneal nerves. MRI of these patients revealed no abnormality or a small amount of ischemic focus (**Figure 1**). About 28.57% (2/7) of the patients had abnormal antibodies in CSF, and all of them responded to immunomodulatory therapy. Neurological sequelae continued up to 90 days after HS and the Barthel index of these patients was 38.75 ± 20.9 (range, 10–100). The conduction velocity of sensorimotor nerves of the three patients in our hospital is shown in **Table 2**. **Figure 2** shows the timeline with relevant data from the episode of care of these three patients.

CASE REPORTS

Case 1

A 57-year-old man was found unresponsive in a workshop on a hot summer day (ambient temperature 36°C). His core

TABLE 1 | Detailed clinical data of patients with Guillain–Barre syndrome induced by heat stroke.

No	Source	Year	Location	Background Diseases	Age	Gender	Tc (°C)	Degree of coma	Duration of coma (day)	GCS scale
1	Our hospital	2020	China	Hypertension	57	Male	42	deep	7	3
2	Our hospital	2018	China	None	41	Male	42.5	light	6	10
3	Our hospital	2021	China	None	56	Male	42	deep	8	3
4	J Neurol Neurosurg Psychiatry, 1999, 66(3):408.	1999	Germany	Drug addict	28	Male	42.5	deep	4	NA
5	Clin Lab, 2017, 63(9):1507-1511.	2017	China	NA	41	male	41.3	moderate	5	NA
6	J Environ Occup Med (China), 2007, 24(3):325-326	2007	China	None	35	male	42	Deep	NA	NA
7	J Binzhou Med College (China), 1998, 21(6):562	1998	China	NA	25	female	39.8	deep	3	NA

No	BP (mmHg)	MOD (Yes/No)	HS to quadriplegia (day)	Pseudo-recovery period (day)	Cranial nerve injury	Both upper limbs strength (MRC grades)	Both lower limbs strength (MRC grades)
1	95/43	Yes	8	1	Dysphagia, facioplegia, dysarthria	0	0
2	92/46	Yes	13	11	Dysphagia, facioplegia, dysarthria	2∼3	0
3	87/36	Yes	16	6	Dysphagia, facioplegia, ophthalmoplegia	0	0
4	85/30	Yes	12	8	Dysphagia, facioplegia	2∼3	1∼2
5	NA	NA	NA	NA	Dysphagia, right blepharoptosis, dysarthria	2	2
6	141/85	Yes	15	NA	Dysphagia, dysarthria	0	0
7	NA	NA	15	12	facioplegia	0∼1	0∼1

No	Protein CONC in CSF (g/l)	WBC in CSF (10^6/L/mm^3)	Antibody in CSF	Treatment	Prognosis/time	The Barthel index
1	0.47∼1.82	0.6	None	Plasma exchange; IVIG; Immune-modulating.	Upper limb strength (MRC grades 3/5); Lower limb strength (MRC grades 2/5); /day 90	10
2	0.62∼0.88	3	IgG (59 mg/L) IgA (2.55 mg/L)	IVIG; Immune-modulating.	Extremities strength (MRC grades 4/5); /day 90	30
3	1.09	3.4	None	IVIG; Immune-modulating.	Upper limb strength (MRC grades 2/5); Lower limb strength (MRC grades 4/5); /day 90	15
4	0.48∼7.3	6	IgM (500 U/l)	IVIG; plasma exchange.	Chair-bound /14 months later	NA
5	0.732	6	NA	IVIG; Immune-modulating.	Recovered /3 months later	100
6	1.005	NA	NA	Immune-modulating.	Extremity muscles weakness /NA.	NA
7	2.85	3	NA	Immune-modulating.	Extremity strength (MRC grades 3/5) /day 35	NA

MOD, multiple organ damage; BP, blood pressure; MRC, Medical Research Council; CONC, concentration; IVIG, intravenous immunoglobulin.

temperature was 42°C within 30 min of admission. He was in deep coma with wide unreactive pupils and without corneal and pharyngeal reflexes. Blood pressure was 95/43 mmHg and the heart rate was 146/min. He developed disseminated intravascular coagulation (DIC), thrombopenia below 1,800 MRD/ml, acute heart/liver/kidney damage, rhabdomyolysis, and metabolic acidosis. He was diagnosed with HS. After 7 days of treatment including hyperbaric oxygen (HBO), correction of electrolyte and acid-base disturbance, antishock, protection of cardiac and hepatorenal function, suppression of excessive gastric acid secretion, etc., his consciousness recovered from coma and his limb muscles had Medical Research Council (MRC) grades 4. But only 1 day later, he complained of fatigue, weakness of limbs, dyspnea, and difficulty in expectoration. He required intensive care and tracheotomy within hours. All limb muscles had MRC grade 0. Facioplegia increased 2 days later. He had no ophthalmoplegia, but having hyporeflexia and stocking glove hypoesthesia for vibratory and cold stimuli. Small ischemic focus in the basal ganglia and cortex was shown through MRI. Protein concentration in CSF was 0.47 g/l at

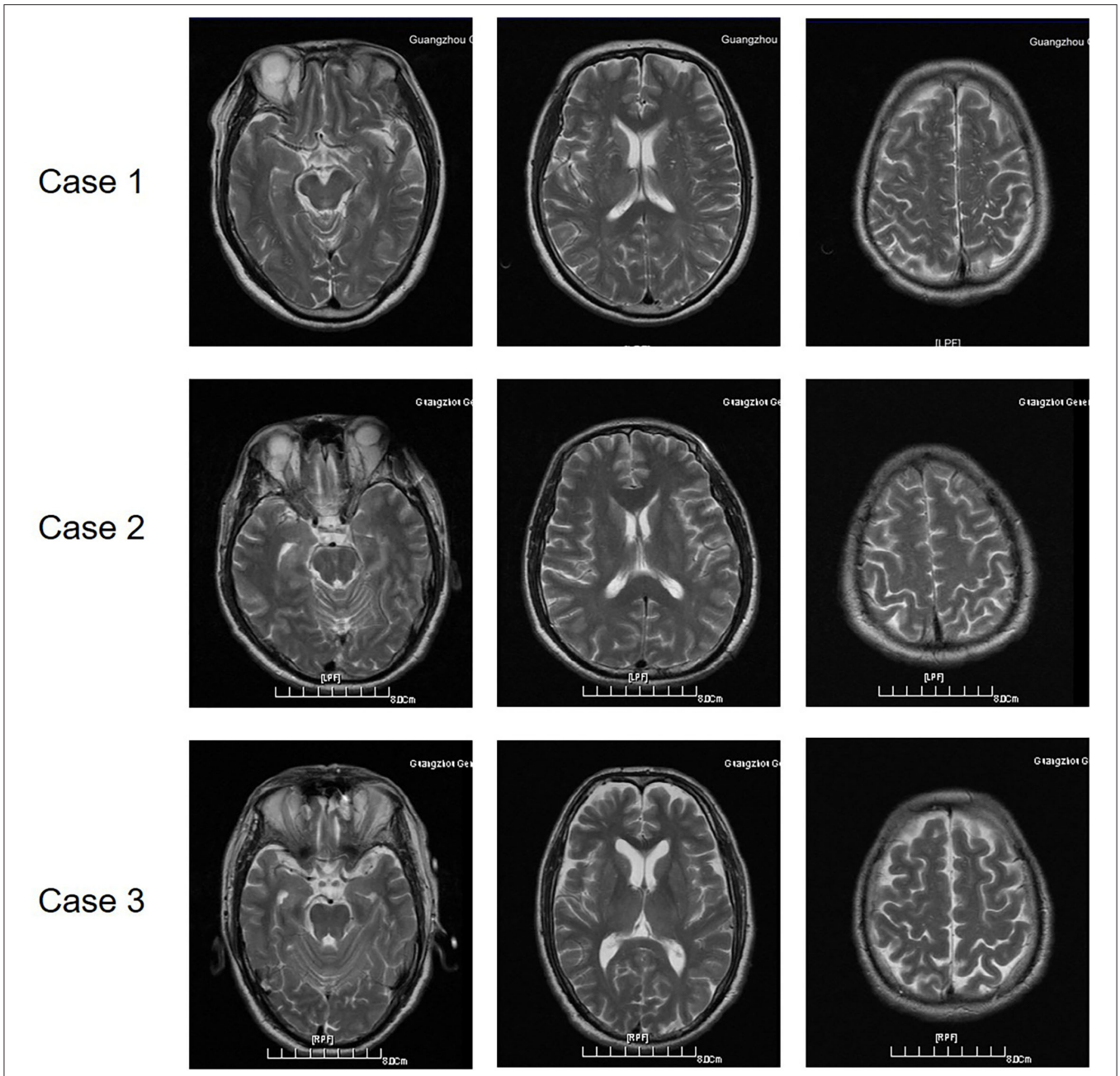

FIGURE 1 | The brain magnetic resonance imaging (MRI) of the three patients with GBS induced by HS.

2 days after tetra paresis and 1.82 g/l 10 days later. White blood cell (WBC) count was 0.60 $\times$ 10^6/L cells/mm^3 at 2 days after tetra paresis and 5.4 $\times$ 10^6/L cells/mm^3 10 days later. Antibody concentration in the CSF and serum was all normal. Compound motor action potentials were<1 mV in all tested nerves at 10 days after HS. Conduction velocities were below 90% of the lower limit of normal in the bilateral tibial nerve and common peroneal nerves. F responses were missing in both median nerves, ulnar nerves, tibial nerves, and common peroneal nerves. A conduction block was present along the both median nerves (right wrist stimulation amplitude 0.67 mV and left 0.56 mV; right elbow stimulation amplitude 0.45 mV and left 0.58 mV) and ulnar nerves (right wrist stimulation amplitude 0.76 mV and left 0.88 mV; right elbow stimulation amplitude 0.69 mV and left 0.87 mV). The sensory potentials of bilateral tibial nerves and common peroneal nerves were not elicited. The amplitude of the sensory potentials of bilateral median nerves and ulnar nerves was reduced. The patient was diagnosed with AIDP and treated with a 2-day course plasma exchange, intravenous immunoglobulin (IVIG) for 5 days, and

TABLE 2 | The conduction velocity of nerves.

	Nerve	Sensory nerve			Motor nerves		
		Latency (ms)	Amplitude (μV)	Conduction velocity (m/s)	Latency (ms)	Amplitude (mV)	Conduction velocity (m/s)
Case 1	Right median nerve	3.52	1.95	47.9	8.35	0.45	46.6
	Left median nerve	3.49	1.71	48.1	8.38	0.58	46.3
	Right ulnar nerve	3.02	2.2	48.7	6.67	0.69	53.7
	Left ulnar nerve	0	0	0	6.65	0.87	54.2
	Right tibial nerve	0	0	0	13	0.61	40.5
	Left tibial nerve	0	0	0	12.9	0.83	41
	Right common peroneal nerve	0	0	0	10.5	0.43	45.6
	Left common peroneal nerve	0	0	0	10.5	0.43	45.4
Case 2	Right median nerve	3.23	5.9	55.1	9	1.42	46
	Left median nerve	3.21	4.9	55.1	8.78	1.42	46.4
	Right ulnar nerve	2.63	6.6	51.6	7.45	1.02	48.3
	Left ulnar nerve	2.69	4.5	51.2	7.03	3.6	49.2
	Right tibial nerve	0	0	0	20.4	0.48	33.6
	Left tibial nerve	0	0	0	20	0.62	34.4
	Right common peroneal nerve	0	0	0	14.7	0.51	36.9
	Left common peroneal nerve	0	0	0	14.5	0.39	36.5
Case 3	Right median nerve	3.45	1.75	43.1	12.35	0.43	37.8
	Left median nerve	3.03	1.75	41.5	15.31	0.51	40.1
	Right ulnar nerve	3.56	1.85	45.3	10.7	0.52	42.3
	Left ulnar nerve	3.58	1.80	42.9	9.81	0.56	41.6
	Right tibial nerve	0	0	0	12.08	0.35	37.8
	Left tibial nerve	0	0	0	13.73	0.39	35.5
	Right common peroneal nerve	0	0	0	8.76	0.40	43.3
	Left common peroneal nerve	0	0	0	12.58	0.38	40.9

The conduction velocity of motor nerves of median nerve and ulnar nerve was recorded through the stimulation from elbow to wrist. The conduction velocity of motor nerves of tibial nerve and common peroneal nerve was recorded through the stimulation from knee to ankle.

then immune-modulating therapy (methylprednisolone). The strength of both upper limbs recovered to MRC grade 1, and the patient was discharged from hospital 29 days after HS. Then, 3 months after HS, upper limb muscles had MRC grade 3 and lower limb muscles had MRC grade 2, which made the patient chair-bound.

Case 2

A 41-year-old man fainted suddenly with projectile vomiting while working on a hot summer day (ambient temperature 35°C). His core temperature was 42.3°C on admission. He was in light coma with corneal, pharyngeal, and pupillary light reflexes. Tachypnoea had induced hypocapnia. Blood pressure was 92/46 mm Hg and the heart rate was 165/min. He had hepatic and renal dysfunction, inflammatory reaction, myocardial ischemia, and coagulation disorders. No abnormalities were found in brain MRI and he was diagnosed with HS. After 2 days of coma, he was conscious and the MRC grades of his limbs were level 5 (normal). But after 8 more days, he complained of fatigue, myalgia, and arthralgia, and 3 days later, he developed fever (38.9°C), tetraplegia, and dysphagia. He required intensive care within hours. Proximal arm muscles had MRC grades between 2 and 3. All other limb muscles had grade 0 and he developed facioplegia. Protein concentration in CSF was 0.88 g/l and WBC count was 3×10^6/L at 1 day after the onset of tetra paresis. Protein concentration in CSF was 0.62 g/l and WBC count was 1.3×10^6/L at after 2 more days. The concentration of IgG antibody in the CSF was 59 mg/L, and concentration of IgA antibody was 2.55 mg/L at 2 days after the onset of tetra paresis. Compound motor action potentials were <1.5 mV in all tested nerves 14 days after HS. Conduction velocities were below 90% of the lower limit of normal in the bilateral tibial nerves and common peroneal nerves. F responses were missing in both tibial nerves and common peroneal nerves. F responses were decreased in both median nerves and were normal in both ulnar nerves. A conduction block was present along the both median nerves (right wrist stimulation amplitude 1.85 mV and left 1.86 mV; right elbow stimulation amplitude 1.42 mV and left 1.42 mV) and tibial nerves (right ankle stimulation amplitude 0.42 mV and left 0.46 μV; right knee stimulation amplitude 0.48 mV and left 0.62 mV). The sensory potentials of the bilateral tibial nerves and common peroneal nerves were not elicited. The patient was diagnosed with AIDP and treated with IVIG for 5 days and then immune-modulating therapy (methylprednisolone). The

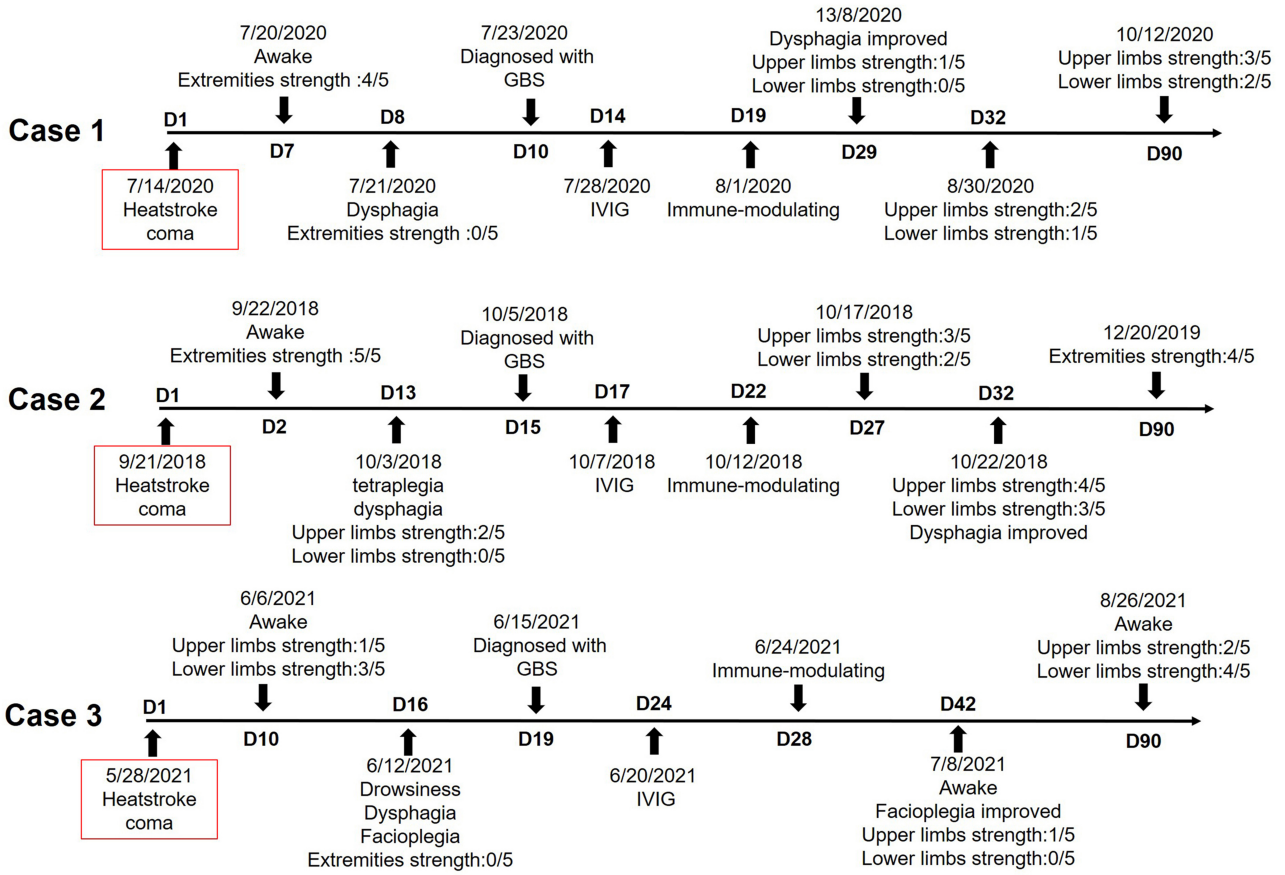

FIGURE 2 | The timeline of the disease and treatment of these three patients with GBS induced by HS.

strength of the limbs recovered to MRC grade 3, and the patient was recovered from facioplegia 32 days after HS. The patient was relieved from tracheotomy and could stand up with walking aid 90 days after HS.

Case 3

A 56-year-old man felt dizziness and fatigue while working in a hot environment (ambient temperature 33°C). Immediately, the patient developed blurred consciousness, irritability, and progressed to coma and accompanied by great sweating. He was admitted to emergency room immediately. His core temperature was 42°C, with a blood pressure of 87/36 mm Hg and the pulse rate of 164/min. He was in a deep comatose state, hepatorenal dysfunction, hypokalemia, elevated inflammatory reaction, myocardial ischemia associated with increased myocardial enzymes, coagulation disorders, and rhabdomyolysis. No abnormalities were found in brain MRI. He was diagnosed with HS and was treated by cooling, antishock, and intubation. He was conscious after 10 days of coma. The strength of his upper limbs had MRC grade 1 and the lower limb muscles had grade 3. His hepatorenal dysfunction, inflammatory reaction, myocardial ischemia, and coagulation disorders were alleviated after 12 days. But after 6 more days, the patient developed drowsiness, tetraplegia with MRC grade 0 of the muscle strength, dys-expectoration, and required tracheotomy. Protein concentration in CSF was 1.09 g/l and WBC count was 3.4×10^6/L at 3 days after tetra paresis. Immunoglobulin in CSF and serum was normal. Compound motor action potentials were<1 mV in all tested nerves at day 18. Conduction velocities were below 90% of the low limit of the normal value in both median nerves and ulnar nerves. F responses were missing in tibial nerves, ulnar nerves, and common peroneal nerves. A conduction block was present along the both median nerves (right wrist stimulation amplitude 0.78 mV and left 0.56 μV; right elbow stimulation amplitude 0.43 mV and left 0.51 mV) and tibial nerves (right ankle stimulation amplitude 0.53 mV and left 0.55 mV; right knee stimulation amplitude 0.35 mV and left 0.39 mV). The sensory potentials of the bilateral tibial nerves, ulnar nerves, median nerves, and common peroneal nerves were not elicited. The patient was diagnosed with AIDP at 19 days after HS and treated with a 5-day course IVIG and then immune-modulating therapy (methylprednisolone). He was sober 21 days after HS and his upper limbs had MRC grade 1 at 42 days after HS. His upper limb strength had MRC grade 2 and lower limb strength had MRC grade 4 at 90 days after HS.

DISCUSSION

These patients in our hospital developed an acute neuropathy that met clinical and neurophysiological criteria for Guillain–Barré syndrome. Currently, similar reports are very rare, but we have treated three cases of such disease in the recent 5 years. Neurological dysfunction is an important clinical feature of heat stroke. Patients with cerebellar injury account for the majority of neurological sequelae induced by HS (10). GBS-like neuropathies have been reported from Saudi Arabia, where the temperature is high and HS is common (11). In this study, 85.7% (6/7) of the cases were from China. GBS symptoms developed almost 10 days after HS. The patients with GBS all had consciousness disorders at the early stage of HS and limb weakness often developed after patients regained consciousness. Moreover, patients with mild degree of disorder of consciousness had better prognosis. The mechanism may be related to cerebral hypoxia and secondary neuron death induced by HS.

Different from other peripheral nerve injuries induced by HS, there was a "pseudo-recovery period" after these patients recovered from coma after HS. In the "pseudo-recovery period," the extremity sensorimotor function of these patients was improved. Tetraplegia and dysphagia usually developed after the "pseudo-recovery period." Protein cell separation was shown in the CSF of all these patients, which is a typical characteristic of GBS. The results of electromyography and clinical presentation supported the diagnosis of GBS. GBS is an acute polyradiculoneuropathy that typically presents with progressive monophasic generalized and symmetric weakness classically involving bilateral upper and lower extremities and associated with hyporeflexia. A total of three patients in this study were diagnosed with AIDP. AIDP is the most common GBS variant, with electrophysiological studies primarily showing demyelination and variants showing primary dysfunction or loss of peripheral nervous system axons (12). The immunological cascade that may trigger and induce demyelination in peripheral nerves in AIDP patients is complex and incompletely understood (12). Heat stroke and its progression to nervous system injury are due to a complex interplay among the acute physiological alterations associated with hyperthermia (including circulatory failure and hypoxia), the direct cytotoxicity of heat, cell apoptosis, and the inflammatory and coagulation responses of the host. The mechanism of AIDP after HS may be related to demyelination induced by hyperthermia. Axonal excitability can be reduced, and conduction block of motor and sensory axons may occur during hyperthermia (13). However, the particular mechanism of demyelination induced by HS is still less studied.

Compared with classical presentation of GBS, the disease progressed rapidly and relieved within 14 to 26 days of onset. But the prognosis was poor and almost totally reliant on others. Sural sparing pattern is a typical symptom of GBS, which strongly supports the diagnosis of GBS in half to two-thirds of patients (14, 15). About 38% of patients with AIDP showed sensory nerve conduction abnormalities in the sural nerves (16). A total of three patients in our hospital had abnormal sensory nerve conduction of common peroneal and tibial nerves, and sural nerve conduction was moderately slowed in Case 4. It suggested that peripheral nerve injury induced by GBS after HS might be more serious than classical GBS. Although the sural-sparing pattern has not yet been included in the electrodiagnostic criteria, it plays a well-established role in GBS diagnosis (17). The lack of sural nerve examination was a limitation of this study. These patients were treated with methylprednisolone following plasma exchange or IVIG. Although corticosteroids given alone do not significantly hasten recovery from GBS (18), intravenous methylprednisolone combination with IVIG may hasten recovery but does not significantly affect the long-term outcome (19). In this study, the symptoms of these three patients improved significantly after treatment, suggesting the effect of combination therapy of GBS after HS.

Acute inflammatory demyelinating polyradiculoneuropathy has a relatively better prognosis than axonal forms of GBS. In this study, the MRC grades of extremities strength of these patients were increased 90 days after HS, and cranial nerve disturbances were relieved. But they were still chair-bound. Therefore, GBS should be identified, diagnosed, and treated early when the patient develops extremity sensorimotor disturbances after regaining consciousness from HS.

CONCLUSION

To our knowledge, the most cases of GBS induced by HS have been reported in this study in the recent 5 years. Clinicians should pay attention to heat stroke patients with sustained coma. When extremity weakness, tetraplegia, and dysphagia develop after the patient recover consciousness, early, exact, and timely diagnosis and treatment should be performed, to accelerate recovery and improve prognosis.

DATA AVAILABILITY STATEMENT

The original contributions presented in the study are included in the article/supplementary material, further inquiries can be directed to the corresponding author.

ETHICS STATEMENT

Written informed consent was obtained from the individual(s) for the publication of any potentially identifiable images or data included in this article.

AUTHOR CONTRIBUTIONS

XXN: data curation and writing-original draft preparation. CLW: data curation. YQG: methodology. ZFL: writing and reviewing and editing. All authors contributed to the article and approved the submitted version.

FUNDING

This work was supported by grants from the National Natural Science Foundation of China [No. 82072143],

Natural Science Foundation of Guangdong Province of China [No. 2021A1515010170], the PLA Logistics Research Project of China [18CXZ030, BLJ20J006], and the PLA Medical Science and Technology Youth Development Programme [21QNPY122].

ACKNOWLEDGMENTS

The authors would like to extend their heartfelt thanks to Prof. Lei Su for his insightful guidance in the course of this research.

REFERENCES

1. Hifumi T, Kondo Y, Shimizu K, Miyake Y. Heat stroke. *J Intensive Care.* (2018) 6:30–38. doi: 10.1186/s40560-018-0298-4
2. Shimada T, Miyamoto N, Shimada Y, Watanabe M, Shimura H, Ueno Y, et al. Analysis of clinical symptoms and brain MRI of heat stroke: 2 case reports and a literature review. *J Stroke Cerebrovasc Dis.* (2019) 29:104511. doi: 10.1016/j.jstrokecerebrovasdis.2019.104511
3. Malek E, Salameh J. Guillain-barre syndrome. *Semin Neurol.* (2019) 39:589–95. doi: 10.1055/s-0039-1693005
4. Shahrizaila N, Lehmann HC, Kuwabara S. Guillain-Barré syndrome. *Lancet.* (2021) 397:1214–28. doi: 10.1016/S0140-6736(21)00517-1
5. Huang C, Zhang Y, Deng S, Ren Y, Lu W. Trauma-related Guillain-Barré syndrome: systematic review of an emerging concept. *Front Neurol.* (2020) 11:588290. doi: 10.3389/fneur.2020.588290
6. Ge R, Chen F. A Case report of guillain-barre syndrome induced by heat stroke. *J Binzhou Med College (China).* (1998) 21:562.
7. Pfeiffer G, Steffen W. Guillain-Barré syndrome after heat stroke. *J Neurol Neurosurg Psychiatry.* (1999) 66:408. doi: 10.1136/jnnp.66.3.408
8. Qin H, Xu Q. A case report of occupational severe heatstroke complicated with guillain-barre syndrome. *J Environ Occup Med (China).* (2007) 24:325–6. doi: 10.3969/j.issn.1006-3617.2007.03.036
9. Wen H. Guillain-barre syndrome induced by heat stroke: a case report and literature review. *Clin Lab.* (2017) 63:1507–11. doi: 10.7754/Clin.Lab.2017.170231
10. Lawton EM, Pearce H, Gabb GM. Environmental heatstroke and long-term clinical neurological outcomes: a literature review of case reports and case series 2000–2016. *Emerg Med Australas.* (2019) 31:163–73. doi: 10.1111/1742-6723.12990
11. Bouges F, Vijayan G, Jaufeerally F. Peripheral neuropathy after heatstroke. *Lancet.* (1987) 1:224. doi: 10.1016/S0140-6736(87)90045-6
12. Liu S, Dong C, Ubogu EE. Immunotherapy of Guillain-Barré syndrome. *Hum Vaccin Immunother.* (2018) 14:2568–79. doi: 10.1080/21645515.2018.1493415
13. Howells J, Czesnik D, Trevillion L, Burke D. Excitability and the safety margin in human axons during hyperthermia. *J Physiol.* (2013) 591:3063–80. doi: 10.1113/jphysiol.2012.249060
14. Derksen A, Ritter C, Athar P, Kieseier BC, Mancias P, Hartung HP, et al. Sural sparing pattern discriminates Guillain-Barré syndrome from its mimics. *Muscle Nerve.* (2014) 50:780–4. doi: 10.1002/mus.24226
15. Umapathi T, Koh JS, Cheng YJ, Goh EJH, Lim CSJ. The utility of sural-sparing pattern in the electrodiagnosis of regional subtypes of Guillain-Barré Syndrome. *Clin Neurophysiol Pract.* (2020) 5:43–4. doi: 10.1016/j.cnp.2019.12.002
16. Kuwabara S, Ogawara K, Misawa S, Mizobuchi K, Sung JY, Kitano Y, et al. Sensory nerve conduction in demyelinating and axonal Guillain-Barré syndromes. *Eur Neurol.* (2004) 51:196–8. doi: 10.1159/000078485
17. Freiha J, Zoghaib R, Makhoul K, Maalouf N, Riachi N, Chalah MA, et al. The value of sensory nerve conduction studies in the diagnosis of Guillain-Barré syndrome. *Clin Neurophysiol.* (2021) 132:1157–62. doi: 10.1016/j.clinph.2021.02.013
18. Hughes RA, Brassington R, Gunn AA, Doorn PA. Corticosteroids for Guillain-Barré syndrome. *Cochrane Database Syst Rev.* (2016) 10:CD001446. doi: 10.1002/14651858.CD001446.pub5
19. Hughes RAC, Swan AV, Koningsveld R, Doorn PA. Corticosteroids for Guillain-Barré syndrome. *Cochrane Database Syst Rev.* (2006) 19:CD001446. doi: 10.1002/14651858.CD001446.pub2

Conflict of Interest: The authors declare that the research was conducted in the absence of any commercial or financial relationships that could be construed as a potential conflict of interest.

Publisher's Note: All claims expressed in this article are solely those of the authors and do not necessarily represent those of their affiliated organizations, or those of the publisher, the editors and the reviewers. Any product that may be evaluated in this article, or claim that may be made by its manufacturer, is not guaranteed or endorsed by the publisher.

Copyright © 2022 Ni, Wang, Guo and Liu. This is an open-access article distributed under the terms of the Creative Commons Attribution License (CC BY). The use, distribution or reproduction in other forums is permitted, provided the original author(s) and the copyright owner(s) are credited and that the original publication in this journal is cited, in accordance with accepted academic practice. No use, distribution or reproduction is permitted which does not comply with these terms.

frontiers | Frontiers in Neurology

CASE REPORT
published: 24 June 2022
doi: 10.3389/fneur.2022.905613

The Combined Efficacy of a Two-Year Period of Cybernic Treatment With a Wearable Cyborg Hybrid-Assistive Limb and Leuprorelin Therapy in a Patient With Spinal and Bulbar Muscular Atrophy: A Case Report

Hideaki Nakatsuji[1,2], *Tetsuhiko Ikeda*[3], *Atsushi Hashizume*[2], *Masahisa Katsuno*[2], *Gen Sobue*[4,5] *and Takashi Nakajima*[3]*

[1] Department of Clinical Research, National Hospital Organization Niigata National Hospital, Kashiwazaki, Japan, [2] Department of Neurology, Nagoya University Graduate School of Medicine, Nagoya, Japan, [3] Department of Neurology, National Hospital Organization Niigata National Hospital, Kashiwazaki, Japan, [4] Brain and Mind Research Center, Nagoya University, Nagoya, Japan, [5] Aichi Medical University, Nagakute, Japan

OPEN ACCESS

Edited by:
Giovanni Meola,
University of Milan, Italy

Reviewed by:
Yuishin Izumi,
Tokushima University, Japan
Maria Pennuto,
University of Padua, Italy
Davide Pareyson,
Fondazione IRCCS, Istituto Neurologico Carlo Besta, Italy
Gianni Sorarù,
University of Padua, Italy
Valeria Crippa,
University of Milan, Italy

***Correspondence:**
Takashi Nakajima
nakajima-md@mqb.biglobe.ne.jp

Specialty section:
This article was submitted to Neuromuscular Disorders and Peripheral Neuropathies, a section of the journal Frontiers in Neurology

Received: 27 March 2022
Accepted: 25 May 2022
Published: 24 June 2022

Citation:
Nakatsuji H, Ikeda T, Hashizume A, Katsuno M, Sobue G and Nakajima T (2022) The Combined Efficacy of a Two-Year Period of Cybernic Treatment With a Wearable Cyborg Hybrid-Assistive Limb and Leuprorelin Therapy in a Patient With Spinal and Bulbar Muscular Atrophy: A Case Report. Front. Neurol. 13:905613. doi: 10.3389/fneur.2022.905613

Spinal and bulbar muscular atrophy (SBMA), also known as Kennedy's disease, is a rare, slowly progressive, incurable, and hereditary neurodegenerative disease caused by the testosterone-dependent accumulation of pathogenic polyglutamine-expanded androgen receptor protein. After extensive review, two treatments for SBMA have recently been approved in Japan; this decision was based on the results of randomized controlled trials: First, anti-androgen therapy using leuprorelin acetate (leuprorelin), a disease-modifying drug that can inhibit the progression of dysphagia but has not yet been proved to improve gait function; second, cybernic treatment with a wearable cyborg hybrid assistive limb (HAL®) (Cyberdyne Inc. Tsukuba, Japan). The HAL is an innovative walking exercise system that has been shown to significantly improve gait function in eight neuromuscular diseases without reduction in muscle function, including SBMA. It is possible that the combination of these two approaches might yield better outcomes. However, the long-term effects of such a combined approach have yet to be clinically evaluated. Here, we describe the case of a 39-year-old male with SBMA who commenced anti-androgen therapy with leuprorelin 1 year previously; this was followed by cybernic treatment with HAL. The duration of walking exercise with HAL was 20–30 min a day in one session. Over 2 weeks, the patient underwent nine sessions (one course). The efficacy of HAL was evaluated by gait function tests before and after one course of cybernic treatment. Then, leuprorelin treatment was combined with cybernic sessions every 2 months for 2 years (13 courses in total). Walking ability, as evaluated by the 2-min walk test, improved by 20.3% in the first course and peaked 10 months after the commencement of combined therapy (a 59.0% improvement). Walking function was maintained throughout the period. Generally, SBMA is characterized by moderately increased serum levels of creatine kinase (CK), reflecting neuromuscular damage; interestingly, the patient's CK levels decreased dramatically with combined therapy, indicating remarkable functional

improvement. Long-term combined therapy improved the patient's gait function with a steady reduction in CK levels. The combination of leuprorelin with cybernic treatment can, therefore, improve and maintain gait function without damaging the motor unit and may also suppress disease progression.

Keywords: spinal and bulbar muscular atrophy, hybrid assistive limb, cybernic treatment, leuprorelin acetate, anti-androgen therapy, creatine kinase, case report

INTRODUCTION

Spinal and bulbar muscular atrophy (SBMA) was first described by Kennedy et al. in 11 patients from two families as a progressive proximal spinal and bulbar muscular atrophy of the late onset and described this as a sex-linked recessive trait; this condition is now known as Kennedy's disease (1). SBMA is a rare neuromuscular lower motor neuron disease with estimated prevalence of 1–2 per 100,000 males globally (2, 3). SBMA is associated with some of the features of primary myopathy and is characterized by high serum levels of creatine kinase (CK) prior to the onset of symptoms (4, 5).

Over time, SBMA gradually impairs gait function, thus leading to the need for patients to use a wheelchair ∼20 years after the onset (6). Bulbar palsy symptoms occur in almost all patients, and the most common cause of death is aspiration pneumonia caused by dysphagia. Considering these symptoms, the treatment strategy for SBMA is to prevent aspiration and maintain ambulatory function. Furthermore, this disease is characterized by a slow progressive deterioration of various motor functions, thus resulting in a prolonged and gradually increasing burden on the patient. For this reason, there is a clear need to establish treatments that can alleviate each symptom and potentially cure the disease completely.

SBMA is caused by the abnormal expansion of CAG repeats in the androgen receptor (*AR*) gene on the X chromosome (7). In addition, previous neuropathological examination of 11 autopsied cases showed that the loss of lower motor neurons is associated with the nuclear accumulation of polyglutamine-expanded AR protein (8). These findings led to the development of a therapeutic strategy to prevent the nuclear accumulation of abnormal AR proteins. Further research, involving a mouse model of SBMA, showed that castration improved phenotypic expression by reducing the levels of testosterone to undetectable levels. These data indicated that the pathogenesis of this disease depends on the levels of testosterone, a known ligand for AR (9). Therefore, it was hoped that the anti-androgen therapy with leuprorelin acetate (leuprorelin), which has been used previously in the treatment of prostate and breast cancer, could be used as drug repositioning therapy without the need for castration in humans (10).

Randomized controlled clinical trials of leuprorelin for the treatment of SBMA ultimately demonstrated the benefit of this drug for the preservation of swallowing function in a patient treatment group (11, 12). In addition, some patients receiving leuprorelin exhibited a significant reduction in the accumulation of mutant ARs in scrotal skin biopsies (11).

These findings showed that leuprorelin was a potential disease-modifying drug, and, in 2017, leuprorelin was approved in Japan as an orphan drug to improve the swallowing dysfunction of patients with SBMA (13). However, the lack of improvement in limb muscle weakness and gait function in patients with SBMA remained problematic (14). Further research showed that, although leuprorelin improved dysphagia when compared to a control group, it did not improve gait function (12, 15). Consequently, leuprorelin was not considered to be a perfect disease-modifying drug (14). There was also concern that even if treatment led to an improvement in dysphagia, if muscle weakness and walking function did not improve, the patient would fall more frequently; this would lead to bone fractures and reduce the patient's quality of life and life expectancy.

There are cases of patients with SBMA being treated with various exercise therapies, ranging from high to low intensity. However, there have been no reports of improvement in terms of gait function in these cases (16–18). Furthermore, findings suggested that, when patients with SBMA are treated with conventional exercise therapy, the remaining motor neurons may activate more frequently, thus resulting in overexcitement in the motor unit and a likelihood of neuronal loss.

Sankai et al. considered the potential medical application of cybernics, an innovative technology that connects humans and devices electrically and mechanically to enhance their movements (19). Based on cybernic technology, Sankai and Nakajima developed a completely new exercise therapy that incorporated a wearable cyborg hybrid-assistive limb (HAL) for neurorehabilitation, featuring "interactive biofeedback" (iBF), which they named cybernic treatment (20) (**Figure 1**). The HAL and the wearer's movements are controlled by three hybrid mechanisms (20): cybernic voluntary control (CVC), cybernic autonomous control (CAC), and cybernic impedance control (CIC). The HAL controls the torque of the electric power unit based on the wearer's motor unit potentials (CVC). The wearer can walk without overloading the lower limbs. Simultaneously, the HAL and the wearer can move the lower limbs with HAL's built-in ideal gait pattern based on force plate signals and joint angle measurements (CAC). *Via* proprioception, the wearer senses that the gait patterns close to the ideal have been achieved using CIC. These mechanisms allow the wearer to repeat the successful gait in a safe manner without fatigue, thus promoting motor learning and the regeneration of walking function.

Prior to the invention of HAL, it had been thought that exercise therapy might cause the overexcitement of motor units and exacerbate diseases, such as SBMA, spinal muscular atrophy (SMA), amyotrophic lateral sclerosis (ALS), and Duchenne muscular dystrophy (DMD).

FIGURE 1 | A photograph showing a hybrid-assisted limb (HAL) for medical use (lower limb type) (20). For safety reasons, we also used a mobile hoist (All-in-One®, Ropox A/S, Denmark) to prevent falls during cybernic treatment with HAL.

However, a randomized controlled clinical trial (NCY-3001) demonstrated that innovative HAL-based gait exercise, or cybernic treatment, was safe and efficacious when used to treat eight neuromuscular diseases, including SBMA (20). As a result, cybernic treatment was officially approved in Japan and the USA in 2015 and 2020, respectively.

As with the limitations of leuprorelin therapy when used alone (12, 15), we considered that, without the combined effect of a disease-modifying drug, such as leuprorelin, the effect of HAL alone would not last long enough to inhibit disease progression (20). Therefore, we hypothesized that the combination of leuprorelin and HAL might overcome the limitations of each of the two therapies alone, thus resulting in a synergistic effect.

Therefore, we focused on the lack of efficacy for leuprorelin when used alone to treat gait disturbance in SBMA. We hypothesized that the combination of leuprorelin and HAL would further enhance the efficacy of disease-modifying drugs, including leuprorelin. At present, Japan is the only country in which both therapies are officially approved. Clinicians are, therefore, in a unique position in that they can use leuprorelin and HAL simultaneously to treat patients with SBMA. Since conducting a randomized clinical trial of such a combined treatment is not easy, we believe that a well-designed observational study like ours is essential and have reported our data here as a case report.

CASE DESCRIPTION

A 39-year-old man with SBMA noticed an inability to run 12 years previously. A few years after this initial observation, the patient exhibited limb weakness with elevated levels of creatine kinase (CK), a nasal voice, tongue atrophy, hand tremor, and muscle fasciculation. None of the patient's blood relatives exhibited symptoms that were suggestive of SBMA. The patient received genetic counseling and psychological support. Genetic testing of the *AR* gene revealed 60 CAG repeats (the normal number of repeats is 9–34). Thus, the patient was diagnosed with SBMA at 29 years of age. At 38 years of age, the patient needed a railing to climb the stairs. Until then, he had never received any medical or motor exercise therapy. At this time, anti-androgen therapy was initiated; every 12 weeks, the patient was subcutaneously administered with leuprorelin acetate (11.25 mg) using a Leuplin SR Injection Kit (Takeda Pharmaceutical Company Ltd. Japan) (13). The patient's serum testosterone levels were quickly suppressed and maintained below the lower limit of the normal range. Half a year later, the patient noticed progressive limb weakness, indicating the anti-anabolic effect of the anti-androgen therapy. During this time, the patient received no form of physical therapy. One year after the patient's first injection of leuprorelin, the patient started intensive and innovative motor learning in the form of cybernic treatment with HAL; this treatment took place in a hospital with specialized rehabilitation facilities for neuromuscular diseases. At this time, the following neurological findings were noted. There was mild muscle weakness in the oris muscles and slight atrophy of the tongue. Dysarthria only involved a slight nasal voice; there was no dysphagia. The patient had a slight tremor in both upper limbs. There was mild weakness in the proximal muscles of the extremities, and the tendon reflexes of the extremities were slightly attenuated. There were no pathological reflexes, cerebellar symptoms, sensory disturbances, or autonomic symptoms. There was no joint deformity or limitations in the range of motion. At this time, his Barthel index was 100, indicating complete independence, although he used a cane to walk long distances.

Walking exercise therapy with the HAL (Medical Use Lower Limb Type; Cyberdyne Inc., Tsukuba, Japan) (21) commenced after fitting the device and adjusting the torque and signal sensitivity of the motor unit potentials (**Figure 1**). The duration of the walking exercise with HAL was 20–30 min per day in one session. The patient completed nine HAL sessions (one course) in ∼2 weeks with regular physiotherapy. Gait function was assessed by two standardized gait function tests: the 2-min walk test (2MWT), which indicates walk endurance, and the 10-min walk test (10MWT), which indicates walk speed (20). As shown in **Figure 2**, the patient's walking ability improved with clinical significance after the first course of cybernic

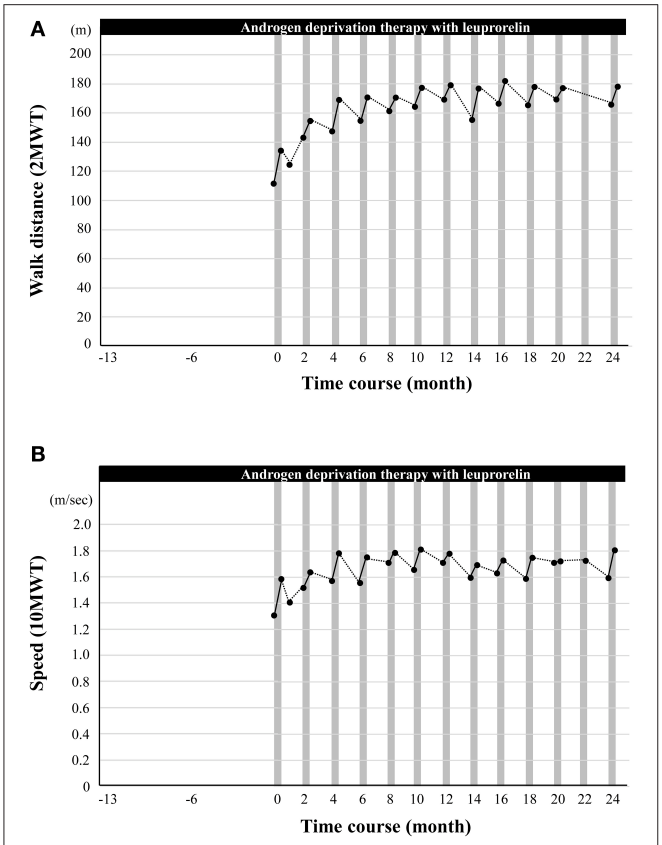

FIGURE 2 | The effect of cybernic treatment with a hybrid-assisted limb (HAL) on gait function. **(A)** The black dots indicate the measured walk distance (a 2-min walk test, 2MWT). **(B)** The black dots indicate the speed (a 10-min walk test, 10MWT). Vertical gray bars indicate one course of cybernic treatment with HAL.

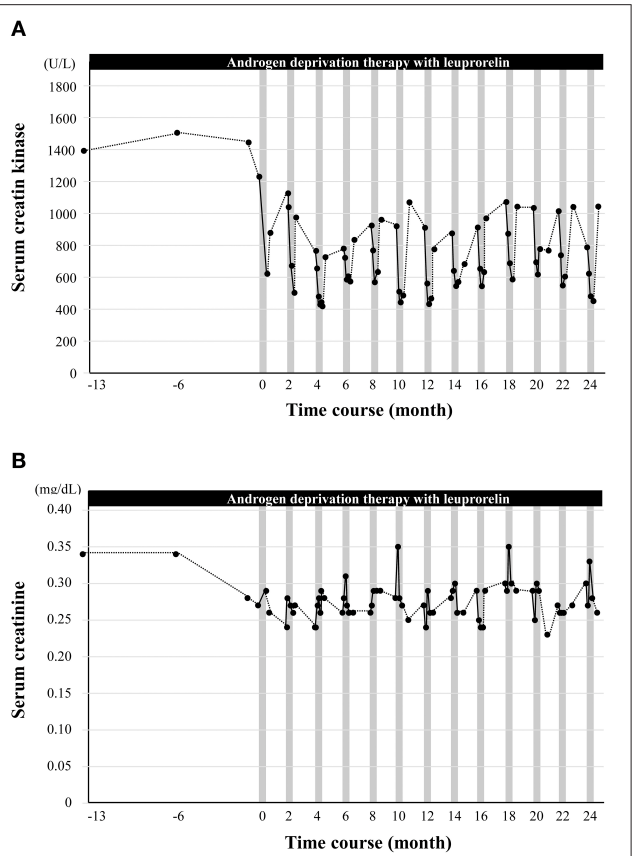

FIGURE 3 | The effect of cybernic treatment with a hybrid-assisted limb (HAL) on the serum levels of creatine kinase and creatinine. **(A)** The black dots indicate the serum levels of creatine kinase. **(B)** The black dots indicate the serum levels of creatinine. Vertical gray bars indicate one course of cybernic treatment with HAL.

treatment; the 2MWT improved from 111.5 m at the baseline to 134.2 m (+20.3%) after the first course (**Figure 2A**). His walking speed also improved from 1.31 to 1.58 m/s (+21.2%) (**Figure 2B**). These improvements are comparable to those published previously in the NCY-3001 clinical trial (20). Initially, his walking pattern was characterized by unnatural swaying while lifting his waist and legs. After the treatment, he felt the driving force of walking from behind and the swaying of his body axis decreased; furthermore, his walking became more natural. This initial improvement was highly evident. However, despite self-training at home, both the 2MWT and the 10MWT worsened mildly after 1 month (**Figure 2**). Fortunately, even with this deterioration, these data were better than before the onset of HAL treatment.

For the first 10 months, the gait tests prior to cybernic treatment were moderately lower than immediately after the last course of cybernic treatment. Following each course of cybernic treatment, the gait tests improved steadily to a level that was higher than immediately after the previous treatment. Ten months after the initiation of HAL, the 2MWT reached a peak at 177.3 m (+59.0%) (**Figure 2A**; **Supplementary Video 1**). From 18 months to 2 years, the 2MWT was maintained between 165 m (+46.7%) and 178 m (+59.6%). Regular cybernic treatment with HAL, combined with leuprorelin, was continued every 2 months for 2 years (13 courses in total), with the patient's willingness and satisfaction. The peak 10MWT was observed slightly earlier than in the 2MWT. The rate of improvement in the 2MWT over 2 years was higher than that in the 10MWT (+59.6% vs. +38.2%) (**Figures 2A,B**). Therefore, this implied that the walking endurance continued to improve with long-term cybernic treatment. Consequently, regular cybernic treatment with HAL appears to improve and maintain walking function.

Serum levels of CK reflect muscle damage and are elevated in neuromuscular diseases, including SBMA (22). The patient's serum CK levels decreased from 1,230 to 622 U/L after his first course of cybernic treatment with HAL (**Figure 3A**). Then, the levels rose back to 878 U/L; this was still rather low at approximately two-thirds of the original baseline. Moreover, with continued cybernic treatments, the levels of CK gradually declined, corresponding to an improvement in the 2MWT. This trend was consistent in every course. Using a pedometer, the patient's total physical activity was also measured during his hospital stay; this recorded ∼3,800 steps and was similar to

the patient's ordinary level of daily activity. Our clinical team quickly rejected the idea that rest and immobility had reduced the patient's CK levels, which may be the case during hospitalization for acute illness. Instead, we concluded that the combination of leuprorelin therapy and HAL reduced the CK levels due to HAL's therapeutic effect and efficacy in improving gait. Conversely, the patient's serum creatinine level, a biomarker of muscle mass in SBMA (23), was maintained (**Figure 3B**). The improvement and maintenance of gait function, the repeated drastic reduction in serum CK levels, and the increase and maintenance of serum creatinine levels were observed only after the combined therapy of HAL and leuprorelin, and not during the period of leuprorelin monotherapy (from −13 to 0 months).

DISCUSSION

This report describes the first successful case in the history of SBMA treatment in which the improvement and maintenance of ambulatory motor function were observed over 2 years. Furthermore, we also observed a reduction in serum CK levels as a biomarker of muscle damage, and the maintenance of serum creatinine levels as a biomarker of muscle volume retention. Our interpretation is that these outcomes are the result of the combination of leuprorelin and HAL.

Thus far, none of the existing pharmaceutical agents, including leuprorelin, have achieved functionally efficacy with regard to muscle weakness or gait in patients with SBMA (12, 24). Consequently, it has remained unclear as to whether the levels of serum CK and creatinine, as key biomarkers, correspond to a response to treatment (5). Leuprorelin alone has been previously reported to reduce serum CK levels by ∼20% after 48 weeks of treatment (24). In the present case, the reduction in CK levels after 1 year of leuprorelin administration alone was not comparable. However, we found that the levels of CK decreased from 1,230 to 622 IU/L (−51%) when combined with HAL treatment. After returning to daily life, the levels of CK only increased by a small extent. Serum creatinine data did not indicate a reduction in muscle mass; furthermore, pedometer data did not show a reduction in muscle damage due to rest. Moreover, a decreasing trend of CK was observed after each course of HAL. In other words, we can assume that the levels of CK were reduced by the combined therapeutic effects of leuprorelin and HAL. The NCY-3001 study has previously tested the effects and safety of cybernic treatment for progressive neuromuscular diseases, including SBMA but did not confirm muscle damage directly by measuring serum CK levels. In the present case report, the safety of HAL treatment combined with leuprorelin was further reinforced by the reduction in serum CK levels. However, in the patient described herein, we found that the combination of leuprorelin and HAL reduced serum CK levels and maintained the levels of creatinine; these effects correlated with an improvement in gait function. Therefore, the results of this case study suggest that these simultaneous changes in serum CK and creatinine are valid therapeutic indicators for SBMA (5).

Our results indicate a clear therapeutic effect on the pathological mechanism of SBMA, i.e., the suppression of motor neurons and muscle fiber injury were correlated with an improvement in function. We believe that this fact may be explained by the therapeutic mechanism, especially the iBF. The iBF selects the neural network that inhibits higher central controls to the pathological motor units and increases commands to the healthier motor units (20, 25, 26). Cybernic treatment might improve motor function and inhibit the degeneration of motor neurons.

Furthermore, this combined treatment led to an improvement of ambulatory function that was maintained for 2 years, with high levels of patient satisfaction. During a previous study of the natural history of SBMA, the 6-min walk test (6MWT) was found to decrease by 11.3% per year (27). The 2MWT is a simplified version of the 6MWT that correlates accurately with a lower patient burden (28); the rate of decrease is expected to be similar. We found that the 2MWT at the start of HAL was 111.5 m. If we apply a rate of decrease based on the natural history of this disease, we can estimate that the 2MWT would have decreased to ∼88 m after 2 years. However, the actual value increased to 178.0 m; this was +102% of the estimated value and, therefore, represents a remarkable treatment effect.

Leuprorelin was approved in Japan for the treatment of SBMA (13) primarily because of its biological mechanism as a disease-modifying agent that acts on the primary etiology of SBMA and, secondly, because of its proven clinical efficacy for dysphagia in clinical trials (12, 24). Clinical trials of leuprorelin monotherapy did not demonstrate any improvement in ambulatory function.

In addition to SMBA, similar problems were observed in the lack of improvement in gait function, following the administration of exon-skipping therapy after the onset of DMD (29) and the lack of effect of SMN protein-enhancing treatment in patients with SMA several years after the onset (30). Therefore, to significantly amplify the efficacies of disease-modifying drugs acting on the primary etiologies of DMD and SMA, it is essential that we combine drug therapy and cybernic treatment with HAL.

This observational single case report clarifies the clinical efficacy of a combination of leuprorelin treatment for dysphagia and HAL treatment for gait disturbance. However, there is a limitation to be considered in that this combination of therapies was not compared statistically to monotherapies, HAL or leuprorelin. Therefore, it is still unclear whether the combined treatment of leuprorelin and HAL can constantly reduce serum CK levels and maintain ambulatory function over the long term. Consequently, it appears to be crucial that we conduct future RCTs to compare the combined treatment to HAL monotherapy with regard to changes in 2MWT, serum CK, and creatinine as outcome measures. However, this type of randomized trial may be challenging in a region where both treatments are officially approved. A comparative study may be possible in observational cohorts with more patients in Japan.

CONCLUSION

In this case report, the novel form of combined therapy overcame the apparent limitations of disease-modifying drugs acting on primary etiology and improved the gait function of patients with

SBMA over the long term. Although this is only a single case report, the results are groundbreaking. If this phenomenon can be generalized, it may be possible to improve the treatment efficacy of DMD and SMA, as well as SBMA, by introducing combined therapy with HAL.

DATA AVAILABILITY STATEMENT

The original contributions presented in the study are included in the article/**Supplementary Material**, further inquiries can be directed to the corresponding author.

ETHICS STATEMENT

The studies involving human participants were reviewed and approved by the Ethics Committee of National Hospital Organization Niigata National Hospital. The patients/participants provided their written informed consent to participate in this study. Written informed consent was obtained from the individual(s) for the publication of any potentially identifiable images or data included in this article.

AUTHOR CONTRIBUTIONS

HN drafted and revised the manuscript and was responsible for the acquisition of data, the analysis of data, the interpretation of data, research project execution, study design, and concept. TI and AH acquired the data. MK revised the manuscript and analyzed/interpreted the data. GS was responsible for analysis/interpretation of the data. TN revised the manuscript, acquired/analyzed/interpreted the data, executed the research project, and was also involved with the study design and concept. All authors contributed to the article and approved the submitted version.

FUNDING

This research was supported by Grants-in Aid from the Research Committee of CNS Degenerative Diseases (Reference: 20FC1049), Research on Dissemination of Best Practicable Care for Muscle Dystrophy (Reference: 21FC1006), and Research on Policy Planning and Evaluation for Rare and Intractable Diseases, Health, Labour and Welfare Sciences Research Grants, the Ministry of Health, Labour and Welfare, Japan.

ACKNOWLEDGMENTS

The authors would like to thank Mr. Kazuyuki Kishimoto and Mr. Kazuhiko Hasegawa, both physiotherapists in National Hospital Organization Niigata National Hospital and Mr. Andrew Paul Wood and Charlesworth Author Services for reviewing the manuscript and providing editing support.

SUPPLEMENTARY MATERIAL

The Supplementary Material for this article can be found online at: https://www.frontiersin.org/articles/10.3389/fneur.2022.905613/full#supplementary-material

Supplementary Video 1 | Changes in gait speed and endurance in the 2MWT after commencing combined therapy. This video clip compares the baseline (an upper row) with a time point 10 months after the commencement of treatment (a lower row). The first 20 s (a left column) and the last 20 s (a right column) of the test can be observed. The lower left video (10 months later and the first 20 s in the 2MWT) shows dramatic gait improvement in speed compared to the baseline (the upper left video). The lower right video shows a dramatic improvement in gait endurance compared to the baseline (the upper right video). The patient used a mobile hoist (All-in-One®, Ropox A/S, Denmark) to prevent falls during the 2MWT. In this video, the same person in the team of evaluators pulls the mobile hoist according to the patient's gait but is careful to never strain the patient's sling and never affect the patient's gait.

REFERENCES

1. Kennedy WR, Alter M, Sung JH. Progressive proximal spinal and bulbar muscular atrophy of late onset. A sex-linked recessive trait. *Neurology.* (1968) 18:671–80. doi: 10.1212/WNL.18.7.671
2. Guidetti D, Sabadini R, Ferlini A, Torrente I. Epidemiological survey of X-linked bulbar and spinal muscular atrophy, or Kennedy disease, in the province of Reggio Emilia, Italy. *Eur J Epidemiol.* (2001) 17:587–91. doi: 10.1023/A:1014580219761
3. Finsterer J. Perspectives of Kennedy's disease. *J Neurol Sci.* (2010) 298:1–10. doi: 10.1016/j.jns.2010.08.025
4. Sorenson EJ, Klein CJ. Elevated creatine kinase and transaminases in asymptomatic SBMA. *Amyotroph Lateral Scler.* (2007) 8:62–4. doi: 10.1080/17482960600765040
5. Querin G, Bede P, Marchand-Pauvert V, Pradat PF. Biomarkers of spinal and bulbar muscle atrophy (SBMA): acomprehensive review. *Front Neurol.* (2018) 9:844. doi: 10.3389/fneur.2018.00844
6. Atsuta N, Watanabe H, Ito M, Banno H, Suzuki K, Katsuno M, et al. Natural history of spinal and bulbar muscular atrophy (SBMA): a study of 223 Japanese patients. *Brain.* (2006) 129:1446–55. doi: 10.1093/brain/awl096
7. La Spada AR, Wilson EM, Lubahn DB, Harding AE, Fischbeck KH. Androgen receptor gene mutations in X-linked spinal and bulbar muscular atrophy. *Nature.* (1991) 352:77–9. doi: 10.1038/352077a0
8. Adachi H, Katsuno M, Minamiyama M, Waza M, Sang C, Nakagomi Y, et al. Widespread nuclear and cytoplasmic accumulation of mutant androgen receptor in SBMA patients. *Brain.* (2005) 128:659–70. doi: 10.1093/brain/awh381
9. Katsuno M, Adachi H, Kume A, Li M, Nakagomi Y, Niwa H, et al. Testosterone reduction prevents phenotypic expression in a transgenic mouse model of spinal and bulbar muscular atrophy. *Neuron.* (2002) 35:843–54. doi: 10.1016/S0896-6273(02)00834-6
10. Katsuno M, Adachi H, Doyu M, Minamiyama M, Sang C, Kobayashi Y, et al. Leuprorelin rescues polyglutamine-dependent phenotypes in a transgenic mouse model of spinal and bulbar muscular atrophy. *Nat Med.* (2003) 9:768–73. doi: 10.1038/nm878
11. Banno H, Katsuno M, Suzuki K, Takeuchi Y, Kawashima M, Suga N, et al. Phase 2 trial of leuprorelin in patients with spinal and bulbar muscular atrophy. *Ann Neurol.* (2009) 65:140–50. doi: 10.1002/ana.21540
12. Hashizume A, Katsuno M, Suzuki K, Banno H, Takeuchi Y, Kawashima M, et al. Efficacy and safety of leuprorelin acetate for subjects with spinal and bulbar muscular atrophy: pooled analyses of two randomized-controlled trials. *J Neurol.* (2019) 266:1211–21. doi: 10.1007/s00415-019-09251-x
13. PMDA. *Leuplin SR Injection Kit 11.25mg.* (2017). Available online at: https://www.pmda.go.jp/PmdaSearch/iyakuDetail/400256_2499407G3030_1_07 (accessed February 6, 2022).

14. Arnold FJ, Merry DE. Molecular mechanisms and therapeutics for SBMA/Kennedy'sdisease. *Neurotherapeutics.* (2019) 16:928–47. doi: 10.1007/s13311-019-00790-9
15. Hashizume A, Katsuno M, Suzuki K, Hirakawa A, Hijikata Y, Yamada S, et al. Long-term treatment with leuprorelin for spinal and bulbar muscular atrophy: natural history-controlled study. *J Neurol Neurosurg Psychiatry.* (2017) 88:1026–32. doi: 10.1136/jnnp-2017-316015
16. Preisler N, Andersen G, Thogersen F, Crone C, Jeppesen TD, Wibrand F, et al. Effect of aerobic training in patients with spinal and bulbar muscular atrophy (Kennedy disease). *Neurol.* (2009) 72:317–23. doi: 10.1212/01.wnl.0000341274.61236.02
17. Shrader JA, Kats I, Kokkinis A, Zampieri C, Levy E, Joe GO, et al. A randomized controlled trial of exercise in spinal and bulbar muscular atrophy. *Ann Clin Transl Neurol.* (2015) 2:739–47. doi: 10.1002/acn3.208
18. Heje K, Andersen G, Buch A, Andersen H, Vissing J. High-intensity training in patients with spinal and bulbar muscular atrophy. *J Neurol.* (2019) 266:1693–7. doi: 10.1007/s00415-019-09316-x
19. Sankai Y, Suzuki K, Hasegawa Y. *Cybernics: Fusion of Human, Machine and Information Systems*. Tokyo: Springer (2014).
20. Nakajima T, Sankai Y, Takata S, Kobayashi Y, Ando Y, Nakagawa M, et al. Cybernic treatment with wearable cyborg Hybrid Assistive Limb (HAL) improves ambulatory function in patients with slowly progressive rare neuromuscular diseases: a multicentre, randomised, controlled crossover trial for efficacy and safety (NCY-3001). *Orphanet J Rare Dis.* (2021) 16:304. doi: 10.1186/s13023-021-01928-9
21. PMDA. *HAL For Medical Use (Lower Limb Type).* (2015). Available online at: https://www.pmda.go.jp/files/000216634.pdf (accessed February 6, 2022).
22. Soraru G, D'Ascenzo C, Polo A, Palmieri A, Baggio L, Vergani L, et al. Spinal and bulbar muscular atrophy: skeletal muscle pathology in male patients and heterozygous females. *J Neurol Sci.* (2008) 264:100–5. doi: 10.1016/j.jns.2007.08.012
23. Hijikata Y, Hashizume A, Yamada S, Inagaki T, Ito D, Hirakawa A, et al. Biomarker-based analysis of preclinical progression in spinal and bulbar muscular atrophy. *Neurol.* (2018) 90:e1501–e9. doi: 10.1212/WNL.0000000000005360
24. Katsuno M, Banno H, Suzuki K, Takeuchi Y, Kawashima M, Yabe I, et al. Efficacy and safety of leuprorelin in patients with spinal and bulbar muscular atrophy (JASMITT study): a multicentre, randomised, double-blind, placebo-controlled trial. *Lancet Neurol.* (2010) 9:875–84. doi: 10.1016/S1474-4422(10)70182-4
25. Nakajima T. Nerve function recovery mechanism by the robot suit. *Clin Neurosci.* (2016) 34:936–7. Available online at: https://scholar.google.com/scholar?cluster=1089814798738094105
26. Nakajima T. Innovative technology, clinical trials and the subjective evaluation of patients: the cyborg-type robot HAL and the treatment of functional regeneration in patients with rare incurable neuromuscular diseases in Japan. In: Brucksch S, Sasaki K, editors. *Humans and Devices in Medical Contexts: Case Studies From Japan*. Singapore: Springer Singapore (2021). p. 281–310.
27. Takeuchi Y, Katsuno M, Banno H, Suzuki K, Kawashima M, Atsuta N, et al. Walking capacity evaluated by the 6-minute walk test in spinal and bulbar muscular atrophy. *Muscle Nerve.* (2008) 38:964–71. doi: 10.1002/mus.21077
28. Andersen LK, Knak KL, Witting N, Vissing J. Two- and 6-minute walk tests assess walking capability equally in neuromuscular diseases. *Neurology*. (2016) 86:442–5. doi: 10.1212/WNL.0000000000002332
29. Randeree L, Eslick GD. Eteplirsen for paediatric patients with Duchenne muscular dystrophy: a pooled-analysis. *J Clin Neurosci.* (2018) 49:1–6. doi: 10.1016/j.jocn.2017.10.082
30. Mercuri E, Darras BT, Chiriboga CA, Day JW, Campbell C, Connolly AM, et al. Nusinersen versus sham control in later-onset spinal muscular atrophy. *N Engl J Med.* (2018) 378:625–35. doi: 10.1056/NEJMoa1710504

Conflict of Interest: AH and GS received royalties from Takeda Pharmaceutical Co., Ltd. MK received a speaker's fee, a research grant, and royalties from Takeda Pharmaceutical Co., Ltd.

The remaining authors declare that the research was conducted in the absence of any commercial or financial relationships that could be construed as a potential conflict of interest.

Publisher's Note: All claims expressed in this article are solely those of the authors and do not necessarily represent those of their affiliated organizations, or those of the publisher, the editors and the reviewers. Any product that may be evaluated in this article, or claim that may be made by its manufacturer, is not guaranteed or endorsed by the publisher.

Copyright © 2022 Nakatsuji, Ikeda, Hashizume, Katsuno, Sobue and Nakajima. This is an open-access article distributed under the terms of the Creative Commons Attribution License (CC BY). The use, distribution or reproduction in other forums is permitted, provided the original author(s) and the copyright owner(s) are credited and that the original publication in this journal is cited, in accordance with accepted academic practice. No use, distribution or reproduction is permitted which does not comply with these terms.

frontiers | Frontiers in Neurology

CASE REPORT
published: 04 July 2022
doi: 10.3389/fneur.2022.937989

A Remarkable Case of Acute Motor-Sensory Axonal Polyneuropathy (AMSAN) Variant of Guillain Barré Syndrome, in a Diabetic Patient Infected With COVID-19: A Case Report and Review of the Literature

Sajjad Ali[1†], *Alvina Karam*[2], *Aarish Lalani*[1], *Sadia Jawed*[1], *Musfirah Moin*[3], *Zain Douba*[4,5*†] *and Murtaza Ali*[6†]

[1] Department of Medicine, Ziauddin Medical University, Karachi, Pakistan, [2] Department of Medicine, Khyber Medical College, Peshawar, Pakistan, [3] Department of Medicine, Liaquat National Hospital and Medical College, Karachi, Pakistan, [4] Faculty of Medicine, University of Aleppo, Aleppo, Syria, [5] CME Office, Faculty of Medicine, University of Aleppo, Aleppo, Syria, [6] Department of Medicine, Dr. Ruth K.M. Pfau, Civil Hospital Karachi, Karachi, Pakistan

Background: Severe acute respiratory syndrome coronavirus 2 (SARS-CoV-2), which causes coronavirus disease- 2019 (COVID-19), has been a global epidemic in our healthcare system. SARS-CoV-2 primarily affects the respiratory system, but neurological involvement has also been reported, including Guillain–Barré syndrome (GBS) development.

Case Presentation: A 58-year-old male with known co-morbid hypertension and type 2 diabetes mellitus presented to the emergency room with complaints of worsening shortness of breath, dry cough, and fever for the past 10 days. On day 20 of hospitalization, he developed neurological symptoms after being tested positive for COVID-19. A neuroelectrophysiology study was conducted to evaluate neurological symptoms and suggested that the patient suffers from acute motor-sensory axonal polyneuropathy (AMSAN). CSF analysis showed elevated protein levels that confirmed the diagnosis of GBS. He was subsequently treated with oral prednisolone and IVIG, which improved neurological symptoms.

Conclusion: Ever since the emergence of COVID-19, GBS has surfaced as to its potentially dangerous outcome. Healthcare professionals should be mindful of GBS and should rule it out in anyone having sensory symptoms or weakness during or after a COVID-19 infection. Its early detection and treatment can result in improved clinical outcomes.

Keywords: Guillain-Barré syndrome, coronavirus, COVID-19, neuroelectrophysiological characteristics, neuroinfection

OPEN ACCESS

Edited by:
Giovanni Meola,
University of Milan, Italy

Reviewed by:
Luis Del Carpio-Orantes,
Instituto Mexicano del Seguro Social, Mexico
Mostafa Meshref,
Al-Azhar University, Egypt

***Correspondence:**
Zain Douba
zaindouba97.zd@gmail.com
orcid.org/0000-0001-9662-9492

†*Supervisor*

Specialty section:
This article was submitted to Neuromuscular Disorders and Peripheral Neuropathies, a section of the journal Frontiers in Neurology

Received: *06 May 2022*
Accepted: *09 June 2022*
Published: *04 July 2022*

Citation:
Ali S, Karam A, Lalani A, Jawed S, Moin M, Douba Z and Ali M (2022) A Remarkable Case of Acute Motor-Sensory Axonal Polyneuropathy (AMSAN) Variant of Guillain Barré Syndrome, in a Diabetic Patient Infected With COVID-19: A Case Report and Review of the Literature. Front. Neurol. 13:937989. doi: 10.3389/fneur.2022.937989

INTRODUCTION

Severe acute respiratory syndrome coronavirus 2 (SARS-CoV-2), which causes coronavirus disease- 2019 (COVID-19), has been a global epidemic in our healthcare system with 276,939,345 cases worldwide and 5,389,206 deaths, as of December 22, 2021 (1). The most common clinical presentations of COVID-19 are fever, headache, vomiting, malaise, and respiratory symptoms, ranging from a mild cough to severe pneumonia (2). If not promptly managed, life-threatening complications such as acute respiratory distress syndrome (ARDS), multi-organ failure, and even death can occur. Moreover, due to the complexity of COVID-19, multiple systemic manifestations have also been documented (3). SARS-CoV-2 primarily affects the respiratory system, but neurological involvement has also been reported, including Guillain–Barré syndrome (GBS) (4).

GBS is a life-threatening inflammatory/autoimmune condition in which the immune system targets healthy nerve cells in the peripheral nervous system (PNS). Usually, an infectious illness triggers the condition, such as gastroenteritis or a lung infection. Progressive ascending motor impairment with reduced reflexes and cranial nerve involvement is the hallmark clinical sign of GBS, which can persist from a few days to several weeks (5). Acute inflammatory demyelinating polyneuropathy (AIDP) is the most common type of GBS in the western part of the world; acute motor axonal neuropathy (AMAN) is the most common form in the Asian region, and Miller-Fisher syndrome (MFS) is the least common form in the western world. In addition, there are overlap syndromes (GBS-MFS overlap) (6).

In light of the clinical relevance of COVID-19 during pandemic times, the authors have presented a suspected case of GBS in a COVID-19 patient in a tertiary care hospital.

CASE PRESENTATION

A 58-year-old male with a known co-morbid of hypertension and type 2 diabetes mellitus (compliant with medications) presented to the emergency room on September 25, 2021, with complaints of worsening shortness of breath, dry cough, and intermittent fever for the past 10 days. On general physical examination, his respiratory rate was 50 breaths per minute, along with the use of accessory muscles. He had 90% oxygen saturation on high-low oxygen. With worsening respiratory symptoms, he was shifted to the Critical Care Unit (CCU).

On admission, baseline laboratory investigations were carried out (**Table 1**). He had low hemoglobin levels, low leucocyte count, and significantly high C-reactive protein (CRP) and Creatinine (Cr) levels. He was further tested positive for SARS-CoV-2 by polymerase chain reaction (PCR), despite being fully vaccinated for COVID-19.

On detailed investigation, a High-resolution Computer Tomography (HRCT) scan of the chest was done and revealed patchy bilateral areas of ground-glass opacity along with lobular septal thickening. In addition, there were bilateral extensive fibrotic patches in sub-pleural and central locations, together with pleural thickening. The above findings represent pulmonary fibrosis with interstitial lung disease due to sequelae of COVID-19 pneumonia.

TABLE 1 | Baseline investigations of the patient on admission.

Parameters	Result	Normal range
Complete blood count		
Hb (g/dl)	11.7	13.5–16.5
MCV (fl)	84.7	78.1–95.3
MCH (pg)	25.5	25.3–31.7
MCHC (Gm/dL)	30.2	30.3–34.4
Total leukocyte count (/L)	10,500	4,600–10,800
Lymphocytes (%)	22	17.5–45
Neutrophils (%)	67.8	34.9–76.2
Platelets count (counts/uL)	263,000	154,000–450,000
Inflammatory markers		
CRP (mg/dL)	319.4	< 10
ESR (mm/h)	76	≤ 20
Biochemical profile		
Sodium (mEq/L)	150	135–145
Potassium (mEq/L)	3.7	3.5–5.0
Chloride (mEq/L)	115	95–105
Calcium (mEq/L)	8.9	8.5–10.2
Magnesium (mg/dl)	1.9	1.5–2.0
Phosphorous (mg/dl)	5.5	3.0–4.5
BUN (mg/dL)	39	6–24
Cr (mg/dl)	6.3	0.6–1.2
Urine direct report		
pH	6	4.5–8
Specific gravity	1.03	1.005–1.025
Protein (mg/day)	+	≤ 150
Glucose (mmol/L)	+++	0–0.8
Blood (RBCs)	++	≤ 3
RBCs (per hpf)	20	≤ 2
Pus cells	2–3	0–4
Yeast cells	+++	none

The patient was intubated during the CCU hospitalization due to worsening hypoxemic respiratory failure that was refractory to noninvasive positive pressure ventilation. He was given an entire course of remdesivir and dexamethasone during the intubation period. On the 15th day of hospitalization, he was extubated and was shifted out of the CCU.

On the 20th day of hospitalization (30 days after onset of COVID-19 symptoms), the patient developed bilateral lower limb weakness. Given the concern for the neurological nature of the complaint was evaluated by an on-call neurologist. His physical exam revealed intact cranial nerves and sensations but a power of 3/5 in lower limbs bilaterally along with absent lower limb reflexes and mute plantar reflex. To rule out etiologies of polyneuropathy, a magnetic resonance imaging (MRI) scan of the cervical was done which showed to be insignificant.

On further investigation, neuroelectrophysiology (**Table 2**) was done whose report showed decreased compound muscle action potential (CMAP) amplitude and sensory nerve action

TABLE 2 | Neuro-electrophysiology report of the patient.

Motor nerve conduction study								
Nerve	**Recording Site**	**CMAPS amplitude (mV)**		**Distal latency (m/s)**		**Proximal latency (m/s)**		**Conduction velocity (m/s)**	
		Lt.	**Normal value**	**Lt.**	**Normal value**	**Lt.**	**Normal value**	**Lt.**	**Normal value**
Median	APB	1.2	>4	3.2	<4.5	8.0		50.3	45–55
Ulnar	ADM	1.7	>4	2.8	<4.2	8.4		48.9	45–55
Radial	EIP		>5		1.9–2.9				55–67
Peroneal	EDB	N/R	>2	N/R	<6.5			N/R	40
Tibial	AHB	N/R	>3	N/R	<6.5	N/R		N/R	40
Peroneal	TA		>2		<3	N/R			40

Sensory nerve conduction study				
Nerve	**Latency**		**Snaps Amplitude UV**	
	Recording value	**Normal range**	**Recording value**	**Normal range**
Left Median	3.0	2.9–3.5	7.3	>15
Left Ulnar	2.8	2.9–3.5	7.0	>15
Left Radial		1.9–2.8		>10
Left Sural	NR	<4.2	NR	>5

Electromyography study					
Muscles	**Insertion activity**	**Spontaneous activity**	**Motor unit potential**		
			Amplitude (uV)	**Duration (m/s)**	**Morphology**
Left Biceps	-	Nill	Normal	Normal	Bi,tri
Left FDI	-	Fibs+ve	Few	MUAPS	
Left Quadriceps	-	Nill	Normal	Normal	Bi,Tri
Left. TA.	-	Fibs+ve	Few	MUAPS	

APB, Abductor pollicis brevis; ADM, abductor digiti minimi; EIP, extensor indicis proprius; EDB, extensor digitorum brevis; AHB, abductor halluces brevis; TA, tibialis anterior; FDI, (first dorsal interrossei; TA, tibialis anterior; MUAP, motor unit action potential; fibs, fibrillation.

potential (SNAP) amplitude in the left median and ulnar nerves. Moreover, electromyography (EMG) showed few motor unit action potential (MUAP) along with fibrillation in the left first dorsal interosseous and left tibialis anterior muscles. In conclusion, the reports suggested acute motor-sensory axonal polyneuropathy (AMSAN).

Moreover, a detailed cerebrospinal fluid (CSF) analysis was carried out which revealed to have isolated elevated protein levels (71 mg/dL), while the rest of the components were in the normal range such as pH, specific gravity, glucose. No white blood cells or red blood cells were noted. Culture and sensitivity, and gram staining were both negative. Increased protein levels is a hallmark of GBS.

Based on clinical findings, neurophysiological studies, CSF analysis, and MRI of the cervical, the patient was diagnosed with GBS associated with COVID-19.

Initially, the patient was given oral glucocorticoid (prednisolone) for 5 days and was tapered off when symptoms began to improve. He further received intravenous immunoglobulins (IVIG) for 6 days continuously. His vitals were stable throughout the rest of the hospital stay, and he had no signs of distress. After receiving this treatment, the patient's symptoms significantly improved, and he was discharged on October 21, 2021, to home with regular physiotherapy advised by the on-call doctor.

The present paper has been reported in accordance with the CARE guidelines (7).

DISCUSSION

GBS is an immune-mediated polyneuropathy that is most often preceded by infection. It has been linked with many infectious disease-causing organisms such as Campylobacter jejuni, cytomegalovirus, Epstein-Barr virus, Zika virus, as well as previous coronaviruses i.e., Middle East respiratory syndrome (MERS) and severe acute respiratory syndrome (SARS) (8, 9). In our case report, we have discussed a case of GBS in a 58-year-old male, which was caused by an aberrant immunological

TABLE 3 | Review of the literature for AMSAN-GBS associated with COVID-19.

Age, gender	Onset of disease	Clinical Features	CSF findings	Treatment	Outcome
Seventy years, Female (10)	Ten days after COVID-19 symptoms	Quadriplegia, hypotonia, areflexia and bilateral positive Lasègue sign	Increased protein level at 1 g/L Normal white blood cell count	Intravenous immunoglobulin (2 g/kg for 5 days) Hydroxychloroquine (600 mg per day) and Azithromycine	No significant neurological improvement was seen after 1 week of treatment.
Sixty years, Male (11)	Day 20 of hospitalization	Acute weakness in lower limbs with distal distribution Foot drop on the right side. Gastroplegia, paralytic ileus, and loss of blood pressure control	Oligoclonal bands seen. Increased ratio IgG/albumin in CSF (170) Normal total protein level	Intravenous immunoglobulin (0.4 g/kg/day)	After 5 days, the vegetative symptomatology significantly improved, with the remission of gastroplegia and recovery of intestinal functions. Persistence of osteotendinous hyporeflexia but slight improvement in the right foot drop.
Sixty-five years, Male (12)	Two weeks after hospitalization	Acute progressive symmetric ascending quadriparesis	N.A	Intravenous Immunoglobulin (0.40 g/kg/day) for 5 days	N.A
Fifty-five years, Female (13)	Day 26 of hospitalization	Acute progressive lower limb weakness	Average glucose, cell count, and protein (57 mg/dL protein)	The patient started on intravenous immunoglobulin (20 g IV daily for 5 days)	On the third day of IVIG treatment, she developed acute respiratory distress syndrome (ARDS).
Seventy-seven years, Female (14)	Seven days after COVID-19 symptoms	Tetraplegia, areflexia, paresthesia in upper limbs, facial diplegia, dysphagia, tongue weakness, and respiratory failure.	Albuminocytological dissociation	Two cycles of intravenous immunoglobulin	Persistence of severe upper-limb weakness, dysphagia, and lower-limb paraplegia.
Twenty-three years, Male (14)	Ten days after COVID-19 symptoms	Facial diplegia, areflexia, lower limbs paresthesia, and ataxia	Albuminocytological dissociation Protein level: 123 mg/dl no cells negative PCR assay for SARS-CoV-2	Intravenous immunoglobulin received	Had improvements, including decrease in ataxia and mild decrease in facial weakness.
Fifty-seven years, Male (15)	Twelve days after the resolution of COVID-19 symptoms	Numbness and tingling in the hands and feet. Over 10 days, the patient developed distal limb weakness and severe gait impairment	Normal cell count and normal proteins Normal CSF/serum albumin ratio Absence of oligoclonal banding	Intravenous immunoglobulin cycle at 0.4 g/kg/day over 5 days	Significant improvement of the weakness in the upper limbs and the left foot but a poor benefit on the right foot and gait ataxic. Slowly improvement by physiotherapy and, after 1 month, able to walk without aid and was discharged.
Seventy-six years, Male (16)	Five to Seven days after COVID-19 symptoms	Diarrhea, coughing, and a history of 1-week common cold. Unable to move lower limbs and not able to stand or walk	High Protein: 76 mg/dL	Intravenous immunoglobulin (20 g/day for 5 days concomitant anti-COVID treatment	Discharged to home with good recovery.
Fifty-four years, Male (17)	Afebrile	Ascending progression of weakness. afebrile and severe dysautonomia	No albumino-cytological dissociation in CSF	Intravenous immunoglobulin and invasive ventilation	Passed away
Thirty-six years, Female (17)	Twelve days after COVID-19 symptoms	Ascending progression of weakness	Albuminocytological dissociation	Intravenous immunoglobulin	Discharged with good improvement.
Sixty-six years, Male (18)	One month after the COVID symptoms	Progressive ascending weakness	High protein 0.6 g/L (0.15–0.45 g/L) High glucose 3.97 mmol/L (2.2–3.9 mmol/L) Normal cell counts	Started on intravenous immunoglobulin at (0.4 g/kg IV) once daily for 5 days	Improved clinically, with power 4/5 in the upper extremities and 3/5 in of the lower extremities. The patient was discharged.

(Continued)

TABLE 3 | Continued

Age, gender	Onset of disease	Clinical Features	CSF findings	Treatment	Outcome
Fifty-five year, Female (19)	Twenty-six day after hospitalization	Decreased muscle strength in lower limbs	Glucose: 78 mg/dL Protein: 48,4 mg/dL (normal value: < 50 mg/dL), No white blood cells (WBCs).	Intravenous immunoglobulin	Passed away due to acute respiratory distress syndrome (ARDS) before the medication could start its effect.
Sixty-one year, Male (20)	A month after COVID-19 symptoms	Flaccidity in all of the upper and lower limb muscles	N.A	Started on intravenous immunoglobulin (400 mg/kg body weight daily, for 5 days)	Significant clinical alleviation of symptoms with improvement in respiratory functions, oxygen saturation, and return of muscle power, recovering to 4/5 power in the upper and lower limbs on both sides.

N.A, Not available; CSF, Cerebrospinal Fluid.

response following 20th days of hospitalization post-COVID-19 infection. GBS was confirmed after assessing clinical features and nerve conduction investigation revealing motor-sensory axonal polyneuropathy.

Despite being a rare GBS variant in the western world, AMSAN is more commonly associated with COVID-19 infection in Asia. We have reviewed and compiled all of the AMSAN type of GBS cases that have been associated with SARS-CoV-2, looking at their clinical presentations, the average latency period until GBS symptoms appear, the CSF findings, as well as their treatment plans and outcomes. In addition, we did a thorough literature search on the PubMed database for all studies with full text available in English and original data on GBS patients with recent COVID infection published between June 2020 and October 29, 2021. We searched using the following keywords: Guillain–Barré syndrome, GBS, COVID-19, SARS-CoV2, and AMSAN. As a result, we found a total of 11 published articles with 13 AMSAN-GBS cases associated with COVID-19 (**Table 3**).

A study by Toscano et al. (14) showcased five patients, three having an axonal type of GBS and two having demyelinating neuropathy. However, electrophysiological tests revealed demyelinating polyneuropathy in the majority of published cases, with axonal neuropathy in only four patients (12). Diabetes mellitus (DM) is prevalent comorbidity in some of these individuals, as it was in our case (12, 21). The clinical and electrophysiological aspects of concurrent peripheral neuropathies, including GBS, are worsened by underlying DM. The specific mechanism causing DM-induced aggravation is unknown; however, it could be linked to chronic inflammatory disorders associated with DM, as well as peripheral nerve neurovascular deterioration (22).

So far, three cases have been documented in the literature, two with sphincter dysfunction and one with hypertension (23). However, there were no symptoms suggestive of autonomic system disturbance in our patient or the five cases reported from Italy (9). In addition to the conventional post-infectious pattern, numerous instances of GBS post-COVID-19 had followed a para-infectious course (24).

Various case reports and series have been published, suggesting a possible association between SARS-CoV-2 infection and GBS (2), although the actual mechanism is still unknown. According to one explanation, nerve tissue injury is linked to the virus's direct neuronal invasion by directly binding to ACE2 receptors. Another theory explains immune-mediated indirect neuron injury by claiming that the immune system is overstimulated, leading to increased interleukin-6 (IL-6) production and the emergence of an autoimmune reaction (25). SARS-CoV-2 has been shown to promote an overactive immunological response, activate inflammatory cells, and enhance the production of cytokines such as IL6, resulting in neural tissue damage. As a result, it is possible that these immunological processes are to blame for COVID-19 individuals' neurological symptoms. COVID19 patients with severe symptoms and a rapidly deteriorating clinical status are also more likely to experience serious neurological events, according to the research. It is currently unclear if COVID-19 causes the production of autoantibodies against specific gangliosides, as found in other GBS types. In the future, more research into the pathophysiologic mechanism of GBS in COVID-19 patients will be needed.

CONCLUSION

Healthcare professionals should be conscious of GBS, an uncommon complication related to COVID-19. In asymptomatic patients or those who have had a mild respiratory ailment weeks earlier, diagnosis might be challenging and time-consuming. GBS should be ruled out in anyone with sensory symptoms or weakness during or after a COVID-19 infection. Clinical outcomes can be improved by early detection and treatment.

DATA AVAILABILITY STATEMENT

The original contributions presented in the study are included in the article/supplementary material, further inquiries can be directed to the corresponding author.

ETHICS STATEMENT

Written informed consent was obtained from the individual(s) for the publication of any potentially identifiable images or data included in this article.

AUTHOR CONTRIBUTIONS

SA conceived, designed, supervised the study, responsible for data collection, and literature review. AK, AL, and MM analyzed and/or interpreted the data. AK, AL, SJ, and MM wrote the initial manuscript. ZD critically revised the manuscript. MA provided detailed insights of the patient's history and supervised the study. All authors have read the final manuscript.

ACKNOWLEDGMENTS

We would like to thank the patient for his participation in this study.

REFERENCES

1. Worldometers.info. *COVID Live-Coronavirus Statistics–Worldometer*. (2021). Available online at: https://www.worldometers.info/coronavirus/ (accessed on December 22, 2021).
2. Hoang A, Chorath K, Moreira A, Evans M, Burmeister-Morton F, Burmeister F, et al. COVID-19 in 7780 pediatric patients: a systematic review. *EClinicalMedicine*. (2020) 24:100433. doi: 10.1016/j.eclinm.2020.100433
3. Papri N, Hayat S, Mohammed A, Afsar M, Hasan I, Rahman A, et al. Guillain-Barré syndrome associated with SARS-CoV-2 infection: a case report with long term follow up. *J. Neuroimmunol.* (2021) 356:577590. doi: 10.1016/j.jneuroim.2021.577590
4. Fragiel M, Miró Ò, Llorens P, Jiménez S, Piñera P, Burillo G, et al. Incidence, clinical, risk factors and outcomes of Guillain-Barré in Covid-19. *Ann Neurol.* (2021) 89:598–603. doi: 10.1002/ana.25987
5. Sejvar J, Baughman A, Wise M, Morgan O. population incidence of guillain-barré syndrome: a systematic review and meta-analysis. *Neuroepidemiology*. (2011) 36:123–133. doi: 10.1159/000324710
6. Mantefardo B, Gube AA, Awlachew E, Sisay G. Novel coronavirus (COVID-19)-associated guillain-barre' syndrome: case report. *Int Med Case Rep J.* (2021) 14:251–253. doi: 10.2147/IMCRJ.S305693
7. Gagnier JJ, Kienle G, Altman DG, Moher D, Sox H, Riley D, et al. The CARE guidelines: consensus-based clinical case reporting guideline development. *J Med Case Reports.* (2013) 7:223. doi: 10.1186/1752-1947-7-223
8. Kamel W, Ibrahim Ismail I, Al-Hashel J. Guillain-Barre syndrome following COVID-19 infection: first case report from kuwait and review of the literature. *Dubai Med J.* (2021) 4:107–11. doi: 10.1159/000513382
9. Tsai L, Hsieh S, Chao C, Chen YC, Lin YH, Chang SC, et al. Neuromuscular disorders in severe acute respiratory syndrome. *Arch Neurol.* (2004) 61:1669–73. doi: 10.1001/archneur.61.11.1669
10. El Otmani H, El Moutawakil B, Rafai MA, El Benna N, El Kettani C, Soussi M, et al. Covid-19 and Guillain-Barré syndrome: more than a coincidence!. *Rev Neurol (Paris).* (2020) 176:518–9. doi: 10.1016/j.neurol.2020.04.007
11. Assini A, Benedetti L, Di Maio S, Schirinzi E, Del Sette M. New clinical manifestation of COVID-19 related Guillain-Barrè syndrome highly responsive to intravenous immunoglobulins: two Italian cases. *Neurol Sci.* (2020) 41:1657–8. doi: 10.1007/s10072-020-04484-5
12. Sedaghat Z, Karimi N. Guillain Barre syndrome associated with COVID-19 infection: a case report. *J Clin Neurosci.* (2020) 76:233–5. doi: 10.1016/j.jocn.2020.04.062
13. Mozhdehipanah H, Paybast S, Gorji R. Guillain–Barré syndrome as a neurological complication of COVID-19 infection: a case series review of the literature. *Clin Neurosci J.* (2020) 7:156–61. doi: 10.34172/icnj.2020.18
14. Toscano G, Palmerini F, Ravaglia S, Ruiz L, Invernizzi P, Cuzzoni MG, et al. Guillain-Barré syndrome associated with SARS-CoV-2. *N Engl J Med.* (2020) 382:2574–76. doi: 10.1056/NEJMc2009191
15. Zito A, Alfonsi E, Franciotta D, Todisco M, Gastaldi M, Ramusino MC, et al. COVID-19 and Guillain-Barré syndrome: a case report and review of literature. *Front Neurol.* (2020) 11:909. doi: 10.3389/fneur.2020.00909
16. Eslamian F, Taleschian-Tabrizi N, Izadseresht B, Shakouri SK, Gholian S, Rahbar M. Electrophysiologic findings in patients with COVID-19 and quadriparesia in the northwest of Iran, a case series study and literature review. *Caspian J Intern Med.* (2021) 12(Suppl 2):S451–9. doi: 10.22088/cjim.12.0.451
17. Chakraborty U, Hati A, Chandra A. Covid-19 associated Guillain-Barré syndrome: a series of a relatively uncommon neurological complication. *Diabetes Metab Syndr.* (2021) 15:102326. doi: 10.1016/j.dsx.2021.102326
18. Miyajan KF, Alyamani NA, Zafer DO, Tawakul AA. Guillain-Barré syndrome in an elderly patient as a complication of COVID-19 infection. *Cureus.* (2021) 13:e19154. doi: 10.7759/cureus.19154
19. Agha Abbaslou M, Karbasi M, Mozhdehipanah H. A rare axonal variant of guillain-barré syndrome as a neurological complication of COVID-19 infection. *Arch Iranian Med.* (2020) 23:718–21. doi: 10.34172/aim.2020.93
20. Haidary AM, Noor S, Hamed E, Baryali T, Rahmani S, Ahmad M, et al. Acute motor-sensory axonal polyneuropathy variant of Guillain-Barre syndrome complicating the recovery phase of coronavirus disease 2019 infection: a case report. *J Med Case Rep.* (2021) 15:379. doi: 10.1186/s13256-021-02988-y
21. Alberti P, Beretta S, Piatti M, Karantzoulis A, Piatti ML, Santoro P, et al. Guillain-Barré syndrome related to COVID-19 infection. *Neurol Neuroimmunol Neuroinflamm.* (2020) 7:e741. doi: 10.1212/NXI.0000000000000741
22. Bae JS, Kim YJ, Kim JK. Diabetes mellitus exacerbates the clinical and electrophysiological features of Guillain-Barré syndrome. *Eur J Neurol.* (2016) 23:439–46. doi: 10.1111/ene.12885
23. Ellul M, Benjamin L, Singh B, Lant S, Michael B, Kneen R, et al. Neurological associations of COVID-19. *Lancet Neurol.* (2020) 19:767–83. doi: 10.1016/S1474-4422(20)30221-0
24. Zhao H, Shen D, Zhou H, Liu J, Chen S. Guillain-Barré syndrome associated with SARSCoV-2 infection: causality or coincidence? *Lancet Neurol.* (2020) 19:383–4. doi: 10.1016/S1474-4422(20)30109-5
25. Ascierto PA, Fu B. Wei HIL-6 modulation for COVID-19: the right patients at the right time? *J Immuno Therapy Cancer.* (2021) 9:e002285. doi: 10.1136/jitc-2020-002285

Conflict of Interest: The authors declare that the research was conducted in the absence of any commercial or financial relationships that could be construed as a potential conflict of interest.

Publisher's Note: All claims expressed in this article are solely those of the authors and do not necessarily represent those of their affiliated organizations, or those of the publisher, the editors and the reviewers. Any product that may be evaluated in this article, or claim that may be made by its manufacturer, is not guaranteed or endorsed by the publisher.

Copyright © 2022 Ali, Karam, Lalani, Jawed, Moin, Douba and Ali. This is an open-access article distributed under the terms of the Creative Commons Attribution License (CC BY). The use, distribution or reproduction in other forums is permitted, provided the original author(s) and the copyright owner(s) are credited and that the original publication in this journal is cited, in accordance with accepted academic practice. No use, distribution or reproduction is permitted which does not comply with these terms.

frontiers | Frontiers in Neurology

CASE REPORT
published: 11 July 2022
doi: 10.3389/fneur.2022.889894

Case Report: A 72-Year-Old Woman With Progressive Motor Weakness, Dry Eyes and High Levels of Serum Neurofilament Light Chain

Maria Janina Wendebourg[1,2], *Jens Kuhle*[1,2] *and Martin Hardmeier*[1]*

[1] Department of Neurology, University Hospital Basel, Basel, Switzerland, [2] Department of Clinical Research, University of Basel, Basel, Switzerland

Background: Diagnosis of Amyotrophic Lateral Sclerosis (ALS) is challenging as initial presentations are various and diagnostic biomarkers are lacking. The diagnosis relies on the presence of both upper and lower motor neuron signs and thorough exclusion of differential diagnoses, particularly as receiving an ALS diagnosis has major implications for the patient. Sjögren's syndrome may mimic peripheral ALS phenotypes and should be considered in the work-up.

Case: A 72-year-old female presented with a mono-neuropathy of the right leg and a complaint of dry eyes and mouth. Initial diagnostic work-up confirmed a regional sensorimotor neuropathy and a Sjögren's syndrome; a causal relationship was assumed. However, motor symptoms spread progressively despite immunosuppressive treatment, eventually including both legs, both arms and the diaphragm. Clinically, unequivocal central signs were lacking, but further along in the disease course, the atrophy pattern followed a split phenotype and deep tendon reflexes were preserved. Nerve biopsy did not show vasculitic infiltration; however, serum neurofilament light chain (sNfL) concentrations were and remained persistently highly elevated despite immunosuppressive treatment. Electrodiagnostic re-evaluation confirmed denervation in 3 regions. A diagnosis of familial ALS was finally confirmed by a C9*orf*72 repeat expansion. Stationary sensory symptoms were best explained by a neuropathy associated with concomitant Sjögren's syndrome

Discussion: Our instructive case shows the difficulties of diagnosing ALS in the setting of a peripheral symptom onset and a concurrent but unrelated condition also causing neuropathy. Such cases require high clinical vigilance and readiness to reappraise diagnostic findings if the disease course deviates from expectation. Recently proposed simplified diagnostic criteria, genetic testing and body fluid biomarkers such as sNfL may facilitate the diagnostic process and lead to an earlier diagnosis of ALS.

Keywords: case report, neuromuscular disorders, peripheral neuropathies, C9*orf*72, serum neurofilament light chain (sNfL), Amyotrophic Lateral Sclerosis, Sjögren's disease

OPEN ACCESS

Edited by:
Giovanni Meola,
University of Milan, Italy

Reviewed by:
Michael Swash,
Queen Mary University of London, United Kingdom
Tim W. Rattay,
University of Tübingen, Germany

***Correspondence:**
Martin Hardmeier
martin.hardmeier@usb.ch

Specialty section:
This article was submitted to Neuromuscular Disorders and Peripheral Neuropathies, a section of the journal Frontiers in Neurology

Received: *04 March 2022*
Accepted: *13 June 2022*
Published: *11 July 2022*

Citation:
Wendebourg MJ, Kuhle J and Hardmeier M (2022) Case Report: A 72-Year-Old Woman With Progressive Motor Weakness, Dry Eyes and High Levels of Serum Neurofilament Light Chain. Front. Neurol. 13:889894. doi: 10.3389/fneur.2022.889894

INTRODUCTION

Amyotrophic Lateral Sclerosis (ALS) is a fatal neurodegenerative disease characterized by the degeneration of upper (UMN) and lower motor neurons (LMN), leading to the combination of muscle weakness, atrophy, and spasticity with exaggerated deep tendon reflexes (1), and may include frontal lobe dysfunction. Its prevalence is 2.6–3.0/100,000 in populations of European descent. Death occurs mainly from respiratory failure. The mean time of survival is 2–3 years, but in some cases, patients live for more than 10 years. There are considerable differences in symptom presentation and clinical course. While the majority of cases present with a limb-onset spinal type, others present with bulbar symptoms such as dysarthria and dysphagia, or primarily with signs of UMN dysfunction (1).

Diagnosis of ALS is still mostly clinically based on the El Escorial criteria and their revisions (2, 3), and, more recently, on the Gold Coast criteria (4) (see **Table 1**). The latter require progressive motor impairment, the clinical presence of UMN and LMN signs or LMN signs in two regions as well as the thorough exclusion of ALS mimics.

Diagnostic biomarkers other than electromyoneurography (ENMG) to objectify LMN (3) are currently not part of diagnostic criteria. However, UMN dysfunction may be shown by increased cortical excitability as determined by transcranial magnetic stimulation (5, 6), particularly in early stages of the disease, or on imaging, where atrophy of the precentral gyri and alterations of the cortico-spinal tract in various MRI measures has been reported (7, 8).

Furthermore, several studies have recently shown that neurofilament light (NfL) chain levels are highly increased in CSF and serum of patients with ALS and they have been repeatedly shown to harbor independent prognostic information besides potentially qualifying as a diagnostic biomarker (9–11). However, NfL is not disease specific but quantitatively captures neuro-axonal damage in inflammatory, neurodegenerative, vascular and traumatic brain diseases (12), as well as in peripheral disorders such as vasculitic and other polyneuropathies (13, 14).

Genetic analyses may assist diagnosis as about 5%−15% of ALS cases are familial (fALS) with autosomal dominant inheritance. The most prevalent mutations concern a repeat expansion of the C9*orf*72 gene (Chromosome 9 open reading frame 72; 30−40%), the SOD1 gene (superoxide dismutase 1, 10−20%), the TDP-43 gene (transactive response DNA-binding protein 43; 5%), and the FUS gene (fused-in sarcoma, 5%) (15). A C9*orf*72 repeat expansion is found in 7−19% of apparent sporadic ALS cases.

Differential diagnoses comprise, among others, multifocal motor neuropathy, Kennedy disease, lead intoxication and spinal stenosis. A recent study highlighted Sjögren's motor neuropathy as a further entity to consider (16). Mimics may cause up to 10% false ALS diagnosis (17), but likewise, ALS may not be diagnosed in first place due to the presence of other diseases.

We present the case of a patient with sicca symptoms and a progressive, predominantly flaccid, motor paralysis with mild sensory symptoms who was diagnosed with Sjögren's syndrome and associated neuropathy but eventually turned out to be a familial ALS with a C9*orf*72 repeat expansion.

Our case highlights the challenges in diagnosing ALS in the presence of a treatable co-existing disease and we discuss the differential diagnostic considerations during progression and evolution of symptoms as well as the value of biomarkers.

CASE DESCRIPTION

A 70-year-old woman presented with persistent weakness of the right leg after a fall and fracture of the right ankle 10 months before. She had no pain but complained of dry eyes and a dry mouth. Personal history was remarkable for a colon carcinoma operated 30 years ago, a metabolic syndrome and endoprosthesis of both knees. Only in the later follow-up, the patient reported that her mother had died from bulbar ALS. There was no known history of autoimmune disease in the family. The time course of both, clinical evolution and results of ancillary examinations are depicted in **Figure 1**.

At first outpatient consultation, we saw an overweight woman (BMI 43 kg/m^2) in otherwise good health. The cranial nerve examination was unremarkable. Upper limbs and the left leg were normal including preserved deep tendon reflexes and reported normal sensory function. The right leg showed a distally pronounced weakness (right/left, Medical Research Council (MRC) grades): hip flexion 2/5, hip extension 4/5, hip adduction 5/5, hip abduction 2/5, knee flexion 2/5, knee extension 4/5, foot dorsal extension 0/5, foot plantar flexion 3/5. Deep tendon reflexes were absent in the right leg and plantar responses were flexor bilaterally. We observed no fasciculations. The right lateral lower leg and dorsal foot showed a marked sensory deficit while vibration sense was only minimally impaired (7/8 at both halluces).

Neurographies in the right leg were abnormal: The peroneal compound muscle action potential (CMAP) was absent, the tibial CMAP and the sural sensory nerve action potential (SNAP) showed markedly reduced amplitudes without conduction block (CB). The left leg showed a slightly decreased peroneal CMAP and otherwise normal neurographies. Myography showed severe signs of acute denervation in the right anterior tibial, gastrocnemius, and rectus femoris muscle with fasciculations, positive sharp waves and fibrillation potentials. Plain MRI of the lumbar spine showed no abnormalities. An asymmetric sensorimotor axonal neuropathy was diagnosed.

Further work-up included laboratory screening for treatable causes of neuropathy, a spinal tap and measurement of sNfL levels. Anti-SSA/ro antibodies (55 U/ml; cut-off <10 U/ml), anti-GM1 (116%; cut-off 50%), anti-GD1a (130%; cut-off 50%) and anti-GD1b (98%; cut-off 50%) were elevated. Anti-SSB/la antibodies, cryoglobulines, blood sedimentation rate and the remainder of the laboratory screening including serum creatine kinase (CK) levels were normal. Cerebrospinal fluid (CSF) analysis showed a normal cell count, negative CSF-specific oligoclonal bands (OKBs) and only slightly elevated total protein (515 g/L, reference: 150–500 mg/L; quotient albumin CSF/serum: normal). Serum NfL levels were markedly elevated [141.5 pg/ml;

TABLE 1 | Comparison of the El Escorial (2), Awaji (3), and Gold Coast criteria (4) for Amyotrophic Lateral Sclerosis.

	El Escorial criteria (2)	Awaji criteria (3)	Gold Coast criteria (4)
	Progressive spread of symptoms or signs **AND**		Progressive motor impairment **AND**
Possible ALS	UMN and LMN signs in 1 region	UMN and LMN signs in 1 region	UMN and LMN signs in at least 1 region or LMN signs in at least 2 regions
Probable ALS	UMN and LMN signs in 2 regions	UMN and LMN signs in 2 regions	
Probable ALS (laboratory supported)	UMN signs in 1 region + electrophysiologic evidence of LMN signs in 2 regions		
Definite ALS	UMN and LMN signs in 3 regions	UMN and LMN signs in 3 regions	
	Mandatory: Exclusion of other etiologies explaining clinical symptoms		

In Awaji criteria, ENMG can substitute clinical evidence of LMN involvement on each diagnostic level. Regions are defined as: bulbar, cervical, thoracic, and lumbar. UMN, upper motor neuron; LMN, lower motor neuron.

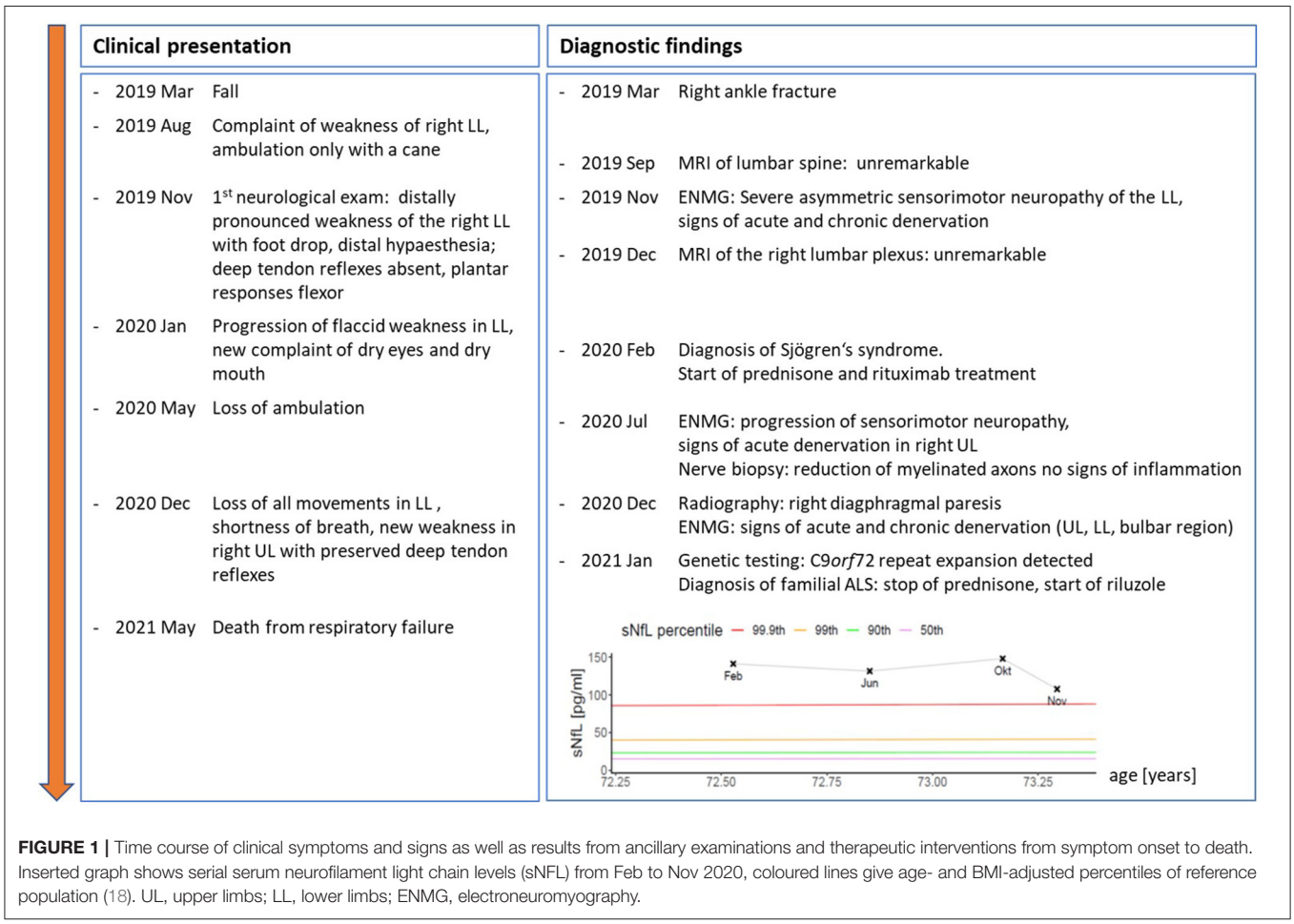

FIGURE 1 | Time course of clinical symptoms and signs as well as results from ancillary examinations and therapeutic interventions from symptom onset to death. Inserted graph shows serial serum neurofilament light chain levels (sNFL) from Feb to Nov 2020, coloured lines give age- and BMI-adjusted percentiles of reference population (18). UL, upper limbs; LL, lower limbs; ENMG, electroneuromyography.

>99.9th percentile (18)] indicating severe ongoing neuro-axonal injury. Nerve ultrasound had limited validity due to the patient's obesity but showed no detectable abnormalities.

The clinical suspicion of Sjögren's disease was supported by a positive Schirmer test and sialometry showing pathologic reductions of tear and saliva production. On lip biopsy, interstitial fibrosis and lymphatic invasion of small saliva glands was demonstrated and a diagnosis of Sjögren's disease was made according to the ACR criteria (19).

At this stage, the neuropathy was considered to be attributable to Sjögren's disease. Prednisone (80 mg/day, with tapering) as well as Rituximab treatment was established. Treatment

was expected to improve or at a least stabilize motor (and sensory) function.

Contrarily, the weakness progressed further over the course of the next months, spreading to the left leg, rendering the patient wheelchair bound. Moreover, she began to complain of shortness of breath. Upon re-admission, the clinical examination was normal for cognition and cranial nerve function. In the upper limbs, we found focal atrophies of the right first dorsal interosseous (FDI), abductor pollicis brevis (APB) and intrinsic hand muscles with a relatively preserved abductor digiti mini muscle (ADM), a pattern classically known as a "split hand", as well as slight weakness of the right arm (MRC, right/left): Deltoid 4/5, biceps 4/5, brachioradial 4/5, triceps 5-/5, wrist extension 5/5, finger extension 5/5, wrist flexion 5-/5, hand grip 5/5, APB 4/5. Deep tendon reflexes were now brisk in the upper limbs, and there were no signs of sensory impairment. Lower limbs were nearly completely paralyzed with an MRC grade of 0 in most proximal and distal muscles apart from left foot plantar and toe flexion (MRC grade 3). All deep tendon reflexes were absent; plantar response was flexor on both sides. Vibration sense was reduced (right/left 4/8 and 5/8), while the sensory deficit in the right lower extremity remained largely unchanged. Pulmonary work-up revealed a right diaphragmatic paresis. Sensory and motor neurographies were normal in the right ulnar nerve but unobtainable in the lower limbs. Motor evoked potentials to the upper extremities showed no abnormalities. Electromyography showed progressive signs of severe acute denervation in the upper limbs and the sternocleidomastoid muscle, with sparing of the tongue. A biopsy of the left superficial peroneal nerve revealed a reduction of myelinated fibers without signs of vasculitis. Serum NfL levels remained highly elevated and only slightly decreased at last follow-up [107.9 pg/ml; >99.9th percentile (see **Figure 1**)].

At this point, the clinical course was clearly deviating from expectance with deterioration under immunotherapy, brisk reflexes in wasted muscles, split hand, and split leg characteristics (20), bulbar involvement on myography and a nerve biopsy negative for vasculitis. This presentation allowed a diagnosis of laboratory supported probable ALS according to the El Escorial/Awaji criteria (2, 3) and a diagnosis of ALS according to the Gold Coast criteria (4) (see **Table 1**). The sensory involvement was most likely explained by coincidental, probably Sjögren's associated, sensory neuropathy.

Because of the patient's family history, genetic panel testing for motor neuron diseases was performed. It revealed a pathological repeat expansion in the C9*orf*72 gene confirming a familial ALS. During the following months, the patient experienced a further decline in motor function and died from respiratory failure 26 months after symptom onset.

DISCUSSION

The pathological hallmark of ALS spectrum diseases is an abnormal nuclear clearance and development of cytoplasmatic inclusion of TDP-43 (21). Increased cortical excitability is thought to induce neurodegeneration through glutamate-mediated excitotoxicity. The predominant affection of monosynaptic projections may explain the differential involvement of muscle groups at the same joint resulting in the "split hand" or more generally, "split limb" phenotypes (20).

As there are no disease-specific biomarkers, the diagnosis of ALS is challenging and may be delayed due to comorbidities providing an alternative explanation of symptoms. However, a high level of diagnostic certainty should be attained, before confronting the patient with a diagnosis of a fatal disease without a curative treatment option, especially in cases in which the differential diagnosis is treatable.

The initial clinical picture presented by our patient was suggestive for a lesion in the proximal part of the peripheral nervous system involving motor and sensory fibers. Restriction to one side had suggested plexopathy, but asymmetric presentations of polyradiculopathy and mononeuritis multiplex were also considered. Extensive work-up revealed a Sjögren's syndrome. At that point in time, the monomelic presentation including sensory deficits was attributed to an assumed vasculitic neuropathy, where high levels of sNfL may also be found (13).

Neuropathies in Sjögren's syndrome can be axonal, demyelinating, and mixed, they predominantly involve sensory fibers with and without pain, but autonomous and motor fibers as well as cranial nerves may also be affected (23). Severe forms of motor neuropathy may even mimic ALS (17). Histopathologically, sensory neuropathies show an infiltration of dorsal root sensory ganglia, while motor neuropathies rather seem to be caused by vasculitis and micro-infarction of nerves (22).

Interestingly, an association of a variety of auto-inflammatory diseases with ALS has been described, among them rheumatologic diseases like Sjögren's syndrome (23). On the other hand, coincident sensory neuropathy may be found in ALS, in C9*orf*72 ALS in up to 38% of subjects (24).

In our case, there are several hints, which retrospectively fit well with the final diagnosis. In particular, painless progressive spread of motor symptoms and a partly "split limb" phenotype are typical characteristics of ALS. The high concentrations of sNfL in the context of a nerve biopsy negative for vasculitis, absence of rapid progressive dementia and no other plausibleexplanation is a strong indicator for ALS as the likely cause of neuro-axonal damage. Furthermore, sNfL remained high despite immunosuppressive treatment while markers indicating activity of Sjögren's disease were low from the beginning. In the case of a vasculitic neuropathy, sNfL would have been expected to typically decrease when treated successfully (13), while in ALS levels usually remain stable over the disease course until the later stages (9, 25). These findings further substantiated doubts on a causative relationship between Sjögren's disease and the motor neuropathy. Nevertheless, UMN signs could only be found clinically several months later with brisk reflexes in wasted muscles. Studies of cortical excitability *via* transcranial magnetic stimulation as a candidate marker of UMN dysfunction early in the disease had not been performed. Imaging of brain and entire spinal cord showed only unspecific changes even late in the disease course.

Genetic testing at an earlier time point would have helped to shorten the diagnostic uncertainty, and the patient would not have been exposed to the risks and side effects of an

immunosuppressive treatment. However, genetic testing is not yet done routinely. Furthermore, the C9*orf*72 repeat expansion is intronic and only detectable by using repeat-primed PCR techniques, which are not included in common panel exome analysis and have to be ordered explicitly (26).

In conclusion, our case shows the difficulties of diagnosing ALS in the setting of a potentially relevant alternative diagnosis. Moreover, it highlights the need for diagnostic biomarkers as well as the role of genetic testing. These tools are important for development of disease-modifying therapies and for early diagnosis when future treatments may most efficaciously prevent disease progression.

DATA AVAILABILITY STATEMENT

The original contributions presented in the study are included in the article/supplementary material, further inquiries can be directed to the corresponding author/s.

ETHICS STATEMENT

Ethical review and approval was not required for the study on human participants in accordance with the local legislation and institutional requirements. The patients/participants provided their written informed consent to participate in this study. Written informed consent was obtained from the individual(s) for the publication of any potentially identifiable images or data included in this article.

AUTHOR CONTRIBUTIONS

MJW: clinical and electrophysiological examinations and manuscript writing. JK: manuscript editing and analysis of serum biomarkers. MH: supervision of the clinical and examinations and supervision and editing of the writing process. All authors contributed to the article and approved the submitted version.

REFERENCES

1. van Es MA, Hardiman O, Chio A, Al-Chalabi A, Pasterkamp RJ, Veldink JH, et al. Amyotrophic lateral sclerosis. *Lancet.* (2017) 390:2084–98. doi: 10.1016/S0140-6736(17)31287-4
2. Brooks BR, Miller RG, Swash M, Munsat TL, World Federation of Neurology Research Group on Motor Neuron Diseases. El Escorial revisited: revised criteria for the diagnosis of amyotrophic lateral sclerosis. *Amyotroph Lateral Scler Other Motor Neuron Disord.* (2000) 1:293–9. doi: 10.1080/146608200300079536
3. Carvalho MD, Swash M. Awaji diagnostic algorithm increases sensitivity of El Escorial criteria for ALS diagnosis. *Amyotroph Lateral Scler.* (2009) 10:53–7. doi: 10.1080/17482960802521126
4. Shefner JM, Al-Chalabi A, Baker MR, Cui LY, de Carvalho M, Eisen A, et al. A proposal for new diagnostic criteria for ALS. *Clin Neurophysiol.* (2020) 131:1975–8. doi: 10.1016/j.clinph.2020.04.005
5. Geevasinga N, Menon P, Özdinler PH, Kiernan MC, Vucic S. Pathophysiological and diagnostic implications of cortical dysfunction in ALS. *Nat Rev Neurol.* (2016) 12:651–61. doi: 10.1038/nrneurol.2016.140
6. Zoccolella S, Mastronardi A, Scarafino A, Iliceto G, D'Errico E, Fraddosio A, et al. Motor-evoked potentials in amyotrophic lateral sclerosis: potential implications in detecting subclinical UMN involvement in lower motor neuron phenotype. *J Neurol.* (2020) 267:3689–95. doi: 10.1007/s00415-020-10073-5
7. Grolez G, Moreau C, Danel-Brunaud V, Delmaire C, Lopes R, Pradat PF, et al. The value of magnetic resonance imaging as a biomarker for amyotrophic lateral sclerosis: a systematic review. *BMC Neurol.* (2016) 16:155. doi: 10.1186/s12883-016-0672-6
8. Jin J, Hu F, Zhang Q, Jia R, Dang J. Hyperintensity of the corticospinal tract on FLAIR: a simple and sensitive objective upper motor neuron degeneration marker in clinically verified amyotrophic lateral sclerosis. *J Neurol Sci.* (2016) 367:177–83. doi: 10.1016/j.jns.2016.06.005
9. Poesen K, De Schaepdryver M, Stubendorff B, Gille B, Muckova P, Wendler S, et al. Neurofilament markers for ALS correlate with extent of upper and lower motor neuron disease. *Neurology.* (2017) 88:2302–9. doi: 10.1212/WNL.0000000000004029
10. Verde F, Silani V, Otto M. Neurochemical biomarkers in amyotrophic lateral sclerosis. *Curr Opin Neurol.* (2019) 32:747–57. doi: 10.1097/WCO.0000000000000744
11. Vacchiano V, Mastrangelo A, Zenesini C, Masullo M, Quadalti C, Avoni P, et al. Plasma and CSF neurofilament light chain in amyotrophic lateral sclerosis: a cross-sectional and longitudinal study. *Front Aging Neurosci.* (2021) 13:753242. doi: 10.3389/fnagi.2021.753242
12. Khalil M, Teunissen CE, Otto M, Piehl F, Sormani MP, Gattringer T, et al. Neurofilaments as biomarkers in neurological disorders. *Nat Rev Neurol.* (2018) 14:577–89. doi: 10.1038/s41582-018-0058-z
13. Bischof A, Manigold T, Barro C, Heijnen I, Berger CT, Derfuss T, et al. Serum neurofilament light chain: a biomarker of neuronal injury in vasculitic neuropathy. *Ann Rheum Dis.* (2018) 77:1093–4. doi: 10.1136/annrheumdis-2017-212045
14. Wieske L, Smyth D, Lunn MP, Eftimov F, Teunissen CE. Fluid biomarkers for monitoring structural changes in polyneuropathies: their use in clinical practice and trials. *Neurotherapeutics.* (2021) 18:2351–67. doi: 10.1007/s13311-021-01136-0
15. Mathis S, Goizet C, Soulages A, Vallat JM, Masson GL. Genetics of amyotrophic lateral sclerosis: a review. *J Neurol Sci.* (2019) 399:217–26. doi: 10.1016/j.jns.2019.02.030
16. Seeliger T, Prenzler NK, Gingele S, Seeliger B, Körner S, Thiele T, et al. Neuro-Sjögren: peripheral neuropathy with limb weakness in Sjögren's syndrome. *Front Immunol.* (2019) 10:1600. doi: 10.3389/fimmu.2019.01600
17. Traynor BJ, Codd MB, Corr B, Forde C, Frost E, Hardiman O. Amyotrophic lateral sclerosis mimic syndromes: a population-based study. *Arch Neurol.* (2000) 57:109–13. doi: 10.1001/archneur.57.1.109
18. Benkert P, Meier S, Schaedelin S, Manouchehrinia A, Yaldizli Ö, Maceski A, et al. Serum neurofilament light chain for individual prognostication of disease activity in people with multiple sclerosis: a retrospective modelling and validation study. *Lancet Neurol.* (2022) 21:246–57. doi: 10.1016/S1474-4422(22)00009-6
19. Shiboski CH, Shiboski SC, Seror R, Criswell LA, Labetoulle M, Lietman TM, et al. 2016 American College of Rheumatology/European League against rheumatism classification criteria for primary Sjögren's syndrome: a consensus and data-driven methodology involving three international patient cohorts. *Arthritis Rheumatol.* (2017) 69:35–45. doi: 10.1002/art.39859
20. Ludolph AC, Emilian S, Dreyhaupt J, Rosenbohm A, Kraskov A, Lemon RN, et al. Pattern of paresis in ALS is consistent with the physiology of the corticomotoneuronal projections to different muscle groups. *J Neurol Neurosurg Psychiatry.* (2020) 91:991–8. doi: 10.1136/jnnp-2020-323331
21. Eisen A, Braak H, Del Tredici K, Lemon R, Ludolph AC, Kiernan MC. Cortical influences drive amyotrophic lateral sclerosis. *J Neurol Neurosurg Psychiatry.* (2017) 88:917–24. doi: 10.1136/jnnp-2017-315573

22. Mori K, Iijima M, Koike H, Hattori N, Tanaka F, Watanabe H, et al. The wide spectrum of clinical manifestations in Sjögren's syndrome-associated neuropathy. *Brain*. (2005) 128(Pt 11):2518–34. doi: 10.1093/brain/awh605
23. Turner MR, Goldacre R, Ramagopalan S, Talbot K, Goldacre MJ. Autoimmune disease preceding amyotrophic lateral sclerosis: an epidemiologic study. *Neurology*. (2013) 81:1222–5. doi: 10.1212/WNL.0b013e3182a6cc13
24. Pegat A, Bouhour F, Mouzat K, Vial C, Pegat B, Leblanc P, et al. Electrophysiological characterization of C9ORF72-associated amyotrophic lateral sclerosis: a retrospective study. *Eur Neurol*. (2019) 82(4–6):106–12 doi: 10.1159/000505777
25. Menke RA, Gray E, Lu CH, Kuhle J, Talbot K, Malaspina A, et al. CSF neurofilament light chain reflects corticospinal tract degeneration in ALS. *Ann Clin Transl Neurol*. (2015) 2:748–55. doi: 10.1002/acn3.212
26. Cooper-Knock J, Kirby J, Highley R, Shaw PJ. The spectrum of C9orf72-mediated neurodegeneration and amyotrophic lateral sclerosis. *Neurotherapeutics*. (2015) 12:326–39. doi: 10.1007/s13311-015-0342-1

Conflict of Interest: The authors declare that the research was conducted in the absence of any commercial or financial relationships that could be construed as a potential conflict of interest.

The reviewer TR declared a past co-authorship with one of the authors JK to the handling editor.

Publisher's Note: All claims expressed in this article are solely those of the authors and do not necessarily represent those of their affiliated organizations, or those of the publisher, the editors and the reviewers. Any product that may be evaluated in this article, or claim that may be made by its manufacturer, is not guaranteed or endorsed by the publisher.

Copyright © 2022 Wendebourg, Kuhle and Hardmeier. This is an open-access article distributed under the terms of the Creative Commons Attribution License (CC BY). The use, distribution or reproduction in other forums is permitted, provided the original author(s) and the copyright owner(s) are credited and that the original publication in this journal is cited, in accordance with accepted academic practice. No use, distribution or reproduction is permitted which does not comply with these terms.

frontiers | Frontiers in Neurology

CASE REPORT
published: 12 July 2022
doi: 10.3389/fneur.2022.930039

Case Reports: Novel Missense Variants in the Filamin C Actin Binding Domain Cause Variable Phenotypes

Daniele Velardo[1], Maria Grazia D'Angelo[2], Andrea Citterio[3], Elena Panzeri[3], Laura Napoli[1], Claudia Cinnante[4,5], Maurizio Moggio[1], Giacomo Pietro Comi[1,6], Dario Ronchi[6] and Maria Teresa Bassi[3]*

[1] Fondazione IRCCS Ca' Granda Ospedale Maggiore Policlinico, Neuromuscular and Rare Diseases Unit, Department of Neuroscience, Milan, Italy, [2] NeuroMuscular Unit, Scientific Institute for Research, Hospitalization and Healthcare (IRCCS) E. Medea, Bosisio Parini, Italy, [3] Laboratory of Molecular Biology, Scientific Institute for Research, Hospitalization and Healthcare (IRCCS) E. Medea, Bosisio Parini, Italy, [4] Fondazione IRCCS Ca' Granda Ospedale Maggiore Policlinico, Neuroradiology Unit, Milan, Italy, [5] Department of Radiology, Istituto Auxologico Italiano, Scientific Institute for Research, Hospitalization and Healthcare (IRCCS), Milan, Italy, [6] Department of Pathophysiology and Transplantation, Dino Ferrari Center, Neuroscience Section, University of Milan, Milan, Italy

Filamin C is a large dimeric actin-binding protein, most prevalent in skeletal and cardiac muscle Z-discs, where it participates in sarcomere mechanical stabilization and intracellular signaling, interacting with numerous binding partners. Dominant heterozygous mutations of Filamin C gene cause several forms of myopathy and structural or arrhythmogenic cardiomyopathy. In this report we describe clinical and molecular findings of two Italian patients, in whom we identified two novel missense variants located within the Filamin C actin binding domain. Muscle imaging, histological and ultrastructural findings are also reported. Our results underline the extreme inter- and intrafamilial variability of clinical manifestations, hence the need to extend the investigation also to asymptomatic relatives, and the relevance of a broad diagnostic approach involving muscle electron microscopy, skeletal muscle magnetic resonance imaging and next generation sequencing techniques.

Keywords: Filamin C, actin binding domain, distal myopathy, muscle electron microscopy, muscle magnetic resonance imaging, next generation sequencing

OPEN ACCESS

Edited by:
Thomas O. Krag,
Department of Neurology,
Rigshospitalet, Denmark

Reviewed by:
Chiara Fiorillo,
Giannina Gaslini Institute (IRCCS), Italy
Parijat Kabiraj,
Mayo Clinic, United States
Corrado Italo Angelini,
University of Padua, Italy
Frieder Schoeck,
McGill University, Canada

****Correspondence:***
Daniele Velardo
velardo.daniele@gmail.com

Specialty section:
This article was submitted to Neuromuscular Disorders and Peripheral Neuropathies, a section of the journal Frontiers in Neurology

Received: *27 April 2022*
Accepted: *22 June 2022*
Published: *12 July 2022*

Citation:
Velardo D, D'Angelo MG, Citterio A, Panzeri E, Napoli L, Cinnante C, Moggio M, Comi GP, Ronchi D and Bassi MT (2022) Case Reports: Novel Missense Variants in the Filamin C Actin Binding Domain Cause Variable Phenotypes. Front. Neurol. 13:930039. doi: 10.3389/fneur.2022.930039

INTRODUCTION

Heterozygous defects in the human Filamin C gene (*FLNC*) located on chromosome 7q32.1 result in clinical forms of myopathy and cardiomyopathy with marked phenotypic variability (1, 2). FLNC-related myopathies comprise three main presentations, according to type and location of the molecular defect: (i) missense or splice site changes affecting the rod domain result in late onset, progressive, proximal muscular weakness with large sarcoplasmic inclusions; (ii) frameshift mutations in the rod domain cause distal myopathy without sarcoplasmic inclusions; (iii) missense variants in the actin-binding domain (ABD) result in proximal or distal myopathy with non-specific myopathic changes (3–5). More recently, patients displaying restrictive, hypertrophic, dilated and arrhythmogenic cardiomyopathies have been found harboring truncating and missense *FLNC* mutations (6). Here we describe two novel *FLNC* variants located in the actin-binding domain associated with different phenotypes in two distinct Italian families.

CASE DESCRIPTIONS

Samples collection and studies were performed with informed consent from the patients according to approvals given by Ethic Committee of the Scientific Institute IRCCS Eugenio Medea, Bosisio Parini, Lecco, Italy and IRCCS Ca' Granda Foundation, Ospedale Maggiore Policlinico, Milan, Italy. The complete timeline of relevant clinical signs and symptoms and of diagnostic assessments performed during disease progression is reported in **Supplementary Figure 1**.

Patient 1

Patient 1 is a 53-year-old man, born to non-consanguineous parents, who had noticed mild hand and triceps brachii muscles wasting without corresponding weakness at the age of 28. Before then, he had practiced sport at a competitive level. At the age of 31 he started to complain fatigue and weakness in the legs and arms, impairing daily activities. Muscle cramps were present, mostly in the lower limbs.

Neurological examination at the age of 39 revealed forearm pronators, finger flexors and intrinsic hand muscles moderate weakness and wasting with mild asymmetry, a selective moderate weakness of the ankle plantar flexors and posterior leg muscles wasting, while all other lower limbs muscles showed only mild strength reduction. As the disease was progressing, weakness and wasting became more widespread and involved more proximal muscles. Last clinical examination at the age of 52 showed a severe muscle atrophy of lower and upper limbs (**Figure 1**) with moderate-severe muscle weakness more evident at distal upper than lower limbs. Mild facial muscular weakness was evident together with mild dysphonia. The patient is still able to stand with support but not to walk.

No cardiac or respiratory involvement were present. Creatine kinase (CK) levels were only moderately increased (range along time from 300 to 850 UI/L, normal values: 24–195) and electromyography displayed chronic myopathic signs with distal neuropathic signs at upper and lower limbs muscles.

The patient performed three muscle biopsies along time: all of them revealed an increased variability in muscle fibers diameter, a small number of centralized nuclei, central areas with reduced oxidative enzyme activity in both fiber types and increased subsarcolemmal activity in some type I fibers (**Figures 1A,B**). Immunostaining of muscle membrane proteins (Dystrophin, Caveolin-3, sarcoglycans) was normal.

Electron microscopy showed the presence of unstructured fibers, as the normal sarcomeric organization is no longer distinguishable (in some fields only a residual Z-disk was present) and small vacuoles with loose material inside, without evidence of collections of filamentous material; several mitochondria with altered or elongated shape, sometimes collected in small groups, and cytoplasmic dilations within several fibers were also noted (**Figures 2A–D**).

Muscle imaging through magnetic resonance of the lower limbs (performed at the age of 47) showed diffuse and severe muscle atrophy more evident in the posterior portion of the legs and signs of fatty substitution of the paravertebral muscles.

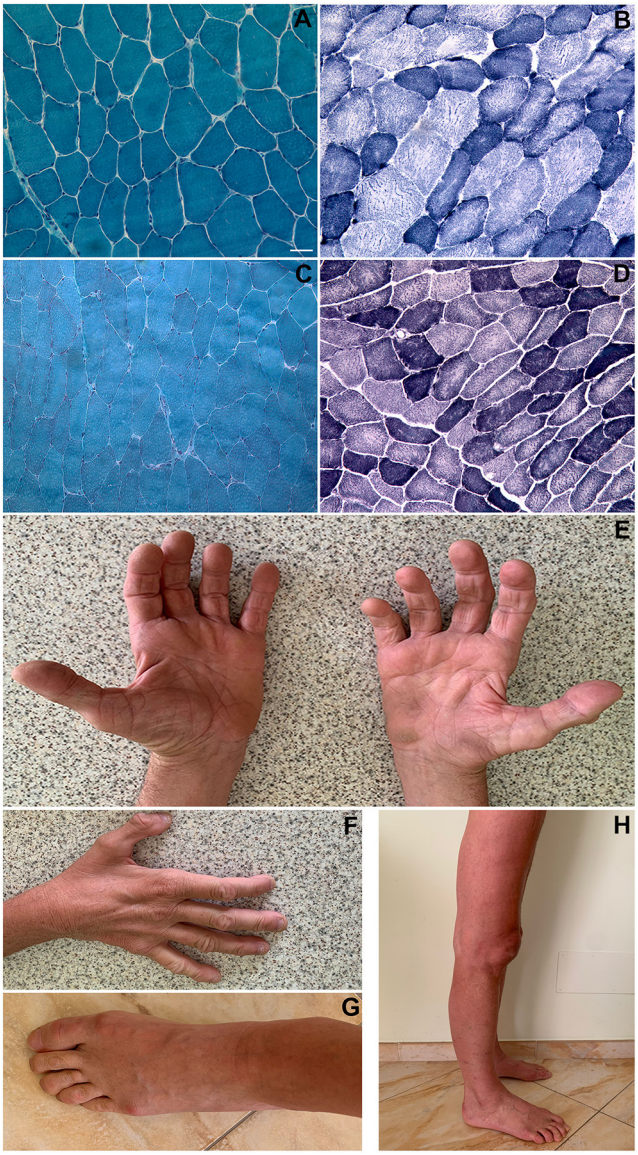

FIGURE 1 | Histopathological findings. Patient 1 (biceps brachii muscle; magnification: 200x): Gomori trichrome stain showing a slightly increased variability in muscle fibers diameter; no rimmed vacuoles and no sarcoplasmic or intranuclear inclusions were present **(A)**. NADH-TR stain showing "moth-eaten" or "core-like" areas of oxidative enzyme activity reduction in both fiber types and increased subsarcolemmal activity in some type I fibers (darker blue areas) **(B)**. Patient 2 (vastus lateralis muscle; magnification: 200x): Gomori trichrome stain showing an almost normal fiber variability pattern; no rimmed vacuoles and no inclusions were present **(C)**. NADH-TR stain shows slightly "core-like" reduction of central oxidative enzyme activity in both fiber types **(D)**. Patient 1 pictures showing intrinsic hand, foot, leg and thigh muscles wasting **(E–H)**. Scale bar: 25 μm.

Sanger sequencing of genes encoding Calpain 3, Lamin A/C, Selenoprotein, Valosin Containing Protein (VCP), Fukutin related protein (FKRP), Dysferlin, Anoctamin 5, GNE, dynactin subunit 1 (DCTN1) and testing for Survival Motor Neuron (SMN1) deletions were negative. Exome sequencing performed

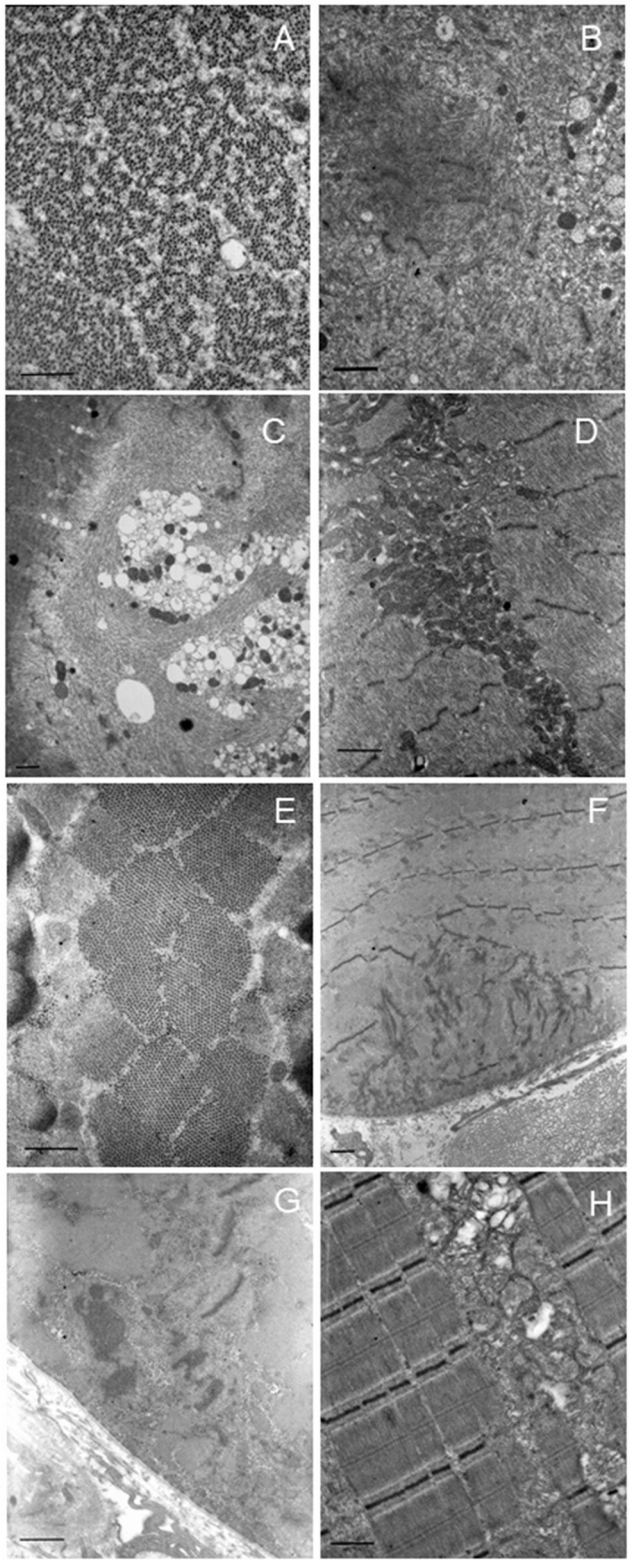

FIGURE 2 | Electron microscopy. Representative images of patients 1 **(A–D)** and 2 **(E–H)**. Patient 1: altered ultrastructural sarcomere pattern in transverse section **(A)**. Degeneration of sarcomere structure with extended area of

(Continued)

FIGURE 2 | myofibrillar disorganization in the sarcoplasm **(B,C)**. Also, many cytoplasmic vacuoles **(C)**. Collection and increase of intermyofibrillar mitochondria with normal morphology **(D)**. Patient 2: normal appearance of sarcomere pattern **(E)**. Degeneration of sarcomere structure with extended area of myofibrillar disorganization at the sub-sarcolemma level **(F)**. Area of myofibrillar disorganization with cytoplasmic bodies **(G)**. Abnormal mitochondrial accumulation, some mitochondria are swollen or with altered cristae **(H)**. Scale bar: short dash 463 nm, long dash 926 nm.

on the Trio revealed a novel *de novo* heterozygous missense variant c.665T>C in the *FLNC* gene (NM_001458, exon 3) leading to p.Met222Thr substitution in the actin binding region of the Filamin c protein (**Figure 3**). No other suspicious variants were detected in other distal myopathy-related genes (and included in the relative curated gene list of Panel App).

The Met222 residue is evolutionary conserved from human to Xenopus and different prediction tools support a likely pathogenic effect of the identified variant (**Supplementary Table 1**). The patient's asymptomatic siblings tested negative for the *FLNC* variant.

Patient 2

A 33-year-old man came to our attention with a clinical history of fatigue and progressive bilateral hypotrophy of the posterior thigh muscles and distal quadriceps, with associated foot plantar flexion weakness, lasting about 3 years. Currently, he is no longer able to lift himself on his toes and has suspended sports activity.

Electromyography showed predominantly myopathic changes in the proximal muscles of the four limbs (i.e., ileo-psoas, quadriceps femoris, deltoid) with additional aspects of active denervation in the triceps surae muscles (positive sharp waves, atypical repetitive discharges) and mixed neuropathic and myopathic features in the tibialis anterior.

Neurological examination revealed bilateral mild weakness of opponens pollicis and extensor digitorum and severe weakness of the gastrocnemius muscles, tibio-tarsal joint tension bilaterally, wasting of the posterior thigh and leg muscles. Creatine kinase levels were moderately elevated (652 UI/L). Echocardiography excluded structural cardiac alterations; there were no symptoms or signs of respiratory involvement.

The patient underwent open biopsy of the right vastus lateralis muscle. Histological examination showed mild muscular alterations, characterized by a diffuse reduction of oxidative enzyme activity with moth-eaten or core-like appearance (**Figures 1C,D**). Electron microscopy showed Z disk alterations (streaming or loss) in some fields, small subsarcolemmal or endomysial collections of mitochondria, in some cases of elongated shape (**Figures 2E–H**).

Lower limbs muscle MRI showed discrete muscle wasting of the posterior region of the lower legs and mild atrophy of the distal portion of quadriceps and hamstring muscles. Signs of adipose replacement are present in the same muscles, particularly in the leg (**Figures 4A–D**).

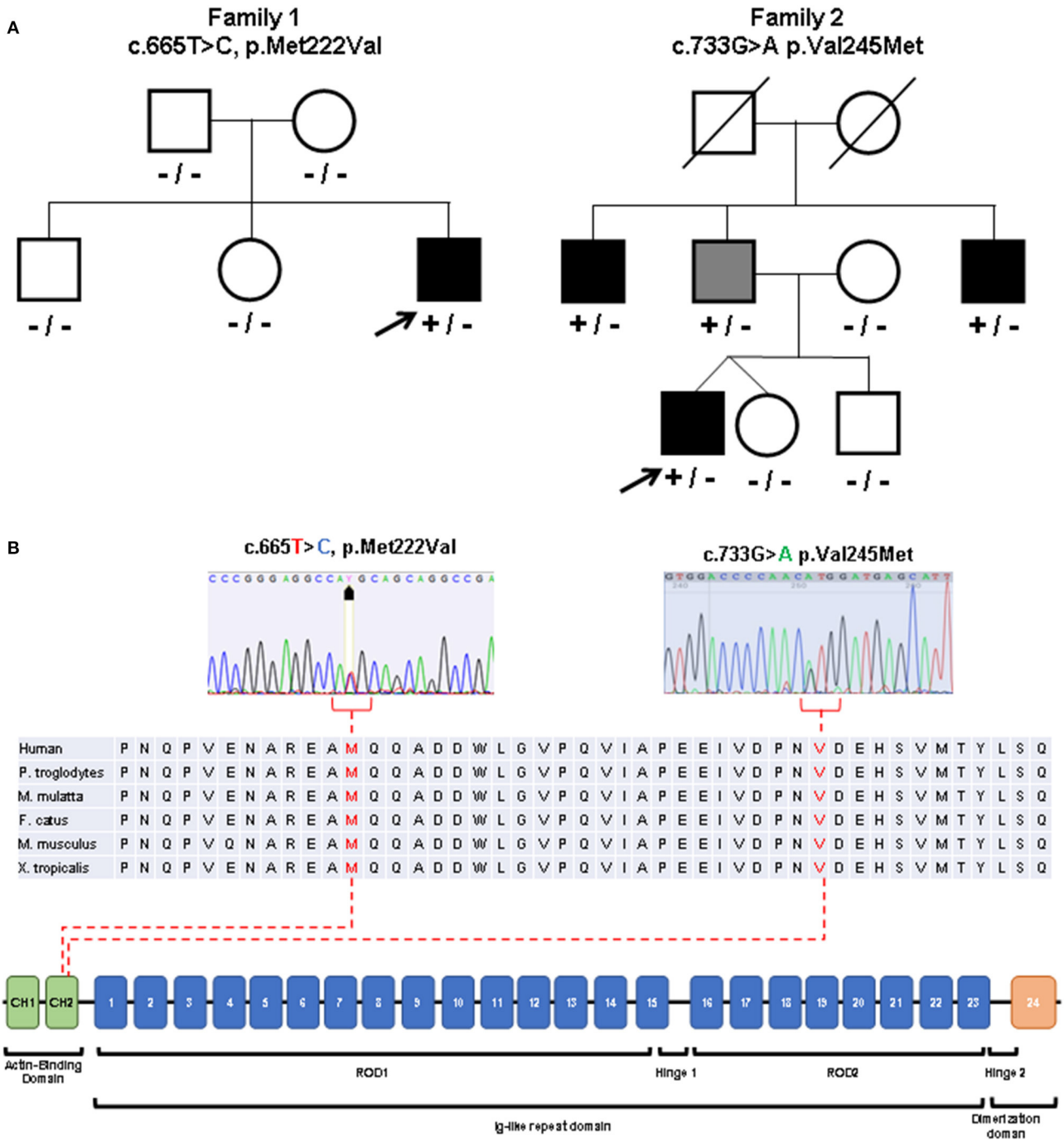

FIGURE 3 | Molecular studies. **(A)** Pedigrees of the described families. Index patients are indicated with arrows. Black symbols indicate clinically affected subjects. Gray symbol indicates subclinical involvement. Available genotypes are reported under the corresponding subjects. [**(B)**, top] Variants identified in the patients (sequence electropherograms) affecting conserved amino acidic residues within the actin binding domain. [**(B)**, bottom] Diagram showing the structure of FLNC gene and the protein domains observed in the encoded protein (Filamin-c).

Patient 2 underwent NGS-based panel sequencing targeting main genes involved in muscular dystrophies and distal myopathies (**Supplementary Table 2**). NGS analysis disclosed the novel heterozygous *FLNC* actin-binding domain missense variant c.733G>A (exon 4, p.Val245Met) (**Figure 3**), predicted as pathogenic (**Supplementary Table 1**). The same variant was identified in the clinically asymptomatic 65-year-old patient's father who displayed normal CK levels (51 UI/L), mixed

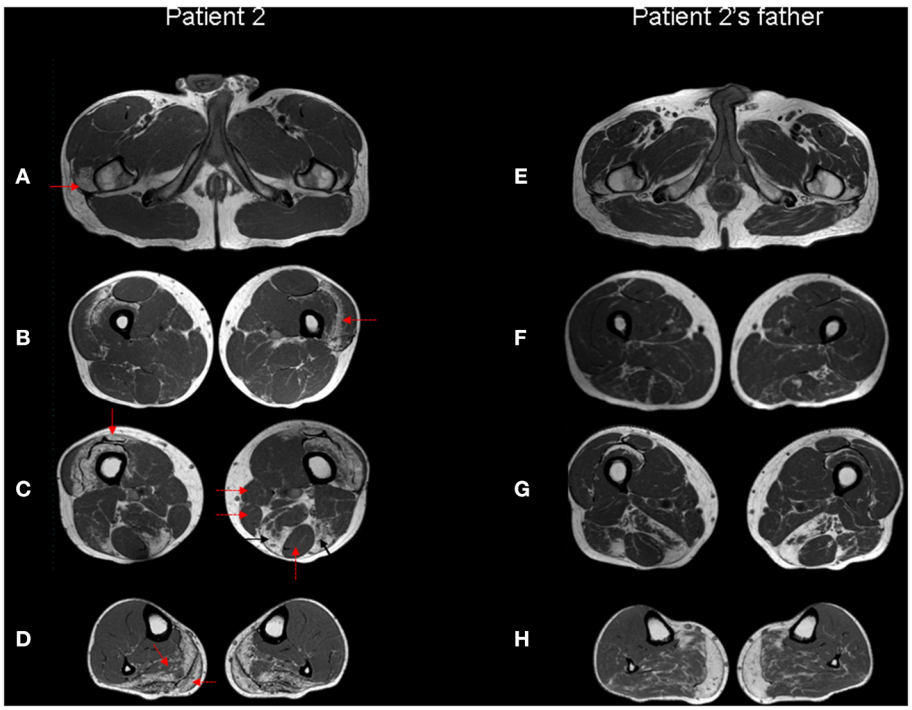

FIGURE 4 | Muscle MRI. Patient 2 **(A–D)** and patient 2's father **(E–H)** Turbo Spin Echo (TSE) axial T1 MRI images from thigh **(A–C, E–G)** to leg **(D,H)**. The patient's images show bilateral symmetric selective fatty degeneration of the distal insertion of the gluteus medius muscle [**(A)**, red arrow], subfascial fatty degeneration of vastus lateralis and intermedius muscles [**(B)**, red dotted arrow], with a relative sparing of rectus femoris, involved only at the distal insertion [**(C)**, red arrow]; fatty degeneration and wasting of semimembranosus and long head of biceps femoris muscle [**(C)**, black arrows] with relative preservation of gracilis, sartorious and semitendinosus muscles [**(C)**, red dotted arrows]. In the lower leg, there is a predominant fibroadipose replacement of the posterior muscles, primarily affecting the soleus and the medial gastrocnemius muscles [**(D)**, red dotted arrows]. The same involvement pattern of selected muscle groups can also be observed in the patient's father, although it is less pronounced except at the level of the distal leg.

neurogenic and myopathic motor unit potentials at the level of the medial gastrocnemius muscle bilaterally, chronic myogenic potentials in the four limbs' proximal muscles, with normal nerve conduction velocities. Muscle MRI displayed the same pattern of adipose replacement, albeit to a lower degree, previously observed in Patient 2 (**Figures 4E–H**). The dizygotic twin sister and the brother of the patient tested negative for the *FLNC* variant. Finally, the c.733G>A change was detected in two paternal uncles. One of them is a 60 years old man who is unable to lift on his toes. His CK levels are modestly increased (215 UI/L) and his neurophysiologic examination shows chronic sensory-motor mixed neuropathic signs and mixed neurogenic and, especially, myopathic motor unit potentials in the distal legs muscles. The second paternal uncle, aged 57 years, is affected by dilated cardiomyopathy without apparent skeletal muscle involvement. He was tested on a gene panel containing 42 genes currently known to be associated with monogenetic cardiomyopathy (http://www.umcutrecht.nl/NGS; panel car01 version 21.1) which disclosed the same c.733G>A (p.Val245Met) *FLNC* variant. No other clinical information is available.

In silico prediction tools including CADD scores supported the pathogenic role of the variants identified in the patients (**Supplementary Table 2**).

DISCUSSION

In the present report we identified two novel *FLNC* variants affecting conserved residues in the ABD. The clinical, radiological and histological findings contribute to expand the heterogenous phenotypic manifestations and skeletal muscle involvement observed in patients with filaminopathies.

A distal myopathy phenotype has to date been associated with missense variants in the calponin homology 2 (CH2) domain of the ABD (5, 7) or frameshift variants in the immunoglobulin-like domain 15 of ROD1 domain of *FLNC* gene (8, 9).

Distal ABD-filaminopathy usually presents with handgrip weakness followed by posterior leg muscles involvement with slow clinical progression (5, 10). Gemelli and co-authors previously described a variant (c.664>G; p.M222V, the same residue found mutated in Patient 1) in two siblings presenting progressive distal myopathy starting in their third decade (7). Although presenting a similar age at onset, our case is characterized by an initial involvement of the upper limbs, an earlier involvement of the lower limbs, and raised CK levels. The clinical features of Patient 2 overlaps those described in other patients with ABD Filamin-c mutations, except for the higher CK levels (5). However, differently from previous reports, heterogenous presentations ranging from subclinical

involvement of the distal leg muscles to apparently isolated cardiac involvement were observed in his family members harboring the same defect. Reduced penetrance and variable expressivity had been also previously described for *FLNC* variants associated with cardiac involvement (11, 12).

The histopathology of distal ABD-filaminopathy shows unspecific myopathic changes (10). In accordance with these data, and unlike the case already described in the literature (7), muscle biopsy findings in Patient 1 did not include myofibrillar aggregates nor intracytoplasmic or subsarcolemmal vacuoles. Likewise, immunohistochemical analysis of the Patient 2's muscle biopsy with antibodies directed against Desmin, Myotilin and αB-crystallin and ultrastructural analysis did not detect the characteristic protein aggregates of myofibrillar myopathies (1, 3).

Mixed myogenic and neurogenic pattern and spontaneous activity (positive sharp waves) in the anterior tibial muscle, with normal motor nerve conduction velocities, have already been described in Filamin C distal myopathy (8). An initial axonal motor neuropathy, with no significant abnormalities at the muscle needle exam, was suspected in another patient carrying a substitution in the Filamin C ABD causing a distal myofibrillar myopathy (7). Although in both our patients nerve conduction studies did not show reduced velocities and muscle biopsies did not reveal signs of neurogenic damage, concomitant neuropathy cannot be completely ruled out, as previously discussed (1).

The available muscle MRI data in filaminopathy show the following features: in the pelvis, initial changes are relatively mild. In the thigh, semimembranosus, adductor magnus and longus, long head of biceps femoris, vastus intermedius and medialis are most affected, whereas semitendinosus, rectus femoris, sartorius, and gracilis are relatively spared. In the lower leg, the soleus muscle shows pronounced fatty changes; tibialis anterior and medial gastrocnemius muscles are involved later, while peroneal muscles and lateral gastrocnemius are relatively spared even in more advanced disease (2, 13, 14). Although in Patient 1 the degree of fibroadipose replacement at the time of MRI is too advanced to recognize a peculiar pattern, this is certainly identifiable in Patient 2 and, more importantly, allows the identification of subclinical muscle involvement in his clinically asymptomatic father.

Our study contributes to expand the number of ABD variants of Filamin C associated with distal myopathy. Even in the absence of obvious alterations at standard microscopy, ultrastructural analysis might show the subversion of the intermyofibrillar network and mitochondrial alterations associated with myofibrillar myopathies (15, 16) but without protein aggregates. Muscle MRI is advised to recognize specific patterns of muscle involvement in affected patients and asymptomatic carriers.

DATA AVAILABILITY STATEMENT

The original contributions presented in the study are included in the article/**Supplementary Material**, further inquiries can be directed to the corresponding author/s.

ETHICS STATEMENT

The studies involving human participants were reviewed and approved by Comitato Etico Milano Area 2 Fondazione IRCCS Ca' Granda Ospedale Maggiore Policlinico (Milan, Italy). The patients/participants provided their written informed consent to participate in this study. Written informed consent was obtained from the individual(s) for the publication of any potentially identifiable images or data included in this article.

AUTHOR CONTRIBUTIONS

DV and MD'A interpreted the results, conceived the idea, revised the literature, wrote the manuscript, and made the clinical evaluation. DR, AC, and EP performed genetic analysis. LN performed ultrastructural studies. CC performed muscle MRI studies. MM, DR, GC, and MB performed a critical revision of the manuscript for important intellectual content. All authors have read and approved the manuscript.

FUNDING

This study was (partially) funded by Italian Ministry of Health—Current research IRCCS. The work was supported by funds from the Fondazione Regionale Lombarda per la Ricerca Biomedica (FRRB) grant Care4Neurorare (to MB). This work is generated within the European Reference Network for Neuromuscular Diseases.

ACKNOWLEDGMENTS

The authors wish to thank the patients and their families for participating in the work.

SUPPLEMENTARY MATERIAL

The Supplementary Material for this article can be found online at: https://www.frontiersin.org/articles/10.3389/fneur.2022.930039/full#supplementary-material

REFERENCES

1. Vorgerd M, van der Ven PF, Bruchertseifer V, Löwe T, Kley RA, Schröder R, et al. A mutation in the dimerization domain of filamin c causes a novel type of autosomal dominant myofibrillar myopathy. *Am J Hum Genet.* (2005) 77:297–304. doi: 10.1086/431959

2. Fürst DO, Goldfarb LG, Kley RA, Vorgerd M, Olivé M, van der Ven PF. Filamin C-related myopathies: pathology and mechanisms. *Acta Neuropathol.* (2013) 125:33–46. doi: 10.1007/s00401-012-1054-9

3. Kley RA, Serdaroglu-Oflazer P, Leber Y, Odgerel Z, van der Ven PF, Olivé M, et al. Pathophysiology of protein aggregation and extended phenotyping in filaminopathy. *Brain.* (2012) 135:2642–60. doi: 10.1093/brain/aws200

4. Borch JS, Eisum AV, Krag T, Vissing J. Expanding the phenotype of filamin-C-related myofibrillar myopathy. *Clin Neurol Neurosurg.* (2019) 176:30–3. doi: 10.1016/j.clineuro.2018.11.013
5. Duff RM, Tay V, Hackman P, Ravenscroft G, McLean C, Kennedy P, et al. Mutations in the N-terminal actin-binding domain of filamin C cause a distal myopathy. *Am J Hum Genet.* (2011) 88:729–40. doi: 10.1016/j.ajhg.2011.04.021
6. Verdonschot JAJ, Vanhoutte EK, Claes GRF, Helderman-van den Enden ATJM, Hoeijmakers JGJ, Hellebrekers DMEI, et al. A mutation update for the FLNC gene in myopathies and cardiomyopathies. *Hum Mutat.* (2020) 41:1091–111. doi: 10.1002/humu.24004
7. Gemelli C, Prada V, Fiorillo C, Fabbri S, Maggi L, Geroldi A, et al. A novel mutation in the N-terminal acting-binding domain of Filamin C protein causing a distal myofibrillar myopathy. *J Neurol Sci.* (2019) 398:75–78. doi: 10.1016/j.jns.2019.01.019
8. Guergueltcheva V, Peeters K, Baets J, Ceuterick-de Groote C, Martin JJ, Suls A, et al. Distal myopathy with upper limb predominance caused by filamin C haploinsufficiency. *Neurology.* (2011) 77:2105–14. doi: 10.1212/WNL.0b013e31823dc51e
9. Rossi D, Palmio J, Evilä A, Galli L, Barone V, Caldwell TA, et al. A novel FLNC frameshift and an OBSCN variant in a family with distal muscular dystrophy. *PLoS ONE.* (2017) 12:e0186642. doi: 10.1371/journal.pone.0186642
10. Savarese M, Sarparanta J, Vihola A, Jonson PH, Johari M, Rusanen S, et al. Panorama of the distal myopathies. *Acta Myol.* (2020) 39:245–65. doi: 10.36185/2532-1900-028
11. Valdés-Mas R, Gutiérrez-Fernández A, Gómez J, Coto E, Astudillo A, Puente DA, et al. Mutations in filamin C cause a new form of familial hypertrophic cardiomyopathy. *Nat Commun.* (2014) 29:5326. doi: 10.1038/ncomms6326
12. Tucker NR, McLellan MA, Hu D, Ye J, Parsons VA, Mills RW, et al. Novel mutation in FLNC (Filamin C) causes familial restrictive cardiomyopathy. *Circ Cardiovasc Genet.* (2017) 10:e001780. doi: 10.1161/CIRCGENETICS.117.001780
13. Fischer D, Kley RA, Strach K, Meyer C, Sommer T, Eger K, et al. Distinct muscle imaging patterns in myofibrillar myopathies. *Neurology.* (2008) 2:758–65. doi: 10.1212/01.wnl.0000324927.28817.9b
14. Wattjes MP, Kley RA, Fischer D. Neuromuscular imaging in inherited muscle diseases. *Eur Radiol.* (2010) 20:2447–60. doi: 10.1007/s00330-010-1799-2
15. Jackson S, Schaefer J, Meinhardt M, Reichmann H. Mitochondrial abnormalities in the myofibrillar myopathies. *Eur J Neurol.* (2015) 22:1429–35. doi: 10.1111/ene.12814
16. Schröder R, Schoser B. Myofibrillar myopathies: a clinical and myopathological guide. *Brain Pathol.* (2009) 19:483–92. doi: 10.1111/j.1750-3639.2009.00289.x

Conflict of Interest: The authors declare that the research was conducted in the absence of any commercial or financial relationships that could be construed as a potential conflict of interest.

Publisher's Note: All claims expressed in this article are solely those of the authors and do not necessarily represent those of their affiliated organizations, or those of the publisher, the editors and the reviewers. Any product that may be evaluated in this article, or claim that may be made by its manufacturer, is not guaranteed or endorsed by the publisher.

Copyright © 2022 Velardo, D'Angelo, Citterio, Panzeri, Napoli, Cinnante, Moggio, Comi, Ronchi and Bassi. This is an open-access article distributed under the terms of the Creative Commons Attribution License (CC BY). The use, distribution or reproduction in other forums is permitted, provided the original author(s) and the copyright owner(s) are credited and that the original publication in this journal is cited, in accordance with accepted academic practice. No use, distribution or reproduction is permitted which does not comply with these terms.

frontiers | Frontiers in Neurology

TYPE Case Report
PUBLISHED 23 September 2022
DOI 10.3389/fneur.2022.1011956

Check for updates

OPEN ACCESS

EDITED BY
Giovanni Meola,
University of Milan, Italy

REVIEWED BY
Yuto Uchida,
Johns Hopkins Medicine, United States
Tomoya Kubota,
Osaka University, Japan

*CORRESPONDENCE
Ann Cordenier
ann.cordenier@uzbrussel.be

SPECIALTY SECTION
This article was submitted to Neuromuscular Disorders and Peripheral Neuropathies, a section of the journal Frontiers in Neurology

RECEIVED 04 August 2022
ACCEPTED 05 September 2022
PUBLISHED 23 September 2022

CITATION
Cordenier A, Flamez A, de Ravel T, Gheldof A, Pannone L, De Asmundis C, Pappaert G and Bissay V (2022) Case report: Coexistence of myotonia congenita and Brugada syndrome in one family. *Front. Neurol.* 13:1011956. doi: 10.3389/fneur.2022.1011956

COPYRIGHT
© 2022 Cordenier, Flamez, de Ravel, Gheldof, Pannone, De Asmundis, Pappaert and Bissay. This is an open-access article distributed under the terms of the Creative Commons Attribution License (CC BY). The use, distribution or reproduction in other forums is permitted, provided the original author(s) and the copyright owner(s) are credited and that the original publication in this journal is cited, in accordance with accepted academic practice. No use, distribution or reproduction is permitted which does not comply with these terms.

Case report: Coexistence of myotonia congenita and Brugada syndrome in one family

Ann Cordenier[1]*, Anja Flamez[1], Thomy de Ravel[2], Alexander Gheldof[2], Luigi Pannone[3], Carlo De Asmundis[3], Gudrun Pappaert[3] and Véronique Bissay[1]

[1]Department of Neurology, Center for Neurosciences, Vrije Universiteit Brussel (VUB), UZ-Brussel, Brussels, Belgium, [2]Center for Medical Genetics, Vrije Universiteit Brussel (VUB), UZ-Brussel, Brussels, Belgium, [3]Heart Rhythm Management Centre, Vrije Universiteit Brussel (VUB), UZ-Brussel, Brussels, Belgium

Myotonia congenita is a rare neuromuscular disorder caused by *CLCN1* mutations resulting in delayed muscle relaxation. Extramuscular manifestations are not considered to be present in chloride skeletal channelopathies, although recently some cardiac manifestations have been described. We report a family with autosomal dominant myotonia congenita and Brugada syndrome. Bearing in mind the previously reported cases of cardiac arrhythmias in myotonia congenita patients, we discuss the possible involvement of the CLCN1-gene mutations in primary cardiac arrhythmia.

KEYWORDS

myotonia congenita, Brugada, cardiac arrhythmia, CLCN1, channelopathies

Introduction

Non-dystrophic myotonias (NDMs) are rare genetic neuromuscular disorders caused by dysfunctional ion channels expressed in the skeletal muscle cell membrane and, depending on the ion channel involved, referred to as chloride or sodium channelopathies.

Myotonia congenita is a chloride channelopathy with autosomal dominant or recessive inheritance, leading to Thomsen's or Becker's disease, respectively. Chloride channels (ClC-1), encoded by the *CLCN1* gene, play an essential role in restoring and maintaining the electrical stability of skeletal muscle cells. Up till now, more than 150 different *CLCN1* mutations, resulting in a reduced conductance of the ClC-1, have been described (1–3). Sodium channelopathies are caused by mutations in the *SCN4A* gene, resulting in an impaired inactivation of the alpha-subunit of the skeletal muscle NaV1.4 channel. Two autosomal dominant inherited phenotypes are recognized, paramyotonia congenita (PMC) and sodium channel myotonia (SCM) (1, 3). Both ion channelopathies lead to hyperexcitability of the sarcolemma membrane, causing myotonia, characterized by delayed skeletal muscle relaxation after voluntary or evoked muscle contraction. The first symptoms usually appear in the first or second decade but may also emerge later in life. MC is characterized by muscle stiffness (myotonia) upon initiating movement, and alleviated by repeated muscle contractions, known as the "warm-up" phenomenon.

Transient muscle weakness after initiating movements as well as muscle hypertrophy can be part of the phenotype. Symptoms in Becker's disease are often more severe (4). In contrast to *SCN4A*-associated myotonia, face and hand muscles are less involved in MC, and no or minimal cold sensitivity is reported. However, distinguishing SCM from MC can be challenging since there is some clinical overlap (1). Diagnosis is made by medical history, physical examination, neurophysiological tests, and genetic analysis. Most NDM patients present myotonic discharges on needle electromyography (nEMG). In addition, Fournier's short exercise test (SET) can be performed to differentiate sodium and chloride channelopathies based on postexercise changes in compound muscle action potential (CMAP) amplitude obtained by supramaximal nerve stimulation. In most MC cases, the CMAP amplitude decreases instantaneously after a short effort and quickly returns to baseline, classified as pattern II (5). However, in a minority of autosomal dominant MC cases, the CMAP amplitude is not altered by exercise, resembling the pattern III characteristics of SCM (5).

NDMs are skeletal muscle disorders without extramuscular manifestations. However, in 2016 our study group reported four families with coexisting Brugada syndrome (BrS) and NDM. Three families were diagnosed with genetically confirmed SCM and one with autosomal dominant MC (Thomsen disease) (6). BrS is another rare inherited channelopathy, due to alterations of ion currents at the level of the cardiac sarcolemma, predisposing to life-threatening ventricular arrhythmias and sudden cardiac death (SCD). The estimated prevalence is 1 in 2000 people worldwide. The diagnosis is confirmed on spontaneous or Ajmaline-induced ST segment elevation on the electrocardiogram (ECG) with a type I morphology of $>$ 2 mm in more than one lead among the right precordial leads (V1-V3) (7, 8). Approximately 20–30% of BrS cases are attributed to a mutation in the *SCN5A* gene. Other genes are assumed to be causative in an additional 10% of cases. However, most cases remain genetically unsolved. We hereby present a second family with MC and coexisting BrS.

Case presentation

The index patient, a 52-year-old man (A1, Table 1), was referred to our neurology department. He complained of chronic painful muscle stiffness, mainly involving the shoulder and pelvic girdle and, to a lesser degree, the hands. He reported a warm-up phenomenon. Stress and preceding rest periods were exacerbating factors. Cold exposure, on the other hand, was not. He never experienced muscle weakness. These muscle complaints had been until now, attributed to fibromyalgia. Most importantly, there was a history of symptomatic BrS for which an ICD was implanted (Table 1). Upon physical examination diffuse hypertrophy was noted. When the patient tried to get up from a chair, initially we observed marked muscle stiffness of the lower limbs, which progressively improved upon repetition of the task. No other clinical myotonia was detected, including during the evaluation of hand grip, and eye closure. No percussion myotonia or lid lag could be elicited. Muscle strength was normal, and Gower's sign was negative. nEMG showed myotonic discharges mostly exceeding 1 second of duration in all muscles tested, without any myopathic features. The short exercise test was normal at room temperature and after cooling (pattern III). Genetic testing revealed that the patient was heterozygous carrier for a c.2287C>A, p.(Gln763Lys) variant in exon 19 of the *CLCN1* gene, which is classified as a variant of unknown significance (VUS). Other genetic causes of myotonia, including myotonic dystrophy type 1 (*DMPK*) and 2 (*ZNF9*) and sodium channelopathies (*SCN4A)*, were excluded. Subsequently we screened three relatives of our index patient, 2 of whom had BrS, for the presence of myotonia.

The eldest sister (A2) complained of muscle stiffness in the 4 limbs, especially after a period of rest, or after heavy exercise. There was no aggravation with exposure to cold. She had normal muscle strength and no signs of muscle hypertrophy. Although no clinical myotonia was detected, nEMG did reveal brief (100–200 msec duration) myotonic discharges in several muscles. The short exercise test was normal at room temperature and after cooling (pattern III). Sequencing the *CLCN1* gene, the same heterozygous c.2287C>A, p.(Gln763Lys) variant in exon 19 was detected. No Brugada syndrome was diagnosed since she had a negative Ajmaline challenge test. The second sister (A3) had been diagnosed with Brugada Syndrome following a malignant cardiac event requiring an ICD implantation. She did not complain of muscle stiffness, myalgia, or delayed muscle relaxation. She mentioned sporadic muscle cramps, not preventing her from exercising. The neurological exam was normal, and no muscle hypertrophy nor clinical myotonia was present. During nEMG no myotonic discharges were observed. However, a slightly prolonged random insertional activity, was found in the intrinsic hand muscles and not in the other tested muscles, including the tibial anterior and biceps brachii. These findings were interpreted as a cramp and not as myotonic discharges. This was supported by the fact that at the same time, the patient experienced a slight painful cramping sensation at the site of the needle insertion. A short exercise test was also normal at room temperature and after cooling of the investigated muscle. Based on these clinical and electrophysiological features, no myotonic phenotype was retained. In the context of genetic screening of this family, the analysis of *CLCN1*, *SCN4A*, and *DMPK* genes was normal in this patient (A3). The son of our index patient A1 (A4) had a first negative Ajmaline challenge test at the age of 11 which turned positive when he was 19 years old, confirming the diagnosis of BrS. He never had any cardiac or neurological symptoms. No clinical or electrical abnormalities were detected during physical examination and nEMG. His genetic screening showed no variants in the *CLCN1* gene. No *SCN5A* variant was found in this family. A primary cardiac

arrhythmia gene panel was performed of the index patient (A1) and his son (A4). They both returned normal. The following genes were tested in this panel: ANK3, CACNA1c, CACNA2D1, CACNB2b, GPD1L, HCN4, KCNA3, KCNA4, KCNA7, KCNC4, KCND2, KCND3, KCNE1L (KCNE5), KCNE3, KCNH2, KCNJ8, RANGRF (MOG1), SCN1B, SCN2B, SCN3B, SCN5A, SCN7A (Nav.2.1), SGK1, SGK3, SLMAP, SNTG2, TRPM4. The clinical and paraclinical features of the 4 relatives are summarized in Table 1. The nEMG findings are shown in Figure 1.

Discussion

We report a family with a clinical and electrophysiological phenotype of NDM and the presence of a heterozygous c.2287C>A (p.Gln763Lys) *CLCN1* gene variant. Although this variant was previously reported as likely benign by Brugnoni et al. we believe that in our family this variant is probably pathogenic (13). Indeed, Thomsen's disease is the most probable diagnosis based on the presence of cold-insensitive predominant lower limb muscle stiffness and associated warm-up phenomenon, muscle hypertrophy, myotonic discharges without myopathic features on nEMG, further supported by segregation analysis of this pedigree, and the absence of other gene mutations related to familial myotonic syndromes, including *SCN4A*, *DMPK*, and *ZNF9* (14–16). Some family members of this pedigree were previously diagnosed with BrS. *SCN5A* sequencing and the primary cardiac arrhythmia panel analysis were normal. However, a causative role of the detected *CLCN1* variant in relation to the arrythmia can be ruled out since two relatives (A3, A4) were diagnosed with BrS and did not carry this *CLCN1* variant.

In 2016, our study group reported the first large family with Thomsen's disease due to a novel described *CLCN1* mutation and coexisting BrS. Thirteen relatives with BrS were reported, of whom 11 carried the NM_198056.3(SCN5A): c.2632C>T, p.(Arg878Cys) variant of unknown significance (VUS), and five had a genetically confirmed MC due to the NM_000083.3(CLCN1): c.744+1G>A;[=] pathogenic variant. Remarkably, two relatives who showed a positive Ajmaline challenge test without a history of malignant cardiac events, carried the *CLCN1* variant and not the *SCN5A* VUS (6).

Despite the absence of similar cases in the literature reporting the coexistence of BrS and MC, other cardiac arrhythmias and conduction disturbances have recently been described in patients with MC. Vereb et al. reported six MC patients who exhibited arrhythmias or conduction disorders, some of whom requiring a pacemaker (9). Wang et al. described nine autosomal dominant and recessive MC patients with cardiac arrhythmia resulting in minor cardiac symptoms. However, genetic analyses exploring primary cardiac arrhythmias were not specified in this article (10). Two additional case reports described the coexistence of MC and cardiac arrhythmia, including Wolff-Parkinson-White syndrome (11, 12). An overview of reported cases of cardiac arrhythmias in myotonia congenita patients is given in Table 2.

It is unclear whether *CLCN1* mutations may contribute to primary arrhythmias or conduction disorders. The ClC-1 channels are mainly expressed in the skeletal muscle, but low levels are also found in the kidney, heart, liver, smooth muscle, and the central nervous system (16–18). Other chloride channel isoforms, including ClC-2 and ClC-3 voltage-gated chloride channels, have been implicated in cardiac arrhythmias (19). By contrast, no clear link has been reported between cardiac ClC-1 channels and cardiac arrhythmias, including BrS. However, for several reasons our clinical data may support a potential role of *CLCN1* in the pathogenesis of cardiac arrhythmia, especially BrS. First, since the likelihood of cardiac and muscular channelopathies occurring together in patients is extremely low, given their rare prevalence in the general population, a pathophysiological link between *CLCN1* mutations and cardiac arrhythmias can be suspected. Second, we can assume that the prevalence of *CLCN1*-associated myotonia is underestimated in the BrS population, due to the rather unspecific symptoms, especially in mild cases. Patients may complain of chronic muscle stiffness and myalgia without muscle weakness. Because those symptoms are unspecific and common, NDM is rarely suspected, and diagnosis is often delayed. This is clearly illustrated by the history of our family cases A1 and A2, where in the former symptoms were attributed to an earlier fibromyalgia diagnosis, and, in the latter, mild muscular symptoms were not even reported. Thanks to increasing awareness of the presence of subtle muscular symptoms in myotonia, the rhythmology team referred the BrS patient (A1) to our neurology department. The NDM diagnosis would probably not yet have been made in other circumstances. Finally, the Mendelian model for BrS, characterized by single gene disease, has been recently challenged by an oligogenic model referring to a possible cumulative role of common and rare genetic variants (20). A possible explanation could be that *CLCN1* variants contribute to the BrS phenotype. On the other hand, it cannot be excluded that it is a simple coexistence of two separate pathologies and that the gene responsible for Brugada syndrome in these patients is not yet known.

A parallel can be drawn with the *SCN4A* gene recently added to the list of minor genes associated with BrS (7, 8). In 2016, our study group reported 3 families with *SCN4A*-associated NDM and coexisting BrS, with this gene presumably acting as a modifier gene. Some of these patients had few muscle complaints, despite the presence of a deleterious variant in the *SCN4A* gene (6). The expression of the skeletal *SCN4A* isoform in cardiac muscle was also described (21, 22).

Even though current data are not sufficient to advocate a systematic cardiac work-up in patients with NDM, there is increasing evidence of an overlap between skeletal

TABLE 1 Clinical and paraclinical features of the 4 relatives.

			Neurological				Cardiological						
Patient	**Age (Y)**	**Sex**	**Clinical findings**	**MD on nEMG**	**SET room temp/ cooling**	**Genetic tests**	**Clinical findings**	**Baseline ECG**	**Ajm**	**BrS diagnosis**	**EPS**	**Genetic result**	**ICD**
A1	53	M	MS, myalgiaWUP MH	+ All tested muscles	Type III/III	HZc of NM_000083.3(CLCN1): c.2287C>A, p.(Gln763Lys) SCN4A: WT DMPK: WT ZNF9: WT	Palpitations syncope	Nl	Type 1 pattern	Confirmed	Nl	SCN5A: WT BRSGP: WT	+
A2	60	F	MS, WUP	+ All tested muscles	Type III/III	HZc of NM_000083.3(CLCN1): c.2287C>A, p.(Gln763Lys) SCN4A: WT	aS	Nl	Nl	-No BrS diagnosis	NP	NP	-
A3	56	F	aSp	-*	Type III /III	CLCN1: WT SCN4A: WT DMPK: WT	Aborted SCD	Nl	Type 1 pattern	Confirmed	NP	SCN5A: WT	+
A4	24	M	aS	-	NP	CLCN1: WT	aS	Nl	Type 1 pattern	Confirmed	Nl	BRSGP: WT	-

Ajm, Ajmaline challenge test; aS, asymptomatic; aSp, aspecific muscular symptoms; BrS, Brugada syndrome; BRSGP, Brugada syndrome gene panel; DMPK, Myotonic Dystrophy Protein Kinase gene; ECG, electrocardiogram; EPS, electrophysiological study; F, female; HZc, Heterozygous carrier; ICD, implantable cardioverter defibrillator; M, male; MD, myotonic discharges; MH, muscle hypertrophy; MS, muscle stiffness; nEMG, needle-electromyography; Nl, Normal; NP, not-performed; SCD, sudden cardiac death; SET, short exercise test of Fournier; VUS, variant of unknown significance; WUP, warm-up phenomenon; WT, Wild Type; Y, Years.

*Muscle cramp in intrinsic hand muscle, not in the other tested muscles. +, present; −, absent.

10.3389/fneur.2022.1011956

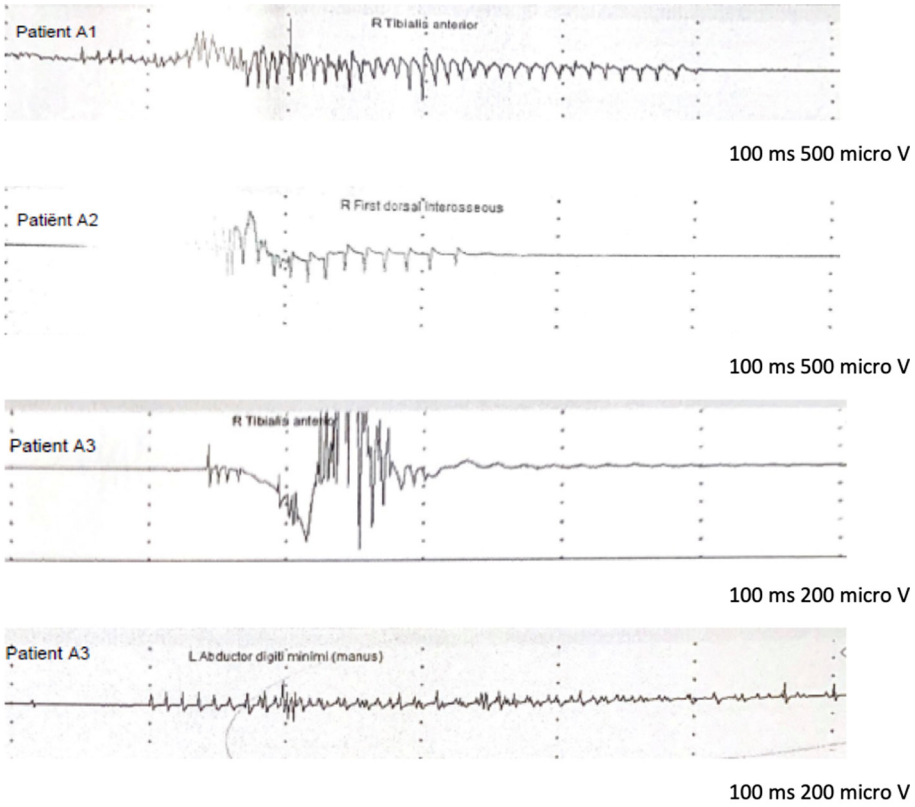

A1, A2: Myotonic discharge

A3 1. Normal insertion activity (tibialis anterior) - 2. Muscle cramp (abductor digiti minimi).

FIGURE 1
nEMG findings.

TABLE 2 Reported cases of cardiac arrhythmias in myotonia congenita patients.

Study	N	Muscular features	Cardiac features
Bissay et al. (6)	5	none, sporadic muscle stiffness at the thumb, sporadic cramps calf at night	+ Ajmaline test in 5 patients: asymptomatic, RBBB, VF
Vereb et al. (9)	48	Myotonia, myalgia, cramps, paresis, muscle hypertrophy	6 of 48 patients: RBBB (2), cardiac arrhythmia (2), AV-block II, AV-block III, pacemaker implantation (3)
Wang et al. (10)	17	Muscle stiffness, muscle hypertrophy, warm-up phenomenon	9 of 17 patients: Sinus tachycardia (2), atrial premature beats (2), ventricular premature beats (2), sinus arrythmia (2)
Caballero (11)	1	Myotonia, transient weakness, muscular hypertrophy	Wolf-Parkinson-White-Syndrome
Anderson (12)	1	Myotonia of grip and percussion	AV- block II with Wenckebach conduction disturbance

muscle and cardiac ion channelopathies. Therefore, we propose to perform at least a thorough cardiac history assessment and a 12-lead ECG in NDM patients. A history of palpitations, syncopes, conduction disorders, or a family history of sudden cardiac death should prompt an immediate referral to a cardiologist. Conversely, patients with primary cardiac arrhythmias, especially those with BrS, should be systematically asked about presence of muscle stiffness, myalgia, muscle weakness, and if indicated, be referred to the neurology department.

Sodium channel blockers are used in the symptomatic treatment of myotonia. Mexiletine, a class 1B antiarrhythmic drug, seems to be a safe anti-myotonic therapy in the presence of Brugada syndrome (23, 24). However, the use of Flecainide, a class 1C antiarrhythmic drug, should be started with caution, based on a case report in which BrS was unmasked after initiating this treatment in an SCM patient who had never experienced cardiac symptoms before (25). Considering this and the previously reported family with concomitant MC and BrS, the use of class 1C antiarrhythmic drug to alleviate myotonia seems less appropriate for MC patients as well (6).

Of course, our data need to be confirmed by new designed clinical and genome wide association studies in larger patient cohorts, as well as functional studies in order to further clarify the involvement of *CLCN1* gene in cardiac arrhythmias.

Data availability statement

The datasets presented in this article are not readily available because of ethical and privacy restrictions. Requests to access the datasets should be directed to the corresponding author.

Ethics statement

Written informed consent was obtained from the individual(s) for the publication of any potentially identifiable images or data included in this article.

Author contributions

AC: data collection, review of the literature, and article writing. VB: review of literature, article writing, and article editing. AF, TR, AG, LP, CD, and GP: article editing. All authors contributed to the article and approved the submitted version.

Conflict of interest

The authors declare that the research was conducted in the absence of any commercial or financial relationships that could be construed as a potential conflict of interest.

Publisher's note

All claims expressed in this article are solely those of the authors and do not necessarily represent those of their affiliated organizations, or those of the publisher, the editors and the reviewers. Any product that may be evaluated in this article, or claim that may be made by its manufacturer, is not guaranteed or endorsed by the publisher.

References

1. Statland JM, Barohn JB. Muscle channelopathies: the nondystrophic myotonias and periodic paralyses. *Continuum.* (2013) 19:1598–614. doi: 10.1212/01.CON.0000440661.49298.c8

2. Morales F, Pusch M. An up-to-date overview of the complexity of genotype-phenotype relationships in myotonic channelopathies. *Front Neurol.* (2019) 10:1404. doi: 10.3389/fneur.2019.01404

3. Vivekanandam V, Männikkö R, Mathew E, Hanna MG. Improving genetic diagnostics of skeletal muscle channelopathies. *Expert Rev Mol Diagn.* (2020) 20:725–36. doi: 10.1080/14737159.2020.1782195

4. Sun C, Tranebjaerg L, Torbergsen T, Homgren G, Van Ghelue M. Spectrum of CLCN1 mutations in patients with myotonia congenita in Northern Scandinavia. *Eur J Hum Genet.* (2001) 9:903–9. doi: 10.1038/sj.ejhg.5200736

5. Fournier E, Arzel M, Sternberg D, Vicart S, Laforet P, Eymard B, et al. Electromyography guides toward subgroups of mutations in muscle channelopathies. *Ann Neurol.* (2004) 56:650–61. doi: 10.1002/ana.20241

6. Bissay V, Van Malderen SCH, Keymolen K, Lissens W, Peeters U, Daneels D, et al. SCN4A variants and Brugada syndrome: phenotypic and genotypic overlap between cardiac and skeletal muscle sodium channelopathies. *Eur J Hum Gene.* (2016) 24:400–7. doi: 10.1038/ejhg.2015.125

7. Campuzano O, Sarquella-Brugada G, Cesar S, ARbelo E, Brugada J, Brugada R. Update on genetic basis of brugada syndrome: monogenic, polygenic or oligogenic? *Int J Mol Sci.* (2020) 21:7155 doi: 10.3390/ijms21197155

8. Campuzano O, Sarquella-Brugada G, Fernandez-Falgueras A, Cesar S, Coll M, Mates J, et al. Genetic interpretation and clinical translation of minor genes related to Brugada syndrome. *Hum Mutat.* (2019) 40:749–64. doi: 10.1002/humu.23730

9. Vereb N, Montagnese F, Gläser D, Schoser B. Non-dystrophic myotonias: clinical and mutation spectrum of 70 German patients. *J Neurol.* (2021) 268:1708–20. doi: 10.1007/s00415-020-10328-1

10. Wang Q, Zhao Z, Shen H, Bing Q, Li N, Hu J. The clinical, myopathological, and genetic analysis of 20 patients with non-dystrophic myotonia. *Front Neurol.* (2022) 13:830707. doi: 10.3389/fneur.2022.830707

11. Caballero PE. Becker myotonia congenita associated with Wolff-Parkinson-White syndrome. *Neurologist.* (2011) 17:38–40. doi: 10.1097/NRL.0b013e3181d35c93

12. Anderson M. Probable Thomsen's disease with cardiac involvement. *J Neurol.* (1977) 214:301–4. doi: 10.1007/BF00316576

13. Brugnoni R, Kapetis D, Imbrici P, Pessia M, Canioni E, Colleoni L, et al. A large cohort of myotonia congenita probands: novel mutations and a high-frequency mutation region in exons 4 and 5 of the CLCN1 gene. *J Hum Genet.* (2013) 589:581–7. doi: 10.1038/jhg.2013.58

14. Bissay V, Van Malderen SC. What the internist should know about hereditary muscle channelopathies. *Acta Clin Belg.* (2018) 73:1–6. doi: 10.1080/17843286.2017.1396674

15. Matthews E, Fialho D, Tan SV, Venance SL, Cannon SC, Sternberg D, et al.The non-dystrophic myotonias: molecular pathogenesis diagnosis and treatment. *Brain.* (2010) 133:9–22. doi: 10.1093/brain/awp294

16. Imbrici P, Altamura C, Pessia M, Mantegazza R, Desaphy JF, Conte Camerino D. ClC-1 chloride channels: state-of-the-art research and future challenges. *Front Cell Neurosc.* (2015) 9:156. doi: 10.3389/fncel.2015.00156

17. Steinmeyer K, Ortland C, Jentsch TJ. Primary structure and functional expression of a developmentally regulated skeletal muscle chloride channel. *Nature*. (1991) 354:301–4. doi: 10.1038/354301a0

18. Chen TT, Klassen TL, Goldman AM, Marini C, Guerrini R, Noebels JL. Novel brain expression of ClC-1 chloride channels and enrichment of CLCN1 variants in epilepsy. *Neurology*. (2013) 80:1078–85. doi: 10.1212/WNL.0b013e31828868e7

19. Duan D. Phenomics of cardiac chloride channels: the systematic study of chloride channel function in the heart. *J Physiol*. (2009) 587:2163–77. doi: 10.1113/jphysiol.2008.165860

20. Monasky MM, Micaglio E, Ciconte G, Pappone C. Brugada syndrome: oligogenic or mendelian disease? *Int J Mol Sci*. (2020) 21:1687. doi: 10.3390/ijms21051687

21. Pereon Y, Lande G, Demolombe S, Nguyen The Tich S, Sternberg D, Le Marec H, et al. Paramyotonia congenita with an SCN4A mutation affecting cardiac repolarization. *Neurology*. (2003) 60:340–2. doi: 10.1212/01.WNL.0000042093.96309.5A

22. Kaufmann SG, Westenbroeck RE, Maass AH, Lange V, Renner A, Wischmeyer E, et al. Distribution and function of sodium channel subtypes in human atrial myocardium. *J Mol Cell Cardiol*. (2013) 61:133–41. doi: 10.1016/j.yjmcc.2013.05.006

23. Vicart S, Franques J, Bouhour F, Magot A, Péréon Y, Sacconi S, et al. Efficacy and safety of mexiletine in non-dystrophic myotonias: a randomised, double-blind, placebo-controlled, cross-over study. *Neuromuscul Disord*. (2021) 31:1124–35. doi: 10.1016/j.nmd.2021.06.010

24. Modoni A, D'Amico A, Primiano G, Capozzoli F, Desaphy JF, Lo Monaco M. Long-term safety and usefulness of mexiletine in a large cohort of patients affected by non-dystrophic myotonias. *Front Neurol*. (2020) 11:300. doi: 10.3389/fneur.2020.00300

25. Cavalli M, Fossati B, Vitale R, Brigonzi E, Ricigliano V, Saraceno L, et al. Flecainide-induced Brugada syndrome in a patient with skeletal muscle sodium channelopathy: a case report with critical therapeutical implications and review of the literature. *Front Neurol*. (2018) 9:385. doi: 10.3389/fneur.2018.00385

frontiers | Frontiers in Neurology

TYPE Case Report
PUBLISHED 23 September 2022
DOI 10.3389/fneur.2022.937885

Check for updates

OPEN ACCESS

EDITED BY
Giovanni Meola,
University of Milan, Italy

REVIEWED BY
Andrea Legati,
IRCCS Carlo Besta Neurological Institute Foundation, Italy
Alessia Nasca,
IRCCS Carlo Besta Neurological Institute Foundation, Italy
Daniele Ghezzi,
University of Milan, Italy

*CORRESPONDENCE
Arnaud Chevrollier
arnaud.chevrollier@univ-angers.fr
Isabelle Maystadt
isabelle.maystadt@ipg.be

†These authors share last authorship

SPECIALTY SECTION
This article was submitted to Neuromuscular Disorders and Peripheral Neuropathies, a section of the journal Frontiers in Neurology

RECEIVED 06 May 2022
ACCEPTED 01 September 2022
PUBLISHED 23 September 2022

CITATION
Lhuissier C, Wagner BE, Vincent A, Garraux G, Hougrand O, Van Coster R, Benoit V, Karadurmus D, Lenaers G, Gueguen N, Chevrollier A and Maystadt I (2022) Case report: Thirty-year progression of an EMPF1 encephalopathy due to defective mitochondrial and peroxisomal fission caused by a novel *de novo* heterozygous *DNM1L* variant. *Front. Neurol.* 13:937885. doi: 10.3389/fneur.2022.937885

COPYRIGHT
© 2022 Lhuissier, Wagner, Vincent, Garraux, Hougrand, Van Coster, Benoit, Karadurmus, Lenaers, Gueguen, Chevrollier and Maystadt. This is an open-access article distributed under the terms of the Creative Commons Attribution License (CC BY). The use, distribution or reproduction in other forums is permitted, provided the original author(s) and the copyright owner(s) are credited and that the original publication in this journal is cited, in accordance with accepted academic practice. No use, distribution or reproduction is permitted which does not comply with these terms.

Case report: Thirty-year progression of an EMPF1 encephalopathy due to defective mitochondrial and peroxisomal fission caused by a novel *de novo* heterozygous *DNM1L* variant

Charlène Lhuissier[1], Bart E. Wagner[2], Amy Vincent[3], Gaëtan Garraux[4,5], Olivier Hougrand[6], Rudy Van Coster[7], Valerie Benoit[8], Deniz Karadurmus[8], Guy Lenaers[1,9], Naïg Gueguen[1,10], Arnaud Chevrollier[1*†] and Isabelle Maystadt[8,11*†]

[1]MitoLab Team, UMR CNRS 6015-INSERM U1083, Unité MitoVasc, SFR ICAT, Université d'Angers, Angers, France, [2]Department of Histopathology, Royal Hallamshire Hospital, Sheffield, United Kingdom, [3]Wellcome Centre for Mitochondrial Research, Faculty of Medical Sciences, Translational and Clinical Research Institute, Newcastle University, Newcastle upon Tyne, United Kingdom, [4]GIGA-CRC in vivo Imaging, University of Liège, Liège, Belgium, [5]Department of Neurology, CHU Liège, Liège, Belgium, [6]Département d'Anatomie Pathologique, CHU Liège, Liège, Belgium, [7]Division of Pediatric Neurology and Metabolism, Department of Pediatrics, Ghent University Hospital, Ghent, Belgium, [8]Institut de Pathologie et de Génétique, Gosselies, Belgium, [9]Service de Neurologie, Centre Hospitalier Universitaire d'Angers, Angers, France, [10]Service de Biochimie et Biologie Moléculaire, CHU Angers, Angers, France, [11]Faculté de Médecine, URPhyM, Université de Namur, Namur, Belgium

Mutations in *DNM1L* (*DRP1*), which encode a key player of mitochondrial and peroxisomal fission, have been reported in patients with the variable phenotypic spectrum, ranging from non-syndromic optic atrophy to lethal infantile encephalopathy. Here, we report a case of an adult female patient presenting with a complex neurological phenotype that associates axonal sensory neuropathy, spasticity, optic atrophy, dysarthria, dysphasia, dystonia, and ataxia, worsening with aging. Whole-exome sequencing revealed a heterozygous *de novo* variant in the GTPase domain of *DNM1L* [NM_001278464.1: c.176C>A p.(Thr59Asn)] making her the oldest patient suffering from encephalopathy due to defective mitochondrial and peroxisomal fission-1. *In silico* analysis suggested a protein destabilization effect of the variant Thr59Asn. Unexpectedly, Western blotting disclosed profound decrease of DNM1L expression, probably related to the degradation of DNM1L complexes. A detailed description of mitochondrial and peroxisomal anomalies in transmission electron and 3D fluorescence microscopy studies confirmed the exceptional phenotype of this patient.

KEYWORDS

mitochondrial fission, DRP1, *DNM1L*, encephalopathy, EMPF1

Introduction

DNM1L is located on chromosome 12p11.21 and encodes the 81.8 kDa human dynamin-1-like protein (DNM1L), formerly called dynamin-related protein 1 (DRP1). DNM1L protein belongs to the conserved family of dynamins and plays a key role in the regulation of mitochondrial and peroxisomal fission (1–5). As for other dynamins, DNM1L comprises a large GTPase domain, including the GTP-binding motifs that are needed for guanine nucleotide binding and hydrolysis, and two additional domains, the middle domain and the GTPase effector domain (GED), which are involved in oligomerization and regulation of the GTPase activity. DNM1L forms homodimers which are recruited to the outer membrane of the mitochondria and to the surface of peroxisomes, where they induce mitochondrial or peroxisomal fission, by wrapping around the scission site to constrict and sever the membrane through a GTP-hydrolysis-dependent mechanism (6). Excessive activation and upregulation of DNM1L has been found to be associated with aberrant mitochondrial fragmentation, causing neuronal damage in various neurodegenerative diseases, such as Alzheimer's disease, Parkinson's disease, Huntington's disease, and amyotrophic lateral sclerosis (7). Furthermore, a neural cell specific Drp1-/- mice model emphasized the role of Drp1 in embryonic forebrain development and synapse formation (8).

In humans, heterozygous *DNM1L* variants were reported in isolated autosomal dominant optic atrophy type 5 (OPA5, MIM#610708), and monoallelic or biallelic variants were associated with encephalopathy due to defective mitochondrial and peroxisomal fission (EMPF1, MIM#614388). Thirty-eight EMPF1 patients have been reported to date, showing a wide phenotypic spectrum and a variable degree of severity, ranging from early death to slowly progressive encephalopathy with hypotonia and developmental delay (9–11), while seizures were inconstantly reported. Dystonia, dysarthria, spasticity, microcephaly, insensitivity to pain, peripheral neuropathy, ataxia, optic atrophy, and brain anomalies (dysmyelination, corpus callosum anomalies, and T2 hyperintensities mainly in the cortex and the basal ganglia) are common clinical features associated with *DNM1L* variants.

Here, we report the oldest EMPF1 patient, whose clinical presentation recapitulates the entire phenotypic spectrum of *DNM1L*-related encephalopathy, except for the microcephaly and brain MRI anomalies, emphasizing the pejorative evolution of the clinical presentation. Heterozygous mutations in the GTPase domain usually affect *DNM1L* enzymatic activity without affecting its abundance, but here the p.(Thr59Asn) variant induced the full loss of *DNM1L* normal forms probably following the degradation of the DNM1L complexes. We confirmed, with a detailed description of mitochondrial and peroxisomal anomalies in transmission electron and 3D fluorescence microscopy studies, the abnormal cellular features of this patient.

Case report

The 32-year-old female patient is the only child of healthy non-consanguineous Caucasian parents (Supplementary Figure 1). Pregnancy was uncomplicated. She was born at 38-week gestation by cesarean section due to narrow maternal pelvis, with a weight of 2,950 g (P45), height of 47.5 cm (P35), and normal head circumference (precise measure not known). Neonatal adaptation was correct (APGAR score 9 at 1 min). During the first month, sucking difficulties and poor weight gain were noticed. The patient showed hypotonia and global developmental delay. She walked autonomously at 24 months, with a tendency to tiptoe and with ataxic gait, despite intensive physiotherapy. She progressively developed a tetrapyramidal syndrome. A diagnostic hypothesis of cerebral palsy was suggested, but CT scan revealed no brain anomalies. She spoke the first intelligible words at 3.5 years and built sentences at 4 years. During childhood, she had behavioral problems, such as tantrums, which decreased with aging. She had high pain tolerance. She had learning difficulties and required a school for special educational needs. At the age of 7, global IQ was estimated around 66 at the Wechsler scale. She can read and write, but mathematics remains a challenge. Since age 10, her neurological status deteriorated with increasing gait disturbances, dysarthria, and dysphagia. At the age of 12 years, clinical examination revealed a scoliosis, which was treated with a brace. She also had an ophthalmological follow-up for nystagmus and bilateral optic atrophy (Table 1). Her puberty was delayed, with the first menstrual cycle beginning at 16 years. At the age of 18 years, she developed tonic–clonic epileptic generalized seizures. Epilepsy was well controlled with lamotrigine treatment. At age 27, sleep study revealed severe dyssomnia, with fragmented sleep and a periodic limb movement disorder, treated with clonazepam.

At clinical examination at 29 years, the patient's height was 155 cm (P3) and weight was 42 kg (−3SD). Her head circumference was 54.5 cm (P55). She had a long and asymmetric face with deep-set eyes, divergent strabismus, high nasal bridge, and high arched palate (Supplementary Figure 1). Standard X-ray showed scoliosis that was 35 degrees with a Risser index of 4. Neurological examination revealed spastic quadriparesis with brisk tendon reflexes, a pseudobulbar syndrome with dysarthria and dysphagia, dystonia, ataxia, and lower limbs proprioception deficit.

Currently, at 32 years, the patient daily presents with drop attack of the lower limbs, without loss of consciousness. Spasticity, contractures, ataxia, peripheral neuropathy, dysarthria, and dysphagia are worsening with aging. She uses a wheelchair and requires assistance with activities of daily life, but can still feed herself. Her treatment consists in lamotrigine, coenzyme Q10, clonazepam, sotalol, alprazolam, and levetiracetam. She is receiving speech therapy, physiotherapy, occupational therapy, and psychological support.

TABLE 1 Summary of the clinical and genetic features of the patient in this study compared with EMPF1 patients described with a *de novo* heterozygous mutation in the GTPase domain of DNM1L.

	Trujillano et al. (12)	Whitley et al. (13)	Verrigni et al. (14)	Longo et al. (15)	Keller et al. (9)	Liu et al. (10)	Wei et al. (16)	This study
Mutation	c.607G>A p.(Val203Ile)	c.95 G>C p.(Gly32Ala)	c.668G>T p.(Gly223Val)	c.436G>A p.(Asp146Asn)	c.115A>G p.(Ser39Gly)	c.116G>A p.(Ser39Asn)	c.445G>A p.(Gly149Ar)	c.176C>A p.(Thr59Asn)
Inheritance	*de novo*	*de novo*	*de novo*	*de novo*	*de novo*	*de novo*	*de novo*	*de novo*
Gender	female	female	female	female	male	male	male	female
Age	8 months	7 years	6 years	5 years	10 years	3 years	4.5 years	32 years
Early developmental delay	+	+	-	+	+	+	+	+
Hypotonia	NA	+	-	++	+	+	+	+
Spasticity	+	+	NA	+	-	+	-	++
Dystonia	+	NA	NA	NA	+	NA	NA	+
Seizures	-	-	++ (>2.5 y)	-	+ (>8 y)	-	-	**+ (>18 y)**
Peripheral neuropathy	+ (unspecified)	+ (sensory)	NA	++ (axonal, sensory)	+ (axonal, sensory)	NA	+ (axonal, sensory)	++ (axonal, sensory)
Feeding difficulties/failure to thrive	+	+	NA	+	++	NA	NA	+
Ataxia	NA	+	+	+	NA	NA	+	+
Nystagmus	+	+	NA	+	-	NA	-	+
Optic nerve atrophy	-	+	NA	-	-	NA	NA	+
Facial dysmorphism	NA	+	NA	NA	+	NA	-	+
Microcephaly	NA	+	NA	-	+	+	NA	-
Brain MRI anomalies	Abnormal myelination, cerebral white matter atrophy	-	T2 hyperintensities in the posterior white matter regions and in the cortical areas. Global cerebral and cerebellar atrophy	-	Left cerebellar venous angioma (non specific)	T2 hyperintensity of basal ganglia, ventriculomegaly	Delayed myelination, thin corpus callosum	-
Scoliosis	NA	+	NA	-			NA	+
Other	Areflexia, Tongue fasciculations, Craniosynostosis, Chorea, Recurrent respiratory infections, Bilateral vocal cord paralysis	aphthous ulcers			Mitral valva insufficiency		Strabismus, mild cognitive impairment, dysarthria, equinous foot deformity	Insensitivity to pain, dysarthria, delayed menarche

10.3389/fneur.2022.937885

Brain MRI, performed in childhood, was controlled at adulthood and remained unremarkable. A fluorodeoxyglucose (FDG)-positron emission tomography (PET) revealed basal ganglia hypermetabolism compared to cerebral cortex. At adult age, lumbar puncture showed normal intracranial pressure and normal glucose and cells in cerebrospinal fluid. Metabolic screening (plasma and urinary amino acids, very-long-chain fatty acid) was unremarkable, except for increased lactate:pyruvate and 3-hydroxybutyrate:acetoacetate ratios, which were more pronounced post-prandially (lactate 2.41 mmol/L, nl 0.4–1.8; L:P 18.5, nl <15; 3OHB:AA 3.5, nl <1). At 23 years, a severe axonal sensory neuropathy was detected in the four limbs by nerve conduction studies (NCS).

Genetic investigations

The patient underwent serial genetic investigations (molecular karyotyping, *POLG* sequencing, spino-cerebellar-ataxia/Friedreich/dentatorubral-pallidoluysian triplet expansions analyses) that were unremarkable. Clinical exome sequencing was performed on DNA extracted from the whole blood of the patient and her parents, with Illumina NextSeq technology, according to the manufacturer's protocol (Supplementary material and method). In the proband, a heterozygous *DNM1L* c.176C>A p.(Thr59Asn) (Chr12(GRCh38): g.32701488 C>A) variant was detected (NM_001278464.1). The ClinVar accession number is SCV001780462. The variant was confirmed by PCR and direct Sanger sequencing. The primer sequences and reaction conditions are available upon request. This variant is not listed in genomic variant database (GnomAD). Paternity and maternity were molecularly confirmed, and the variant was not found in the parents suggesting that it arose *de novo* (paternal coverage 146X; maternal coverage 99X) (Supplementary Figure 2). The pathogenicity of the variant was assessed *in silico* using multiple prediction software, with results strongly supporting his deleterious and damaging effect, classified as class 5 variant by the American College of Medical Genetics ACMG prediction program (PS2, PS3, PP2, PP3, PP5). DNA next-generation sequencing did not detect any additional variant nor CNV on the second *DNM1L* allele (coverage 100% >20X). Moreover, no additional candidate causal variant was identified by clinical exome (in particular, no mutation was detected in the *OPA1* gene with a coverage of 99.95% >20X). In the proband, cDNA short- and long-range amplification and sequencing revealed that the mutant and the wide-type *DNML1* alleles are both expressed, in similar proportion (50%-50%), in blood extracted lymphocytes, in lymphoblastoid cells, and in fibroblasts (Supplementary Figure 2 and Supplementary material and method).

In addition, mitochondrial genome sequencing performed with Illumina MiSeq technology showed the m.10254G>A p.(Asp66Asn) variant in *MT-ND3* (NC_012920) at 1.5% heteroplasmy in blood, at 9.9% heteroplasmy in urine, and at 1.3% heteroplasmy in skeletal muscle. This variant has no frequency in MitoMap and is classified as pathogenic in ClinVar (accession number VCV000155887). In the mother, this mitochondrial variant was found at 1.3% heteroplasmy in urine but was not significantly detected in blood (Supplementary Figure 2).

Biochemical and histological characterizations

The Thr59Asn substitution is located in the GTPase domain, within a stretch of highly conserved residues of the switch I essential for the ligand binding, the catalytic activity of the enzyme, and the interaction with other domains, such as the switch 2 (5). *In silico* structural modeling of DNM1L Thr59Asn and comparison with the wild-type, nucleotide-free structure (PDB:4H1U) indicated conformational changes in the switch s1, $\alpha E1^G$ helix, and two disorders loop, the 80-loop and the loop connecting $\alpha E1^G$ and the β2A sheet (Figure 1A). In addition, bioinformatics tests predicted that the Thr59Asn variant affects the stability of DNM1L (Supplementary Figure 3). While contradictory results were obtained according to the predictive tools used for the nucleotide-free structure, the Thr59Asn substitution is predicted to destabilize the protein in its nucleotide-bound state, particularly in the GDP-bound one (Supplementary Figure 3B). We characterized the skin fibroblasts from the patient carrying the DNM1L p.Thr59Asn mutation to explore its pathogenic nature. Unexpectedly, by Western blot, we showed a strong decrease of DNM1L protein expression (Figure 1B), with the very faint of signal corresponding to the two 81-83Kda bands generally revealed by DNM1L immunostaining. In a process that remains to be understood, the mutated DNML1 form would complex with the wide-type DNML1 form and be degraded. Interestingly, in the patient fibroblasts, the profile of OPA1 isoforms is also different, although no mutation or splicing alteration was detected by NGS and long-range *OPA1* RNA studies (data not shown).

As loss of DNM1L function leads to a block in mitochondrial and peroxisomal fission, we conducted microscopic organelles' imaging by fluorescent MitoTracker Green probe and immunostaining against the peroxisomal membrane protein 70, respectively. Normal skin fibroblasts show a set of dynamic tubular networks with some isolated mitochondria that we could fragment by bioenergetic stress (Figure 2A). 3D analysis and morphometric measurements revealed a hyper-connected mitochondrial network (Figure 2A) without any isolated mitochondria. After antimycin/oligomycin treatment, which induces a mitochondrial stress by the inhibition of complexes III and V, the mitochondrial network remained tubular with some swollen elements. As hyper-fusion requires

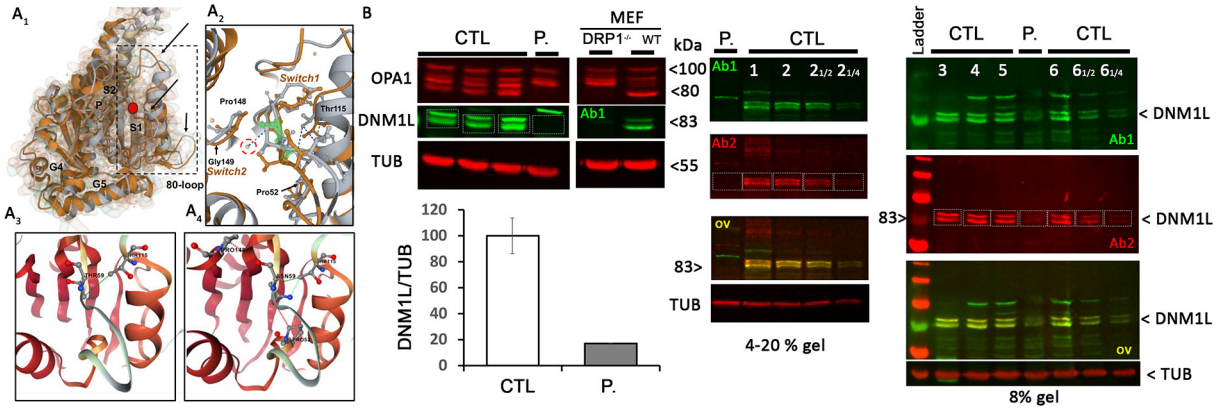

FIGURE 1
DNM1L/DRP1 immunostaining shows the loss of *DNM1L* normal forms in patient fibroblasts. **(A_1)** Comparison of the GTPase domain structure of nucleotide-free, wild-type (orange, pdb code 4H1U) and mutated THR59ASN DNM1L (gray) in ribbon and Gaussian volume representation, using RCSB pairwise structure alignment tool. The mutation site is indicated by a red circle. Modeling indicates a disorganization of the switch 1 in which the mutation is located, but also in the unique 80-loop, $\alpha E1^G$ helix and the loop connecting $\alpha E1^G$ and the β2A sheet (indicated by black arrow). **(A_2)** Close-up view of the switch1 in the nucleotide-free structure of the WT (orange) and mutated (gray) DNM1L. ASN59 is underlined in green. Water molecules are represented in yellow. The catalytic water molecule connecting switch I (THR59) with switch II (GLY149) by hydrogen bonds is circled in red. This interaction is lost with the amino acid switch THR59ASN. Amino acids interacting with THR59 or ASN59 are indicated. Detailed view of amino acid interactions in nucleotide-free wild-type **(A_3)** and mutated **(A_4)** protein structures. Hydrophobic interaction is in green, hydrogen bonds in red, and VDW in blue. Analysis was performed using Dynamut2. **(B)** OPA1 and DNM1L/DRP1 protein quantification and α-tubulin (TUB) as loading control in control (CTL) and patient (P.) fibroblasts. Control and DRP1 knock out MEFs: Mouse embryonic Fibroblasts models. On the right, overlay yellow staining of 2 DNM1L/DRP1 antibodies Ab1 and 2 indicates specific staining. ≪ ½ ≫ and ≪ ¼ ≫: controls were charged at 1/2 and ¼ to control the linearity range of DNM1L signal detection.

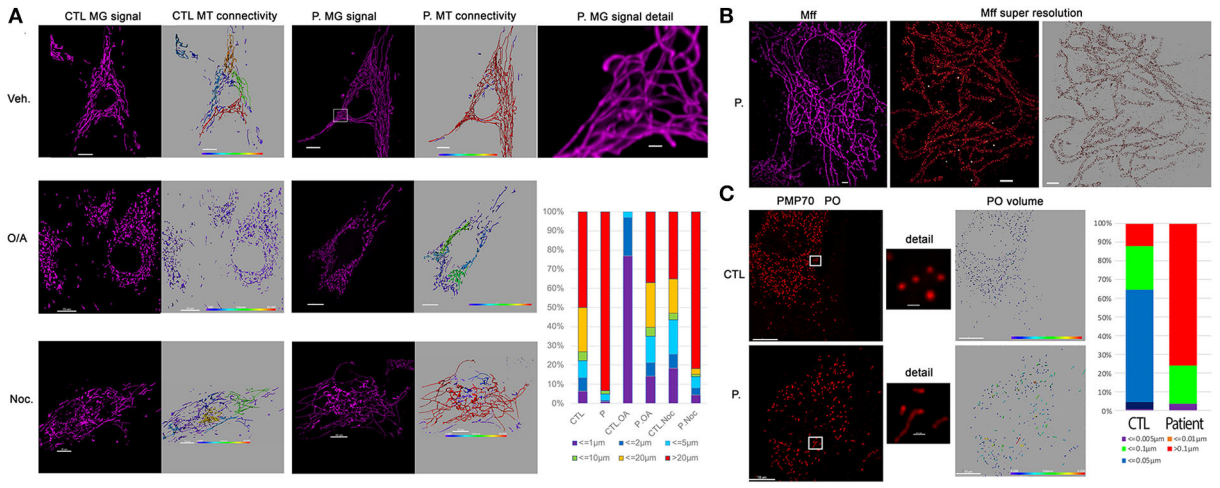

FIGURE 2
Patient fibroblasts show highly connected mitochondrial network and elongation of peroxisome compare to control. **(A)** Representative fluorescent images of mitochondrial network structure (in purple) in control (CTL) and patient (P.) fibroblasts. Mitochondrial volume was assessed using the MitoTracker Green fluorescent signal which was analyzed using Imaris software. The color code highlights the different lengths of the mitochondrial tubules with short isolated mitochondria in violet and connected network in red. To present the changes in mitochondrial morphology in patient's cells, types of mitochondria were classified into six groups according to mitochondrial volume, for example, red color represents mitochondria > 20 μm^3. Oligomycin 4 μg/ml coupled to antimycin 2 μg/ml (O/A) treatment leads to mitochondrial fission within 4 h in CTL cells. 6 h nocodazole (Noc), 10 μM disrupts microtubules. **(B)** Immunostaining against mitochondrial Mff DRP1 receptor. Representative TIRF image of mitochondria (left, in purple) shows the hyper-connectivity of the network. Single-molecule localization microscopy dSTORM was used to analyze mitochondrial MFF distribution. The white dots are the fiducial signals used to control drift during acquisition. Scale bar: 2 μm. **(C)** Immunostaining against peroxisomal PMP70 protein. Peroxisome (PO) volume was assessed using fluorescent signal by Imaris software and color-coded. To present the changes in peroxisome morphology in patient's cells, types of Peroxisomes were classified into five groups according to peroxisome volume, for example, red color represents peroxisomes > 20 μm^3. Scale bar = 10 μm; Scale bar in details 1 μm.

mitochondria to be brought together, the microtubule network was chemically disrupted using nocodazole to prevent mitochondrial movements. Following cytoskeletal depolymerization, the mitochondrial network remained abnormally connected in the patient's fibroblasts suggesting an absence of fission. We performed immunostaining of Mff, the mitochondrial outer membrane DRP1 receptor, by super-resolution microscopy and confirmed normal Mff distribution on mitochondrial hyper-connected network of the mutated fibroblasts (Figure 2B). Compared to control fibroblasts, disclosing small and abundant peroxisomes, mutated fibroblasts showed a decreased number of peroxisomes, which appeared significantly elongated (Figure 2C). These results strongly suggest a defect in DRP1 function, with downstream consequences on mitochondrial fission and peroxisomal shape in the DNM1L p.Thr59Asn fibroblasts.

Transmission electron microscopy (TEM) pictures of patient fibroblasts confirmed the presence of enlarged peroxisomes (17) with many peroxisomes in autophagic vacuoles and longer mitochondria than in control cells (Figure 3A). Immunohistological studies of a muscle biopsy revealed no specific anomaly, and only one ragged red fiber was detected. However, muscle TEM disclosed elongated mitochondria, with long slender protrusions from some mitochondria, likely corresponding to mitochondrial nano-tunnels. No ultrastructure defect was evidenced, with normal cristae distribution, apart from a couple of mitochondrial profiles with some degenerated cristae. Subsarcolemmal concentric laminated bodies and several multiple degenerative myelinoid intramitochondrial foci were identified (Figure 3B). No respiratory chain complex enzymatic deficiency was shown in muscle and skin biopsy.

Discussion

Here, we report the oldest EMPF1 patient, whose clinical presentation recapitulates the entire phenotypic spectrum of *DNM1L*-related encephalopathy, except for the microcephaly and brain MRI anomalies (Table 1). This patient shows a complex neurological phenotype associating developmental delay, progressive spastic quadriplegia, dystonia, dysarthria, dysphagia, axonal neuropathy, ataxia, nystagmus, optic atrophy, epilepsy, low sensitivity to pain, scoliosis, delayed menarche, and learning difficulties. Peripheral neuropathy, usually described as axonal with predominant sensory loss, is constantly reported in EMPF1 patients harboring a heterozygous DNM1L variant in the GTPase domain. This peripheral neuropathy is progressive, as confirmed by electroneuromyography examinations of the patient, which showed a drastic decrease of the sensory nerve action potentials and worsening of muscle denervation signs between ages 7 and 23. Interestingly, delayed menarche described in our patient may also be part of the *DNM1L*-related phenotypic spectrum as it was already reported in another 27-year-old female harboring a *de novo* heterozygous *DNM1L* variant in the GED domain (18).

The first case of lethal EMPF1 encephalopathy due to defective mitochondrial and peroxisomal fission was described in 2007, in a new-born girl harboring a *de novo* heterozygous mutation in DRP1 middle domain, and presenting with microcephaly, abnormal brain development, optic atrophy, persistent lactic acidemia, and mildly elevated plasma concentration of very-long-chain fatty acids (19). Additional descriptions of severe lethal forms of EMPF1 associated with *de novo* heterozygous variants located in DRP1 middle domain were reported (9, 11, 20–22). Outside the DRP1 middle domain, *DNM1L* variants were also reported in the GTPase domain, initially at a heterozygous state associated with isolated autosomal dominant optic atrophy and at compound heterozygous state associated with autosomal recessive EMPF1 (23). More recently, several patients suffering from encephalopathy due to defective mitochondrial and peroxisomal fission-1 were described with *de novo* heterozygous variants located in the GTPase domain, as observed in our patient (9, 10, 12–16) (Table 1). Interestingly, most of the mutated amino acids in this latter cohort (Ser39, Asp146, Gly149) were reported as the most relevant residues of the five GTP-binding stretches, as the Thr59 residue mutated in our patient (5).

A dominant-negative mechanism is classically hypothesized for heterozygous mutations located in the GTPase domain, as they affect the enzymatic domain of the protein without altering the capacity of the protein to homopolymerize, leading to a loss of function of the wild-type protein within the homopolymers (24). This dominant-negative effect was also suggested by the functional experiments on DNM1L/DRP1 (Thr59Asn) mutant cells and model organism studies (2, 5, 25, 26). However, the present study revealed an almost complete loss of DNM1L protein in the mutated fibroblasts, which suggests the degradation of the mutated and non-mutated DNM1L proteins. As the complete loss of DNM1L/DRP1 in mice is embryonic lethal, our results raise questions concerning DNM1L/DRP1 complex instability within different tissues and its downstream consequences on this patient's clinical presentation.

In addition, the phenotype of our proband might be influenced by the heteroplasmic presence of the m.10254G>A p.(Asp66Asn) variant in *MT-ND3*. This variant was reported at 90% heteroplasmy in the muscle sample of a patient presenting with a severe Leigh syndrome associated with early developmental regression and ophthalmoplegia (27). However, the 1.3% heteroplasmy level measured in muscle sample of our patient is very low, and no necrotic lesion in the brainstem, basal ganglia, or thalamus, and characteristic of the Leigh syndrome was observed by brain MRI. Consequently, the contribution of this mitochondrial variant to the DNM1L patient clinical presentation is most likely not preponderant.

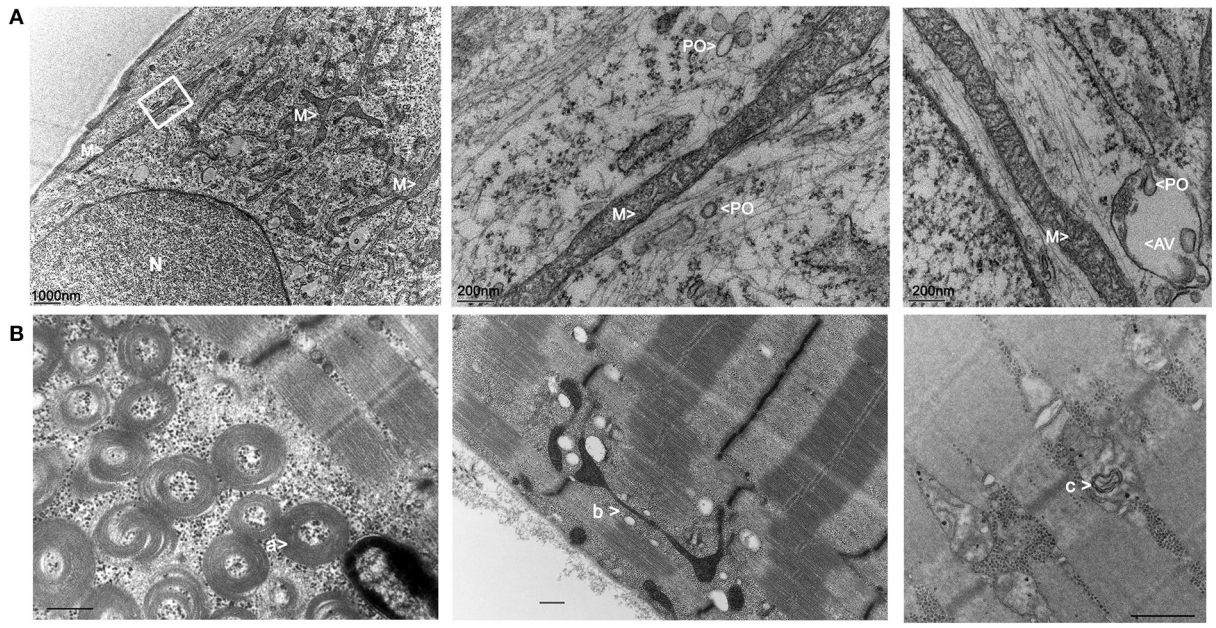

FIGURE 3
Electron microscopy imaging of the patient fibroblasts and muscle. **(A)** Skin fibroblasts: M, mitochondria; PO, peroxisomes; N, nucleus; AV, autophagic vacuole. **(B)** Muscle biopsy: a: concentric laminated bodies; b: mitochondrial nano-tunnel; c multiple degenerative myelinoid intramitochondrial foci.

EMPF1 phenotype overlaps with the clinical spectrum of other diseases linked to proteins involved in mitochondrial dynamics fusion (MFN2, OPA1) and fission (MFF, MID49/MIEF2, DNM2). EMPF1 is clinically very similar to Behr's syndrome (OMIM #210000) due to biallelic *OPA1* mutations (28) and to EMPF2 (OMIM #614785) due to biallelic *MFF* mutations (29). Mitochondrial morphology is maintained through the opposing forces of fission and fusion, and this balance is crucial in muscles and neurons. Interestingly, functional studies have already demonstrated the essential role of threonine-59 in Drp1. In *C. elegans DNM1L/DRP1* ortholog gene, the analogous Thr61Asn mutation has a strong dominant-negative effect on mitochondrial morphology, by inhibiting the mitochondrial outer membrane fission (25). Moreover, in COS-7 cells transfected with the DNM1L/DRP1 (Thr59Asn) allele, the mitochondrial network invariably collapsed into large perinuclear aggregates, composed of clustered mitochondrial tubules, reflecting a defective distribution of the fused mitochondrial network throughout the cell (26).

In this respect, reconstruction of 3D fluorescence microscopy images showed a hyper-connected mitochondrial network in the patient fibroblasts, compared to control, and a defect of fragmentation in mitochondrial stress context. This was well described in *DNM1L*-related optic atrophy or encephalopathy, contrasting with hyper-fragmentation observed in *OPA1*-related optic atrophy (14, 15, 19, 30). In muscle, the long slender double-membrane protrusions from mitochondria likely correspond to nano-tunnels that connect the matrices of non-adjacent mitochondria, which might emphasize immobilized mitochondria "in distress" (31). These protrusions are observed in normal tissue but are more abundant in presence of mtDNA mutations (32). Similarly, TEM analyses of the patient muscle revealed the presence of concentric laminated bodies that are common to other mitochondrial myopathies (33). Altogether, these peculiar observations reflect mitochondrial stress in our patient and should be confirmed in future by additional muscle sample analyses of EMPF1 patients.

DNM1L protein also mediates peroxisomal fission. Peroxisomes are dynamic and multifunctional organelles involved in the beta-oxidation of the very-long-chain fatty acids and in the formation of plasmalogen, which is an important component of the myelin. Very-long-chain fatty acid dosages performed in our DNM1L/DRP1 (Thr59Asn) patient showed normal results (data not shown), while our data revealed a decreased number of significantly elongated peroxisomes, as already reported for other DNM1L patients (15). Additional studies demonstrated that DNM1L/DRP1 is recruited by PEX11 to the peroxisome membranes to induce their division and that the dominant-negative DNM1L/DRP1 (Thr59Asn) mutant reduces peroxisome abundance (2). More recently, X-ray structure analyses of DNM1L confirmed that threonine-59 is located in the switch I motif and is essential for the GTPase reaction involved in mitochondrial and peroxisome

segregations (5). The great impact of the p.(Thr59Asn) mutation on peroxisomal network and shape is thus a central contribution to the severity of the clinical phenotype reported here (15, 19, 24).

This work evidences a novel *de novo* heterozygous *DNM1L* mutation causing an original adult presentation of encephalopathy due to defective mitochondrial and peroxisomal fission-1 EMPF1. Structural anomalies of mitochondria and peroxisomes observed in the primary cell culture from skin biopsy attest the main impact of *DNM1L*/DRP1 (Thr59Asn) mutation on mitochondrial and peroxisomal dynamics, which has to be correlated with the original post-translational modifications of DNM1L and OPA1, emphasizing the complexity of DRP1 regulation and its role in causing EMPF1 pathogenicity.

Data availability statement

The datasets presented in this study can be found in online repositories. The name of the repository and accession number can be found below: National Center for Biotechnology Information (NCBI) CinVar, https://www.ncbi.nlm.nih.gov/clinvar/, VCV001195874.1, (accessed May 6, 2022).

Ethics statement

The studies involving human participants were reviewed and approved by Institutional Review Board Committee of the University Hospital of Angers Authorization number: AC-2012-1507. The patients/participants provided their written informed consent to participate in this study. Written informed consent was obtained from the individual(s) for the publication of any potentially identifiable images or data included in this article.

Author contributions

IM, CL, and AC: drafting of the manuscript. IM, CL, AC, NG, and GL: revision of the manuscript. IM and AC: study concept or design. GG, AC, VB, DK, RV, OH, CL, and NG: acquisition of data. AC, CL, VB, BW, AV, and CL: interpretation of data. All authors contributed to the article and approved the submitted version.

Funding

This work was supported by "Université d'Angers." AV is supported by a Henry Wellcome Fellowship (215888/Z/19/Z).

Acknowledgments

We are thankful to the patient and her family for participating in the study. We thank Katharina DULIEU from the Department of Physical and Rehabilitation Medicine, Libramont, Belgium, for the clinical follow-up of the patient. We thank the University of Angers, SCIAM Microscopy Core Facility, SFR ICAT, F-49000 Angers, France.

Conflict of interest

The authors declare that the research was conducted in the absence of any commercial or financial relationships that could be construed as a potential conflict of interest.

Publisher's note

All claims expressed in this article are solely those of the authors and do not necessarily represent those of their affiliated organizations, or those of the publisher, the editors and the reviewers. Any product that may be evaluated in this article, or claim that may be made by its manufacturer, is not guaranteed or endorsed by the publisher.

Supplementary material

The Supplementary Material for this article can be found online at: https://www.frontiersin.org/articles/10.3389/fneur.2022.937885/full#supplementary-material

References

1. Koch A, Thiemann M, Grabenbauer M, Yoon Y, McNiven MA, Schrader M. Dynamin-like protein 1 is involved in peroxisomal fission. *J Biol Chem.* (2003) 278:8597–605. doi: 10.1074/jbc.M211761200

2. Li X, Gould SJ. The dynamin-like GTPase DLP1 is essential for peroxisome division and is recruited to peroxisomes in part by PEX11. *J Biol Chem.* (2003) 278:17012–20. doi: 10.1074/jbc.M212031200

3. Bonekamp NA, Vormund K, Jacob R, Schrader M. Dynamin-like protein 1 at the Golgi complex: a novel component of the sorting/targeting machinery en route to the plasma membrane. *Exp Cell Res.* (2010) 316:3454–67. doi: 10.1016/j.yexcr.2010.07.020

4. Kraus F, Roy K, Pucadyil TJ, Ryan MT. Function and regulation of the divisome for mitochondrial fission. *Nature.* (2021) 590:57–66. doi: 10.1038/s41586-021-03214-x

5. Wenger J, Klinglmayr E, Fröhlich C, Eibl C, Gimeno A, Hessenberger M, et al. Functional mapping of human dynamin-1-like GTPase domain based on x-ray structure analyses. *PLoS ONE.* (2013) 8:e71835. doi: 10.1371/journal.pone.0071835

6. Koirala S, Guo Q, Kalia R, Bui HT, Eckert DM, Frost A, et al. Interchangeable adaptors regulate mitochondrial dynamin assembly for membrane scission. *Proc Natl Acad Sci U S A.* (2013) 110:E1342–1351. doi: 10.1073/pnas.1300855110

7. Joshi AU, Minhas PS, Liddelow SA, Haileselassie B, Andreasson KI, Dorn GW, et al. Fragmented mitochondria released from microglia trigger A1 astrocytic response and propagate inflammatory neurodegeneration. *Nat Neurosci.* (2019) 22:1635–48. doi: 10.1038/s41593-019-0486-0

8. Ishihara N, Nomura M, Jofuku A, Kato H, Suzuki SO, Masuda K, et al. Mitochondrial fission factor Drp1 is essential for embryonic development and synapse formation in mice. *Nat Cell Biol.* (2009) 11:958–66. doi: 10.1038/ncb1907

9. Keller N, Paketci C, Edem P, Thiele H, Yis U, Wirth B, et al. novo DNM1L variant presenting with severe muscular atrophy, dystonia and sensory neuropathy. *Eur J Med Genet.* (2021) 64:104134. doi: 10.1016/j.ejmg.2020.104134

10. Liu X, Zhang Z, Li D, Lei M, Li Q, Liu X, et al. DNM1L-related mitochondrial fission defects presenting as encephalopathy: a case report and literature review. *Front Pediatr.* (2021) 9:626657. doi: 10.3389/fped.2021.626657

11. Piccoli C, Scrima R, D'Aprile A, Chetta M, Cela O, Pacelli C, et al. Pathogenic DNM1L Variant (1085G>A) linked to infantile progressive neurological disorder: evidence of maternal transmission by germline mosaicism and influence of a contemporary in cis variant (1535T>C). *Genes (Basel).* (2021) 12:1295. doi: 10.3390/genes12091295

12. Trujillano D, Bertoli-Avella AM, Kumar Kandaswamy K, Weiss ME, Köster J, Marais A, et al. Clinical exome sequencing: results from 2819 samples reflecting 1000 families. *Eur J Hum Genet.* (2017) 25:176–82. doi: 10.1038/ejhg.2016.146

13. Whitley BN, Lam C, Cui H, Haude K, Bai R, Escobar L, et al. Aberrant Drp1-mediated mitochondrial division presents in humans with variable outcomes. *Hum Mol Genet.* (2018) 27:3710–9. doi: 10.1093/hmg/ddy287

14. Verrigni D, Di Nottia M, Ardissone A, Baruffini E, Nasca A, Legati A, et al. Clinical-genetic features and peculiar muscle histopathology in infantile DNM1L-related mitochondrial epileptic encephalopathy. *Hum Mutat.* (2019) 40:601–18. doi: 10.1002/humu.23729

15. Longo F, Benedetti S, Zambon AA, Sora MGN, Di Resta C, De Ritis D, et al. Impaired turnover of hyperfused mitochondria in severe axonal neuropathy due to a novel DRP1 mutation. *Hum Mol Genet.* (2020) 29:177–88. doi: 10.1093/hmg/ddz211

16. Wei Y, Qian M. Case report: a novel *de novo* mutation in DNM1L presenting with developmental delay, ataxia, and peripheral neuropathy. *Front Pediatr.* (2021) 9:604105. doi: 10.3389/fped.2021.604105

17. Kors S, Hacker C, Bolton C, Maier R, Reimann L, Kitchener EJA, et al. Regulating peroxisome-ER contacts via the ACBD5-VAPB tether by FFAT motif phosphorylation and GSK3β. *J Cell Biol.* (2022) 221:e202003143. doi: 10.1083/jcb.202003143

18. Assia Batzir N, Bhagwat PK, Eble TN, Liu P, Eng CM, Elsea SH, et al. De novo missense variant in the GTPase effector domain (GED) of DNM1L leads to static encephalopathy and seizures. *Cold Spring Harb Mol Case Stud.* (2019) 5:a003673. doi: 10.1101/mcs.a003673

19. Waterham HR, Koster J, van Roermund CWT, Mooyer PAW, Wanders RJA, Leonard JV, et al. lethal defect of mitochondrial and peroxisomal fission. *N Engl J Med.* (2007) 356:1736–41. doi: 10.1056/NEJMoa064436

20. Ladds E, Whitney A, Dombi E, Hofer M, Anand G, Harrison V, et al. De novo DNM1L mutation associated with mitochondrial epilepsy syndrome with fever sensitivity. *Neurol Genet.* (2018) 4:e258. doi: 10.1212/NXG.0000000000000258

21. Ryan CS, Fine AL, Cohen AL, Schiltz BM, Renaud DL, Wirrell EC, et al. *De novo* DNM1L variant in a teenager with progressive paroxysmal dystonia and lethal super-refractory myoclonic status epilepticus. *J Child Neurol.* (2018) 33:651–8. doi: 10.1177/0883073818778203

22. Schmid SJ, Wagner M, Goetz C, Makowski C, Freisinger P, Berweck S, et al. Novo dominant negative mutation in DNM1L causes sudden onset status epilepticus with subsequent epileptic encephalopathy. *Neuropediatrics.* (2019) 50:197–201. doi: 10.1055/s-0039-1685217

23. Gerber S, Charif M, Chevrollier A, Chaumette T, Angebault C, Kane MS, et al. Mutations in DNM1L, as in OPA1, result in dominant optic atrophy despite opposite effects on mitochondrial fusion and fission. *Brain.* (2017) 140:2586–96. doi: 10.1093/brain/awx219

24. Gerber S, Charif M, Chevrollier A, Chaumette T, Angebault C, Kane S, et al. Reply: The expanding neurological phenotype of DNM1L-related disorders. *Brain.* (2018) 141:e29. doi: 10.1093/brain/awy027

25. Labrousse AM, Zappaterra MD, Rube DA, van der Bliek AM. C elegans dynamin-related protein DRP-1 controls severing of the mitochondrial outer membrane. *Mol Cell.* (1999) 4:815–26. doi: 10.1016/S1097-2765(00)80391-3

26. Smirnova E, Griparic L, Shurland DL, van der Bliek AM. Dynamin-related protein Drp1 is required for mitochondrial division in mammalian cells. *Mol Biol Cell.* (2001) 12:2245–56. doi: 10.1091/mbc.12.8.2245

27. Leshinsky-Silver E, Lev D, Malinger G, Shapira D, Cohen S, Lerman-Sagie T, et al. Leigh disease presenting in utero due to a novel missense mutation in the mitochondrial DNA-ND3. *Mol Genet Metab.* (2010) 100:65–70. doi: 10.1016/j.ymgme.2010.02.002

28. Bonneau D, Colin E, Oca F, Ferré M, Chevrollier A, Guéguen N, et al. Early-onset Behr syndrome due to compound heterozygous mutations in OPA1. *Brain.* (2014) 137:e301. doi: 10.1093/brain/awu184

29. Koch J, Feichtinger RG, Freisinger P, Pies M, Schrödl F, Iuso A, et al. Disturbed mitochondrial and peroxisomal dynamics due to loss of MFF causes Leigh-like encephalopathy, optic atrophy and peripheral neuropathy. *J Med Genet.* (2016) 53:270–8. doi: 10.1136/jmedgenet-2015-103500

30. Chevrollier A, Guillet V, Loiseau D, Gueguen N, de Crescenzo M-AP, Verny C, et al. Hereditary optic neuropathies share a common mitochondrial coupling defect. *Ann Neurol.* (2008) 63:794–8. doi: 10.1002/ana.21385

31. Vincent AE, Turnbull DM, Eisner V, Hajnóczky G, Picard M. Mitochondrial Nanotunnels. *Trends Cell Biol.* (2017) 27:787–99. doi: 10.1016/j.tcb.2017.08.009

32. Vincent AE, White K, Davey T, Philips J, Ogden RT, Lawless C, et al. Quantitative 3D Mapping of the Human Skeletal Muscle Mitochondrial Network. *Cell Rep.* (2019) 26:996–1009.e4. doi: 10.1016/j.celrep.2019.03.051

33. Vincent AE, Ng YS, White K, Davey T, Mannella C, Falkous G, et al. The Spectrum of Mitochondrial Ultrastructural Defects in Mitochondrial Myopathy. *Sci Rep.* (2016) 6:30610. doi: 10.1038/srep30610

frontiers | Frontiers in Neurology

TYPE Case Report
PUBLISHED 19 October 2022
DOI 10.3389/fneur.2022.1016393

Check for updates

OPEN ACCESS

EDITED BY
Giovanni Meola,
University of Milan, Italy

REVIEWED BY
Mohamed Kazamel,
University of Alabama at Birmingham, United States
Angelo Torrente,
University of Palermo, Italy

*CORRESPONDENCE
Yan Wang
wangyanwang@bjmu.edu.cn
Gui-Qiang Wang
john131212@126.com

SPECIALTY SECTION
This article was submitted to Neuromuscular Disorders and Peripheral Neuropathies, a section of the journal Frontiers in Neurology

RECEIVED 10 August 2022
ACCEPTED 23 September 2022
PUBLISHED 19 October 2022

CITATION
Cheng H, Lv H, Wang Y and Wang G-Q (2022) Case report: Wallerian degeneration: The innate-immune response to adult-onset Still's disease peripheral nerve injury. *Front. Neurol.* 13:1016393. doi: 10.3389/fneur.2022.1016393

COPYRIGHT
© 2022 Cheng, Lv, Wang and Wang. This is an open-access article distributed under the terms of the Creative Commons Attribution License (CC BY). The use, distribution or reproduction in other forums is permitted, provided the original author(s) and the copyright owner(s) are credited and that the original publication in this journal is cited, in accordance with accepted academic practice. No use, distribution or reproduction is permitted which does not comply with these terms.

Case report: Wallerian degeneration: The innate-immune response to adult-onset Still's disease peripheral nerve injury

Hao Cheng[1], He Lv[2], Yan Wang[1]* and Gui-Qiang Wang[1]*

[1]Department of Infectious Diseases and the Center for Liver Diseases, Peking University First Hospital, Beijing, China, [2]Department of Neurology, Peking University First Hospital, Beijing, China

Peripheral nerve injury is one of the rare complications of adult-onset Still's disease (AOSD). We report a 20-year-old woman diagnosed with AOSD combined with severe sensory neuropathy. She presented with a sore throat, joint pain, rash, and lymphadenopathy. After receiving glucocorticoid therapy, her fever, rash, and inflammatory markers improved. Unexpectedly, 3 weeks after the onset, she experienced sudden paresthesia in her extremities, decreased muscle strength, and diminished tendon reflexes. The electrophysiological examination and peripheral nerve biopsy confirmed immune-mediated severe sensory neuropathy. For the first time, we report typical Wallerian degeneration in AOSD patients with sensory neuropathy by nerve biopsy. Compared with other common symptoms, the delayed aggravation of neurological symptoms may be an important characteristic of sensory neuropathy secondary to AOSD. We emphasize that intensive attention to neurological symptoms after general symptoms control, administration of adequate and appropriate prolonged immunosuppressive therapy, and long-term follow-up are essential for these patients.

KEYWORDS

adult-onset Still's disease, sensory neuropathy, sensory ganglionopathy, Wallerian degeneration, delayed aggravation, innate-immune response

Introduction

Peripheral nerve injury is a rare complication of adult-Onset Still's Disease (AOSD). Wallerian degeneration was observed in distal myelinated fibers, which may cause the delayed aggravation of neurological symptoms during glucocorticoid treatment in an AOSD patient.

The rapidly progressive clinical deterioration of the AOSD patient presented here posed a diagnostic challenge requiring an extensive diagnostic workup. In the literature, only a few case reports describe the main manifestations of AOSD with sensory neuropathy, while most were short of pathological evidence.

For the first time, we report typical Wallerian degeneration in AOSD patients with severe sensory neuropathy by nerve biopsy. Careful distinction and prompt diagnosis are critical for adherence to immunosuppressive therapy.

Case description

A 20-year-old woman was presented to the emergency clinic with fever and sore throat for one week and joint pain, weakness in limbs, and slight numbness of fingertips and tongue. She denied any tobacco or alcohol (illicit drugs) use, and her family history was not notable. After admission, she continued to experience a high fever (T_{max} 40°C). One week after her admission, scattered congestive pinpoint itching rashes appeared on her chest, abdomen, back, and limbs, without ulceration or scaling, accompanied by liver function abnormalities (alanine aminotransferase, ALT_{max} 227 IU/L, reference range of 7–40 IU/L; aspartate transaminase, AST_{max} 193 IU/L, reference range of 13–35 IU/L). The rash was noticeable when the body temperature rose and faded when the body temperature dropped. Inflammatory markers such as serum ferritin (max to >7,500 ng/ml, reference range 11–306.8 ng/ml), erythrocyte sedimentation rate (ESR, max to 50 mm/h, reference range 0–20 mm/h), C-reactive protein (CRP, max to 104 mg/L, normal <5 mg/L), and lactate dehydrogenase (LDH, max to 900 IU/L, reference range 100–240 IU/L) were all significantly elevated. The lymph node ultrasound revealed extensive enlarged superficial lymph nodes (Figure 1).

The clinical diagnosis of AOSD is generally reached by exclusion while investigating a patient with a fever of unknown origin. We carried out detailed screenings for infectious diseases, autoimmune diseases, and tumors. Laboratory examinations for common pathogens (respiratory pathogens, such as influenza virus, mycoplasma, chlamydia, legionella, adenovirus, etc.) and specific disease-related pathogens (cytomegalovirus/Epstein-Barr virus, mycobacterium tuberculosis, rickettsia of typhus, *Coxiella burnetii* of Q fever, Salmonella typhi, Brucella, etc.) were all negative. The blood culture was repeatedly negative, and screening tests for AIDS, hepatitis B, hepatitis C, and syphilis were negative. Antibodies that indicate some autoimmune diseases, such as the anti-double-stranded DNA antibody, antineutrophil cytoplasmic antibodies (ANCA), anti-extractable nuclear antigen (ENA) antibodies, immunoglobulins, protein electrophoresis, immunofixation electrophoresis, complements, rheumatoid factor were all no meaningful found. No significant findings were found in tumor markers, bone marrow biopsy, and imaging examinations of underlying malignant tumors. According to the Yamaguchi criteria (1), the patient was diagnosed with AOSD.

Methylprednisolone (60 mg Q.D.) was administrated as starting dose with subsequent tapering. After glucocorticoid treatment, her main symptoms were relieved, and inflammatory markers rapidly decreased, but the paresthesia and decreased sensation in her extremities decreased muscle strength with MRC (Medical Research Council) grades 2–3, tendon reflexes diminished to the disappearance, and imbalance progressed remarkably so that she was not able to walk or write; even words started slurring in the third week. We ordered an MRI of the spine with no positive findings, excluding the possibility of the patient's lumbosacral ganglion compression. Heavy metal and toxicants blood tests were negative. Head MRI and cerebrospinal fluid (CSF) examination were normal. The anti-ganglioside GQ1b antibody was negative in both serum and cerebrospinal fluid. Polymyositis antibodies, and paraneoplastic syndrome-related antibodies (Hu, Yo, and Ri antibodies) showed no meaningful findings. We performed the electrophysiological examination, and nerve and muscle biopsy revealed immune-mediated extensive peripheral nerve injury (Supplementary Figures 1–3). Intriguingly, electron microscopy images of nerve biopsy demonstrate the typical manifestation of distal axonal degeneration due to nerve injury—Wallerian degeneration (Figure 2). Paresthesia, muscle weakness, and tendon reflexes were fully recovered with MRC grades five after 9 months of glucocorticoid therapy in the patient, and slight numbness of the fingers and toes remained. She got fully recovered after more than 3 years of regular follow-up.

Discussion

Neurological complications of AOSD are rare (2), usually seizures, cranial nerve palsy, aseptic meningoencephalitis, and Miller-Fisher syndrome, of which immune-mediated peripheral nerve injury has been reported minimally. We summarized previous case reports of AOSD combined with peripheral nerve injuries in Table 1. The delayed onset of peripheral nerve injury involving medium and large myelinated sensory fibers occurred 2 weeks to 3 years after the onset of the early symptoms, which was a great challenge for early identification and accurate diagnosis.

We confirmed the patient's severe immune-mediated sensory neuropathy by electrophysiological examination and pathological findings from nerve and muscle biopsies. For etiologies of sensory nerve injury, sensory ganglionopathy should be ruled out. After detailed examinations and long-term follow-up observation, we excluded the common causes of sensory ganglionopathies, such as lumbosacral ganglion compression, paraneoplastic sensory ganglionopathy, and sensory ganglionopathy secondary to Sjögren disease.

Guillain-Barré syndrome was the disease we focused on differential diagnosis in the diagnosis of sensory neuropathy in this patient. Although we found that this patient had a number of inconsistencies with the common Guillain-Barré syndrome and its common variants, for example, we found no obvious antecedent events such as infection, vaccination, and

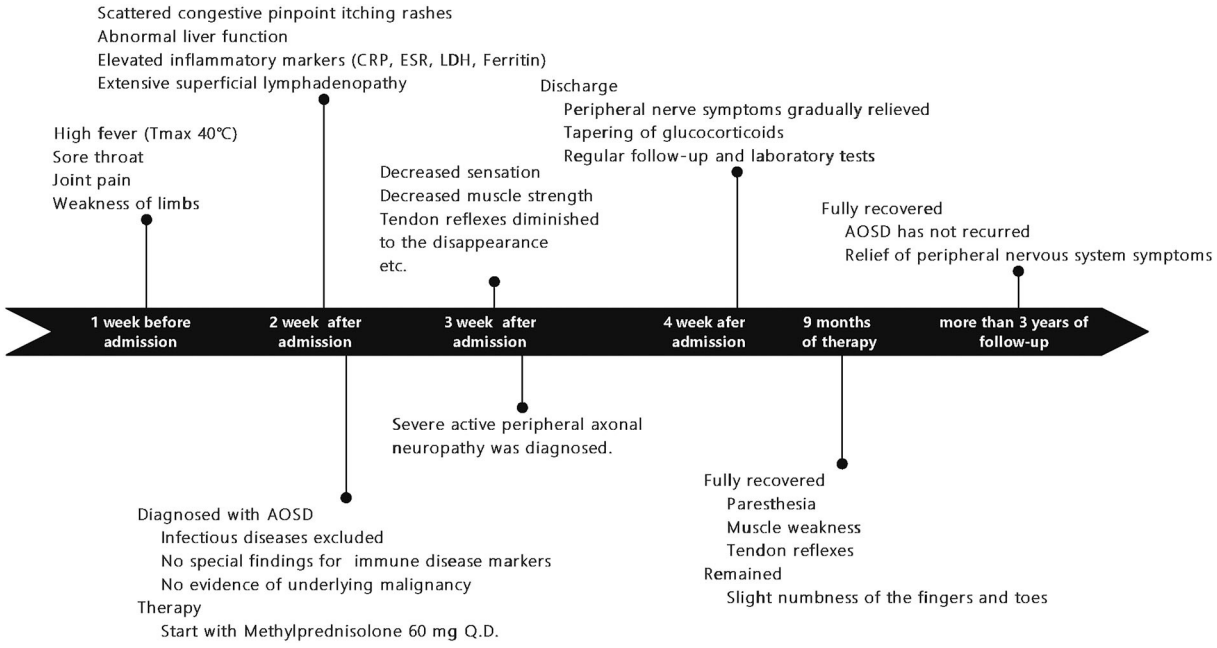

FIGURE 1
A timeline showing symptoms and exams/interventions performed on the patient. AOSD, Adult-onset Still's disease; CRP, C-reactive protein; LDH, lactate dehydrogenase, ESR, erythrocyte sedimentation rate.

other predisposing factors such as drugs, surgery, radiation, chemotherapy, etc. that contributed to the Guillain-Barré syndrome. The patient had normal CSF cell count and protein levels, negative for anti-ganglioside GQ1b antibody, and the patient's response to glucocorticoid therapy was good. However, based on the results of the nerve conduction study and nerve and muscle pathology, theoretically, we cannot in an absolute sense rule out the possibility of the Guillain-Barre syndrome, since both Guillain-Barre syndrome and sensory neuropathy secondary to AOSD are peripheral nervous system damage due to autoimmune abnormalities. From the perspective of disease "monism," combined with the patient's symptoms, auxiliary examination and treatment response, and long-term regular follow-up monitoring, we currently tend to believe that the patient's severe sensory neuropathy is secondary to AOSD.

Although the pathogenesis of sensory neuropathy and AOSD is unclear, the possible mechanism of its peripheral nerve damage may be related to both inflammatory response and autoimmune response. The enhanced inflammatory factors may directly attack the dorsal root ganglion, anterior horn motor neurons, interstitial structure, myelin, and axons, or infringement of nerve nourishing blood vessels cause peripheral nerve lesions (7). The autoimmune response can directly cause disease or facilitate potential pathogenic conditions, resulting in peripheral nerve lesions similar to the Guillain-Barré syndrome. Although AOSD diagnosis requires exclusion of infection, it has also been suggested that one of the possible pathogenesis of peripheral nerve injury is triggered by multiple infectious factors in an autoimmune background. They may become potentially invasive antigens to trigger peripheral neuroimmune damage, which causes the immune recognition system to misjudge and trigger autoimmune attacks. The delayed aggravation of peripheral nerve injury symptoms is consistent with this kind of autoimmune injury characterized by a prodromal period (8).

Most previous case reports lack pathological evidence; only one of the case reports showed axonal damage with mild demyelination changes by nerve biopsy. For the first time, we report typical Wallerian degeneration in AOSD patients with sensory neuropathy by neuromuscular biopsy. Wallerian degeneration is a common pathological feature of neurological disorders. It has been said that Wallerian degeneration is an active and dynamic cellular process that provides a chance for axons to reconnect, rather than rebuilding the entire nerve projection by axon regeneration, which was regulated at molecular and cellular levels (9). In response to immune-mediated injury, Wallerian degeneration showed as an orchestrated interplay between innate-immune cells and molecules produced by immune and non-immune cells.

Previous studies reported that activation of innate immunity plays a major role in the pathogenesis of AOSD, and innate immunity is also proven to contribute to the mechanism of Wallerian degeneration. All the symptoms, including that of peripheral nerve injury, were recovered by long-term glucocorticoid therapy. Delayed aggravation of the patient's

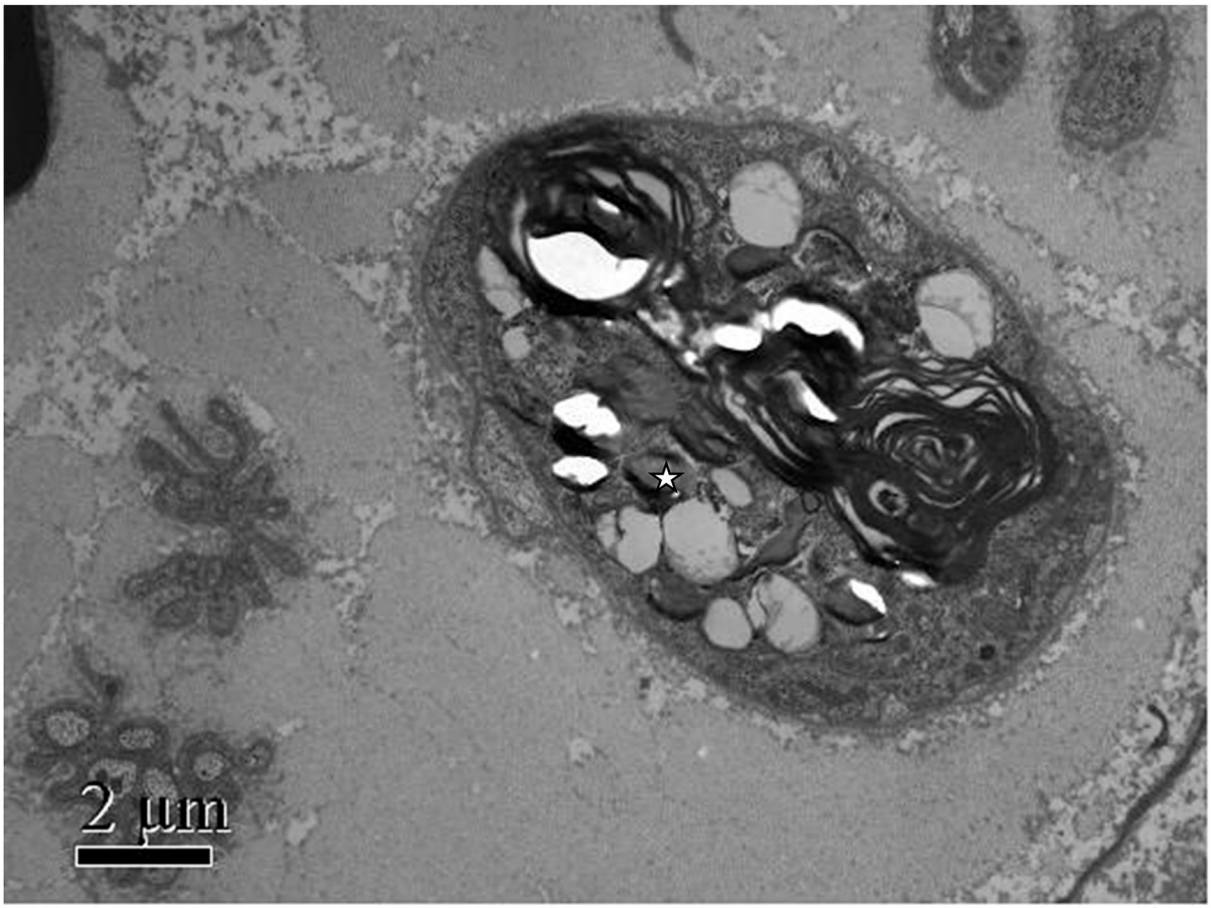

FIGURE 2
Patient's photograph of the sural nerve biopsy specimen. Electron microscopic findings: Myelinated nerve fibers were extensively destroyed. Wallerian degeneration could be observed (white star), and Schwann cells and macrophages were not observed. Scale bars: 2μm.

peripheral nervous system symptoms may be due to Wallerian degeneration and dynamic self-destruction progress, which is a response to active systemic immunity in AOSD. Effective innate immune response to Wallerian degeneration after the injury is key to neurological recovery.

Since reports of sensory neuropathy secondary to AOSD are rare, there is currently no unified treatment recommendation. The patient started immunosuppressive therapy for AOSD. After a diagnosis of severe sensory neuropathy, we recommended glucocorticoids in combination with cyclophosphamide (CTX), but the patient refused because of concerns about the side effects of CTX. Due to economic reasons, the patient refused to use intravenous immunoglobulin (IVIG) and plasma exchange therapy and maintained glucocorticoids alone, followed by long-term tapering and eventually got remission. Combined with the above immunopathological mechanisms of AOSD and Wallerian degeneration, we believe that immunotherapy, in addition to glucocorticoids, such as glucocorticoids combined with other immunosuppressive agents, IVIG, or plasma exchange, may improve patient outcomes. Therefore, attention to neurological symptoms, early diagnosis, and initiation of adequate immunosuppressive therapy is critical to improving prognosis in patients with such severe sensory neuropathy.

Conclusion

In conclusion, we present the rare case of a 20-year-old woman who was diagnosed with AOSD with severe sensory neuropathy. For the first time, we report typical Wallerian degeneration found in the patient by neuromuscular biopsy. By elucidating possible autoimmune mechanisms and reviewing previous reports, we conclude that Wallerian degeneration is the innate immune response to AOSD peripheral nerve injury, which may cause the delayed aggravation of neurological

TABLE 1 Summary of literature on adult-onset Still's disease* with peripheral nerve injury.

Author, year of publication	Case characteristics						
	Gender/ age	Clinical symptoms	Peripheral nerve lesion and the time of onset	Electrophysiological examination and pathological biopsy	CSF examination	Treatment	Prognosis/follow-up
Marie (3)/1999	M/17	High fever, sore throat, myalgia, headache	Left facial nerve palsy and weakened tendon reflex occurred three weeks after onset	NA	White blood cell count 25 × 10^6/L, Protein quantitative 1 g/L	aspirin 3 g/d	All symptoms disappeared after anti-inflammatory treatment / no recurrence after seven months of follow-up
Desai (4)/2002	F/23	Joint pain, rash, fever	Miller-Fisher syndrome occurred three years after the onset, and tendon reflexes were weakened	Prolonged F wave latency of right tibial nerve	Cell count is negative; protein quantification is 0.41 g/L	Intravenous injection of immunoglobulin,2 mg/kg*d, for three days	After one week of immunotherapy, Miller-Fisher syndrome disappeared, and there was still persistent fatigue. /The follow-up results were not reported.
Zhao (5)/2008	M/60	High fever, joint pain	Five months after the onset of illness, bilateral limb weakness	Sensory nerve conduction velocity slows down, and sural nerve biopsy shows axonal damage with mild demyelination changes	No positive findings	Intravenous maintenance dose of prednisone, 20 mg/d	The right muscle weakness disappeared after eight days of hormone shock/All symptoms disappeared after four months of follow-up.
LI (6)/2009	F/62	High fever, joint pain, skin sheal	Numbness and pain in both lower limbs occurred more than two weeks after the onset	Electromyography suggests peripheral nerve damage in both lower limbs	NA	Low-dose glucocorticoids and tripterygium glycosides, etc.	After hormone and immunosuppressive treatment, the skin lesions, fever, joint pain, and skin lesions subsided, and the remaining symptoms were numbness of the lower limbs. No further follow-up was reported.

*All the cases are in line with Yamaguchi criteria. CSF, cerebrospinal fluid.

10.3389/fneur.2022.1016393

symptoms during glucocorticoid treatment in an AOSD patient. We emphasize that intensive attention to neurological symptoms, administration of adequate and appropriate prolonged immunosuppressive therapy, and long-term follow-up are particularly important for these patients.

Data availability statement

The raw data supporting the conclusions of this article will be made available by the authors, without undue reservation.

Ethics statement

Written informed consent was obtained from the individual(s) for the publication of any potentially identifiable images or data included in this article.

Author contributions

HC wrote this case report, including the concept of this article, the definition of intellectual content, and data acquisition. HL guided the microphotograph identification of the patient's sural nerve biopsy specimens and the discussion on sensory neuropathy. YW and G-QW designed and reviewed the manuscript for its intellectual content. YW is the principal investigator. HC, HL, and G-QW are the main participants in the project. All authors contributed to the article and approved the submitted version.

Funding

This work was supported by the National Natural Science Foundation of China (#82070605) and the Science and Technology Department of Xinjiang Uygur Autonomous Region (#2020A03004-3).

Conflict of interest

The authors declare that the research was conducted in the absence of any commercial or financial relationships that could be construed as a potential conflict of interest.

Publisher's note

All claims expressed in this article are solely those of the authors and do not necessarily represent those of their affiliated organizations, or those of the publisher, the editors and the reviewers. Any product that may be evaluated in this article, or claim that may be made by its manufacturer, is not guaranteed or endorsed by the publisher.

Supplementary material

The Supplementary Material for this article can be found online at: https://www.frontiersin.org/articles/10.3389/fneur.2022.1016393/full#supplementary-material

References

1. Yamaguchi M, Ohta A, Tsunematsu T, Kasukawa R, Mizushima Y, Kashiwagi H, et al. Preliminary criteria for classification of adult Still's disease. *J Rheumatol.* (1992) 19:424–30.

2. Giacomelli R, Ruscitti P, Shoenfeld Y. A comprehensive review on adult onset Still's disease. *J Autoimmun.* (2018) 93:24–36. doi: 10.1016/j.jaut.2018.07.018

3. Marie I, Levesque H, Perraudin N, Cailleux N, Lecomte F, Courtois H. Aseptic meningitis and cranial nerve palsy revealing adult-onset Still's disease. *Clin Infect Dis.* (1999) 29:220–1. doi: 10.1086/520170

4. Desai SS, Allen E, Deodhar A. Miller Fisher syndrome in adult onset Still's disease: case report and review of the literature of other neurological manifestations. *Rheumatology.* (2002) 41:216–22. doi: 10.1093/rheumatology/41.2.216

5. Zhao H, Yuan Y, Li Y, Si C-W, Tian G-S, Wang G-Q, et al. Encephalic large arteries narrowness and peripheral neuropathy in a patient with adult-onset Still's disease. *Rheumatol Int.* (2008) 28:1261. doi: 10.1007/s00296-008-0599-3

6. Yanxi Li, Zhu Xi. Yang Shi, Diao Qingchun. Adult Still's disease complicated by peripheral neuropathy: a case report. *J Clin Dermatol.* (2009) 38:111–2. doi: 10.3969/j.issn.1000-4963.2009.02.023

7. Callaghan BC, Price RS, Chen KS, Feldman EL. The importance of rare subtypes in diagnosis and treatment of peripheral neuropathy. *JAMA Neurol.* (2015) 72:1510. doi: 10.1001/jamaneurol.2015.2347

8. Hughes RA, Cornblath DR. Guillain-Barré syndrome. *Lancet.* (2005) 366:1653–66. doi: 10.1016/S0140-6736(05)67665-9

9. Zhang K, Jiang M, Fang Y. The drama of Wallerian degeneration: the cast, crew, and script. *Annu Rev Genet.* (2021) 55:93–113. doi: 10.1146/annurev-genet-071819-103917

frontiers | Frontiers in Neurology

TYPE Case Report
PUBLISHED 24 October 2022
DOI 10.3389/fneur.2022.905725

Check for updates

OPEN ACCESS

EDITED BY
Giovanni Meola,
University of Milan, Italy

REVIEWED BY
Kishore Raj Kumar,
Garvan Institute of Medical Research, Australia
Chiara Fiorillo,
University of Genoa, Italy

*CORRESPONDENCE
Adrian Rodriguez-Hernandez
adrianrodriguez@health.fau.edu

SPECIALTY SECTION
This article was submitted to Neuromuscular Disorders and Peripheral Neuropathies, a section of the journal Frontiers in Neurology

RECEIVED 27 March 2022
ACCEPTED 30 September 2022
PUBLISHED 24 October 2022

CITATION
Rodriguez-Hernandez A, Mayo M, Jauregui L and Patel P (2022) Autosomal dominant GDAP1 mutation with severe phenotype and respiratory involvement: A case report. *Front. Neurol.* 13:905725. doi: 10.3389/fneur.2022.905725

COPYRIGHT
© 2022 Rodriguez-Hernandez, Mayo, Jauregui and Patel. This is an open-access article distributed under the terms of the Creative Commons Attribution License (CC BY). The use, distribution or reproduction in other forums is permitted, provided the original author(s) and the copyright owner(s) are credited and that the original publication in this journal is cited, in accordance with accepted academic practice. No use, distribution or reproduction is permitted which does not comply with these terms.

Autosomal dominant GDAP1 mutation with severe phenotype and respiratory involvement: A case report

Adrian Rodriguez-Hernandez[1]*, Meagan Mayo[2], Lilibeth Jauregui[2] and Pooja Patel[1,3]

[1]Department of Neurology, Charles E. Schmidt College of Medicine, Florida Atlantic University, Boca Raton, FL, United States, [2]Department of Internal Medicine, Charles E. Schmidt College of Medicine, Florida Atlantic University, Boca Raton, FL, United States, [3]Department of Neurology, Marcus Neuroscience Institute, Boca Raton, FL, United States

Charcot Marie Tooth (CMT) is a heterogeneous group of genetic disorders characterized by progressive motor and sensory neuropathy. CMT is a multi-gene disorder with several possible mutations responsible for a wide range of clinical presentations. A specific mutation of the ganglioside-induced-differentiation-associated protein 1 (*GDAP1*) gene is associated with the axonal subtype of CMT (CMT2K) which is inherited in an autosomal dominant fashion, as well as the demyelinating subtype (CMT4A) which is inherited in an autosomal recessive pattern. Phenotypic disease expression is largely dependent on these inheritance patterns. While the autosomal recessive form (CMT4A) exhibits severe disease with an early onset, the autosomal dominant variant (CMT2K) tends to have milder phenotypes and a later onset. We describe an atypical presentation of a patient with severe CMT2K with rapidly progressive polyneuropathy, respiratory failure, and dysphonia. We suggest that this case will inspire further evaluation of disease heterogeneity and variants.

KEYWORDS

Charcot Marie Tooth, GDAP1, case report, CMT2K, neuropathy

Introduction

Charcot Marie Tooth (CMT) is characterized by a clinically and genetically miscellaneous group of neuropathies, spanning a variety of Mendelian inheritance patterns. Greater than 1,000 different mutations in 80 disease-associated genes have been identified (1). Mutations in the ganglioside-induced-differentiation-associated protein 1 gene (*GDAP1*) are responsible for a subgroup of the hereditary motor and sensory neuropathies seen in Charcot Marie Tooth (2).

GDAP1-related mutations may be inherited in an autosomal recessive pattern (more common) or in an autosomal dominant pattern. *GDAP1* autosomal recessive inherited mutations, termed CMT4A, are characterized by demyelinating, axonal, or intermediate disease forms. CMT4A causes an early-onset, severe neuropathy that affects

all extremities and frequently leads to wheelchair dependence in young adult life (second-third decade). In the advanced stages of the disease, most of these patients acquire vocal cord paresis (unilateral or bilateral) and diaphragmatic weakness. On the other hand, autosomal dominant inherited mutations, termed CMT2K, are characterized by axonal disease and tend to have a more benign presentation characterized by slow progression, adult-onset, and more distal involvement. Most of these patients remain ambulant throughout their lives (3, 4). In isolated patients, CMT2K has been associated with characteristics more commonly associated with CMT4A, such as dysphonia or dysautonomia (5).

This case report describes an atypical course of CMT2K with rapidly progressive polyneuropathy, dysphonia, and respiratory failure in a patient with adult-onset, autosomal dominant disease.

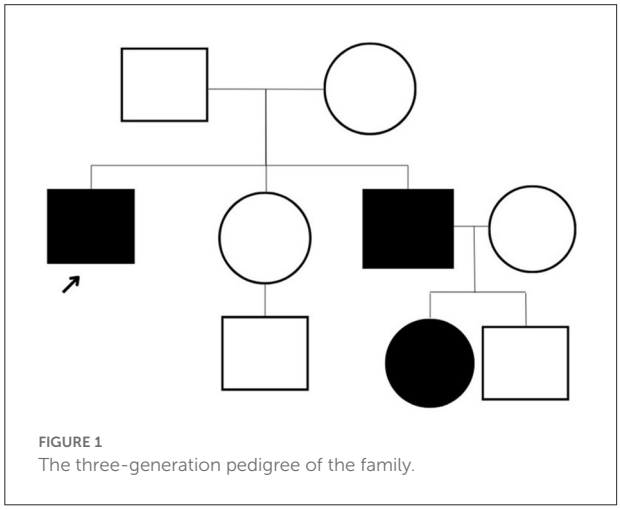

FIGURE 1
The three-generation pedigree of the family.

Case presentation

A previously healthy and physically active 63-year-old male presented to the hospital due to a sensation of chest "heaviness" and dysphonia. Further history revealed that for the past 2 years, the patient had progressive paresthesias, cramping, and weakness beginning in the right lower extremity and then spreading to the left lower extremity and distal upper extremities bilaterally. He was now mostly confined to a wheelchair after being diagnosed with CMT 1 year ago.

The patient underwent a comprehensive screen of 81 genes associated with peripheral neuropathies. Genomic deoxyribonucleic acid (gDNA) was isolated from the patient's whole blood. Sequence enrichment of the targeted coding exons and adjacent intronic nucleotides was carried out by a bait capture methodology using long biotinylated oligonucleotide probes followed by polymerase chain reaction (PCR) and Next-Generation sequencing. A compound heterozygous p. R120W mutation (also known as c.358C > T) was found at exon 3 of the *GDAP1* gene (NM_018972.4); resulting from a C to T substitution at nucleotide position 358. This mutation

TABLE 1 Motor and sensory nerve conduction studies of the bilateral upper and lower extremities.

Nerve	Stimulation site	Distance (cm)	Recording site	Latency (ms)			Amplitude (CMAP Mv; SNAP uV)			Velocity (m/s)		
	Motor			R	L	NL	R	L	NL	R	L	NL
Median	Wrist	22.5	APB	5.2	5	<4.2	0.3	0.8	> 5	52	47	>50
Median	Elbow		APB	9.5	9.8		0.3	0.9				
Ulnar	Wrist	22	ADM	4.5	3.4	<4.2	2	4.3	> 5	50	49	>53
Ulnar	B elbow	10	ADM	8.9	7.9		2	3.4		59	53	>53
Ulnar	A Elbow		ADM	10.6	9.8		2.4	3.9				
Peroneal	Fib Head		EDB	*NR	*NR	<6.1	*NR	*NR	>2.5	*NR	*NR	>40
Peroneal	Pop fossa	10	EDB	*NR	*NR		*NR	*NR		*NR	*NR	
Tibial	Ankle		AHB	*NR	*NR	<6.1	*NR	*NR	>3.0	*NR	*NR	>35
Tibial	Pop fossa		AHB	*NR	*NR		*NR	*NR		*NR	*NR	
Sensory												
Median	Wrist	14	Dig II	4	3.6	<3.6	38.4	28.5	>10	35	39	>39
Ulnar	Wrist	14	Dig V	4.1	3.1	<3.7	11.2	22.9	>15	34	45	>38
Radial	Forearm		Wrist	2.2	2	<3.1	26.5	24.4	>15			
Sural	Calf		Ankle	4.4	4.6	<4.0	6.1	4.7	>5.0	32	30	>35

ADM, abductor digiti minimi; AHB, abductor hallucis brevis; APB, abductor pollicis brevis; cm, centimeters; Dig, digit; EDB, extensor digitorum brevis; Fib, fibular; L, left; m/s, meters per second; ms, millisecond; NL, normal limit; Pop, popliteal; R, right; SNAP, sensory nerve action; uV, microvolt; NR, no response.

TABLE 2 Chronological clinical course of the patient.

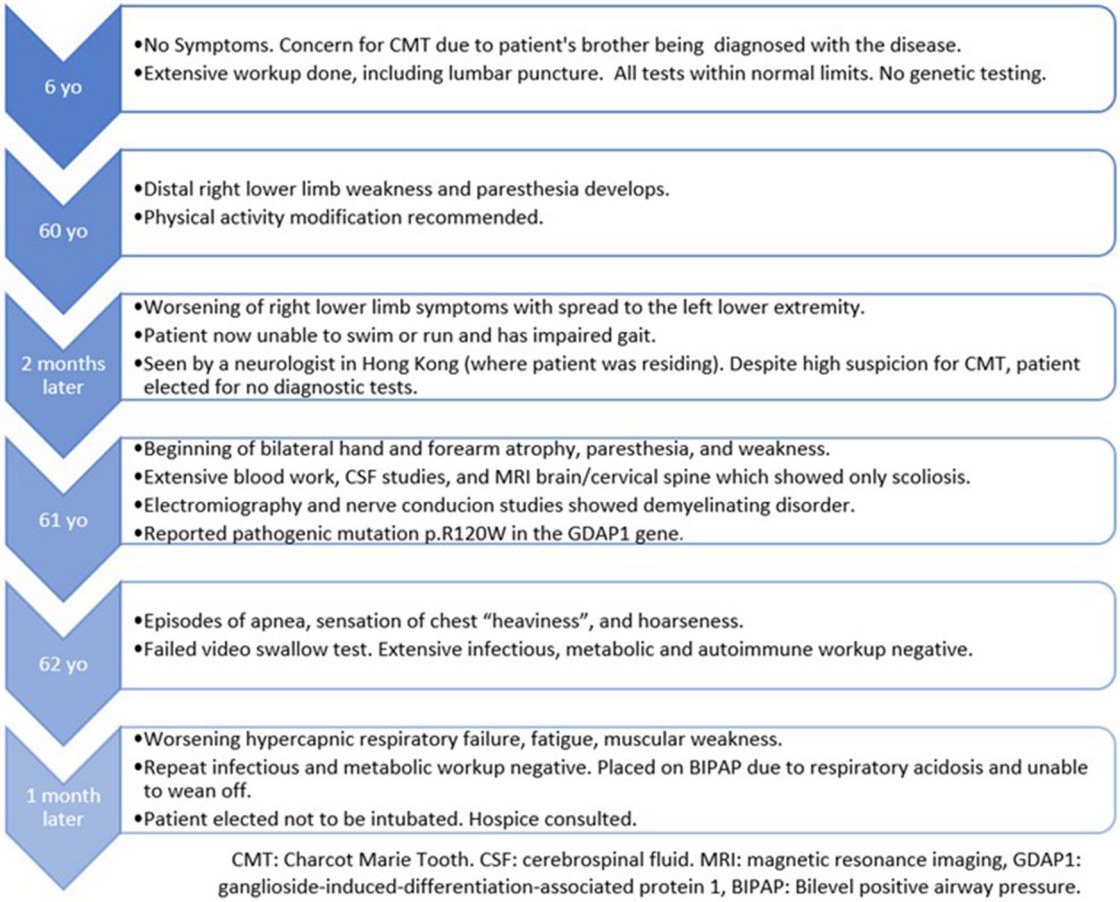

CMT: Charcot Marie Tooth. CSF: cerebrospinal fluid. MRI: magnetic resonance imaging, GDAP1: ganglioside-induced-differentiation-associated protein 1, BIPAP: Bilevel positive airway pressure.

is described as "Pathogenic" (class 5) according to the ACMG guideline. A survey of the patient's family history also revealed an extensive incidence of CMT consistent with an autosomal dominant inheritance pattern. Disease was absent in both parents, with the patient's brother diagnosed at age five and the brother's daughter at age four. However, these family members presented with milder symptoms such as difficulty walking, arched feet, and wasting of the muscles in the lower extremities (Figure 1).

The patient's neurological examination revealed weakness of the bilateral upper extremities, bilateral intrinsic hand muscles, and right wrist extensors with compromised handwriting. Additionally, the patient had bilateral proximal leg weakness, including impaired foot flexion and dorsiflexion. There was generalized areflexia with reduced pinprick, vibration, and thermic sensation in all extremities (up to the knees and wrists). Based on these findings, the patient was assigned a CMT neuropathy scale of 24/36, which indicates severe neuropathy. In regard to the patient's initial concern of "chest heaviness", chest X-ray was without abnormalities, although the patient was mildly tachypneic with the use of accessory muscles of respiration. The cardiac examination was unremarkable.

Laboratory tests did not reveal any acute abnormalities. Infections and acute coronary syndrome were excluded. Notably, there was an absence of paraprotein and a normal creatinine kinase. Anti-Ach binding, anti-Ach blocking, antineuronal, antiganglioside, and anti-myelin-associated glycoprotein precursor antibodies were all negative. The patient refused lumbar puncture for cerebrospinal fluid (CSF) studies (he verbally explained normal CSF results from 1 year ago, although we were unable to obtain this report). MRI of the brain and cervical spine, as well CT of the chest, were without abnormalities.

On further workup, nerve conduction studies (NCS) demonstrated evidence of right median axonopathy, left median and right ulnar mixed type neuropathy, and demyelinating left ulnar neuropathy. There was also evidence of a severe generalized sensory and motor neuropathy of the lower extremities with an absence of F and H waves (Table 1). Due to the patient's decreased phonation and weak cough, intrahospital speech therapy suggested outpatient follow up for formal evaluation of probable vocal cord impairment.

With imminent threat to life ruled out, the patient was ultimately discharged. Unfortunately, he was lost to follow up

TABLE 3 Clinical characteristics of patients with various autosomal dominant mutations in the ganglioside induced differentiation associated protein 1 (GDAP1) gene.

Study	Kim et al. (6)	Pakhrin et al. (7)	Sivera et al. (8)	Fu et al. (9)	Pezzini et al. (5)	Auranen et al. (10)	Chung et al. (11)
Country	Korea	China	Spain	China	Italy	Finland	Korea
Number of Patients	7	9	58	3	26	14	2
Mutation(s)	R120W Q218E R226K	V219G Q38R	R120W R22GK T157P	R120W C240Y	R120W R226S Q218E H123R Arg120Gly	H123R V795I (MFN2)	Q218E
Age onset (mean)	19.7 yrs	15.8 yrs	23.8 yrs	3 yrs	19.8 yrs	33.5 yrs	24.5 yrs
FDS Score (mean)	2.2	NA	1.3	NA	NA	NA	NA
CMTNS (mean/range)	11.1/6–25	NA/3–13	7.3/0–26	12.5/12–13	NA	NA	NA
Muscle Weakness	All LL weakness (R22K > R120W) Hand weakness (in 5/7 patients)	Mild in LL Severe in hands (Q38R mutation only)	Distal LL	Distal and proximal LL > UL	Distal LL Distal UL (in 4/26 patients)	Distal > proximal	Moderate in distal LL and UL
Wheelchair bound (number of patients)	No	Yes (1)	No	Yes (1)	No	NA	No
Foot deformities (percentage of patients)	Yes	Yes	Yes (85.2%)	Yes (80%)	Yes (<50%)	Yes	Yes
Sensory loss	V = P (28%) V > P (58%) Normal (14%)	Motor only	Non-specific sensory (57.1%)	V (33%)	NA	Motor only	Distal V and P
Vocal cord paresis diaphragmatic weakness hoarseness	No	No	No	No	No	Yes (1). Dysphonia (in MFN2 mutation)	No
Electrophysiological studies	CMAP: normal (UL), decreased (LL) MNCV: decreased (LL) SNAP: decreased (LL > UL)	MNCV: 40.9 m/s CMAP 2.1 mV	CMAP: decreased SNAP: decreased	MNCV/CMAP in 2 patients (mean): 56.1 m/s/2.1 mv	CMAP: Decreased (LL > UL)	SNAP: Decreased (LL > UL) MNCV: normal MNCV: normal	MNCV: mildly reduced/normal CMAP: mildly reduced/normal SNCV: normal.

CMTNS, charcot marie tooth examination score; FDS, functional disability score; LL, lower limbs; UL, upper limbs; V, vibration; P, pain; NA, not available; yrs, years; CMAP, compound muscle action potential; MNCV, motor nerve conduction velocity; SNAP, sensory nerve action potential; SNCV, sensory nerve conduction velocity; m/s, meter/second; mV, millivolts.

10.3389/fneur.2022.905725

and returned to the hospital 3 weeks later with worsening respiratory failure and dysphonia. At this time, arterial blood gas revealed persistent hypercapnia with hypoxemia, requiring Bilevel Positive Airway Pressure (BIPAP). Chest X-ray showed mild elevation of the left hemidiaphragm. An extensive workup for respiratory insufficiency excluded electrolyte abnormalities, myasthenia, autoimmune disease, substance abuse, infection, pulmonary embolism, spinal cord injury, and structural brain abnormalities. The patient developed worsening mental status in the setting of refractory hypercapnia and respiratory muscle fatigue. Per his wishes, the patient was not intubated and ultimately was transitioned to hospice care within 6 weeks of his initial presentation to this hospital (Table 2).

Discussion

Charcot-Marie Tooth presents heterogeneously with progressive motor and sensory polyneuropathy leading to weakness, muscle atrophy, loss of sensation, loss of deep tendon reflexes, and foot deformities. Mutations in the *GDAP1* gene are responsible for both an autosomal recessive early-onset severe demyelinating form of CMT (CMT4A) and a late-onset dominant form (CMT2K)—such as was seen in our patient. Specifically, our patient possessed a p.R120w mutation located in coding exon 3 in the *GDAP1* gene. This pathogenic mutation is the most common variant seen within CMT2K (3, 8). However, the severity of our patient's clinical presentation was inconsistent with current knowledge of this CMT2K subtype (Table 3).

Although the clinical phenotype within CMT genotypes may differ between individuals in one family, this patient's rapidly progressive disease in his 6th decade of life is a unique presentation of CMT2K. As described by Silveira et al. (8), the CMT2K usually does not present with respiratory failure, stridor, or vocal cord dysfunction. Rather, these are common characteristics of recessive forms (CMT4A). Therefore, extensive workup to rule out neuromuscular, infectious, toxic, cardiac, and metabolic etiologies of respiratory failure is essential in such atypical presentations. Although Abbousonan et al. (12) described multiple disorders of pulmonary function, sleep, and upper airway in patients with other CMT variants, these have not been documented in the CMT2K form. We believe our patient had a rapidly progressive restrictive pulmonary impairment secondary to diaphragmatic nerve dysfunction, as well as vocal cord impairment secondary to peripheral neuropathy affecting the vagus nerve and its laryngeal branches.

CMT2K is responsible for axonal neuropathy that is associated with (relatively) normal nerve conduction velocities (NCV), loss of myelinated axons, and regenerative sprouting. On the other hand, CMT4A causes demyelinating, axonal, or mixed type CMT that is characterized by segmental demyelination with a diffuse reduction in NCV (13). In additional to an unusually rapid onset and severe disease course, our patient also had an atypical neuropathy consisting of a mainly mixed pattern with a probable right concomitant carpal tunnel syndrome.

To our knowledge, we present the only documented case of CMT2K with adult-onset rapidly progressive respiratory failure and acute vocal cord dysfunction with evidence of mixed demyelinating and axonal neuropathy. This suggests that the phenotypic presentations of various types of CMT may extend beyond our current genotypic cognizance. This case will hopefully serve to motivate further research, disease understanding, and treatment optimization for those diagnosed with Charcot Marie Tooth.

Data availability statement

The original contributions presented in the study are included in the article/supplementary material, further inquiries can be directed to the corresponding author.

Ethics statement

Written informed consent was obtained from the individual(s) for the publication of any potentially identifiable images or data included in this article.

Author contributions

AR-H, MM, LJ, and PP contributed to the writing of the manuscript and critical revision of the manuscript. All authors gave important contributions to the final form of the manuscript.

Conflict of interest

The authors declare that the research was conducted in the absence of any commercial or financial relationships that could be construed as a potential conflict of interest.

Publisher's note

All claims expressed in this article are solely those of the authors and do not necessarily represent those of their affiliated organizations, or those of the publisher, the editors and the reviewers. Any product that may be evaluated in this article, or claim that may be made by its manufacturer, is not guaranteed or endorsed by the publisher.

References

1. Timmerman V, Strickland AV, Züchner S. Genetics of Charcot-Marie-Tooth (CMT) disease within the frame of the human genome project success. *Genes.* (2014) 5:13–32. doi: 10.3390/genes5010013

2. Cuesta A, Pedrola L, Sevilla T, García-Planells J, Chumillas MJ, Mayordomo F, et al. The gene encoding ganglioside-induced differentiation-associated protein 1 is mutated in axonal Charcot-Marie-Tooth type 4A disease. *Nat Genet.* (2002) 30:22–5. doi: 10.1038/ng798

3. Zimoń M, Baets J, Fabrizi GM, Jaakkola E, Kabzińska D, Pilch J, et al. Dominant GDAP1 mutations cause predominantly mild CMT phenotypes. *Neurology.* (2011) 77:540–8. doi: 10.1212/WNL.0b013e318228fc70

4. Sevilla T, Jaijo T, Nauffal D, Collado D, Chumillas MJ, Vilchez JJ, et al. Vocal cord paresis and diaphragmatic dysfunction are severe and frequent symptoms of GDAP1-associated neuropathy. *Brain.* (2008) 131(Pt 11):3051–61. doi: 10.1093/brain/awn228

5. Pezzini I, Geroldi A, Capponi S, Gulli R, Schenone A, Grandis M, et al. GDAP1 mutations in Italian axonal Charcot-Marie-Tooth patients: Phenotypic features and clinical course. *Neuromuscul Disord.* (2016) 26:26–32. doi: 10.1016/j.nmd.2015.09.008

6. Kim HS, Kim HJ, Nam SH, Kim SB, Choi YJ, Lee KS, et al. Clinical and neuroimaging features in Charcot-Marie-Tooth patients with GDAP1 mutations. *J Clin Neurol.* (2021) 17:52–62. doi: 10.3988/jcn.2021.17.1.52

7. Pakhrin PS, Xie Y, Hu Z, Li X, Liu L, Huang S, et al. Genotype-phenotype correlation and frequency of distribution in a cohort of Chinese Charcot-Marie-Tooth patients associated with GDAP1 mutations. *J Neurol.* (2018) 265:637–46. doi: 10.1007/s00415-018-8743-9

8. Sivera R, Frasquet M, Lupo V, García-Sobrino T, Blanco-Arias P, Pardo J, et al. Distribution and genotype-phenotype correlation of GDAP1 mutations in Spain. *Sci Rep.* (2017) 7:6677. doi: 10.1038/s41598-017-06894-6

9. Fu J, Dai S, Lu Y, Wu R, Wang Z, Yuan Y, et al. Similar clinical, pathological, and genetic features in Chinese patients with autosomal recessive and dominant Charcot-Marie-Tooth disease type 2K. *Neuromuscul Disord.* (2017) 27:760–5. doi: 10.1016/j.nmd.2017.04.001

10. Auranen M, Ylikallio E, Toppila J, Somer M, Kiuru-Enari S, Tyynismaa H. Dominant GDAP1 founder mutation is a common cause of axonal Charcot-Marie-Tooth disease in Finland. *Neurogenetics.* (2013) 14:123–32. doi: 10.1007/s10048-013-0358-9

11. Chung KW, Kim SM, Sunwoo IN, Cho SY, Hwang SJ, Kim J, et al. A novel GDAP1 Q218E mutation in autosomal dominant Charcot-Marie-Tooth disease. *J Hum Genet.* (2008) 53:360–4. doi: 10.1007/s10038-008-0249-3

12. Aboussouan LS, Lewis RA, Shy ME. Disorders of pulmonary function, sleep, and the upper airway in Charcot-Marie-Tooth disease. *Lung.* (2007) 185:1–7. doi: 10.1007/s00408-006-0053-9

13. Shy ME. Charcot-Marie-Tooth disease: an update. *Curr Opin Neurol.* (2004) 17:579–85. doi: 10.1097/00019052-200410000-00008

frontiers | Frontiers in Neurology

TYPE Case Report
PUBLISHED 14 November 2022
DOI 10.3389/fneur.2022.1033327

Check for updates

OPEN ACCESS

EDITED BY
Giovanni Meola,
University of Milan, Italy

REVIEWED BY
Yuan Xue,
Shandong Provincial Hospital Affiliated to Shandong First Medical University, China
Jowy Tani,
Taipei Medical University, Taiwan

*CORRESPONDENCE
Tao Li
ltll@163.com

†These authors have contributed equally to this work

SPECIALTY SECTION
This article was submitted to Neuromuscular Disorders and Peripheral Neuropathies, a section of the journal Frontiers in Neurology

RECEIVED 31 August 2022
ACCEPTED 23 September 2022
PUBLISHED 14 November 2022

CITATION
Dong M-X, Wang Q, Xu J-F, Hu L, Yu Y and Li T (2022) Case report: Recreational nitrous oxide abuse triggered peripheral neuropathy possibly through the immune-mediated pathogenesis. *Front. Neurol.* 13:1033327. doi: 10.3389/fneur.2022.1033327

COPYRIGHT
© 2022 Dong, Wang, Xu, Hu, Yu and Li. This is an open-access article distributed under the terms of the Creative Commons Attribution License (CC BY). The use, distribution or reproduction in other forums is permitted, provided the original author(s) and the copyright owner(s) are credited and that the original publication in this journal is cited, in accordance with accepted academic practice. No use, distribution or reproduction is permitted which does not comply with these terms.

Case report: Recreational nitrous oxide abuse triggered peripheral neuropathy possibly through the immune-mediated pathogenesis

Mei-Xue Dong[1†], Qing Wang[2†], Jun-Feng Xu[3†], Ling Hu[1], Ying Yu[1] and Tao Li[1*]

[1]Department of Neurology, Renmin Hospital of Wuhan University, Hubei General Hospital, Wuhan, China, [2]Department of Neurology, Wuhan No. 9 Hospital, Wuhan, China, [3]Department of Neurology, Ezhou Central Hospital, Ezhou, China

Nitrous oxide (N_2O), commonly known as laughing gas, is widely used in clinical practice and food industry. However, an increasing number of young people have been abusing N_2O for recreational purpose, resulting in many functional disorders and sometimes irreversible nerve damage. We present the case of a 20-year-old N_2O abuser who gradually developed peripheral neuropathy after continuously inhaling N_2O for 2 months. The neurological symptoms of the patient had kept exacerbation for the next 2 months until she came for medical care sitting in a wheelchair. We suggested the patient halting N_2O intake and supplementing methylcobalamine according to the standardized protocol. Her symptoms had partly recovered during the following 2 weeks but remained unchanged in another 2 weeks. Antibodies against ganglioside complexes were detected and anti-GM1 IgM antibodies were positive in both cerebrospinal fluid and serum. Intravenous immunoglobulin was given as an additional treatment and the patient's symptoms had significantly recovered further. The patient discharged walking by herself. Then she has been continuously followed up in outpatient department for the next 4 months and taking steroid hormone as well as methylcobalamine. Her symptoms gradually disappeared and all the electrophysiological parameters significantly improved. With this case we were able to show that N_2O-related peripheral neuropathy is not only a metabolic disorder but also an immune-mediated disease. N_2O intake can trigger a mimic Guillain-Barré syndrome.

KEYWORDS

nitrous oxide, peripheral neuropathy, ganglioside complexes, Guillain-Barré syndrome, immunoglobin, steroid hormone

Introduction

Nitrous oxide (N_2O), commonly known as laughing gas, is a colorless, non-irritating gas with a sweetish smell. It is widely used as an anesthetic in clinical practice and can also be easily obtained in the catering industry for whipping cream preparation and in the motor industry as a fuel booster (1). In the recent years, an increasing number of young people have been abusing N_2O for recreational purpose. In the UK, N_2O was the eighth most commonly used substance and its lifetime prevalence was about 38.6% (2). The N_2O abuse can cause hypotension, lung injury, apnea, and any other accidental injuries with a large dose in a short time. The chronic toxicities of N_2O are megaloblastic anemia, psychiatric syndromes and neurological injuries, including subacute combined degeneration, myeloneuropathy, myelopathy and peripheral neuropathy (3). To date, the mechanism of N_2O toxicity has not been clearly elucidated and vitamin B12 deficiency is the most extensively studied mechanism. Vitamin B12 is an important cofactor for methionine synthetase and methylmalonyl coenzyme A mutase and its deficiency can lead to a decrease of methionine, tetrahydrofolate, and S-adenosylmethionine, and an increase of homocysteine, 5-methyltetrahydrofolate, and methylmalonic acid, resulting in nerve demyelination and injury (4). In addition, N_2O can lead to NMDA antagonism, alteration of cerebral blood flow, and inhibition of the synthesis and release of xanthine and monoamines (5). Here we present the case of a 20-year-old N_2O abuser mimicking Guillain-Barré syndrome (GBS) with significant immune disturbances.

Case description

The patient was a 20-year-old camgirl without any other medical history and occasionally inhaled N_2O for fun in the last 2 years (Figure 1A). She had kept inhaling N_2O (about 10 whippets daily) after a failed investment 4 months ago. Two months later she gradually felt numbness and weakness in her lower limbs. She didn't pay attention to it and kept inhaling N_2O without any treatments. The numbness and weakness kept being heavier and her upper limbs also suffered. The superficial sensation had significantly decreased of both hands and legs below knees. She couldn't feed herself with hands (muscular strength: 3/5) nor stand up (proximal muscular strength: 3/5; distal muscular strength: 0/5), and came for medical care sitting in a wheelchair. Her limbs' muscular tone had decreased and all the tendon reflexes were disappeared while the overall muscle bulks were normal. The deep sensations of vibration, position, and movement stayed normal. Romberg sign and Babinski sign were negative. She had no defecation problems, psychiatric disorders, headache, epilepsy, cognition impairment, or any other neurological symptoms. She also had no history of vaccine injection, enteritis, or influenza in the last year.

Blood tests indicated slightly decreased hemoglobin (129 g/L) and increased mean corpuscular volume (97.8 fL). Plasma homocysteine level was significantly elevated (24.67 μmol/L) while the serum levels of folic acid, vitamin B12, and any other vitamins were normal. Magnetic resonance imaging hadn't found demyelination or any other abnormal focuses in both brain and spinal cord. Electromyography examination showed extensive peripheral nerve damage, involving motor nerve, sensory nerve, and nerve root. Axonal injuries were especially obvious and nerve damages of the lower limbs were significant heavier than that of upper limbs (Table 1).

N_2O-related peripheral neuropathy was diagnosed according to the medical history of N_2O abuse, typical clinical manifestations, and the above auxiliary examinations. Guillain-Barré syndrome (especially acute motor axonal neuropathy, AMAN) should also be considered as differential diagnosis. After all, the patient was suggested to halt N_2O intake and use methylcobalamine for supplementation according to the standardized protocol. The patient's symptoms had partly recovered during the following 2 weeks. The muscular strength of upper limbs increased to 4/5 while superficial sensation and muscular strength of lower limbs recovered slightly. These syndromes remained unchanged after another 2 weeks.

To obtain optimal treatments further, lumbar puncture was performed and cerebrospinal fluid (CSF) was obtained for tests. The leukocyte count of CSF was 3 cells per μl while the protein level was 0.23 g/L. Antibodies against ganglioside complexes were also detected using a commercial ELISA kit and anti-GM1 IgM antibodies were positive in both serum and CSF while anti-GM1 IgG antibodies were negative (Figure 1B). Intravenous immunoglobulin (0.4g/kg × 5 days) was then given as an additional treatment. The patient's symptoms had significantly improved a week later. Her muscular strength of upper limbs and proximal lower limbs increased to 5/5 when the distal lower limbs increased to 1/5. Her superficial sensation had also partly recovered. The patient discharged from the hospital and could walk independently with a steppage gait and take good care of herself.

Then she has been continuously followed up in outpatient department. Considering the amazing treatment outcome of immunoglobin, she accepted the injection of methylprednisolone (1,000 mg qd × 5 days) and orally took prednisone (60 mg qd × 5 days, 30 mg × 5 days, 15 mg qd × 5 days, 10 mg × 5 days) as follows. After that, she has been continuously taking prednisone 5 mg daily. Four months after the discharge from hospital, her numbness gradually disappeared and the muscular strength of distal lower limbs increased to 4/5. Her gait was almost normal and all the electrophysiological parameters significantly improved. The latencies of motor nerves, sensory nerves, and F waves had extensively decreased while the amplitudes had increased. The

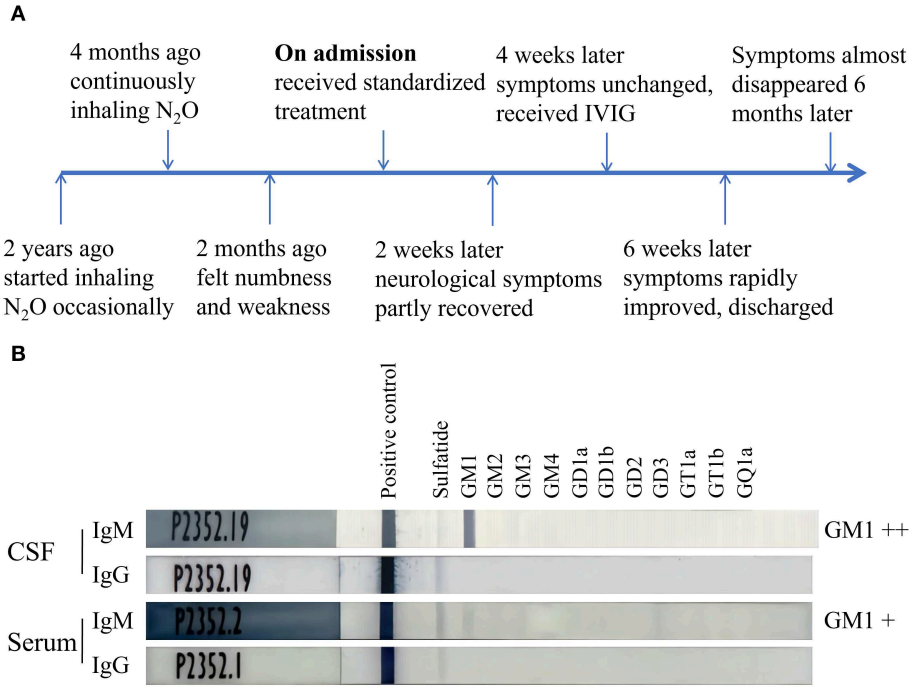

FIGURE 1
Timeline of the case and ELISA results of antibodies against ganglioside complexes. **(A)** The patient started inhaling N_2O occasionally 2 years ago, felt numbness and weakness 2 months ago, significantly improved after receiving the treatment of IVIG, and almost recovered 6 months after the admission. **(B)** ELISA tests indicated the anti-GM1 IgM antibodies were positive in both CSF and serum while anti-GM1 IgG antibodies were negative. IVIG, intravenous immunoglobulin; CSF, cerebrospinal fluid.

incidences of F waves also had significantly increased (Table 2). The patient and her parents were aware of the whole process and pleased with the treatment outcome in spite of the injury induced by lumbar puncture, high price of immunoglobulin, and potential side effects of prednisone.

Discussion

Commonly, recreational N_2O abuse is recognized to cause metabolic disorders with vitamin B12 deficiency. However, vitamin B12 deficiency is not sufficient to account for N_2O-induced peripheral neuropathy as these patients showed prominent motor superexcitability changes and less prominent sensory superexcitability changes in nerve excitability test when compared to patients with vitamin B12 deficiency (6). Here, we present the case of a 20-year-old N_2O abuser suffering peripheral neuropathy mimicking GBS with immune disturbances.

Peripheral neuropathy is the most common N_2O-related neurological disorder with a morbidity up to 97% (7). These patients primarily exhibited limb numbness or weakness, especially the lower limbs. Decreased muscle strength, superficial sensory disturbances, and decreased tendon reflex were the most common neurological signs according to the published report (7). Increased plasma homocysteine level is more sensitive than plasma vitamin B12 level for clinical diagnosis, as N_2O mainly consumes vitamin B12 in tissue but not blood (3). Electromyography of these patients indicated mixed axonal and demyelination injury, including motor and sensory nerves simultaneously. Abnormal F wave and H reflex were also found in the majority of N_2O abuser (8). All in all, the case we presented was a typical N_2O-related peripheral neuropathy according to these characteristics.

However, without the medical history of N_2O abuse, these patients were usually misdiagnosed as GBS (9). The absent medical history of vaccine injection, enteritis, or influenza before the onset didn't support the diagnosis of GBS. The course of disease progression of the patient was also significantly longer than the natural history of GBS (2–4 weeks). To our knowledge, GBS is more likely to occur in the middle-aged or aged population but not the youth. The electrophysiological features of N_2O abuser were dramatically different from those in acute inflammatory demyelinating polyradiculoneuropathy (a GBS variant), but exactly similar to another GBS variant (AMAN). It's difficult to differentiate N_2O abuse and AMAN according to those electrophysiological findings (10). Meanwhile, the injury severity of lower limbs

TABLE 1 Electrophysiological parameters of the case before the treatment with intravenous immunoglobulin.

Motor nerve	Segment	Lat (ms)	Amp (mV)	CV (m/s)	Dist (mm)
Medianus (L)	Wrist-APB	4.00	3.6		55.0
	Elbow-Wrist	8.75	3.6	48.4	230
Medianus (R)	Wrist-APB	4.29	5.1		55.0
	Elbow-Wrist	8.92	4.7	47.5	220
Peroneus (L)	Ankle-EDB	Null	Null		
	Fib.head-Ankle	Null	Null		
Peroneus (R)	Ankle-EDB	Null	Null		
	Fib.head-Ankle	Null	Null		
Tibialis (L)	Ankle-Abd hal	Null	Null		
Tibialis (R)	Ankle-Abd hal	Null	Null		
Ulnaris (L)	Wrist-ADM	3.23	4.4		55.0
	Elbow-Wrist	7.31	4.9	52.7	215
Ulnaris (R)	Wrist-ADM	3.05	5.0		55.0
	Elbow-Wrist	6.79	5.3	56.1	210
Sensory nerve	**Segment**	**Peak lat (ms)**	**Amp (uV)**	**CV (m/s)**	**Dist (mm)**
Medianus (L)	Wrist-Dig II	2.35	27.0	48.9	115
Medianus (R)	Wrist-Dig II	2.64	22.3	47.3	125
Radialis (L)	EPL tendon-Wrist	1.65	20.9	54.5	90.0
Radialis (R)	EPL tendon-Wrist	1.50	20.9	66.7	100
Superficial peroneal (L)	Lower leg-Ankle	2.56	3.9	35.2	90.0
Superficial Peroneal (R)	Lower leg-Ankle	2.64	5.4	36.0	95.0
Suralis (L)	Mid.lower leg-Lat.Malleolus	2.19	4.4	38.8	85.0
Suralis (R)	Mid.lower leg-Lat.Malleolus	2.07	3.7	38.6	80.0
Ulnaris (L)	Wrist-Dig V	1.98	24.3	48.0	95.0
Ulnaris (R)	Wrist-Dig V	2.14	26.9	49.1	105
F wave	**Segment**	**M-Lat (ms)**	**F-Lat (ms)**	**Amp (uV)**	**F (%)**
Medianus (L)	Wrist-APB	3.5	31.4	59.1	33.3
Medianus (R)	Wrist-APB	4.1	28.5	153	73.3
Tibialis (L)	Ankle-Abd hal	Null	Null		
Tibialis (R)	Ankle-Abd hal	Null	Null		
Ulnaris (L)	Wrist-ADM	2.6	30.2	156	100
Ulnaris (R)	Wrist-ADM	3.3	28.4	224	100

"Null" indicates that no signal can be detected; Lat, latency; ms, millisecond; Amp, amplitude; mV, millivolt; CV, conduction velocity; Dist, distance; L, left; R, right; APB, abductor pollicis brevis; EDB, extensor digitorum brevis; Abd hal, abductor hallucis; Fib.head, fibular head; ADM, abductor digiti minimi; Mid.lower leg, the middle of lower leg; Dig, digitus; EPL, extensor pollicis longus.

is usually heavier than the upper limbs in N_2O abuser while it is similar in patient with GBS (11). The difference in the distal and proximal compound muscle action potential amplitudes of the upper limbs can be a parameter for differential diagnosis between the N_2O abuser and AMAN patients, as the axonal injury was more severe in AMAN patients than N_2O abuser, especially upper limbs (10). GBS is an immune-mediated disease while N_2O-related neurological syndromes are deemed as metabolic disorders. Albuminocytologic dissociation and antibodies against ganglioside complexes in CSF were the specific characteristics of GBS. However, the potential pathogenesis seemed to be more complicated as the motor neuropathy of young N_2O abuser remained disabled with methylcobalamine supplementation in follow-up research (12).

Here, although the patient was suggested to halt N_2O intake and supplement methylcobalamine according to the current standardized protocol, her syndromes had only partly recovered without further progress. Lumbar puncture was performed and CSF was tested. Albuminocytologic dissociation was not found in CSF while we were the first to report positive anti-GM1 IgM antibodies in both CSF and serum. Gangliosides are specifically enriched in nervous system plasma membranes while GM1 is mainly expressed at nodes of Ranvier and motor nerve terminals (13). When GM1 or its mimicry, *Campylobacter jejuni* strains,

TABLE 2 Electrophysiological parameters of the case 4 months after the discharge from hospital.

Motor nerve	Segment	Lat (ms)	Amp (mV)	CV (m/s)	Dist (mm)
Medianus (L)	Wrist-APB	3.58	7.1		65.0
	Elbow-Wrist	7.06	6.9	57.5	200
Medianus (R)	Wrist-APB	3.75	8.5		65.0
	Elbow-Wrist	7.54	7.9	60.7	230
Peroneus (L)	Ankle-EDB	Null	Null		
	Fib.head-Ankle	Null	Null		
Peroneus (R)	Ankle-EDB	Null	Null		
	Fib.head-Ankle	Null	Null		
Tibialis (L)	Ankle-Abd hal	5.37	0.082		70.0
Tibialis (R)	Ankle-Abd hal	4.74	0.22		70.0
Ulnaris (L)	Wrist-ADM	2.63	7.2		60.0
	Elbow-Wrist	5.64	7.2	61.5	185
Ulnaris (R)	Wrist-ADM	2.54	10.0		60.0
	Elbow-Wrist	5.31	9.3	61.4	170
Sensory nerve	**Segment**	**Peak lat (ms)**	**Amp (uV)**	**CV (m/s)**	**Dist (mm)**
Medianus (L)	Wrist-Dig II	2.25	44.2	55.6	125
Medianus (R)	Wrist-Dig II	2.48	39.1	52.4	130
Radialis (L)	EPL tendon-Wrist	1.51	26.7	59.6	90.0
Radialis (R)	EPL tendon-Wrist	1.35	28.8	66.7	90.0
Superficial Peroneal (L)	Lower leg-Ankle	1.73	14.5	49.1	85.0
Superficial Peroneal (R)	Lower leg-Ankle	1.84	13.1	43.5	80.0
Suralis (L)	Mid.lower leg-Lat.Malleolus	1.87	7.6	42.8	80.0
Suralis (R)	Mid.lower leg-Lat.Malleolus	1.66	11.7	42.2	70.0
Ulnaris (L)	Wrist-Dig V	1.73	45.4	54.9	95.0
Ulnaris (R)	Wrist-Dig V	1.84	43.8	59.8	110
F wave	**Segment**	**M-Lat (ms)**	**F-Lat (ms)**	**Amp (uV)**	**F (%)**
Medianus (L)	Wrist-APB	3.4	26.7	267	76.9
Medianus (R)	Wrist-APB	3.6	26.8	463	91.7
Tibialis (L)	Ankle-Abd hal	Null	Null		
Tibialis (R)	Ankle-Abd hal	Null	Null		
Ulnaris (L)	Wrist-ADM	2.5	27.3	189	100
Ulnaris (R)	Wrist-ADM	2.4	25.6	185	100

"Null" indicates that no signal can be detected; Lat, latency; ms, millisecond; Amp, amplitude; mV, millivolt; CV, conduction velocity; Dist, distance; L, left; R, right; APB, abductor pollicis brevis; EDB, extensor digitorum brevis; Abd hal, abductor hallucis; Fib.head, fibular head; ADM, abductor digiti minimi; Mid.lower leg, the middle of lower leg; Dig, digitus; EPL, extensor pollicis longus.

are exposed to the autoimmune system, anti-GM1 antibodies are produced and activate the complement cascade, leading to either reversible conduction failure or axonal degeneration in AMAN patients (14). Anti-GM1 IgM antibodies have also been found in multifocal motor neuropathy, autoimmune limbic encephalitis, Bickerstaff brainstem encephalitis, and any other patients with neuronal or glial damage, resulting in the exposure of GM1 to autoimmune system (15). The disturbed immunological system of the patient with positive anti-GM1 IgM antibodies were probably primarily caused by N_2O or secondary to the peripheral neuropathy by N_2O. After all, the favorable prognosis with intravenous immunoglobin and steroid hormone further validated our supposes that immunological system was involved in the N_2O-related peripheral neuropathy (12). The effect of N_2O on the neuroimmune system is possibly through vitamin B12 deficiency or any other unclear pathways to be clarified in future (16).

Conclusion

With this case we were able to show that recreational N_2O abuse can cause immune-mediated disorder besides metabolic disorder. N_2O-related peripheral neuropathy is a mimic of GBS

with many similar characteristics. We therefore encouraged all clinicians to perform CSF tests of antibodies against ganglioside complexes when encountering N_2O abusers. The potential immunological pathogenesis should be clarified to find novel treatments for these patients.

Data availability statement

The raw data supporting the conclusions of this article will be made available by the authors, without undue reservation.

Ethics statement

The studies involving human participants were reviewed and approved by the Local Ethics Committee of Renmin Hospital of Wuhan University. The patients/participants provided their written informed consent to participate in this study.

Author contributions

M-XD and TL designed the study and analyzed the patient data. QW, J-FX, LH, and YY collected the original clinical data. M-XD wrote the first draft of the manuscript. All authors commented on previous versions of the manuscript and read and approved the final manuscript.

Funding

This work was supported by the Open Fund of Hubei Key Laboratory of Renmin Hospital of Wuhan University (2021KFY040).

Conflict of interest

The authors declare that the research was conducted in the absence of any commercial or financial relationships that could be construed as a potential conflict of interest.

Publisher's note

All claims expressed in this article are solely those of the authors and do not necessarily represent those of their affiliated organizations, or those of the publisher, the editors and the reviewers. Any product that may be evaluated in this article, or claim that may be made by its manufacturer, is not guaranteed or endorsed by the publisher.

Supplementary material

The Supplementary Material for this article can be found online at: https://www.frontiersin.org/articles/10.3389/fneur.2022.1033327/full#supplementary-material

References

1. Inquimbert C, Maitre Y, Moulis E, Gremillet V, Tramini P, Valcarcel J, et al. Recreational nitrous oxide use and associated factors among health profession students in France. *Int J Environ Res Public Health*. (2022) 19:5237. doi: 10.3390/ijerph19095237

2. Kaar SJ, Ferris J, Waldron J, Devaney M, Ramsey J, Winstock AR. Up: the rise of nitrous oxide abuse. An international survey of contemporary nitrous oxide use. *J Psychopharmacol.* (2016) 30:395–401. doi: 10.1177/0269881116632375

3. Bao L, Li Q, Li Q, Chen H, Zhang R, Shi H, et al. Clinical, electrophysiological and radiological features of nitrous oxide-induced neurological disorders. *Neuropsychiatr Dis Treat.* (2020) 16:977–84. doi: 10.2147/NDT.S236939

4. Largeau B, Karam A, Potey C, Caous AS, Tard C, Carton L, et al. Myeloneuropathy induced by recreational nitrous oxide use with variable exposure levels. *Eur J Neurol.* (2022) 29:2173–80. doi: 10.1111/ene.15370

5. Xiang Y, Li L, Ma X, Li S, Xue Y, Yan P, et al. Recreational nitrous oxide abuse: prevalence, neurotoxicity, and treatment. *Neurotox Res.* (2021) 39:975–85. doi: 10.1007/s12640-021-00352-y

6. Tani J, Weng HY, Chen HJ, Chang TS, Sung JY, Lin CS, et al. Elucidating unique axonal dysfunction between nitrous oxide abuse and vitamin B12 deficiency. *Front Neurol.* (2019) 10:704. doi: 10.3389/fneur.2019.00704

7. Yu M, Qiao Y, Li W, Fang X, Gao H, Zheng D, et al. Analysis of clinical characteristics and prognostic factors in 110 patients with nitrous oxide abuse. *Brain Behav.* (2022) 12:e2533. doi: 10.1002/brb3.2533

8. Li Y, Dong J, Xu R, Feng F, Kan W, Ding H, et al. Clinical epidemiological characteristics of nitrous oxide abusers: a single-center experience in a hospital in China. *Brain Behav.* (2021) 11:e2416. doi: 10.1002/brb3.2416

9. Beal JC, Cheng Y, Merchant S, Zarnegar R. An acute, severe axonal sensorimotor polyneuropathy in the setting of nitrous oxide abuse. *Neurohospitalist.* (2020) 10:293–6. doi: 10.1177/1941874420910648

10. Li Y, Zhang X, Zhao C. Electrophysiological characteristics of patients with nitrous oxide abuse. *Neurol Res.* (2021) 43:793–801. doi: 10.1080/01616412.2021.1935101

11. Jiang J, Shang X, Wang X, Chen H, Li W, Wang Y, et al. Nitrous oxide-related neurological disorders: clinical, laboratory, neuroimaging, and electrophysiological findings. *Brain Behav.* (2021) 11:e2402. doi: 10.1002/brb3.2402

12. Berling E, Fargeot G, Aure K, Tran TH, Kubis N, Lozeron P, et al. Nitrous oxide-induced predominantly motor neuropathies: a follow-up study. *J Neurol.* (2022) 269:2720–6. doi: 10.1007/s00415-021-10858-2

13. McGonigal R, Campbell CI, Barrie JA, Yao D, Cunningham ME, Crawford CL, et al. Schwann cell nodal membrane disruption triggers bystander axonal degeneration in a Guillain-Barré syndrome mouse model. *J Clin Investig.* (2022) 132:e158524. doi: 10.1172/JCI158524

14. Yanaka S, Yogo R, Watanabe H, Taniguchi Y, Satoh T, Komura N, et al. On-membrane dynamic interplay between anti-GM1 IgG antibodies and complement component C1q. *Int J Mol Sci.* (2019) 21:147. doi: 10.3390/ijms21010147

15. Oktar AÇ, Selçuk Ö, Tunç C, Işildak S, Sanli E, Yilmaz V, et al. Serum anti-ganglioside antibodies in patients with autoimmune limbic encephalitis. *Turk J Med Sci.* (2021) 51:2570–4. doi: 10.3906/sag-2101-348

16. Mohsenzadegan M, Kourosh Arami M, Oshaghi M, Sedigh Maroufi S. A. review of the effects of the anesthetic gas nitrous oxide on the immune system; a starting point for future experiences. *Immunopharmacol Immunotoxicol.* (2020) 42:179–86. doi: 10.1080/08923973.2020.1735412

frontiers | Frontiers in Neurology

TYPE Case Report
PUBLISHED 01 December 2022
DOI 10.3389/fneur.2022.1018529

Check for updates

OPEN ACCESS

EDITED BY
Giovanni Meola,
University of Milan, Italy

REVIEWED BY
Hipólito Nzwalo,
University of Algarve, Portugal
Daria Diodato,
Bambino Gesù Children's Hospital (IRCCS), Italy

*CORRESPONDENCE
Ming-Fan Hong
hmf9001@163.com

SPECIALTY SECTION
This article was submitted to Neuromuscular Disorders and Peripheral Neuropathies, a section of the journal Frontiers in Neurology

RECEIVED 13 August 2022
ACCEPTED 09 November 2022
PUBLISHED 01 December 2022

CITATION
Diao S-P, Chen S-F, Liu A-Q, Zhou Z-H, Peng Z-X and Hong M-F (2022) Elderly onset of MELAS in a male: A case report. *Front. Neurol.* 13:1018529. doi: 10.3389/fneur.2022.1018529

COPYRIGHT
© 2022 Diao, Chen, Liu, Zhou, Peng and Hong. This is an open-access article distributed under the terms of the Creative Commons Attribution License (CC BY). The use, distribution or reproduction in other forums is permitted, provided the original author(s) and the copyright owner(s) are credited and that the original publication in this journal is cited, in accordance with accepted academic practice. No use, distribution or reproduction is permitted which does not comply with these terms.

Elderly onset of MELAS in a male: A case report

Sheng-Peng Diao, Song-Fa Chen, Ai-Qun Liu, Zhi-Hua Zhou, Zhong-Xing Peng and Ming-Fan Hong*

Department of Neurology, College of Clinical Medicine, The First Affiliated Hospital, Guangdong Pharmaceutical University, Guangzhou, China

Background: Mitochondrial encephalomyopathy with lactic acidosis and stroke-like episodes (MELAS) is one of the most common maternally inherited mitochondrial diseases which rarely affects elderly people.

Case presentation: We reported the case of a 61-year-old male patient with MELAS. He was experiencing acute migraine-like headaches as the first symptoms. Laboratory data showed elevated lactate and creatine kinase levels. Brain magnetic resonance imaging (MRI) found a high signal intensity lesion in the left occipital-temporal-parietal lobe on diffusion-weighted imaging (DWI). Magnetic resonance angiography (MRA) revealed reversible vasoconstriction of the middle cerebral arteries and superficial temporal arteries. A muscle biopsy suggested minor muscle damage. A genetic study revealed a mitochondrial DNA A3243G mutation.

Conclusion: Elderly onset of MELAS is rare and easily misdiagnosed as an ischemic stroke. MELAS with the onset of stroke-like episodes should be considered in adult or elderly patients with imaging findings that are atypical for cerebral infarction. The use of multimodal MRI in the clinical diagnosis of MELAS could be extremely beneficial.

KEYWORDS

MELAS, stroke-like episodes, magnetic resonance angiography (MRA), migraine, magnetic resonance imaging (MRI)

Background

Mitochondrial encephalomyopathy with lactic acidosis and stroke-like episodes (MELAS) is one of the most common maternally inherited mitochondrial diseases (1). MELAS is typically characterized by stroke-like episodes and hyperlactic acidemia. Nevertheless, only approximately half of patients show typical clinical manifestations, with significant heterogeneity in genetics and clinical manifestations (2, 3), which leads to difficulty in diagnosis and even misdiagnosis.

Only 1–6% of patients develop the disease after 40 years of age (4). It is even rare in patients after 60 years of age, and there have been only a few cases reported in female patients (5–7). In this report, we described the case of a 61-year-old male patient with MELAS. The clinical and imaging features of the patient helped us in understanding the clinical manifestations of MELAS in the elderly and making a precise diagnosis.

Case presentation

First attack

A previously healthy 61-year-old male patient presented with sudden onset of a left-sided migraine-like headache (December 26, 2019) and developed a right-sided migraine-like headache after 2 days. He was immediately admitted to a local hospital for treatment. The results of the brain CT scan (data not shown) showed acute cerebral infarction of the left occipital-parietal lobe, and he was diagnosed with acute ischemic cerebral infarction. The patient was then treated with aspirin (100 mg/day), atorvastatin (20 mg/day), and citicoline (0.6 g/day). However, he had weakness in his right limb and could not walk for 7 days after onset. He subsequently showed emotional irritability and hallucinations 8 days after onset. There was no history of blurred vision, hearing impairment, migraine headaches, or gastroenteritis. In addition, there was no history of diabetes, hypertension, or a family history of stroke, and no history of smoking or drinking. No one in his family had a similar medical history.

The patient was admitted to our hospital 11 days after onset (6 January 2020). On physical examination, his blood pressure was 112/69 mmHg, and he had lethargy and a lag in response with slow speech. He also had right homonymous hemianopia, which was shown by a slight wrinkle on the right frontal, a slight nasolabial groove on the right, and his mouth was skewed to the left with a tongue extended into the middle. The patient was given grade 1 for right upper extremity strength, grade 3 for right lower extremity strength, and grade 5 for left extremity strength, with reduced tendon reflex of the limbs. The pathological sign was negative. His score was 10 according to the United States National Institutes of Health Stroke Scale (NIHSS).

After 12 days of onset, clinical chemistry analysis revealed fasting blood glucose levels of 6.6 mmol/L, glycated hemoglobin levels of 6.1%, creatine kinase levels of 448 U/L, high sensitivity C-reactive protein levels of 42.1 mg/L, and arterial blood lactic acid levels of 3.3 mmol/L. The results of routine hematological tests, homocysteine, blood lipids, four coagulation tests, erythrocyte sedimentation rate, antinuclear antibodies, anti-cardiolipin antibodies, anti-neutrophil antibodies, protein C, and protein S were all within the normal range. The results of the cerebrospinal fluid (CSF) assay showed a value of 4.13 mmol/L for lactic acid, and routine biochemistry did not reveal any abnormalities.

The first magnetic resonance imaging (MRI) examination was performed 12 days after onset (7 January 2020) (Figure 1A), and diffusion-weighted imaging (DWI) showed a high signal intensity (Figures 1A, 3). Magnetic resonance angiography (MRA) showed dilation of the left middle cerebral artery, posterior cerebral artery, and bilateral superficial temporal arteries (Figure 2A). Arterial spin labeling (ASL) indicated hyperperfusion in the left occipital-temporal-parietal focal areas (Figure 2D). There was a double inverted lactate peak at 1.33 ppm detected by magnetic resonance spectroscopy (MRS) (Figure 2F).

Electroencephalogram (EEG) monitoring revealed several high amplitudes and sharp slow-wave activities in the left and right hemispheres, varying during waking and sleeping. A muscle biopsy was performed on the patient. The modified gomori trichrome (MGT) staining was negative (Figure 3). The succinate dehydrogenase (SDH)/c oxidase (COX) double staining showed a blue fiber, no positive result of blood vessel wall strength, and no obvious abnormality of muscle fiber under the electron microscope (Figure 3) (8). Next, 3 ml of peripheral venous blood from the patient was drawn for genotypic detection analysis, and the results indicated mitochondrial 3243A>G mutation (Figure 2G), which is a pathogenic mutation (2). The proportion of the m.3243A>G mutation in blood was 15%.

Remission

The patient was diagnosed with MELAS by gene testing. After initial treatment (adenosine triphosphate disodium 60 mg/day, coenzyme Q10 30 mg/day, and L-arginine 20 g/day), the patient's condition showed significant improvement, and he was able to live independently. The second MRI examination was performed 27 days after the first onset (22 January 2020). DWI showed that the high signal intensity of the left occipital-temporal-parietal lobe was reduced (Figure 1B). In addition, MRA showed that the bilateral superficial temporal arteries were retracted (Figure 2B).

Recurrence

Unfortunately, the patient relapsed 68 days after the first onset (3 March 2020). There was a twitch on the left limb of the patient; his limbs were weak, and he was unable to walk. The third MRI examination was performed on 3 March 2020. DWI revealed a high signal intensity (Figure 1C), and ASL showed hyperperfusion in the right occipital-temporal-parietal focus areas (Figure 2E). In addition, according to MRA, the left middle cerebral artery was normal, whereas the right middle cerebral artery was dilated (Figure 2C). His limb convulsions did not recur after treatment with lamotrigine (50 mg/day), coenzyme Q10 (30 mg/day), and L-arginine (20 g/day), and his limb muscle strength weakness was improved, but he developed dementia and currently requires family care.

Discussion

Mitochondrial encephalomyopathy with lactic acidosis and stroke-like episodes is the most common clinical form of mitochondrial encephalomyopathy, with stroke-like episodes

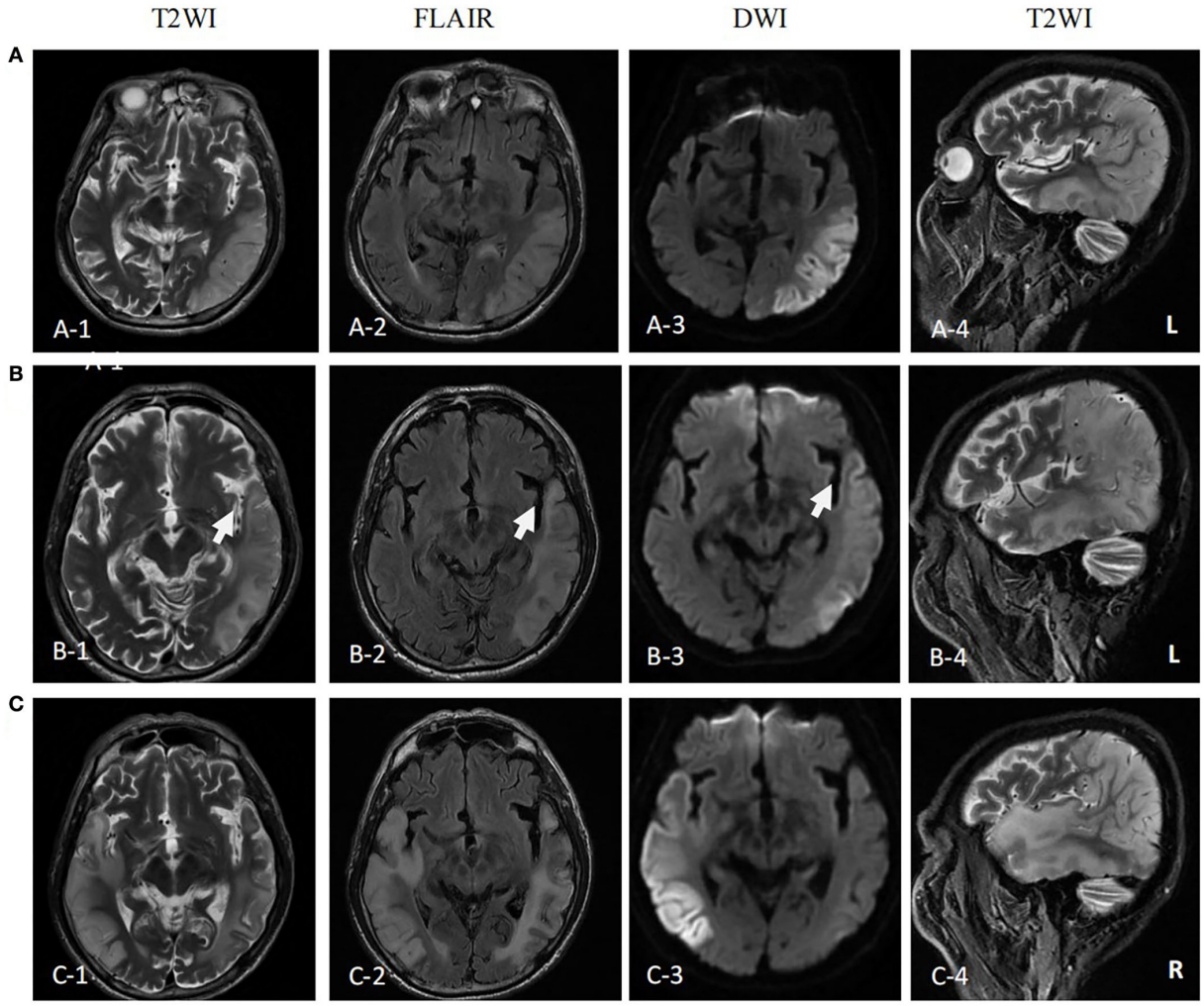

FIGURE 1
MR images of the patient. **(A)** MR images performed on the first attack (12 days after onset) showed high signal intensity in occipital-temporal-parietal lobe hyperextension on T2-weighted, fluid attenuation inversion recovery (FLAIR), and diffusion-weighted imaging (DWI). **(B)** MR images performed on the remission (27 days after the first onset) showed a high signal intensity of DWI, FLAIR, and T2WI of the left occipital-temporal-parietal lobe was reduced. The focus of the temporal lobe is enlarged (arrow). **(C)** MR images performed on the recurrence (68 days from the first onset) showed new high signal intensity in the right occipital-temporal-parietal lobe hyperextension on T2-weighted, FLAIR, and DWI.

and hyperlactic acidemia as the primary clinical features, which was first reported by Pavlakis et al. (9). The clinical manifestations of MELAS are usually sudden stroke-like symptoms such as limb weakness, cortical blindness, mental disturbance, mental retardation, epilepsy, headache, and neural deafness (10). MELAS is common in adolescents and rarely seen in the elderly. Some scholars believe that MELAS with onset in over 50-year-old patients is seldom seen and has atypical clinical manifestations (11), making it difficult to diagnose. Only a few cases of this disease have been reported in older women, and there is less knowledge about this disease in the elderly (5–7). There are no case reports of MELAS in elderly men, and one of the factors that make diagnosing MELAS in geriatric-onset patients difficult is the lack of adequate knowledge about MELAS in men aged above 60 years. We herein presented the case of a 61-year-old male patient with MELAS.

As the first symptom, the older man experienced acute migraine-like headaches. The CT scan of the left occipital-parietal lobe at the local hospital revealed low-density lesions. At our hospital, a hyperintense lesion was seen in the left occipital-temporal-parietal lobe on a brain MRI.

This patient was easily misdiagnosed with ischemic cerebrovascular disease. However, MRA did not indicate stenosis or occlusion of the corresponding cerebral responsible vessels. As a result, we suspected the diagnosis of ischemic cerebral infarction and other diseases, such as MELAS. Then,

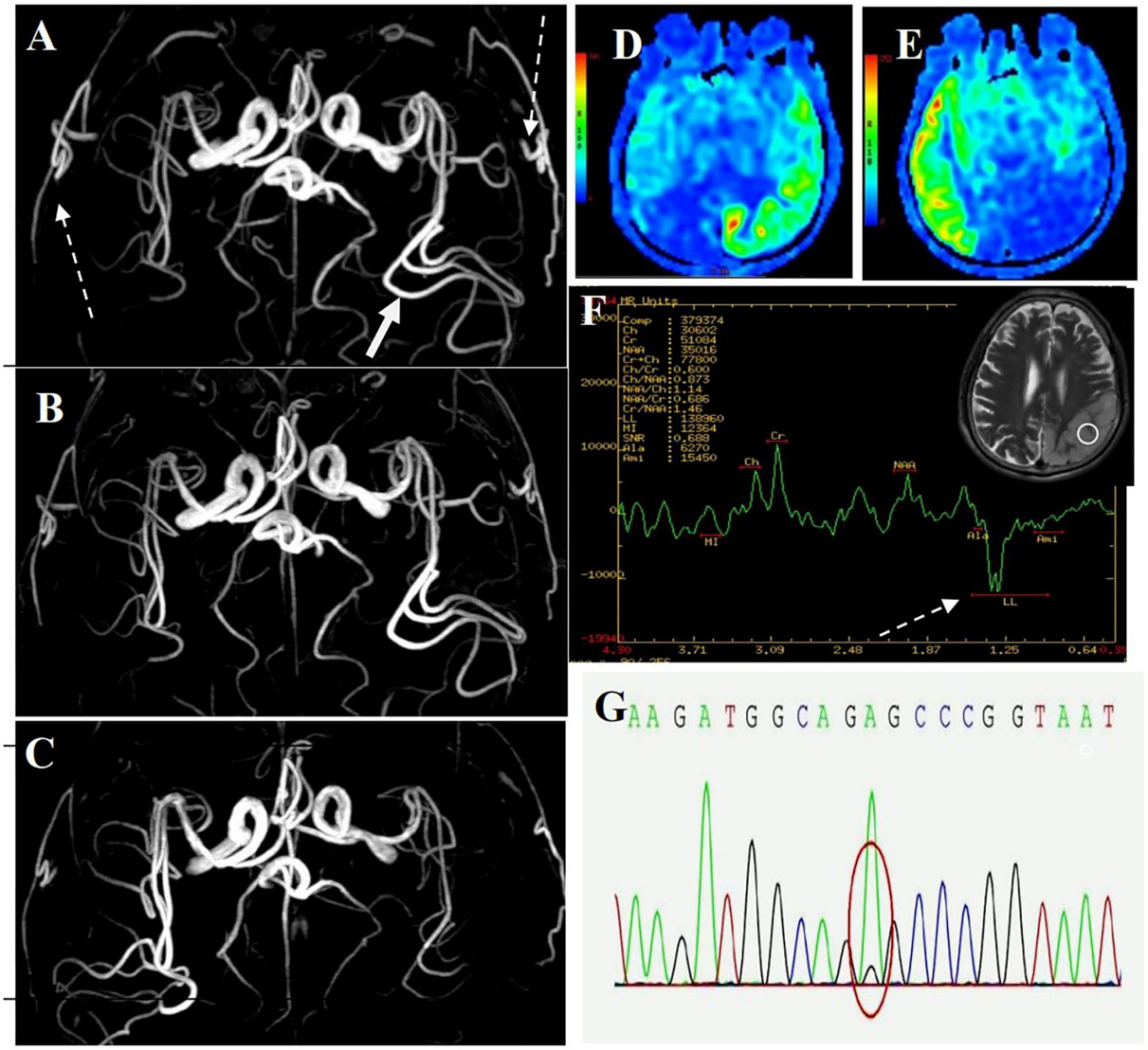

FIGURE 2
MR images of the patient. **(A)** MRA image of first onset period, 12 days after onset. MRA showed dilation of the left middle cerebral artery (long-tail arrow), with apparent dilation of superficial temporal arteries (long dotted arrow). **(B)** MRA image of remission period, 27 days after onset. MRA showed that the superficial temporal arteries were retracted. **(C)** MRA images of recurrence period, 68 days after onset. MRA showed that the left middle cerebral artery appeared normal, and the right middle cerebral artery was dilated. **(D)** ASL image of first onset period, 12 days after onset. ASL showed hyperperfusion in the left occipital-temporal-parietal focal areas. **(E)** ASL images of recurrence period, 68 days after onset. ASL showed hyperperfusion in the right occipital-temporal-parietal focal regions. **(F)** MRS image of first onset period, 12 days after onset. MRS showed a double inverted lactate peak at 1.33 ppm (short dotted arrow). **(G)** Genotypic detection analysis showed mitochondrial mutation (m.3243A >G).

laboratory data showed elevated lactate and creatine kinase levels, and genetic analysis revealed a mitochondrial DNA A3243G mutation. MELAS was confirmed after the patient met the clinical diagnostic criteria (12).

This case has some essential and specific MRA imaging features. MRA revealed reversible vasoconstriction of the middle cerebral arteries and superficial temporal arteries bilaterally. In patients presenting with the acute stage of MELAS, the accumulation of lactate in the lesion results in local arterial dilatation (12). Some blood vessels suffer from chronic damage to the vessel wall, episodic spasm, and intimal hyperplasia as the disease progresses. The angiogram showed normalization progression and reduction in blood vasculature (13). The cerebral blood vessels in the focal area dilated during the initial attack and recurrence stages and retracted during remission. However, there was no such vascular change during acute

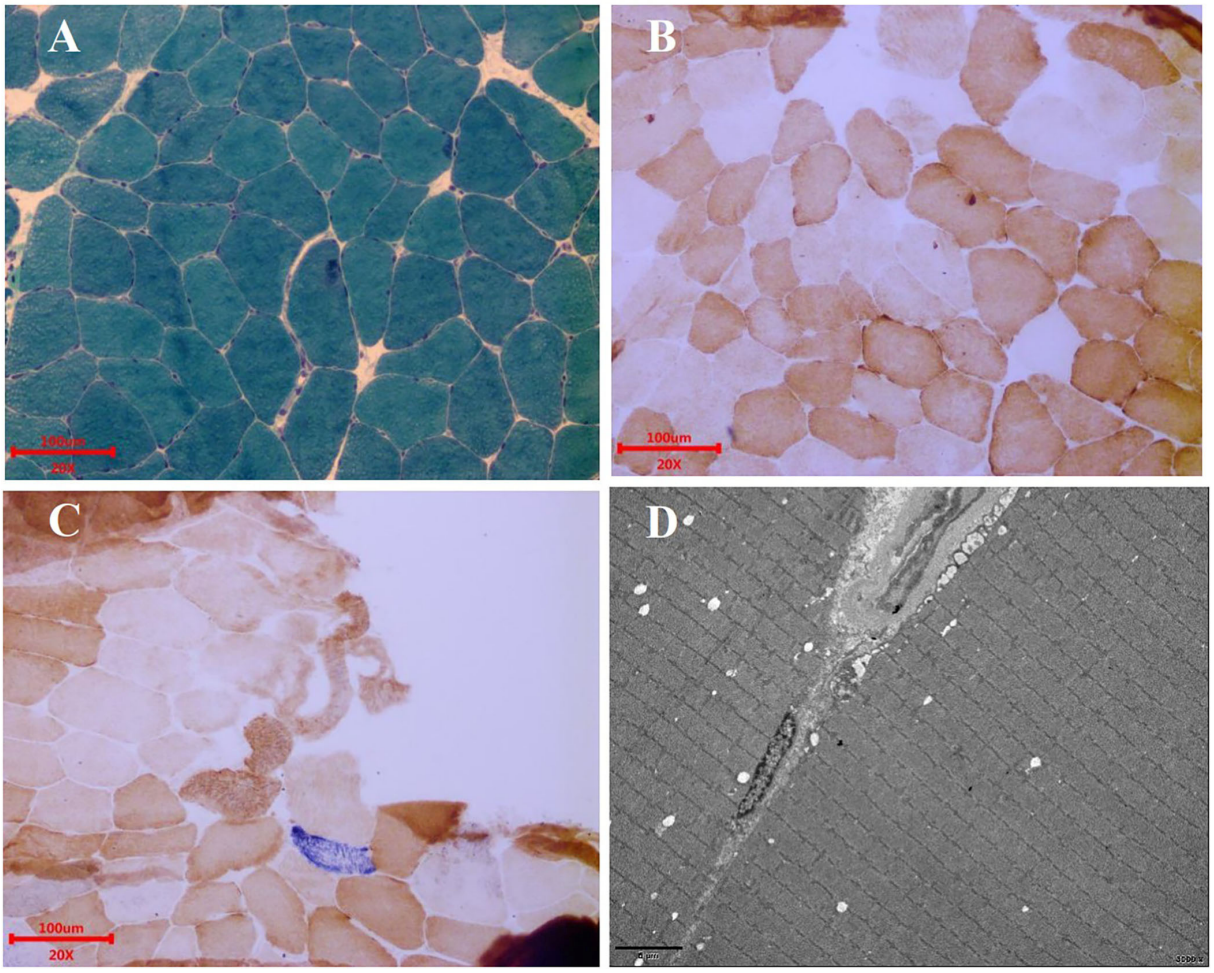

FIGURE 3
Muscle biopsy. **(A)** MGT staining showed no ragged red fibers. Scale bars: 100 μm. **(B)** COX staining showed no significant decrease in myofibrillase activity. Scale bars: 100 μm. **(C)** SDH/COX double staining found one blue fiber. Scale bars: 100 μm. **(D)** Under the electron microscope, the basic arrangement of myofibrils was regular, the sarcolemma was shrunken, and no special ultrastructural and pathological changes were found. Scale bars: 5 μm.

ischemic stroke. MELAS can be diagnosed and evaluated using MRA, which can detect the cerebrovascular imaging characteristics of MELAS.

Acute migraine-like headaches were the first symptoms that the patient experienced. MRA indicated apparent dilation of the bilateral superficial temporal arteries in the acute phase. The headache gradually disappeared after the treatment. Subsequent MRA showed that the bilateral superficial temporal arteries were slowly retracted and appeared normal. Migraine attacks are thought to be caused by an increase in blood flow through the superficial temporal artery during the acute phase of migraine (14, 15). In recent years, mitochondrial dysfunction has been proven to play an essential role in the pathogenesis of migraine (16). The patient was found to have a mitochondrial DNA A3243G point mutation. The findings of this case suggest that mitochondrial dysfunction may contribute to migraine pathogenesis.

Myopathic symptoms are also manifestations of MELAS, mainly including myasthenia, myalgia, and exercise intolerance (8). The patient underwent a muscle biopsy, and MGT staining was found negative. SDH/COX double staining showed a blue fiber. There was no positive result of blood vessel wall strength and no obvious abnormality of muscle fiber under the electron microscope. A muscle biopsy suggested minor muscle damage. The possibility of missed diagnoses and delayed treatment exists. However, there is a limited correlation between muscle biopsies and the diagnosis of MELAS (17). The presence of mitochondrial disease cannot be ruled out by a normal muscle biopsy (18). In contrast, gene detection plays a vital role in diagnosing MELAS when muscle biopsy fails to diagnose it, and it is the diagnostic gold standard for MELAS (19).

This patient was detected to carry the m.3243A>G mutation, a pathogenic variant of MELAS. The proportion of the m.3243A>G mutation in the blood test was low (15%). More than 80% of the patients have the mitochondrial DNA (mtDNA) 3243A>G mutation (4). Patients with MELAS have obvious heterogeneity and various clinical manifestations, and even monozygotic twins with the m.3243A>G mutation can also be found. The age of onset and clinical phenotype are different (20). Studies have shown that the mtDNA mutation rate of patients with MELAS having ragged red fibers is significantly higher than that of patients without ragged red fibers (18). The mtDNA mutation rate has been confirmed to be related to the age of onset of MELAS, and the later the onset, the lower the mutation rate of mtDNA (21). The low mutation rate of m.3243A>G in this patient may explain the patient's late onset and absence of obvious lesions in muscle biopsy.

Conclusion

We reported a rare case of elderly onset male MELAS. Stroke-like episodes in elderly patients with MELAS are easily misdiagnosed as ischemic stroke and should be considered in the differential diagnoses when imaging findings are inconsistent with ischemic infarction. In this case, superficial temporal artery dilatation with MRA during a stroke-like migraine-like attack enriched our understanding of the clinical and imaging features of MELAS. Multimodal MRI during stroke-like episodes in MELAS can provide significant clues to a final diagnosis.

Data availability statement

The datasets presented in this article are not readily available because of ethical and privacy restrictions. Requests to access the datasets should be directed to the corresponding author/s.

Ethics statement

The studies involving human participants were reviewed and approved by the Ethics Committee of the First Affiliated Hospital, Guangdong Pharmaceutical University. This enrolled patient provided written, informed consent to be included in the study. All methods were performed in accordance with the relevant guidelines and regulations. The patients/participants provided their written informed consent to participate in this study.

Author contributions

M-FH and Z-XP contributed to the conception of the study. Z-HZ, A-QL, and S-FC contributed significantly to the analysis and manuscript preparation. S-PD performed the data analyses and wrote the manuscript. All authors contributed to the article and approved the submitted version.

Acknowledgments

We would like to acknowledge the subject who participated in this study.

Conflict of interest

The authors declare that the research was conducted in the absence of any commercial or financial relationships that could be construed as a potential conflict of interest.

Publisher's note

All claims expressed in this article are solely those of the authors and do not necessarily represent those of their affiliated organizations, or those of the publisher, the editors and the reviewers. Any product that may be evaluated in this article, or claim that may be made by its manufacturer, is not guaranteed or endorsed by the publisher.

References

1. Scaglia F, Northrop JL. The mitochondrial myopathy encephalopathy, lactic acidosis with stroke-like episodes (MELAS) syndrome. *CNS Drugs.* (2006) 20:443–64. doi: 10.2165/00023210-200620060-00002

2. Kaufmann P, Engelstad K, Wei Y, Kulikova R, Oskoui M, Battista V, et al. Protean phenotypic features of the A3243G mitochondrial DNA mutation. *Arch Neurol.* (2009) 66:85–91. doi: 10.1001/archneurol.2008.526

3. Mancuso M, Orsucci D, Angelini C, Bertini E, Carelli V, Comi GP, et al. The m.3243A>G mitochondrial DNA mutation and related phenotypes. A matter of gender? *J Neurol.* (2014) 261:504–10. doi: 10.1007/s00415-013-7225-3

4. El-Hattab AW, Adesina AM, Jones J, Scaglia F. MELAS syndrome: Clinical manifestations, pathogenesis, and treatment options. *Mol Genet Metab.* (2015) 116:4–12. doi: 10.1016/j.ymgme.2015.06.004

5. Sinnecker T, Andelova M, Mayr M, Rüegg S, Sinnreich M, Hench J, et al. Diagnosis of adult-onset MELAS syndrome in a 63-year-old patient with suspected recurrent strokes - a case report. *BMC Neurol.* (2019) 19:91. doi: 10.1186/s12883-019-1306-6

6. Aurangzeb S, Vale T, Tofaris G, Poulton J, Turner MR. Mitochondrial encephalomyopathy with lactic acidosis and stroke-like episodes (MELAS) in the older adult. *Pract Neurol.* (2014) 14:432–6. doi: 10.1136/practneurol-2014-000853

7. Mukai M, Nagata E, Mizuma A, Yamano M, Sugaya K, Nishino I, et al. Adult-onset mitochondrial myopathy, encephalopathy, lactic acidosis, and stroke (MELAS)-like encephalopathy diagnosed based on the complete sequencing of mitochondrial DNA extracted from biopsied muscle without any myopathic changes. *Intern Med.* (2017) 56:95–9. doi: 10.2169/internalmedicine.56.7301

8. Van Adel BA, Tarnopolsky MA. Metabolic myopathies: update 2009. *J Clin Neuromuscul Dis.* (2009) 10:97–121. doi: 10.1097/CND.0b013e3181903126

9. Pavlakis SG, Phillips PC, DiMauro S, De Vivo DC, Rowland LP. Mitochondrial myopathy, encephalopathy, lactic acidosis, and stroke like episodes: a distinctive clinical syndrome. *Ann Neurol.* (1984) 16:481–8. doi: 10.1002/ana.410160409

10. Goldstein A, Servidei S. *Mitochondrial Encephalomyopathy, Lactic Acidosis, and Stroke-Like Episodes (MELAS)[M]//Diagnosis and Management of Mitochondrial Disorders*. Cham: Springer (2019) 81-100. doi: 10.1007/978-3-030-05517-2_5

11. Hirano M, Pavlakis SG. Mitochondrial myopathy, encephalopathy, lactic acidosis, and stroke-like episodes (MELAS): current concepts. *J Child Neurol.* (1994) 9:4–13. doi: 10.1177/088307389400900102

12. Iizuka T, Sakai F, Suzuki N, Hata T, Tsukahara S, Fukuda M, et al. Neuronal hyperexcitability in stroke-like episodes of MELAS syndrome. *Neurology*. (2002) 59:816–24. doi: 10.1212/wnl.59.6.816

13. Ikawa M, Yoneda M, Muramatsu T, Matsunaga A, Tsujikawa T, Yamamoto T, et al. Detection of pre-clinically latent hyperperfusion due to stroke-like episodes by arterial spin-labeling perfusion MRI in MELAS patients. *Mitochondrion.* (2013) 13:676–880. doi: 10.1016/j.mito.2013.09.007

14. Ho TW, Edvinsson L, Goadsby PJ. CGRP. and its receptors provide new insights into migraine pathophysiology. *Nat Rev Neurol.* (2010) 6:573–82. doi: 10.1038/nrneurol.2010.127

15. Cutrer FM. Pathophysiology of migraine. *Semin Neurol.* (2010) 30:120–30. doi: 10.1055/s-0030-1249222

16. Dong X, Guan X, Chen K, Jin S, Wang C, Yan L, et al. Abnormal mitochondrial dynamics and impaired mitochondrial biogenesis in trigeminal ganglion neurons in a rat model of migraine. *Neurosci Lett.* (2017) 636:127–33. doi: 10.1016/j.neulet.2016.10.054

17. Baek MS, Kim SH, Lee YM. The usefulness of muscle biopsy in initial diagnostic evaluation of mitochondrial encephalomyopathy, lactic acidosis, and stroke-like episodes. *Yonsei Med J.* (2019) 60:98–105. doi: 10.3349/ymj.2019.60.1.98

18. Lorenzoni PJ, Werneck LC, Kay CS, Silvado CE, Scola RH. When should MELAS (mitochondrial myopathy, encephalopathy, lactic acidosis, and stroke-like episodes) be the diagnosis? *Arq Neuropsiquiatr.* (2015) 73:959–67. doi: 10.1590/0004-282X20150154

19. Finsterer J. Genetic data are a prerequisite for interpreting clinical and muscle biopsy findings in MELAS. *Yonsei Med J.* (2019) 60:399–400. doi: 10.3349/ymj.2019.60.4.399

20. Maeda K, Kawai H, Sanada M, Terashima T, Ogawa N, Idehara R, et al. Clinical phenotype and segregation of mitochondrial 3243A > G mutation in 2 pairs of monozygotic twins. *JAMA Neurol.* (2016) 73:990–3. doi: 10.1001/jamaneurol.2016.0886

21. Qi Y, Zhang Y, Wang Z, Yang Y, Yuan Y, Niu S, et al. Screening of common mitochondrial mutations in Chinese patients with mitochondrial encephalomyopathies. *Mitochondrion.* (2007) 7:147–50. doi: 10.1016/j.mito.2006.11.019

frontiers | Frontiers in Neurology

TYPE Case Report
PUBLISHED 12 December 2022
DOI 10.3389/fneur.2022.1066040

Check for updates

OPEN ACCESS

EDITED BY
Giovanni Meola,
University of Milan, Italy

REVIEWED BY
Hatice Tankisi,
Aarhus University Hospital, Denmark
Hiroshi Takashima,
Kagoshima University, Japan

*CORRESPONDENCE
Louise Sloth Kodal
louise.boensdorff.sloth.01@regionh.dk

SPECIALTY SECTION
This article was submitted to Neuromuscular Disorders and Peripheral Neuropathies, a section of the journal Frontiers in Neurology

RECEIVED 10 October 2022
ACCEPTED 15 November 2022
PUBLISHED 12 December 2022

CITATION
Kodal LS, Hammer-Hansen S, Holm-Yildiz S, Grønskov K, Karstensen HG and Dysgaard T (2022) Case report: A novel variant in *SLC25A46* causing sensorimotor polyneuropathy and optic atrophy. *Front. Neurol.* 13:1066040. doi: 10.3389/fneur.2022.1066040

COPYRIGHT
© 2022 Kodal, Hammer-Hansen, Holm-Yildiz, Grønskov, Karstensen and Dysgaard. This is an open-access article distributed under the terms of the Creative Commons Attribution License (CC BY). The use, distribution or reproduction in other forums is permitted, provided the original author(s) and the copyright owner(s) are credited and that the original publication in this journal is cited, in accordance with accepted academic practice. No use, distribution or reproduction is permitted which does not comply with these terms.

Case report: A novel variant in *SLC25A46* causing sensorimotor polyneuropathy and optic atrophy

Louise Sloth Kodal[1]*, Sophia Hammer-Hansen[2], Sonja Holm-Yildiz[1], Karen Grønskov[2], Helena Gásdal Karstensen[2] and Tina Dysgaard[1]

[1]Department of Neurology, Copenhagen Neuromuscular Center, Rigshospitalet, University of Copenhagen, Copenhagen, Denmark, [2]Department of Clinical Genetics, Rigshospitalet, University of Copenhagen, Copenhagen, Denmark

SLC25A46 is a mitochondrial protein involved in mitochondrial dynamics. Recently, bi-allelic variants have been identified as a pathogenic cause in a spectrum of neurological syndromes. We report a novel homozygous *SLC25A46* variant in two siblings, originating from Iraq. Both presented with optic atrophy and varying neurological symptoms. The neurological examination and nerve conduction studies were consistent with sensorimotor polyneuropathy, one having mild polyneuropathy and the other pronounced polyneuropathy. The cases illustrate the disease spectrum and provide substantial information to the knowledge of polyneuropathy caused by *SLC25A46* variants. It further highlights the diagnostic potentials of whole exome sequencing which can improve future understanding of disease mechanisms.

KEYWORDS

hereditary neuropathy, whole exome sequencing, polyneuropathy, optic atrophy, case report

Introduction

SLC25A46 is a part of the Solute Carrier 25 (SLC25) family of transporters (1), a large family of more than 50 transporters varying in both size and transported substrates. The specific function is unknown, but it is thought to function as a transport protein in the outer mitochondrial membrane interacting with the inner membrane thereby contributing to mitochondrial dynamics involved in fusion and fission (2). Only a few patients with biallelic pathogenic variants in *SLC25A46* have been described in the literature. Patients can present with either Leigh syndrome (3), progressive myoclonic ataxia (4), or optic atrophy (OA), and limb spasticity (5).

Only a few patients have been described with OA and axonal peripheral neuropathy (PN) due to variants in *SLC25A46* (6), and only one patient with OA, PN, and ataxia has been reported (7).

In this case report, we present the medical history and clinical and molecular genetic findings of two sisters, both presenting with decreased vision in varying degrees since childhood and varying PN symptoms due to homozygosity for a novel *SLC25A46* variant.

Case description

Two sisters aged 26 (Patient A) and 34 (Patient B) were referred for genetic evaluation and diagnostic clarification due to childhood-onset optic atrophy.

Family history and molecular genetics

The patients were originally from Iraq and of consanguineous parents. Patients A and B had seven siblings of which a brother also had optic atrophy since childhood and one sister experienced problems with balance.

Molecular genetic analysis of *OPA1* using gene-panel sequencing (NGS) and multiplex ligation-dependent probe amplification (MLPA) as well as PCR and Sanger sequencing of three mitochondrial variants [ND1 (m.3460G>A), ND4 (m.11778G>A), and ND6 (m.14484T>C)] was normal. Therefore, whole-exome sequencing (trio analysis with patient A as the proband) was performed revealing homozygosity for a novel *SLC25A46* variant [GRCh37, chr5:110,097,073, NM_138773.3:c.848A>C, p.(Gln283Pro)] in the proband, which was confirmed by Sanger Sequencing (Figure 1). Subsequently, patient B, as well as the affected brother were found to be homozygous for the variant. The variant has been reported in ClinVar in an affected individual (Accession number VCV001679272.1) and has not been reported in healthy controls [Genome Aggregation Database (version 2.1.1) or the UK biobank]. *In silico* models categorize the variant as pathogenic (CADD = 26, REVEL:0.758). A different missense variant at the same position (p.Gln283His) has been reported but has been classified as a variant of unknown significance in ClinVar. The variant was therefore classified as likely pathogenic according to ACMG guidelines for variant classification (PS4_sup; PM2_sup, PM3_sup, PP1_mod, PP3_sup) (8). The genetic testing of relatives was challenged and timely as some relatives lived abroad and contact was scarce. Both parents were tested and found to be heterozygous carriers and a symptomatic sibling was found to be homozygous (Figure 2).

Following genetic diagnosis, the two sisters were referred for neurological evaluation. The other sibling did not wish for further clinical workup.

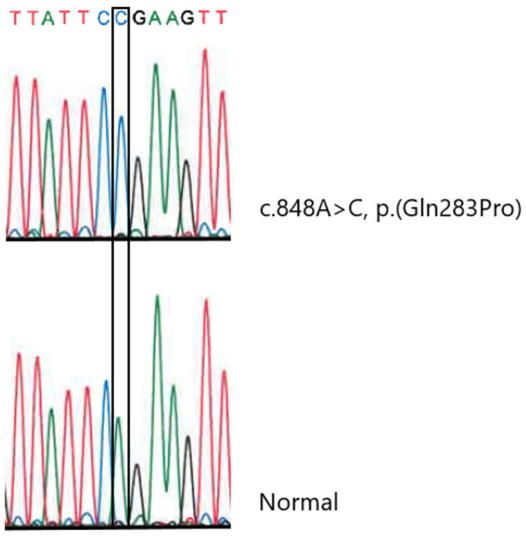

FIGURE 1
Sanger sequencing confirming the *SLC25A46* variant (NM_138773.3:c.848A>C, p.Gln283Pro).

Patient A

A 26-year-old woman was seen in the Neuromuscular Clinic after referral. The patient was diagnosed with optic atrophy around the age of 13 years with symptoms since the age of 10 years but had not experienced progression in adult life. Patient A described herself as clumsier compared to her peers in childhood. The patient had since the age of 15 experienced sensibility disturbances lateral in the upper extremities and tingling and prickling sensation in the lower extremities and a general "weakness" when carrying heavy objects as well as impaired balance. She experienced a progression of sensibility disturbances and balance throughout the years (For timeline, see Supplementary material 2).

She had until recently worked as an ergo therapist and had now started a Master's degree. She experienced some cognitive symptoms with slightly impaired memory especially concerning numbers without worsening throughout the years. She was otherwise healthy and did not have diabetes or any use of medication except contraceptives. Patient A did not have any children yet but had thoughts about whether potential children would inherit the patient's symptoms. This had been the main concern for Patient A since adolescence and she had a wish for diagnostic clarification.

Neurological evaluation revealed diffuse slightly decreased muscle strength in the right hand (the patient was righthanded), impaired pinprick, and light touch sensations lateral on both arms. The Utah Early Neuropathy Scale (UENS) score was 0

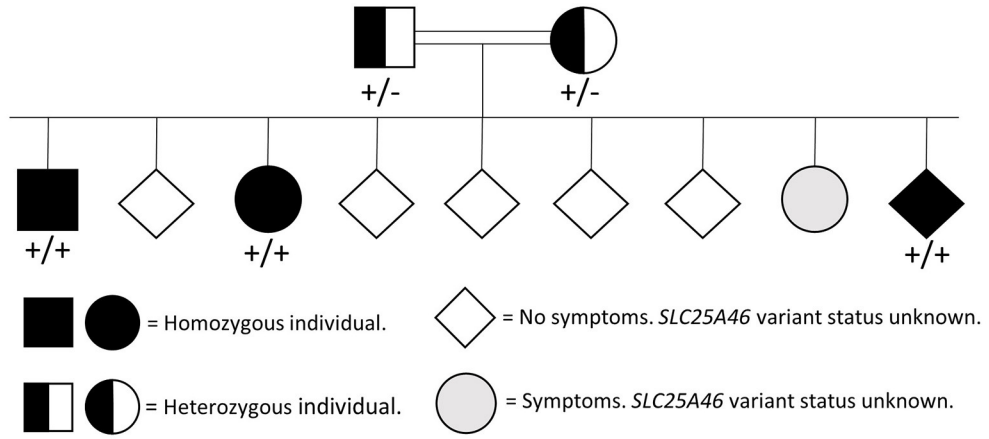

FIGURE 2
Pedigree showing the presence of the *SLC25A46* variant (NM_138773.3:c.848A>C, p.Gln283Pro) within the family.

TABLE 1 Nerve conduction studies.

Nerve	Patient A's values	Interpretation	Patient B's values	Interpretation
Median L/R				
Amplitude (μV)	NA/8.1	Abnormal	NA/2.3	Abnormal
CV (m/s)	NA/58	Normal	NA/52	Normal
Ulnar L/R				
Amplitude (μV)	15.1/17.3	Normal	NA	
CV (m/s)	57/57	Abnormal	NA	
Sural L/R				
Amplitude (μV)	1.7/1.2	Abnormal	%/%	
CV (m/s)	50/52	Normal	%/%	No certain response
Tibial L/R				
Amplitude (μV)	19.1/16.5	Normal	%/1.0	No certain response on left side. Severely reduced amplitude and CV on right side.
CV (m/s)	46/44	Normal	%/39	

CV, conduction velocity; L/R, left/right; NA, not applicable. %, no certain response to stimuli.

out of a maximum of 42 points. A slightly unsteady gait when walking as on a tightrope was seen. Otherwise, the examination was normal.

Laboratory screening for treatable causes of neuropathy was normal including normal HbA1c. A nerve conduction study (NCS) showed reduced sensory nerve action potential in the median (up to the wrist) and sural nerves. No certain response was found in the peroneal nerves. Motor nerve studies were normal except for slowed conduction velocity in both ulnar nerves. The NCS was consistent with a predominantly sensory PN (Table 1). Cerebral MRI was normal.

The patient was seen by a neuro-ophthalmologist where bilateral optic atrophy was confirmed and decreased vision was found (vision 6/12–6/18). The patient was recommended glasses and yearly follow-ups.

The patient was referred to the cardiology department, where an electrocardiogram (ECG), Holter monitoring, and heart ultrasound were performed. Holter monitoring and echocardiogram were normal with an ejection fraction (EF) of 60% and a global longitudinal strain (GLS) of 19. ECG was with abnormal unspecific changes and the patient is followed at a local cardiology clinic with annual controls including Holter.

No medical treatment exists for polyneuropathy due to an *SLC25A46* variant. Patient A was offered a referral to physiotherapy but did not feel a need for it.

One year later, the patient's ophthalmological, cardiological, and neurological symptoms were stationary. The patient is still followed yearly at the Neuromuscular Clinic as well as the Department of Cardiology and the Department of Ophthalmology.

Patient B

A 34-year-old woman described herself as healthy except for a medical history of migraine with aura and decreased vision since early childhood. In school, she had problems reading what the teacher wrote on the blackboard and could not read books. She did not experience any problems with balance or gait and was a fast runner compared to her peers in school.

At the age of 25 years, she experienced increasing problems with balance and a tendency to have leg cramps (for timeline, see Supplementary material 2). Further, she experienced tinnitus with unknown debut without hearing loss. She had no complaints of sensibility disturbances or decreased muscle strength. The balance problems had increased slowly over the last 10 years, but her primary complaint was impaired vision. She was trained as a masseuse but is currently unemployed.

The cranial nerve examination was unremarkable except for a divergent eye axis and impaired vision with the ability to count fingers in half a meter's distance and the inability to read at a normal distance. The neurological examination of the upper extremities was normal with intact sensibility, motor function, and reflexes. No ataxia was found in the upper extremities. Hammertoes were observed and the neurological examination of the lower extremities revealed impaired vibration and position sense up to ankles, discrete sensory ataxia when performing the heel–knee–shin test, and decreased deep tendon reflexes in both ankles. The UENS score was 8. Romberg's sign was positive, and the gait was wide based on the ability to walk on a tightrope.

Blood screening showed a slightly increased kappa-free light chain test, 23.2 (reference interval 3.3–19.4), normal kappa/lambda ratio, and was interpreted without clinical significance. HbA1C was normal.

A nerve conduction study showed reduced amplitude in median nerves, loss of response in sural nerves, and severely reduced and no certain motor response in right and left tibial nerves. The NCS was consistent with a pronounced axonal sensory-motor PN (Table 1). Cerebral MRI showed slight vermis atrophy in the cerebellum (Figure 3). Otherwise, the cerebral MRI was normal.

Ophthalmological examination found optic atrophy consistent with the previous OA diagnosis and significantly impaired vision (vision 6/60). The patient uses an enlarging TV system (CCTV).

ECG and echocardiography were normal with EF at 60% and GLS at 21. Audiological testing was performed because of the unspecific tinnitus, and normal hearing was found with an audiometry discrimination score of 96/96. The patient was referred to physiotherapy due to impaired balance and ataxia.

One year later the neurological symptoms as well as the neurological examination were stationary. Patient B is still followed in the neuromuscular clinic with yearly controls as well as yearly controls at the Department of Cardiology and the Department of Ophthalmology.

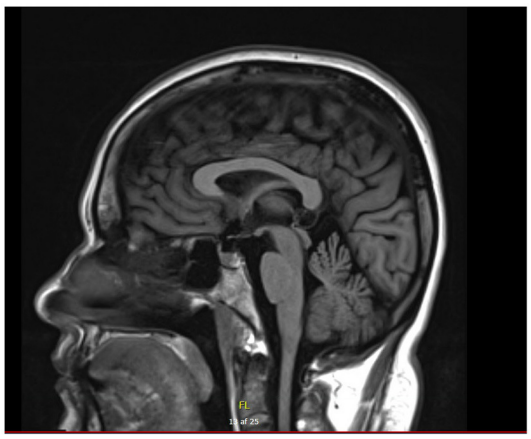

FIGURE 3
Cerebral MRI of patient B with cerebellar atrophy involving vermis.

Discussion

We report two patients with optic atrophy and polyneuropathy of varying degrees.

The patients had clinically been diagnosed with optic atrophy since childhood but did not have a genetic diagnosis for several years. The diagnosis was challenged as the patients were originally from Iraq and came to Denmark later in life which enhance cultural and language barriers. Furthermore, the family was spread across countries, and contact with some relatives was scarce. Patient A was initially tested for the gene *OPA1*, a more common gene related to hereditary optic atrophy. Due to a great wish for diagnostic clarification whole exome sequencing was performed and the patients were found to be homozygous for a novel, likely pathogenic *SLC25A46* variant (NM_138773.3:c.848A>C, p.Gln283Pro). Both parents were heterozygous carriers, and a symptomatic sibling was found to be homozygous for the *SLC25A46* variant.

Recently, the *SLC25A46*-associated PN has been classified as Charcot–Marie–Tooth Disease Type 6B, CMT6B, (9) and different variants in *SLC25A46* have been identified in different neurological syndromic forms with optic atrophy and axonal PN in four unrelated families in the United Kingdom, Palestine, Pakistan, the United States, and Italy (4, 7). However, the different phenotypes and clinical presentations including prognosis are still uncertain.

Patient A presented with mild OA at the age of 10 and a mild predominately sensory PN was found on ENG consistent with the neurological examination and the history of mild symptoms. Patient B presented with OA in early childhood and progressive

balance impairment from the age of 25. A pronounced sensory-motor PN was found at the neurological examination and confirmed by nerve conduction studies. A cerebral MRI scan showed cerebellar atrophy. The cases illustrate the spectrum of the disease and confirm the previously described phenotypes in other variants of *SLC25A46*.

Patient A had a great wish for genetic testing and diagnostic clarification. She expressed concern about the disease and the risk of potential future children inheriting the disease. After investigation and diagnostic clarification, the patient was informed about the expected recessive trait and that Patient A's potential children will be carriers, but that the likelihood of symptomatic disease is very small with an unrelated partner. Patient B's main concern was visual impairment, and the diagnostic genetic clarification did not bring any further information for the patient as there is currently no treatment for the disease.

Our findings and genetic evaluation make the novel *SLC25A46* variant likely pathogenic and the varying phenotype with optic atrophy and polyneuropathy is supported by literature on other variants in *SLC25A46* where different neurological syndromes have been described (3–7).

Whole-exome sequencing can give diagnostic clarification and answers to patients even though the phenotype and prognosis may still be uncertain. Furthermore, it can improve understanding of disease mechanisms associated with polyneuropathy and CMT, which is needed to address relevant therapeutic areas.

Conclusion

We present two sisters with varying polyneuropathy symptoms and symptomatic optic nerve atrophy due to a novel *SLC25A46* variant. The relatively late polyneuropathy diagnosis despite a known history of OA and consanguineous family history highlights the importance of thorough investigation as well as the diagnostic challenges in young patients. It further highlights the possibilities of whole exome sequencing which can improve future understanding of disease mechanisms.

Data availability statement

The datasets presented in this article are not readily available because of ethical and privacy restrictions. Requests to access the datasets should be directed to the corresponding author.

Ethics statement

Written informed consent was obtained from the individual(s) for the publication of any potentially identifiable images or data included in this article.

Author contributions

LK: writing an initial manuscript draft, clinical examination, and manuscript editing and preparation. SH-H: clinical genetic workup and counseling, genetic data, and manuscript editing. SH-Y: clinical examination and manuscript editing. TD: conceiving the idea, supervising clinical examination and investigation, and editing the manuscript. KG: genetic data and manuscript editing. HK: genetic data and manuscript editing. All authors contributed to the article and approved the submitted version.

Conflict of interest

The authors declare that the research was conducted in the absence of any commercial or financial relationships that could be construed as a potential conflict of interest.

Publisher's note

All claims expressed in this article are solely those of the authors and do not necessarily represent those of their affiliated organizations, or those of the publisher, the editors and the reviewers. Any product that may be evaluated in this article, or claim that may be made by its manufacturer, is not guaranteed or endorsed by the publisher.

Supplementary material

The Supplementary Material for this article can be found online at: https://www.frontiersin.org/articles/10.3389/fneur.2022.1066040/full#supplementary-material

SUPPLEMENTARY MATERIAL 1
Completed CARE checklist submitted as a supplementary file.

SUPPLEMENTARY MATERIAL 2
Timeline of historical and current information for Patient A and Patient B.

References

1. Haitina T, Lindblom J, Renström T, Fredriksson R. Fourteen novel human members of mitochondrial solute carrier family 25 (SLC25) widely expressed in the central nervous system. *Genomics.* (2006) 88:779–90. doi: 10.1016/j.ygeno.2006.06.016

2. Terzenidou ME, Segklia A, Kano T, Papastefanaki F, Karakostas A, Charalambous M, et al. Novel insights into SLC25A46-related pathologies in a genetic mouse model. *PLoS Genet.* (2017) 13:e1006656. doi: 10.1371/journal.pgen.1006656

3. Janer A, Prudent J, Paupe V, Fahiminiya S, Majewski J, Sgarioto N, et al. *SLC 25A46* is required for mitochondrial lipid homeostasis and cristae maintenance and is responsible for Leigh syndrome. *EMBO Mol Med.* (2016) 8:1019–38. doi: 10.15252/emmm.201506159

4. Charlesworth G, Balint B, Mencacci NE, Carr L, Wood NW, Bhatia KP. *SLC25A46* mutations underlie progressive myoclonic ataxia with optic atrophy and neuropathy. *Mov Disord.* (2016) 31:1249–51. doi: 10.1002/mds.26716

5. Sulaiman RA, Patel N, Alsharif H, Arold ST, Alkuraya FS, A. novel mutation in SLC25A46 causes optic atrophy and progressive limb spasticity, with no cerebellar atrophy or axonal neuropathy. *Clin Gen.* (2017) 92:230–1. doi: 10.1111/cge.12963i

6. Abrams AJ, Hufnagel RB, Rebelo A, Zanna C, Patel N, Gonzalez MA, et al. Mutations in SLC25A46, encoding a UGO1-like protein, cause an optic atrophy spectrum disorder. *Nat Genet.* (2015) 47:926–32. doi: 10.1038/ng.3354

7. Abrams AJ, Fontanesi F, Tan NBL, Buglo E, Campeanu IJ, Rebelo AP, et al. Insights into the genotype-phenotype correlation and molecular function of SLC25A46. *Hum Mutat.* (2018) 39:1995–2007. doi: 10.1002/humu.23639

8. Richards S, Aziz N, Bale S, Bick D, Das S, Gastier-Foster J, et al. Standards and guidelines for the interpretation of sequence variants: a joint consensus recommendation of the American College of Medical Genetics and Genomics and the Association for Molecular Pathology. *Genet Med May.* (2015) 17:405–24. doi: 10.1038/gim.2015.30

9. https://omim.org/entry/616505?search=slc25a46&highlight=slc25a46

frontiers | Frontiers in Neurology

TYPE Case Report
PUBLISHED 15 December 2022
DOI 10.3389/fneur.2022.991060

Check for updates

OPEN ACCESS

EDITED BY
Giovanni Meola,
University of Milan, Italy

REVIEWED BY
Claudia Vinciguerra,
University of Salerno, Italy
Fengdan Wang,
Peking Union Medical College Hospital (CAMS), China

*CORRESPONDENCE
Limin Wang
wanglimingd@126.com

†These authors have contributed equally to this work

SPECIALTY SECTION
This article was submitted to Neuromuscular Disorders and Peripheral Neuropathies, a section of the journal Frontiers in Neurology

RECEIVED 11 July 2022
ACCEPTED 01 September 2022
PUBLISHED 15 December 2022

CITATION
Tian H, Zhong Y, Liu Z, Wei L, Yuan Y, Zhang Y and Wang L (2022) Lipid storage myopathy due to late-onset multiple Acyl-CoA dehydrogenase deficiency with novel mutations in ETFDH: A case report. *Front. Neurol.* 13:991060. doi: 10.3389/fneur.2022.991060

COPYRIGHT
© 2022 Tian, Zhong, Liu, Wei, Yuan, Zhang and Wang. This is an open-access article distributed under the terms of the Creative Commons Attribution License (CC BY). The use, distribution or reproduction in other forums is permitted, provided the original author(s) and the copyright owner(s) are credited and that the original publication in this journal is cited, in accordance with accepted academic practice. No use, distribution or reproduction is permitted which does not comply with these terms.

Lipid storage myopathy due to late-onset multiple Acyl-CoA dehydrogenase deficiency with novel mutations in ETFDH: A case report

Huihong Tian[1,2†], Yi Zhong[1], Zhihua Liu[1,3], Liping Wei[1,4], Yanbo Yuan[1], Yuhu Zhang[1] and Limin Wang[1*†]

[1]Department of Neurology, Guangdong Provincial People's Hospital, Guangdong Neuroscience Institute, Guangdong Academy of Medical Sciences, Guangzhou, China, [2]Shantou University Medical College, Shantou, China, [3]South China University of Technology School of Medicine, Guangzhou, China, [4]The Second School of Clinical Medicine, Southern Medical University, Guangzhou, China

Background: Lipid storage myopathy (LSM) is an autosomal recessive inherited lipid and amino metabolic disorder with great clinical heterogeneity. Variations in the electron transfer flavoprotein dehydrogenase (ETFDH) gene cause multiple acyl-CoA dehydrogenase deficiency (MADD), and have a manifestation of LSM. Muscle biopsy helps clarify the diagnosis of LSM, and next-generation sequencing (NGS) can be useful in identifying genomic mutation sites. The diagnosis of MADD contributes to targeted therapy.

Case presentation: We report on a teenager who appeared to have muscle weakness and exercise intolerance at the onset. Before the referral to our hospital, he was unsuccessfully treated with glucocorticoid for suspected polymyositis. The next-generation sequencing of the proband and his parents revealed heterozygous variations, c.365G>A (p.G122D) inherited from the father, c.176-194_176-193del, and c.832-316C>T inherited from the mother in the ETFDH gene. The tandem mass spectrometry identified the mutations to be pathogenic. However, his parents and his younger sister who were detected with a mutation of c.365G>A presented no clinical symptoms. This indicates that the combination of the three compound heterozygous mutations in ETFDH is significant. After MADD was diagnosed, a dramatic clinical recovery and biochemical improvement presented as riboflavin was given to the patient across a week, which further confirmed the diagnosis of MADD.

Conclusion: Our observations extend the spectrum of ETFDH variants in Chinese the population and reinforce the role of NGS in diagnosis of MADD. Early diagnosis and appropriate treatment of LSM lead to great clinical efficacy and avoid some lethal complications.

KEYWORDS

lipid storage myopathy, multiple acyl-CoA dehydrogenase deficiency, ETFDH, riboflavin, whole genome sequencing

Introduction

Lipid storage myopathy (LSM) is an inherited autosomal recessive disease caused by disorders in lipid and amino acid metabolism (1). Multiple acyl-CoA dehydrogenase deficiency (MADD), also called glutaric aciduria type II, is the most common type and accounts for ∼90% of LSM in China. Other types of LSM include primary carnitine deficiency (PCD), neutral lipid storage disease with ichthyosis (NLSDI), and neutral lipid storage disease with myopathy (NLSDM) (2). The pathologic manifestation is deposition of lipid droplets in muscle fibers (3). MADD is related to mutations in genes encoding the electron transfer flavoprotein alpha and beta (ETFA and ETFB) proteins or the electron transfer flavoprotein dehydrogenase (ETFDH) protein (4). MADD could be simply divided into neonatal-onset and late-onset MADD. Ninety percent of late-onset MADD is caused by mutations in ETFDH, while neonatal-onset MADD is related to ETFA or ETFB (5).

Herein, we discuss a young male patient who complained of muscle weakness and exercise intolerance. Three novel compound heterozygous mutations are located in one exon and two introns. He was misdiagnosed with polymyositis and treated with a glucocorticoid, resulting in worse parameters of muscle enzyme. After confirmation of the diagnosis of LSM (MADD), the patient received riboflavin replacement therapy accompanied by coenzyme Q10 and levocarnitine, and had a full recovery.

Case report

A 17-year-old boy was admitted to our hospital because of progressive muscle weakness and exercise intolerance for over 6 months. Initially, he had difficulty standing up from squatting and climbing stairs. He had to stop to rest when climbing three to four floors. On admission, he could only climb one floor or walk 20–30 m. Gradually, his upper extremities and jaw were also affected; he could not lift heavy weights and had trouble chewing. He was diagnosed with inflammatory myopathy and treated with corticosteroid in the first hospital. However, his symptoms were not alleviated. For all we know, his siblings and parents did not present similar symptoms.

The physical examination showed moderate muscle weakness (grade 3/5 for the proximal lower limbs, grade 4/5 for the distal lower limbs, grade 4/5 for the upper limbs) according to the Medical Research Council scale, he had a waddling gait, and there was no knee jerk reflex. Cranial nerves were examined and found to be normal including functions of chewing and swallowing. On admission, myocardial enzyme levels were elevated markedly, and creatine kinase (CK), lactate dehydrogenase (LDH), hydroxybutyrate-dehydrogenase (HBDH) were 2,387 (range 50–310 U/L), 1,185 (range 120–250 U/L), and 1,049 U/L (range 72–182 U/L), respectively. Alanine aminotransferase (ALT) was 85 U/L (range 9–50 U/L), and aspartate aminotransferase (AST) was 178 U/L (range 15–40 U/L). Uric acid was 640 umol/L (range 208–428). Rheumatic immune indexes were negative. Although one of the eight myositis antibodies related to idiopathic inflammatory myopathies, antialanyl tRNA synthetase (PL-12), was positive, we think it was not clinically significant for the following reasons. The patient did not have muscle pain and tenderness, and the muscle biopsy did not show inflammatory infiltrates; what is more, he had no response to the glucocorticoid treatment. Antialanyl tRNA synthetase (PL-12) was positive, while other immunity indexes were negative. The electromyography revealed myogenic damage, while the magnetic resonance imaging showed no abnormalities of the bilateral quadriceps femoris. The magnetic resonance imaging of the head was normal, and the electroencephalogram was approximately normal. An abdominal ultrasound scan demonstrated that he had a fatty liver.

Muscle biopsies of the biceps brachii and quadriceps femoris revealed increased deposition of lipid droplets in muscle fibers stained with Oil Red O (ORO) (Figure 1A), which indicated lipid storage myopathy (Figure 1). However, succinate dehydrogenase (SDH) (Figure 1B) and nicotinamide adenine dinucleotide-tetrazolium reductase (NADH-TR) (Figure 1C) were negative for fat vacuole deposition. The hematoxylin and eosin (H and E) (Figure 1D) stain showed a little inflammatory cell infiltration, and abundant small vacuoles were observed in a large number of muscle fibers. Electron microscopy demonstrated that lipid droplets increased in subsarcomembrane and of myofibrils.

The genetic testing (next-generation sequencing) of the boy and his parents confirmed novel compound heterozygous mutations of the ETFDH gene: (OMIM:231675, NM_004453), c.365G>A (p.G122D), c.176-194_176-193del, and c.832-316 C>T, which were predicted to be deleterious in chromosome 4. The exome sequencing of his father showed a compound heterozygous mutation, c.365G>A (p.G122D), in exon 4, while his mother carried compound heterozygous mutations, c.17 6-194_176-193del and c.832-316C>T, in intron 4. The result of the gene test showed that the mutations of ETFDH in the proband came from his patients and were consistent with the pattern of autosomal recessive inheritance. His 6-year-old sister was asymptomatic, and her NGS test showed mutation of c.365G>A (p.G122D), which was inherited from the father. None of the mutations were reported in previous studies; that is, the mutations of the proband are not identified in the Human Gene Mutation Database (HGMD). Meanwhile, the significance of these mutations is not clear. To solve this problem, tandem mass spectrometry and gas chromatography-mass spectrometry of urinary organic acids was conducted in the 1-year follow-up, and we found that the mutations had pathogenicity. To the best of our knowledge, this is the first report on three compound heterozygous variants of ETFDH involved in a patient. In addition, this is the first study that reports gene

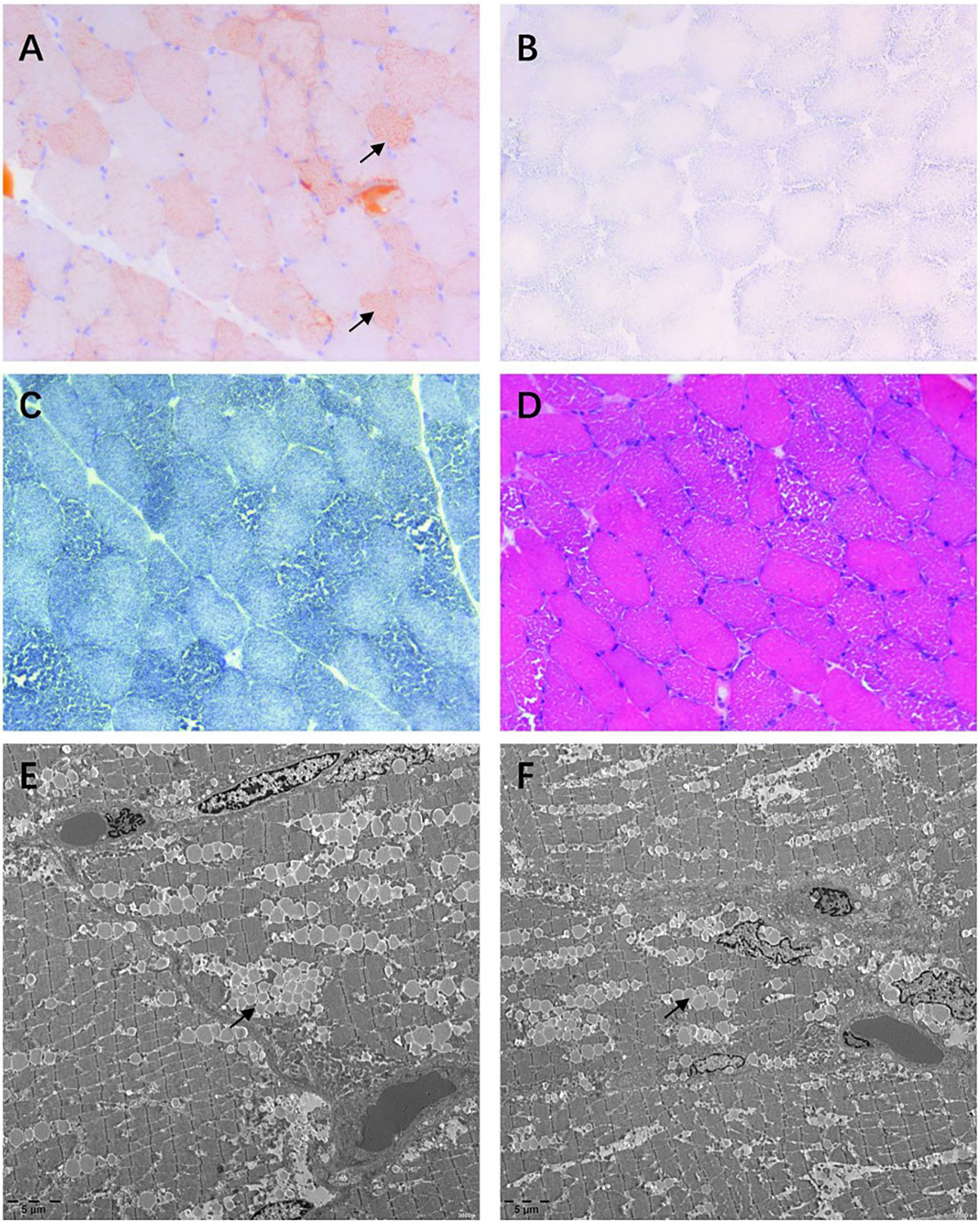

FIGURE 1
Muscle biopsy of the quadriceps femoris. **(A)** Oil Red O (ORO) stain showing lipid droplets deposited in some muscle fibers. **(B,C)** Lipid droplet is almost invisible in succinate dehydrogenase (SDH) and nicotinamide adenine dinucleotide (NADH) stains. **(D)** Hematoxylin and eosin (H and E) stain demonstrating abundant vacuoles appearing in most fibers. **(E,F)** Considerable lipid droplets are observed by transmission electron microscopy.

mutation in a intron, which may benefit from the development of technology.

After confirming the diagnosis of MADD, a combination of riboflavin (60 mg/day), levocarnitine (30 ml/day), and CoQ10 (30 mg/day) was administered to the patient with great improvement in muscle weakness and exercise intolerance in 1 week. In addition, his CK and CK-MB levels were obviously decreased (CK: 5,023 to 864 U/L, CK-MB: 129 to 37 U/L) after having taken the medicines for 4 days. However, CK and CK-MB rose to 9,204 and 70.5 U/L, respectively, in 1 month because of the withdrawal of drugs aalone. The patient adhered to the medication for the next 2 months, the muscle weakness and exercise intolerance completely disappeared, and the creatine kinase values went back to normal (CK: 123 U/L, CK-MB: 11 U/L), as well as the other myocardial enzymes (LDH: 184 U/L, HBDH: 131 U/L, ALT: 34 U/L, AST: 22 U/L). Besides, his uric acid level was decreased to 500 umol/L, a near-normal value. Except for the medications, the patient adhered to a low-fat, high-protein, and low-purine diet. In addition, he did regular low-intensity exercises after discharge. The patient was re-examined by electromyography 1 year post incidence, which suggested myogenic damage but the manifestations of muscles were better than before.

Discussion

Late-onset MADD is mainly caused by homozygous or compound heterozygous mutations in the ETFDH gene. According to previously published articles, several mutation sites are the most common spots: c.250G > A (p.A84T), c.770A > G (p.Y257C), and c.1227A > C (p.L409F) (6, 7).

In this case, the patient was diagnosed with hyperuricemia in the first hospital, but his uric acid decreased gradually after taking riboflavin without using a uric acid-lowering drug. A study involving eight patients with LSM complicated by hyperuricemia found that men with LSM are more likely to develop hyperuricemia than women with LSM because of the benefit of estrogen (8). The cause of hyperuricemia is mainly related to decreased uric acid excretion, which could be explained by renal tubular disorder. The article points out that in young patients who experience muscle weakness and hyperuricemia, LSM should be considered as a differential diagnosis.

Previous literature found that the clinical manifestation of patients with later-onset MADD often involves hepatomegaly, encephalopathy, rhabdomyolysis, vomiting, hypoglycemia, and so on (7, 9–11). Symmetric proximal muscle weakness of the lower extremities was the main complaint of the patient. He was diagnosed with fatty liver by the abdominal ultrasound scan despite being a teenager and keeping a healthy lifestyle. We suspected that his fatty liver was related to MADD.

Before his diagnosis of LSM, low-dose dexamethasone had been used for a week, resulting in worse outcomes of muscle enzyme and no improvement in muscle strength. It may be because the disease continued to progress and the treatment was useless. However, a case reported that a young woman with proximal tetraparesis and myalgia was diagnosed with MADD and had a surprising response to treatment of plasmapheresis and intravenous immunoglobulin (IVIg) (12). It indicates that guidelines for treatment should be refined. Except for invasive muscle biopsy, muscle magnetic resonance imaging can also be conducted to distinguish between MADD and immune-mediated necrotizing myopathy (13). The MRI of the quadriceps femoris muscle of this patient revealed no abnormality, this result may be attributed to the short duration. The mechanism of how immunomodulatory treatment works is not clear. Therefore, further research on the pathophysiology of MADD is needed.

The diagnosis of MADD is based on combination of clinical presentations, acylcarnitines and urine organic acids, muscle biopsy, and genetic analysis. Muscle biopsy is the main criterion for diagnosis of LSM, and genetic diagnosis is conducive to a more accurate diagnosis and future gene-targeted therapy. Meanwhile, muscle MRI can be a complementary and differential examination technique, as it is non-invasive. In this case, because of his symptom of muscle weakness and the positive myositis-specific autoantibody, anti-alanyl tRNA synthetase (anti-PL-12), we gave him dexamethasone as a diagnosis of polymyositis was considered, but it had little clinical efficacy. The biopsy confirmed the diagnosis of LSM, and the gene screening confirmed MADD through mutations of ETFDH. Almost all cases of late-onset MADD is related to variants of the ETFDH gene and riboflavin response (6). MADD is potentially lethal but curable after timely treatment with full-dose riboflavin. Thus, it is essential to diagnose the disease as early as possible. The limitation of our study is that it is hard to define which drug mainly produced a curative effect while three drugs were being applied simultaneously, namely, riboflavin, coenzyme Q10, and levocarnitine. According to previous studies, a dosage of 100–400 mg/d of riboflavin is needed (1). However, the patient was relieved with only 60 mg of riboflavin and CoQ10, and L-carnitine. The use of CoQ10 and L-carnitine in MADD is controversial. MADD may cause secondary carnitine and CoQ 10 deficiency (14).

Conclusion

We have identified a novel compound heterozygous mutation in the ETFDH gene from a patient with late-onset riboflavin-responsive multiple acyl-CoA dehydrogenase deficiency, which expands the spectrum of mutations found in patients with MADD. Late-onset MADD is a curable hereditary disease. Besides, early diagnosis and treatment could reduce complications, so this article can help improve the knowledge of LSM.

Data availability statement

The datasets presented in this article are not readily available because of ethical and privacy restrictions. Requests to access the datasets should be directed to the corresponding author.

Author contributions

All authors listed have made a substantial, direct, and intellectual contribution to the work and approved it for publication.

Funding

This study was supported by the Natural Science of Guangdong Province (Grant No. 2018A030313427) and Guangzhou Science and Technology Planning Project (Grant No. 202002030393).

Conflict of interest

The authors declare that the research was conducted in the absence of any commercial or financial relationships that could be construed as a potential conflict of interest.

Publisher's note

All claims expressed in this article are solely those of the authors and do not necessarily represent those of their affiliated organizations, or those of the publisher, the editors and the reviewers. Any product that may be evaluated in this article, or claim that may be made by its manufacturer, is not guaranteed or endorsed by the publisher.

References

1. Vasiljevski ER, Summers MA, Little DG, Schindeler A. Lipid storage myopathies: Current treatments and future directions. *Prog Lipid Res.* (2018) 72:1–17. doi: 10.1016/j.plipres.2018.08.001

2. Angelini C, Pennisi E, Missaglia S, Tavian D. Metabolic lipid muscle disorders: biomarkers and treatment. *Ther Adv Neurol Disord.* (2019) 12:175628641984335. doi: 10.1177/1756286419843359

3. Missaglia S, Coleman R, Mordente A, Tavian D. Neutral lipid storage diseases as cellular model to study lipid droplet function. *Cells.* (2019) 8:187. doi: 10.3390/cells8020187

4. Liu XY, Wang ZQ, Wang DN, Lin MT, Wang N. A historical cohort study on the efficacy of glucocorticoids and riboflavin among patients with late-onset multiple Acyl-CoA dehydrogenase deficiency. *Chin Med J.* (2016) 129:142–6. doi: 10.4103/0366-6999.173438

5. Dernoncourt A, Bouchereau J, Acquaviva-Bourdain C, Wicker C, De Lonlay P, Gourguechon C, et al. Myogenic disease and metabolic acidosis: consider multiple acyl-coenzyme a dehydrogenase deficiency. *Case Rep Crit Care.* (2019) 2019:1–7. doi: 10.1155/2019/1598213

6. Xi J, Wen B, Lin J, Zhu W, Luo S, Zhao C, et al. Clinical features and ETFDH mutation spectrum in a cohort of 90 Chinese patients with late-onset multiple acyl-CoA dehydrogenase deficiency. *J Inherit Metab Dis.* (2014) 37:399–404. doi: 10.1007/s10545-013-9671-6

7. Wang ZQ, Chen XJ, Murong SX, Wang N, Wu ZY. Molecular analysis of 51 unrelated pedigrees with late-onset multiple acyl-CoA dehydrogenation deficiency (MADD) in southern China confirmed the most common ETFDH mutation and high carrier frequency of c.250G>A. *J Mol Med.* (2011) 89:569–76. doi: 10.1007/s00109-011-0725-7

8. Han J, Song X, Lu S, Ji G, Xie Y, Wu H. Adolescent hyperuricemia with lipid storage myopathy: a clinical study. *Med Sci Monit.* (2019) 25:9103–11. doi: 10.12659/MSM.918841

9. Grünert SC. Clinical and genetical heterogeneity of late-onset multiple acyl-coenzyme A dehydrogenase deficiency. *Orphanet J Rare Dis.* (2014) 9:117. doi: 10.1186/s13023-014-0117-5

10. Chen HZ, Jin M, Cai NQ, Lin XD, Liu XY, Xu LQ, et al. Rhabdomyolysis and respiratory insufficiency due to the common ETFDH mutation of c.250G>A in two patients with late-onset multiple acyl-CoA dehydrogenase deficiency. *Chin Med J.* (2019) 132:1615–8. doi: 10.1097/CM9.0000000000000288

11. Zhu M, Zhu X, Qi X, Weijiang D, Yu Y, Wan H, et al. Riboflavin-responsive multiple Acyl-CoA dehydrogenation deficiency in 13 cases, and a literature review in mainland Chinese patients. *J Hum Genet.* (2014) 59:256–61. doi: 10.1038/jhg.2014.10

12. Kleefeld F, Renesse A, Dittmayer C, Harms L, Radke J, Radbruch H, et al. Successful plasmapheresis and immunoglobulin treatment for severe lipid storage myopathy: doing the right thing for the wrong reason. *Neuropathol Appl Neurobiol.* (2022) 48:e12731. doi: 10.1111/nan.12731

13. Zhao YW, Liu XJ, Zhang W, Wang ZX, Yuan Y. Muscle magnetic resonance imaging for the differentiation of multiple Acyl-CoA dehydrogenase deficiency and immune-mediated necrotizing myopathy. *Chin Med J.* (2018) 131:144–50. doi: 10.4103/0366-6999.222323

14. Gempel K, Topaloglu H, Talim B, Schneiderat P, Schoser BGH, Hans VH, et al. The myopathic form of coenzyme Q10 deficiency is caused by mutations in the electron-transferring-flavoprotein dehydrogenase (ETFDH) gene. *Brain.* (2007) 130:2037–44. doi: 10.1093/brain/awm054

frontiers | Frontiers in Neurology

TYPE Case Report
PUBLISHED 16 January 2023
DOI 10.3389/fneur.2023.1056341

Check for updates

OPEN ACCESS

EDITED BY
Jian-Quan Shi,
Nanjing Medical University, China

REVIEWED BY
Tomas Marek,
Mayo Clinic, United States
Jiu Chen,
Nanjing University, China

*CORRESPONDENCE
Xinhong Feng
✉ fxha01071@btch.edu.cn

SPECIALTY SECTION
This article was submitted to Neuromuscular Disorders and Peripheral Neuropathies, a section of the journal Frontiers in Neurology

RECEIVED 28 September 2022
ACCEPTED 02 January 2023
PUBLISHED 16 January 2023

CITATION
Chen M, Li X and Feng X (2023) Case report: Brachial plexopathy caused by malignant peripheral nerve sheath tumor and review of the literature. *Front. Neurol.* 14:1056341. doi: 10.3389/fneur.2023.1056341

COPYRIGHT
© 2023 Chen, Li and Feng. This is an open-access article distributed under the terms of the Creative Commons Attribution License (CC BY). The use, distribution or reproduction in other forums is permitted, provided the original author(s) and the copyright owner(s) are credited and that the original publication in this journal is cited, in accordance with accepted academic practice. No use, distribution or reproduction is permitted which does not comply with these terms.

Case report: Brachial plexopathy caused by malignant peripheral nerve sheath tumor and review of the literature

Mengjie Chen, Xiuli Li and Xinhong Feng*

Department of Neurology, Beijing Tsinghua Changgung Hospital, School of Clinical Medicine, Tsinghua University, Beijing, China

Brachial plexopathy (BP) is easily misdiagnosed due to its complexity and varying clinical presentation. Malignant peripheral nerve sheath tumors (MPNST) can accumulate in the brachial plexus and share symptoms with BP, which may hinder the differential diagnosis between BP induced by radiation or metastases, and MPNST-derived BP, in patients with a history of breast cancer and radiation exposure. A 34-year-old Chinese female presented with MPNST. The tumor involved the brachial plexus. She had a history of breast cancer and radiotherapy. The first consideration was radiation- or breast cancer metastasis-derived BP. Clinical examination was performed. Finally, a diagnosis of MPNST of the brachial plexus was made, which guided an accurate treatment plan. This report highlights the importance of correctly diagnosing BP etiology for guiding precise treatment. BP caused by MPNST needs to be considered in clinical practice, and biopsy plays a central role in the differential diagnosis. Complete local surgical resection can prolong survival of patients with MPNST and improve treatment prognosis.

KEYWORDS

brachial plexopathy, malignant peripheral nerve sheath tumors, diagnosis, EMG, case report

1. Introduction

The brachial plexus provides motor and sensory innervation to the upper extremities. Brachial plexopathy (BP) is a peripheral neuropathy that occurs in the brachial plexus. The prevalence of cancer-associated plexopathy is ∼0.4% in patients with cancer and 2−5% in those treated with radiotherapy, indicating that BP is a rare condition (1). Malignant peripheral nerve sheath tumors (MPNST) are derived from Schwann cells or generated through pluripotent cell differentiation of the neural crest. MPNST are rare and highly aggressive soft-tissue tumors. Type I neurofibromatosis is a major risk factor for MPNST (2, 3). However, ∼45% of MPNST cases are incidental and 10% are due to previous radiation exposure (4, 5). MPNST can involve the brachial plexus and present with clinical features similar to those of BP, which may hinder the differential diagnosis between BP induced by radiation or metastases, and MPNST-derived BP, in patients with a previous history of breast cancer and radiation exposure. Improper treatment due to misdiagnosis can lead to medicolegal disputes and delays in effective treatment of malignant tumors, markedly affecting patient clinical outcome. Therefore, it is recommended that in patients with BP, particularly those with a history of breast cancer and radiotherapy, the diagnosis of the cause should be achieved as it helps determine the accurate treatment decision. A representative case is discussed in the following section.

2. Case presentation

A 34-year-old female patient presented with weakness that progressed over 1 year and progressively involved her entire left upper limb. She had needle-like intermittent pain in left upper limb with visual analog scale (VAS) score of 4-5 points, and attack duration of 1–2 s occurring several times a day but mostly at night. Six months ago, the above symptoms worsened. VAS score was 6–7 points, and there was increased pain frequency. She was unable to lie on her back. Three weeks prior, she could not lift her left arm, and the pain radiating from the left shoulder blade to the fingers worsened. The patient had a history of breast cancer and had undergone standard radiotherapy and chemotherapy. No other pertinent history was noted.

Clinical examination revealed decreased muscle strength and muscle atrophy in the left upper limb. Left biceps and radial reflexes were not elicited; the rest of the neurological examination was normal. Electrophysiological studies were performed to evaluate the brachial plexus. Nerve conduction studies showed that the motor and sensory nerves of the right upper limb were normal, whereas the left brachial plexus was injured with predominant axonal injury. In addition, needle electromyography revealed damage to the left brachial plexus. Laboratory examinations revealed that the blood levels of the tumor marker Squamous Cell Carcinoma Antigen were 2.1 ng/ml (reference value <1.5 ng/ml). Further neuroimaging was performed. Magnetic resonance imaging (MRI) of the brachial plexus revealed thickening and edema of the left brachial plexus (Figure 1). Ultrasound of the left brachial plexus showed significant edema and thickening of the left brachial plexus roots, trunk, and strands, mostly pronounced in the supraclavicular fossa segment, with local thickening showing neuroma-like changes, ultrasound of the left upper arm nerve showed edema of some nerve bundles (Figure 2). The patient was a young woman with an insidious and progressive onset of symptoms, with pain in the left upper limb as the first symptom and progressive weakness affecting the entire upper limb function. She had a history of previous tumor treatment, the possibility of either radiation-induced BP or metastatic BP resulting from breast cancer was considered. Radiation-induced BP, with predominant neurofibromas on the nuclear magnetic structure, was less consistent with this patient's symptomatology. Further, positron emission tomography-computed tomography (PET-CT) revealed increased radioactive uptake in the left brachial plexus (SUV 24.4), indicating a tumor (Figure 3). Finally, we performed a pathological examination of tissue of brachial plexus swelling in the left supraclavicular fossa. The pathological pictures showed a diffuse laminar arrangement of spindle or oval cells with mild-moderate heterogeneity of the nuclei, along with some vitreous changes and chondrogenic differentiation. Morphology and positive immunohistochemical presentations (Vimentin, Ki-67, SOX10, S-100, P120) of nerve biopsy confirmed an MPNST (Figure 4).

Based on our follow-up with the patient, we noted that she had undergone complete local surgical resection at another hospital. After 2 months of post-operative rehabilitation, the patient's severe pain in the left upper limb was relieved and the muscle strength could resist partial resistance. The prognosis of the patient was good.

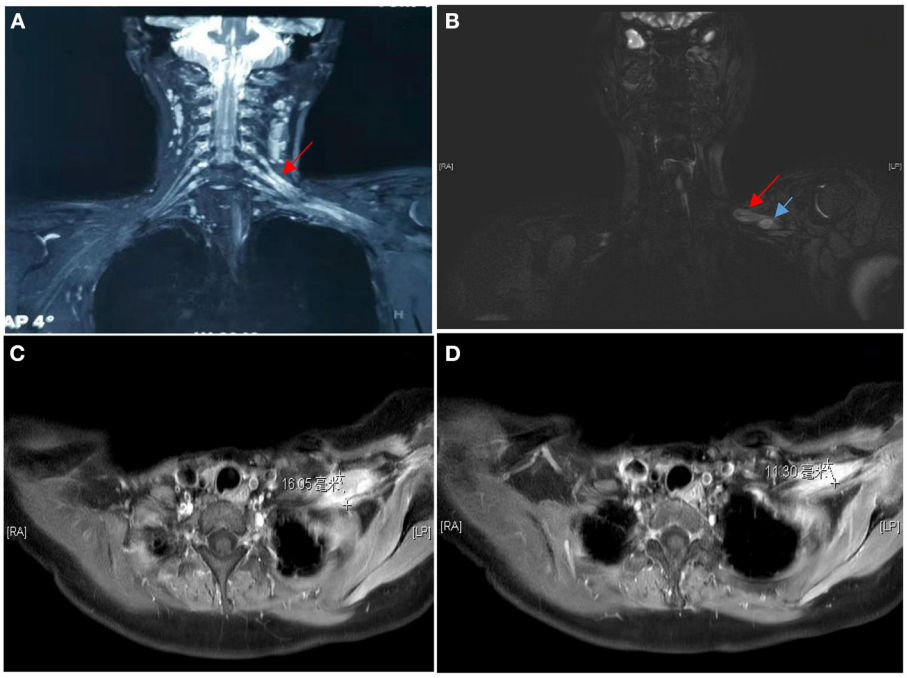

FIGURE 1
MRI of the brachial plexus showed the C5/C6 roots, upper and middle trunks and all strands of the left brachial plexus were significantly swollen and thickened, with T2W high signal, the right brachial plexus had good continuity, with no clear thickening and no signal enhancement **(A)**. MRI showed multiple nodules within the brachial plexus in the left subclavian region **(B)**, the two that could be distinguished were ~16 mm **(C)** and 11 mm **(D)** in diameter respectively.

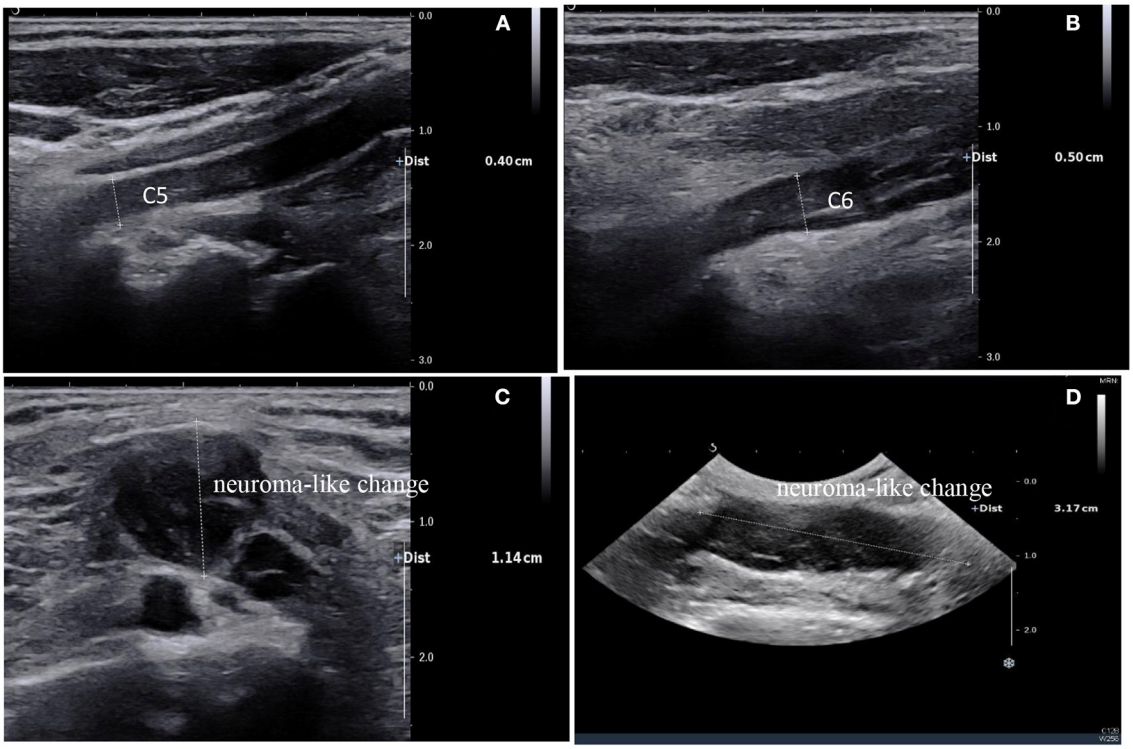

FIGURE 2
Ultrasound of the brachial plexus showed a high degree of thickening of the C5 and C6 nerve roots, ~0.4 cm and 0.5 cm respectively **(A, B)**; diffuse edema of the superior, middle, and inferior trunks were seen in the interosseous sulcus; Brachial plexus neuroma-like change of brachial plexus in the supraclavicular fossa, ~1.14 cm thick at most and 3.17 cm long **(C, D)**.

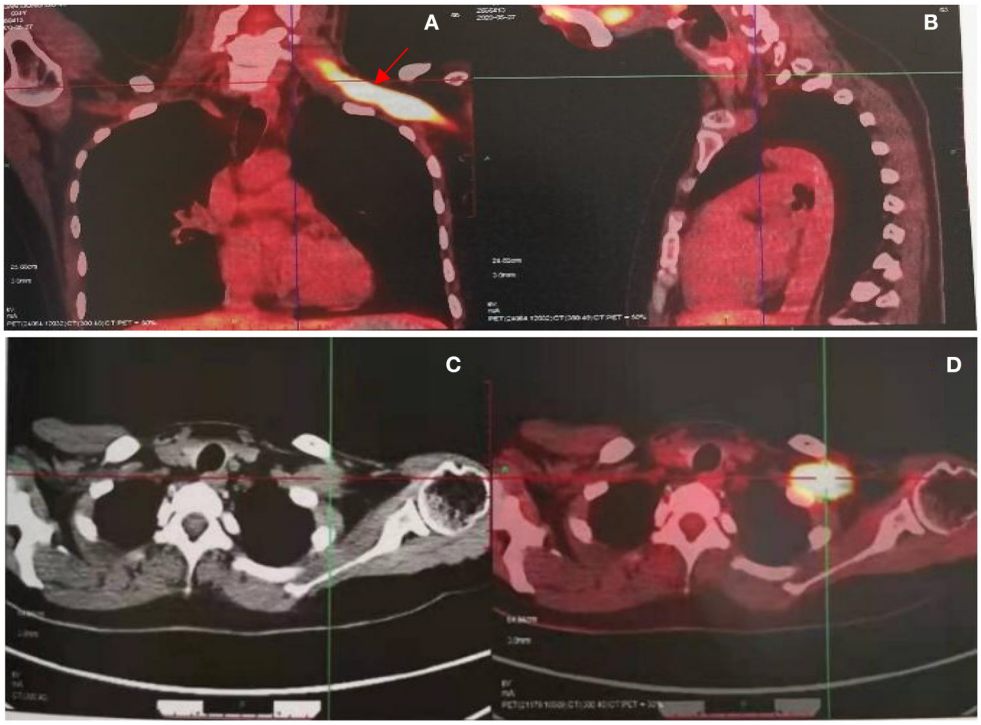

FIGURE 3
PET CT revealed increased radioactive uptake in the left brachial plexus (SUV max 24.4) **(A, B)**, involving a length of 9.3 cm **(C, D)**.

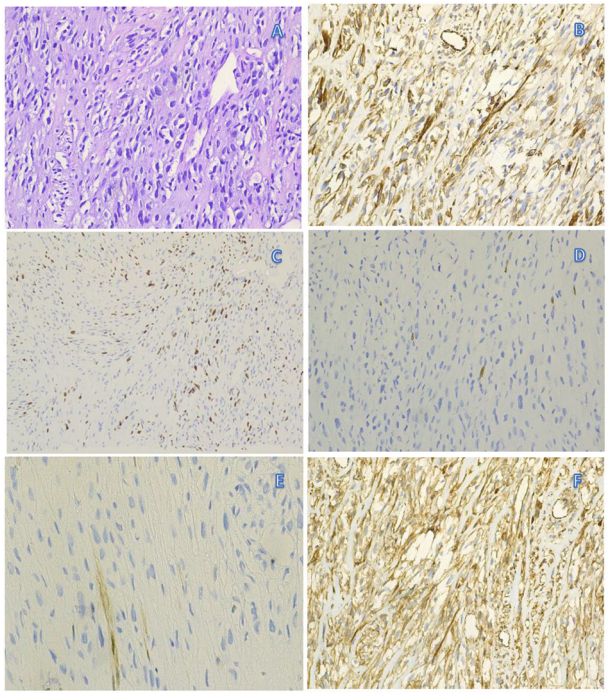

FIGURE 4
Pathology (tissue of brachial plexus swelling in the left supraclavicular fossa): diffuse lamellar arrangement of the spindle or oval cells, mild-moderate heterogeneity of the nuclei, nuclear schism 4/10HPF, some interstitial vitreous changes, chondrogenic differentiation visible in focal areas **(A)**. Immunohistochemistry: Vimentin (+) **(B)**, Ki-67 (25%+) **(C)**, SOX10 (individual cells+) **(D)**, S-100 (individual cells weakly+) **(E)**, P120 (+) **(F)**. In summary, a diagnosis of malignant peripheral schwannoma was considered.

3. Discussion

The brachial plexus comprises the ventral nerves of the C5-T1 spinal nerves and innervates the upper limbs, shoulders, and upper chest. The brachial plexus can be localized based on neurological and neurophysiological examination (6, 7). BP is one of the most severe types of peripheral nerve injury because of its complicated anatomical structure (8). BP is divided into two main categories, traumatic and non-traumatic, depending on the clinical situation (9). Non-traumatic BP usually occurs because of idiopathic brachial neuritis, BP caused by direct tumor invasion or metastasis, radiation-related BP, thoracic outlet syndrome, and iatrogenic injury, all of which can cause partial or complete loss of upper limb function (10).

BP-associated with breast cancer can occur due to radiation injury or metastatic spread of the tumor (11, 12). In our case, the first consideration for diagnosis was the more commonly occurring radiation-induced brachial plexus neuropathy (RIBPN) (10, 13, 14). It should be noted that the differential diagnosis between neoplastic-derived BP and RIBPN is complex in clinical practice. In terms of clinical features, pain is usually more severe in neoplastic BP than that in RIBPN, affects the lower brachial plexus more often, and is more commonly associated with Horner's syndrome (14, 15). In addition, sensory abnormalities and muscle weakness are usually more severe in tumor-induced brachial plexopathies than in RIBPN (16). The presence of myofibrillation on neurophysiological examination supports the diagnosis of RIBPN, together with the presence of myofibrillatory discharges (17–21). An electromyogram (EMG) can detect ~30% of myofibrillatory discharges, which are usually undetectable in cases with tumor infiltration; however, myofibrillatory discharges are not a common feature of RIBPN. MRI is a non-invasive test commonly used to distinguish brachial plexus pathologies (22, 23) and has a higher resolution of anatomical structures compared to other imaging techniques such as ultrasound. Conventional MRI sequences used to evaluate the brachial plexus typically include T1-weighted (T1W) and fat-suppressed T2-weighted (T2W) images. Upon fibrosis within and around neurons due to radiotherapy, T2W images show an equal to low signal relative to that of the muscle. Conversely, T2W sequences show a massy high signal in the presence of brachial plexus tumor infiltration. In addition, nerves with radiological brachial plexus injury show mainly diffuse, homogeneous, and symmetrical swelling on MRI (24). Tumors usually appear on MRI as a heterogeneous, asymmetric enlargement of the lesion and as an enhancing mass (25, 26). Based on these parameters, it is possible to differentiate between radiological brachial plexus injury and a tumor to a certain extent, and diffusion-weighted imaging (DWI) sequences may be effective in differentiating benign or malignant peripheral nerve mass-like or infiltrative lesions (27). In our case, the nerve ultrasound and MRI findings were not consistent with brachial plexus injury after radiotherapy, particularly the nodular and tumor-like thickening of the brachial plexus on ultrasound, suggesting a tumor association (28, 29).

PET is important for identifying the tumor-associated brachial plexus as it can detect the hypermetabolic manifestations of tumors. RIBPN generally reflects a slight avidity. Increased radioactivity uptake in the left brachial plexus on PET suggests the presence of a tumor (26, 30). In conjunction with this case, elevated tumor markers suggest the possibility of tumor-induced BP. However, this patient was treated with a full course of radiotherapy and continued endocrine therapy after breast-conserving surgery, and no tumor recurrence was observed at regular follow-up. The diagnosis of MPNST as the etiology of BP was confirmed with biopsy. The pathological diagnosis of MPNST requires a combination of morphology, immunohistochemistry and clinical history. Under the microscope, MPNSTs are typically infiltrative lesions that show different cell morphologies (including spindle-shaped, epithelioid, pleomorphic, or oval-shaped). Spindle-shaped cells MPNST are often arranged in long fascicles. The nucleus is also diverse in morphology, displaying elongated, conical, curved or wavy shapes. Widespread heterogeneity of the nucleus and nuclear schism are common. Interstitial vitreous changes and chondrogenic differentiation can be found on pathological images (31). These diagnostic pathomorphological manifestations are consistent with our case. Immunohistochemically, as the Schwann differentiation of tumors is highly variable and incomplete, S-100 protein expression is usually more restricted, showing weak positivity (32). Nuclear expression of Sox10 is an essential neural crest transcription factor for specification and maturation of Schwann cells (33). The expression of Ki-67 protein is recognized to be closely related to the cell division cycle and can reflect the malignancy of the tumor (34). Vimentin protein is an important component of the cytoskeleton.

Positive immunohistochemistry indicates that the tumor is likely to originate from mesenchymal tissue (35). P120 is involved in intercellular adhesion and signal transduction in several cell types and is associated with tumor formation (36). Immunohistochemistry is very valuable for the diagnosis of MPSNT.

Breast and lung cancer are the most common cancer types causing BP. Primary brachial plexus tumors (e.g., nerve sheath tumors and neurofibromas) are uncommon and mostly isolated. These tumors rarely cause symptomatic plexopathy (10, 37). However, multiple tumors occur in patients with type I neurofibromatosis, and these are more likely to present as pain with associated functional deficits. Both type I neurofibromatosis and malignant transformation of these tumors are rare. MPSNT accounts for 5–10% of all soft tissue sarcomas and is much less common when it involves the brachial plexus; 10% of MPSNT is due to previous radiation exposure (5, 38, 39). In the present case, a diagnosis of radiation-induced MPNST was considered in the context of the patient's past medical history as a relationship between radiotherapy and MPNST progression had been demonstrated. Radiotherapy causes chromosomal damage and induces abnormal and atypical cytological proliferation of Schwann cells. It accelerates the progression of malignant nerve sheath tumors, particularly in susceptible patients (40, 41). As peripheral nerves are very sensitive to radiotherapy, persistent inflammation after this treatment leads to changes in the peripheral nerve microenvironment and a higher proliferation rate. Radiotherapy can also cause lymphatic obstruction and fibrotic damage to the perineural vessels, allowing mutated Schwann cells to evade immune surveillance and continue to proliferate (42).

Complete local surgical resection can prolong the survival of patients with malignant peripheral schwannomas. For radiation-induced MPNST, the median survival time was 5 months for patients without surgery, 16 months for patients with complete surgical resection, 28.3% for 2-year survival, 12 months for patients with incomplete surgical resection, and 7.5% for 2-year survival. In general, radiation-induced MPNST is associated with poorer prognosis compared with that for sporadic MPNST (43). In these circumstances, EMG can detect abnormal changes in electrical activity that occur during surgery, which may reveal potential nerve damage. Thus, the use of intraoperative neurophysiological monitoring (IONM) for electrical activity ensures the best possible nerve integrity, avoids unnecessary damage, and improves treatment prognosis (44).

In conclusion, a complete diagnostic pathway for BP in a patient with a history of breast cancer and radiotherapy is presented here. This case report highlights the importance of correctly diagnosing the etiology of BP in order to guide precise treatment. MPNST-derived BP, together with RIBPN and BP derived from breast cancer metastases require attention in clinical practice in a patient population with a history of breast cancer and radiotherapy, with biopsy playing a key role in the differential diagnosis. Concerning treatments, complete local surgical resection can prolong the survival of patients with MPNST and improve treatment prognosis. Importantly, the risk of brachial plexus injury secondary to MPNST should be considered before patients are treated with radiotherapy for the primary tumor lesion, and long-term follow-up along with neurological examination of patients after radiotherapy is necessary. It is also pertinent to investigate the molecular mechanisms underlying radiation-induced MPNST.

Data availability statement

The original contributions presented in the study are included in the article/supplementary material, further inquiries can be directed to the corresponding author.

Ethics statement

The studies involving human participants were reviewed and approved by Ethics Committee of the Beijing Tsinghua Changgung Hospital, School of Clinical Medicine, Tsinghua University. The patients/participants provided their written informed consent to participate in this study. Written informed consent was obtained from the individual(s) for the publication of any potentially identifiable images or data included in this article.

Author contributions

MC: drafting/revision of the manuscript for content, including medical writing for content, and analysis or interpretation of data. XL: study concept or design and analysis or interpretation of data. XF: drafting/revision of the manuscript for content, including medical writing for content, major role in the acquisition of data, and study concept or design. All authors contributed to the article and approved the submitted version.

Acknowledgments

The authors acknowledge their gratitude to the patient in this study.

Conflict of interest

The authors declare that the research was conducted in the absence of any commercial or financial relationships that could be construed as a potential conflict of interest.

Publisher's note

All claims expressed in this article are solely those of the authors and do not necessarily represent those of their affiliated organizations, or those of the publisher, the editors and the reviewers. Any product that may be evaluated in this article, or claim that may be made by its manufacturer, is not guaranteed or endorsed by the publisher.

References

1. Jaeckle KA. Neurological manifestations of neoplastic and radiation-induced plexopathies. *Semin Neurol.* (2004) 24:385–93. doi: 10.1055/s-2004-861533

2. Korfhage J, Lombard DB. Malignant peripheral nerve sheath tumors: from epigenome to bedside. *Mol Cancer Res.* (2019) 17:1417–28. doi: 10.1158/1541-7786.MCR-19-0147

3. Uusitalo E, Leppavirta J, Koffert A, Suominen S, Vahtera J, Vahlberg T, et al. Incidence and mortality of neurofibromatosis: a total population study in Finland. *J Invest Dermatol.* (2015) 135:904–6. doi: 10.1038/jid.2014.465

4. Farid M, Demicco EG, Garcia R, Ahn L, Merola PR, Cioffi A, et al. Malignant peripheral nerve sheath tumors. *Oncologist.* (2014) 19:193–201. doi: 10.1634/theoncologist.2013-0328

5. LaFemina J, Qin LX, Moraco NH, Antonescu CR, Fields RC, Crago AM, et al. Oncologic outcomes of sporadic, neurofibromatosis-associated, and radiation-induced malignant peripheral nerve sheath tumors. *Ann Surg Oncol.* 20:66–72. doi: 10.1245/s10434-012-2573-2

6. Ferrante MA, Wilbourn AJ. The utility of various sensory nerve conduction responses in assessing brachial plexopathies. *Muscle Nerve.* (1995) 18:879–89. doi: 10.1002/mus.880180813

7. Ferrante MA. Brachial plexopathies: classification, causes, and consequences. *Muscle Nerve.* (2004) 30:547–68. doi: 10.1002/mus.20131

8. Noland SS, Bishop AT, Spinner RJ, Shin AY. Adult traumatic brachial plexus injuries. *J Am Acad Orthop Surg.* (2019) 27:705–16. doi: 10.5435/JAAOS-D-18-00433

9. Wilbourn AJ. Plexopathies. *Neurol Clin.* (2007) 25:139–71. doi: 10.1016/j.ncl.2006.11.005

10. Gilcrease-Garcia BM, Deshmukh SD, Parsons MS. Anatomy, imaging, and pathologic conditions of the brachial plexus. *Radiographics.* (2020) 40:1686–714. doi: 10.1148/rg.2020200012

11. Wittenberg KH, Adkins MC. MR imaging of nontraumatic brachial plexopathies: frequency and spectrum of findings. *Radiographics.* (2000) 20:1023–32. doi: 10.1148/radiographics.20.4.g00jl091023

12. Kim J, Jeon JY, Choi YJ, Choi JK, Kim SB, Jung KH, et al. Characteristics of metastatic brachial plexopathy in patients with breast cancer. *Supp Care Cancer.* (2020) 28:1913–8. doi: 10.1007/s00520-019-04997-6

13. Delanian S, Lefaix JL, Pradat PF. Radiation-induced neuropathy in cancer survivors. *Radiother Oncol.* (2012) 105:273–82. doi: 10.1016/j.radonc.2012.10.012

14. Kori SH, Foley KM, Posner JB. Brachial plexus lesions in patients with cancer: 100 cases. *Neurology.* (1981) 31:45–50. doi: 10.1212/WNL.31.1.45

15. Mondrup K, Olsen NK, Pfeiffer P, Rose C. Clinical and electrodiagnostic findings in breast cancer patients with radiation-induced brachial plexus neuropathy. *Acta Neurol Scand.* (1990) 81:153–8. doi: 10.1111/j.1600-0404.1990.tb00952.x

16. Ko K, Sung DH, Kang MJ, Ko MJ, Do JG, Sunwoo H, et al. Clinical, electrophysiological findings in adult patients with non-traumatic plexopathies. *Ann Rehabil Med.* (2011) 35:807–15. doi: 10.5535/arm.2011.35.6.807

17. Esteban A, Traba A. Fasciculation-myokymic activity and prolonged nerve conduction block. A physiopathological relationship in radiation-induced brachial plexopathy. *Electroencephalogr Clin Neurophysiol.* (1993) 89:382–91. doi: 10.1016/0168-5597(93)90111-2

18. Roth G, Magistris MR. Neuropathies with prolonged conduction block, single and grouped fasciculations, localized limb myokymia. *Electroencephalogr Clin Neurophysiol.* (1987) 67:428–38. doi: 10.1016/0013-4694(87)90006-X

19. Harper CM Jr, Thomas JE, Cascino TL, Litchy WJ. Distinction between neoplastic and radiation-induced brachial plexopathy, with emphasis on the role of EMG. *Neurology.* (1989) 39:502–6. doi: 10.1212/WNL.39.4.502

20. Thomas JE, Cascino TL, Earle JD. Differential diagnosis between radiation and tumor plexopathy of the pelvis. *Neurology.* (1985) 35:1–7. doi: 10.1212/WNL.35.1.1

21. Lederman RJ, Wilbourn AJ. Brachial plexopathy: recurrent cancer or radiation? *Neurology.* (1984) 34:1331–5. doi: 10.1212/WNL.34.10.1331

22. Martinoli C, Gandolfo N, Perez MM, Klauser A, Palmieri F, Padua L, et al. Brachial plexus and nerves about the shoulder. *Semin Musculoskelet Radiol.* (2010) 14:523–46. doi: 10.1055/s-0030-1268072

23. Lapegue F, Faruch-Bilfeld M, Demondion X, Apredoaei C, Bayol MA, Artico H, et al. Ultrasonography of the brachial plexus, normal appearance and practical applications. *Diagn Interv Imaging.* (2014) 95:259–75. doi: 10.1016/j.diii.2014.01.020

24. Amrami KK, Felmlee JP, Spinner RJ. MRI of peripheral nerves. *Neurosurg Clin N Am.* (2008) 19:559–72. doi: 10.1016/j.nec.2008.07.019

25. Stoll G, Bendszus M, Perez J, Pham M. Magnetic resonance imaging of the peripheral nervous system. *J Neurol.* (2009) 256:1043–51. doi: 10.1007/s00415-009-5064-z

26. Crush AB, Howe BM, Spinner RJ, Amrami KK, Hunt CH, Johnson GB, et al. Malignant involvement of the peripheral nervous system in patients with cancer: multimodality imaging and pathologic correlation. *Radiographics.* (2014) 34:1987–2007. doi: 10.1148/rg.347130129

27. Yuh EL, Jain Palrecha S, Lagemann GM, Kliot M, Weinstein PR, Barbaro NM, et al. Diffusivity measurements differentiate benign from malignant lesions in patients with peripheral neuropathy or plexopathy. *AJNR Am J Neuroradiol.* (2015) 36:202–9. doi: 10.3174/ajnr.A4080

28. Baute V, Strakowski JA, Reynolds JW, Karvelas KR, Ehlers P, Brenzy KJ, et al. Neuromuscular ultrasound of the brachial plexus: a standardized approach. *Muscle Nerve.* (2018) 58:618–24. doi: 10.1002/mus.26144

29. Griffith JF. Ultrasound of the brachial plexus. *Semin Musculoskelet Radiol.* (2018) 22:323–33. doi: 10.1055/s-0038-1645862

30. Meany H, Dombi E, Reynolds J, Whatley M, Kurwa A, Tsokos M, et al. 18-fluorodeoxyglucose-positron emission tomography (FDG-PET) evaluation of nodular lesions in patients with Neurofibromatosis type 1 and plexiform neurofibromas (PN) or malignant peripheral nerve sheath tumors (MPNST). *Pediatr Blood Cancer.* (2013) 60:59–64. doi: 10.1002/pbc.24212

31. Thway K, Fisher C. Malignant peripheral nerve sheath tumor: pathology and genetics. *Ann Diagn Pathol.* (2014) 18:109–16. doi: 10.1016/j.anndiagpath.2013.10.007

32. Hirose T, Hasegawa T, Kudo E, Seki K, Sano T, Hizawa K, et al. Malignant peripheral nerve sheath tumors: an immunohistochemical study in relation to ultrastructural features. *Hum Pathol.* (1992) 23:865–70. doi: 10.1016/0046-8177(92)90396-K

33. Nonaka D, Chiriboga L, Rubin BP. Sox10: a pan-Schwannian and melanocytic marker. *Am J Surg Pathol.* (2008) 32:1291–8. doi: 10.1097/PAS.0b013e3181658c14

34. Menon SS, Guruvayoorappan C, Sakthivel KM, Rasmi RR. Ki-67 protein as a tumour proliferation marker. *Clin Chim Acta.* (2019) 491:39–45. doi: 10.1016/j.cca.2019.01.011

35. Satelli A, Li S. Vimentin in cancer and its potential as a molecular target for cancer therapy. *Cell Mol Life Sci.* (2011) 68:3033–46. doi: 10.1007/s00018-011-0735-1

36. Venhuizen JH, Jacobs FJC, Span PN, Zegers MM. P120 and E-cadherin: double-edged swords in tumor metastasis. *Semin Cancer Biol.* (2020) 60:107–20. doi: 10.1016/j.semcancer.2019.07.020

37. Das S, Ganju A, Tiel RL, Kline DG. Tumors of the brachial plexus. *Neurosurg Focus.* (2007) 22:E26. doi: 10.3171/foc.2007.22.6.27

38. James AW, Shurell E, Singh A, Dry SM, Eilber FC. Malignant peripheral nerve sheath tumor. *Surg Oncol Clin N Am.* (2016) 25:789–802. doi: 10.1016/j.soc.2016.05.009

39. Cai Z, Tang X, Liang H, Yang R, Yan T, Guo W, et al. Prognosis and risk factors for malignant peripheral nerve sheath tumor: a systematic review and meta-analysis. *World J Surg Oncol.* (2020) 18:257. doi: 10.1186/s12957-020-02036-x

40. Scheithauer BW, Erdogan S, Rodriguez FJ, Burger PC, Woodruff JM, Kros JM, et al. Malignant peripheral nerve sheath tumors of cranial nerves and intracranial contents: a clinicopathologic study of 17 cases. *Am J Surg Pathol.* (2009) 33:325–38. doi: 10.1097/PAS.0b013e31818d6470

41. Cavanagh JB. Effects of x-irradiation on the proliferation of cells in peripheral nerve during Wallerian degeneration in the rat. *Br J Radiol.* (1968) 41:275–81. doi: 10.1259/0007-1285-41-484-275

42. de Vries M, Briaire-de Bruijn I, Malessy MJ, de Bruïne SF, van der Mey AG, Hogendoorn PC. Tumor-associated macrophages are related to volumetric growth of vestibular schwannomas. *Otol Neurotol.* (2013) 34:347–52. doi: 10.1097/MAO.0b013e31827c9fbf

43. Yamanaka R, Hayano A. Radiation-induced malignant peripheral nerve sheath tumors: a systematic review. *World Neurosurg.* (2017) 105:961–70.e8. doi: 10.1016/j.wneu.2017.06.010

44. Jung IH, Yoon KW, Kim YJ, Lee SK. Analysis according to characteristics of 18 cases of brachial plexus tumors: a review of surgical treatment experience. *J Korean Neurosurg Soc.* (2018) 61:625–32. doi: 10.3340/jkns.2018.0045

frontiers | Frontiers in Neurology

TYPE Case Report
PUBLISHED 16 January 2023
DOI 10.3389/fneur.2022.1110934

Check for updates

OPEN ACCESS

EDITED BY
Giovanni Meola,
University of Milan, Italy

REVIEWED BY
Corrado Italo Angelini,
University of Padua, Italy
Andreas Brodehl,
Heart and Diabetes Center North Rhine-Westphalia, Germany
Yuwei Da,
Xuanwu Hospital, Capital Medical University, China

*CORRESPONDENCE
Pamela McCombe
✉ pamela.mccombe@uq.edu.au

SPECIALTY SECTION
This article was submitted to Neuromuscular Disorders and Peripheral Neuropathies, a section of the journal Frontiers in Neurology

RECEIVED 29 November 2022
ACCEPTED 30 December 2022
PUBLISHED 16 January 2023

CITATION
Yeow D, Katz M, Henderson R, Prasad S, Denman R, Blum S, Davis M, Robertson T and McCombe P (2023) Phenotypic variability within the desminopathies: A case series of three patients. *Front. Neurol.* 13:1110934. doi: 10.3389/fneur.2022.1110934

COPYRIGHT
© 2023 Yeow, Katz, Henderson, Prasad, Denman, Blum, Davis, Robertson and McCombe. This is an open-access article distributed under the terms of the Creative Commons Attribution License (CC BY). The use, distribution or reproduction in other forums is permitted, provided the original author(s) and the copyright owner(s) are credited and that the original publication in this journal is cited, in accordance with accepted academic practice. No use, distribution or reproduction is permitted which does not comply with these terms.

Phenotypic variability within the desminopathies: A case series of three patients

Dennis Yeow[1], Matthew Katz[2], Robert Henderson[2], Sandhir Prasad[3], Russell Denman[4], Stefan Blum[5], Mark Davis[6], Thomas Robertson[7] and Pamela McCombe[2]*

[1]Department of Neurology, Royal North Shore Hospital, Sydney, NSW, Australia, [2]Department of Neurology, Royal Brisbane and Women's Hospital, Brisbane, QLD, Australia, [3]Department of Cardiology, Royal Brisbane and Women's Hospital, Brisbane, QLD, Australia, [4]Department of Cardiology, The Prince Charles Hospital, Brisbane, QLD, Australia, [5]Department of Neurology, Princess Alexandra Hospital, Brisbane, QLD, Australia, [6]Department of Diagnostic Genomics, Pathwest Laboratory Medicine, Perth, WA, Australia, [7]Department of Pathology, Royal Brisbane and Women's Hospital, Brisbane, QLD, Australia

The *DES* gene encodes desmin, a key intermediate filament of skeletal, cardiac and smooth muscle. Pathogenic *DES* variants produce a range of skeletal and cardiac muscle disorders collectively known as the desminopathies. We report three desminopathy cases which highlight the phenotypic heterogeneity of this disorder and discuss various factors that may contribute to the clinical differences seen between patients with different desmin variants and also between family members with the same variant.

KEYWORDS

desmin, desminopathy, cardiomyopathy, myofibrillar myopathy, splice-site mutation

1. Introduction

Desmin is an intermediate filament which forms links between myofibrils, desmosomes, the nuclear envelope and the sarcolemma within skeletal, cardiac and smooth muscle (1). Structurally it consists of a head domain, a central rod domain with 1A, 1B, 2A, and 2B subunits and a tail domain. Mutations in the desmin gene (*DES*) produce a wide range of phenotypes collectively termed the desminopathies which can present with any combination of skeletal myopathy (myofibrillar myopathy, limb-girdle muscular dystrophy, Kaeser's scapuloperoneal syndrome), cardiomyopathy (dilated cardiomyopathy, hypertrophic cardiomyopathy, restrictive cardiomyopathy, left ventricular non-compaction cardiomyopathy or arrhythmogenic right ventricular cardiomyopathy), ventricular arrhythmia and/or cardiac conduction disease including atrioventricular bock (1, 2). Inheritance is typically autosomal dominant but cases of autosomal recessive inheritance have also been described (3, 4). Many pathogenic *DES* variants, through a toxic gain of function, result in intracellular accumulation of desmin aggregates, which are thought to contribute to disease pathophysiology (5, 6). However, not all pathogenic *DES* variants produce aggregates and it has been hypothesized that both loss of function and toxic gain of function may be contributory disease mechanisms (7).

Here we present three desminopathy cases that illustrate the phenotypic heterogeneity of the disease.

2. Case series

2.1. Case 1

A 54-year-old woman (individual II-1, Figure 1) was referred to our neurology clinic with progressive proximal upper and lower limb weakness over the preceding year. She had a pacemaker inserted at age 30 for complete heart block, previous atrial flutter requiring ablation at age 50 and ongoing paroxysmal atrial fibrillation for which she took amiodarone. Her mother (individual I-1, Figure 1) also required a permanent pacemaker at age 35 for complete heart block.

On examination, there was mild (Medical Research Council grade 4/5), symmetric weakness of shoulder abduction and hip flexion bilaterally with intact reflexes and a normal sensory examination.

Creatine kinase (CK) was mildly elevated at 199 U/L (normal range 34–145 U/L). Electromyography (EMG) revealed early recruitment of myopathic units in proximal muscles. Electrocardiogram (ECG) revealed regular *P* waves and ventricular pacing. Transthoracic echocardiogram (TTE) showed normal left ventricular size and systolic function (ejection fraction 51% by Simpson's biplane method).

Biopsy of the right deltoid revealed marked variation in muscle fiber diameter (ranging from atrophic to hypertrophic), patchy increase in internal nuclei and scattered fibers with basophilic granularity and peripheral basophilic lobular change (Figure 2A). Desmin immunohistochemistry revealed subsarcolemmal and focal central desmin-positive aggregates (Figure 2B). Electron microscopy showed widespread, predominantly subsarcolemmal accumulation of osmiophilic granulofilamentous material (Figure 2C). These findings were consistent with a myofibrillar myopathy.

Genetic testing revealed a novel heterozygous deletion in *DES* (c.735+1delG) that alters the invariant dinucleotide GT splice donor site at the start of intron 3. This variant is absent from the gnomAD database [American College of Medical Genetics (ACMG) criteria PM2]. Different pathogenic variants affecting the same nucleotide (c.735+1G>A, c.735+1G>C, and c.735+1G>T) have been previously reported in desminopathy patients and have been shown to result in skipping of exon 3 leading to an in-frame deletion of 32 amino acids from the rod 1B domain (criteria PS1 and PM4) (8–10). Park et al. (11) showed that this truncated version of desmin forms abnormal aggregates within the cytoplasm in a cell culture model and Brodehl et al. (12) found desmin-positive aggregates within cardiomyocytes from explanted myocardial tissue in a patient with an exon 3 skipping variant. Together these studies support the c.735+1delG variant as being likely pathogenic.

During 9 years of follow up, there was mild progression in proximal muscle weakness but no development of structural cardiomyopathy or ventricular arrhythmias.

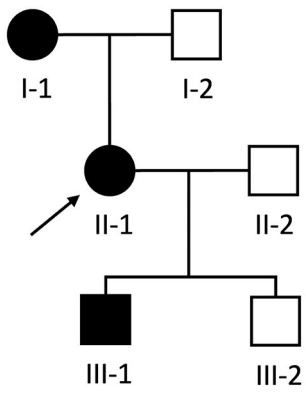

FIGURE 1
Pedigree of Case 1 (II-1) and Case 2 (III-1). Proband is indicated by the black arrow. Black and white shapes indicate clinically affected and unaffected individuals, respectively. Squares and circles indicate males and females, respectively.

2.2. Case 2

During the workup of patient II-1, her then 18-year-old son (individual III-1, Figure 1) was incidentally found to have a systolic murmur and an abnormal ECG during a routine pre-operative assessment prior to elective nasal septoplasty. He was referred to our cardiology clinic and at that time had no dyspnea, palpitations, chest pain or syncope and there was no weakness on neurological examination.

ECG revealed large QRS amplitudes and T-wave inversions in anterolateral leads suggestive of left ventricular hypertrophy but there was no evidence of conduction system disease. TTE revealed concentrically increased left ventricular wall thickness (up to 20 mm) with preserved systolic function (ejection fraction 60–65% by Simpson's biplane method) and mild-moderate diastolic dysfunction (Figures 3A–C). Holter monitor revealed sinus rhythm with nine sinus pauses >2 s (the longest being 3.4 s), which were asymptomatic. Cardiac magnetic resonance imaging (MRI) demonstrated increased left ventricular wall thickness predominantly affecting the anteroseptal and anterolateral walls (Figure 4A). There was increased mid-wall T2 signal and delayed post-gadolinium enhancement within the thickened segments indicating myocardial oedema and fibrosis (Figures 4B, C). CK was normal at 139 U/L.

Given that the clinical phenotype differed from the predominant conduction disease seen in his mother and grandmother, a biopsy of the right quadriceps was performed. This showed findings consistent with a myofibrillar myopathy with frequent subsarcolemmal hyaline inclusions and occasional centrally-placed inclusions (Figure 2D) which stained positively on desmin immunohistochemistry (Figure 2E). Electron microscopy revealed the same osmiophilic granulofilamentous ultrastructure seen in his mother's biopsy (Figure 2F). Genetic testing showed he carried the familial c.735+1delG *DES* variant.

At age 21, he developed intermittent presyncope and a Holter monitor revealed several runs of non-sustained ventricular tachycardia (longest run 17 beats) prompting insertion of an implantable cardioverter-defibrillator (ICD). Concurrently, sequential TTEs documented progressive reduction in left ventricular wall thickness (Figures 3D–F) and decline in left ventricular systolic function such that ejection fraction was 35–40% with global hypokinesis by age 27. At age 27 he had multiple episodes of ventricular tachycardia, which were terminated by defibrillation from his ICD. Serial ECGs also showed progressive conduction system disease with prolongation of the PR interval to 280 ms and QRS duration to 170 ms at age 27. Despite the biopsy finding of myofibrillar myopathy at age 18, there has been no development of clinically appreciable skeletal muscle weakness during follow up.

10.3389/fneur.2022.1110934

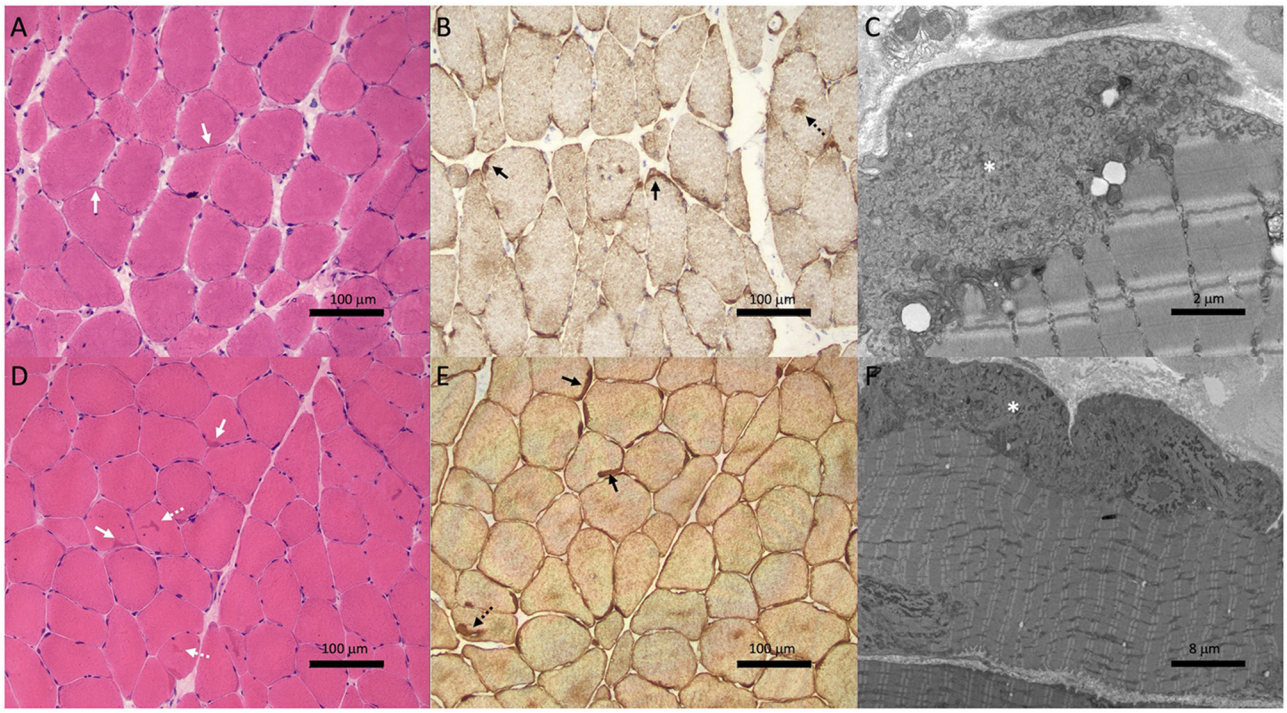

FIGURE 2
Muscle biopsies from Case 1 (II-1; **A**–**C**) and Case 2 (III-1; **D**–**F**) showed features of myofibrillar myopathy. Hematoxylin & eosin staining **(A, D)** showed subtle subsarcolemmal (solid white arrows) and central basophilic hyaline inclusions (dotted white arrows). Variation in muscle fiber size is also noted in patient II-1 **(A)**. Desmin immunohistochemistry **(B, E)** revealed subsarcolemmal (solid black arrows) and central (dotted black arrows) aggregates. Electron microscopy **(C, F)** showed subsarcolemmal osmiophilic granulofilamentous material (asterisk).

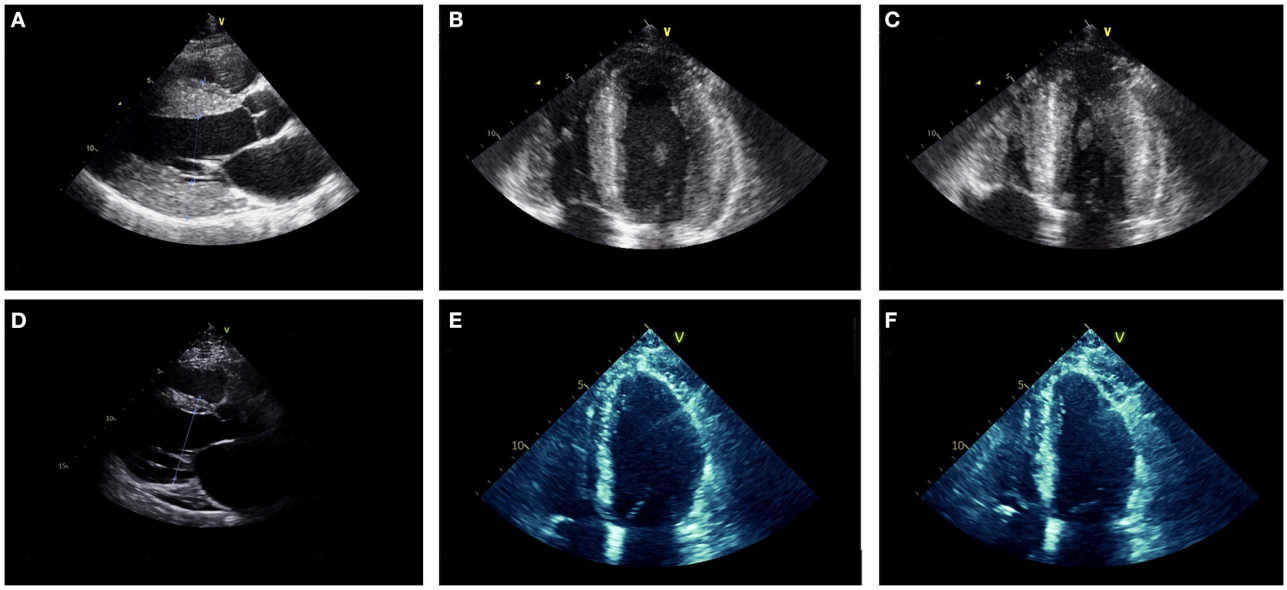

FIGURE 3
Parasternal long axis **(A, D)**, mid-diastolic apical four chamber **(B, E)** and end-systolic apical four chamber **(C, F)** transthoracic echocardiogram images from Case 2 at ages 18 **(A–C)** and 27 **(D–F)**. At age 18, the ventricular (LV) wall was concentrically thickened (interventricular septum 20 mm, posterior LV wall 20 mm) with vigorous systolic function (LV ejection fraction was 60–65% by Simpson's biplane method). At age 27, the LV wall was thin (interventricular septum 10 mm, LV posterior wall 3 mm) and there was moderate-severe LV dysfunction (LV ejection fraction 35–40% by Simpson's biplane method).

2.3. Case 3

A 48-year-old male presented with a 5-year history of facial and proximal upper and lower limb weakness, mild scapular winging and bilateral, asymmetric foot drop. CK was elevated at 712 U/L. His mother had a similar phenotype and both were initially clinically diagnosed with facioscapulohumeral dystrophy, however testing of chromosome 4 DZ4Z repeat length was normal. There was no family history of cardiac disease.

While awaiting further genetic testing to return, he presented acutely to hospital with sudden onset of dizziness and dyspnea. He was found to be in ventricular tachycardia and was successfully cardioverted to sinus rhythm. TTE showed a dilated cardiomyopathy with left ventricular ejection fraction of 35–40% (by Simpson's biplane method) and severe inferolateral hypokinesia. An ICD was implanted.

Genetic testing revealed a heterozygous missense c.5G>T (p.Ser2Ile) variant in the desmin head domain that has been previously reported in multiple patients with myofibrillar myopathy (2, 10, 13). Missense variants are a common cause of disease in the desminopathies (ACMG criteria PP2) (14). The Ser2 residue is conserved in mammals and substitution of serine residues in the head domain for hydrophobic residues (such as isoleucine) appears to be a common pattern amongst pathogenic head domain variants (criteria PM1) (15). This c.5G>T variant is absent from gnomAD (criteria PM2) and is predicted to be pathogenic by several *in silico* meta-scores including BayesDel and MetaRNN (criteria PP3). The p.Ser2Ile protein has been shown to form irregular, entangled intermediate filaments in a cell culture model (PS3) (15). As such, this variant is considered to be likely pathogenic.

During 5 years of follow up, the patient has had recurrent episodes of ventricular tachycardia terminated by the ICD.

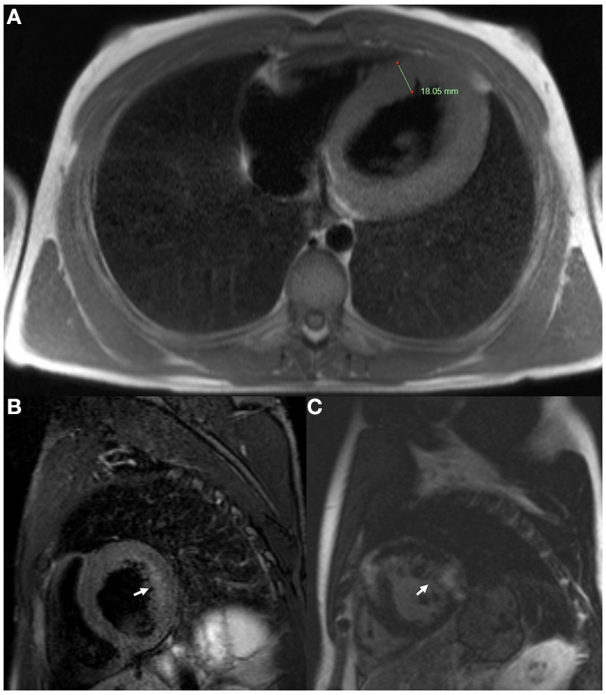

FIGURE 4
Cardiac magnetic resonance imaging of Case 2 (III-1) at age 18. **(A)** Axial T2 sequence showed increased left ventricular wall thickness (18.05 mm). **(B)** Short axis T2 fat saturation sequence showed increased signal in the mid ventricular wall (arrow). **(C)** Short axis T1 post-gadolinium sequence showed delayed gadolinium enhancement within the ventricular myocardium (arrow).

3. Discussion

In this report we present three cases that highlight the well-described clinical heterogeneity of the desminopathies. Despite Case 1 and 2 harboring the same familial variant, Case 1 presented with severe cardiac conduction system disease in early adulthood followed several decades later by a mild limb-girdle pattern of weakness in middle age, whereas Case 2 presented with asymptomatic hypertrophic cardiomyopathy identified in his teenage years which progressed over a few years to dilated cardiomyopathy with ventricular arrhythmias requiring ICD implantation and development of mild conduction system disease. In contrast to Cases 1 and 2 where cardiac symptoms were the initial manifestation of disease, Case 3 initially presented with a combination of facial, scapular and both proximal and distal limb weakness in middle age and then several years later manifested with symptomatic dilated cardiomyopathy and ventricular arrhythmia requiring ICD implantation.

Genotype-phenotype correlations explain some of the phenotypic variability seen in the desminopathies. A systematic review performed by van Spaendonck-Zwarts et al. (14) reviewed 159 patients with 40 different *DES* variants and found that isolated neurologic phenotypes occurred most commonly with variants in the rod 2B domain whereas isolated cardiac phenotypes occurred most commonly with variants in the head or tail domains (14, 16). However, for patients with both neurological and cardiological features, the location of the variant did not seem to predict whether cardiac or neurological features manifested first. More recently, variants in the rod 1B domain (such as the variant in Case 1 and 2) have been linked to a higher likelihood of early onset cardiomyopathy compared to variants in other domains (17). Some of the genotype-phenotype correlation may be explained by the propensity of different *DES* variants to cause loss of function and/or toxic gain of aggregation function (5–7, 17). For example, variants in the desmin tail domain have less propensity to form aggregates (7, 18). The molecular effect of specific variants is also modified by whether they are inherited in isolation (i.e., dominantly) or along with another abnormal allele (i.e., recessively), explaining why phenotype may correlate with mode of inheritance. For example, many dominant gain of function variants present in adulthood whereas some recessive loss of function variants present with severe disease in infancy (3).

Previous attempts at genotype-phenotype correlations may be confounded by several issues relating to the retrospective and cross-sectional nature of these analyses. Firstly, both skeletal myopathy and cardiomyopathy may be present but asymptomatic in an individual, as demonstrated by Case 2 who had biopsy-proven skeletal muscle involvement but no clinical muscle weakness and Case 3 who had dilated cardiomyopathy that had presumably been present for some time before finally manifesting as ventricular tachyarrhythmia. Secondly, the cardiac phenotype may change over time as demonstrated by Case 2 where the initially asymptomatic hypertrophic cardiomyopathy progressed to symptomatic dilated cardiomyopathy with ventricular tachycardia over several years.

Interestingly Gudkova et al. (8) report an almost identical presentation of an initially asymptomatic teenage male with a c.735+1G>A variant who, like Case 2, was identified to have a hypertrophic cardiomyopathy on an incidental basis and then over time progressed to a restrictive and then, finally, a dilated cardiomyopathy with development of frequent ventricular tachycardia. Furthermore, although the study by van Spaendonck-Zwarts et al. (14) did not analyse change in cardiac phenotype over time in individual patients, they did find that, at a group level across all different *DES* variants, both restrictive and hypertrophic cardiomyopathies were diagnosed at significantly earlier ages than dilated cardiomyopathy (mean age 28 vs. 33 vs. 46 years, respectively). The same transformation of cardiac phenotype seen in Case 2 is also seen in a murine *DES* knockout model, which is initially characterized by cardiac hypertrophy with preserved left ventricular systolic function followed at a later stage by ventricular dilatation and impaired ventricular systolic function (5). Prospective registries with systematic and longitudinal assessment of cardiac and neurologic phenotypes at multiple time points would help to address the above-mentioned issues and may yield further insights into genotype-phenotype relationships.

Nevertheless, it remains difficult to explain all components of the observed phenotypic variability based on genotype alone. For example, regarding the distribution and severity of neurological involvement, even accounting for age-related penetrance, patients harboring the same variant may present with different degrees and patterns (e.g., proximal limb/limb-girdle, distal limb, proximal and distal limb, scapuloperoneal, facial, etc.) of muscle weakness (10, 14). Indeed, while Case 3 had facial, scapular and proximal and distal limb weakness by his 40s, a previously reported case with the same p.Ser2Ile variant was reported to have no clinically appreciable skeletal muscles weakness at age 48 (10).

Environmental factors may explain some of the otherwise unexplained phenotypic variability and may also contribute to changes in phenotype over time (19). Desmin expression in skeletal muscle is known to increase following sustained muscle activity in healthy volunteers (20). Furthermore, in a desminopathy skeletal muscle cell culture model generated by Segard et al. (19), thermal, oxidative and mechanical stressors precipitated intracytoplasmic desmin aggregation and this occurred more in cells transfected with desmin with a rod domain variant compared to head and tail domain variants. Separately, in a desminopathy rat model, chronic exercise produced increased desmin aggregation and myofibrillar damage resulting in progressive decline in exercise tolerance over time (21). Collating this data, it is possible then that there is a genotype-environment interaction where environmental stressors, including physical exercise, may upregulate desmin expression and precipitate or accelerate toxic aggregation of desmin and that this may be modulated by the propensity of different *DES* variants toward aggregate formation. However, the effect of different types and levels of intensity of exercise has not been explored thoroughly. Indeed, a low-intensity endurance and resistance regimen has been suggested to be safe and even beneficial in a single human desminopathy case report (22).

Gender is another potential contributor to phenotypic variability and may explain some of the differences seen between Cases 1 and 2. The meta-analysis by van Spaendonck-Zwarts et al. (14) found that, across all the pathogenic *DES* variants analyzed, cardiomyopathy was more common in males compared to females (54 vs. 36%) (14). Furthermore, within large desminopathy families with the same variant, cardiomyopathy has been shown to be more frequent, earlier in onset and more severe, often presenting with sudden cardiac death, in males compared to females (23, 24). Our report of early-onset structural cardiomyopathy with recurrent ventricular arrhythmia as the major presenting feature in a male (Case 2) compared to later onset skeletal myopathy (albeit with early onset cardiac conduction deficits) in his mother in her 50s (Case 1) is consistent with this pattern. Arias et al. (23) hypothesized that this gender effect could be mediated by hormonal factors and/or related to less intense physical activity in female patients (13). Regarding hormonal mechanisms, in a murine model of exercise-induced muscle damage, Komulainen et al. (25) found that female rats exhibited significantly less post-exercise loss of subsarcolemmal desmin expression compared to male rats and hypothesized that this may be due to a protective effect of estrogen on sarcolemmal integrity. Thus, gender-exercise interactions may also modify the desminopathy clinical phenotype.

4. Conclusion

Our three desminopathy cases emphasize that this condition can present with various combinations of limb and/or facial muscle weakness, different forms of structural cardiomyopathy, ventricular arrhythmias and/or cardiac conduction deficit and that the exact combination and temporal sequence of these clinical features can vary both between different *DES* variants and also within families with the same variant. It is likely that multiple factors including the location of the specific variant within the *DES* gene, mode of inheritance, environmental stressors and gender interact to produce this phenotypic heterogeneity. We also reconfirmed a previous finding that the cardiac phenotype may evolve over time from an initial hypertrophic cardiomyopathy to a dilated cardiomyopathy at later stages indicating that age at time of clinical assessment is another factor that may contribute to apparent variability in the clinical manifestation of this disorder.

Data availability statement

The datasets presented in this article are not readily available because of ethical and privacy restrictions. Requests to access the datasets should be directed to PM, pamela.mccombe@uq.edu.au.

Ethics statement

Ethical review and approval was not required for the study on human participants in accordance with the local legislation and institutional requirements. The patients/participants provided their written informed consent to participate in this study.

Author contributions

DY: drafting of article, study conceptualization, and collection of clinical data. MK, RH, and PM: revision of article, examination of patients, collection of clinical data, and study conceptualization. SP, RD, and SB: revision of article, examination of patients, and collection of clinical data. MD: revision of article and genetic analysis. TR:

revision of article, histology, and electron microscopy. All authors contributed to the article and approved the submitted version.

Conflict of interest

The authors declare that the research was conducted in the absence of any commercial or financial relationships that could be construed as a potential conflict of interest.

Publisher's note

All claims expressed in this article are solely those of the authors and do not necessarily represent those of their affiliated organizations, or those of the publisher, the editors and the reviewers. Any product that may be evaluated in this article, or claim that may be made by its manufacturer, is not guaranteed or endorsed by the publisher.

References

1. Azzimato V, Genneback N, Tabish AM, Buyandelger B, Knoll R. Desmin, desminopathy and the complexity of genetics. *J Mol Cell Cardiol.* (2016) 92:93–5. doi: 10.1016/j.yjmcc.2016.01.017

2. Selcen D, Ohno K, Engel AG. Myofibrillar myopathy: clinical, morphological and genetic studies in 63 patients. *Brain.* (2004) 127:439–51. doi: 10.1093/brain/awh052

3. Pinol-Ripoll G, Shatunov A, Cabello A, Larrode P, de la Puerta I, Pelegrin J, et al. Severe infantile-onset cardiomyopathy associated with a homozygous deletion in desmin. *Neuromuscul Disord.* (2009) 19:418–22. doi: 10.1016/j.nmd.2009.04.004

4. Brodehl A, Pour Hakimi SA, Stanasiuk C, Ratnavadivel S, Hendig D, Gaertner A, et al. Restrictive cardiomyopathy is caused by a novel homozygous desmin (DES) mutation p.Y122H leading to a severe filament assembly defect. *Genes (Basel).* (2019) 10:918. doi: 10.3390/genes10110918

5. Milner DJ, Taffet GE, Wang X, Pham T, Tamura T, Hartley C, et al. The absence of desmin leads to cardiomyocyte hypertrophy and cardiac dilation with compromised systolic function. *J Mol Cell Cardiol.* (1999) 31:2063–76. doi: 10.1006/jmcc.1999.1037

6. Kedia N, Arhzaouy K, Pittman SK, Sun Y, Batchelor M, Weihl CC, et al. Desmin forms toxic, seeding-competent amyloid aggregates that persist in muscle fibers. *Proc Natl Acad Sci USA.* (2019) 116:16835–40. doi: 10.1073/pnas.1908263116

7. Brodehl A, Gaertner-Rommel A, Milting H. Molecular insights into cardiomyopathies associated with desmin (DES) mutations. *Biophys Rev.* (2018) 10:983–1006. doi: 10.1007/s12551-018-0429-0

8. Gudkova A, Kostareva A, Sjoberg G, Smolina N, Turalchuk M, Kuznetsova I, et al. Diagnostic challenge in desmin cardiomyopathy with transformation of clinical phenotypes. *Pediatr Cardiol.* (2013) 34:467–70. doi: 10.1007/s00246-012-0312-x

9. Fan P, Lu CX, Dong XQ, Zhu D, Yang KQ, Liu KQ, et al. A novel phenotype with splicing mutation identified in a Chinese family with desminopathy. *Chin Med J.* (2019) 132:127–34. doi: 10.1097/CM9.0000000000000001

10. Shelly S, Talha N, Pereira NL, Engel AG, Johnson JN, Selcen D. Expanding spectrum of desmin-related myopathy, long-term follow-up, and cardiac transplantation. *Neurology.* (2021) 97:e1150–8. doi: 10.1212/WNL.0000000000012542

11. Park KY, Dalakas MC, Goebel HH, Ferrans VJ, Semino-Mora C, Litvak S, et al. Desmin splice variants causing cardiac and skeletal myopathy. *J Med Genet.* (2000) 37:851–7. doi: 10.1136/jmg.37.11.851

12. Brodehl A, Hain C, Flottmann F, Ratnavadivel S, Gaertner A, Klauke B, et al. The desmin mutation *DES*-c.735G>C causes severe restrictive cardiomyopathy by inducing in-frame skipping of exon-3. *Biomedicines.* (2021) 9:1400. doi: 10.3390/biomedicines9101400

13. Wahbi K, Behin A, Charron P, Dunand M, Richard P, Meune C, et al. High cardiovascular morbidity and mortality in myofibrillar myopathies due to DES gene mutations: a 10-year longitudinal study. *Neuromuscul Disord.* (2012) 22:211–8. doi: 10.1016/j.nmd.2011.10.019

14. van Spaendonck-Zwarts KY, van Hessem L, Jongbloed JD, de Walle HE, Capetanaki Y, van der Kooi AJ, et al. Desmin-related myopathy. *Clin Genet.* (2011) 80:354–66. doi: 10.1111/j.1399-0004.2010.01512.x

15. Sharma S, Mucke N, Katus HA, Herrmann H, Bar H. Disease mutations in the "head" domain of the extra-sarcomeric protein desmin distinctly alter its assembly and network-forming properties. *J Mol Med.* (2009) 87:1207–19. doi: 10.1007/s00109-009-0521-9

16. Bar H, Goudeau B, Walde S, Casteras-Simon M, Mucke N, Shatunov A, et al. Conspicuous involvement of desmin tail mutations in diverse cardiac and skeletal myopathies. *Hum Mutat.* (2007) 28:374–86. doi: 10.1002/humu.20459

17. Silva AMS, Rodrigo P, Moreno CAM, Mendonca RH, Estephan EP, Camelo CG, et al. The location of disease-causing DES variants determines the severity of phenotype and the morphology of sarcoplasmic aggregates. *J Neuropathol Exp Neurol.* (2022) 81:746–57. doi: 10.1093/jnen/nlac063

18. Brodehl A, Dieding M, Cakar H, Klauke B, Walhorn V, Gummert J, et al. Functional characterization of desmin mutant pP419S. *Eur J Hum Genet.* (2013) 21:589–90. doi: 10.1038/ejhg.2012.212

19. Segard BD, Delort F, Bailleux V, Simon S, Leccia E, Gausseres B, et al. N-acetyl-L-cysteine prevents stress-induced desmin aggregation in cellular models of desminopathy. *PLoS ONE.* (2013) 8:e76361. doi: 10.1371/journal.pone.0076361

20. Woolstenhulme MT, Jutte LS, Drummond MJ, Parcell AC. Desmin increases with high-intensity concentric contractions in humans. *Muscle Nerve.* (2005) 31:20–4. doi: 10.1002/mus.20170

21. Mossakowski AA, Langer HT, Bizieff A, Avey AM, Zbinden-Foncea H, Hellerstein M, et al. Increased remodeling and impaired adaption to endurance exercise in desminopathy. *bioRxiv.* (2021). doi: 10.1101/2021.10.03.462939

22. Monje C, Jannas-Vela S, Baar K, Zbinden-Foncea H. Case report of an exercise training and nutritional intervention plan in a patient with A350P mutation in DES gene. *Clin Case Rep.* (2020) 8:283–8. doi: 10.1002/ccr3.2607

23. Arias M, Pardo J, Blanco-Arias P, Sobrido MJ, Arias S, Dapena D, et al. Distinct phenotypic features and gender-specific disease manifestations in a Spanish family with desmin L370P mutation. *Neuromuscul Disord.* (2006) 16:498–503. doi: 10.1016/j.nmd.2006.05.011

24. Maddison P, Damian MS, Sewry C, McGorrian C, Winer JB, Odgerel Z, et al. Clinical and myopathological characteristics of desminopathy caused by a mutation in desmin tail domain. *Eur Neurol.* (2012) 68:279–86. doi: 10.1159/000341617

25. Komulainen J, Koskinen SO, Kalliokoski R, Takala TE, Vihko V. Gender differences in skeletal muscle fibre damage after eccentrically biased downhill running in rats. *Acta Physiol Scand.* (1999) 165:57–63. doi: 10.1046/j.1365-201x.1999.00481.x

frontiers | Frontiers in Neurology

TYPE Case Report
PUBLISHED 17 January 2023
DOI 10.3389/fneur.2022.1078784

Check for updates

OPEN ACCESS

EDITED BY
Giovanni Meola,
University of Milan, Italy

REVIEWED BY
Roope Mannikko,
University College London, United Kingdom
Macarena Cabrera-Serrano,
Virgen del Rocío University Hospital, Spain

*CORRESPONDENCE
Banghui Xiao
✉ 562842630@qq.com

SPECIALTY SECTION
This article was submitted to Neuromuscular Disorders and Peripheral Neuropathies, a section of the journal Frontiers in Neurology

RECEIVED 17 November 2022
ACCEPTED 28 December 2022
PUBLISHED 17 January 2023

CITATION
Zhang Z and Xiao B (2023) Case report: SCN4A p.R1135H gene variant in combination with thyrotoxicosis causing hypokalemic periodic paralysis. *Front. Neurol.* 13:1078784. doi: 10.3389/fneur.2022.1078784

COPYRIGHT
© 2023 Zhang and Xiao. This is an open-access article distributed under the terms of the Creative Commons Attribution License (CC BY). The use, distribution or reproduction in other forums is permitted, provided the original author(s) and the copyright owner(s) are credited and that the original publication in this journal is cited, in accordance with accepted academic practice. No use, distribution or reproduction is permitted which does not comply with these terms.

Case report: SCN4A p.R1135H gene variant in combination with thyrotoxicosis causing hypokalemic periodic paralysis

Zhi Zhang and Banghui Xiao*

Department of Endocrinology and Metabolism, Affiliated Hospital of Guizhou Medical University, Guiyang, China

Hypokalemic periodic paralysis (HPP) is a heterogeneous group of diseases characterized by intermittent episodes of delayed paralysis of skeletal muscle with episodes of hypokalemia, caused by variants in CACNA1S or SCN4A genes, or secondary to thyrotoxicosis, Sjogren syndrome, primary aldosteronism, etc. HPP may be the only presentation in Andersen–Tawil syndrome in which the majority of cases are caused by pathogenic variants in the KCNJ2 gene. We present a case of a 29-year-old male with hypokalemic periodic paralysis. The patient began to experience recurrent weakness of the extremities at the age of 26, which was effectively treated with potassium supplementation. He had recently developed dry mouth, palpitations, weight loss, and even dyspnea, with a serum potassium level as low as 1.59 mmol/L. The results of auxiliary examinations showed Graves' disease, and genetic testing indicated a missense variant, NM_000334.4 (SCN4A):c.3404G>A (p.R1135H). He did not experience periodic paralysis during follow-up after lifestyle guidance and treatment of thyrotoxicosis with radioactive iodine. It is a rare case of SCN4A p.R1135H gene variant combined with hyperthyroidism resulting in HPP with respiratory muscle paralysis to raise awareness of the disease and avoid misdiagnosis and missed diagnosis.

KEYWORDS

hypokalemic periodic paralysis, SCN4A gene, thyrotoxic periodic paralysis, hyperthyroidism, therapy

Introduction

Hypokalemic periodic paralysis (HPP) is a rare ion channel disorder and is one of the most common forms of periodic paralysis. The incidence of HPP is ~1 in 100,000 (1). Since Musgrave proposed HPP in 1,727 (2), there has been a growing understanding of the disease. HPP is caused primarily by variants in genes encoding skeletal muscle ion channels that reduce the excitability of the muscle membrane, leading to susceptibility to episodes of paralysis (3). The disease is genetically heterogeneous, and the known variants are mainly in the CACNA1S gene, which encodes a voltage-gated calcium channel in skeletal muscle, and the SCN4A gene, which encodes a sodium channel, among which the CACNA1S gene variant predominates, accounting for about 60% of all variants and the SCN4A gene variant for 20% (4). Approximately 20% of HPP remain unidentified genetically. The disease is generally autosomal dominant and is more common in non-Hispanic Caucasians, known as familial HPP (FPP) (5). Non-familial HPP includes thyrotoxic periodic paralysis (TPP) and sporadic periodic paralysis (SPP), which are more common in Asians and Hispanics (5). The incidence of SPP in Asian populations is lower than that of TPP which is about 2% in Asian populations with thyrotoxicosis (6). Graves' disease (GD) is the most common cause of TPP (7). The pathogenesis of sporadic periodic paralysis

is unclear. Sung et al. conducted a study to clarify whether sporadic HPP and familial HPP have similar genotypes and showed that all FPPs contained variants in the CACNA1S or SCN4A genes, whereas only 4 of 60 participants with SPP were detected with variants in the CACNA1S or SCN4A genes, and there was no significant difference in phenotype between SPP and FPP with variants, except for the later age of onset of SPP (8). The mechanism of hyperthyroidism leading to HPP is also not clear. TPP is associated with elevated thyroid hormone-stimulated Na^+-K^+ ATPase activity. TPP was suggested to be an ion channelopathy, and variants in KCNJ18 encoding potassium channel Kir2.6 were reported in some TPP patients (9–11). Interestingly, variants in the KCNJ18 gene were also reported in patients with SPP (10). There are now substantial studies showing that variants in SCN4A or CACNA1S gene are not associated with TPP (12). The combination of coexisting HPP caused by SCN4A gene variants and thyrotoxic periodic paralysis is very rare. We present an exceptionally rare case of the coexistence of HPP caused by variants in SCN4A genes and TPP.

Case description

A 29-year-old Chinese male patient, who started to experience recurrent weakness in the morning or after staying up late at the age of 26, was diagnosed with HPP associated with a genetic variant after a complete examination at a local hospital, but the specific gene was not clear. We were unable to retrieve detailed data on relevant laboratory parameters at that time, but he remembered clearly the thyroid function was normal. Treatment with potassium supplementation was effective, but recurrent episodes persisted. He was admitted to the local hospital 12 days before he came to our hospital due to an increased frequency of attacks, muscle pain, dry mouth, palpitation, and profuse sweating. The serum potassium level was 1.59 mmol/L. Intravenous potassium supplementation was not effective, and he had chest tightness, inability to speak, and dyspnea. Blood gases suggested PH 7.18, PCO_2 54.8 mmHg, and PO_2 134 mmHg. After endotracheal intubation, mechanical ventilation, and potassium supplementation, the above symptoms improved, but they still recurred and his weight dropped by 2 kg. He denied any past medical history and taking other medications. His parents were healthy and he was an only child, and there were no similar symptoms in his family.

Physical examination showed that vital signs all remain stable and in a normal range. The heart was in rhythm, no significant murmurs were heard in all valve auscultation areas, and his muscle strength and tone were normal.

Laboratory examination revealed thyroid-stimulating hormone (TSH) of 0.01 mIU/L (reference interval, RI:0.27–4.20), free thyroxine (FT4) of 28.42 pmol/L (RI:12.00–22.00), free triiodothyronine (FT3) of 9.98 pmol/L (RI:3.10–6.80), thyrotropin receptor antibody (TRAb) of 20.82 IU/L (RI:0.00–1.75), serum potassium of 2.93 mmol/L (RI:3.5–5.3), sodium of 142.35 mmol/L (RI:137–147), chloride of 110.41 mmol/L (96–108), calcium of 2.09 mmol/L (RI:2.11–2.52), magnesium of 0.69 mmol/L (RI:0.75–1.02), inorganic phosphate of 1.19 mmol/L (RI:0.85–1.51), and carbon dioxide combining power of 20.32 mmol/L (RI:22–29). Hepatic and renal function, serum muscle enzymes, blood glucose, cortisol, renin, and aldosterone were within normal limits. Antinuclear antibody, SSA, SSB, anti-thyroglobulin antibody, and antithyroid peroxidase antibody were negative. Electrocardiogram showed sinus rhythm and marked T depression in leads I, aVL, II, III, aVF and V5–V6, and abnormal U-wave. Static thyroid imaging showed the fullness of the thyroid gland bilaterally with diffuse hyperintensity, consistent with "hyperthyroidism." The thyroid ultrasound did not show any significant abnormalities. The iodine uptake rate of the thyroid gland was higher than normal. Genetic testing revealed a pathogenic heterozygous variant, NM_000334.4 (SCN4A):c.3404G>A (p.R1135H) after obtaining the patient's informed consent. Regretfully, due to distance, the patient's parents failed to undergo genetic testing.

TABLE 1 Thyroid function before treatment and during follow-up.

Variable	Before treatment	3 months at follow-up	9 months at follow-up
TSH (mIU/L)	0.01	236.40	66.34
FT4 (pmol/L)	28.42	<0.30	2.17
FT3 (pmol/L)	9.98	17.70	5.11

Based on these results, we diagnosed the patient with hypokalemic periodic paralysis, caused by a variant in the SCN4A gene combined with Graves' disease. Lifestyle education was given, and treatment with radioactive iodine was administered. The patient was followed up at 3 and 9 months after discharge. He stated no recurrence of muscle pain and weakness after discharge and became hypothyroid (Table 1), and he is now being given 100 μg of levothyroxine replacement therapy.

Discussion

Hypokalemic periodic paralysis associated with variants in the CACNA1S or SCN4A genes, also known as primary HPP and thyrotoxic hypokalemic periodic paralysis, did not differ in terms of attack characteristics, with prodromal symptoms including muscle pain, fatigue, and paresthesia. Weakness usually begins in the proximal muscles of the lower extremities and may progress to flaccid tetraplegia. Episodes of HPP have certain triggers, including ingestion of carbohydrates or alcohol intake, and rest after strenuous exercise. The paralytic attack rate of primary HPP is highest between the ages of 15 and 35 years and decreases after the age of 35 years. The muscle weakness can be focal or generalized, with the ocular, bulbar, and respiratory muscles usually unaffected, lasting several hours (sometimes up to several days) and then gradually subsiding (1, 2). TPP usually occurs in people around 20–40 years of age, with gender differences, with a male-to-female ratio of about 20:1 (12). A case accompanied by ventricular tachycardia and acute respiratory failure has been reported (13), but life-threatening complications have rarely been seen in clinical practice.

In this case, the patient had typical clinical features of HPP. He was a young Asian man, with typical muscle aches and pains during attacks, triggered by staying up late, and potassium supplementation was effective. The patient was initially diagnosed with HPP associated with a gene variant at a local medical unit. As the patient grew older, the frequency of episodes did not decrease, and he developed symptoms of hyperthyroidism such as dry mouth, palpitation, and weight loss. In addition, potassium can even be as low as

1.59 mmol/L, and respiratory muscles were involved, leading to respiratory muscle paralysis.

The diagnosis of primary HPP is based on a history of flaccid paralysis episodes, a positive family history, characteristic changes in serum potassium, and the exclusion of secondary causes. Whereas, genetic testing is the gold standard for confirming the diagnosis, a significant number of patients have no identifiable variants (3). Diagnostic clues for TPP include adult male, no familial hypokalemic periodic paralysis, no familial history of hyperthyroidism, or hypophosphatemia at the time of the episode, blood acid–base balance is relatively normal (12), and thyrotoxicosis is a prerequisite for the diagnosis of TPP. For our patient, the possibility of HPP due to Sjogren syndrome, Cushing syndrome, and primary aldosteronism was excluded. There were no hyperthyroid symptoms, the thyroid function was normal at that time of onset, and he had no clues at the time to suggest secondary periodic paralysis.

The main sodium channel expressed in skeletal muscles is Nav1.4, which alpha subunit is encoded by SCN4A (4). The alpha subunit of the sodium channel consists of four homologous domains, designated DI to DIV. Each domain is composed of six transmembrane helical segments named S1 to S6, and segments S1–4 form the voltage-sensing domain (14). Since Bulman et al. found that the variant of R669H of SCN4A was associated with the pathogenesis of HPP in 1999 (15), 10 SCN4A variants have been linked to HPP, and HPP caused by variants in SCN4A genes is inherited with an autosomal dominant trait (4). Functional studies suggest that the most likely pathomechanism consists of the creation of an aberrant pore beside the normal ion conduction pathway. This gating pore permits small leakage of cationic currents at rest, favoring membrane depolarization in hypokalemia that, in turn, inactivates sodium channels and rends the fiber inexcitable (4). The variant (c.3404G>A: p.R1135H) is in the S4 segment of domain III and causes HPP by neutralizing arginine residues in S4 segments (16). The variant was classified as variants of pathogenic according to ClinVar. Functional studies with native R1135H muscle fibers showed that the variant increases the probability of depolarized resting membrane potentials under normal conditions and reduced extracellular potassium compatible with the diagnosis (17). R1135H has been reported in heterozygous patients with FPP and also can be *de novo* variants in SPP patients (8, 16, 17). The prevalence study of genetically defined skeletal muscle channelopathies in England showed that the frequency of R1135H in 95 HPP patients was 4% (18). The individuals with the variants had typical HPP phenotype, and the age at onset of attacks was in the second decade, with attacks usually occurring at night or in the early morning, and associated with low serum potassium levels or with provocative factors (16).

Although the results of gene testing at the time of onset were not known, we still considered that the cause of the periodic paralysis initial episode due to a genetic variant associated with primary HPP (c.3404G>A: p.R1135H in SCN4A), exacerbated by hyperthyroidism even leading to dyspnea.

This reminds us that although we identified the cause of HPP through gene testing, we still need to pay attention to whether the patient has other causes leading to changes in the condition, and we need to dynamically monitor other indicators to prevent life-threatening situations.

Treatment of primary HPP should be multifaceted, beginning with lifestyle and behavioral changes, such as identification and avoidance of triggers and avoidance of high carbohydrate intake (3). Pharmacologic treatment for HPP currently focuses on potassium supplementation, potassium-preserving diuretics, and carbonic anhydrase inhibitors (including acetazolamide and dichlorphenamide). Of these, oral or intravenous potassium supplementation is the only way to abort the paralysis. Acetazolamide and dichlorphenamide are commonly used for the prevention of periodic paralytic episodes, but the mechanism of action remains unclear. Acetazolamide has been the most commonly used drug for the treatment of HPP since 1968. A retrospective study in the UK showed that only about 50% of patients with primary HPP responded to acetazolamide, and patients with the CACNA1S variant had a greater chance of benefit than patients with the SCN4A variant (19), while exacerbations have been reported with acetazolamide in patients with the SCN4A variant (20). Dichlorphenamide was the first drug in the US to be approved for use in patients with primary hypokalemic periodic paralysis, and several clinical trials have shown that dichlorphenamide is effective in reducing the frequency of episodes of primary HPP (21), and in improving the quality of life of patients with HPP and maintaining its efficacy over time, despite the relationship between genetic background and the effectiveness of dichlorphenamide remains unknown (22). However, common side effects of using carbonic anhydrase inhibitors include abnormal sensation, fatigue, mild cognitive impairment, and kidney stones (3). Potassium-preserving diuretics have also been effective in primary HPP in patients who are intolerant to carbonic anhydrase inhibitors. Some studies have suggested bumetanide as a potential treatment for periodic paralysis, but the sample size of the relevant studies is small, so the potential use of this drug for the treatment of HPP requires further study (23). Treatment of TPP includes potassium chloride supplementation, non-selective β-blockers to prevent episodes of TPP by inhibiting sodium–potassium ATPase activity, antithyroid drugs, radioactive iodine, surgical control of hyperthyroidism, and avoidance of precipitating factors. In contrast, acetazolamide, a classic drug for primary hypokalemic periodic paralysis, can induce recurrent episodes of TPP (12). Because the treatment methods are different, it is very important to identify the cause. A study showed that to minimize future relapses, more definitive primary treatment such as radioactive iodine or surgery is preferred over ATD alone (24). For this patient, as a young male patient with SCN4A gene variant combined with Graves' disease, the symptoms were severe at the time of the attack; hence, we ultimately recommended that the patient's symptoms improve with lifestyle interventions, treatment with radioactive iodine for thyrotoxicosis, and he did not experience attacks of periodic paralysis.

Conclusion

We present an exceptionally rare case of hypokalemic paralysis caused by a variant, NM_000334.4 (SCN4A):c.3404G>A (p.R1135H), combined with hyperthyroidism. From this case, we conclude that even after the genetic diagnosis is clear that the variant causes hypokalemic periodic paralysis, it is still necessary to pay attention to dynamic monitoring of thyroid function and other causes of periodic paralysis in order to avoid life-threatening exacerbation of the patient's condition and to reduce misdiagnosis and underdiagnosis.

Data availability statement

The original contributions presented in the study are included in the article/supplementary material, further inquiries can be directed to the corresponding author.

Ethics statement

Ethical review and approval was not required for the study on human participants in accordance with the local legislation and institutional requirements. The patients/participants provided their written informed consent to participate in this study. Written informed consent was obtained from the individual(s) for the publication of any potentially identifiable images or data included in this article.

Author contributions

ZZ and BX substantially contributed to the collection of the data, participated in drafting, and approved the final version for publication. All authors agree to be accountable for the content of the work. All authors contributed to the article and approved the submitted version.

Acknowledgments

The authors thank the patient for participating in this study.

Conflict of interest

The authors declare that the research was conducted in the absence of any commercial or financial relationships that could be construed as a potential conflict of interest.

Publisher's note

All claims expressed in this article are solely those of the authors and do not necessarily represent those of their affiliated organizations, or those of the publisher, the editors and the reviewers. Any product that may be evaluated in this article, or claim that may be made by its manufacturer, is not guaranteed or endorsed by the publisher.

References

1. Venance SL, Cannon SC, Fialho D, Fontaine B, Hanna MG, Ptacek LJ, et al. The primary periodic paralyses: diagnosis, pathogenesis and treatment. *Brain*. (2006) 129(Pt 1):8–17. doi: 10.1093/brain/awh639

2. Finsterer J. Primary periodic paralyses. *Acta Neurol Scand*. (2008) 117:145–58. doi: 10.1111/j.1600-0404.2007.00963.x

3. Phillips L, Trivedi JR. Skeletal muscle channelopathies. *Neurotherapeutics*. (2018) 15:954–65. doi: 10.1007/s13311-018-00678-0

4. Maggi L, Bonanno S, Altamura C, Desaphy JF. Ion channel gene mutations causing skeletal muscle disorders: pathomechanisms and opportunities for therapy. *Cells*. (2021) 10:1521. doi: 10.3390/cells10061521

5. Lin SH, Huang CL. Mechanism of thyrotoxic periodic paralysis. *J Am Soc Nephrol*. (2012) 23:985–8. doi: 10.1681/ASN.2012010046

6. Hsieh MJ, Lyu RK, Chang WN, Chang KH, Chen CM, Chang HS, et al. Hypokalemic thyrotoxic periodic paralysis: clinical characteristics and predictors of recurrent paralytic attacks. *Eur J Neurol*. (2008) 15:559–64. doi: 10.1111/j.1468-1331.2008.02132.x

7. Kung AW. Clinical review: thyrotoxic periodic paralysis: a diagnostic challenge. *J Clin Endocrinol Metab*. (2006) 91:2490–5. doi: 10.1210/jc.2006-0356

8. Sung CC, Cheng CJ, Lo YF, Lin MS, Yang SS, Hsu YC, et al. Genotype and phenotype analysis of patients with sporadic periodic paralysis. *Am J Med Sci*. (2012) 343:281–5. doi: 10.1097/MAJ.0b013e31822b430c

9. Ryan DP, da Silva MR, Soong TW, Fontaine B, Donaldson MR, Kung AW, et al. Mutations in potassium channel Kir2.6 cause susceptibility to thyrotoxic hypokalemic periodic paralysis. *Cell*. (2010) 140:88–98. doi: 10.1016/j.cell.2009.12.024

10. Cheng CJ, Lin SH, Lo YF, Yang SS, Hsu YJ, Cannon SC, et al. Identification and functional characterization of Kir2.6 mutations associated with non-familial hypokalemic periodic paralysis. *J Biol Chem*. (2011) 286:27425–35. doi: 10.1074/jbc.M111.249656

11. Noso S, Babaya N, Hiromine Y, Ito H, Taketomo Y, Yoshida S, et al. Contribution of Asian haplotype of KCNJ18 to susceptibility to and ethnic differences in thyrotoxic periodic paralysis. *J Clin Endocrinol Metab*. (2019) 104:6338–44. doi: 10.1210/jc.2019-00672

12. Lin S-H. Thyrotoxic periodic paralysis. *Mayo Clin Proc*. (2005) 80:99–105. doi: 10.1016/S0025-6196(11)62965-0

13. Wu C-Z, Wu Y-K, Lin J-D, Kuo S-W. Thyrotoxic periodic paralysis complicated by acute hypercapnic respiratory failure and ventricular tachycardia. *Thyroid*. (2008) 18:1321–4. doi: 10.1089/thy.2008.0232

14. de Lera Ruiz M, Kraus RL. Voltage-gated sodium channels: structure, function, pharmacology, and clinical indications. *J Med Chem*. (2015) 58:7093–118. doi: 10.1021/jm501981g

15. Bulman DE, Scoggan KA, van Oene MD, Nicolle MW, Hahn AF, Tollar LL, et al. A novel sodium channel mutation in a family with hypokalemic periodic paralysis. *Neurology*. (1999) 53:1932–6. doi: 10.1212/WNL.53.9.1932

16. Matthews E, Labrum R, Sweeney MG, Sud R, Haworth A, Chinnery PF, et al. Voltage sensor charge loss accounts for most cases of hypokalemic periodic paralysis. *Neurology*. (2009) 72:1544–7. doi: 10.1212/01.wnl.0000342387.65477.46

17. Groome JR, Lehmann-Horn F, Fan C, Wolf M, Winston V, Merlini L, et al. NaV1.4 mutations cause hypokalaemic periodic paralysis by disrupting IIIS4 movement during recovery. *Brain*. (2014) 137(Pt 4):998–1008. doi: 10.1093/brain/awu015

18. Horga A, Raja Rayan DL, Matthews E, Sud R, Fialho D, Durran SC, et al. Prevalence study of genetically defined skeletal muscle channelopathies in England. *Neurology*. (2013) 80:1472–5. doi: 10.1212/WNL.0b013e31828cf8d0

19. Matthews E, Portaro S, Ke Q, Sud R, Haworth A, Davis MB, et al. Acetazolamide efficacy in hypokalemic periodic paralysis and the predictive role of genotype. *Neurology*. (2011) 77:19604. doi: 10.1212/WNL.0b013e31823a0cb6

20. Sternberg D, Maisonobe T, Jurkat-Rott K, Nicole S, Launay E, Chauveau D, et al. Hypokalaemic periodic paralysis type 2 caused by mutations at codon 672 in the muscle sodium channel gene SCN4A. *Brain*. (2001) 124:1091–9. doi: 10.1093/brain/124.6.1091

21. Greig SL. Dichlorphenamide: a review in primary periodic paralyses. *Drugs*. (2016) 76:501–7. doi: 10.1007/s40265-016-0559-2

22. Sansone VA, Burge J, McDermott MP, Smith PC, Herr B, Tawil R, et al. Randomized, placebo-controlled trials of dichlorphenamide in periodic paralysis. *Neurology*. (2016) 86:1408–16. doi: 10.1212/WNL.0000000000002416

23. Jitpimolmard N, Matthews E, Fialho D. Treatment updates for neuromuscular channelopathies. *Curr Treat Options Neurol*. (2020) 22:34. doi: 10.1007/s11940-020-00644-2

24. Chang RY, Lang BH, Chan AC, Wong KP. Evaluating the efficacy of primary treatment for graves' disease complicated by thyrotoxic periodic paralysis. *Int J Endocrinol*. (2014) 2014:949068. doi: 10.1155/2014/949068

frontiers | Frontiers in Neurology

TYPE Case Report
PUBLISHED 27 January 2023
DOI 10.3389/fneur.2023.1055639

Check for updates

OPEN ACCESS

EDITED BY
Giovanni Meola,
University of Milan, Italy

REVIEWED BY
Edoardo Malfatti,
Hôpitaux Universitaires Henri Mondor, France
Andrea Legati,
IRCCS Carlo Besta Neurological Institute Foundation, Italy
Xin-Ming Shen,
Mayo Clinic, United States
Kaihui Zhang,
Fudan University, China

*CORRESPONDENCE
Matthew Katz
✉ matthew.katz@health.qld.gov.au

SPECIALTY SECTION
This article was submitted to Neuromuscular Disorders and Peripheral Neuropathies, a section of the journal Frontiers in Neurology

RECEIVED 05 October 2022
ACCEPTED 12 January 2023
PUBLISHED 27 January 2023

CITATION
Katz M, Waddell LB, Yuen M, Bryen SJ, Oates E, Garton FC, Robertson T, Henderson RD, Cooper ST and McCombe PA (2023) Case report: Adult-onset limb girdle muscular dystrophy in sibling pair due to novel homozygous *LAMA2* missense variant. *Front. Neurol.* 14:1055639. doi: 10.3389/fneur.2023.1055639

COPYRIGHT
© 2023 Katz, Waddell, Yuen, Bryen, Oates, Garton, Robertson, Henderson, Cooper and McCombe. This is an open-access article distributed under the terms of the Creative Commons Attribution License (CC BY). The use, distribution or reproduction in other forums is permitted, provided the original author(s) and the copyright owner(s) are credited and that the original publication in this journal is cited, in accordance with accepted academic practice. No use, distribution or reproduction is permitted which does not comply with these terms.

Case report: Adult-onset limb girdle muscular dystrophy in sibling pair due to novel homozygous *LAMA2* missense variant

Matthew Katz[1]*, Leigh B. Waddell[2,3], Michaela Yuen[2,3], Samantha J. Bryen[2,3], Emily Oates[4], Fleur C. Garton[5], Thomas Robertson[6,7], Robert David Henderson[1], Sandra T. Cooper[2,3,8] and Pamela A. McCombe[1,9]

[1]Department of Neurology, Royal Brisbane and Women's Hospital, Herston, QLD, Australia, [2]Kids Research, Kids Neuroscience Centre, The Children's Hospital at Westmead, Sydney, NSW, Australia, [3]Discipline of Child and Adolescent Health, Faculty of Medicine and Health, The University of Sydney, Sydney, NSW, Australia, [4]School of Biotechnology and Biomolecular Sciences, University of New South Wales, Sydney, NSW, Australia, [5]Institute for Molecular Biosciences, The University of Queensland, St Lucia, QLD, Australia, [6]Department of Pathology, Royal Brisbane and Women's Hospital, Herston, QLD, Australia, [7]School of Biomedical Sciences, The University of Queensland, St Lucia, QLD, Australia, [8]The Children's Medical Research Institute, Sydney, NSW, Australia, [9]Centre for Clinical Research, The University of Queensland, Herston, QLD, Australia

Recessive pathogenic variants in the laminin subunit alpha 2 (*LAMA2*) gene cause a spectrum of disease ranging from severe congenital muscular dystrophy to later-onset limb girdle muscular dystrophy (LGMDR23). The phenotype of LGMDR23 is characterized by slowly progressive proximal limb weakness, contractures, raised creatine kinase, and sometimes distinctive cerebral white matter changes and/or epilepsy. We present two siblings, born to consanguineous parents, who developed adult-onset LGMDR23 associated with typical cerebral white matter changes and who both later developed dementia. The male proband also had epilepsy and upper motor neuron signs when he presented at age 72. Merosin immunohistochemistry and Western blot on muscle biopsies taken from both subjects was normal. Whole exome sequencing revealed a previously unreported homozygous missense variant in *LAMA2* [Chr6(GRCh38):g.129297734G>A; NM_000426.3:c.2906G>A; p.(Cys969Tyr)] in the proband. The same homozygous *LAMA2* variant was confirmed by Sanger sequencing in the proband's affected sister. These findings expand the genotypic and phenotypic spectrum of LGMDR23.

KEYWORDS

limb girdle muscular dystrophy, genotype, phenotype, *LAMA2*, whole exome sequencing

Introduction

Laminin subunit alpha 2 (*LAMA2*) encodes the α2 subunit of merosin (laminin-2), a glycoprotein critical for linking the sarcolemma to the extracellular matrix (1). Recessive pathogenic *LAMA2* variants cause a wide spectrum of dystrophic muscle disease ranging from severe congenital muscular dystrophy to later-onset limb girdle muscular dystrophy (LGMDR23), which presents after 12 months of age (2). LGDMR23 is a rare form of LGMD, accounting for only about 2% of all patients in Western European LGMD cohorts (3, 4). Most cases of LGMDR23 are caused by missense variants that result in partial merosin deficiency (2).

LGMDR23 typically presents in childhood with slowly progressive proximal limb weakness, contractures and raised creatine kinase (CK) (2). Motor milestones can be delayed, though nearly all patients achieve independent ambulation, which is typically maintained throughout life (2).

Central nervous system (CNS) complications feature prominently in LGMDR23, with distinctive cerebral white matter signal changes reported in almost all cases and epilepsy in some (2).

Here we describe a proband aged 72 years who presented in his early thirties with LGMD and progressed to develop severe dementia, which began manifesting in his mid-sixties, and diffuse upper motor neuron (UMN) signs without a clear alternative explanation for these features. His sister also had a history of LGMD followed by the development of dementia in her late fifties. Whole exome sequencing (WES) in the proband identified a previously unreported homozygous missense variant in *LAMA2* [Chr6(GRCh38):g.129297734G>A; NM_000426.3:c.2906G>A; p.(Cys969Tyr)]. The same homozygous *LAMA2* variant was confirmed by Sanger sequencing in the proband's affected sister. Although cerebral white matter changes are common, UMN findings and severe cognitive impairment have not previously been reported in association with LGMDR23.

Methods

Ethics

Ethical approval for use of muscle tissue and DNA from probands and controls were obtained from the Human Research Ethics Committees of the Children's Hospital at Westmead, Australia (2019/ETH11736) and all study participants (or their guardians) provided informed, written consent.

Genetic testing

Whole exome sequencing was performed for the proband as part of a previous study, where the proband remained undiagnosed (5). The WES data was reanalysed in the present study. Variant filtering and analysis was performed in seqr (6) using a minor allele frequency cut-off of 0.001 from the gnomAD database (7) and genes associated with neuromuscular disorders in publicly available gene lists (8) (Supplementary Table 1). Sanger sequencing was performed to confirm the *LAMA2* variant in the proband and his affected sister, using the primers; LAMA2ex21F: 5'-agttcctctgttcccacctg-3' and LAMA2ex21R: 5'-cgttgtatcaatctgtgcttcc-3.'The chromosomal microarray (CMA) was performed using the Illumina Whole-Genome Infinium CytoSNP 850K Array v1.1. Results were analyzed with BlueFuse Multiversion 4.4, using genome reference sequence GRCh37/hg19.

Muscle immunohistochemistry and western blot

Cryopreserved muscle tissue was sectioned at 8 µm thickness and collected in pre-cooled microcentrifuge tubes for western blot or on microscopic slides (SuperFrost® Plus, Menzel, Germany) for immunostaining.

Immunostaining was performed on non-fixed tissue as described previously (9) using α-merosin (laminin α2) antibodies (MAb1922, Chemicon, 1:20000; NCL-Merosin, Novocastra, 1:200) and α-spectrin antibody (NCL-SPEC1, Novocastra, 1:300). Slides were imaged on a Leica DMi8 microscope and figures prepared using Adobe Illustrator.

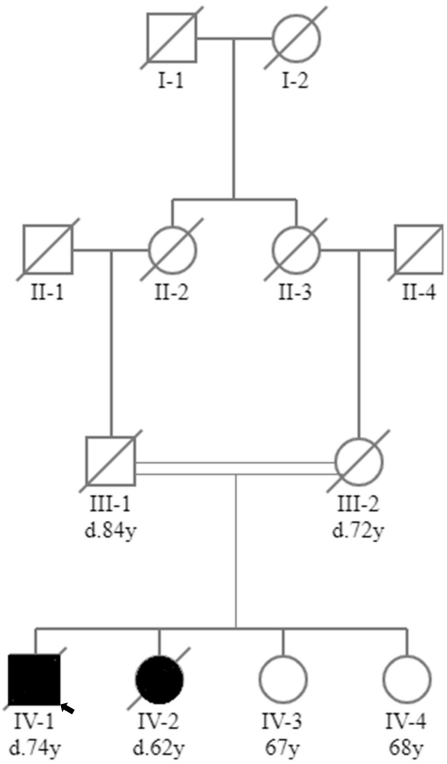

FIGURE 1
Family tree. Family tree showing that the proband (IV-1) and his affected sister (IV-2) were born to consanguineous first cousin parents (III-1 and III-2). Two sisters in their 60s were unaffected (IV-3 and IV-4). Square, male; circle, female; black circle or square, clinically affected; white circle or square, clinically unaffected; line through circle or square, deceased (age of death, where known, given below circle or square as denoted by d.); double line, consanguinity; small black arrow, proband.

Protein sample preparation and western blot was performed as previously described (10). Protein samples were separated on a 4–12% 1 mm NuPAGE™ Bis-Tris gel (Life Technologies) using MOPS running buffer at 150 V and transferred onto a PVDF membrane (Merck Millipore Immobilon™-P, 0.45 µm) for 1 h at 400 mA in Tris-Glycine buffer containing 0.075% sodium dodecyl sulfate and 15% methanol. Total protein was detected using Revert™ 700 total protein stain (LI-COR Biosciences) according to manufacturer's instructions.

Membranes were cut at the 115kD marker band and probed with an α-merosin antibody (bottom half, MAB1922, Chemicon, 1:500) and α-dystrophin antibody (top half, NCL-DYS3, Novocastra, 1:100) overnight at 4°C. Antibody binding was detected using an α-mouse HRP secondary antibody (Merck, 1:1000 for DYS3 detection and 1:2000 for merosin detection) for 2 h at room-temperature. Blots were imaged using the Odyssey CLx imaging system (LI-COR Biosciences) and analyzed using ImageJ. Merosin protein levels were normalized to actin (from total protein stain) and dystrophin. Dystrophin protein levels were also normalized to total protein. The average of 2–3 experiments for each sample was plotted on the graph.

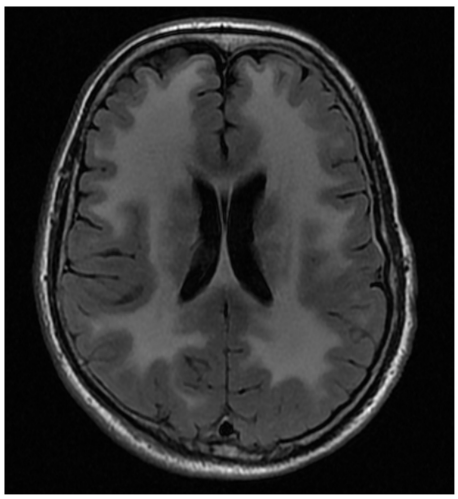

FIGURE 2
MRI brain of proband. Axial FLAIR* image from MRI brain of proband at 64 years of age showing confluent, bilateral white matter T2# hyper intensity with involvement of the corpus callosum *FLAIR, Fluid-attenuated inversion recovery; #T2, transverse relaxation time.

Case report

The male proband (IV-1) was the first child of consanguineous first cousin parents (III-1 and III-2) (Figure 1). He had three sisters (IV-2, IV-3 and IV-4). He had a history of normal childhood motor and language development and was University educated. He presented at age 36 years with a several year history of frequent falls, initially attributed to pelvic fractures sustained from a previous mining accident. He experienced slowly progressive limb weakness with elevated CK (400–600 U/L; normal range <171 U/L). Cognitive issues manifested in his mid-60 s, with family members reporting poor decision making, reduced insight and memory problems. There were no visual hallucinations. Progressive cognitive impairment and severe weakness necessitated high-level nursing home care. Tonic-clonic epileptic seizures, without clear focal onset, began in his late 60 s. Magnetic resonance imaging (MRI) of the brain aged 64 showed confluent, bilateral white matter T2 hyperintensity with involvement of the corpus callosum (Figure 2). There was no significant cerebral or hippocampal atrophy. At around 70 years of age the proband became dependent upon the use of a wheelchair, non-verbal and incontinent.

The proband had a history of well-controlled type II diabetes mellitus, hypothyroidism, depression, paroxysmal atrial fibrillation, and recurrent squamous cell carcinomas. His regular medications at age 72 included sodium valproate 600 mg twice daily, aspirin 100 mg daily, thyroxine 50 mcg 5/7 days and 100 mcg 2/7 days, metformin 500 mg daily, vitamin D 25 mcg daily, insulin glargine 25 units subcutaneously daily, Movicol sachet daily, docusate sodium with senna two tablets twice a day, paracetamol 500 mg two tablets four times a day and risperidone 2 mg as needed.

Examination at the age of 72 showed that he could only follow basic one-step commands and was non-verbal precluding more formal cognitive testing. There was diffuse limb muscle wasting with fixed flexion contractures of the elbows, fingers, hips, and knees. There was Medical Research Council (MRC) grade ≤3 weakness of the proximal and distal limb muscles that could be tested. There was calf pseudohypertrophy. Limb tone was difficult to assess due to the presence of contractures, but pathologic clonus was elicited at the ankles. The reflexes were brisk, and the plantar responses were equivocal. Sensory examination was challenging but the patient appeared to feel sharp sensation in all four limbs. His pupils were equal and reactive to light. Detailed examination of eye movements was not possible due to his difficulty in following instructions and sustaining attention. No facial weakness was observed. The proband was unable to stand or walk.

There was no record of a previous electroencephalogram, nerve conduction study/electromyogram (EMG), transthoracic echocardiogram or respiratory function test. Given the degree of his disability and advanced dementia these were not pursued as the results would not have changed management. The proband continued to decline and poor control of his tonic-clonic seizures resulted in an escalation of his anti-seizure medications. The proband succumbed to aspiration pneumonia at the age of 74.

His younger sister (IV-2) died at the age of 62 from pneumonia in the setting of early onset dementia. She presented to another facility with slowly progressive limb weakness with elevated CK (400-650 U/L) and gait dysfunction from the age of 50. Poor decision making and impairments in working memory were noted in her late 50 s. A limited EMG of her biceps muscle showed myopathic changes characterized by small amplitude motor units without abnormal spontaneous activity. Neuroimaging showed extensive cerebral white matter disease (not shown). From the age of 59 there was a more rapid deterioration in her cognitive and physical function culminating in her being bedbound, mute, and doubly incontinent for the 12 months prior to her death. She did not have a history of epilepsy. The other two sisters in their 60 s (IV-3 and IV-4) were unaffected. There was no other family history of neuromuscular disease or dementia.

Genetic testing

Genetic testing, including targeted sequencing of *FKRP, DNM2* and *LARGE* genes, failed to identify causative genetic variants. Whole exome sequencing, performed from blood of proband (IV-1) identified a previously unreported homozygous missense variant [NM_000426.3:c.2906G>A;p.(Cys969Tyr)] in exon 21 of *LAMA2* (Table 1) [submitted to ClinVar–https://www.ncbi.nlm.nih.gov/clinvar/variation/1693116/?oq=LAMA2%5bgene%5$+$p.Cys969Tyr&m=NM_000426.4(LAMA2):c.2906G$>$A%20(p.Cys969Tyr)]. Sanger sequencing confirmed the *LAMA2* variant was homozygous in the proband and his affected sister (IV-2). The two unaffected sisters (IV-3 and IV-4) were not available for genetic testing for segregation analysis. A chromosomal microarray detected multiple long contiguous stretches of homozygosity (LCSH), including the *LAMA2* locus on chromosome 6.

Muscle histopathology

A quadriceps muscle biopsy obtained from the proband at age 56 years showed myopathic changes with marked replacement of muscle with adipose tissue (Figure 3Ai). The remaining muscle fibers showed marked variation in myofibre diameter with numerous severely atrophic fibers.

TABLE 1 Genetic summary table for novel variant.

Gene	Transcript reference	hg38	Codon variant	Amino acid change	POPmax	*In silico* prediction*	ACMG-AMP classification
LAMA2	NM_000426.3	6:129297734	c.2906G>A	p.Cys969Tyr	NR	DDD	Likely pathogenic (PM2, PM3#, PP1, PP3)

hg38, human reference genome; POPmax, maximum allele frequency in each reference population from 1000G, ExAC, gnomAD and ESP; ACMG-AMP, American College of Medical Genetics and Genomics - Association for Molecular Pathology (version: 8.4.7 from Varsome); NR, allele not previously reported.

*Meta SVM, Meta LR and M-Cap in silico prediction ("D" = deleterious).

#assumed parental carriers due to consanguinity (first cousins), confirmed in case with LCSH via chromosomal microarray.

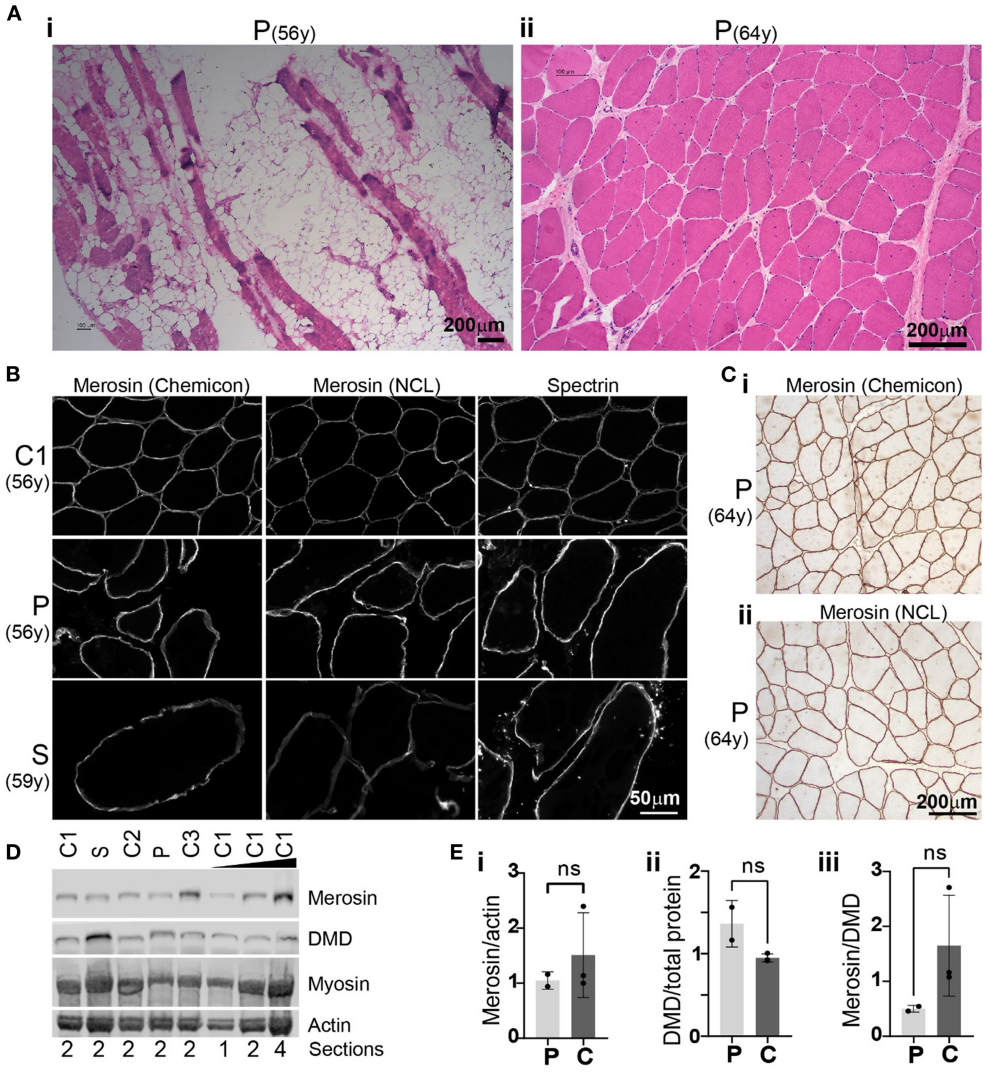

FIGURE 3
Histology, immunohistochemistry and Western blot analysis. **(A)** Haematoxylin and eosin (H&E) staining of muscle biopsies obtained from the proband (P) at age 56 years (i; quadriceps) and 64 years (ii; biceps). Unstained areas observed in (i) represent adipose tissue infiltrates while muscle fibers appear pink in H&E-stained sections. **(B)** Merosin immunohistochemical staining of proband (P) quadriceps muscle biopsies and a muscle biopsy obtained from the proband's sister (S) at 59 years demonstrating membrane-staining comparable to control 1 (C1). Immunostaining for spectrin, another membrane-associated protein, showed a staining pattern similar to merosin. **(C)** Immunohistochemical staining of proband biceps muscle obtained at age 64 years with two merosin antibodies (i: Chemicon MAb1922; ii: NCL-merosin Novocastra) demonstrated membrane-associated staining pattern of merosin similar to **(B)**. **(D)** Western blot of muscle from the proband (P; 56y) and his sister (S; 59y) showed merosin protein levels similar to those detected in three control samples: C1 = 56y (female), C2 = 57y (female), C3 = 59y (male). **(E)** Bar graphs of merosin protein levels normalized to actin (measured from total protein stain) (i), dystrophin protein levels normalized to total protein (ii) and merosin protein levels normalized to dystrophin (iii). Average ± standard deviation for proband and sister (collectively denoted as P) and controls (C) are shown. Groups were compared by using a t-test and found to be not significantly different (ns, i; p = 0.4848, ii; 0.0734, iii; 0.1926).

A biceps muscle biopsy taken subsequently, aged 64 years, showed less severe myopathic changes compared to his quadriceps biopsy with increased internal nuclei, variation in myofibre diameters including hypertrophic and atrophic fibers, but no adipose tissue infiltration (Figure 3Aii). A quadriceps muscle biopsy of the proband's sister at age 59 years showed myopathic changes similar to the quadriceps muscle biopsy from her brother at the age of 56 with severe variation in myofibre diameter, numerous atrophic fibers and significant replacement of skeletal muscle with fibroadipose tissue (not shown).

To determine whether the homozygous missense variant in *LAMA2* results in abnormal subcellular localization and abnormal protein levels of the encoded protein merosin, we performed immunohistochemistry and western blot analysis. Merosin immunohistochemistry on two biopsies from the proband (age 56 and 64 years) and one biopsy from the sister (age 59 years) demonstrated membrane-associated staining pattern comparable to control muscle (Figures 3B, C). Merosin protein levels as determined by Western blot were also comparable to controls (three age matched controls were used) in both subjects (Figure 3D). Merosin protein levels were found to be lower in the proband and sister compared to controls when normalized to actin and dystrophin but this difference was not statistically significant (Figure 3Ei, iii). There was a small increase in dystrophin protein levels when normalized to total protein in the proband and sister compared to controls but this difference was also not statistically significant (Figure 3Eii).

Discussion

The phenotypic and genotypic spectrum of *LAMA2* muscular dystrophy is wide. Here we report a novel homozygous *LAMA2* variant in two siblings born to consanguineous parents. The *LAMA2* variant was not reported in several large reference population databases (7, 11, 12) and *in silico* analyses (13, 14) predicted the variant to have a deleterious impact on protein function (Table 1). The affected sister harbored the same variant in a homozygous state. Whilst genetic testing of the parents was not possible the LCSH on chromosomal microarray would support the novel variant occurring *in trans* due to known parental consanguinity. Collective clinical and genetic evidence supports classification of NM_000426.3:c.2906G>A;p.(Cys969Tyr) as likely pathogenic as per the ACMG-AMP criteria (15) (Table 1). A limitation of our report is the lack of *in vitro* or *in vivo* functional studies to assess for any damaging effect of this variant on the gene product. The variant identified in our study affects a highly conserved cysteine residue within the laminin-type epidermal growth factor (EGF)-like domain (16). Cysteines in this domain are critical for disulfide bond formation (16) and the variant is thus likely to affect the integrity of this rigid rod-like structure, which could destabilize the sarcolemma-extracellular matrix connections facilitated by the laminin-α2 protein (17). A study reporting 61 new LAMA2 variants and reviewing LAMA2 variants in the Leiden Open Variation Database (18) (https://www.LOVD.nl/LAMA2) found that 25% of deleterious missense variants affect cysteine residues within EGF-like repeats (17). A very rare missense variant [p.(Cys969Ser)] in the same amino acid position as our variant has been reported in the gnomAD database in the hetereozygous state without clinical disease (7).

The proband's clinical presentation was notable for profound weakness, severe joint contractures, extensive cerebral white matter changes, UMN findings, epilepsy, and dementia. Cerebral white matter changes are seen in nearly all patients with *LAMA2* muscular dystrophy (1, 2). In patients with adult onset LGMDR23, epilepsy is uncommon and cognition is usually intact despite the striking white matter abnormalities on brain MRI (1, 2). Mild deficits in executive function and mild cognitive impairment have been reported in a few older patients with adult onset LGMDR23 (19, 20). More significant cognitive impairment, in the form of intellectual disability, has been reported in LGMDR23 but only in younger patients with childhood onset disease (20, 21). The dementia seen in the proband and his sister could represent an extension of the LGMDR23 phenotype. However, as they were born to consanguineous parents it is possible that the dementia is due to the inheritance of another, albeit unrecognized, recessive pathogenic variant, especially given the LCSH seen on chromosomal microarray.

The finding of brisk reflexes and pathologic ankle clonus in the proband implies co-existent UMN pathology. This could be related to the extensive white matter changes, but UMN signs have not been described in other patients with *LAMA2* muscular dystrophy most of whom have similar white matter abnormalities on brain MRI.

The muscle biopsies from our subjects showed non-specific myopathic and dystrophic features consistent with the muscle biopsy findings in other LGMD23 cases (2, 4, 19, 20). However, most LGMD23 cases show at least partial merosin deficiency on immunohistochemistry and Western blot (2). Significant variability of merosin immunostaining in cases of LGMDR23 is well recognized and often depends on the antibodies used (22). However, the finding of normal merosin immunostaining, as seen in our subjects, is atypical. Normal merosin immunostaining is not unprecedented and has been described in two cases of genetically confirmed LGMDR23 using the same antibodies (MAb1922, Chemicon and NCL-merosin, Novocastra) (20, 23). Like our subjects, both cases had a late onset of symptoms with one case developing LGMD in their forties (20). In one of these cases, a subtle reduction of merosin immunostaining was only detected when the antibody directed against the N-terminal 300-kDa fragment of laminin-α2 (4H8, Alexis) was used (23). This differential immunostaining is consistent with the findings in other cases of LGMDR23 where staining with the N-terminal antibody often shows more abnormal results compared to staining with the antibody against the C-terminal 80-kDa fragment (MAb1922, Chemicon) (22). This could provide a possible explanation for the "normal" merosin immunostaining seen in our subjects as the N-terminal antibody was not used.

To our knowledge the findings of normal merosin Western blot in muscle despite clinical and genetic evidence of *LAMA2* muscular dystrophy has not been described. It is possible that a small change in merosin protein levels is not detected by our Western blot. Merosin protein levels were lower in the proband and his sister compared to controls when normalized to actin and dystrophin but these differences were not statistically significant (Figure 3Ei, iii). It is possible that the *LAMA2* variant [p.(Cys969Tyr)] could cause disease by conferring a toxic gain-of-function effect at the protein level, although this phenomenon would be extremely rare in the setting of a recessive disorder. Alternatively, the variant may reduce the activity of the laminin type EGF-like

domain as postulated above but not significantly impact overall protein levels.

In the absence of published diagnostic criteria for *LAMA2* muscular dystrophy the finding of rare predicted to be pathogenic recessive variants in the *LAMA2* gene is currently considered to be the gold standard for establishing a diagnosis (1, 2). The presence of limb girdle muscle weakness, contractures, raised CK and cerebral white matter changes in the proband and his sister combined with likely pathogenic *LAMA2* variants are highly suggestive of LGMDR23. In particular, the finding of cerebral white matter changes in both subjects provides a compelling argument that the recessive *LAMA2* variants are the cause for their muscle weakness, as cerebral white matter changes appear to be unique to this sub-type of LGMD.

Conclusion

This case report expands the genotypic and phenotypic spectrum of LGMDR23 through the identification of a novel homozygous *LAMA2* variant in a sibling pair with typical LGMD23 features including white matter signal changes–along with upper motor neuron findings and dementia. This finding highlights the utility of WES in aiding the diagnosis of rare neuromuscular disorders, particularly where the muscle biopsy results are inconclusive.

Data availability statement

The datasets presented in this study can be found in online repositories. The names of the repository/repositories and accession number(s) can be found in the article/Supplementary material.

Ethics statement

The studies involving human participants were reviewed and approved by Human Research Ethics Committees of the Children's Hospital at Westmead, Australia (2019/ETH11736). The patients/participants provided their written informed consent to participate in this study.

Author contributions

MK was responsible for conception, organization, and writing of manuscript. LW and SB were responsible for obtaining initial muscle and genetic data and assisted with editing of the manuscript. MY assisted preparation of the methods section on muscle immunohistochemistry and western blot and provided Figure 3 on muscle histopathology results and helped edit the manuscript. FG assisted with Table 1 on genetic variant, submission of genetic variant to ClinVar database, and helped edit the manuscript. SC was responsible for supervising collection, interpretation of muscle and genetic data, and assisted with editing of the manuscript. EO, TR, RH, and PM helped with editing of the manuscript. All authors contributed to the article and approved the submitted version.

Acknowledgments

Acknowledgment to the Queensland Medical Laboratory (QML) for performing the chromosomal microarray and interpreting the results.

Conflict of interest

The authors declare that the research was conducted in the absence of any commercial or financial relationships that could be construed as a potential conflict of interest.

Publisher's note

All claims expressed in this article are solely those of the authors and do not necessarily represent those of their affiliated organizations, or those of the publisher, the editors and the reviewers. Any product that may be evaluated in this article, or claim that may be made by its manufacturer, is not guaranteed or endorsed by the publisher.

Supplementary material

The Supplementary Material for this article can be found online at: https://www.frontiersin.org/articles/10.3389/fneur.2023.1055639/full#supplementary-material

References

1. Oliveira J, Freixo JP, Santos M, Coelho T. *LAMA2 Muscular Dystrophy*. GeneReviews® (2012). Available online at: https://www.ncbi.nlm.nih.gov/books/NBK97333/

2. Sarkozy A, Foley AR, Zambon AA, Bönnemann CG, Muntoni F. LAMA2-related dystrophies: clinical phenotypes, disease biomarkers, and clinical trial readiness. *Front Mol Neurosci.* (2020) 13:1–11. doi: 10.3389/fnmol.2020.00123

3. Sframeli M, Sarkozy A, Bertoli M, Astrea G, Hudson J, Scoto M, et al. Congenital muscular dystrophies in the UK population: Clinical and molecular spectrum of a large cohort diagnosed over a 12-year period. *Neuromuscul Disord.* (2017) 27:793–803. doi: 10.1016/j.nmd.2017.06.008

4. Løkken N, Born AP, Duno M, Vissing J. LAMA2-related myopathy: Frequency among congenital and limb-girdle muscular dystrophies. *Muscle and Nerve.* (2015) 52:547–53. doi: 10.1002/mus.24588

5. Ghaoui R, Cooper ST, Lek M, Jones K, Corbett A, Reddel SW, et al. Use of whole-exome sequencing for diagnosis of limb-girdle muscular dystrophy: outcomes and lessons learned. *JAMA Neurol.* (2015) 72:1424–32. doi: 10.1001/jamaneurol.2015.2274

6. Pais L, Snow H, Weisburd S, B, Zhang Baxter S, Ditroia S, et al. seqr: a web-based analysis and collaboration tool for rare disease genomics. *Hum Mutat.* (2022) 43:698–707. doi: 10.1002/humu.24366

7. Karczewski KJ, Francioli LC, Tiao G, Cummings BB, Alföldi J, Wang Q, et al. The mutational constraint spectrum quantified from variation in 141,456 humans. *Nature.* (2020) 581:434–43. doi: 10.1038/s41586-020-2308-7

8. Cohen E, Bonne G, Rivier F, Hamroun D. The 2022 version of the gene table of neuromuscular disorders (nuclear genome). *Neuromuscul Disord.* (2021) 31:1313–57. doi: 10.1016/j.nmd.2021.11.004

9. Lo HP, Cooper ST, Evesson FJ, Seto JT, Chiotis M, Tay V, et al. Limb-girdle muscular dystrophy: Diagnostic evaluation, frequency and clues to pathogenesis. *Neuromuscul Disord.* (2008) 18:34–44. doi: 10.1016/j.nmd.2007.08.009

10. Cooper ST, Lo HP, North KN. Single section Western blot: Improving the molecular diagnosis of the muscular dystrophies. *Neurology.* (2003) 61:93–7. doi: 10.1212/01.WNL.0000069460.53438.38

11. Auton A, Abecasis GR, Altshuler DM, Durbin RM, Bentley DR, Chakravarti A, et al. A global reference for human genetic variation. *Nature.* (2015) 526:68–74. doi: 10.1038/nature15393

12. Lek M, Karczewski KJ, Minikel E V, Samocha KE, Banks E, Fennell T, et al. Analysis of protein-coding genetic variation in 60,706 humans. *Nature.* (2016) 536:285–91. doi: 10.1038/nature19057

13. Dong C, Wei P, Jian X, Gibbs R, Boerwinkle E, Wang K, et al. Comparison and integration of deleteriousness prediction methods for nonsynonymous SNVs in whole exome sequencing studies. *Hum Mol Genet.* (2015) 24:2125–37. doi: 10.1093/hmg/ddu733

14. Jagadeesh KA, Wenger AM, Berger MJ, Guturu H, Stenson PD, Cooper DN, et al. M-CAP eliminates a majority of variants of uncertain significance in clinical exomes at high sensitivity. *Nat Genet.* (2016) 48:1581–6. doi: 10.1038/ng.3703

15. Richards S, Aziz N, Bale S, Bick D, Das S, Gastier-Foster J, et al. Standards and guidelines for the interpretation of sequence variants: a joint consensus recommendation of the American College of Medical Genetics and Genomics and the Association for Molecular Pathology. *Genet Med.* (2015) 17:405–24. doi: 10.1038/gim.2015.30

16. Abe Y, Odaka M, Inagaki F, Lax I, Schlessinger J, Kohda D. Disulfide bond structure of human epidermal growth factor receptor. *J Biol Chem.* (1998) 273:11150–7. doi: 10.1074/jbc.273.18.11150

17. Oliveira J, Gruber A, Cardoso M, Taipa R, Fineza I, Gonçalves A, et al. LAMA2 gene mutation update: Toward a more comprehensive picture of the laminin-α2 variome and its related phenotypes. *Hum Mutat.* (2018) 39:1314–37. doi: 10.1002/humu.23599

18. Fokkema IFAC, Taschner PEM, Schaafsma GCP, Celli J, Laros JFJ, den Dunnen JT, et al. v. 20: The next generation in gene variant databases. *Hum Mutat.* (2011) 32:557–63. doi: 10.1002/humu.21438

19. Gavassini BF, Carboni N. Nielsen JøE, Danielsen ER, Thomsen C, Svenstrup K, et al. Clinical and molecular Characterization of limb-girdle muscular dystrophy due to LAMA2 mutations. *Muscle and Nerve.* (2011) 44:703–9. doi: 10.1002/mus.22132

20. Magri F, Brusa R, Bello L, Peverelli L, Del BR, Govoni A, et al. Limb girdle muscular dystrophy due to LAMA2 gene mutations: new mutations expand the clinical spectrum of a still challenging diagnosis. *Acta Myol.* (2020) 39:67–82. doi: 10.36185/2532-1900-009

21. Deodato F, Sabatelli M, Ricci E, Mercuri E, Muntoni F, Sewry C, et al. Hypermyelinating neuropathy, mental retardation and epilepsy in a case of merosin deficiency. *Neuromuscul Disord.* (2002) 12:392–8. doi: 10.1016/S0960-8966(01)00312-1

22. Jones KJ, Morgan G, Johnston H, Tobias V, Ouvrier RA, Wilkinson I, et al. The expanding phenotype of laminin α2 chain (merosin) abnormalities: case series and review. *J Med Genet.* (2001) 38:649–57. doi: 10.1136/jmg.38.10.649

23. Rajakulendran S, Parton M, Holton JL, Hanna MG. Clinical and pathological heterogeneity in late-onset partial merosin deficiency. *Muscle and Nerve.* (2011) 44:590–3. doi: 10.1002/mus.22196

frontiers | Frontiers in Neurology

TYPE Case Report
PUBLISHED 27 January 2023
DOI 10.3389/fneur.2023.1087421

Check for updates

OPEN ACCESS

EDITED BY
Giovanni Meola,
University of Milan, Italy

REVIEWED BY
Curtis R. Coughlin II,
University of Colorado Anschutz Medical Campus, United States
Corrado Italo Angelini,
University of Padua, Italy

*CORRESPONDENCE
Liqiang Yu
✉ yuliqiang@suda.edu.cn
Qi Fang
✉ Fangfangqi_008@126.com

†These authors have contributed equally to this work and share first authorship

SPECIALTY SECTION
This article was submitted to Neuromuscular Disorders and Peripheral Neuropathies, a section of the journal Frontiers in Neurology

RECEIVED 02 November 2022
ACCEPTED 10 January 2023
PUBLISHED 27 January 2023

CITATION
Zhu S, Ding D, Jiang J, Liu M, Yu L and Fang Q (2023) Case report: Novel *ETFDH* compound heterozygous mutations identified in a patient with late-onset glutaric aciduria type II. *Front. Neurol.* 14:1087421. doi: 10.3389/fneur.2023.1087421

COPYRIGHT
© 2023 Zhu, Ding, Jiang, Liu, Yu and Fang. This is an open-access article distributed under the terms of the Creative Commons Attribution License (CC BY). The use, distribution or reproduction in other forums is permitted, provided the original author(s) and the copyright owner(s) are credited and that the original publication in this journal is cited, in accordance with accepted academic practice. No use, distribution or reproduction is permitted which does not comply with these terms.

Case report: Novel *ETFDH* compound heterozygous mutations identified in a patient with late-onset glutaric aciduria type II

Sijia Zhu[1†], Dongxue Ding[1†], Jianhua Jiang[1], Meirong Liu[1], Liqiang Yu[2*] and Qi Fang[1*]

[1]Department of Neurology, The First Affiliated Hospital of Soochow University, Suzhou, China, [2]Department of General Medicine, The First Affiliated Hospital of Soochow University, Suzhou, China

Glutaric aciduria type II (GA II) is an autosomal recessive metabolic disorder of fatty acid, amino acid, and choline metabolism. The late-onset form of this disorder is caused by a defect in the mitochondrial electron transfer flavoprotein dehydrogenase or the electron transfer flavoprotein dehydrogenase (*ETFDH*) gene. Thus far, the high clinical heterogeneity of late-onset GA II has brought a great challenge for its diagnosis. In this study, we reported a 21-year-old Chinese man with muscle weakness, vomiting, and severe pain. Muscle biopsy revealed myopathological patterns of lipid storage myopathy, and urine organic acid analyses showed a slight increase in glycolic acid. All the aforementioned results were consistent with GA II. Whole-exome sequencing (WES), followed by bioinformatics and structural analyses, revealed two compound heterozygous missense mutations: c.1034A > G (p.H345R) on exon 9 and c.1448C>A (p.P483Q) on exon 11, which were classified as "likely pathogenic" according to American College of Medical Genetics and Genomics (ACMG). In conclusion, this study described the phenotype and genotype of a patient with late-onset GA II. The two novel mutations in *ETFDH* were found in this case, which further expands the list of mutations found in patients with GA II. Because of the treatability of this disease, GA II should be considered in all patients with muscular symptoms and acute metabolism decompensation such as hypoglycemia and acidosis.

KEYWORDS

glutaric aciduria type II, ETFDH, compound heterozygous mutations, functional analysis, ACMG, riboflavin supplement

Introduction

Glutaric aciduria type II (GA II), also called multiple acyl-CoA dehydrogenase deficiency or ethylmalonic-adipic aciduria (MADD; OMIM 231680), is a very rare autosomal recessively inherited disorder with an inborn error of metabolism of amino acid, fatty acid, and choline (1) due to functional defects in either electron transfer flavoprotein (ETF) encoded by the alpha- or beta-subunit ETF gene (*ETFA*, OMIM 608053; *ETFB*, OMIM 130410) or ETF-ubiquinone oxidoreductase (ETF: QO) encoded by the ETF dehydrogenase (*ETFDH*, OMIM 231675) gene (2, 3).

The clinical phenotype of GA II is substantially heterogeneous, from relatively mild late-onset to severe birth defects, including myopathy, cardiomyopathy, pancreatitis, and congenital anomalies (4, 5). It has been categorized into three sub-groups based on these different manifestations: neonatal onset with congenital abnormalities (type 1, OMIM 608053), neonatal onset without abnormalities (type 2, OMIM 231680), and mild and/or later onset (type 3, OMIM 231680) (3, 6, 7). Defects in genes *ETFA*, *ETFB,* and *ETFDH* are responsible for these three types, respectively (7). Individuals with severe forms always have a rapidly fatal course. Diagnosis of these severe forms mainly relied on the acylcarnitine pattern in dried blood/plasma including short-, medium-, and long-chain acylcarnitine change detected by tandem mass spectrometry (MS/MS) and urine organic acid (UOA) profile (8). However, the milder form, type 3 GA II, caused by the *ETFDH* gene, can present at any age and always show diverse manifestations including fluctuating proximal muscle weakness, intermittent rhabdomyolysis and other nerve neuropathy, weakened or disappeared tendon reflex, and fatty liver (9, 10). Moreover, many patients may present with an episodic illness that poses a great challenge for its diagnosis (11–13). Under these circumstances, molecular studies and genetic testing are required to make a definitive diagnosis.

The therapeutic strategy usually involves a restricted diet including the avoidance of fasting to prevent hypoglycemia and metabolic acidosis, as well as a diet low in protein and fat together with carnitine, ubiquinone, and riboflavin supplement, especially for those with severe forms (14, 15). Patients with milder late-onset forms always have an obvious improvement both in clinical symptoms and metabolic profile with riboflavin supplementation. Recent studies show that these patients, termed riboflavin-responsive MADD (RR-MADD), have been seen to harbor *ETFDH* variants encoding ETF:QO (16, 17).

Herein, we report a 21-year-old male patient who is molecularly confirmed as late-onset GA II. Whole-exome sequencing (WES) revealed a compound heterozygous mutation for two variants in the *ETFDH* gene, namely, a c.1034A>G (p.H345R) in exon 9 and a c.1448C>A (p.P483Q) in exon 11, respectively, located in the FAD-binding domain and UQ-binding domain. In addition, we predict the protein structural changes caused by these mutations, and the results proved these two novel mutations to be very likely pathogenic based both on the clinical findings and protein changes.

Case report

The patient was a 21-year-old man who came from a non-consanguineous family in Anhui Province. He was admitted to our department due to limb weakness and severe pain accompanied by vomiting for 2 months. In the last 2 weeks, after suffering from influenza, progressive limb weakness reoccurred. He had difficulty walking long distances and climbing the stairs and was too weak to lift his hands to strip or comb the hair. Ten days before admission, he experienced acid reflux, and then repeated nausea and vomiting with gastric contents and bile, with no improvement after fasting and resting up. One week ago, the symptom of limb weakness, pain, and vomiting was noted to have obviously aggravated. Blood test results in the local hospital showed 16,969 u/L creatine kinase (CK) and 2,000 ng/ml myoglobin. Therefore, he was suspected to have gotten rhabdomyolysis in the local hospital and was sent to our department. The patient had normal development during the fetal and infant periods. From 5 years old, he was unable to exercise vigorously because of muscle soreness and aches after activities. Since 2015, he has experienced intermittent acid reflux, nausea, and vomiting; gastroscopy showed chronic superficial gastritis. He had two hospitalizations due to severe vomiting, both occurred in winter. He reported a history of hepatitis carriers for 3 years and denied any history of diabetes and kidney disease. Neurological examination showed limb muscle tenderness, and neck and proximal muscle weakness (manual muscle testing (MMT) score: 4/5 in the neck, 4/5 in upper limbs, and 3/5 in lower limbs).

Besides the elevated level of CK and myoglobin, other parameters were also significantly increased including alanine aminotransferase (ALT) 242 U/L (normal 7–40 U/L), aspartate aminotransferase (AST) 1,745 U/L (normal 13–35 U/L), creatine kinase-MB (CK-MB) 1,425.5 U/L (normal 0–16), myoglobin 2,000 ng/mL (normal 27–70 ng/mL), and lactate dehydrogenase (LDH) 1,813 U/L (normal 120–250 U/L). Urine routine: urine protein (+), urine ketone body (KET) (4+), and urine latent blood (BLD) (3+).

Muscle MRI T2 of lower limbs revealed high signal intensity areas in the bilateral lower limb muscles, indicating diffuse muscle injury (Figures 1A–D). Abdomen ultrasound images showed obvious signs of fatty liver (Figure 1E).

On admission, he was initially diagnosed with rhabdomyolysis or inflammatory myopathy and was treated with methylprednisolone (40 mg for 2 days, followed by 20 mg for another 2 days). After renal function results returned to normal, the muscle biopsy was performed. The results suggested vacuole myopathy with the formation of vacuoles in muscle fibers (Figures 2A, B). The oil red O staining showed diffuse fat granule aggregation, and periodic acid-Schiff (PAS) staining showed no excessive glycogen content (data not shown). The pathological results were consistent with the manifestation of lipid-storage myopathy. UOA analysis showed that glycolic acid slightly increased to 9.0 (normal 0–8), and no significant increase was observed in the rest results. Blood acylcarnitine analysis showed an increase in octanoyl carnitine (C8) and decanoyl carnitine (C10), while the test results may come after glutaric acid-type II treatment.

Whole-exome sequencing (WES) revealed a compound heterozygous mutation in the *ETFDH* gene in the proband: c.1034A > G (p.H345R) on exon 9 and c.1448C>A (p.P483Q) on exon 11. Sanger sequencing showed that these two mutations, respectively, come from the proband's father and mother (Figure 3). No mutations were identified in other related genes such as ETFA or ETFB gene.

Both mutations were not reported in the Human Gene Mutation Database and were not found in 100 healthy Chinese control individuals. ETF:QO was shown to have three functional domains: FAD-binding domain, 4Fe−4S cluster domain, and UQ-binding domain. The p.H345R and p.P483Q, respectively, lied in the FAD-binding domain and UQ-binding domain. Bioinformatic and structural analysis was conducted to predict the effect of the revealed variants on the functional properties of the proteins.

The missense mutation c.1034A > G led to the change from histidine to arginine at 345th amino acid, with no physical and chemical properties change. Multiplex sequence alignment of the *ETFDH* protein across eight different species and 100 vertebrate genomes showed that Histidine (H) at codon 345 was highly

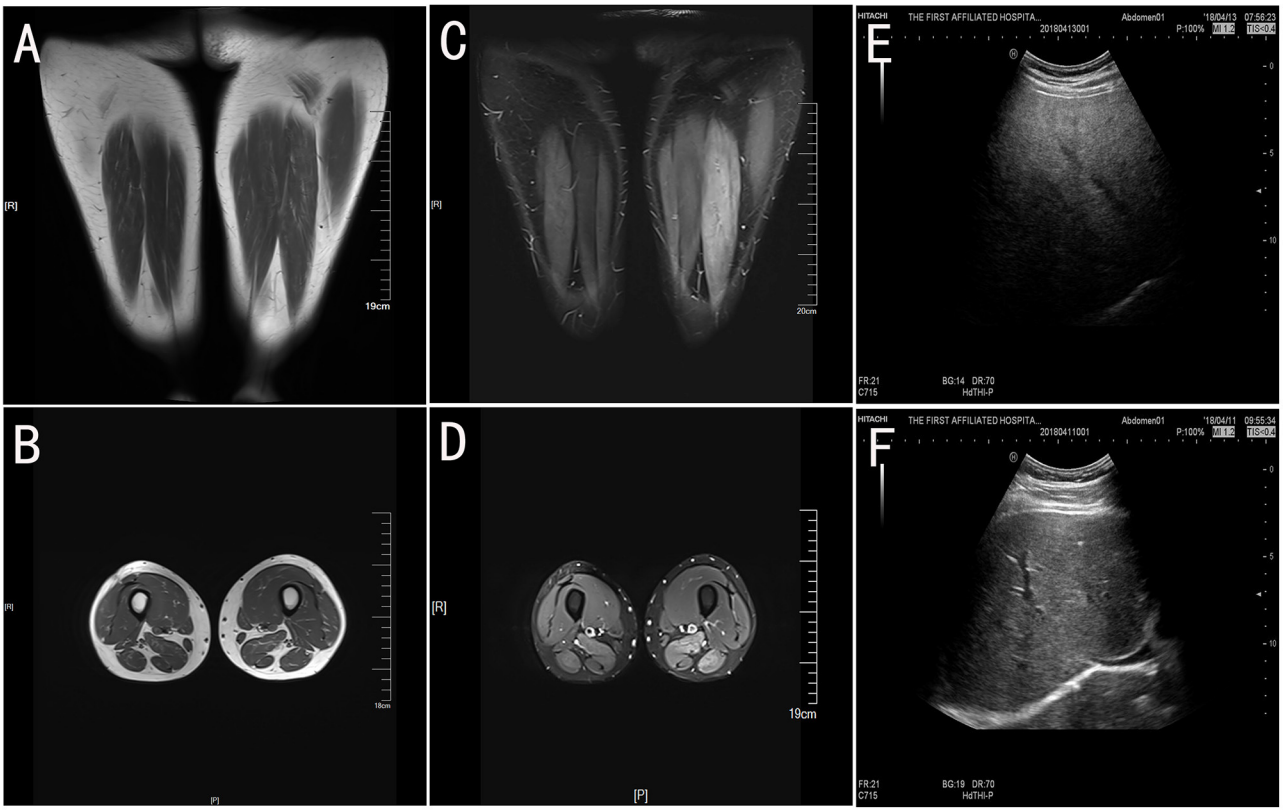

FIGURE 1
The muscle MRI of lower limbs and abdomen ultrasound. The T1-weight images **(A, B)** showed slightly atrophy of bilateral lower limbs. Fat suppression (T2-weighted short tau inversion recovery, T2-STIR) images **(C, D)** have high signal intensity in the bilateral limb muscles, which indicates muscle injury. The abdomen ultrasound **(E)** showed obvious signs of a fatty liver compared with the health control **(F)**.

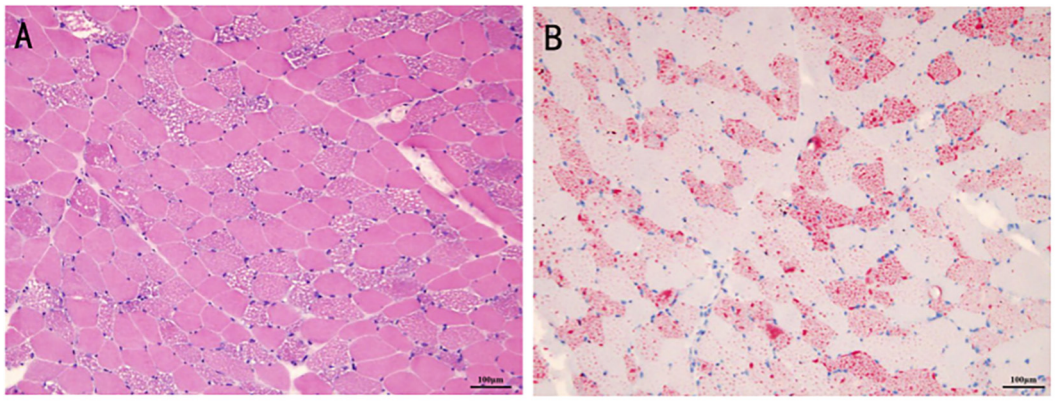

FIGURE 2
The histopathologic manifestation of the patient's muscle. The formation of vacuoles was found in the muscle fibers for hematoxylin-eosin staining **(A)**. The oil red O staining showed diffuse fat granule aggregation **(B)**.

conserved among species (Figure 4A). This mutation was graded as variant uncertain significance (VUS) according to ACMG. Results predicted by MutationTaster and SIFT supported that p.H345R of *ETFDH* was a tolerated mutation, while Polyphen-2 identified it as benign. The structural analysis showed a polar interaction change between the wild-type and mutant structures of the *ETFDH* protein (Figure 4B).

The missense mutation c.1448C>A led to the change from proline to glutamine at 483rd amino acid, and the physical and chemical properties change included the size of the side chain change, resulting in the amino acids weight change from 115 to 146. Multiplex sequence alignment also showed that Proline (P) at codon 483 was highly conserved among species (Figure 4C). The mutation was graded as likely pathogenic according to ACMG.

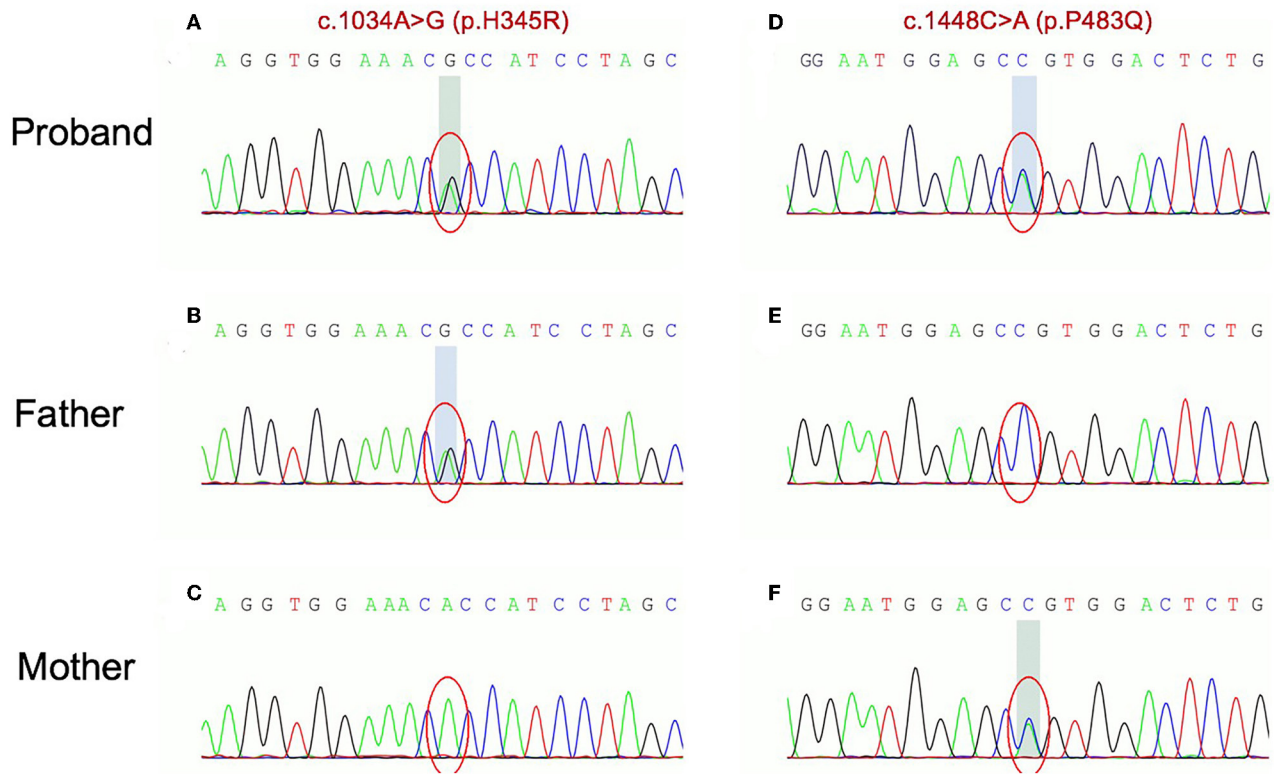

FIGURE 3
Sanger traces for PCR products of the proband and his parents. Sanger traces for PCR products of the proband indicated a compound heterozygous mutation in ETFDH gene: c.1034A > G (p.H345R) on exon 9 **(A)** and c.1448C>A (p.P483Q) on exon 11 **(B)**. Sanger traces for PCR of his parents. The c.1034A > G (p.H345R) on exon 9 and c.1448C>A (p.P483Q) on exon 11 come from the father and mother **(C–F)**, respectively.

Results of Polyphen-2, MutationTaster, and SIFT all supported that p.P483Q of *ETFDH* was a deleterious mutation. The structural analysis revealed a polar interaction change (Figure 4D) and a stability decrease between the wild-type and mutant structures of the *ETFDH* protein.

The patient received a high dose of riboflavin (150 mg/day) with a low-fat diet (lipid restricted to 25% of total calories) after diagnosis. Symptoms of muscle weakness were progressively relieved in 3 weeks and recovered completely in 2 months. In addition, routine blood examinations such as CK, AST, and ALT decreased to normal values at the 6-month follow-up. Until now, the patient remained on riboflavin treatment (150 mg/day) and a low-fat diet. Fortunately, he had no muscle weakness recurrence and was competent for daily life during the 3-year follow-up.

Discussion

Glutaric aciduria type II is a highly heterogeneous disease characterized by various manifestations with different degrees. RR-MADD, caused by *ETFDH* gene mutations, is the most common phenotype (18). In this study, we described a patient with two novel compound heterozygous mutations in the *ETFDH* gene: c.1034A > G (p.H345R) on exon 9 and c.1448C>A (p.P483Q) on exon 11.

The electron transfer flavoprotein dehydrogenase gene is located on chromosome 4q32.1 and consists of 13 exons. To date, more than 200 mutations in the *ETFDH* gene have been identified in Human Gene Mutation Database (HGMD), including various types such as missense, nonsense, insertion, deletion, and splicing mutations (19). The following hot spot mutations were the most frequently identified mutations in Chinese: c.250G > A (p.A84T), c.770A > G (p.Y257C), and c.1227A > C (p.L409F) with a frequency of 12.2%, 15.0%, and 12.2%, respectively (20). Some reports have revealed that the genotype of GA II patients with *ETFDH* mutations was correlated with their diverse phenotype (21). For example, nonsense mutations in both alleles of the *ETFDH* gene resulting in truncation may affect protein structure or stability, which always presents with more severe manifestations. However, the definite correlation between the genotype and phenotype of *ETFDH* mutated late-onset mild GA II has not been fully confirmed due to limited patients and other factors such as infections and poor nutrition. Missaglia described five GA II patients with various *ETFDH* mutations and varying degrees of clinical symptom severity. Similar to our patient, most patients had two compound missense mutations and mainly presented with muscle weakness or exercise intolerance. In addition, our patient had extra-muscle symptoms such as vomiting and fatty liver, while some previously reported patients presented with severe neurological symptoms and metabolic disorders, which further illustrated the high heterogeneity of the disease (22). Therefore, inherited metabolic disease should be considered in clinical work when patients have unexplained myasthenia, exercise intolerance, or other extra-muscle symptoms such as vomiting, seizure, encephalopathy, and hypoglycemia. Blood acylcarnitine analysis and urine organic acid tests could be performed to screen for GA II. Genetic testing should be further conducted to confirm the diagnosis (23).

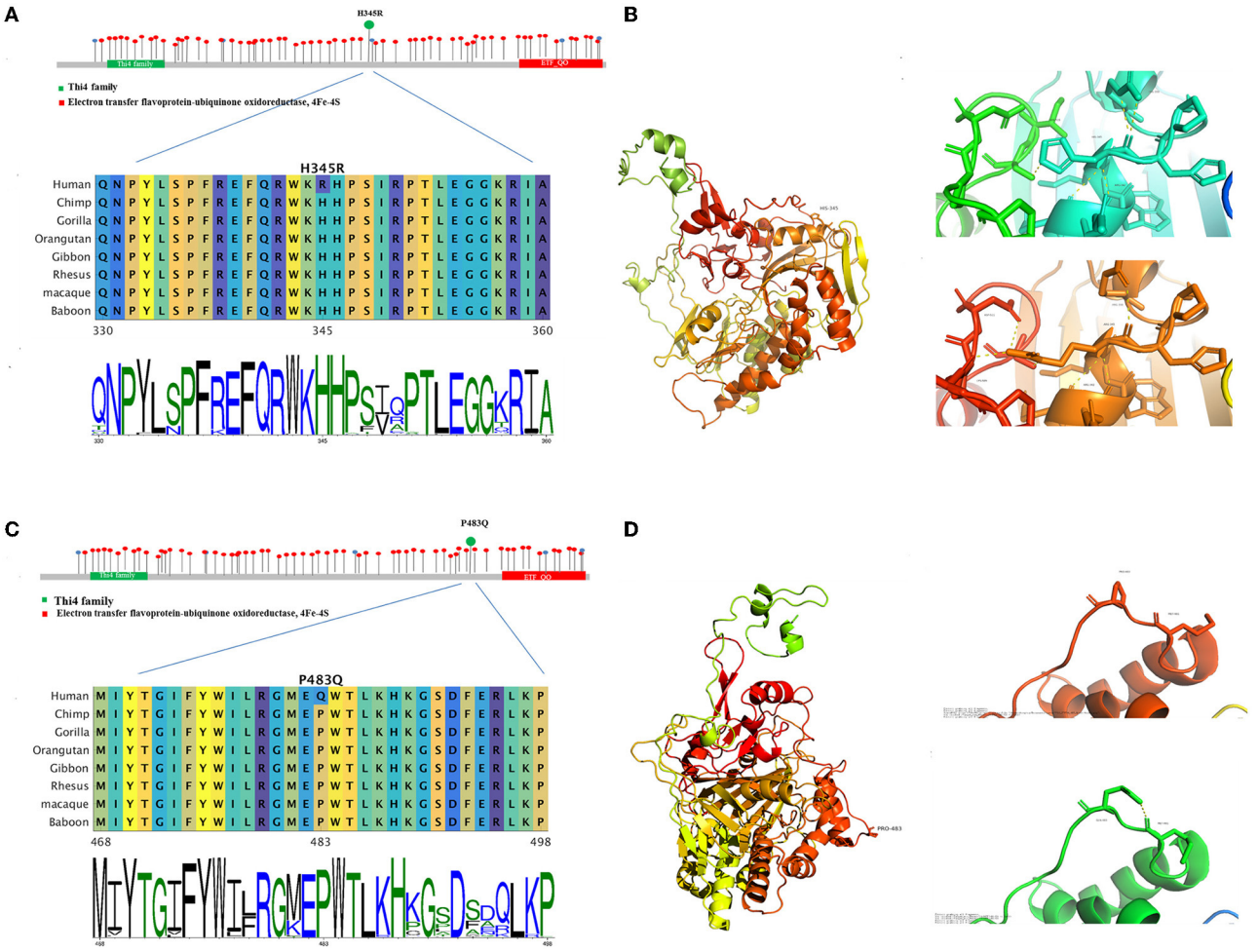

FIGURE 4
The bioinformatic analysis of the two mutations observed in the proband. Allelic spectrum and location by the functional domain of reported pathogenic mutations of the ETFDH gene were shown. Multiplex sequence alignment of the ETFDH protein across eight different species shows that H345 and P483 are highly conserved among species **(A, C)**. The structure **(B, D)** was built by means of homology modeling based on 2 gmh with Identity 95. The structure is modeled by RosettaCM. The partial 3D structures of both mutations revealed polar interaction changes in the ETFDH protein.

As a component of the electron-transfer system in mitochondria, the ETF:QO protein forms a short pathway to mediate ATP production by electron transfer from over nine mitochondrial flavin-containing dehydrogenases to the respiratory ubiquinone pool (24–26). It is composed of a 4Fe-4S cluster and one molecule of flavin adenine dinucleotide (FAD) binding domain and the UQ-binding domain (5). It has been reported that regions in the FAD domain could decrease protein stability. While the lack of part of the UQ-binding region and 4Fe4S cluster severely affected the *ETFDH*-mediate electron-transfer pathway (27). The two mutations c.1034A > G (p.H345R) on exon 9 and c.1448C>A (p.P483Q) detected in our study were, respectively, located in the FAD-binding domain and UQ-binding domain. For the first mutation, the structural analysis showed a polar change for the *ETFDH* protein and the second mutation revealed a polar change and stability alteration for this protein. As a previous study reported, *ETFDH* missense variants could cause the misfolding of related proteins, thus inducing structural instability in the protein (28, 29).

According to ACMG guidelines, the pieces of evidence for pathogenic or likely pathogenic variants are graded as four levels: very strong (PVS1), strong (PS1–4), moderate (PM1–6), and supporting (PP1–5) (19). The first mutation affects the amino acid residue 345 causing a substitution of histidine to arginine, putatively affecting the FAD-binding domain. The acid 345H is located in the FAD-binding domain and 15 DMs were located within 30 residues around this residue, indicating that this area is a mutational hot spot related to the disease (PM1). Furthermore, this mutation was absent in Exome Aggregation Consortium (ExAC) or 1,000 Genomes Project (PM2). The multiplex sequence alignment of the *ETFDH* protein across eight different species and 100 vertebrates showed that Histidine (H) at codon 345 in the *ETFDH* gene is highly conserved among species, which indicated that this mutation might have a relatively negative impact. The homology modeling of *ETFDH* protein showed that there were five polar interactions in the wild type, while the mutant H345R had six, which cause the protein structural change. Multiple lines of computational evidence were found to support the deleterious effect on the gene, including the conservation and evolutionary analysis, structural modeling, and computational prediction such as MutationTaster and SIFT (PP3). In this case, the patient's phenotype is highly specific for GA II (PP4). Based on these findings, it could

be classified as "likely pathogenic" according to ACMG (2 PM + 2 PP).

The second mutation affects the amino acid residue 483 causing proline to glutamine. The acid 483P is located in the UQ-binding domain and 19 DMs were located within 30 residues around P483, also indicating a mutational hot spot (PM1). This mutation was not found in ExAC or 1000 Genomes Project (PM2). In the ClinVar database, a different mutation c.1448C>T (p.P483L) at the same amino acid was reported to be "likely pathogenic" (PM5). Furthermore, the Proline (P) at codon 483 is also highly conserved among species. The homology modeling of the *ETFDH* protein showed that there was no polar interaction in the wild type, while the mutant P483Q had one, which could cause the protein structural change. Furthermore, we found that the 483rd Proline mutated to other 19 amino acids could cause a significant rise of the structural folding free energy, resulting in a decline of thermodynamic stability. The deleterious effect was supported by the conservation and evolutionary analysis, structural modeling, and computational prediction including MutationTaster, Polyphen2, and SIFT (PP3). Considering the patient's phenotype (PP4), this mutation should be classified as "likely pathogenic" (3 PM + 2 PP).

Similar to most patients with late-onset GA II, our patient showed a good response to riboflavin treatment. Riboflavin, commonly known as vitamin B2, is the precursor of flavin cofactors, which exists extensively in our daily food and is metabolized to (FMN) and FAD (30). Thus, the role of riboflavin in stabilizing certain forms of ETF: QO variant proteins is undoubted. The common view supports long-term, high-dose therapy of riboflavin. However, a recent study showed that most patients did not need continuous high-dose riboflavin treatment. Patients had a low risk of recurrence with intermittent and low-dose riboflavin treatment. Some patients even remained asymptomatic after discontinuation of riboflavin. A hypothesis is that riboflavin increased FAD-binding flavoproteins, which could release more FAD to the mitochondrial matrix during degradation, remaining a larger circulating FAD pool even after discontinuation of riboflavin (5). In addition to riboflavin treatment, a low-fat, low-protein, and high-carbohydrate diet should be provided to reduce metabolic disorders and ensure an adequate energy supply. L-carnitine and coenzyme Q10 can also be given to patients with carnitine deficiency and coenzyme Q10 deficiency, respectively (31). Since the high clinical heterogeneity and treatability of late-onset GA II, screening the hot spot mutations in Chinese patients clinically suspected of GA II could be beneficial for its early diagnosis and treatment, during which the WES strategy would be a great tool to identify novel pathogenic spots.

Conclusion

In summary, we described the phenotype and genotype of a patient with late-onset GA II. Two novel likely pathogenic mutations, c.1034A > G (p.H345R) and c.1448C>A (p.P483Q) mutations were identified, enriching the spectrum of *ETFDH* mutations associated with GA II. Due to its atypical symptoms and its good responsibility to riboflavin of late-onset mild GA II, the precise diagnosis is of great importance, and genetic testing would be useful to avoid misdiagnosis and missed diagnosis.

Data availability statement

The original contributions presented in the study are included in the article/supplementary material, further inquiries can be directed to the corresponding authors.

Ethics statement

The studies involving human participants were reviewed and approved by the First Affiliated Hospital of Soochow University. The patients/participants provided their written informed consent to participate in this study. Written informed consent was obtained from the individual(s) for the publication of any potentially identifiable images or data included in this article.

Author contributions

SZ and DD conducted the case series and drafted the manuscript. SZ, DD, and JJ participated in the collection and collation of clinical data. ML conducted the muscle biopsy and pathological analysis. LY and DD were responsible for data analysis of genetic testing and Sanger sequencing. LY and QF were involved in revising the manuscript critically and have given final approval for the version to be published. All authors have read and approved the manuscript.

Funding

This study was supported by the National Natural Science Foundation of China (82071300, 82001219) and the Gusu Health Talents Training Project (GSWS2020002).

Acknowledgments

The authors would like to thank all the subjects for their participation in this study.

Conflict of interest

The authors declare that the research was conducted in the absence of any commercial or financial relationships that could be construed as a potential conflict of interest.

Publisher's note

All claims expressed in this article are solely those of the authors and do not necessarily represent those of their affiliated organizations, or those of the publisher, the editors and the reviewers. Any product that may be evaluated in this article, or claim that may be made by its manufacturer, is not guaranteed or endorsed by the publisher.

References

1. Goodman SI, Binard RJ, Woontner MR, Frerman FE. Glutaric acidemia type II: gene structure and mutations of the electron transfer flavoprotein:ubiquinone oxidoreductase (ETF:QO) gene. *Mol Genet Metab.* (2002) 77:86–90. doi: 10.1016/S1096-7192(02)00138-5

2. Gregersen N, Kølvraa S, Rasmussen K, Christensen E, Brandt NJ, Ebbesen F, et al. Biochemical studies in a patient with defects in the metabolism of acyl-CoA and sarcosine: another possible case of glutaric aciduria type II. *J Inherit Metab Dis.* (1980) 3:67–72. doi: 10.1007/BF02312527

3. Swigonová Z, Mohsen A-W, Vockley J. Acyl-CoA dehydrogenases: dynamic history of protein family evolution. *J Mol Evol.* (2009) 69:176–93. doi: 10.1007/s00239-009-9263-0

4. Zhu M, Zhu X, Qi X, Weijiang D, Yu Y, Wan H, et al. Riboflavin-responsive multiple Acyl-CoA dehydrogenation deficiency in 13 cases, and a literature review in mainland Chinese patients. *J Hum Genet.* (2014) 59:256–61. doi: 10.1038/jhg.2014.10

5. Wen B, Tang S, Lv X, Li D, Xu J, Olsen RKJ, et al. Clinical, pathological and genetic features and follow-up of 110 patients with late-onset MADD: a single-center retrospective study. *Hum Mol Genet.* (2022) 31:1115–29. doi: 10.1093/hmg/ddab308

6. Goodman SI, Frerman FE. Glutaric acidaemia type II (multiple acyl-CoA dehydrogenation deficiency). *J Inherit Metab Dis.* (1984) 7:33–7. doi: 10.1007/BF03047371

7. Olsen RKJ, Andresen BS, Christensen E, Bross P, Skovby F, Gregersen N. Clear relationship between ETF/ETFDH genotype and phenotype in patients with multiple acyl-CoA dehydrogenation deficiency. *Hum Mutat.* (2003) 22:12–23. doi: 10.1002/humu.10226

8. Grünert SC. Clinical and genetical heterogeneity of late-onset multiple acyl-coenzyme A dehydrogenase deficiency. *Orphanet J Rare Dis.* (2014) 9:117. doi: 10.1186/s13023-014-0117-5

9. Yamada K, Kobayashi H, Bo R, Takahashi T, Purevsuren J, Hasegawa Y, et al. Clinical, biochemical and molecular investigation of adult-onset glutaric acidemia type II: characteristics in comparison with pediatric cases. *Brain Dev.* (2016) 38:293–301. doi: 10.1016/j.braindev.2015.08.011

10. Macchione F, Salviati L, Bordugo A, Vincenzi M, Camilot M, Teofoli F, et al. Multiple acyl-COA dehydrogenase deficiency in elderly carriers. *J Neurol.* (2020) 267:1414–9. doi: 10.1007/s00415-020-09729-z

11. Henriques BJ, Rodrigues JV, Olsen RK, Bross P, Gomes CM. Role of flavinylation in a mild variant of multiple acyl-CoA dehydrogenation deficiency: a molecular rationale for the effects of riboflavin supplementation. *J Biol Chem.* (2009) 284:4222–9. doi: 10.1074/jbc.M805719200

12. Köppel S, Gottschalk J, Hoffmann GF, Waterham HR, Blobel H, Kölker S. Late-onset multiple acyl-CoA dehydrogenase deficiency: a frequently missed diagnosis? *Neurology.* (2006) 67:1519. doi: 10.1212/01.wnl.0000240065.35635.a6

13. Lian L, Chen D, Li J, Tan S, Que J, Feng H, et al. Late-onset MADD in Yemen caused by a novel ETFDH mutation misdiagnosed as ADEM. *Mult Scler Relat Disord.* (2021) 48:102689. doi: 10.1016/j.msard.2020.102689

14. Cornelius N, Frerman FE, Corydon TJ, Palmfeldt J, Bross P, Gregersen N, et al. Molecular mechanisms of riboflavin responsiveness in patients with ETF-QO variations and multiple acyl-CoA dehydrogenation deficiency. *Hum Mol Genet.* (2012) 21:3435–48. doi: 10.1093/hmg/dds175

15. Rosa M, Pascarella A, Parenti G, Buono S, Romano A, Della Casa R, et al. Developmental evolution in a patient with multiple acyl-coenzymeA dehydrogenase deficiency under pharmacological treatment. *Eur J Paediatr Neurol.* (2012) 16:203–5. doi: 10.1016/j.ejpn.2011.07.003

16. Olsen RKJ, Olpin SE, Andresen BS, Miedzybrodzka ZH, Pourfarzam M, Merinero B, et al. ETFDH mutations as a major cause of riboflavin-responsive multiple acyl-CoA dehydrogenation deficiency. *Brain.* (2007) 130:2045–54. doi: 10.1093/brain/awm135

17. Wen B, Dai T, Li W, Zhao Y, Liu S, Zhang C, et al. Riboflavin-responsive lipid-storage myopathy caused by ETFDH gene mutations. *J Neurol Neurosurg Psychiatry.* (2010) 81:231–6. doi: 10.1136/jnnp.2009.176404

18. Missaglia S, Tavian D, Moro L, Angelini C. Characterization of two ETFDH mutations in a novel case of riboflavin-responsive multiple acyl-CoA dehydrogenase deficiency. *Lipids Health Dis.* (2018) 17:1–8. doi: 10.1186/s12944-018-0903-5

19. Richards S, Aziz N, Bale S, Bick D, Das S, Gastier-Foster J, et al. Standards and guidelines for the interpretation of sequence variants: a joint consensus recommendation of the American College of Medical Genetics and Genomics and the Association for Molecular Pathology. *Genet Med.* (2015) 17:405–24. doi: 10.1038/gim.2015.30

20. Xi J, Wen B, Lin J, Zhu W, Luo S, Zhao C, et al. Clinical features and ETFDH mutation spectrum in a cohort of 90 Chinese patients with late-onset multiple acyl-CoA dehydrogenase deficiency. *J Inherit Metab Dis.* (2014) 37:399–404. doi: 10.1007/s10545-013-9671-6

21. Wang Z-Q, Chen X-J, Murong S-X, Wang N. Wu Z-Y. Molecular analysis of 51 unrelated pedigrees with late-onset multiple acyl-CoA dehydrogenation deficiency (MADD) in southern China confirmed the most common ETFDH mutation and high carrier frequency of c250G. *A J Mol Med.* (2011) 89:569–76. doi: 10.1007/s00109-011-0725-7

22. Missaglia S, Tavian D, Angelini C, ETF. dehydrogenase advances in molecular genetics and impact on treatment. *Crit Rev Biochem Mol Biol.* (2021) 56:360–72. doi: 10.1080/10409238.2021.1908952

23. Angelini C, Burlina A, Blau N, Ferreira CR. Clinical and biochemical footprints of inherited metabolic disorders: X. Metabolic myopathies. *Mol Genet Metab.* (2022) 137:213–22. doi: 10.1016/j.ymgme.2022.09.004

24. Schwarz JM, Cooper DN, Schuelke M, Seelow D. MutationTaster2: mutation prediction for the deep-sequencing age. *Nat Methods.* (2014) 11:361–2. doi: 10.1038/nmeth.2890

25. El-Gebali S, Mistry J, Bateman A, Eddy SR, Luciani A, Potter SC, et al. The Pfam protein families database in 2019. *Nucleic Acids Res.* (2019) 47:D427–D32. doi: 10.1093/nar/gky995

26. Rohl CA, Strauss CEM, Misura KMS, Baker D. Protein structure prediction using Rosetta. *Methods Enzymol.* (2004) 383:66–93. doi: 10.1016/S0076-6879(04)83004-0

27. Er T-K, Chen C-C, Liu Y-Y, Chang H-C, Chien Y-H, Chang J-G, et al. Computational analysis of a novel mutation in ETFDH gene highlights its long-range effects on the FAD-binding motif. *BMC Struct Biol.* (2011) 11:43. doi: 10.1186/1472-6807-11-43

28. Sato K, Nishina Y, Shiga K. In vitro refolding and unfolding of subunits of electron-transferring flavoprotein: characterization of the folding intermediates and the effects of FAD and AMP on the folding reaction. *J Biochem.* (1996) 120:276–85. doi: 10.1093/oxfordjournals.jbchem.a021410

29. Gregersen N, Bross P, Vang S, Christensen JH. Protein misfolding and human disease. *Annu Rev Genomics Hum Genet.* (2006) 7:103–24. doi: 10.1146/annurev.genom.7.080505.115737

30. Henriques BJ, Olsen RK, Bross P, Gomes CM. Emerging roles for riboflavin in functional rescue of mitochondrial β-oxidation flavoenzymes. *Curr Med Chem.* (2010) 17:3842–54. doi: 10.2174/092986710793205462

31. Li Q, Yang C, Feng L, Zhao Y, Su Y, Liu H, et al. Glutaric acidemia, pathogenesis and nutritional therapy. *Front Nutr.* (2021) 8:704984. doi: 10.3389/fnut.2021.704984

frontiers | Frontiers in Neurology

TYPE Systematic Review
PUBLISHED 01 February 2023
DOI 10.3389/fneur.2023.1107474

Check for updates

OPEN ACCESS

EDITED BY
Giovanni Meola,
University of Milan, Italy

REVIEWED BY
Tracey Anne Willis,
Robert Jones and Agnes Hunt Orthopaedic Hospital NHS Trust, United Kingdom
Delia Gagliardi,
University of Milan, Italy

*CORRESPONDENCE
Jaffer Shah
✉ jaffer.shah@kateb.edu.af

SPECIALTY SECTION
This article was submitted to Neuromuscular Disorders and Peripheral Neuropathies, a section of the journal Frontiers in Neurology

RECEIVED 24 November 2022
ACCEPTED 10 January 2023
PUBLISHED 01 February 2023

CITATION
Elhalag RH, Motawea KR, Talat NE, Rouzan SS and Shah J (2023) Efficacy of vamorolone in treatment of Duchene muscle dystrophy. A meta-analysis. *Front. Neurol.* 14:1107474. doi: 10.3389/fneur.2023.1107474

COPYRIGHT
© 2023 Elhalag, Motawea, Talat, Rouzan and Shah. This is an open-access article distributed under the terms of the Creative Commons Attribution License (CC BY). The use, distribution or reproduction in other forums is permitted, provided the original author(s) and the copyright owner(s) are credited and that the original publication in this journal is cited, in accordance with accepted academic practice. No use, distribution or reproduction is permitted which does not comply with these terms.

Efficacy of vamorolone in treatment of Duchene muscle dystrophy. A meta-analysis

Rowan H. Elhalag[1], Karam R. Motawea[1], Nesreen Elsayed Talat[1], Samah S. Rouzan[1] and Jaffer Shah[2]*

[1]Faculty of Medicine, Alexandria University, Alexandria, Egypt, [2]New York State Department of Health, New York, NY, United States

Background and aim: Recent studies evaluated the role of vamorolone in treating Duchenne muscular dystrophy (DMD), so we aimed in our Meta-analysis to assess the efficacy of vamorolone in comparison with placebo and corticosteroids for treating DMD patients.

Methods: We searched PubMed, Web of Science, Scopus, and Cochrane library databases. We included any randomized control trials and controlled observational studies that investigated the role of vamorolone in treating DMD patients. We used RevMan software, version 5.4. to perform our meta-analysis.

Results: After a search of the literature, 4 studies were included in the meta-analysis; the total number of patients included in the study is 277 patients, 125 patients in the vamorolone group, 106 in the glucocorticoids group, and 46 in placebo (steroid naïve) group. The pooled analysis showed a statistically significant association between the vamorolone group and increased TTSTAND velocity, TTRW velocity and TTCLIMB velocity compared with the placebo group (MD = 0.04, 95% CI = 0.02–0.07, $p = 0.002$), (MD = 0.24, 95% CI = 0.11–0.37, $p = 0.0003$), and (MD = 0.06, 95% CI = 0.05–0.06, $p < 0.00001$), respectively. Also, the analysis showed a statistically significant association between vamorolone and increased TTRW velocity and increased Height percentile for age compared with the glucocorticoid group (MD = −0.14, 95% CI = −0.26 to −0.01, $p = 0.03$) and (MD = 17.82, 95% CI = 3.89–31.75, $p = 0.01$), respectively.

Conclusion: Our study revealed a significant association between vamorolone and increased TTSTAND velocity, TTRW velocity, and TTCLIMB velocity compared with the placebo (steroid naïve), also showed a statistically significant association between increased TTRW velocity and increased Height percentile for age compared with the glucocorticoid that enhances the privilege of vamorolone over glucocorticoid in treating DMD patients. More multicenter randomized studies are needed to support our results.

KEYWORDS

Duchene muscular dystrophy (DMD), vamorolone, neuromuscular, glucocorticoids, steroid naïve

Introduction

Duchenne muscular dystrophy (DMD), an X-linked progressive neuromuscular condition, has reported a worldwide incidence of 1 in 3,500 to 1 in 5,000 live male births which equals 200 per million births, the onset appears in early childhood and ends with death in late teens (1). It is caused by mutations in DMD (encoding dystrophin) that prevent the production of the muscle isoform of dystrophin (Dp427m) (2). DMD is a severe, progressive muscle-wasting disease with early symptoms that includes difficulties in climbing stairs, a waddling gate, and

repeated falls; patients first develop these symptoms between 2 and 3 years old. Most patients become wheelchair-dependent around the age of 10–12 years and require assisted ventilation at ∼20 years of age. With optimal care, most DMD patients die between the age of 20 and 40 years from cardiac and/or respiratory failure (3).

Current medical treatment focuses on symptoms linked to the degeneration-regeneration cycle. Corticosteroids are considered the gold standard therapy for DMD and potentially effective in symptom reduction, while the exact mechanism is unknown, corticosteroids are supposed to predominantly reduce inflammation (4, 5). A systematic review revealed that prednisone enhances strength and pulmonary function in patients with DMD. Additionally, prednisone can improve motor function, postpone cardiomyopathy, and decrease the need for scoliosis surgery. Additional corticosteroids might also be beneficial in DMD; Deflazacort has the same effectiveness as prednisone with the distinct benefit of increasing survival at 5–15 years of follow-up (6–8). Unfortunately, glucocorticoid therapy is attributed to side effects like immunosuppression, muscle weakness, and Cushingoid look, as well as long-term harmful sequelae like osteopenia and stunted growth (9). Several corticosteroids, such as prednisone and deflazacort, act as agonists of the mineralocorticoid receptor, raising blood pressure, and volume *via* the renin-angiotensin system. In contrast, vamorolone is a strong antagonist of the mineralocorticoid receptor, similar to eplerenone and spironolactone in activity (9).

Vamorolone has a different mechanism of action from traditional corticosteroid anti-inflammatory medications as it holds the distinct NF-B inhibitory (anti-inflammatory) activities while losing the gene transcriptional activities connected to glucocorticoid response element binding and activation. It also has powerful antagonist activity for the mineralocorticoid receptor (5, 10–12). Vamorolone and corticosteroids both suppress the NF-B-related cell damage pathways, which are known to be one of the initial molecular disorders of dystrophin-deficient muscle in (DMD) patients (13). Previous studies (14–16) showed that vamorolone may be a safer alternative than prednisone as fewer physician-reported adverse effects (AEs) occurred with vamorolone than have been reported for treatment with prednisone and deflazacort, moreover that vamorolone therapy did not result in the growth stunting that is common with these corticosteroids indicating that vamorolone might be a suitable option for treating DMD. And to verify these findings, we performed a meta-analysis to determine whether vamorolone is more effective than corticosteroids.

Methods

Preferred Reporting Items for Systematic Reviews and Meta-Analyses (PRISMA) guidelines and the Cochrane handbook were followed to perform this meta-analysis (17).

Study design

This is a meta-analysis study that aimed to investigate the efficacy of vamorolone vs. placebo (steroid naïve) and corticosteroids for the treatment of DMD patients.

Search strategy

(Vamorolone) AND (Glucocorticoids OR Prednisone OR placebo) AND (Duchenne muscular dystrophy OR Becker's Muscular Dystrophy OR Cardiomyopathy, Dilated, X-Linked OR Childhood Pseudo hypertrophic Muscular Dystrophy), we looked for relevant randomized control trials and observational studies in PubMed, Web of Science, Scopus and Cochrane library databases from inception to 17 November 2022.

Eligibility criteria

Any randomized control trials and controlled observational studies such as Cross-sectional, prospective, or retrospective cohort and case-control studies that investigated the efficacy of vamorolone vs. placebo (steroid naïve) and corticosteroids for the treatment of DMD patients, so the PICO will be:

1- Population: DMD patient.
2- Intervention: vamorolone.
3- Control: placebo (steroid naïve) or corticosteroids.
4- Outcome: TTSTAND velocity, TTRW velocity, TTCLIMB velocity, Height percentile for age, and BMI Z score.

Exclusion criteria

We exclude animal studies, case reports, case series, editorials, and reviews.

Study selection process

Two independent authors (RHE and KRM) revised the titles and/or abstracts of the searched papers to determine suitable studies. Then, the two authors revised the full texts of the retrieved reports independently. Any conflicts between authors were solved by the first author.

Data extraction and management

Two independent authors used an excel sheet to extract the following data: the first author's name, year of publication, age, sex, study design, country of the study, number of patients, Outcome measurements: TTSTAND velocity, TTRW velocity, TTCLIMB velocity, Height percentile for age and BMI Z score in Vamorolone vs. Placebo (steroid naïve) and Vamorolone vs. Glucocorticoids. Two authors performed data extraction of outcomes and any conflicts were solved by the first author (RHE).

Quality assessment

Newcastle Ottawa scale tool was used to assess the quality because most of the included studies were non randomized studies; each study was given a score and ranked as good, fair, or poor quality.

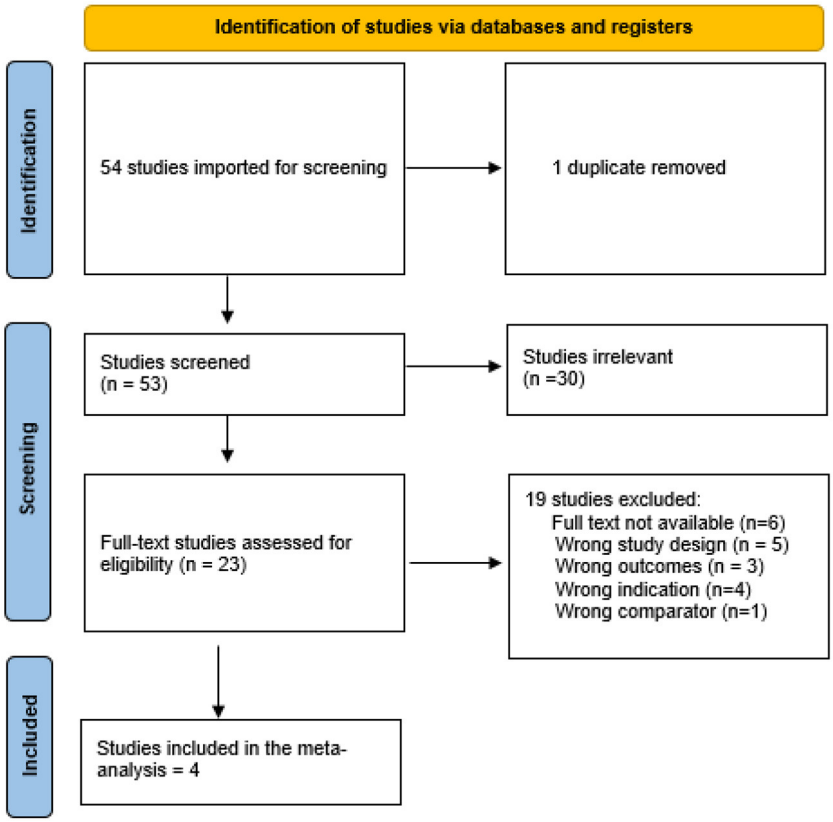

FIGURE 1
Prisma.

Data synthesis

Data were analyzed using RevMan software, version 5.4. Sensitivity analysis (leave-one-out test) was used. Continuous data were presented as mean difference (MD) with a 95% confidence interval (CI). If no heterogeneity was observed, results were presented in a fixed effect model and a random effect model was used if significant heterogeneity was observed. Results were considered significant if the $p < 0.05$.

Results

Summary of studies

After a search of the literature, 54 studies resulted, and then became 53 were eligible for title and abstract screening after duplicate removal. Of the 53, 30 were irrelevant and 23 studies were eligible for full-text screening. Finally, four studies were included in the meta-analysis after the full-text screening, as shown in the PRISMA in Figure 1.

The overall quality was good in the four included studies, as shown in Table 1.

The total number of patients included in the study is 277 patients, 125 patients in the vamorolone group, 106 in the glucocorticoids group, and 46 in the placebo (steroid naïve) group. Other baseline data are shown in Table 2.

Outcomes

Vamorolone vs. placebo

TTSTAND velocity

The pooled analysis showed a statistically significant association between the vamorolone group and increased TTSTAND velocity compared with the placebo group (MD = 0.04, 95% CI = 0.02–0.07, $p = 0.002$). We observed no significant heterogeneity between the two studies ($P = 0.79$, $I^2 = 0\%$, Figure 2).

TTRW velocity

The pooled analysis showed a statistically significant association between the vamorolone group and increased TTRW velocity compared with the placebo group (MD = 0.24, 95% CI = 0.11–0.37, $p = 0.0003$). We observed no significant heterogeneity between the two studies ($P = 0.35$, $I^2 = 0\%$, Figure 3).

TTCLIMB velocity

The pooled analysis showed a statistically significant association between the vamorolone group and increased TTCLIMB velocity compared with the placebo group (MD = 0.06, 95% CI = 0.05–0.06, $p < 0.00001$). We observed no significant heterogeneity between the two studies ($P = 0.38$, $I^2 = 0\%$, Figure 4).

10.3389/fneur.2023.1107474

TABLE 1 Quality assessment.

ID	Selection				Comparability	Exposure			Total point	AHRQ Standards
	(1) Representativeness	(2) Selection of the non-exposed cohort	(3) Ascertainment of exposure	(4) Demonstration that outcome of interest was not present at start of study	(1) Comparability of cohorts	(1) Assessment of outcome	(2) Was follow-up long enough for outcomes to occur	(3) Adequacy of follow up of cohorts		
Smith et al. [16]	1	1	1	0	2	1	1	1	8	Good
Mah et al. [15]	1	1	1	0	1	1	1	1	7	Good
Hoffman et al. [29]	1	1	1	0	2	1	1	1	8	Good
Guglieri et al. [14]	1	1	1	0	2	1	1	1	8	Good

Vamorolone vs. glucocorticoids

TTSTAND velocity

The pooled analysis showed no statistically significant difference between the vamorolone group and the Glucocorticoid group (MD = 0.00, 95% CI = −0.08–0.09, $p = 0.94$). We observed a significant heterogeneity between the two studies ($P = 0.02$, $I^2 = 83\%$, Figure 5).

TTRW velocity

The pooled analysis showed a statistically significant association between the vamorolone group and increased TTRW velocity compared with the glucocorticoid group (MD = −0.14, 95% CI = −0.26 to −0.01, $p = 0.03$). We observed no significant heterogeneity between the two studies ($P = 0.26$, $I^2 = 20\%$, Figure 6).

TTCLIMB velocity

The pooled analysis showed no statistically significant difference between the vamorolone group and the glucocorticoid group (MD = −0.03, 95% CI = −0.06–0.01, $p = 0.12$). We observed no significant heterogeneity between the two studies ($P = 0.36$, $I^2 = 0\%$, Figure 7).

Height percentile for age

The pooled analysis showed no statistically significant difference between the vamorolone group and the glucocorticoid group (MD = −6.45, 95% CI = −61.82–48.92, $p = 0.82$). We observed a significant heterogeneity among the studies ($P < 0.00001$, $I^2 = 99\%$). It was solved by leave-one-out test by removing ((14); $P = 0.21$, $I^2 = 35\%$), and the analysis showed a statistically significant association between the vamorolone group and increased height percentile for age compared with the glucocorticoid group (MD = 17.82, 95% CI = 3.89–31.75, $p = 0.01$, Figure 8).

BMI *Z* score

The pooled analysis showed no statistically significant difference between the vamorolone group and the glucocorticoids group (MD = 0.21, 95% CI = −0.22–0.64, $p = 0.33$). We observed a significant heterogeneity among studies ($P = 0.002$, $I^2 = 80\%$). It was solved by leave-one-out test by removing ((15); $P = 0.19$, $I^2 = 39\%$), and the analysis showed no statistically significant difference between the vamorolone group and glucocorticoid group (MD = −0.01, 95% CI = −0.29–0.30, $p = 0.97$, Figure 9).

Discussion

The pooled analysis revealed a statistically significant association between the vamorolone group and increased TTSTAND velocity, increased TTRW velocity, and increased TTCLIMB velocity compared with the placebo group. Similarly, the pooled analysis showed a statistically significant association between the vamorolone group and increased TTRW velocity compared with the glucocorticoid group. However, the pooled analysis showed no statistically significant difference between the vamorolone group and the glucocorticoid group regarding TTSTAND velocity and TTCLIMB velocity. Also, the analysis showed a statistically significant association between the vamorolone group and increased

TABLE 2 Baseline characteristics.

		Hoffman et al. (29)	Smith et al. (16)	Mah et al. (15)	Guglieri et al. (14)
Number of patients in each group	Vamorolone	48	23	23	58
	GC	14	80	185	31
	Placebo or GC naivee	31	19	N/A	28
Age (years)	Vamorolone	4.9 ± 0.9	5.2 ± 0.90	5.83 ± 0.88	5.4 ± 0.9
	GC	5.7 ± 0.7	5.9 ± 0.65	6.03 ± 0.8	5.5 ± 0.9
	Placebo or GC naivee	4.9 ± 0.8	5.03 ± 0.55	N/A	5.4 ± 0.8
Weight in kg	Vamorolone	N/A	19.5 ± 2.5	21.98 ± 3.78	19 ± 3.5
	GC		20.53 ± 3.4	20.35 ± 3.55	21 ± 3
	Placebo or GC naivee		18.3 ± 2	N/A	20 ± 3
Height in cm	Vamorolone		107 ± 6.8	111.80 ± 6.94	26.6 ± 27.14
	GC		109.4 ± 5.8	109.86 ± 6.86	37 ± 29
	Placebo or GC naivee		105.4 ± 5.1	N/A	33 ± 29
BMI (kg/m^2)	Vamorolone	16.9 ± 1.2	17 ± 0.9	17.68 ± 1.23	16.4 ± 1.3
	GC	16.3 ± 1.7	17.1 ± 1.9	16.68 ± 1.55	16.8 ± 1.3
	Placebo or GC naivee	15.2 ± 1.6	16.4 ± 0.9	N/A	16.8 ± 1.1
TTSTAND	Vamorolone	M = 0.0452 (SD = 0.053)	M = 0.241 (SD = 0.076)	M = 0.2 (SD = 0.13)	M = 0.0448 (SD = 0.0804)
	GC	M = 0.01 (SD = 0.068)		M = 0.25 (SD = 0.13)	
	Placebo or GC naivee		M = 0.205 (SD = 0.102)		M = −0.01 (SD = 0.06)
TTRW	Vamorolone	M = 0.1604 (SD = 0.2508)	M = 2.061 (SD = 0.347)	M = 1.87 (SD = 0.63)	M = 0.2212 (SD = 0.2612)
	GC	M = −0.01 (SD = 0.256)		M = 1.89 (SD = 0.71)	
	Placebo or GC naivee		M = 1.717 (SD = 0.46)		M = 0.02 (SD = 0.33)
TTCLIMB	Vamorolone	M = 0.0448 (SD = 0.0759)	M = 0.331 (SD = 0.127)	M = 0.32 (SD = 0.19)	M = 0.0619 (SD = 0.0198)
	GC	M = 0.01 (SD = 0.062)		M = 0.33 (SD = 0.18)	
	Placebo or GC naivee		M = 0.242 (SD = 0.108)		M = 0.0056 (SD = −0.0078)
Height percentile for age	Vamorolone		M = 35.24 (SD = 29.82)	M = 37.03 (SD = 31.14)	M = 2.026 (SD = 8.003)
	GC		M = 26.14 (SD = 24.21)	M = 13.42 (SD = 18.62)	M = −1.88 (SD = 8.81)
	Placebo or GC naivee		M = 27.16 (SD = 21.17)		
BMI *z* score	Vamorolone	M = 0.2582 (SD = 0.5576)	M = 1.46 (SD = 0.62)	M = 1.52 (SD = 0.66)	M = 0.46 (SD = 0.54)
	GC	M = 0.543 (SD = 0.6646)	M = 1.068 (SD = 1.05)	M = 0.79 (SD = 1.11)	M = 0.41 (SD = 0.51)
	Placebo or GC naivee		M = 0.36 (SD = 0.77)		

height percentile for age compared with the glucocorticoid group. Additionally, the pooled analysis showed no statistically significant difference between the vamorolone group and glucocorticoid group regarding BMIZ score.

One of the initial molecular pathologies of dystrophin-deficient muscle in Duchenne muscular dystrophy (DMD) patients is known to be the activation of NFκB-related cell damage pathways, and vamorolone and corticosteroids both suppress these pathways (13). Numerous inflammatory genes are regulated by NFκB in immune cells as well as muscle fibers (18–21) and the invasion and activation of these cells can result in the death of muscle cells (22, 23). Vamorolone is a first-in-class steroidal anti-inflammatory drug (24), it lacks an 11-carbon oxygen group (hydroxyl or carbonyl), one of five molecular interaction sites with the glucocorticoid receptor, which sets it apart from the other 33 medications in the corticosteroid class (25, 26). Vamorolone retains the anti-inflammatory properties of steroid medications while lacking its side effects (AEs), such as growth retardation, bone morbidities, and muscular atrophy (25, 27). Vamorolone inhibiting NFκB-associated proinflammatory signals in a ligand/receptor monomeric state rather than the more conventional molecular models of ligand/receptor dimeric complexes is consistent with the retention of anti-inflammatory activity and absence of side effects in preclinical models (28). Numerous corticosteroids, such as prednisone and deflazacort, act as agonists of the mineralocorticoid receptor, raising blood pressure and volume *via* the renin-angiotensin system. In contrast, vamorolone has the same activity as eplerenone and spironolactone as a powerful antagonist of the mineralocorticoid receptor (11). Vamorolone

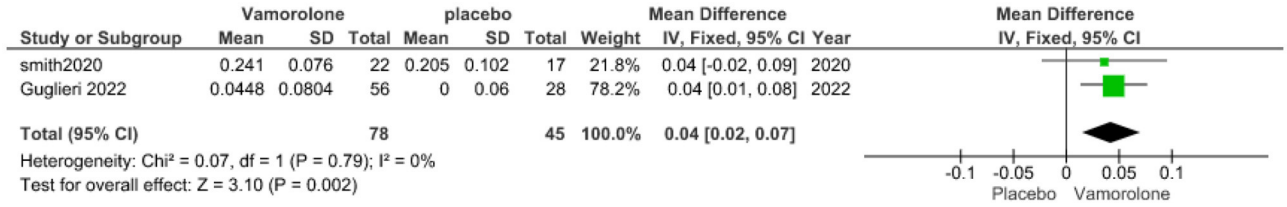

FIGURE 2
TTSTAND outcome vamorolone vs. placebo.

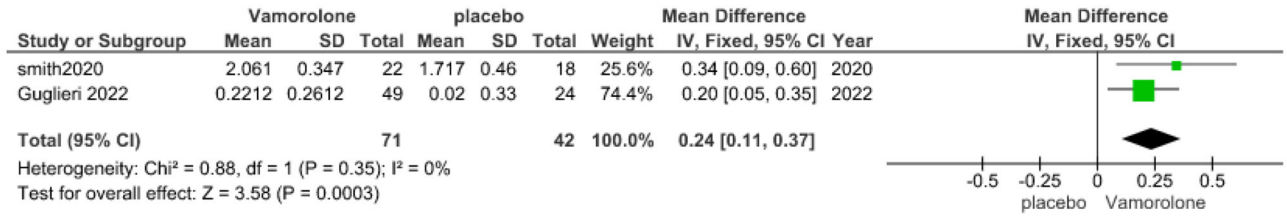

FIGURE 3
TTRW outcome vamorolone vs. placebo.

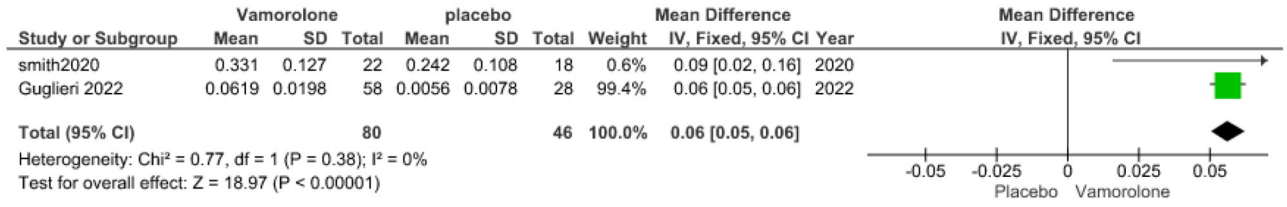

FIGURE 4
TTCLIMB vamorolone vs. placebo.

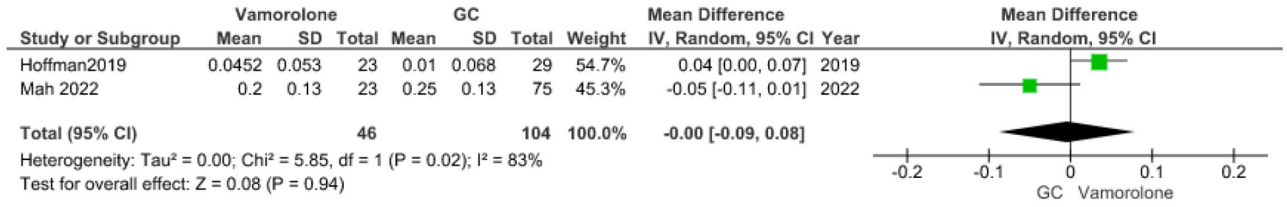

FIGURE 5
TTSTAND outcome vamorolone vs. glucocorticoids.

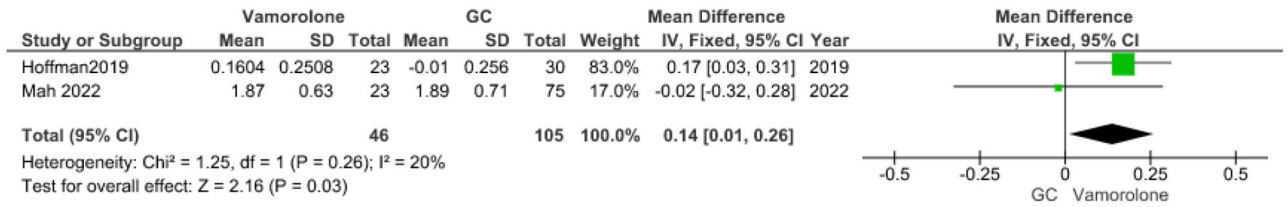

FIGURE 6
TTRW outcome vamorolone vs. glucocorticoids.

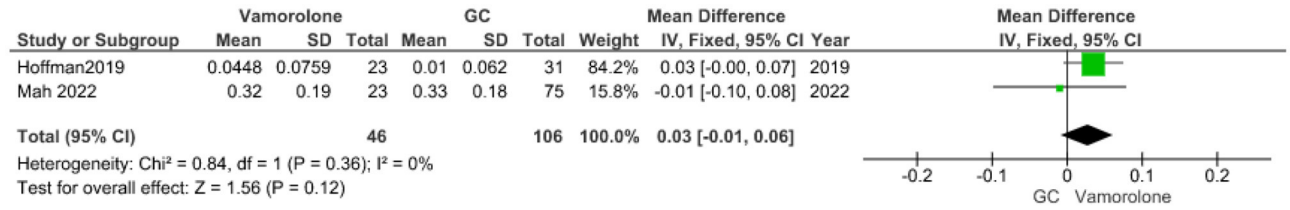

FIGURE 7
TTCLIMB outcome vamorolone vs. glucocorticoids.

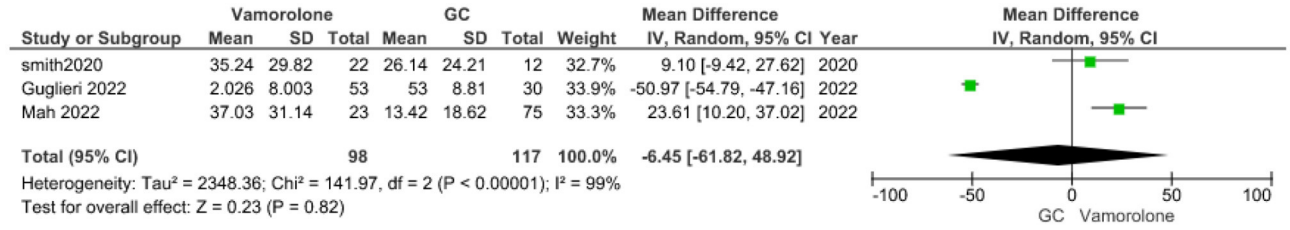

FIGURE 8
Height percentile for age outcome vamorolone vs. glucocorticoids.

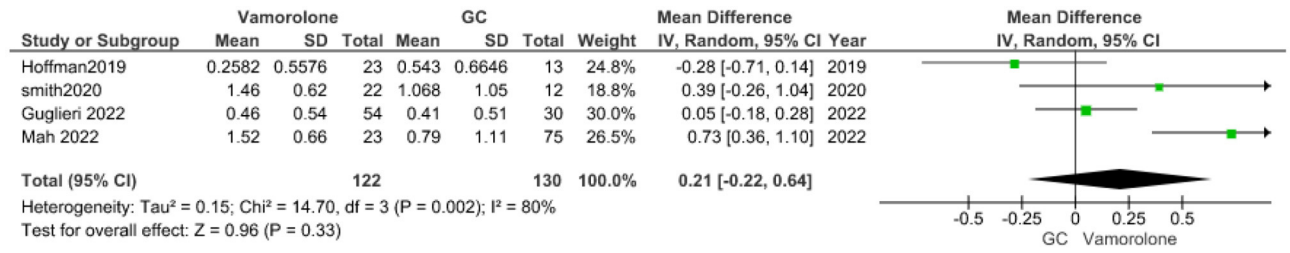

FIGURE 9
BMI z score outcome vamorolone vs. glucocorticoids.

optimizes traditional steroidal anti-inflammatory activities: retains the distinct NFκB inhibitory (anti-inflammatory) activities while losing the gene transcriptional activities connected to glucocorticoid response element binding and activation, is a powerful antagonist for the mineralocorticoid receptor, and has superior membrane stabilization properties (5, 10–12).

Our findings agree with the findings of Hoffman et al. (29) who concluded that oral administration of vamorolone in individuals with DMD over the course of a 24-week therapy term was safe, effective, and well-tolerated at all tested doses. When they used vamorolone at doses of 2.0 and 6.0 mg/kg/d for a period of 24 weeks, the drug met the primary efficacy outcome of improved muscle function. They also discovered that the majority of the negative effects of glucocorticoids are not present in vamorolone including bone turnover and insulin resistance improvement and less weight gain. Serum osteocalcin is a reliable indicator of bone production and turnover in children that is essential to growth (30). Improvements in bone density and bone geometry have been demonstrated to be predicted by increases in serum osteocalcin (31). Prednisone and deflazacort both dramatically lower serum osteocalcin levels (32, 33). Vamorolone, on the other hand, boosted osteocalcin levels, indicating a reduction of deleterious bone effects (29). The lack of deleterious alterations in bone turnover indicators in DMD patients receiving vamorolone treatment raises the possibility of losing the bone morbidities usually associated with glucocorticoids (29). They also found evidence of adrenal suppression (29).

Our results also support those of Guglieri et al. (14), who discovered that vamorolone is effective and safe in the treatment of boys with DMD at a wide dose range (2–6 mg/kg per day) and throughout a 24-week course of therapy. They also discovered that vamorolone is a safer alternative than prednisone in this disease as it is a dissociative steroid, which means that it isolates safety issues (growth deceleration, bone biomarkers abnormalities) from efficacy (improving motor results in DMD). Their results confirmed earlier research that showed vamorolone-treated DMD youngsters had normal development trajectories across 18 months (16) and 30 months (15). Prednisone medication, on the other hand, reduced development trajectories in this 24-week experiment, supporting numerous studies of corticosteroid treatment in DMD (15, 34, 35). Furthermore, neither of the vamorolone dose groups showed mean reductions in any of the bone turnover markers, supporting the enhanced safety profile

of vamorolone on bone health. The favorable bone biomarker profile observed in the vamorolone-treated groups compared with corticosteroids is explained by vamorolone not being a substrate for 11β-hydroxysteroid dehydrogenase enzymes which are necessary for corticosteroid-induced bone morbidities in mice, as it lacks the 11βmoiety acted upon by these enzymes (36, 37). Additionally, Guglieri et al. incidentally found an unexpectedly high incidence of adrenal insufficiency at baseline in boys with DMD in both vamorolone-treated and corticosteroids-treated groups using both ACTH-stimulation and morning cortisol measurements, as corticosteroid medications (including endogenous cortisol) potently, widely, and rapidly block the hypothalamic-pituitary-adrenal (HPA) axis and long-term use can result in adrenal insufficiency (38), this finding with the vamorolone-treated group requires additional investigation.

Similar to our findings, Mah et al. (15) discovered that among boys with DMD who were 4–7 years old at enrolment, vamorolone therapy was not connected to a change in TTSTAND velocity from baseline to 30 months. However, long-term vamorolone therapy at doses up to 6.0 mg/kg/d showed to be safe and effective based on clinical and laboratory outcomes. Additionally, over a 30 month treatment period, subjects receiving larger doses of vamorolone (i.e., ≥2 mg/kg/d) continued to show improvement in their motor function as measured by the TTCLIMB, TTRW, NSAA, and 6MWT distance. They also discovered that boys treated with vamorolone experienced significantly less bone age delay in relation to chronological age than boys treated with corticosteroid therapy. Additionally, unlike traditional corticosteroid medication, vamorolone does not have the same association with insulin resistance; however, long-term vamorolone therapy may be linked to adrenal suppression (16). Similarly, Smith et al. (16) discovered that over the course of the 18 month treatment period, boys receiving vamorolone showed improvements from baseline in all five motor evaluations (TTSTAND, TTRW, TTCLIMB, NSAA, and 6MWT). Contrary to those who received corticosteroids, those who received vamorolone did not show any signs of growth stunting. Moreover, comparing published trials of deflazacort- and prednisone-treated DMD patients, doctors found that participants receiving vamorolone experienced fewer other corticosteroid-related safety issues, such as weight gain, Cushingoid appearance, behavior change (mood disturbance), and hirsutism.

Future implications

Our analysis results revealed that vamorolone treatment was associated with improvements in some motor outcomes like TTRW velocity and increased height percentile for age compared with the glucocorticoid group. Our analysis suggests that vamorolone can be used in the treatment of patients with DMD as it is more effective and safer than corticosteroids.

Strengths and limitations

The overall quality was good in all of the studies included in our analysis. The short study period and small sample size are limitations of our analysis. In addition, most of our studies were clinical trials but not randomized. Therefore, to support our findings and further evaluate the efficacy and safety of vamorolone treatment in DMD patients, prospective randomized clinical trial studies with larger sample sizes and longer follow-up durations are required.

Conclusion

Our pooled analysis revealed a statistically significant association between the vamorolone group and increased TTSTAND velocity, increased TTRW velocity, and increased TTCLIMB velocity compared with the placebo group. Similarly, the pooled analysis showed a statistically significant association between the vamorolone group and increased TTRW velocity, and increased height percentile for age compared with the glucocorticoid group. However, the pooled analysis showed no statistically significant difference between the vamorolone group and the glucocorticoid group regarding TTSTAND velocity, TTCLIMB velocity, and BMIZ score. Therefore, we suggest that vamorolone can be used in treating patients with DMD. More randomized clinical trials are needed to support our findings.

Data availability statement

The original contributions presented in the study are included in the article/supplementary material, further inquiries can be directed to the corresponding author.

Author contributions

RE: idea-screening-data extraction and analysis. KM: screening-quality assessment and writing. NT: data extraction and writing. SR: writing. JS: screening and reviewing. All authors contributed to the article and approved the submitted version.

Conflict of interest

The authors declare that the research was conducted in the absence of any commercial or financial relationships that could be construed as a potential conflict of interest.

Publisher's note

All claims expressed in this article are solely those of the authors and do not necessarily represent those of their affiliated organizations, or those of the publisher, the editors and the reviewers. Any product that may be evaluated in this article, or claim that may be made by its manufacturer, is not guaranteed or endorsed by the publisher.

References

1. Yiu EM, Kornberg AJ. Duchenne muscular dystrophy. *J. Paediatr Child Health.* (2015) 51:759–64. doi: 10.1111/jpc.12868

2. Aartsma-Rus A, Van Deutekom JC, Fokkema IF, Van Ommen GJB, Den Dunnen JT. Entries in the Leiden Duchenne muscular dystrophy mutation database: an overview of mutation types and paradoxical cases that confirm the reading-frame rule. *Muscle Nerve.* (2006) 34:135–44. doi: 10.1002/mus.20586

3. Mercuri E, Bönnemann CG, Muntoni F. Muscular dystrophies. *Lancet.* (2019) 394:2025–38. doi: 10.1016/S0140-6736(19)32910-1

4. Buyse GM, Goemans N, Van Den Hauwe M, Meier T. Effects of glucocorticoids and idebenone on respiratory function in patients with duchenne muscular dystrophy. *Pediatr Pulmonol.* (2013) 48:912–20. doi: 10.1002/ppul.22688

5. Heier CR, Damsker JM, Yu Q, Dillingham BC, Huynh T, Van der Meulen JH, et al. VBP15, a novel anti-inflammatory and membrane-stabilizer, improves muscular dystrophy without side effects. *EMBO Mol Med.* (2013) 5:1569–85. doi: 10.1002/emmm.201302621

6. Biggar W, Harris V, Eliasoph L, Alman B. Long-term benefits of deflazacort treatment for boys with Duchenne muscular dystrophy in their second decade. *Neuromuscul Disord.* (2006) 16:249–55. doi: 10.1016/j.nmd.2006.01.010

7. Lebel DE, Corston JA, McAdam LC, Biggar WD, Alman BA. Glucocorticoid treatment for the prevention of scoliosis in children with Duchenne muscular dystrophy: long-term follow-up. *JBJS.* (2013) 95:1057–61. doi: 10.2106/JBJS.L.01577

8. Schram G, Fournier A, Leduc H, Dahdah N, Therien J, Vanasse M, et al. All-cause mortality and cardiovascular outcomes with prophylactic steroid therapy in Duchenne muscular dystrophy. *J Am Coll Cardiol.* (2013) 61:948–54. doi: 10.1016/j.jacc.2012.12.008

9. Fuhlbrigge AL, Kelly HW. Inhaled corticosteroids in children: effects on bone mineral density and growth. *Lancet Respir Med.* (2014) 2:487–96. doi: 10.1016/S2213-2600(14)70024-4

10. Garvin LM, Chen Y, Damsker JM, Rose MC. A novel dissociative steroid VBP15 reduces MUC5AC gene expression in airway epithelial cells but lacks the GRE mediated transcriptional properties of dexamethasone. *Pulm Pharmacol Ther.* (2016) 38:17–26. doi: 10.1016/j.pupt.2016.04.004

11. Heier CR, Yu Q, Fiorillo AA, Tully CB, Tucker A, Mazala DA, et al. Vamorolone targets dual nuclear receptors to treat inflammation and dystrophic cardiomyopathy. *Life Sci Allian.* (2019) 2:e201800186. doi: 10.26508/lsa.201800186

12. Sreetama SC, Chandra G, Van der Meulen JH, Ahmad MM, Suzuki P, Bhuvanendran S, et al. Membrane stabilization by modified steroid offers a potential therapy for muscular dystrophy due to dysferlin deficit. *Mol Ther.* (2018) 26:2231–42. doi: 10.1016/j.ymthe.2018.07.021

13. Chen Y-W, Nagaraju K, Bakay M, McIntyre O, Rawat R, Shi R, et al. Early onset of inflammation and later involvement of TGFβ in Duchenne muscular dystrophy. *Neurology.* (2005) 65:826–34. doi: 10.1212/01.wnl.0000173836.09176.c4

14. Guglieri M, Clemens PR, Perlman SJ, Smith EC, Horrocks I, Finkel RS, et al. Efficacy and safety of vamorolone vs placebo and prednisone among boys with Duchenne muscular dystrophy: a randomized clinical trial. *JAMA Neurol.* (2022) 79:1005–14. doi: 10.1001/jamaneurol.2022.2480

15. Mah JK, Clemens PR, Guglieri M, Smith EC, Finkel RS, Tulinius M, et al. Efficacy and safety of vamorolone in Duchenne muscular dystrophy: a 30-month nonrandomized controlled open-label extension trial. *JAMA Netw Open.* (2022) 5:e2144178. doi: 10.1001/jamanetworkopen.2021.44178

16. Smith EC, Conklin LS, Hoffman EP, Clemens PR, Mah JK, Finkel RS, et al. Efficacy and safety of vamorolone in Duchenne muscular dystrophy: an 18-month interim analysis of a non-randomized open-label extension study. *PLoS Med.* (2020) 17:e1003222. doi: 10.1371/journal.pmed.1003222

17. Higgins J, Green S. *Cochrane Handbook for Systematic Reviews of Interventions, Version 5.0.* The Cochrane Collaboration, 2009 (2010).

18. Acharyya S, Villalta SA, Bakkar N, Bupha-Intr T, Janssen PM, Carathers M, et al. Interplay of IKK/NF-κB signaling in macrophages and myofibers promotes muscle degeneration in Duchenne muscular dystrophy. *J Clin Invest.* (2007) 117:889–901. doi: 10.1172/JCI30556

19. Dogra C, Changotra H, Wergedal JE, Kumar A. Regulation of phosphatidylinositol 3-kinase (PI3K)/Akt and nuclear factor-kappa B signaling pathways in dystrophin-deficient skeletal muscle in response to mechanical stretch. *J Cell Physiol.* (2006) 208:575–85. doi: 10.1002/jcp.20696

20. Kumar A, Boriek AM. Mechanical stress activates the nuclear factor-kappaB pathway in skeletal muscle fibers: a possible role in Duchenne muscular dystrophy. *FASEB J.* (2003) 17:386–96. doi: 10.1096/fj.02-0542com

21. Loop T, Pahl H. Activators and target genes of Rel/NF-κB transcription factors. *Nucl Fact κB.* (2003) 1–48. doi: 10.1007/978-94-010-0163-2_1

22. Spencer MJ, Montecino-Rodriguez E, Dorshkind K, Tidball JG. Helper (CD4+) and cytotoxic (CD8+) T cells promote the pathology of dystrophin-deficient muscle. *Clin Immunol.* (2001) 98:235–43. doi: 10.1006/clim.2000.4966

23. Spencer MJ, Tidball JG. Do immune cells promote the pathology of dystrophin-deficient myopathies? *Neuromuscl Disord.* (2001) 11:556–64. doi: 10.1016/S0960-8966(01)00198-5

24. Reeves EK, Hoffman EP, Nagaraju K, Damsker JM, McCall JM. VBP15: preclinical characterization of a novel anti-inflammatory delta 9, 11 steroid. *Bioorg Med Chem.* (2013) 21:2241–9. doi: 10.1016/j.bmc.2013.02.009

25. Liu X, Wang Y, Gutierrez JS, Damsker JM, Nagaraju K, Hoffman EP, et al. Disruption of a key ligand-H-bond network drives dissociative properties in vamorolone for Duchenne muscular dystrophy treatment. *Proc Natl Acad Sci USA.* (2020) 117:24285–93. doi: 10.1073/pnas.2006890117

26. Liu X, Wang Y, Ortlund EA. First high-resolution crystal structures of the glucocorticoid receptor ligand-binding domain–peroxisome proliferator-activated γ coactivator 1-α complex with endogenous and synthetic glucocorticoids. *Mol Pharmacol.* (2019) 96:408–17. doi: 10.1124/mol.119.116806

27. Damsker JM, Cornish MR, Kanneboyina P, Kanneboyina I, Yu Q, Lipson R, et al. Vamorolone, a dissociative steroidal compound, reduces collagen antibody-induced joint damage and inflammation when administered after disease onset. *Inflamm Res.* (2019) 68:969–80. doi: 10.1007/s00011-019-01279-z

28. Hudson WH, Vera IMSd, Nwachukwu JC, Weikum ER, Herbst AG, Yang Q, et al. Cryptic glucocorticoid receptor-binding sites pervade genomic NF-κB response elements. *Nat Commun.* (2018) 9:1337. doi: 10.1038/s41467-018-03780-1

29. Hoffman EP, Schwartz BD, Mengle-Gaw LJ, Smith EC, Castro D, Mah JK, et al. Vamorolone trial in Duchenne muscular dystrophy shows dose-related improvement of muscle function. *Neurology.* (2019) 93:e1312–23. doi: 10.1212/WNL.0000000000008168

30. Szulc P, Seeman E, Delmas P. Biochemical measurements of bone turnover in children and adolescents. *Osteoporos Int.* (2000) 11:281–94. doi: 10.1007/s001980070116

31. Pye SR, Ward KA, Cook MJ, Laurent MR, Gielen E, Borghs H, et al. Bone turnover predicts change in volumetric bone density and bone geometry at the radius in men. *Osteoporos Int.* (2017) 28:935–44. doi: 10.1007/s00198-016-3816-z

32. Babadjanova G, Allolio B, Vollmer M, Reincke M, Schulte H. Comparison of the pharmacodynamic effects of deflazacort and prednisolone in healthy subjects. *Euro J Clin Pharmacol.* (1996) 51:53–7. doi: 10.1007/s002280050160

33. Saviola G, Abdi. Ali L, Shams. Eddin S, Coppini A, Cavalieri F, Campostrini L, et al. Compared clinical efficacy and bone metabolic effects of low-dose deflazacort and methyl prednisolone in male inflammatory arthropathies: a 12-month open randomized pilot study. *Rheumatology.* (2007) 46:994–8. doi: 10.1093/rheumatology/kem030

34. Bello L, Gordish-Dressman H, Morgenroth LP, Henricson EK, Duong T, Hoffman EP, et al. Prednisone/prednisolone and deflazacort regimens in the CINRG Duchenne natural history study. *Neurology.* (2015) 85:1048–55. doi: 10.1212/WNL.0000000000001950

35. Griggs RC, Herr BE, Reha A, Elfring G, Atkinson L, Cwik V, et al. Corticosteroids in Duchenne muscular dystrophy: major variations in practice. *Muscle Nerve.* (2013) 48:27–31. doi: 10.1002/mus.23831

36. Fenton C, Martin C, Jones R, Croft A, Campos J, Naylor AJ, et al. Local steroid activation is a critical mediator of the anti-inflammatory actions of therapeutic glucocorticoids. *Ann Rheumat Dis.* (2021) 80:250–60. doi: 10.1136/annrheumdis-2020-218493

37. Fenton CG, Doig CL, Fareed S, Naylor A, Morrell AP, Addison O, et al. 11beta-HSD1 plays a critical role in trabecular bone loss associated with systemic glucocorticoid therapy. *Arthritis Res Ther.* (2019) 21:188. doi: 10.1186/s13075-019-1972-1

38. Roy R, Soldin SJ, Stolze B, Barbieri M, Tawalbeh SM, Rouhana N, et al. Acute serum protein and cytokine response of single dose of prednisone in adult volunteers. *Steroids.* (2022) 178:108953. doi: 10.1016/j.steroids.2021.108953

frontiers | Frontiers in Neurology

TYPE Case Report
PUBLISHED 02 February 2023
DOI 10.3389/fneur.2022.1067418

Check for updates

OPEN ACCESS

EDITED BY
Giovanni Meola,
University of Milan, Italy

REVIEWED BY
Gregory Carter,
Washington State University, United States
Nilo Riva,
IRCCS "Carlo Besta" Neurological Institute, Italy

*CORRESPONDENCE
Katherine M. Burke
✉ Katherine.Burke@mgh.harvard.edu

SPECIALTY SECTION
This article was submitted to Neuromuscular Disorders and Peripheral Neuropathies, a section of the journal Frontiers in Neurology

RECEIVED 11 October 2022
ACCEPTED 30 December 2022
PUBLISHED 02 February 2023

CITATION
Burke KM, Ellrodt AS, Joslin BC, Sanpitak PP, MacAdam C, Deo P, Ozment K, Shea C, Johnson SA, Ho D, Chu SK, Babu AN, Franz CK and Paganoni S (2023) Ultrasound-guided glenohumeral joint injections for shoulder pain in ALS: A case series. *Front. Neurol.* 13:1067418. doi: 10.3389/fneur.2022.1067418

COPYRIGHT
© 2023 Burke, Ellrodt, Joslin, Sanpitak, MacAdam, Deo, Ozment, Shea, Johnson, Ho, Chu, Babu, Franz and Paganoni. This is an open-access article distributed under the terms of the Creative Commons Attribution License (CC BY). The use, distribution or reproduction in other forums is permitted, provided the original author(s) and the copyright owner(s) are credited and that the original publication in this journal is cited, in accordance with accepted academic practice. No use, distribution or reproduction is permitted which does not comply with these terms.

Ultrasound-guided glenohumeral joint injections for shoulder pain in ALS: A case series

Katherine M. Burke[1]*, Amy S. Ellrodt[1], Benjamin C. Joslin[2], Pia P. Sanpitak[2], Claire MacAdam[1], Prabhav Deo[3,4], Kevin Ozment[3,4], Cristina Shea[5], Stephen A. Johnson[1], Doreen Ho[1], Samuel K. Chu[3,4], Ashwin N. Babu[5,6], Colin K. Franz[2,3,4] and Sabrina Paganoni[1,5,7]

[1]Sean M. Healey & AMG Center for ALS at Massachusetts General Hospital, Department of Neurology, Harvard Medical School, Boston, MA, United States, [2]Ken and Ruth Davee Department of Neurology, Northwestern University Feinberg School of Medicine, Chicago, IL, United States, [3]Shirley Ryan AbilityLab, Chicago, IL, United States, [4]Physical Medicine and Rehabilitation, Northwestern University Feinberg School of Medicine, Chicago, IL, United States, [5]Department of Physical Medicine and Rehabilitation, Spaulding Rehabilitation Hospital, Boston, MA, United States, [6]Massachusetts General Hospital Department of Orthopedics, Sports Medicine, Boston, MA, United States, [7]VA Boston Healthcare System, Boston, MA, United States

Introduction: Shoulder pain is a common secondary impairment for people living with ALS (PALS). Decreased range of motion (ROM) from weakness can lead to shoulder pathology, which can result in debilitating pain. Shoulder pain may limit PALS from participating in activities of daily living and may have a negative impact on their quality of life. This case series explores the efficacy of glenohumeral joint injections for the management of shoulder pain due to adhesive capsulitis in PALS.

Methods: People living with ALS and shoulder pain were referred to sports medicine-certified physiatrists for diagnostic evaluation and management. They completed the Revised ALS Functional Rating Scale and a questionnaire asking about their pain levels and how it impacts sleep, function, and quality of life at baseline pre-injection, 1-week post-injection, 1 month post-injection, and 3 months post-injection.

Results: We present five cases of PALS who were diagnosed with adhesive capsulitis and underwent glenohumeral joint injections. Though only one PALS reported complete symptom resolution, all had at least partial symptomatic improvement during the observation period. No complications were observed.

Conclusions: People living with ALS require a comprehensive plan to manage shoulder pain. Glenohumeral joint injections are safe and effective for adhesive capsulitis in PALS, but alone may not completely resolve shoulder pain. Additional therapies to improve ROM and reduce pain should be considered.

KEYWORDS

amyotrophic lateral sclerosis, motor neuron disease, shoulder pain, frozen shoulder, adhesive capsulitis

1. Introduction

Amyotrophic lateral sclerosis (ALS) is a fatal neurodegenerative disease (1). The management of ALS is largely focused on symptom management as current FDA-approved treatments to slow disease progression have modest efficacy (1).

Amyotrophic lateral sclerosis symptoms include muscle weakness and atrophy, reduced range of motion, spasticity, and cramping leading to progressive disability. Pain is a common secondary complication of ALS from musculoskeletal dysfunction due to limited mobility, loss

of range of motion, and difficulty with positioning in bed, chairs, or wheelchairs (2). Progressive, often non-uniform, weakness likely also contributes by disrupting agonist-antagonist muscle pair equilibrium leading to increased stress on the joint and surrounding structures. Pain negatively affects the quality of life for both PALS and their caregivers (2–7) The most commonly reported loci of pain in PALS are the lower back, neck, legs, and shoulders (2, 8) Shoulder pain is reported by ∼20% of the total ALS population (8). Many PALS develop shoulder pain due to weakness of the periscapular muscles with subsequent loss of range of motion, subluxation, and development of shoulder pathology, including adhesive capsulitis or "frozen shoulder."

Adhesive capsulitis is a complex disorder that involves pain and restricted range of motion (ROM) of the shoulder (9–11) and can lead to considerable disability. The capsule surrounding the glenohumeral (GH) joint stiffens and becomes inflamed, which results in a decreased range of motion (ROM) at the shoulder. There are overlapping stages of adhesive capsulitis. In the earlier stages, patients present with severely restricted ROM and significant pain, often in the absence of injury. In the later stages, restrictions in ROM remain, but with improvements in pain. As ROM and pain improve, there may be continued evidence of a tight joint space, but no evidence of synovitis (10). Adhesive capsulitis is largely a clinical diagnosis, with any imaging done to exclude other potential diagnoses (9).

For individuals without ALS, the management of adhesive capsulitis involves exercises and supervised physical therapy focused on gentle ROM and periscapular stabilization. First-line medications typically prescribed to treat pain in ALS are non-steroidal anti-inflammatory agents (NSAIDs) and non-opioid analgesics (4, 12). Early corticosteroid injection to the GH joint should be considered for moderate to severe symptoms (13, 14), as there is evidence suggesting improved outcomes with earlier steroid injection (15). This in-clinic procedure is fast and safe. It is routinely performed in the seated position, which is preferable for PALS who may be in a power wheelchair and/or have limited tolerance for the supine position. Adverse effects such as bleeding or infection are rare when performed with proper clean technique. In cases where conservative measures are ineffective, surgical interventions such as arthroscopic release and manipulation under anesthesia are considered, especially in the early stages when the pain can be debilitating (16, 17).

To the best of our knowledge, there is no evidence from controlled trials that would substantiate a standard best practice for addressing shoulder pain in people with ALS. Thus, the management of shoulder pain has long been based on the individual clinician's experience and preferences with very little empirically-derived evidence to support the implementation of one therapeutic method over another. When PALS present with progressive shoulder pain, accompanying restrictions in ROM, and no history of trauma, referral to physiatry can help to assess the pain generator (e.g., adhesive capsulitis vs. other shoulder pathology) and help guide the intervention. There is growing evidence to support the use of GH steroid injections for adhesive capsulitis for those without ALS (13–17).

The purpose of this study was to assess the efficacy of ultrasound-guided GH joint injections for treating shoulder pain due to adhesive capsulitis in PALS. We present a case series of five patients referred for physiatric evaluation and consideration of GH joint injections as part of their clinical care. Participants completed surveys pre- and post-injections regarding their pain levels and impact on function.

2. Methods

Participants were recruited from the Sean M. Healey & AMG Center for ALS at Massachusetts General Hospital and the Northwestern University Feinberg School of Medicine ALS Clinic. Eligible participants were informed of the study and study staff consented interested participants. Both the Mass General Brigham Institutional Review Board (IRB) and the Northwestern IRB approved this study.

Participants were asked to participate in this study if they had ALS and a clinical suspicion of adhesive capsulitis (pain with restricted ROM, without a history of trauma). Participants were seen by physiatrists certified in Sports Medicine by the American Board of Physical Medicine and Rehabilitation for diagnostic confirmation and consideration of GH steroid injections. The physiatrists completed a history, physical, and ultrasound examinations to assess the likelihood of adhesive capsulitis vs. other common shoulder pathologies (such as rotator cuff or biceps tendinopathy, periscapular myofascial pain, etc.). Once a clinical diagnosis of adhesive capsulitis was established, an ultrasound-guided GH joint injection was performed. For Cases 1–3, a solution of 4 ml of 1% Lidocaine and 1 ml (40 mg) of Kenalog was injected into the affected joints. For Cases 4 and 5, a solution of 2 ml of 1% Lidocaine, 2 ml of 0.25% Bupivacaine, and 1 ml (40 mg) of Kenalog was injected into the involved joints. Differences were due to the preference of the physiatrist performing the intervention. The study duration was from May 2019 to August 2021. Enrollment was limited by the COVID-19 pandemic, as sites had temporary holds on the observational studies, and patient care shifted to telemedicine visits.

Participants were asked to complete the revised ALS Functional Rating Scale (ALSFRS-R) and a questionnaire that assessed pain, sleep, function, and quality of life (Supplementary material) at baseline before undergoing the GH joint injections. They were then asked to complete the same questionnaires at 1-week post-injection and 1-month post-injection. There was an optional phone call at 3 months to complete the same questionnaires.

Electronic medical record review was available for all participants, from which information regarding their ALS diagnosis, disease duration, and current functional status was gathered.

3. Results

Of nine participants enrolled in the study, three initially agreed but ultimately declined the referral for GH joint injections and were provided with ROM and stretching exercises by the clinic's physical therapists. Follow-up of these individuals was not pursued as part of this study. Another participant was seen by physiatry: diagnostic evaluation pointed to myofascial pain with muscle spasms as the most likely pain generator. For this reason, the participant underwent bilateral trapezius, infraspinatus, and levator scapulae trigger point injections rather than GH joint injections. This participant did have resolution of his shoulder pain 18 days post-injection, but this was not sustained 2 months post-injection. We

report on the remaining five participants who were diagnosed by sports medicine-certified physiatrists with adhesive capsulitis and did undergo ultrasound-guided GH joint steroid injections. None of the participants experienced procedure-related complications. Average pain scores and impact on sleep and quality of life for each participant are shown in Table 1. Complete data for each participant are shown in Supplementary Tables 1–5.

3.1. Case 1

The participant was a 41-year-old woman with upper motor neuron predominant limb onset sporadic ALS, meeting El Escorial criteria for definite ALS. She used a wheelchair for mobility and was dependent on caregivers for activities of daily living (ADLs). ALS symptom onset was over 3 years prior with left-hand weakness and clawing. She had bilateral upper and lower extremity weakness with atrophy (left greater than right), and spasticity throughout her extremities. She presented with atraumatic bilateral shoulder pain, right greater than left, with passive range of motion restrictions. She was taking NSAIDs as needed and undergoing physical therapy with shoulder range of motion and stretching exercises. Physiatry evaluation confirmed the diagnosis of adhesive capsulitis, and she underwent a right GH joint injection with ultrasound guidance. Post-injection, she demonstrated improvements in shoulder pain, which were sustained at the 3-month visit, as well as sustained improvements in sleep, function, and quality of life (Supplementary Table 1).

3.2. Case 2

The participant was a 42-year-old man with limb onset sporadic ALS, meeting El Escorial criteria for probable ALS—laboratory supported. He was ambulatory with a single-point cane and had modified independence with ADLs. ALS onset was over 2 years prior with lower extremity weakness. He presented with upper and lower extremity weakness and atrophy, with brisk reflexes in bilateral lower extremities. He reported atraumatic right shoulder pain that started a few months before, with limited ROM. He was not taking any medications and was not participating in physical therapy. He had been prescribed shoulder range of motion and stretching exercises at a multidisciplinary clinic but was unable to perform them due to pain. Physiatry evaluation confirmed the diagnosis of adhesive capsulitis and he underwent a right GH joint injection with ultrasound guidance. Post-injection, he demonstrated improvements in shoulder pain, which were sustained at the 1-month visit, as well as improvements in sleep, function, and quality of life (Supplementary Table 2). He initiated a stretching program for bilateral shoulders post-injection.

3.3. Case 3

The participant was a 57-year-old man with limb onset sporadic ALS, meeting El Escorial criteria for probable ALS—laboratory supported. ALS symptom onset was over 3 years prior with lower extremity weakness. He was ambulatory without an assistive device and required assistance with ADLs due to bilateral upper extremity weakness. He had bilateral upper and lower extremity weakness, with increased reflexes in bilateral lower and left upper extremities. He presented with bilateral atraumatic shoulder pain, left greater than right. He had been prescribed shoulder range of motion and stretching exercises at a multidisciplinary clinic but was unable to perform them due to pain. He was not taking any pain medications. Physiatry evaluation confirmed the diagnosis of adhesive capsulitis and he underwent bilateral GH joint injections with ultrasound guidance. Overall, the pain was improved in bilateral shoulders post-injection, and this was sustained at the 3-month visit. At 1 month, the pain was not impacting sleep, function, and quality of life, but this was not sustained at 3 months (Supplementary Table 3). He was stretching at the 1-month mark, but this was not sustained at 3 months.

3.4. Case 4

The participant was a 49-year-old man with upper motor neuron predominant limb onset sporadic ALS, meeting El Escorial criteria for probable ALS—laboratory supported. He presented with mild bilateral upper extremity weakness without muscle atrophy, as well as diffuse muscle spasticity characterized by a slight catch at the end range of the passive range of motion. He was power wheelchair dependent for community mobility and used either a cane or a power wheelchair for household mobility. He had modified independence with ADLs. He presented with 6 months of progressively worsening atraumatic bilateral anterolateral shoulder pain and stiffness, left greater than right. He had passive and active ROM restrictions bilaterally. He had been taking ibuprofen as needed for several years. He had been prescribed shoulder range of motion and stretching exercises at a multidisciplinary clinic but was not able to comply with them due to pain. He underwent bilateral GH joint injections with ultrasound guidance. He exhibited improvements in the impact of shoulder pain that lasted only 1 month, but the improvements in his quality of life and function were largely sustained at the 3-month follow-up (Supplementary Table 4).

3.5. Case 5

The participant is a 58-year-old woman with upper motor neuron predominant limb onset ALS, meeting El Escorial criteria for definite ALS. Despite having no family history of ALS or dementia, she was later found to carry a hexanucleotide repeat expansion in the C9orf72 gene (>145 repeats). She had some hand intrinsic muscle atrophy and moderate bilateral arm weakness (right worse than left). She had diffusely increased muscle tone treated with oral baclofen. She was ambulatory and required assistance with ADLs due to upper extremity weakness. She presented with atraumatic left shoulder pain and stiffness for 2 months. She managed her pain with a nightly dose of ibuprofen and had not yet started physical therapy before the initial referral for injection. She had limited active and passive shoulder ROM.

TABLE 1 Pain and impact on sleep, function, and quality of life.

	Case 1	Case 2	Case 3	Case 4	Case 5
Average pain 0–10 (R/L)					
Pre-injection (days from baseline)	7/7 (−19)	7/0 (−22)	3/4 (−3)	6/5 (−18)	1/7 (0)
1st follow-up (days from baseline)	4/7 (7)	2/0 (7)	0/0 (7)	1/2 (10)	0/0 (11)
2nd follow-up (days from baseline)	5/7 (28)	2/0 (21)	2/3 (25)	4/4 (31)	0/0 (28)
3rd follow-up (days from baseline)	0/0 (74)	Not collected	0/0 (87)	6/6 (87)	0/0 (87)
Max pain 0–10 (R/L)					
Pre-injection	9/9	9/0	4/5	8/8	1/8
1st follow-up	8/7	4/0	5/5	4/4	0/0
2nd follow-up	8/8	5/0	2/3	8/8	0/0
3rd follow-up	5/5	Not collected	10/10	8/6	0/0
My shoulder pain keeps me from getting enough sleep at night					
Pre-injection	Often	Sometimes	Rarely	Always	Always
1st follow-up	Never	Rarely	Rarely	Never	Never
2nd follow-up	Never	Sometimes	Never	Never	Never
3rd follow-up	Never	Not collected	Never	Never	Never
My shoulder pain limits my ability to complete daily hygiene					
Pre-injection	Always	Often	Always	Always	Never
1st follow-up	Often	Rarely	Always	Never	Never
2nd follow-up	Sometimes	Sometimes	Never	Never	Never
3rd follow-up	Rarely	Not collected	Always	Never	Never
My shoulder pain limits my ability to get dressed each day					
Pre-injection	Always	Often	Always	Always	Always
1st follow-up	Often	Sometimes	Always	Rarely	Never
2nd follow-up	Sometimes	Sometimes	Never	Rarely	Never
3rd follow-up	Always	Not collected	Always	Sometimes	Never
My shoulder pain limits me from leaving the house for other activities					
Pre-injection	Always	Rarely	Often	Sometimes	Never
1st follow-up	Never	Rarely	Always	Rarely	Never
2nd follow-up	Never	Sometimes	Never	Rarely	Never
3rd follow-up	Never	not collected	Rarely	Rarely	Never
My shoulder pain has a negative impact on my quality of life					
Pre-injection	Always	Often	Always	Always	Never
1st follow-up	Often	Sometimes	Sometimes	Never	Never
2nd follow-up	Often	Sometimes	Never	Never	Never
3rd follow-up	Always	not collected	Always	Never	Never

She underwent left GH joint injections with ultrasound guidance. In early and late follow-ups, the patient reported the resolution of shoulder pain and it was no longer impacting sleep. This allowed her to engage in a shoulder home exercise program provided by ALS interdisciplinary clinic occupational therapist with assistance from her family. Resolution of pain and impact on sleep, function, and quality of life were sustained at the 3-month visit (Supplementary Table 5).

4. Discussion

In this case series, we present empiric evidence of the benefit of GH joint steroid injections for PALS who present with shoulder pain in the setting of adhesive capsulitis. All study participants presented here reported improvement in their pain levels and a positive impact on sleep, function, or quality of life. One of the participants (Case 5) reported a complete resolution of her shoulder pain. There were no

adverse events reported by the participants in this study. These results demonstrate the safety of, and suggest a role for, ultrasound-guided GH joint steroid injections for PALS with adhesive capsulitis, though additional measures may be needed for further pain management.

The development of shoulder pain from adhesive capsulitis in PALS is likely a secondary effect of their disease resulting from multiple factors such as decreased shoulder muscle strength, muscle atrophy, and reduced activity levels. The progressive lack of motion may contribute to the inflammation and tightening of the joint capsule. Similar pathology has been reported in both stroke and Parkinson's disease where there is motor dysfunction involving the shoulder (18, 19). Motion is critical to maintain and restore ROM (13, 16). Early in the disease course, PALS meet with physical therapists and occupational therapists in the multidisciplinary clinic to review the importance of a regular range of motion exercise program for all joints, including the shoulders. For individuals with upper extremity weakness, especially the shoulder, the range of motion exercises become even more crucial, and the physical therapists or occupational therapists will review the range of motion and stretching program with patients and train their caregivers if they are not able to complete the exercises on their own. Unfortunately, some PALS still present with shoulder pain. For these PALS, stretching and range of motion exercises are reinforced, and strategies to increase compliance can be helpful (20). Shoulder approximation sleeves can also be used to help support the shoulder and manage pain, as well as modalities such as transcutaneous electrical nerve stimulation (TENS) devices. However, while these tools and strategies have shown promise, these interventions are not always enough to completely relieve pain or improve function (20). Unfortunately, there may be limited ability to complete the recommended exercises due to disease progression or pain. Often, the shoulder will become quite painful, will limit the ability to participate in ADLs, including daily hygiene, and may impact sleep quality and overall quality of life. When pain has become a limiting factor, the provider is challenged to make appropriate recommendations for adequate pain control and to optimize the person's ability to participate in ADLs. This study highlights the need for a multifaceted approach, which may include GH joint injections, as well as education on the cause of shoulder pain and the importance of a long-term stretching program to maintain a functional ROM to minimize risk for re-freezing or ongoing pain.

Referral to musculoskeletal specialists for the consideration for steroid injections should be considered for PALS with shoulder pain. The procedure offers the advantages of being a fast, safe, in-office procedure that requires no ionizing radiation or sedation. Evidence in non-ALS populations shows improved pain relief with steroid injections compared to manual therapy and exercise without injection (21). Shoulder injections have also been shown to be beneficial for hemiplegic shoulder pain in patients status post-stroke (22). With pain relief from the injections, the person may be able to tolerate ROM and stretching exercises, which will restore motion and in turn may further improve pain, and help to restore function and quality of life. Appropriate pain relief with localized steroid injections also offers a strategy to reduce reliance on systemic pain medications with potential GI, renal, and neurologic side effects.

It is important to minimize the delays in referrals to musculoskeletal specialists, given the emerging evidence of improved outcomes with earlier steroid injections in people without ALS, as well as improved efficacy compared to manual therapy with exercise (14, 21). While early diagnosis and intervention is ideal, our cohort suggests that GH joint injection for adhesive capsulitis likely benefits PALS across the progression of ALS. If employed in early ALS, GH injection may allow a person to maintain ROM, functional independence, and participation in active physical therapy programs. In later-stage ALS, GH injection may offer improved passive ROM and caregiver ability to assist with ADLs, such as dressing and bathing. Throughout all ALS stages, the pain-reducing effect of GH injection may have benefits on activity, sleep, and mood.

Our study was limited by the small number of participants and case series design. The ongoing COVID-19 pandemic also limited participation, such that we were not able to collect the range of motion measurements as the participants completed their post-injection visits over the telephone, and many did not present to the clinic again during the study period due to COVID-19 restrictions. Further research is also needed to compare the outcomes between those who choose not to have the injections to those who do choose this intervention. We did not collect this information as part of this study. Finally, as more evidence emerges regarding specific injection techniques and steroid dose for people without ALS, it will be important to explore these same questions in the ALS population.

This case series supports the safety and efficacy of GH joint injections for adhesive capsulitis in PALS. Larger studies to determine the prevalence of adhesive capsulitis vs. other pathologies and to optimize comprehensive management plans aimed at complete shoulder pain resolution are needed.

Data availability statement

The original contributions presented in the study are included in the article/Supplementary material, further inquiries can be directed to the corresponding author.

Author contributions

KB, BJ, and CF: concept and design, data collection, data analysis, drafting of the manuscript, and critical review of the manuscript. AE, AB, and SP: concept and design, data collection, data analysis, and critical review of the manuscript. PS, PD, KO, and SC: data collection, data analysis, and critical review of the manuscript. CM, CS, SJ, and DH: data analysis and critical review of the manuscript. All authors contributed to the article and approved the submitted version.

Acknowledgments

This research would not be possible without the contributions of our patients in taking the time to complete the surveys and provide feedback on the impact of the shoulder injections.

Conflict of interest

DH: compensation for consulting from Alexion pharmaceuticals. SP: Research grants from Amylyx Therapeutics, Revalesio Corporation, Alector Therapeutics, UCB, Biohaven Pharmaceuticals, Clene Nanomedicine, Prilenia Therapeutics, Seelos Therapeutics.

Research grants from the ALS Association, the American Academy of Neurology, the CDC, ALS Finding a Cure, the Salah Foundation, the Spastic Paraplegia Foundation, the Muscular Dystrophy Association, I AM ALS, Tambourine, Target ALS, Columbia University, the Cullen Education and Research Fund. Site PI: Alector Therapeutics, Cytokinetics, Inc., Anelixis Therapeutics. Institutional consulting agreements with Amylyx Therapeutics, Frequency Therapeutics, Sola Biosciences. Personal consulting agreements with Cytokinetics, Inc., Arrowhead Pharmaceuticals, and Orthogonal Neurosciences. Honoraria from Medscape.

The remaining authors declare that the research was conducted in the absence of any commercial or financial relationships that could be construed as a potential conflict of interest.

Publisher's note

All claims expressed in this article are solely those of the authors and do not necessarily represent those of their affiliated organizations, or those of the publisher, the editors and the reviewers. Any product that may be evaluated in this article, or claim that may be made by its manufacturer, is not guaranteed or endorsed by the publisher.

Supplementary material

The Supplementary Material for this article can be found online at: https://www.frontiersin.org/articles/10.3389/fneur.2022.1067418/full#supplementary-material

References

1. Majmudar S, Wu J, Paganoni S. Rehabilitation in amyotrophic lateral sclerosis: why it matters. *Muscle Nerve.* (2014) 50:4–13. doi: 10.1002/mus.24202

2. Paganoni S, Karam C, Joyce N, Bedlack R, Carter GT. Comprehensive rehabilitative care across the spectrum of amyotrophic lateral sclerosis. *NeuroRehabilitation.* (2015) 37:53–68. doi: 10.3233/NRE-151240

3. Chiò A, Mora G, Lauria G. Pain in amyotrophic lateral sclerosis. *Lancet Neurol.* (2017) 16:144–57. doi: 10.1016/S1474-4422(16)30358-1

4. Chiò A, Canosa A, Gallo S, Moglia C, Ilardi A, Cammarosano S, et al. Pain in amyotrophic lateral sclerosis: a population-based controlled study. *Eur J Neurol.* (2012) 19:551–5. doi: 10.1111/j.1468-1331.2011.03540.x

5. Raheja D, Stephens HE, Lehman E, Walsh S, Yang C, Simmons Z. Patient-reported problematic symptoms in an ALS treatment trial. *Amyotroph Lateral Scler Frontotemporal Degener.* (2016) 17:198–205. doi: 10.3109/21678421.2015.1131831

6. Wallace VC, Ellis CM, Burman R, Knights C, Shaw CE, Al-Chalabi A. The evaluation of pain in amyotrophic lateral sclerosis: a case controlled observational study. *Amyotroph Lateral Scler Frontotemporal Degener.* (2014) 15:520–7. doi: 10.3109/21678421.2014.951944

7. Pizzimenti A, Aragona M, Onesti E, Inghilleri M. Depression, pain and quality of life in patients with amyotrophic lateral sclerosis: a cross-sectional study. *Funct Neurol.* (2013) 28:115–9. doi: 10.11138/FNeur/2013.28.2.115

8. Ho DT, Ruthazer R, Russell JA. Shoulder pain in amyotrophic lateral sclerosis. *J Clin Neuromuscul Dis.* (2011) 13:53–5. doi: 10.1097/CND.0b013e31821c5623

9. Fields BK, Skalski MR, Patel DB, White EA, Tomasian A, Gross JS, et al. Adhesive capsulitis: review of imaging findings, pathophysiology, clinical presentation, and treatment options. *Skeletal Radiol.* (2019) 48:1171–84. doi: 10.1007/s00256-018-3139-6

10. Kraal T, Lübbers J, van den Bekerom MP, Alessie J, van Kooyk Y, Eygendaal D, et al. The puzzling pathophysiology of frozen shoulders - a scoping review. *J Exp Orthop.* (2020) 7:91. doi: 10.1186/s40634-020-00307-w

11. Nagy MT, Macfarlane RJ, Khan Y, Waseem M. The frozen shoulder: myths and realities. *Open Orthop J.* (2013) 7:352–5. doi: 10.2174/1874325001307010352

12. Brettschneider, Johannes, Jerome K, Albert L. Drug therapy for pain in amyotrophic lateral sclerosis or motor neuron disease. *Cochrane Database Sys Rev.* (2013) 6:5226. doi: 10.1002/14651858

13. Challoumas D, Biddle M, McLean M, Millar NL. Comparison of treatments for frozen shoulder: a systematic review and meta-analysis. *JAMA Netw Open.* (2020) 3:e2029581. doi: 10.1001/jamanetworkopen.2020.29581

14. Shang X, Zhang Z, Pan X, Li J, Li Q. Intra-articular versus subacromial corticosteroid injection for the treatment of adhesive capsulitis: a meta-analysis and systematic review. *BioMed Res Int.* (2019) 2019:1274790. doi: 10.1155/2019/1274790

15. Sun Y, Liu S, Chen S, Chen J. The effect of corticosteroid injection into rotator interval for early frozen shoulder: a randomized controlled trial. *Am J Sports Med.* (2018) 46:663–70. doi: 10.1177/0363546517744171

16. Chan HB, Pua PY, How CH. Physical therapy in the management of frozen shoulder. *Singapore Med J.* (2017) 58:685–9. doi: 10.11622/smedj.2017107

17. Koh KH. Corticosteroid injection for adhesive capsulitis in primary care: a systematic review of randomized clinical trials. *Singapore Med J.* (2016) 57:646–57. doi: 10.11622/smedj.2016146

18. Zhu Y, Su B, Li N, Jin H. Pain management of hemiplegic shoulder pain post stroke in patients from Nanjing, China. *Neural Regen Res.* (2013) 8:2389–98. doi: 10.3969/j.issn.1673-5374.2013.25.010

19. Sarasua SM, Floyd S, Bridges WC, Pill SG. The epidemiology and etiology of adhesive capsulitis in the US Medicare population. *BMC Musculoskelet Disord.* (2021) 22:828. doi: 10.1186/s12891-021-04704-9 PMID:34579697

20. Burke K, DE Marchi F, Swartz Ellrodt A, Doyle M, Koul M, Comeau O, et al. Exploring the use of educational materials for increasing participation in a stretching program: a quality improvement project in people with motor neuron disease. *Eur J Phys Rehabil Med.* (2021) 57:78–84. doi: 10.23736/S1973-9087.20.06245-0 PMID:32744050

21. Page MJ, Green S, Kramer S, Johnston RV, McBain B, Chau M, et al. Manual therapy and exercise for adhesive capsulitis (frozen shoulder). *Cochrane Database Syst Rev.* (2014) 8:CD011275. doi: 10.1002/14651858.CD011275

22. Lakse E, Gunduz B, Erhan B, Celik EC. The effect of local injections in hemiplegic shoulder pain: a prospective, randomized, controlled study. *Am J Phys Med Rehabil.* (2009) 88:805–11. doi: 10.1097/PHM.0b013e3181b71c65

frontiers | Frontiers in Neurology

TYPE Case Report
PUBLISHED 13 February 2023
DOI 10.3389/fneur.2023.1078151

Check for updates

OPEN ACCESS

EDITED BY
Giovanni Meola,
University of Milan, Italy

REVIEWED BY
Paulo Victor Sgobbi Souza,
Federal University of São Paulo, Brazil
Per Harald Jonson,
University of Helsinki, Finland

*CORRESPONDENCE
Song Tan
✉ tansong@med.uestc.edu.cn

SPECIALTY SECTION
This article was submitted to Neuromuscular Disorders and Peripheral Neuropathies, a section of the journal Frontiers in Neurology

RECEIVED 24 October 2022
ACCEPTED 24 January 2023
PUBLISHED 13 February 2023

CITATION
Wang D-Z, Li B-H, Ma Q, Yu Z, Chen K, He Y and Tan S (2023) Novel compound heterozygous mutations of LAMA2-limb–girdle muscular dystrophy: A case report and literature review. *Front. Neurol.* 14:1078151. doi: 10.3389/fneur.2023.1078151

COPYRIGHT
© 2023 Wang, Li, Ma, Yu, Chen, He and Tan. This is an open-access article distributed under the terms of the Creative Commons Attribution License (CC BY). The use, distribution or reproduction in other forums is permitted, provided the original author(s) and the copyright owner(s) are credited and that the original publication in this journal is cited, in accordance with accepted academic practice. No use, distribution or reproduction is permitted which does not comply with these terms.

Novel compound heterozygous mutations of LAMA2-limb–girdle muscular dystrophy: A case report and literature review

Duo-Zi Wang[1], Bing-Hu Li[1], Qiong Ma[2], Zhou Yu[3], Kai Chen[1], Ying He[3] and Song Tan[1,4,5]*

[1]Department of Neurology, Sichuan Provincial People's Hospital, University of Electronic Science and Technology of China, Chengdu, China, [2]Department of Neurology, The First People's Hospital of Liangshan in Yi Autonomous Prefecture, Xichang, China, [3]Department of Psychosomatic Medicine, Sichuan Provincial People's Hospital, University of Electronic Science and Technology of China, Chengdu, China, [4]Sichuan Provincial Key Laboratory for Human Disease Gene Study, Chengdu, China, [5]Chinese Academy of Sciences Sichuan Translational Medicine Research Hospital, Chengdu, Sichuan, China

The laminin α2 (LAMA2) gene pathogenic variants can lead to limb–girdle muscular dystrophy (known as LGMDR23), which is rarely reported and characterized by proximal weakness in the limbs. We present the case of a 52-year-old woman who gradually developed weakness in both lower extremities since the age of 32 years. Magnetic resonance imaging (MRI) brain showed symmetrical sphenoid wings-like white matter demyelination in bilateral lateral ventricles. Electromyography showed quadriceps muscle damage on the bilateral lower extremity. Next-generation sequencing (NGS) found two loci variations in the LAMA2 gene, i.e., c.2749 + 2dup and c.8689C>T. This case highlights the importance of considering LGMDR23 in patients presenting with weakness and white matter demyelination on MRI brain and further expands the gene variants spectrum of LGMDR23.

KEYWORDS

limb-girdle muscular dystrophy, LAMA2, merosin, case report, MDC1A, LGMDR23

1. Introduction

The laminin α2 (LAMA2) gene localizes on chromosome 6q22-q23, encoding the laminin-α2 chain, which connects with laminin-γ1 and -β1 chains and forms the heterotrimeric laminin-211 protein (1). The LAMA2 pathogenic variants can lead to merosin-deficient congenital muscular dystrophy type 1A (MDC1A) and limb–girdle muscular dystrophy (known as LGMDR23). Together, these two dystrophy types are jointly known as LAMA2-related muscular dystrophy. The former is mainly found in infants and characterized by the early onset of muscle weakness, hypotonia, and joint contractures appearing in infancy or before the first year after birth (2). The latter, while rarely reported, is mainly found in older children and even in adults characterized by proximal weakness of the limbs. In the case report, we reported novel compound heterozygous mutations of the LAMA2 gene in a middle-aged woman with LGMDR23.

2. Clinical presentation

A 52-year-old woman presented with dizziness for several days. A few days before the presentation, the patient developed dizziness but denied visual rotation and tinnitus, and denied gait disturbance. Further analysis of medical history revealed that the patient was developmentally normal, with her motor milestones similar to her peers. Since the age of

32 years, the weakness in both lower extremities gradually appeared, but it did not affect her daily life and work. Her son (aged 23 years) and parents had no weakness.

The examination was notable for muscle atrophy of both lower extremities (especially right gluteus maximus) with symmetric proximal weakness (right/left; Medical Research Council [MRC]): deltoids (5/5), biceps (5/5), hip flexors (4/4), hip abductors (4/4), knee flexors (4+/4+), knee extensors (4+/4+). Distal strength of both upper and lower limbs was intact (abductor pollicis brevis [5/5], first dorsal interosseous [5/5], abductor digiti minimi [5/5], finger extensors [5/5], tibialis anterior [5/5], tibialis posterior [5/5], and peroneus longus and brevis [5/5]) and neck flexion/extension was normal. No bulbar muscle weakness or dysarthria were noted. The tone was normal and no fasciculations and clinical myotonia were observed. Deep tendon reflexes were 1+ throughout with flexor plantar responses bilaterally. The remainder of the examination including cranial nerves, sensory modalities, and cerebellar testing was normal. She scored 27 out of 30 on Mini-Mental State Examination (primary school education; ≤20 reflects cognitive impairment), with the following subscores: orientation,

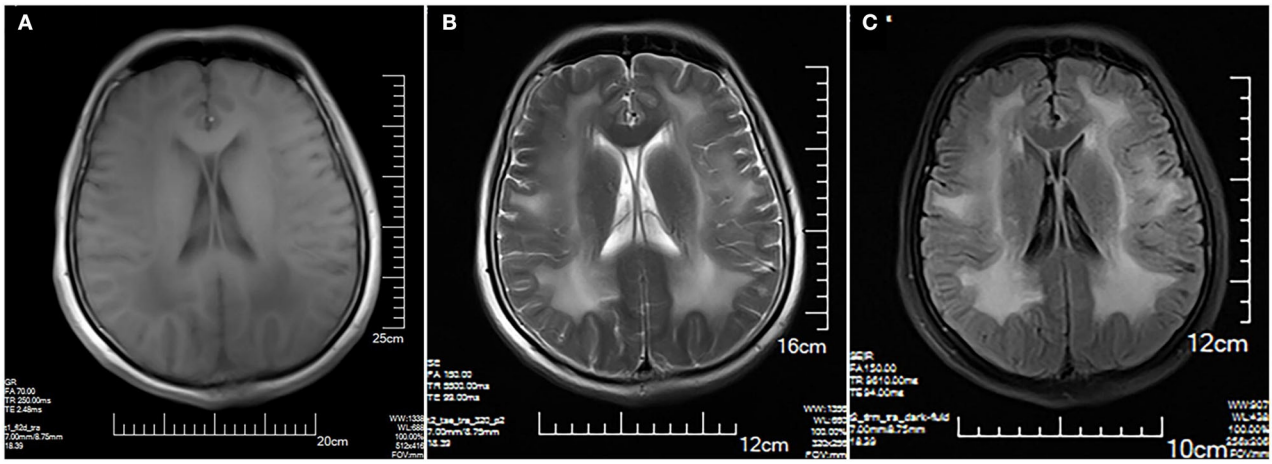

FIGURE 1
Brain MRI. Symmetrical sphenoid wings-like lesions are shown in bilateral lateral ventricles with slight hypointensity on axial T1 **(A)**; slight hyperintensity on axial T2 **(B)** and FLAIR **(C)**. No obvious abnormality in the sulcus and the gyrus was shown.

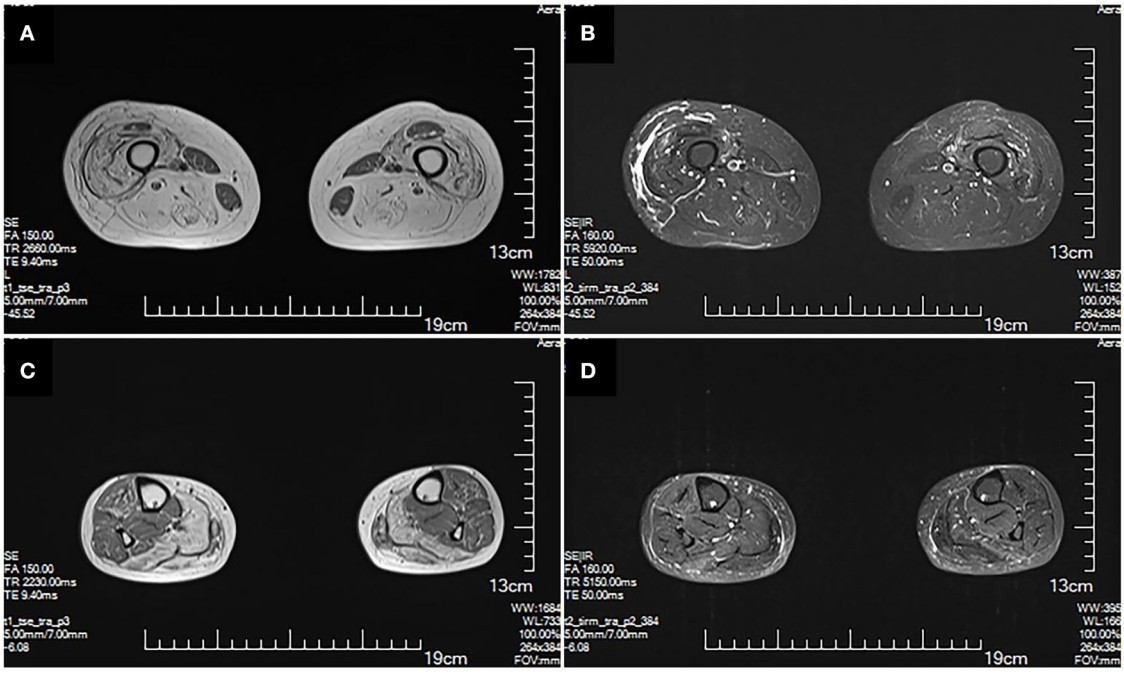

FIGURE 2
MRI of lower extremities. Muscle MRI T1 **(A)** and T2 **(B)** show diffuse atrophy and fatty degeneration within thigh muscles; the sartorius, the gracilis, and the rectus femoris muscles are selectively preserved. MRI T1 **(C)** and T2 **(D)** of calf muscles show diffuse atrophy and fatty degeneration in the soleus and the lateral head of gastrocnemius muscles. No signs of inflammation and edema are shown.

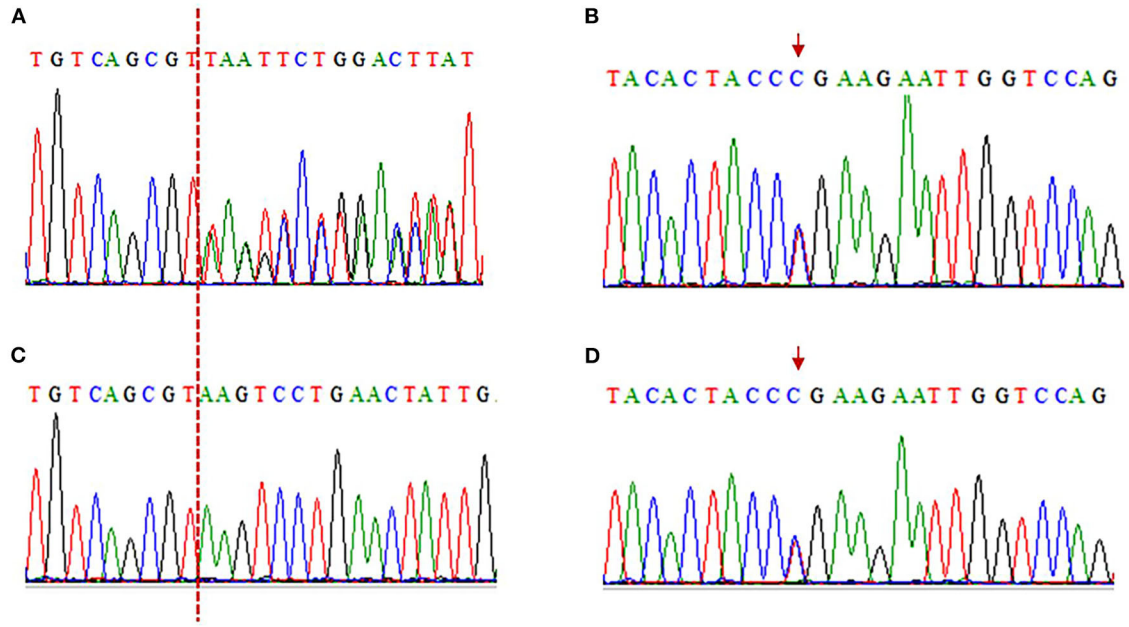

FIGURE 3
Electropherograms of sanger sequencing results. **(A, C)** The c.2749 + 2dup mutation is shown in the patient, while her son is wild type (A: patient, C: son). The red dotted line indicates the insertion position. c.2749 + 2dup (Reference sequence: TGTCAGCGT(-)AAGTCCTGAACTATTG; Mutated sequence: TGTCAGCGT(**T**)AAGTCCTGAACTATT). **(B, D)** The c.8689C>T truncated mutation is in the patient and her son (B: patient, D: son). The red arrows indicate mutation position. c.8689C>T (Reference sequence: TACACTACC**C**GAAGAATTGGTCCAG; Mutated sequence: TACACTACC**T**GAAGAATTGGTCCAG).

7/10; calculation, 5/5; recall, 6/6; language, 5/5; execute, 3/3; and visuospatial, 1/1.

The MRI brain showed symmetrical sphenoid wings-like lesions in bilateral lateral ventricles with slight hypointensity on T1 and slight hyperintensity on T2 and FLAIR (Figure 1). The MRI muscle showed diffuse atrophy and fatty degeneration in thigh muscles, soleus, and the lateral head of gastrocnemius muscles; the sartorius, the gracilis, and the rectus femoris muscles were selectively preserved (Figure 2).

Electromyography shows bilateral lower extremity quadriceps muscle damage. The muscle enzymes are slightly elevated (creatine kinase: 445 U/L; normal: 40–200 U/L). Next-generation sequencing (NGS) shows two loci variations in the LAMA2 gene, i.e., c.2749 + 2dup and c.8689C>T (Figure 3). The final diagnosis of LGMDR23 was made.

3. Discussion

The possible localizations in this patient with symmetrical lower extremity proximal weakness while lack of sensory involvement include anterior horn cells, motor nerve roots, neuromuscular junction, and muscles. The lack of fasciculations and fatigability makes anterior horn cell conditions (spinal muscular atrophy types 3 and 4) and neuromuscular junction disease (myasthenia gravis) less likely. The chronic condition with adolescence onset makes an inherited myopathy most likely, especially muscular dystrophy. Combined with white matter demyelination, both myotonic dystrophy (MD) (3) and LGMDR23 should be considered. MD is characterized by myotonia, progressive muscle weakness, and atrophy, and it can be genetically classified into MD 1 (caused by an expanded CTG triplet in DMPK on chromosome 19) and MD 2 (caused by the expansion of a CCTG tetramer in CNBP on chromosome 3). The former is characterized by weakness in the distal predominant limbs and grip myotonia, while the latter is characterized by progressive weakness in the proximal and distal limbs and variable mild grip myotonia (4). However, a lack of clinical myotonia makes MD less likely.

LGMDR23 is characterized by proximal weakness in childhood or even adulthood. Patients with LGMDR23 show a mild phenotype with late-onset proximal muscle weakness and delayed motor milestones but achieve independent ambulation (5, 6). As seen in this patient, the weakness rarely affects their life. In terms of the complaint of "dizziness," we do not believe it is the unique manifestation of LGMDR23 as it disappeared during her follow-up period.

The prevalence of LGMDR23 is unknown; however, it is considered to be very rare. A Chinese study of 130 patients with LAMA2-related muscular dystrophy reported that the frequency of LGMDR23 was 10.8% (14/130) (6). In one study including 128 patients with limb–girdle muscular dystrophy (LGMD), only three patients were due to the mutation of the LAMA2 gene (5). Another study that included 370 patients with LGMD showed that only five patients were due to the mutation of the LAMA2 gene (7). According to previous studies, the age of disease onset ranges from 1 to 56 years. All the reported patients showed mild symptoms and gained independent ambulation and remained ambulatory even in 69-year-old patients. All the reported patients presented with high levels of creatine kinase when diagnosed [from 600 U/L (8) to 2,000 U/L (5)]. A previous study showed the absence of merosin staining in MDC1A, but low levels of residual merosin can be seen in LGMDR23 (5). Unfortunately, immunohistochemistry staining of merosin has not been performed in this case. A few patients showed the involvement of the respiratory and cardiovascular systems.

TABLE 1 Results of bioinformatic analyses.

DNA Variant	Protein variant	Pathogenicity prediction							Splicing prediction
		LRT		MutationTaste		Fathmm-MKL_coding		CADD	SpliceAI
		Score	Pred	Score	Pred	Score	Pred		
c.2749 + 2dup	splicing	—	—	—	—	—	—	—	0.99
c.8689C>T	p.R2897X	0	D	1	A	0.847	D	58	0.01
Threshold		D: Deleterious; N: Neutral; U: Unknown		A: Disease causing automatic; D: Disease causing; N: Polymorphism; P: Polymorphism automatic		D: Deleterious; T: Tolerated		>10	>0.5

Score of LRT, MutationTaster, Fathmm-MKL_coding and SpliceAI: 0-1.
CADD, Combined Annotation Dependent Department; threshold: 10, the higher the value, the higher the probability that the mutation site is a harmful mutation.

However, most of the patients showed white matter anomalies on brain MRI. In addition, a recent study suggested that diffuse fatty infiltration can be seen in the adductor magnus and in the long head of the biceps femoris selectively.

With respect to the mutations in LGMDR23, the known pathogenic variants included frameshift, nonsense, copy number variations, splicing, missense, and small amino acid deletions, among which the splicing variant was previously assumed to be more common in patients with LGMDR23 (9). In a Chinese LGMDR23 cohort of 14 patients, 23 variants have been reported, among which 8 out of 23 were missense, 7 out of 23 were frameshift, 3 out of 23 were nonsense, 3 out of 23 were copy number variations, 1 out of 23 was splicing, and 1 out of 23 was small amino acid deletions (6). Next-generation sequencing (NGS) found two loci variations in the LAMA2 gene, i.e., c.2749 + 2dup and c.8689C>T in our patient. Both mutations are not reported in the HGMD database (Human Gene Mutation Database). The c.2749 + 2dup is a splicing mutation: a T was inserted between c.2749 + 1 and c.2749 + 2, which is equivalent to the occurrence of T duplication at c.2749 + 2. The c.2749 + 2dup mutation is located in the splicing region, which may cause a splicing change. Aprevious study reported that c.2749 + 2dup might be related to white matter abnormalities (10). In addition, we have made *in silico* analysis by spliceAI, which yielded a score of 0.99 (Table 1), suggesting that this mutation may affect splicing. The c.8689C>T is a truncation mutation, in which CGA mutates into TGA, resulting in the 2,897 arginine being changed to the stop codon and termination of translation at this position. Results of *in silico* analyses by LRT, MutationTaster, Fathmm-MKL, and CADD demonstrated that this mutation may be disease-causing (Table 1). Functionally, this mutation is located in exon 61, encoding concanavalin A-like lectin/glucanase domain|laminin G domain. Thus, this mutation may destruct the interaction between laminins and integrin-α7β1 and αβ-dystroglycan protein complexes, thus disrupting the connection between the basal and muscle cell membranes (11). It was reported that homozygous or compound heterozygous mutations were thought to be pathogenic in theory. Unfortunately, we were unable to perform a sequencing analysis of the patient's parents as they had died. However, as the proband's son carries only one of the two variants, it was confirmed that the proband is a compound heterozygous case. Thus, c.2749 + 2dup and c.8689C>T were considered to be responsible for the proximal weakness in the limbs in this case.

This case report highlights the importance of considering LGMDR23 in a patient presenting with weakness and white matter demyelination on an MRI of thr brain. It also highlights the importance of comprehensive physical examination in patients with white matter demyelination to find insidious muscle weakness. Moreover, we reported two potentially pathogenic mutations in a compound heterozygous state (c.2749 + 2dup and c.8689C>T) in the LAMA2 gene responsible for LGMD in a Chinese patient, which further expands the gene variants spectrum of LGMDR23. These results can refine prenatal diagnosis, genetic counseling, and treatments of patients with LGMDR23.

Data availability statement

The datasets presented in this article are not readily available because of ethical and privacy restrictions. Requests to access the datasets should be directed to the corresponding author.

Ethics statement

The studies involving human participants were reviewed and approved by the Ethical Review Board of Sichuan Provincial People's Hospital. Written informed consent to participate in this study was provided by the patients/participants. Written informed consent was obtained from the patient for the publication of any potentially identifiable images or data included in this article.

Author contributions

Drafting the manuscript: D-ZW, B-HL, and ST. Obtaining clinical data, critical reviewing of the manuscript, and final approval: All authors.

Acknowledgments

We thank Amplicongene (Shanghai, China) for the helpful bioinformatics analysis.

Conflict of interest

The authors declare that the research was conducted in the absence of any commercial or financial relationships that could be construed as a potential conflict of interest.

Publisher's note

All claims expressed in this article are solely those of the authors and do not necessarily represent those of their affiliated organizations, or those of the publisher, the editors and the reviewers. Any product that may be evaluated in this article, or claim that may be made by its manufacturer, is not guaranteed or endorsed by the publisher.

References

1. Helbling-Leclerc A, Zhang X, Topaloglu H, Cruaud C, Tesson F, Weissenbach J, et al. Mutations in the laminin alpha 2-chain gene (LAMA2) cause merosin-deficient congenital muscular dystrophy. *Nat Genet.* (1995) 11:216–8. doi: 10.1038/ng1095-216

2. O'Grady GL, Lek M, Lamande SR, Waddell L, Oates EC, Punetha J, et al. Diagnosis and etiology of congenital muscular dystrophy: We are halfway there. *Ann Neurol.* (2016) 80:101–11. doi: 10.1002/ana.24687

3. Minnerop M, Gliem C, Kornblum C. Current progress in CNS imaging of myotonic dystrophy. *Front Neurol.* (2018) 9:646. doi: 10.3389/fneur.2018.00646

4. Hamel JI. Myotonic dystrophy. *Continuum (Minneap Minn).* (2022) 28:1715–34. doi: 10.1212/CON.0000000000001184

5. Løkken N, Born AP, Duno M, Vissing J. LAMA2-related myopathy: Frequency among congenital and limb–girdle muscular dystrophies. *Muscle Nerve.* (2015) 52:547–53. doi: 10.1002/mus.24588

6. Tan D, Ge L, Fan Y, Chang X, Wang S, Wei C, et al. Natural history and genetic study of LAMA2-related muscular dystrophy in a large Chinese cohort. *Orphanet J Rare Dis.* (2021) 16:319. doi: 10.1186/s13023-021-01950-x

7. Magri F, Nigro V, Angelini C, Mongini T, Mora M, Moroni I, et al. The Italian limb–girdle muscular dystrophy registry: Relative frequency, clinical features, and differential diagnosis. *Muscle Nerve.* (2017) 55:55–68. doi: 10.1002/mus.25192

8. Chan SH, Foley AR, Phadke R, Mathew AA, Pitt M, Sewry C, et al. Limb–girdle muscular dystrophy due to LAMA2 mutations: diagnostic difficulties due to associated peripheral neuropathy. *Neuromuscul Disord.* (2014) 24:677–83. doi: 10.1016/j.nmd.2014.05.008

9. Oliveira J, Gruber A, Cardoso M, Taipa R, Fineza I, Gonçalves A, et al. LAMA2 gene mutation update: Toward a more comprehensive picture of the laminin-α2 variome and its related phenotypes. *Hum Mutat.* (2018) 39:1314–37. doi: 10.1002/humu.23599

10. Yamamoto-Shimojima K, Ono H, Imaizumi T, Yamamoto T. Novel LAMA2 variants identified in a patient with white matter abnormalities. *Hum Genome Var.* (2020) 7:16. doi: 10.1038/s41439-020-0103-5

11. Barraza-Flores P, Bates CR, Oliveira-Santos A, Burkin DJ. Laminin and Integrin in LAMA2-Related Congenital Muscular Dystrophy: From Disease to Therapeutics. *Front Mol Neurosci.* (2020) 13:1. doi: 10.3389/fnmol.2020.00001

frontiers | Frontiers in Neurology

TYPE Case Report
PUBLISHED 09 March 2023
DOI 10.3389/fneur.2023.1124540

Check for updates

OPEN ACCESS

EDITED BY
Christian Krarup,
University of Copenhagen, Denmark

REVIEWED BY
Hiroyuki Nodera,
Tenri Hospital, Japan
Yuwei Da,
Xuanwu Hospital, Capital Medical University, China

*CORRESPONDENCE
Yanmin Kan
✉ wuxiny_2009@163.com
Jing Zhang
✉ xiaoyan20110316@126.com

†These authors have contributed equally to this work and share first authorship

SPECIALTY SECTION
This article was submitted to Neuromuscular Disorders and Peripheral Neuropathies, a section of the journal Frontiers in Neurology

RECEIVED 17 December 2022
ACCEPTED 14 February 2023
PUBLISHED 09 March 2023

CITATION
Li Q, Chen Q, Zhang T, Xu Y, Kan Y and Zhang J (2023) Case report: Anti-CNTN1 antibody-associated nodopathies disease with asymmetric onset. *Front. Neurol.* 14:1124540. doi: 10.3389/fneur.2023.1124540

COPYRIGHT
© 2023 Li, Chen, Zhang, Xu, Kan and Zhang. This is an open-access article distributed under the terms of the Creative Commons Attribution License (CC BY). The use, distribution or reproduction in other forums is permitted, provided the original author(s) and the copyright owner(s) are credited and that the original publication in this journal is cited, in accordance with accepted academic practice. No use, distribution or reproduction is permitted which does not comply with these terms.

Case report: Anti-CNTN1 antibody-associated nodopathies disease with asymmetric onset

Qian Li[1,2,3,4†], Qing Chen[5†], Ting Zhang[5], Ying Xu[5], Yanmin Kan[2,3,4,6*] and Jing Zhang[1,2,3,4,5,6*]

[1]Neurology Department, The Third Central Hospital of Tianjin, Tianjin, China, [2]Tianjin Key Laboratory of Extracorporeal Life Support for Critical Diseases, Tianjin, China, [3]Artificial Cell Engineering Technology Research Center, Tianjin, China, [4]Tianjin Institute of Hepatobiliary Disease, Tianjin, China, [5]The Third Central Clinical College of Tianjin Medical University, Tianjin, China, [6]The Third Central Clinical College of Nankai University, Tianjin, China

Anti-contactin-1 (CNTN1) IgG4 antibody-associated nodopathies is an autoimmune antibody-mediated peripheral neuropathy with a unique clinical presentation, pathophysiology, electrophysiology, and therapeutic response. The critical histopathological features are a dense lymphoplasmacytic infiltrate, a storiform pattern of fibrosis, and obliterative phlebitis. Here, a 62-year-old male patient presented with subacute unilateral limb onset, progressive exacerbation, marked weakness of the extremities, cranial, and autonomic nerve involvement. Neurophysiology showed slowed motor nerve conduction velocity (MCV), prolonged distal motor delay (DML), slowed sensory nerve conduction velocity (SCV), decreased sensory nerve activity potential (SNAP) amplitude, decreased amplitude of bilateral neuromotor conduction, abnormal cutaneous sympathetic response (SSR) in both lower extremities, axonal damage, prolonged F-wave latency, and discrete waves. In the initial phase, there was a response to intravenous immunoglobulin (IVIG), and corticosteroids and rituximab were also effective. After 1 year follow-up, the patient improved significantly. This article reports on a patient with nodular disease with anti-contactin-1 (CNTN1) IgG4 antibodies and reviews the literature to improve clinicians' understanding of the disease.

KEYWORDS

contactin-1, Ranvier's, autoimmune nodopathies, paranodal, peripheral neuropathy

1. Introduction

Anti-contactin-1 (CNTN1) IgG4 antibody-associated nodopathies is an autoimmune antibody-mediated peripheral neuropathy. In recent years, some important cell adhesion molecules in the Ranvier's-related region have become the research focus of biomarkers for chronic inflammatory demyelinating polyradiculoneuropathy (CIDP) (1–3). Some scholars put forward the concept of nodo-paranodopathy disease (4, 5) from the perspective of microstructure, however, the latest guidelines (6) clearly state that protein antibody-positive diseases associated with paranodopathy are named autoimmune nodopathies. In this article, we analyzed a patient with positive anti-contactin-1 IgG4 antibody, and reviewed the related literature to improve clinicians' understanding, diagnosis, and treatment of this kind of disease.

TABLE 1 Medical research council (MRC) scale for muscle examination.

Functions assessed
Upper extremity: wrist flexion, forearm flexion, shoulder abduction
Lower extremity: ankle dorsiflexion, knee extension, hip flexion
Score for each movement
0—No visible contraction
1—Visible muscle contraction, but no limb movement
2—Active movement, but not against gravity
3—Active movement against gravity
4—Active movement against gravity and resistance
5—Active movement against full resistance
Maximum score: 60 (four limbs, maximum of 15 points per limb)
Minimum score: 0 (quadriplegia)

2. Case presentation

2.1. Medical history

A 62-year-old man was admitted for treatment of progressive limb weakness over 4 months. He suddenly felt weakness in the right lower limb during farming over 4 months ago, accompanied by pain and cramps in the calf. He received treatment in the community for 4 days, and the above symptoms disappeared. One week after the initial onset of the weakness, the patient began to have left-sided angle of mouth, salivation, chewing difficulties, difficulty in closing the right eye, slurred speech, transient diplopia, ataxia, weakened tendon reflex of the right limb, and the MRC grade of the right limb muscle was 4 (Table 1), with CT examination showing low-density lesions in the bilateral basal ganglia area. The patient's symptoms progressed after antithrombotic treatment, with recurrence of transient diplopia. He was discharged after 2 weeks of hospitalization. At 9 weeks after the initial onset, after suffering from upper respiratory tract infection, pain occurred in the lower parts of both lower limbs, and the distal knuckles and toes of both lower limbs continued to have numbness. The distal numbness of the limbs gradually spread to the proximal end, accompanied by weakness of both feet, followed by weakness of the limbs, mainly the distal limbs. At 13 weeks after initial onset, he had difficulty in passing stool and needed enema to help, and 15 weeks after initial onset, he had difficulty in passing urine. He was in good health in the past and had a history of COVID-19 vaccination 10 days before the onset of symptoms. He did not have a family history of genetic disease or history of exposure to poisons.

2.2. Admission physical examination

Upon admission, the following were observed: normal cognitive function, the speech was unclear, bilateral forehead lines disappeared, could not wrinkle forehead, bilateral eye closure was weak and right side was obvious, the right nasolabial groove was shallow, the bilateral drum gills were weak, the strength of the right side teeth was weak, the angle of mouth was left, the tongue body was thin, the tongue muscle strength was weak, with right tongue muscle tremor. The masticatory muscle was slightly weak, the pharyngeal reflex disappeared, shoulder shrug and neck were powerful, the neck flexion was weak. Limb muscle strength (MRC) grades: proximal left upper limb: V, distal: II+; left lower limb proximal extensor: IV+, flexor: III, distal: II; proximal right upper limb: V, distal: II+; proximal extensor of right lower limb: IV−, flexor: II+, distal: 0. The muscle tension of both lower limbs decreased, the tendon reflex and abdominal wall reflex of the limbs disappeared. The ataxia of both upper limbs was unstable and both lower limbs cannot be completed. Stocking glove hypoesthesia was observed for vibratory and cold stimuli.

2.3. Auxiliary examination

Upon auxiliary examination, the following were observed: blood test examination: blood routine, blood coagulation routine; blood glucose, liver and kidney function, thyroid function, tumor markers, serum protein electrophoresis, and vitamin B12 were not significantly abnormal. Cerebrospinal fluid (CSF) protein level: 618.91 mg/dL (normal value 15–45 mg/dL), white blood cell count: 6/μL (normal value 0–8/μL). The neuroelectrophysiology is shown in Table 2. An MRI of the cervical plexus is shown in Figure 1A, an MRI of the lumbosacral plexus in Figure 1B, and musculoskeletal ultrasounds are shown in Figure 2.

2.4. Admission diagnosis

The diagnosis upon admission was as follows: acute inflammatory demyelinating polyradiculoneuropathy (AIDP)?/ACIDP?/Autoimmune nodopathies? After IVIG treatment, the limb weakness of the patients improved. Blood antibody report: anti-CNTN1 antibody IgG4 positive 1:100, CSF corresponding antibody 1:32. Diagnosis: Autoimmune nodopathies. The treatment was 500 mg methylprednisolone intravenous shock therapy and hormone reduction 5 days after surgery with 48 mg methylprednisolone orally administered. The patient's fatigue symptoms gradually improved, but he was still unable to walk, and improvement of numbness was not obvious.

After discharge, the patient's condition was stable and he was readmitted to the hospital for rituximab treatment because of his inability to walk. Upon follow-up 1 year after onset of disease, he was able to walk normally and felt numbness only in the fingertips. The changes in muscle strength during the three admissions are shown in Table 3. EMG comparisons for the three admissions are shown in Table 2.

3. Discussion

The latest guideline (6) names diseases positive for antibodies against Ranviers-related proteins as autoimmune nodopathies and no longer as a CIDP subtype. Positive antibodies to contactin-1 (CNTN1), a cell adhesion molecule at the axial end of the paracord region, may cause nodopathies disease,

TABLE 2 Results of nerve conduction study and F-wave of the anti-contaction-1 IgG4 antibody associated autoimmune nodopathies.

Nerves	Time of onset			Normal values
	4 months after onset of disease (Left/right)	6 months after onset of disease (Left/right)	11 months after onset of disease (Left/right)	
Median nerve				
CMAP (mV)	1.2 91%↓/1.4 91%↓	ND/1.0 93%↓	3.5 73%↓/3.1 76%↓	≥7.0
DML (ms)	22.40/21.20	ND/19.43	10.57/10.89	≤4.1
MCV (m/s)	18.8 69%↓/18.8 69%↓	ND/20.1 67%↓	40.2 33%↓/36.5 39%↓	≥51.0
SCV (m/s)	ND/32.0 42%↓	34.7 34%↓/ND	26.5 52%↓/30.0 40%↓	≥41.8
SNAP (μV)	ND/5.0 86%↓	2.6 93%↓/ND	1.5 95%↓/2.2 93%↓	≥12.7
F-wave latency (ms)	12.3/ND	ND/27.4	36.4/37.6	≤31.0
F-wave occurrence rat (%)	0/0	ND/25	85/75	≥73
Ulnar nerve				
CMAP (mV)	5.6 67%↓/4.3 75%↓	ND/2.6 80%↓	5.0 58%↓/5.4 55%↓	≥7.0
DML (ms)	4.58 76%↑/6.09 89%↑	ND/10.78	5.31/5.83	≤3.2
MCV (m/s)	–/–	ND/18.1 73%↓	40.0 40%↓/38.0 43%↓	≥56.0
SCV (m/s)	ND/–	–/ND	37.6 31%↓/35.2 35%↓	≥44.2
SNAP (μV)	ND/–	NR/ND	2.3 88%↓/1.5 92%↓	≥6.9
F-wave latency (ms)	71.8/26.9	ND/24.9	ND/36.4	–
F-wave occurrence rat (%)	90/0	ND/45	ND/90	–
Tibial nerve				
CMAP (mV)	ND/ 0.3 97%↓	ND/ND	NR/0.3 98%↓	≥4
DML (ms)	ND/ 34.53	ND/ND	ND/6.41 64%↓	≤5.1
MCV (m/s)	ND/20.6 64%↓	ND/ND	ND/ND	≥40.5
SCV (ms)	ND/ND	ND/ND	ND/ND	≥35.1
SNAP (μV)	ND/–	ND/ND	NR/NR	≥0.4
F-wave latency (ms)	17.1 /65.4	ND/ND	ND/ND	≤51.0
F-wave occurrence rat (%)	10/35	ND/ND	ND/ND	≥80
Peroneal nerve				
CMAP (mV)	ND/–	ND/ND	1.2 91%↓/0.7 95%↓	≥3.6
DML (ms)	ND/NR	ND/ND	5.42/6.04	≤4.75
MCV (m/s)	ND/–	ND/ND	–/–	≥36.8
SCV (ms)	ND/–	ND/ND	ND/ND	≥46.5
NAP (μV)	ND/–	ND/ND	NR/NR	≥0.8
Skin sympathetic reflexes				
DML (ms, Upper limb)	1,350/1,412	NR/NR	NR/NR	–
DML (ms, Lower limbs)	NR/NR	NR/NR	NR/NR	–
Transient reflex				
DML (ms)	5.0/5.94	3.65 / 6.51	2.34/2.92	–
CMAP (mV)	0.2↓/0.1↓	0.2↓/ 0.3↓	0.7/0.7	–

ND, not examined; NR, not elicited; CMAP, compound muscle action potential; DML, motor terminal latency; MCV, motor nerve conduction velocity; SCV, sensory nerve conduction velocity; SNAP, sensory nerve action potential; ↑, higher than normal; ↓, lower than normal; –, none.

with unique clinical manifestations, pathophysiological, and electrophysiological changes. Clinical studies found that among patients with nodopathies, the positive proportion of CNTN1 antibody ranges from 2.4 to 6.5% (7–9). In 2018, Hashimoto et al. (10) reviewed 20 patients with CIDP who were positive for anti-CNTN1 antibodies, and reported a relatively high age

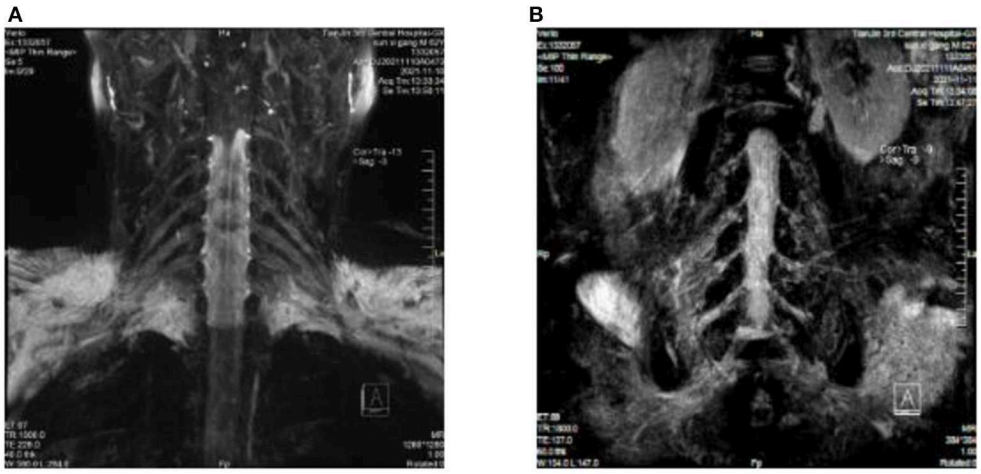

FIGURE 1
(A) Cervical plexus MRI: fluid attenuation inversion recovery (FLAIR) shows slightly thickened bilateral nerve roots at C4/C5–C6/C7. **(B)** Lumbosacral plexus MRI: fluid attenuation inversion recovery (FLAIR) shows bilateral nerve root thickening at the L1/L2–L4/L5 intervertebral space, with slightly higher signal intensity, especially at L2/L3–L4/L5.

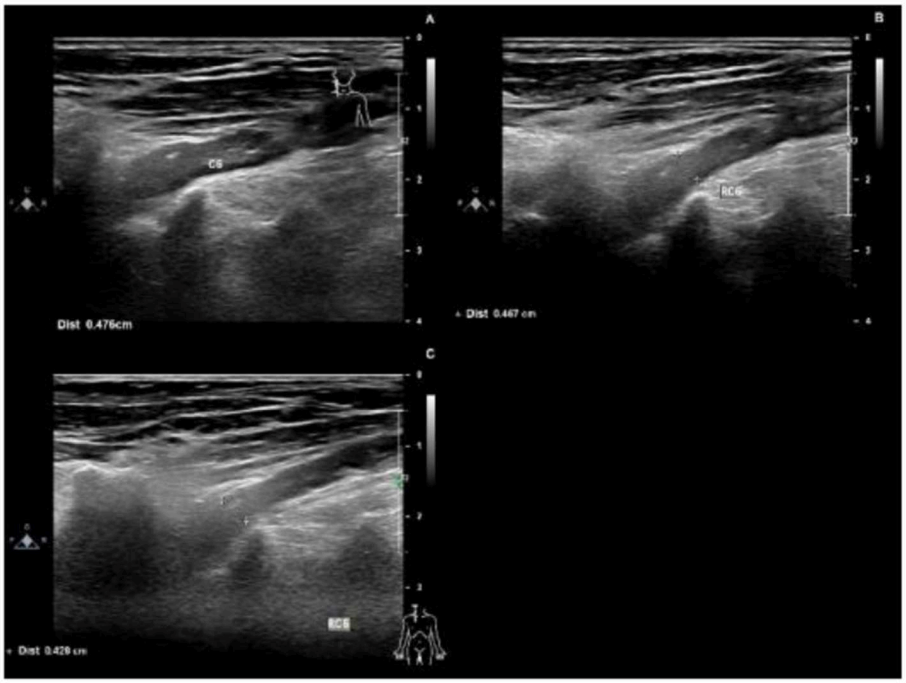

FIGURE 2
Ultrasounds 4 months after the onset of the disease, the right C6 nerve root was thickened, with a thickness of 0.476 cm **(A)**. 6 months after the onset of the disease, the right C6 nerve root was thickened, with a thickness of 0.467 cm **(B)**. 11 months after the onset of the disease, the right C6 nerve root was thickened, with a thickness of 0.426 cm **(C)**.

of onset of 63.0 ± 13.5 years (range 33–81 years, 80% >60 years), with a male-to-female ratio of 2:1. Our patient was an elderly male, consistent with the epidemiological features of the disease. Antecedent infections or vaccinations may also be a trigger for autoimmune nodopathies. In 2022, a NF186+ autoimmune nodopathies case was reported following COVID-19 vaccination (11). Some studies suggest (12, 13) that this may be a result of interactions between the susceptible vaccinated subject and various vaccine components. The mechanisms involved may be molecular patterns, i.e., significant similarities between certain disease-causing elements contained in vaccines and specific human proteins. Our patient developed muscle weakness symptoms after receiving a COVID-19 vaccine, before the onset of the disease, suggesting that COVID-19 vaccination may be the causative agent of CNTN1+, and the speculated mechanism is similar to NF186+, as described above. The clinical manifestation of

TABLE 3 Change in muscle strength between patient admissions.

(Treatment time/muscle strength)	Left upper extremity		Left lower extremity		Right upper extremity		Right lower extremity	
	Proximal	Distal	Proximal	Distal	Proximal	Distal	Proximal	Distal
2021.10.21	V	II–III	III	II	V	II–III	II+	0
2021.10.27 (IVIG treatment for 3 days)	V	III	III+	II	V	III	III-	0
2021.10.30 (Hormone therapy for 3 days)	V	III+	IV-	II	V	III+	III	0
2021.11.04	V	III+	IV-	II	V	III+	III	0
2021.11.14	V	III+	IV-	II	V	III+	III	0
2021.12.15	V	IV	IV-	II	V	IV-	III+	I–II
2021.12.22 (Rituximab treatment for 1 day)	V	IV	IV	II	V	IV+	IV	I–II
2021.12.27	V	IV+	IV+	II	V	IV+	IV	II
2022.09.05	V	IV+	IV+	III	V	IV+	IV+	III

nodopathies with positive anti-CNTN1 antibody is unique and is different from classical CIDP. CNTN1 antibody-positive patients with nodopathies mostly have subacute onset or rapid progression after chronic onset, mainly manifested as symmetrical proximal and distal limb weakness and sensory abnormalities, which may be accompanied by tremors and sensory ataxia (14–16). The clinical symptoms are closely related to the titer of IgG antibody and the deposition density of IgG in node areas (7). Significant sensory ataxia was found in all patients reported in Japan, but not in patients reported in Spain, suggesting that ethnic or genetic factors may affect antibody-binding epitopes, resulting in clinical heterogeneity (14). Cortese et al. (17) found cranial nerve involvement and respiratory failure in 1 of 3 anti-CNTN1 IgG4 antibody-positive patients. The patient in our case had an unusual subacute unilateral limb onset. The course of the disease was a sudden frustration, manifested as remission-relapse-incomplete remission, and finally progressing to bilateral cranial nerve asymmetry and relative symmetrical limb involvement. Not only was there limb weakness and sensory abnormalities, but also symptoms of cranial nerves and autonomic nerve involvement. The course of the patient was not completely consistent with that reported in other literature. The involvement of cranial nerves and autonomic nerves may be a result of by conduction block, and the mechanism is similar to limb motor nerves.

Protein-cell separation is present in 80–90% of typical CIDP patients. The latest literature suggests that the reference upper limit of cerebrospinal fluid total protein (CSF-TP) should be higher than 45 mg/dl (18). The cerebrospinal fluid (CSF) protein of patients with nodopathies associated with positive anti-CNTN1 antibody is more obvious (16). In addition, MRI of CNTN1 antibody-positive patients may show symmetrical diffuse edema, thickening of nerve roots in the brachial plexus and lumbosacral plexus, as well as edema thickening of nerve roots in musculoskeletal ultrasounds. The mechanism for these may be a lack of blood-nerve barrier at the nerve roots, which are highly susceptible to damage by circulating immune antibodies. The cerebrospinal fluid protein of this patient was 618 mg/dl. MRI and musculoskeletal B-ultrasounds were consistent with the above findings. The musculoskeletal ultrasound showed no significant changes before and after treatment (Table 3). Considering that the improvements observed in auxiliary examinations lagged behind the clinical manifestations, further follow-up observations can be made.

The electrophysiological characteristics of anti-CNTN1 antibody-positive patients with nodopathies were as follows: MCV slowed down, DML prolonged, F wave latency prolonged and conduction block occurred, axonal damage appeared in the early stage, SCV slowed down, and SNAP amplitude decreased (15, 19). The pathological basis of these changes is that the structure of the paranodal region is destroyed, which affects the normal conduction of nerve pulses in myelinated fibers. The electrophysiology of this patient showed that MCV slowed down, DML prolonged, SCV slowed down, SNAP amplitude decreased, bilateral nerves motor conduction amplitude decreased, SSR abnormality for both lower limbs, axonal damage, and F wave latencies prolonged. The neurophysiological manifestations were consistent with those of patients with anti-CNTN1 antibody-positive nodopathies diseases.

The typical pathological manifestations of CIDP were not found in the gastrocnemius nerve biopsy of patients with CNTN1 antibody-positive nodopathies. Destruction of the paranodal structure and separation of the myelin sheath from the axon were observed under an electron microscope (20–22), suggesting that attack by the CNTN1 antibody on the paranodal region is the pathogenesis of the disease.

Most CNTN1 antibodies are mainly IgG4 subtype, with lower binding to Fc receptors, and do not participate in the complement activation pathway (23), with the response to IVIG treatment poor. However, IgG1, IgG2, and IgG3 subtypes can also coexist in CNTN1 IgG4 positive patients, and the latter subtype can induce complementary deposition and activation. Therefore, CNTN1 IgG4 positive patients may respond to IVIG treatment at the initial stage (24). Corticosteroids, plasma exchange, and rituximab are effective in patients with CNTN1 antibody-positive nodopathies

disease. According to studies in Japan (14), corticosteroid therapy is effective in 73% of CNTN1 IgG4 positive patients. Plasma exchange improves the treatment rate of CNTN1 antibody-positive patients by removing related antibodies in the plasma. As a targeted drug, rituximab can target the IgG4 antibody, achieving good therapeutic effects by depleting B lymphocytes and downregulating humoral immune responses (25, 26). Our patient had a good response to corticosteroids and rituximab treatment.

4. Conclusion

CNTN1 antibody-positive nodopathies is due to the autoimmune antibody attacking the paranodal region of Ranvier, which destroys the composition of the complex in this region and leads to demyelination of myelinated nerve fibers. Patients with CNTN1 antibody-positive nodopathies have unique clinical manifestations, including unilateral limb onset, motor and sensory system involvement, tremor, sensory ataxia, cranial nerve, and autonomic nerve involvement, significantly increased CSF protein, and increased erythrocyte sedimentation rate. MRI and nerve ultrasound showed symmetrical diffuse edema of brachial and lumbosacral plexus nerve roots, while neuroelectrophysiology showed a slowed MCV, prolonged F wave latencies, and conduction block. Axonal damage can occur in the early stage. Most patients respond poorly to IVIG, but some patients respond well to IVIG in the early stage of the disease. Corticosteroids, plasma exchange, and rituximab are all effective in patients with positive CNTN1 antibody. At present, the clinical understanding of paranodal-related antibodies is still insufficient, and standardized treatment can reduce the disability rate and improve the cure rate. Therefore, in the process of diagnosis and treatment of nodopathies diseases, we should screen the antibodies against paranodal proteins in time, to improve the accuracy of diagnosis and guide treatment.

Data availability statement

The original contributions presented in the study are included in the article/supplementary material, further inquiries can be directed to the corresponding authors.

Ethics statement

The studies involving human participants were reviewed and approved by the Third Central Hospital of Tianjin. The patients/participants provided their written informed consent to participate in this study. Written informed consent was obtained from the individual(s) for the publication of any potentially identifiable images or data included in this article.

Author contributions

All authors contributed to the article and agreed to the submitted version.

Funding

This work was supported by Tianjin Science and Technology Commission Major Special Project for Prevention and Treatment of Major Diseases (19ZXDBSY00100) and National Natural Science Foundation of China Incubation Project, Tianjin Third Central Hospital and Tianjin Key Laboratory of *In Vitro* Life Support for Critical Diseases (2019YNR5).

Conflict of interest

The authors declare that the research was conducted in the absence of any commercial or financial relationships that could be construed as a potential conflict of interest.

Publisher's note

All claims expressed in this article are solely those of the authors and do not necessarily represent those of their affiliated organizations, or those of the publisher, the editors and the reviewers. Any product that may be evaluated in this article, or claim that may be made by its manufacturer, is not guaranteed or endorsed by the publisher.

References

1. Mathey EK, Park SB, Hughes RAC, Pollard JD, Armati PJ, Barnett MH, et al. Chronic inflammatory demyelinating polyradiculoneuropathy: from pathology to phenotype. *J Neurol Neurosurg Psychiatry.* (2015) 86:973–85. doi: 10.1136/jnnp-2014-309697

2. Poliak S, Peles E. The local differentiation of myelinated axons at nodes of Ranvier. *Nat Rev Neurosci.* (2003) 4:968–0. doi: 10.1038/nrn1253

3. Querol L, Illa I. Paranodal and other autoantibodies in chronic inflammatory neuropathies. *Curr Opin Neurol.* (2015) 28:474–9. doi: 10.1097/WCO.0000000000000233

4. Uncini A, Susuki K, Yuki N. Nodo-paranodopathy: beyond the demyelinating and axonal classification in anti-ganglioside antibody-mediated neuropathies. *Clin Neurophysiol.* (2013) 124:1928–34. doi: 10.1016/j.clinph.2013.03.025

5. Uncini A, Kuwabara S. Nodopathies of the peripheral nerve: an emerging concept. *J Neurol Neurosurg Psychiatry.* (2015) 86:1186–95. doi: 10.1136/jnnp-2014-310097

6. Van den Bergh P, van Doorn PA, Hadden R, Avau B, Vankrunkelsven P, Allen JA, et al. European Academy of Neurology/Peripheral Nerve Society guideline on diagnosis and treatment of chronic inflammatory demyelinating polyradiculoneuropathy: report of a joint task force-second revision. *J Peripher Nerv Syst.* (2021) 26:242–68. doi: 10.1111/jns.12455

7. Devaux JJ, Odaka M, Yuki N. Nodal proteins are target antigens in Guillain-Barre syndrome. *J Peripher Nerv Syst.* (2012) 17:62–71. doi: 10.1111/j.1529-8027.2012.00372.x

8. Querol L, Nogales-Gadea G, Rojas-Garcia R, Diaz-Manera J, Pardo J, Ortega-Moreno A, et al. Neurofascin IgG4 antibodies in CIDP associate with disabling tremor and poor response to IVIg. *Neurology.* (2014) 82:879–86. doi: 10.1212/WNL.0000000000000205

9. Devaux JJ, Miura Y, Fukami Y, Inoue T, Manso C, Belghazi M, et al. Neurofascin-155 IgG4 in chronic inflammatory demyelinating polyneuropathy. *Neurology.* (2016) 86:800–7. doi: 10.1212/WNL.0000000000002418

10. Hashimoto Y, Ogata H, Yamasaki R, Sasaguri T, Ko S, Yamashita K, et al. Chronic inflammatory demyelinating polyneuropathy with concurrent membranous nephropathy: an anti-paranode and podocyte protein antibody study and literature survey. *Front Neurol.* (2018) 9:997. doi: 10.3389/fneur.2018.00997

11. Wen S, Huang K, Zhu H, Li P, Zhou L, Feng L. Case report: anti-NF186+ CIDP after receiving the inactivated vaccine for coronavirus disease (COVID-19). *Front Neurol.* (2022) 13:838222. doi: 10.3389/fneur.2022.838222

12. Bagella CF, Corda DG, Zara P, Elia AE, Ruiu E, Sechi E, et al. Chronic Inflammatory Demyelinating Polyneuropathy after ChAdOx1 nCoV-19 Vaccination. *Vaccines-Basel.* (2021) 9:1502. doi: 10.3390/vaccines9121502

13. Vojdani A, Kharrazian D. Potential antigenic cross-reactivity between SARS-CoV-2 and human tissue with a possible link to an increase in autoimmune diseases. *Clin Immunol.* (2020) 217:108480. doi: 10.1016/j.clim.2020.108480

14. Miura Y, Devaux JJ, Fukami Y, Manso C, Belghazi M, Wong AH, et al. Contactin 1 IgG4 associates to chronic inflammatory demyelinating polyneuropathy with sensory ataxia. *Brain.* (2015) 138(Pt 6):1484–91. doi: 10.1093/brain/awv054

15. Doppler K, Appeltshauser L, Wilhelmi K, Villmann C, Dib-Hajj SD, Waxman SG, et al. Destruction of paranodal architecture in inflammatory neuropathy with anti-contactin-1 autoantibodies. *J Neurol Neurosurg Psychiatry.* (2015) 86:720–8. doi: 10.1136/jnnp-2014-309916

16. Querol L, Nogales-Gadea G, Rojas-Garcia R, Martinez-Hernandez E, Diaz-Manera J, Suarez-Calvet X, et al. Antibodies to contactin-1 in chronic inflammatory demyelinating polyneuropathy. *Ann Neurol.* (2013) 73:370–80. doi: 10.1002/ana.23794

17. Cortese A, Lombardi R, Briani C, Callegari I, Benedetti L, Manganelli F, et al. Antibodies to neurofascin, contactin-1, and contactin-associated protein 1 in CIDP: Clinical relevance of IgG isotype. *Neurol-Neuroimmunol.* (2020) 7:e639. doi: 10.1212/NXI.0000000000000639

18. Breiner A, Bourque PR, Allen JA. Updated cerebrospinal fluid total protein reference values improve chronic inflammatory demyelinating polyneuropathy diagnosis. *Muscle Nerve.* (2019) 60:180–3. doi: 10.1002/mus.26488

19. Fehmi J, Scherer SS, Willison HJ, Rinaldi S. Nodes, paranodes and neuropathies. *J Neurol Neurosurg Psychiatry.* (2018) 89:61–71. doi: 10.1136/jnnp-2016-315480

20. Koike H, Katsuno M, Sobue G. Deciphering the mechanism and spectrum of chronic inflammatory demyelinating polyneuropathy using morphology. *Clin Exp Neuroimmunol.* (2018) 9:35–46. doi: 10.1111/cen3.12442

21. Kuwabara S, Misawa S, Mori M. Paranodal destruction and axo-glial dysjunction in a subtype of CIDP with anticontaction-1 antibodies. *J Neurol Neurosurg Psychiatry.* (2015) 86:707. doi: 10.1136/jnnp-2015-310448

22. Koike H, Kadoya M, Kaida K, Ikeda S, Kawagashira Y, Iijima M, et al. Paranodal dissection in chronic inflammatory demyelinating polyneuropathy with anti-neurofascin-155 and anti-contactin-1 antibodies. *J Neurol Neurosurg Psychiatry.* (2017) 88:465–73. doi: 10.1136/jnnp-2016-314895

23. Nirula A, Glaser SM, Kalled SL, Taylor FR. What is IgG4? A review of the biology of a unique immunoglobulin subtype. *Curr Opin Rheumatol.* (2011) 23:119–24. doi: 10.1097/BOR.0b013e3283412fd4

24. Appeltshauser L, Weishaupt A, Sommer C, Doppler K. Complement deposition induced by binding of anti-contactin-1 auto-antibodies is modified by immunoglobulins. *Exp Neurol.* (2017) 287(Pt 1):84–90. doi: 10.1016/j.expneurol.2016.10.006

25. Kira J, Yamasaki R, Ogata H. Anti-neurofascin autoantibody and demyelination. *Neurochem Int.* (2019) 130:104360. doi: 10.1016/j.neuint.2018.12.011

26. Querol L, Devaux J, Rojas-Garcia R, Illa I. Autoantibodies in chronic inflammatory neuropathies: diagnostic and therapeutic implications. *Nat Rev Neurol.* (2017) 13:533–47. doi: 10.1038/nrneurol.2017.84

frontiers | Frontiers in Neurology

TYPE Case Report
PUBLISHED 22 March 2023
DOI 10.3389/fneur.2023.1138668

Check for updates

OPEN ACCESS

EDITED BY
Giovanni Meola,
University of Milan, Italy

REVIEWED BY
Claudia Ricci,
University of Siena, Italy
Dongsheng Fan,
Peking University Third Hospital, China

*CORRESPONDENCE
Ewa Zapalska
✉ ewa.zapalska9@gmail.com

SPECIALTY SECTION
This article was submitted to Neuromuscular Disorders and Peripheral Neuropathies, a section of the journal Frontiers in Neurology

RECEIVED 06 January 2023
ACCEPTED 17 February 2023
PUBLISHED 22 March 2023

CITATION
Zapalska E, Wrzesień D and Stępień A (2023) Case report: Flail leg syndrome in familial amyotrophic lateral sclerosis with L144S *SOD1* mutation. *Front. Neurol.* 14:1138668. doi: 10.3389/fneur.2023.1138668

COPYRIGHT
© 2023 Zapalska, Wrzesień and Stępień. This is an open-access article distributed under the terms of the Creative Commons Attribution License (CC BY). The use, distribution or reproduction in other forums is permitted, provided the original author(s) and the copyright owner(s) are credited and that the original publication in this journal is cited, in accordance with accepted academic practice. No use, distribution or reproduction is permitted which does not comply with these terms.

Case report: Flail leg syndrome in familial amyotrophic lateral sclerosis with L144S *SOD1* mutation

Ewa Zapalska*, Dominika Wrzesień and Adam Stępień

Department of Neurology, Military Institute of Medicine – National Research Institute, Warsaw, Poland

We observed a Polish family with familial amyotrophic lateral sclerosis with heterozygous L144S *SOD1* mutation, which manifested clinically as flail leg syndrome. Flail leg syndrome is a rare phenotype of amyotrophic lateral sclerosis, with slow progression, long survival, and predominance of lower motor neuron signs at onset, as a triad of distal paresis, muscle atrophy, and hyporeflexia/areflexia, confined to the lower limbs for an extended period of time. Although familial amyotrophic lateral sclerosis is usually associated with a worse prognosis than the sporadic form of the disease, the clinical course of the disease in patients with L144S *SOD1* mutation is benign, with slow progression and long survival. This unique case report provides an in-depth clinical analysis of all of the symptomatic members of a family, who were diagnosed with amyotrophic lateral sclerosis in our clinic, including three siblings (two brothers and a deceased sister) with flail leg syndrome and their fraternal aunt, who has been previously misdiagnosed with cervical myelopathy and is living with symptoms of the disease for 15 years. Sanger sequencing of the *SOD1* gene was performed in all of the living patients, revealing an L144S (c.434T>C, p.Leu145Ser) heterozygous mutation. The aim of this case report is to increase the physician's awareness of the atypical phenotypes of amyotrophic lateral sclerosis and hopefully, to encourage further research on the factors responsible for delayed disease progression in patients with L144S *SOD1* mutation.

KEYWORDS

flail leg syndrome, familial ALS (FALS), familial amyotrophic lateral sclerosis, SOD1 mutation, pseudopolyneuritic form, amyotrophic lateral sclerosis (ALS), L144S, phenotype of ALS/MND

1. Introduction

Amyotrophic lateral sclerosis (ALS) is the most common motor neuron disease, which in its classic form is characterized by symptoms of simultaneous upper and lower motor neuron involvement at the onset (1). It has a mean prevalence of 5.4/100.000 in Europe (1) with flail leg syndrome (FLS, also known as pseudopolyneuritic variant) accounting for up to 5% of ALS cases (2), in which lower motor neuron signs predominate at onset, affecting the lower limbs usually as a triad of distal paresis, muscle atrophy, and hyporeflexia/areflexia (3).

Flail leg syndrome was discovered by Pierre Marie and later described by his student Patrikios in 1918 as asymmetric-onset, slowly progressing, distal lower limbs muscle weakness with the absence of lower limb deep tendon reflexes (DTRs) and presence of subtle or late upper motor neuron (UMN) signs (4). FLS is a rare phenotype of ALS, characterized by lower motor neuron (LMN) signs restricted to the lumbosacral region for an extended period of time (which varies in the literature from 12 to 24 months), with a more favorable prognosis than the classic form of ALS in the means of slower progression and longer mean survival between 75.9 and 87 months with diminished and late respiratory involvement (3). The longer the disease is confined to the lumbosacral region, the longer the survival (4).

Up to 10% of ALS cases are familial, with *SOD1* gene mutations involved in 14.8% of familial ALS cases in Europe (5). Risk factors of familial ALS include a positive family history of dementia and neurodegenerative disorders, early age of onset, predominant lower limbs symptoms, or subjective sensory signs at the onset (6, 7). Familial ALS is usually inherited in an autosomal dominant pattern, occurs on average 10 years earlier, and has a worse prognosis than sporadic ALS (8).

According to Kuzma-Kozakiewicz et al. (9), the most common *SOD1* mutation among ALS patients in Poland is K3E, followed by L144S (c.434T>C, p.Leu145Ser) which is a heterozygous, missense mutation located in exon 5 of the *SOD1* gene. The study mentioned 26 cases of L144S mutation worldwide (19 cases in Poland, 3 in Iran, 3 in Brazil, and 1 in the USA), including 10 fALS families and 3 sporadic ALS cases, out of which 66.6% of cases displayed classic ALS phenotype and in the remaining 33.3% of cases, progressive muscular atrophy was diagnosed. The clinical course of ALS in patients with L144S *SOD1* mutation is relatively benign, with slow progression and an average survival of 11 years. Initially, the symptoms are confined to the lower limbs, while bulbar symptoms appear late (9).

This case report provides a unique opportunity to analyze the clinical course of familial ALS with heterozygous L144S *SOD1* mutation in a Polish family, from the physician's point of view.

2. Case description

We present three siblings-two brothers (Case 1 and Case 3) and their deceased sister (Case 4 – retrospective analysis), with a rare phenotype of ALS (flail leg syndrome), and their fraternal aunt (Case 2), suffering from a progressive motor decline over 15 years, previously diagnosed with cervical myelopathy in another hospital and finally diagnosed with ALS in our clinic. Family pedigree has been obtained—other family members are reported to be free of any neurological and cognitive deficits (Figure 1).

Diagnostic workup of the patients included the following: laboratory blood tests, CSF analysis (including antibodies against Borrelia burgdorferi in the serum and CSF, oligoclonal bands in CSF), and MRI of the brain, cervical, and lumbosacral spine, which did not display any significant findings in all of the cases. EMG/ENG study was performed in all of the patients and significantly aided the diagnosis. All patients were diagnosed with ALS and subsequently treated with riluzole.

Sanger sequencing of the *SOD1* gene was performed in all of the living patients in 2022 (Cases 1, 2, and 3) and displayed the presence of L144S (c.434T>C, p.Leu145Ser) mutation in one allele.

The patients were not included in any other study and are presented in the order in which they were treated by the authors. The cases are summarized in Table 1.

2.1. Case 1

In February 2022, a 47-year-old man with no prior medical history was admitted to the neurological clinic due to distal lower limbs muscle weakness progressing over 2 years.

The first symptoms appeared in August 2020 in the form of a shortening of the walking distance, followed by a right foot drop in February 2021. Initially, the patient associated the symptoms with a bilateral foot injury that he suffered in 2008 as a result of a fall from a height accident.

The ENG/EMG study from October 2021 revealed features of significant axonal damage to distal segments of the tibial nerves, without signs of active denervation. After the exclusion of lumbar discopathy as a possible cause of the symptoms, the patient underwent orthopedic surgery in April 2021 (right-sided arthrodesis of the first MTP joint and talocalcaneonavicular joint)—without improvement. Since September 2021, the patient walks with a cane, suffers from trembling hands, and reports fasciculations and needle-like pain localized mostly in the lower limbs, as well as upper limbs and trunk. At the time of the patient's hospitalization, his two siblings were already diagnosed with ALS. The patient has no children.

Neurological examination on admission to the clinic revealed the following: generalized atrophy of the lower limbs muscles (more pronounced in the right calf—girth asymmetry of 3 cm) with numerous fasciculations, subtle atrophy of the left first dorsal interosseous muscle, restless tongue; asymmetric, moderate degree flaccid paraparesis (more pronounced distally, affecting the right lower limb to the greater degree than the left) with trace patellar and ankle DTRs and mildly positive Babinski sign on the left side; very brisk DTRs from the upper limbs, steppage gait.

Laboratory blood tests and CSF analysis did not reveal any significant abnormalities. MRI of the brain, cervical, and lumbosacral spine did not reveal any relevant findings. The EMG and ENG study displayed features of denervation at the C/Th and L-S spinal cord regions. Based on the clinical and electrophysiological features, probable ALS was diagnosed and riluzole was introduced. *SOD1* gene sequencing was performed, demonstrating the presence of the p.Leu145Ser variant in one allele.

2.2. Case 2

In May 2022, a 76-year-old bedridden woman was admitted to the neurological clinic due to progressive muscle weakness in the upper and lower limbs.

The first symptoms appeared about 15 years before as chronic back pain and walking difficulty, caused by muscle weakness affecting the left lower limb at first and then the right lower

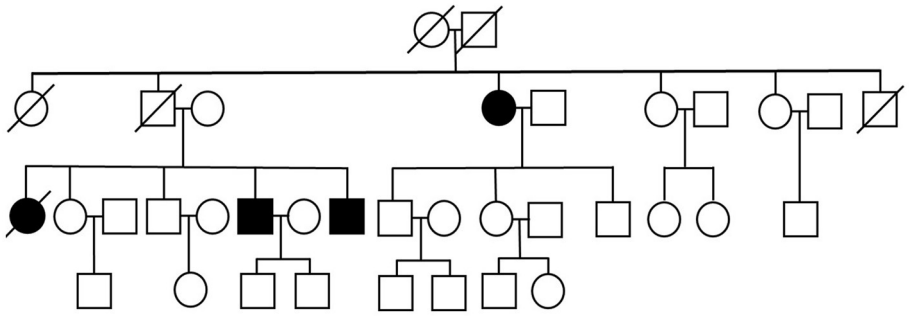

FIGURE 1
Pedigree of the studied polish family.

limb. The patient was walking on straight, stiff legs "as if on stilts"—any attempt to bend the knees resulted in a fall. In 2015, significant deterioration of mobility forced the patient to require the aid of a cane while walking and prompted the patient to seek inpatient neurological care (in another hospital), which resulted in a diagnosis of degenerative disc disease of the cervical and lumbar spine with cervical myelopathy and lumbar stenosis. At the time of the diagnosis, the patient claimed that her family history was positive for multiple sclerosis. In 2016, the patient underwent an L4 laminectomy, which did not result in clinical improvement. The patient did not consent to the surgical treatment of cervical myelopathy. Despite physical rehabilitation, further progression of the symptoms was observed. In addition, muscle weakness in the upper limbs is developing for approximately 3–4 years. For about a year, swallowing difficulty is occurring periodically. Currently, the patient is bedridden and uses a wheelchair with the help of others.

The patient has three children (two sons and a daughter) that are reported to be healthy. Other medical history of the patient includes: microvascular ischemic brain disease, hypertension, thyroid nodules, hypothyroidism, bilateral cataracts, a history of left tibial fracture surgery, and cholecystectomy.

Neurological examination on admission to the clinic revealed the following: bilateral atrophy of the shoulder girdle muscles, biceps and triceps brachii, lumbrical, and interossei muscles; third, fourth, and fifth fingers of both hands were fixed in a flexed position, fasciculations of the left triceps brachii muscle and hand muscles bilaterally, tongue fibrillations, minimal dysarthria, mild dysphagia, spastic paraparesis 1/5 MRC with the absence of patellar and ankle DTRs, the absence of the left plantar reflex, mildly positive Babinski sign on the right side, and paresis of the upper limbs without increased muscle tone (in the left upper limb 2/5 MRC, in the right upper limb proximally 3/5 MRC, distally 4/5 MRC) with normal DTRs.

Laboratory blood tests and CSF analysis did not reveal any significant abnormalities except for elevated TSH and ALT. MRI of the brain revealed numerous chronic microvascular changes within the pons, frontal, and parietal lobes bilaterally as well as crowding of gyri at the vertex/parafalcine region with cortico-subcortical atrophy. MRI of the cervical spine displayed multilevel degenerative disc changes with spinal and foraminal stenosis, with no evidence of cervical myelopathy. The EMG and ENG study revealed features of denervation at three spinal cord regions (C, Th, and L) and slight acute neurogenic damage at the level of the brainstem. Based on the clinical and electrophysiological features, definite ALS was diagnosed and riluzole was introduced. *SOD1* gene sequencing was performed, demonstrating the presence of the p.Leu145Ser variant in one allele.

2.3. Case 3

In June 2022, a 51-year-old man with ALS (diagnosed in 2020) was admitted to the neurological clinic for further diagnostic evaluation.

The first symptoms emerged in 2017 at the age of 46, when the patient started walking with a limp on the right side. The muscle weakness slowly progressed to involve the left lower limb, forcing the patient to walk with a cane from 2019 or 2020. The ENG/EMG study from March 2019 revealed features of significant axonal damage to tibial and deep fibular nerves, without traits of active denervation. From August 2019 to September 2020, the patient was hospitalized three times in the neurological clinic, which culminated in the diagnosis of ALS. Neurological examination revealed flaccid paraparesis, absence of patellar reflex on the right side, lack of ankle DTRs bilaterally, and mildly positive Babinski sign on the left side. MRI of the cervical and lumbar spine displayed degenerative disc changes with no evidence of myelopathy. Gradual progression of electrophysiological findings was observed —at first, features of denervation were present at the lumbosacral region in August 2019 and then spread to C/Th, Th, and L-S regions in September 2020. An additional EMG and ENG study from September 2021 revealed features of denervation at three spinal cord regions (C, Th, and L-S). Since January 2022, the patient walks with the support of a walking cane. The patient has two underage children.

Neurological examination on admission to the clinic revealed the following: fasciculations of deltoid muscles bilaterally, muscle atrophy of the lower limbs (most visible proximally and on the right side), minimal muscle atrophy of the right upper limb, restless tongue; asymmetric flaccid paraparesis—more pronounced in the right lower limb (paresis of hip extensors 2/5 MRC, paresis of

10.3389/fneur.2023.1138668

TABLE 1 Summary of familial ALS cases described in the article.

Case No.	Gender	Mutation/date of genetic testing	Age/year at symptoms' onset	Symptoms at onset	Duration of symptoms' confinement to lower limbs	ALS phenotype	Diagnostic delay	Time from disease onset to bulbar symptoms' onset	Survival
1	M	Heterozygous L144S *SOD1* mutation (02.2022)	46 yo. (2020)	Asymmetric, distal onset lower limb paresis with predominant LMN signs and needle-like pain	2 years - ongoing	Flail leg syndrome	1,5 year	-	2 years - ongoing
2	F	Heterozygous L144S *SOD1* mutation (05.2022)	61 yo. (2007)	Asymmetric-onset, spastic paraparesis with absent patellar and Achilles DTRs	11 years	-	15 years	14 years	15 years - ongoing
3	M	Heterozygous L144S *SOD1* mutation (06.2022)	46 yo. (2017)	Asymmetric, distal onset lower limb paresis with predominant LMN signs	5 years	Flail leg syndrome	3 years	-	5 years - ongoing
4	F	N/A (deceased)	35 yo. (1998)	Distal lower limbs paresis with predominant LMN signs, needle-like thigh pain	4 years	Flail leg syndrome	4 years	5 years	12 years

dorsal flexors 3/5 MRC, paresis of hip flexors and plantar flexors 4/5 MRC), than in the left lower limb (4/5 MRC), lack of patellar and ankle DTRs bilaterally, lack of plantar reflex on the right side, weak plantar reflex on the left side, and discreet paresis of the right upper limb with very brisk DTRs.

Laboratory blood tests revealed mildly increased CK, decreased serum IgM levels, and impaired fasting glycemia. CSF analysis did not display any significant abnormalities except for mild elevation of IgA. MRI of the brain did not reveal any significant findings. *SOD1* gene sequencing was performed, demonstrating the presence of the p.Leu145Ser variant in one allele.

2.4. Case 4

The first symptoms emerged in 1998 at the age of 35, as slowly progressive distal lower limb muscle weakness with intense, needle-like pain in the thighs. The EMG study from 2001 displayed traits of axonal damage to the peripheral nerves (mainly of the lower limbs) at the level of the nerve trunks, with features of denervation and reinnervation in the muscles of the lower and upper limbs, more pronounced distally. MRI of the thoracic and lumbar spine from March 2002 did not reveal any significant findings. In July 2002, the patient was hospitalized in the neurological clinic and presented with moderate degree flaccid paraparesis and muscle atrophy (mainly distal, most pronounced in plantar flexors) with the absence of patellar and ankle DTRs and positive Babinski sign bilaterally; paresis of the fourth and fifth finger of the left hand, duck-like gait. Laboratory blood tests and CSF analysis did not reveal any significant abnormalities except for mildly elevated CK. MRI of the cervical spine was normal. The EMG and ENG study revealed features of denervation at the level of the brainstem, cervical, and lumbar spinal cord regions. Based on the clinical and electrophysiological features, probable ALS was diagnosed and riluzole was introduced.

During hospitalization in the neurological clinic in October 2003, the patient presented with tongue atrophy, mild dysarthria with discreet features of bulbar speech, flaccid quadriparesis (severe paraparesis; the weakness was more pronounced in the right limbs) with upper and lower limb muscle atrophy, trace patellar and ankle DTRs, positive Babinski sign on the left side, and mildly positive Babinski sign on the right side. The EMG and ENG study confirmed features of denervation at cervical and lumbar spinal cord regions. Last recorded neurological consultation from 2008 described flaccid quadriparesis 2/5 MRC with lower limbs areflexia. The patient died in 2011 at the age of 47 due to ALS-related respiratory failure.

3. Discussion

We observed that L144S (c.434T>C, p.Leu145Ser) *SOD1* heterozygous mutation in familial ALS may result in asymmetric-onset lower limb paresis (flaccid or spastic) with trace/absent lower limb DTRs, late bulbar signs, and long survival. Due to limitations of Sanger sequencing, other modifying variants within exon-distant intronic or promoter regions could not be excluded. Lower limb onset and long survival seem to be the defining features of L144S

TABLE 2 Review of L144S *SOD1* cases reported in the literature.

References	Population	Gender	Number of L144S *SOD1* cases/Type of mutation (if specified)	Age of onset	Site of onset	Clinical presentation	Survival (years)
Nel et al. (10)	South African	N/A	($n = 1$)	N/A	N/A	ALS	N/A
Gagliardi et al. (11)	Iranian		1 FALS family ($n = 3$)			ALS	
		F	Homozygous	31	Lower limb	Paresthesia of the toes, followed by painful paresis of upper and lower limbs, dysarthria, dysphagia	2
		M	Homozygous	18	Lower limb	Lower limb paresis, followed by upper limb paresis, dysphagia, respiratory failure	9
		F	Heterozygous	64	Lower limb	Asymmetric-onset, proximal paraparesis with UMN signs predominance, followed with ataxia and numbness of the lower limbs	1+
Chen et al. (12)	Chinese		1 FALS ($n = 1$), 1 SALS				
		F	Familial	50	Lower limb	LMN-dominant ALS of symmetric onset	2.6+
		F	Sporadic	48	Lower limb	Classic ALS of asymmetric onset	3.8+
Kuzma-Kozakiewicz et al. (9)	Polish	79% F, 21% M	5 FALS families ($n = 17$), 2 SALS	39.8 ± 11.0 (mean±SD) ($n = 9$)	Lower limb ($n = 16$)	50% classic ALS, 50% PMA ($n = 8$)	10.34 ± 5.77 (mean±SD) ($n = 14$)
Chadi et al. (13)	Brazilian		3 FALS families ($n = 3$)				
		F		31	Upper limb	UMN-dominant ALS	1+
		M		40	Lower limb	UMN-dominant ALS	25+
		F		22	Lower limb	UMN-dominant ALS	5+
Alavi et al. (14)	Iranian		1 FALS family ($n = 2$), 1 SALS				
		M	Heterozygous, familial	28	Lower limb	ALS	11+
		F	Heterozygous, familial	27	Lower limb	ALS	8+
		M	Heterozygous, sporadic	45	Lower limb	ALS	11+
Cudkowicz et al. (15)	US	N/A	1 FALS family ($n = 2$)	42.5 ± 10.6 (mean±SD)	N/A	ALS	12.3 ± 3.7 (mean±SD)
Sapp et al. (16)	US		1 FALS family ($n = 2$)	42.5 ($n = 2$)			
		N/A				ALS	9
		N/A				ALS	13+

10.3389/fneur.2023.1138668

SOD1 mutation, as depicted in Table 2, resuming the main features of all L144S *SOD1* cases described so far.

Flail leg syndrome is a rare phenotype of ALS which may present with unilateral foot drop, trace deep tendon reflexes from the lower limbs, and waddling gait, which may resemble peripheral neuropathy and lead to a misdiagnosis. According to Wijesekera et al. (4) UK and Melbourne clinical studies, FLS is defined as a progressive, distal onset LMN pattern of weakness and wasting confined solely to the lower limbs for at least 12 months. Deep tendon reflexes from the lower limbs are usually diminished or absent; however, brisk lower limb DTRs or positive Babinski sign do not preclude the diagnosis of FLS, as long as hypertonia and clonus are absent (3, 4). FLS of asymmetric onset may present with brisk DTRs from unaffected limbs (8). During the disease course, the symptoms eventually spread to involve other regions and resemble classic ALS (2).

The siblings (Case 1, Case 3, and Case 4) match the criteria of FLS; however, their fraternal aunt (Case 2) with asymmetric-onset spastic paraparesis and lack of lower limb DTRs does not entirely match the aforementioned diagnostic criteria of FLS due to increased muscle tone in the lower limbs.

A longer clinical course coupled with the atypical presentation at onset may lead to a misdiagnosis, which could prolong the initiation of treatment and may lead to unnecessary interventions including surgeries and hospitalizations (8, 17). An elderly woman with a progressive disability, suffering from chronic back pain does not necessarily have to be diagnosed with cervical myelopathy or lumbar stenosis but may potentially suffer from ALS (as in Case 2), which highlights the importance of careful evaluation of patient's history, neurological examination, and electromyography.

FLS is correlated with the presence of *SOD1* mutation with an odds ratio of 3.75 (18). Therefore, in families affected by familial ALS, a detailed, at least three-generational pedigree should be obtained. Genetic testing should not be performed solely for the purpose of predicting the further clinical course of the disease, because of variable expressivity (one pathogenic variant may manifest as several different phenotypes); however, it does provide limited prognostic information. Predictive testing of minors is considered unethical. First, symptomatic individuals who are willing may undergo full gene sequencing, which is a gold standard for searching the entire coding region of the chosen gene for pathogenic variants. A positive result cannot give a definite answer to whether the individual will develop the disease due to a lack of population-based data on penetrance; however, it may be used to identify at-risk family members and to confirm the diagnosis as clinically definite laboratory-supported familial ALS in patients with clinically suspected or clinically possible ALS and in the light of emerging gene-specific therapies it gives the opportunity to participate in clinical trials (6).

Tofersen is a novel antisense oligonucleotide (ASO) drug administered intrathecally, decreasing the production of SOD1 protein in *SOD1*-ALS. Although it failed to slow down the functional decline of patients at week 28 in a phase 3 trial, it may inhibit neurodegeneration by reducing CSF neurofilament levels (19, 20).

In this case report, we have presented two generations affected by familial ALS, in which the symptoms seem to progress faster in the younger generation, possibly indicating genetic anticipation. Based on the available data from family history, it was not possible to establish the founder, who passed the mutated gene to the affected family members. In our opinion, further research studies are needed to identify the exact factors responsible for delayed ALS progression in patients with L144S *SOD1* mutation, which will certainly aid to unveil the etiology of this currently fatal disease.

4. Conclusion

Amyotrophic lateral sclerosis may present with varying degrees of upper and lower motor neuron involvement at the onset. Flail leg syndrome is one of the rare, atypical phenotypes of ALS with slow progression and long survival, in which lower motor neuron signs predominate for an extended period of time, affecting the lower limbs usually as distal, flaccid paresis (often of asymmetric-onset, including unilateral foot drop), muscle atrophy, and areflexia. In patients presenting lower motor neuron signs of unclear etiology, the EMG/ENG study should always be considered, which will speed up the diagnostic process and enable early treatment, including early enrollment into clinical trials. Subjective sensory symptoms such as "needle-like" pain do not preclude the diagnosis of ALS; on the contrary, they may indicate an atypical phenotype or genetic background of ALS. The role of genetic testing in ALS should be highlighted. Familial ALS with heterozygous L144S *SOD1* mutation is characterized by slow progression and extremely long survival and can manifest clinically as flail leg syndrome.

Data availability statement

The datasets presented in this article are not readily available because of ethical and privacy restrictions. Requests to access the datasets should be directed to the corresponding author.

Ethics statement

Ethical review and approval was not required for the study on human participants in accordance with the local legislation and institutional requirements. The patients/participants provided their written informed consent to participate in this study. Written informed consent was obtained from the individual(s) for the publication of any potentially identifiable images or data included in this article.

Author contributions

EZ served as initiator and supervisor of the project, writer of the manuscript, responsible for the acquisition and analysis of data, treated the patients during hospitalizations, and approved the final version of the manuscript. DW was responsible for the analysis and interpretation of data, physical examination of the patients, provided editorial revisions, and approved the final version of the manuscript. AS served as substantive guidance and support, provided editorial

revisions, and approved the final version of the manuscript. All authors contributed to the article and approved the submitted version.

Conflict of interest

The authors declare that the research was conducted in the absence of any commercial or financial relationships that could be construed as a potential conflict of interest.

Publisher's note

All claims expressed in this article are solely those of the authors and do not necessarily represent those of their affiliated organizations, or those of the publisher, the editors and the reviewers. Any product that may be evaluated in this article, or claim that may be made by its manufacturer, is not guaranteed or endorsed by the publisher.

References

1. Grad LI, Rouleau GA, Ravits J, Cashman NR. Clinical spectrum of amyotrophic lateral sclerosis (ALS). *Cold Spring Harb Perspect Med.* (2017) 7:a024117. doi: 10.1101/cshperspect.a024117

2. Zakharova MN, Abramova AA. Lower and upper motor neuron involvement and their impact on disease prognosis in amyotrophic lateral sclerosis. *Neural Reg Res.* (2022) 17:65. doi: 10.4103/1673-5374.314289

3. Zhang H, Chen L, Tian J, Fan D. Differentiating slowly progressive subtype of lower limb onset ALS from typical ALS depends on the time of disease progression and phenotype. *Front Neurol.* (2022) 13:872500. doi: 10.3389/fneur.2022.872500

4. Wijesekera LC, Mathers S, Talman P, Galtrey C, Parkinson MH, Ganesalingam J, et al. Natural history and clinical features of the flail arm and flail leg ALS variants. *Neurology.* (2009) 72:1087–94. doi: 10.1212/01.wnl.0000345041.83406.a2

5. Mejzini R, Flynn LL, Pitout IL, Fletcher S, Wilton SD. Akkari PA. ALS genetics, mechanisms, and therapeutics: where are we now? *Front Neurosci.* (2019) 13:310. doi: 10.3389/fnins.2019.01310

6. McCluskey L, Ladha SS. *Familial Amyotrophic Lateral Sclerosis.* UpToDate (2022). Available online at: https://www.uptodate.com/contents/familial-amyotrophic-lateral-sclerosis (accessed May, 2022).

7. Mathis S, Goizet C, Soulages A, Vallat JM, Le Masson G. Genetics of amyotrophic lateral sclerosis: a review. *J Neurol Sci.* (2019) 399:217–26. doi: 10.1016/j.jns.2019.02.030

8. Wijesekera LC, Leigh PN. Amyotrophic lateral sclerosis. In: *Orphanet Journal of Rare Diseases, Vol. 4.* Springer Science and Business Media LLC (2009). doi: 10.1186/1750-1172-4-3

9. Kuzma-Kozakiewicz M, Andersen PM, Elahi E, Alavi A, Sapp PC, Morita M, et al. Putative founder effect in the Polish, Iranian and United States populations for the L144S SOD1 mutation associated with slowly uniform phenotype of amyotrophic lateral sclerosis. *Amyotrop Lat Sclerosis Frontotemp Deg.* (2021) 22:80–5. doi: 10.1080/21678421.2020.1803359

10. Nel M, Mahungu AC, Monnakgotla N, Botha GR, Mulder NJ, Wu G, et al. Revealing the mutational spectrum in Southern Africans with amyotrophic lateral sclerosis. *Neurology Genetics.* (2022) 8:e654. doi: 10.1212/NXG.0000000000000654

11. Gagliardi D, Ahmadinejad M, Del Bo R, Meneri M, Comi GP, Corti S, et al. Homozygous SOD1 variation L144S produces a severe form of amyotrophic lateral sclerosis in an Iranian family. *Neurol Genetics.* (2022) 8:e645. doi: 10.1212/NXG.0000000000000645

12. Chen LX, Xu HF, Wang PS, Yang XX, Wu ZY Li HF, et al. SOD1 mutation spectrum and natural history of ALS patients in a 15-year cohort in southeastern China. *Front Genet.* (2021) 12:746060. doi: 10.3389/fgene.2021.746060

13. Chadi G, Maximino JR, Jorge FM, Borba FC, Gilio JM, Callegaro D, et al. Genetic analysis of patients with familial and sporadic amyotrophic lateral sclerosis in a Brazilian Research Center. *Amyotroph Lat Scler Front Deg.* (2017) 18:249–55. doi: 10.1080/21678421.2016.1254245

14. Alavi A, Nafissi S, Rohani M, Zamani B, Sedighi B, Shamshiri H, et al. Genetic analysis and SOD1 mutation screening in Iranian amyotrophic lateral sclerosis patients. *Neurobiol Aging.* (2013) 34:1516–e1. doi: 10.1016/j.neurobiolaging.2012.09.006

15. Cudkowicz ME, McKenna-Yasek D, Sapp PE, Chin W, Geller B, Hayden DL, et al. Epidemiology of mutations in superoxide dismutase in amyotrophic lateal sclerosis. *Annal Neurol Off J Am Neurol.* (1997) 41:210–21. doi: 10.1002/ana.410410212

16. Sapp PC, Rosen DR, Hosler BA, Esteban J, McKenna-Yasek D. O'regan JP, Horvitz HR, Brown Jr RH. Identification of three novel mutations in the gene for CuZn superoxide dismutase in patients with familial amyotrophic lateral sclerosis. *Neuromuscular Disorders.* (1995) 5:353–7. doi: 10.1016/0960-8966(95)00007-A

17. Karakaş P, Koç F, Bozkir MG. Pseudopolyneuritic form of amyotrophic lateral sclerosis with foot drop. In: *Neurosurgery Quarterly, Vol. 23.* Ovid Technologies (Wolters Kluwer Health) (2013). p. 289–93. doi: 10.1097/nq.0b013e318275e317

18. Warner R. Amyotrophic lateral sclerosis in neurodegenerative diseases - molecular mechanisms and current therapeutic approaches *IntechOpen.* (2021) 29:92724. doi: 10.5772/intechopen.92724

19. Brenner D, Freischmidt A. Update on genetics of amyotrophic lateral sclerosis. *Curr Opin Neurol.* (2022) 35:672–7. doi: 10.1097/WCO.0000000000001093

20. Wynford-Thomas R, Robertson NP. Amyotrophic lateral sclerosis: an update on treatments from clinical trials. *J Neurol.* (2023) 2701:1187–9. doi: 10.1007/s00415-022-11553-6

frontiers | Frontiers in Neurology

TYPE Case Report
PUBLISHED 06 April 2023
DOI 10.3389/fneur.2023.1126444

Check for updates

OPEN ACCESS

EDITED BY
Giovanni Meola,
University of Milan, Italy

REVIEWED BY
Xinxing Lai,
Dongzhimen Hospital, Beijing University of Chinese Medicine, China
Jingjing Wei,
Xiyuan Hospital, China Academy of Chinese Medical Sciences, China

*CORRESPONDENCE
Dahua Wu
✉ wdh838692@sina.com

SPECIALTY SECTION
This article was submitted to Neuromuscular Disorders and Peripheral Neuropathies, a section of the journal Frontiers in Neurology

RECEIVED 17 December 2022
ACCEPTED 09 March 2023
PUBLISHED 06 April 2023

CITATION
Xie Y, Li L, Xie L, Jiang J, Yao T, Mao G, Wang S, Lin A, Ge J and Wu D (2023) Beneficial effects and safety of traditional Chinese medicine for chronic inflammatory demyelinating polyradiculoneuropathy: A case report and literature review. *Front. Neurol.* 14:1126444. doi: 10.3389/fneur.2023.1126444

COPYRIGHT
© 2023 Xie, Li, Xie, Jiang, Yao, Mao, Wang, Lin, Ge and Wu. This is an open-access article distributed under the terms of the Creative Commons Attribution License (CC BY). The use, distribution or reproduction in other forums is permitted, provided the original author(s) and the copyright owner(s) are credited and that the original publication in this journal is cited, in accordance with accepted academic practice. No use, distribution or reproduction is permitted which does not comply with these terms.

Beneficial effects and safety of traditional Chinese medicine for chronic inflammatory demyelinating polyradiculoneuropathy: A case report and literature review

Yao Xie[1], Lesang Li[2], Le Xie[1], Junlin Jiang[1], Ting Yao[1], Guo Mao[3], Shiliang Wang[1], Anchao Lin[1], Jinwen Ge[1] and Dahua Wu[1]*

[1]Department of Neurology, Hunan Hospital of Integrated Traditional Chinese and Western Medicine, Changsha, China, [2]Ophthalmology Department, Hunan Want Want Hospital, Changsha, China, [3]Office of Academic Research, Hunan Hospital of Integrated Traditional Chinese and Western Medicine, Changsha, China

Chronic inflammatory demyelinating polyradiculoneuropathy (CIDP) is an immune-mediated neuropathy. First-line treatments for CIDP include corticosteroids, intravenous immunoglobulin, and plasma exchange. However, the application is always limited by high costs, effectiveness, and adverse events. This study investigated a new potentially effective and safe therapeutic treatment to alleviate CIDP symptoms and improve the quality of life. In the present case, a 47-year-old rural woman presented with weakness and numbness of progressive extremities. She was diagnosed with CIDP based on abnormal cerebrospinal fluid and electromyography. The patient was treated with intravenous dexamethasone for 1 week and with Huangqi-Guizhi-Wuwu and Bu-Yang-Huan-Wu decoctions for 90 days. Surprisingly, after the treatment, the weakness and numbness were eliminated, and the quality of life improved. The varying INCAT, MRC, and BI scores also reflected the treatment effects. After 8 months of discharge, the symptoms did not relapse during the follow-up. We also searched "traditional Chinese medicine (TCM)" and "CIDP" in PubMed, EMBASE, the Web of Science, the Cochrane Library, the Chinese National Knowledge Infrastructure Databases, Wanfang Data, and the Chongqing Chinese Science and Technology Periodical Database. Finally, only ten studies were included in the literature review. Three studies were randomized controlled trials, and seven were case reports or case series. There were 419 CIDP patients, but all study sites were in China. Nine TCM formulas involving 44 herbs were reported, with Huang Qi (*Astragalus membranaceus*) being the most important herb. In conclusion, the case and literature demonstrated that TCM treatment might be a more effective, low-cost, and safe option for treating CIDP. Although these preliminary findings are promising, a larger sample size and higher-quality randomized clinical trials are urgently required to confirm our findings.

KEYWORDS

chronic inflammatory demyelinating polyradiculoneuropathy, traditional Chinese medicine, case report, review, *Astragalus membranaceus*

Introduction

Chronic inflammatory demyelinating polyradiculoneuropathy (CIDP) is a rare immune-mediated neuropathy in which an abnormal immune response causes peripheral nerve demyelination and axonal damage (1). It usually results in progressive weakness of the extremities with sensory dysfunction. Symptoms should appear for at least 2 months, and the course can be progressive or relapsing (2). The annual cost of treating CIDP illness can reach USD$ 116,330 per patient, and patients may also experience physical and psychosocial burdens such as impaired physical function, pain, depression, and adverse events (3).

The guidelines recommended intravenous immunoglobulin (IVIg), corticosteroids, and plasma exchange as first-line treatments for CIDP (4, 5). However, the potential side effects of corticosteroids, such as gastric ulceration, diabetes, arterial hypertension, osteoporosis, avascular necrosis of long bones, and cataracts, may outweigh the benefits. Moreover, long-term corticosteroid treatment may cause significant side effects (6). IVIg may result in rapid improvement in disability, but the benefit requires long-term repeated infusions, which carry a significant economic burden, particularly in developing countries (7, 8). Plasma exchange necessitates good vascular access and specialized equipment.

Although first-line treatments can improve symptoms in some patients, they also require ongoing maintenance therapy and the patient's willingness to tolerate the adverse effects or financial burden. The International CIDP Outcome Study (ICOS) revealed that only one-third of CIDP patients were in remission 1 year after the start of first-line treatment, and residual symptoms and deficits were common regardless of treatment (9). There is also a lack of formal efficacy evidence for alternative immunomodulatory agents (4, 10). Because of the side effects, high cost, and limited effectiveness of these treatments, there is an urgent need for new, effective, and safe CIDP treatments.

Traditional Chinese medicine (TCM) has a long history of boosting weakness and sensory dysfunction. TCM treatments have been widely used as a supplement to CIDP treatment in China. Many recent clinical trials have found that TCM treatments can improve clinical symptoms and the quality of life in patients with peripheral neuropathy (PN). Furthermore, TCM therapy can also enhance the sensory nerve conduction velocity (SNCV) and motor nerve conduction velocity (MNCV) in PN (11–13). The therapeutic mechanisms of TCM were elucidated by regulating inflammatory responses and repairing nerve injury (14).

However, no English literature reports the clinical efficacy of Chinese herbs for CIDP. In the present study, we attempted to use short-term corticosteroids combined with Chinese herbs on a patient with CIDP. Surprisingly, we identified that this therapeutic regimen completely relieved limb weakness and numbness and improved the quality of life. A literature review for TCM in CIDP was also conducted.

Case report

This case report was conducted in accordance with the Case Report (CARE) Guidelines (15).

Clinical history

On 25 November 2021, a 47-year-old rural woman complained of progressive weakness and numbness in her extremities. Initially, her symptoms were mild, causing her to experience difficulty grabbing objects or walking. After 3 months, the symptoms gradually worsened; she could not hold anything and only walked with assistance. On 23 February 2022, she was diagnosed with PN at another hospital. However, no IVIg or corticosteroids were administered to her, and her symptoms did not improve. Then, on 10 March 2022, she was transferred to our hospital (Hunan Hospital of Integrated Traditional Chinese and Western Medicine, Changsha, China). Upon arrival, the woman exhibited signs of both fatigue and limb paralysis, and she specifically emphasized that the numbness she was experiencing felt like she was wearing gloves and socks. She had no other particular medical history (Figure 1).

Clinical and laboratory examinations

The proximal end of the upper and lower limbs had grade 3 muscle strength, while the distal end of all limbs had grade 2 muscle strength. Muscular atrophy was observed in the bilateral first dorsal interosseous. Tendon reflexes decreased or disappeared, and limb muscular tension also decreased. Pain and temperature sensibility on the distal limbs decreased. Pyramidal tract signs were not elicited. There was no problem with eye montraosvement, pupil size, or swallowing function.

The cerebrospinal fluid (CSF) result revealed that the white blood cell count was one, and the micro-amount of protein was 652.6 mg/L (normal reference value: 150–450 mg/L). Other anti-ganglioside antibodies in CSF and serum were all negative, except for anti-sulfatide (aSF) IgG in CSF. The erythrocyte sedimentation rate (ESR) was 36 mm/h (normal reference value: 0–20 mm/h). Antinuclear antibodies, rheumatoid factors, HBsAg, HCV-Ab, rapid plasma regain, and HIV-Ab, were all negative. The routine blood, stool, and urine examinations, renal and liver functions, myocardial enzymes, and thyroid functions were all normal.

Electromyography and neuroimaging

Multiple nerves in the upper and lower limbs were observed with decreased MNCV, SNCV, and amplitude during an electromyography (EMG) examination. Demyelination and axonal damage were identified in the bilateral median, ulnar, tibial, and peroneal nerves. Furthermore, no waveforms were elicited from the left peroneal motor nerve, the left median sensory nerve, or the bilateral superficial peroneal sensory nerves (Supplementary Table S1). The brain and spinal MRIs revealed no noticeable abnormalities.

Diagnosis and treatment

Over 8 weeks, the patient developed progressive, symmetric upper- and lower-limb weakness and numbness and reduced tendon reflexes in all limbs. In addition, abnormal CSF and EMG

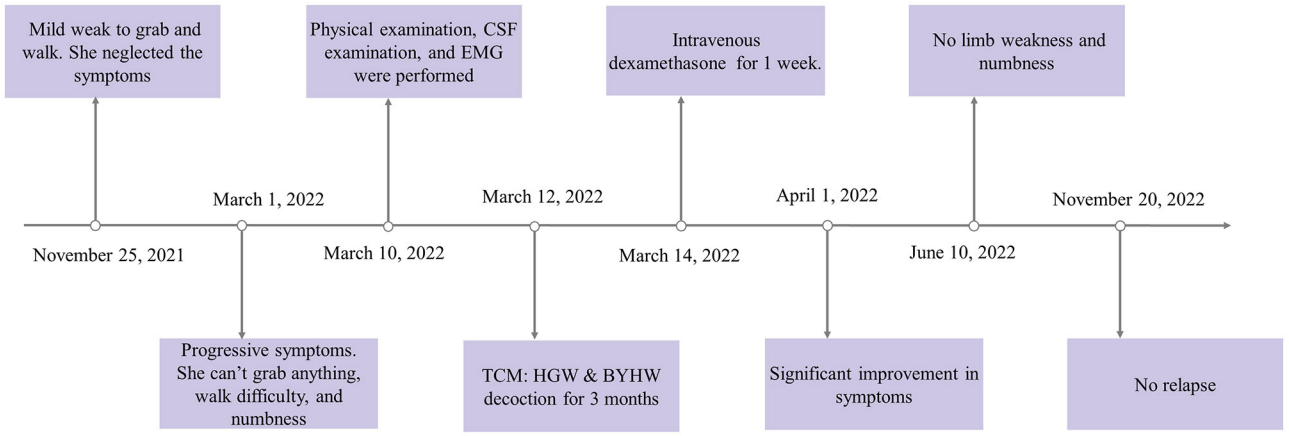

FIGURE 1
Timeline of the case report. HGW and BYHW decoctions, Huangqi-Guizhi-Wuwu and Bu-Yang-Huan-Wu decoctions; CSF, cerebrospinal fluid; EMG, electromyography.

were observed. The patient was diagnosed with CIDP using the EFNS/PNS consensus guideline (4).

Subsequently, intravenous dexamethasone (20 mg daily) was used for 1 week. Simultaneously, the patient was given TCM. The TCM formulas used in this case report were Huangqi-Guizhi-Wuwu and Bu-Yang-Huan-Wu decoctions (HGW and BYHW), which is composed of 12 herbs: Huang Qi (*Astragalus membranaceus*), 60 g; guizhi (Cassia Twig), 10 g; chishao (Radix Paeoniae Rubra), 10 g; danggui (*Angelica sinensis*), 10 g; chuangxiong (*Ligusticum wallichii*), 10 g; dilong (*Lumbricus*), 10 g; weilingxian (Radix Clematidis), 10 g; fuling (Poria Cocos), 10 g; baizhu (Rhizoma Atractylodis macrocephalae), 10 g; dangshen (*Codonopsis pilosula*), 10 g; Roucongrong (Cistanche), 15 g; and gancao (liquorice), 6 g. The quality of these herbs was consistent with the 2020 Chinese Pharmacopeia (16). The decoction was prepared with a standardized procedure, with each formula unit yielding 400 ml of decoction. The HGW and BYHW decoctions were prescribed for 90 days (200 ml orally two times daily).

Follow-up and assessment

Upon admission, the Inflammatory Neuropathy Cause and Treatment (INCAT) Disability Score was 6. The Medical Research Council (MRC) score was 32. The Barthel Index (BI) was 50. After 20 days of treatment, the MRC and BI scores increased to 38 and 60, respectively. However, the INCAT score remained unchanged. Moreover, 3 months later, the patient reported no limb weakness or numbness, and his limb muscle strength could reach grade 5. INCAT, MRC, and BI scores changed to 0, 60, and 100, respectively (Figure 2). After eight months of discharge, the symptoms did not recur during the follow-up.

Most importantly, no side effects were reported. It was unfortunate that she refused to accept an EMG to assess nerve recovery. The patient was delighted with the treatment outcome and was free of adverse events, and the cost was acceptable for a rural family in a developed country. She stated that, after coming to our hospital, her symptoms improved and her quality of life significantly improved. All follow-ups were conducted face to face.

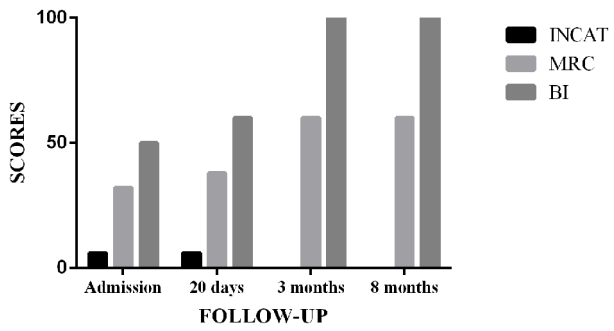

FIGURE 2
Outcome assessment for the CIDP patient in the follow-up. INCAT, Inflammatory Neuropathy Cause and Treatment; MRC, Medical Research Council; BI, Barthel Index.

Literature review

From their inception to 11 November 2022, we screened the following databases for literature reviews: PubMed, EMBASE, Web of Science, the Cochrane Library, the Chinese National Knowledge Infrastructure Databases (CNKI), Wanfang Data, and the Chongqing Chinese Science and Technology Periodical Database (VIP). The search strategy included "traditional Chinese medicine" and "chronic inflammatory demyelinating polyradiculoneuropathy" (Supplementary Table S2).

Supplementary Figure S1 depicts the selection of studies. Finally, only 10 studies were included in the literature review (Table 1) (17–26). Three studies were randomized controlled trials, while seven were case reports or case series (Figure 3). The earliest study was conducted in 1998. A total of 419 CIDP patients were involved, but all study sites were in China. The age of CIPD cases

TABLE 1 Study characteristics.

References	Country	Cases(*n*)	Age	Sex (M/F)	Course	Treatment	Significant findings	Follow-up	Study design
Sha et al. (17)	China	1	6	Girl	3 years	➢ Huangqi-Guizhi-Wuwu decoction: Huangqi 60 g; Guizhi 10 g; Baishao 15 g; Danggui 15 g; Baizhu 20 g; Gegen 10 g; Sangzhi 6 g; Yingyanghuo 6 g; Yangqishi 6 g; Ziheche 3 g; Dihuang 20 g; Gancao 15 g. ➢ Acupuncture ➢ Course of treatment: 3 months	Hughes: 3–0; Barthel Index: 20–95; muscle strength (upper limbs): 4–5; muscle strength (lower limbs): 3–5	16 months	Case report
Jinliang et al. (18)	China	T: 58 C: 57	T: 37.1 C: 34.7	T: 23/31 C: 28/32	T: 17.1 months C: 15.2 months	➢ T: • Guilongtongluo capsule: Huangqi, Dihuang, Jixueteng, Guizhi, Sangzhi, Dilong, Wushaoshe, etc. Six capsules (0.38 g) tid • Prednison, 15 mg, qd ➢ C: Prednison, 15 mg, qd ➢ Course of treatment: 3 months	MCV/SCV/latency were improved Hughes: Motor T/C: $1.23 \pm 1.22/2.13 \pm 1.32$; Sensory T/C: $0.59 \pm 1.02/1.02 \pm 1.28$; Barthel Index $\leq$ 40 (%): T/C: 6.9%/21.1%	3 months	RCT
Kuang and Liu (19)	China	1	14	Boy	3 months	➢ Buzhongyiqi-mahuangfuzixixin decoction: Huangqi 30 g; Fuzi 30 g; Dangsheng 15 g; Xianlingpi 15 g; Tufuling 15 g; Shangyao 20 g; Chenpi 9 g; Tusizi 9 g; Baizhu 10 g; Danggui 10 g; Ganjiang 10 g; Jixueteng 45 g; Mahuang 5 g ➢ Maqianzi 2 capsules (0.2 g), bid ➢ Course of decoction: 6 months ➢ Huangqi injection, 40 ml, ivgtt, qd; and shenfu injection, 30 ml, ivgtt, qd ➢ Acupuncture ➢ Course of other TCM: 1 month	Clinical symptoms were full-recovery. Muscular strength and tendon reflex all turned to normal	6 months	Case report
Wei et al. (20)	China	18	40 ± 6.3	10/8	1 ± 0.45 year	➢ TCM Decoction: Huangqi 30 g; Huangjing 15 g; Yinyanghuo 15 g; Sangjisheng 30 g; Niuxi 15 g; Gegen 15 g ➢ Acupuncture and tuina ➢ Course of treatment: 1 month No immunotherapy	Prineas ($\geq$1): 100% to 33.3%; ADL (independence): 0 to 78%	6 months to 12 months	Case series
Yu et al. (21)	China	7	55.8 ± 5.05	4/3	3–26 months	➢ Bu-Yang-Huan-Wu decoction: Huangqi 60 g; Danggui 10 g; Chuangxiong 10 g; Chishao 20 g; Dilong 15 g; Qinjiao 50 g; Baizhu 15 g; Duhuo 15 g; Niuxi 15 g; Jixueteng 30 g; Yujin 15 g; Ruxiang 5 g; Huangbo 10 g ➢ Acupuncture ➢ Course of TCM: 1 month ➢ Prednosone	Muscular strength increased ($\geq$2) 71.43%; ($\geq$1) 100%	Not report	Case series
Liu et al. (22)	China	1	33	Woman	1 year	➢ Buzhongyiqi decocotion: Huangqi 30 g; Renshen 10 g; Baizhu 10 g; Danggui 10 g; Shengma 10 g; Chaihu 10 g; Chenpi 10 g; Duzhong 10 g; Niuxi 10 g; Suoyang 10 g; Gancao 6 g ➢ Acupuncture and moxibusion ➢ Course of TCM: 1 month ➢ Corticosteroid	Muscular strength was from 2+ to 5–; Numbness and tendon reflex all turned to normal	Not report	Case report

(Continued)

10.3389/fneur.2023.1126444

TABLE 1 (Continued)

References	Country	Cases(*n*)	Age	Sex (M/F)	Course	Treatment	Significant findings	Follow-up	Study design
Hu et al. (23)	China	T: 30 C: 30	T: 35.8± 5.2 C: 36.6± 7.3	T: 18/12 C:20/10	T:11.1±4.5 months C:10.3 ± 4.8 months	➢ T: • Guilongtongluo capsule: Huangqi, Dihuang, Jixueteng, Guizhi, Sangzhi, Dilong, Wushaoshe, etc. Six capsules (0.38 g) tid • Prednison, 15 mg, qd ➢ C: Prednison, 15 mg, qd ➢ Course of treatment: 3 months	MCV/SCV/latency were improved Hughes: Motor T/C: 1.27 ± 1.25/2.06 ± 1.43; Sensory T/C: 0.63 ± 0.93/1.28 ± 1.37; Barthel Index ≤ 40 (%): T/C: 10%/20%	3 months	RCT
Li and Fan (24)	China	15	20–70	10/5		➢ Bu-Yang-Huan-Wu decoction: Huangqi 30 g; Danggui 12 g; Chuangxiong 9 g; Chishao 12 g; Dilong 12 g; Taoren 12 g; Gouji 20 g; Gegen 20 g; Honghua 9 g; Quanxie 9 g, 2 Wugong ➢ Course of treatment: 4 weeks	Prineas (≥1): 100% to 26.7%	6 months	Case series
Lin et al. (25)	China	11	11–65	6/5	1.5 years	➢ Bu-Yang-Huan-Wu decoction: Huangqi 45 g; Danggui 12 g; Chuangxiong 9 g; Chishao 12 g; Dilong 12 g; Taoren 12 g; Gouji 15 g; Mugua 6 g; Honghua 5 g; Gancao 5 g ➢ Course of treatment: 6 months ➢ Intravenous inmmunoglobulin 0.4 mg/kg, ivgtt, qd, 5 days	Prineas (≥1): 100% to 9.1%	6 months—12 months	Case series
Ren et al. (26)	China	T: 20 C: 20	T: 35 ± 2 C: 33 ± 3	T: 12/8 C: 11/9	T: 3–8 months C: 2.5–7 months	➢ T: • Buzhongyiqi decocotion: Huangqi 30 g; Renshen 15 g; Baizhu 10 g; Danggui 10 g; Shengma 10 g; Chaihu 10 g; Chenpi 10 g; Gancao 6 g • Corticosteroid ➢ C: Corticosteroid ➢ Course of treatment: 3 months	Muscular strength increased (≥2) 65%/30%; (≥1) 90%/70%; Relapse rate: T/C: 11.1%/42.9%	12 months	RCT

10.3389/fneur.2023.1126444

ranged from 6 to 70 years, with the most enrolled patients being men. The duration of CIDP disease was 2.5 months to 3 years. Most studies did not report comorbidities.

TCM decoctions were used in all included studies, and the treatment duration ranged from 4 weeks to 6 months. In 60% of the studies, TCM was combined with corticosteroids or IVIg. The average duration of follow-up ranged from 6 months to 16 months. TCM therapies improved muscular strength, sensory disorders (SNCV and MNCV), daily life ability, and relapse rate. However, many studies did not report any adverse event.

There have been reports of nine TCM formulas involving 44 herbs (Supplementary Table S3). The most common herbs were Huang Qi (*Astragalus membranaceus*) (100%), Banggui (*Angelica sinensis*) (77.8%), Baizhu (Rhizoma Atractylodis macrocephalae) (44.4%), and Dilong (*Lumbricus*) (44.4%). We used Gephi 0.9.2 and SPSS Modeler 18.0 to perform a complex network analysis to find the core herb. We identified that Huang Qi was the core herb. The results revealed that the number of triangles, clustering coefficient, and eigenvector centrality were 291, 0.32, and 1, respectively (Figure 3). Furthermore, the dose of Huang Qi in various formulas ranged from 30 to 60 g.

Three RCT studies had sample sizes ranging from 40 to 115. The risk bias assessment tool (RoB2) (27) was used to assess the quality of three RCT studies. The randomization process, deviations from the intended intervention, missing outcome data, outcome measurement, and selection of the reported result were all evaluated. However, the bias in these studies indicated a high risk (Figure 3). Therefore, the efficacy of TCM for CIDP requires further validation in a high-quality RCT.

Discussion

The typical CIDP is a chronic, progressive, monophasic, or recurrent demyelinating polyradiculoneuropathy with progressive weakness, sensory dysfunction, and absent or reduced tendon reflexes (28). CIDP variants include distal, multifocal, focal, motor, and sensory CIDP, all of which share the characteristics of

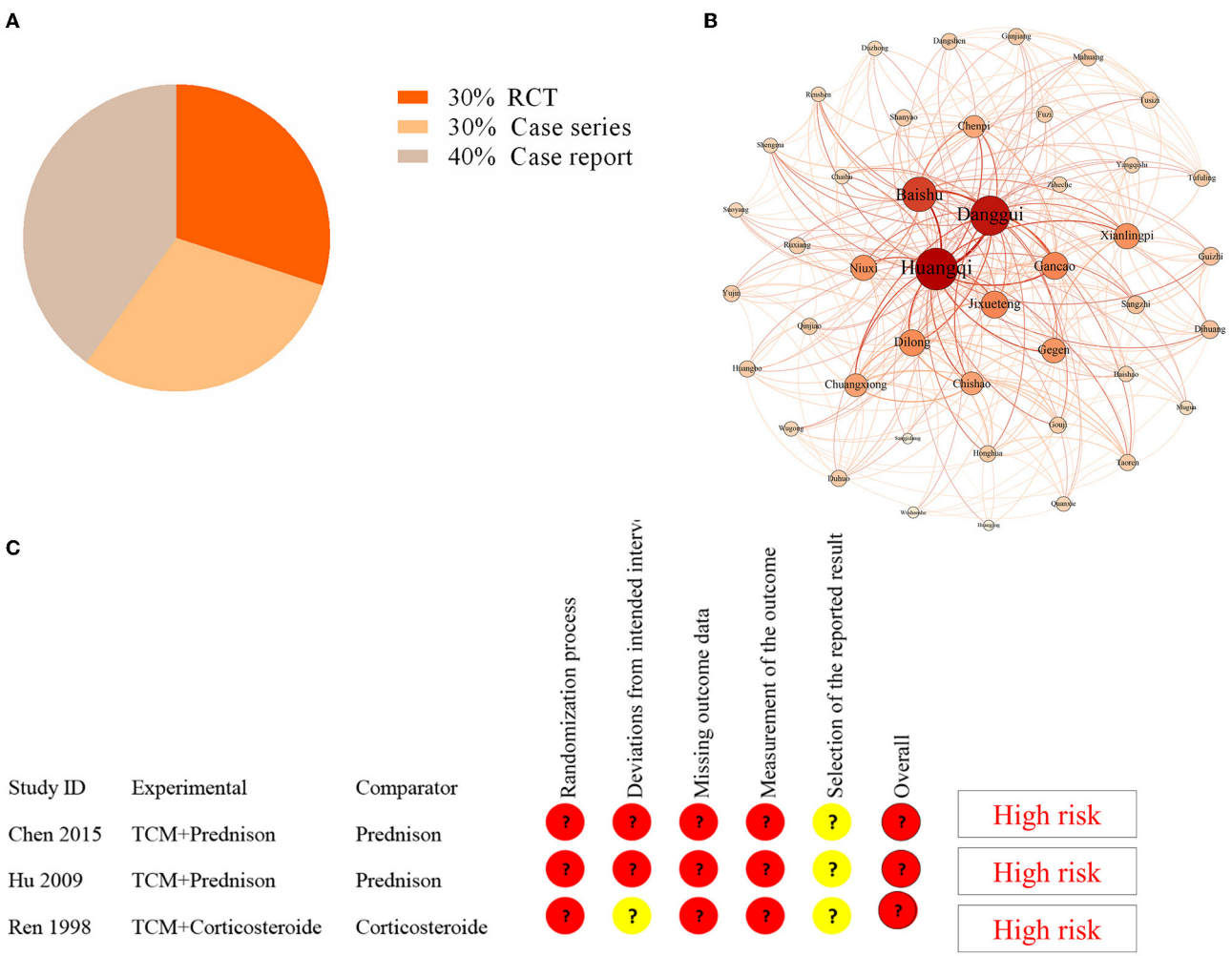

FIGURE 3
Analysis in the literature review. **(A)** The distribution of study design in the included studies. **(B)** Complex network analysis of selected TCM formulas from the included studies. **(C)** The results of the quality assessment of three RCT studies by using the risk bias assessment tool (RoB2).

demyelination and the immune therapy response (4). The diagnosis of CIDP is mainly based on clinical, electrodiagnostic, and laboratory features. However, the heterogeneity of CIDP creates challenges and delays in diagnosis. The ICOS study indicated that the time between disease onset and treatment was 11 months, and delayed-treated patients had a more severe disability (9).

The CIDP patient discussed in the above care report presented with symmetrical and progressive weakness, numbness, loss of tendon reflexes, abnormal protein levels in the CSF, and demyelination on the EMG. The progressive phase lasted more than 3 months. Furthermore, this patient responded to corticosteroid treatment, one of the characteristics of CIDP (29). Therefore, there was sufficient evidence to confirm a CIDP diagnosis for the patient. However, treatment was delayed due to economic hardship and initial mild symptoms.

Interestingly, the patient's CSF ASF-IgG was positive. One of the glycolipid antibodies against the peripheral nerve membrane surface is aSF. Sulfatides constitute a significant class of myelin-specific lipids, and their depletion can result in region-specific effects on non-compact myelin (30). Only 1–3% of CIDP patients had positive aSF (31, 32), raising questions about its diagnostic value. However, aSF-positive patients can exhibit typical clinical symptoms and respond well to immunomodulatory therapy (33), and this case supports the conclusion. The pathological mechanism and clinical significance of aSF should be investigated further.

Almost 20% of the CIDP patients did not respond to first-line therapy (5). Furthermore, 85.7% and 76.9% of CIDP patients experienced worsening after discontinuing IVIg and intravenous methylprednisolone, respectively (34). In addition, the long-term treatment course, high costs, inconvenience, and adverse events limit the application. There is a pressing need to explore alternative therapies that are both effective and safe in order to avoid those problems. Some studies have demonstrated that pulsed high-dose corticosteroid treatment might have fewer side effects and a faster response than daily oral corticosteroid treatment (35, 36). However, the evidence in the guideline is only low to moderate (4).

Meanwhile, some researchers have focused on subcutaneous immunoglobulin, which is well tolerated, effective, and affordable. However, the duration of maintenance treatment is at least 24 weeks, and local reactions at the infusion site are common (37). Better therapies must be explored further.

Traditional Chinese medicine and intravenous dexamethasone were used to treat this case. The intravenous dexamethasone course lasted only 1 week, and TCM was used for 3 months. With no adverse events and an extremely positive response, the combined treatment may be a more effective and safe option. The short-term corticosteroid treatment was well tolerated. Moreover, Chinese herbs were inexpensive, had few or no side effects, and were readily available. In the literature review, 50% of the studies (17, 20–22, and 25) used TCM in combination with corticosteroids, resulting in improvements in weakness, sensory disorder, daily life ability, and relapse rate. Therefore, it can potentially solve the CIDP dilemma, particularly in developing and rural countries. It is generally known that CIDP is an autoimmune disorder that affects peripheral nerve components. Macrophage and T-cell infiltration into peripheral nerves or nerve roots can result in demyelination and axonal damage (2). Corticosteroids are believed to treat CIDP by suppressing various immune components of its presumed autoimmune inflammatory process. Higher concentrations of corticosteroids also interact with DNA recognition sites to activate the transcription of anti-inflammatory genes (6).

Traditional Chinese medicine treatment of this reported CIDP case included Huangqi-Guizhi-Wuwu (HGW) and Bu-Yang-Huan-Wu (BYHW) decoctions, which are the most famous formulas in ancient TCM books. The network pharmacology analysis revealed that HGW could regulate cytokines and the inflammatory response, elements of the cytokine network, the T-cell receptor, NF-kappa B, HIF-1, and PI3K-Akt signaling pathways (14). BYHW can also regulate inflammatory cytokine production and facilitate axonal regeneration (38). Moreover, BYHW may assist in the timely interaction of regenerating axons and distal Schwann cells (39). Furthermore, some studies have indicated that quercetin, formononetin, isorhamnetin, and kaempferol were the main active compounds of HGW, while hydroxysafflor yellow A, astragaloside IV, ferulic acid, ligustrazine, and Z-ligustilide were mainly present in BYHW (40). In the literature review, the herb Huang Qi was used in all studies, with doses ranging from 30 to 60 g in different formulas, and it was used as the core herb in the complex network analysis. This female CIDP patient was also treated with 60 g Huang Qi. More than 100 compounds have been identified in Huang Qi, including flavonoids, saponins, polysaccharides, and amino acids (41). Huangqi can promote the development of immune organs, enhance mucosal immune function, increase the quantity and phagocytic capacity of innate immunity, promote the maturation and differentiation of acquired immunity cells, and improve antibody expression in acquired immunity (42). It appears promising to conduct extensive research on these formulas and Huang Qi for CIDP.

The Inflammatory Neuropathy Cause and Treatment Disability Score, MRC, and BI were used in this case to assess the treatment effect at multiple time points. The INCAT disability score is a valuable tool for evaluating upper and lower limb dysfunctions in inflammatory polyneuropathy studies, with the advantages of feasibility, high face validity, and high reliability (43). The MRC scale was used to assess muscle strength, with a score ranging from 0 for paralysis to 5 for normal and the sum of six pairs of muscles to represent a patient's overall strength. For inflammatory neuropathies, the MRC grading system was frequently used as an outcome measure (44). The BI is a reliable indicator of independence in daily activities. The scale described ten tasks based on the amount of time or assistance the patient requires, with lower scores indicating greater nursing dependency (45, 46). Surprisingly, after 3 months of TCM treatment, the INCAT, MRC, and BI scores were close to normal, and the treatment effect was sustainable. There was no relapse in the 8 months of follow-up.

Adverse effects were common with short-, medium-, and long-term immunotherapy (47). Adverse effects of corticosteroids include diabetes mellitus, hypertension, gastric ulceration, weight gain, osteopenia, and the long-term risk of severe side effects. Transient hypertension, headache, venous thrombosis, and acute renal dysfunction are the common side effects of IVIg. Adverse events associated with citrate use, difficulty with venous access, and hemodynamic changes have been reported in plasma exchange patients. In some cohorts, 60–70% of the CIDP patients reported problems with mobility, self-care, usual activities, pain, or discomfort in IVIg and methylprednisolone (9). It is inspiring to

be here and see how TCM can be used to ensure efficacy and safety in the literature review and case report. Reducing adverse events is particularly important for CIDP patients.

To the best of our knowledge, to date, no English literature has reported the clinical efficacy of Chinese herbs for CIDP. This is the first article to summarize TCM trial or case report findings for CIDP. The article also presented potentially effective herbs or formulas containing specific ingredients. However, evidence of efficacy in case reports is lacking. Longer follow-up efficacy and an EMG exam should be investigated further. All the studies in the review were published in Chinese literature, had a single study site, and had low study quality. Large-sample, multi-center, high-quality studies are required to obtain a high level of evidence for TCM. Therefore, TCM has broad potential applications in CIDP because TCM is well tolerated, effective, inexpensive, and readily available.

Conclusion

In conclusion, the case demonstrated that TCM treatment combined with short-term corticosteroid therapy eliminated the weakness and numbness of CIDP and improved her quality of life. Huangqi (*Astragalus membranaceus*) may be important for regulating the inflammatory response. Although these preliminary findings are promising, larger sample sizes and higher-quality RCTs are urgently required to confirm our findings.

Data availability statement

The original contributions presented in the study are included in the article/Supplementary material, further inquiries can be directed to the corresponding author.

Ethics statement

Ethical review and approval was not required for the study on human participants in accordance with the local legislation and institutional requirements. The patients/participants provided their written informed consent to participate in this study. Written informed consent was obtained from the individual(s) for the publication of any potentially identifiable images or data included in this article.

Author contributions

The idea for this research was proposed by YX. This protocol's drafting was undertaken by YX and LL. DW and JG revised the manuscript for intellectual content. Data collection and illness discussion were performed by YX, LX, JJ, GM, TY, SW, and AL. All authors approved the final version of the manuscript.

Funding

This research was supported by the General Project of the Health Commission of Hunan Province (No. 202218014505), the General Project of the Hunan Administration of Traditional Chinese Medicine (No. D2022060), the Hunan Province Clinical Medical Technology Innovation Guidance Project (No. 2021SK51001), and the Natural Science Foundation of Hunan Province (No. 2022JJ40241).

Conflict of interest

The authors declare that the research was conducted in the absence of any commercial or financial relationships that could be construed as a potential conflict of interest.

Publisher's note

All claims expressed in this article are solely those of the authors and do not necessarily represent those of their affiliated organizations, or those of the publisher, the editors and the reviewers. Any product that may be evaluated in this article, or claim that may be made by its manufacturer, is not guaranteed or endorsed by the publisher.

Supplementary material

The Supplementary Material for this article can be found online at: https://www.frontiersin.org/articles/10.3389/fneur.2023.1126444/full#supplementary-material

References

1. Mathey EK, Park SB, Hughes RA, Pollard JD, Armati PJ, Barnett MH, et al. Chronic inflammatory demyelinating polyradiculoneuropathy: from pathology to phenotype. *J Neurol Neurosurg Psychiatry.* (2015) 86:973–85. doi: 10.1136/jnnp-2014-309697

2. Querol L, Lleixà C. Novel immunological and therapeutic insights in Guillain-Barré syndrome and CIDP. *Neurotherapeutics.* (2021) 18:2222–35. doi: 10.1007/s13311-021-01117-3

3. Querol L, Crabtree M, Herepath M, Priedane E, Viejo VI, Agush S, et al. Systematic literature review of burden of illness in chronic inflammatory demyelinating polyneuropathy (CIDP). *J Neurol.* (2021) 268:3706–16. doi: 10.1007/s00415-020-09998-8

4. Van den Bergh P, van Doorn PA, Hadden R, Avau B, Vankrunkelsven P, Allen JA, et al. European Academy of Neurology/Peripheral Nerve Society guideline on diagnosis and treatment of chronic inflammatory demyelinating polyradiculoneuropathy: report of a joint Task Force-Second revision. *Eur J Neurol.* (2021) 28:3556–83. doi: 10.1111/ene.14959

5. Chinese Society of Neurology, Peripheral Neuropathy Collaboration Group of Chinese Society of Neurology, Chinese Society of Electromyography and Clinical Neuroelectrophysiology, Chinese Society of Neuromuscular Disease. Chinese guidelines for diagnosis and treatment of chronic inflammatory demyelinating polyradiculoneuropathy 2019. *Chin J Neurol.* (2019) 52:883–8. doi: 10.3760/cma.j.issn.1006-7876.2019.11.003

6. Hughes RA, Mehndiratta MM, Rajabally YA. Corticosteroids for chronic inflammatory demyelinating polyradiculoneuropathy. *Cochrane Database Syst Rev.* (2017) 11:D2062. doi: 10.1002/14651858.CD002062.pub4

7. Eftimov F, Winer JB, Vermeulen M, de Haan R, van Schaik IN. Intravenous immunoglobulin for chronic inflammatory demyelinating polyradiculoneuropathy. *Cochrane Database Syst Rev.* (2013) 2013:D1797. doi: 10.1002/14651858.CD001797.pub3

8. Kuwabara S, Mori M, Misawa S, Suzuki M, Nishiyama K, Mutoh T, et al. Intravenous immunoglobulin for maintenance treatment of chronic inflammatory demyelinating polyneuropathy: a multicentre, open-label, 52-week phase III trial. *J Neurol Neurosurg Psychiatry.* (2017) 88:832–8. doi: 10.1136/jnnp-2017-316427

9. Bus S, Broers MC, Lucke IM, Bunschoten C, van Lieverloo G, Adrichem ME, et al. Clinical outcome of CIDP one year after start of treatment: a prospective cohort study. *J Neurol.* (2022) 269:945–55. doi: 10.1007/s00415-021-10677-5

10. Hughes R, Dalakas MC, Merkies I, Latov N, Léger JM, Nobile-Orazio E, et al. Oral fingolimod for chronic inflammatory demyelinating polyradiculoneuropathy (FORCIDP Trial): a double-blind, multicentre, randomised controlled trial. *Lancet Neurol.* (2018) 17:689–98. doi: 10.1016/S1474-4422(18)30202-3

11. Li Z, Jin H, Yan Q, Sun L, Wasan HS, Shen M, et al. The method of activating blood and dredging collaterals for reducing Chemotherapy-Induced peripheral neuropathy: a systematic review and meta-analysis. *Evid Based Complement Alternat Med.* (2019) 2019:1029626. doi: 10.1155/2019/1029626

12. Pang B, Zhao TY, Zhao LH, Wan F, Ye R, Zhou Q, et al. Huangqi Guizhi Wuwu Decoction for treating diabetic peripheral neuropathy: a meta-analysis of 16 randomized controlled trials. *Neural Regen Res.* (2016) 11:1347–58. doi: 10.4103/1673-5374.189202

13. Li QY, Cai FH, Lu Y, Liu H, Wang X, Li FL, et al. External treatment with Chinese herbal medicine for chemotherapy-induced peripheral neuropathy: a systematic review and meta-analysis. *Front Pharmacol.* (2022) 13:764473. doi: 10.3389/fphar.2022.764473

14. Gu JL, Wei GL, Ma YZ, Zhang JZ Ji Y, Li LC, et al. Exploring the possible mechanism and drug targets of Huang-Qi-Gui-Zhi-Wu-Wu decoction for the treatment of Chemotherapy-Induced peripheral neuropathy on network pharmacology. *Evid Based Complement Alternat Med.* (2020) 2020:2363262. doi: 10.1155/2020/2363262

15. Riley DS, Barber MS, Kienle GS, Aronson JK, von Schoen-Angerer T, Tugwell P, et al. CARE guidelines for case reports: explanation and elaboration document. *J Clin Epidemiol.* (2017) 89:218–35. doi: 10.1016/j.jclinepi.2017.04.026

16. Chinese Pharmacopoeia Commission. *Pharmacopoeia of the People's Republic of China.* Beijing: China Medical Science and Technology Press (2020).

17. Sha D, Lingjuan H, Qiliang X, Suicheng X. TCM in the treatment of childhood chronic inflammatory demyelinating polyneuropathy: a case report. *World Chin Med.* (2018) 13:138–41. doi: 10.3969/j.issn.1673-7202.2018.01.035

18. Jinliang C, Xiaoli Y, Junyong HU. Therapy of integrated medicine in the treatment of chronic inflammatory demyelinating polyneuropathy for 58 cases. *Chin Med Modern Distance Educ China.* (2015) 13:71–3. doi: 10.3969/j.issn.1672-2779.2015.17.036

19. Kuang S, Liu C. Discussion on treating chronic Guillain-Barre syndrome with integrated traditional and western medicine. *Shanxi J Trad Chin Med.* (2015) 31:1–3. doi: 10.3969/j.issn.1000-7156.2015.06.001

20. Wei Y, Zhou Z, Liu G, Tang C. Eighteen cases with chronic inflammatory demyelinating polyradiculoneuropathy were treated with traditional Chinese medicine. *Hebei J Trad Chin Med.* (2014): 537-8, 539.

21. Yu S, Yang S, Zheng M. Summary of 7 cases with chronic Guillain-Barre syndrome treated with traditional Chinese medicine therapy. *Hunan J Tradit Chin Med.* (2014) 30:29–30. doi: 10.16808/j.cnki.issn1003-7705.2014.02.015

22. Liu M, Zheng S, Liu J, A. case of chronic Guillain-Barre syndrome was treated with acupuncture and traditional Chinese medicine. *Jiangxi J Tradit Chin Med.* (2012) 43:57–8. doi: 10.3969/j.issn.0411-9584.2012.04.030

23. Hu J, Chen J, Zhang Z. Clinical observation on treatment of 30 patients with chronic inflammatory demyelinating polyneuropathy by Guilong Tongluo capsule combined with prednisone. *Chin J Integr Med.* (2009) 29:649–51. doi: 10.3321/j.issn:1003-5370.2009.07.021

24. Li W, Fan X. Analysis of 15 cases of chronic Guillain-Barre syndrome treated with integrated traditional Chinese and western medicine. *Shanxi Med J.* (2007) 637.

25. Lin X, Wu X, Zhong J. Effect of Buyang-Huanwu decoction combined with gamma globulin therapy on 11 cases of chronic Guillain-Barre syndrome. *J New Chin Med.* (2005) 37:50–1. doi: 10.3969/j.issn.0256-7415.2005.03.023

26. Ren M, Yang R, Wang X, Hu J. Clinical study of integrated traditional Chinese and western medicine in the treatment of chronic inflammatory demyelinating polyradiculoneuropathy. *Chin J Med.* (1998) 55–7.

27. Sterne J, Savović J, Page MJ, Elbers RG, Blencowe NS, Boutron I, et al. RoB 2: a revised tool for assessing risk of bias in randomised trials. *BMJ.* (2019) 366:l4898. doi: 10.1136/bmj.l4898

28. Bunschoten C, Jacobs BC, Van den Bergh P, Cornblath DR, van Doorn PA. Progress in diagnosis and treatment of chronic inflammatory demyelinating polyradiculoneuropathy. *Lancet Neurol.* (2019) 18:784–94. doi: 10.1016/S1474-4422(19)30144-9

29. Shije J, Brannagan TR. Chronic inflammatory demyelinating polyradiculoneuropathy. *Semin Neurol.* (2019) 39:596–607. doi: 10.1055/s-0039-1693008

30. Palavicini JP, Wang C, Chen L, Ahmar S, Higuera JD, Dupree JL, et al. Novel molecular insights into the critical role of sulfatide in myelin maintenance/function. *J Neurochem.* (2016) 139:40–54. doi: 10.1111/jnc.13738

31. Nobile-Orazio E, Giannotta C, Briani C. Anti-ganglioside complex IgM antibodies in multifocal motor neuropathy and chronic immune-mediated neuropathies. *J Neuroimmunol.* (2010) 219:119–22. doi: 10.1016/j.jneuroim.2009.11.012

32. Giannotta C, Di Pietro D, Gallia F, Nobile-Orazio E. Anti-sulfatide IgM antibodies in peripheral neuropathy: to test or not to test? *Eur J Neurol.* (2015) 22:879–82. doi: 10.1111/ene.12658

33. Klehmet J, Märschenz S, Ruprecht K, Wunderlich B, Büttner T, Hiemann R, et al. Analysis of anti-ganglioside antibodies by a line immunoassay in patients with chronic-inflammatory demyelinating polyneuropathies (CIDP). *Clin Chem Lab Med.* (2018) 56:919–26. doi: 10.1515/cclm-2017-0792

34. Nobile-Orazio E, Cocito D, Jann S, Uncini A, Messina P, Antonini G, et al. Frequency and time to relapse after discontinuing 6-month therapy with IVIg or pulsed methylprednisolone in CIDP. *J Neurol Neurosurg Psychiatry.* (2015) 86:729–34. doi: 10.1136/jnnp-2013-307515

35. van Schaik IN, Eftimov F, van Doorn PA, Brusse E, van den Berg LH, van der Pol WL, et al. Pulsed high-dose dexamethasone versus standard prednisolone treatment for chronic inflammatory demyelinating polyradiculoneuropathy (PREDICT study): a double-blind, randomised, controlled trial. *Lancet Neurol.* (2010) 9:245–53. doi: 10.1016/S1474-4422(10)70021-1

36. Eftimov F, Vermeulen M, van Doorn PA, Brusse E, van Schaik IN. Long-term remission of CIDP after pulsed dexamethasone or short-term prednisolone treatment. *Neurology.* (2012) 78:1079–84. doi: 10.1212/WNL.0b013e31824e8f84

37. van Schaik IN, Bril V, van Geloven N, Hartung HP, Lewis RA, Sobue G, et al. Subcutaneous immunoglobulin for maintenance treatment in chronic inflammatory demyelinating polyneuropathy (PATH): a randomised, double-blind, placebo-controlled, phase 3 trial. *Lancet Neurol.* (2018) 17:35–46. doi: 10.1016/S1474-4422(17)30378-2

38. Kim KJ, Namgung U. Facilitating effects of Buyang Huanwu decoction on axonal regeneration after peripheral nerve transection. *J Ethnopharmacol.* (2018) 213:56–64. doi: 10.1016/j.jep.2017.10.036

39. Kim KJ, Hwang J, Park JY, Namgung U. Augmented Buyang Huanwu Decoction facilitates axonal regeneration after peripheral nerve transection through the regulation of inflammatory cytokine production. *J Ethnopharmacol.* (2020) 260:113063. doi: 10.1016/j.jep.2020.113063

40. Wang K, Lei L, Cao J, Qiao Y, Liang R, Duan J, et al. Network pharmacology-based prediction of the active compounds and mechanism of Buyang Huanwu Decoction for ischemic stroke. *Exp Ther Med.* (2021) 22:1050. doi: 10.3892/etm.2021.10484

41. Fu J, Wang Z, Huang L, Zheng S, Wang D, Chen S, et al. Review of the botanical characteristics, phytochemistry, and pharmacology of *Astragalus membranaceus* (Huangqi). *Phytother Res.* (2014) 28:1275–83. doi: 10.1002/ptr.5188

42. Chen Z, Liu L, Gao C, Chen W, Vong CT, Yao P, et al. Astragali Radix (Huangqi): a promising edible immunomodulatory herbal medicine. *J Ethnopharmacol.* (2020) 258:112895. doi: 10.1016/j.jep.2020.112895

43. Breiner A, Barnett C, Bril V. INCAT disability score: a critical analysis of its measurement properties. *Muscle Nerve.* (2014) 50:164–9. doi: 10.1002/mus.24207

44. Vanhoutte EK, Faber CG, Merkies IS. 196Th ENMC international workshop: outcome measures in inflammatory peripheral neuropathies 8–10 February 2013, Naarden, the Netherlands. *Neuromuscul Disord.* (2013) 23:924–33. doi: 10.1016/j.nmd.2013.06.006

45. Collin C, Wade DT, Davies S, Horne V. The Barthel ADL Index: a reliability study. *Int Disabil Stud.* (1988) 10:61–3. doi: 10.3109/09638288809164103

46. Quinn TJ, Langhorne P, Stott DJ. Barthel index for stroke trials: development, properties, and application. *Stroke.* (2011) 42:1146–51. doi: 10.1161/STROKEAHA.110.598540

47. Oaklander AL, Lunn MP, Hughes RA, van Schaik IN, Frost C, Chalk CH. Treatments for chronic inflammatory demyelinating polyradiculoneuropathy (CIDP): an overview of systematic reviews. *Cochrane Database Syst Rev.* (2017) 1:D10369. doi: 10.1002/14651858.CD010369.pub2

frontiers | Frontiers in Neurology

TYPE Original Research
PUBLISHED 09 May 2023
DOI 10.3389/fneur.2023.1113404

Check for updates

OPEN ACCESS

EDITED BY
Giovanni Meola,
University of Milan, Italy

REVIEWED BY
David Lutz,
Ruhr-University Bochum, Germany
Massimo Costanza,
Fondazione IRCCS Istituto Neurologico Carlo Besta, Italy

*CORRESPONDENCE
Bitao Bu
bubitao@tjh.tjmu.edu.cn

RECEIVED 01 December 2022
ACCEPTED 20 April 2023
PUBLISHED 09 May 2023

CITATION
Ma X, Gao H, Xu L, Bi Z, Ji S and Bu B (2023) Increased expression of cell adhesion molecules in myofasciitis.
Front. Neurol. 14:1113404.
doi: 10.3389/fneur.2023.1113404

COPYRIGHT
© 2023 Ma, Gao, Xu, Bi, Ji and Bu. This is an open-access article distributed under the terms of the Creative Commons Attribution License (CC BY). The use, distribution or reproduction in other forums is permitted, provided the original author(s) and the copyright owner(s) are credited and that the original publication in this journal is cited, in accordance with accepted academic practice. No use, distribution or reproduction is permitted which does not comply with these terms.

Increased expression of cell adhesion molecules in myofasciitis

Xue Ma[1,2], Huajie Gao[2], Li Xu[2], Zhuajin Bi[2], Suqiong Ji[2] and Bitao Bu[2]*

[1]Department of Neurology, Air Force Medical University Tangdu Hospital, Xi'an, China, [2]Department of Neurology, Tongji Hospital, Tongji Medical College, Huazhong University of Science and Technology, Wuhan, China

Background: Myofasciitis is a heterogeneous group of diseases pathologically characterized by inflammatory cell infiltration into the fascia. Endothelial activation plays a critical role in the pathogenesis of the inflammatory response. However, the expression of cellular adhesion molecules (CAMs) in myofasciitis has not been investigated.

Methods: Data on clinical features, thigh magnetic resonance imaging, and muscle pathology were collected from five patients with myofasciitis. Immunohistochemical (IHC) staining and Western blot (WB) of the muscle biopsies from patients and healthy controls were performed.

Results: Increased levels of serum pro-inflammatory cytokines, including IL-6, TNF-α, and IL-2R, were detected in four patients. IHC staining and WB indicated significantly increased expression of cell adhesion molecules in blood vessels or inflammatory cells within the perimysium in muscle and fascia tissues of patients with myofasciitis compared to controls.

Conclusion: The up-regulation of CAMs in myofasciitis indicates endothelial activation, which may be potential therapy targets for the treatment of myofasciitis.

KEYWORDS

myofasciitis, dysregulated immune response, cell adhesion molecules, endothelial activation, myopathy

Introduction

Myofasciitis is recognized as a connective disease disorder (CTD) clinically characterized by symmetrical, painful swelling and progressive induration of the extremities and trunk. As a heterogeneous group of diseases, myofasciitis primarily consists of eosinophilic fasciitis (EF) (1), macrophagic myofasciitis (2), immune checkpoint inhibitor-induced myofasciitis (3), infection-associated myofasciitis (4), necrotizing fasciitis (5), chronic graft-versus-host disease-related myofasciitis (6), sarcoid myofasciitis (7), and unknown risk factors-associated myofasciitis. The pathological features of myofasciitis include fascial thickening, marked vasculitis, and inflammatory infiltration by lymphocytes, macrophages, and plasma cells (8).

Cell adhesion molecules (CAMs), including intercellular adhesion molecule 1 (ICAM-1), vascular cell adhesion molecule 1 (VCAM-1), platelet endothelial cell adhesion molecule (PECAM-1/CD31), and CD146, are expressed on vascular endothelial cells and are essential mediators of leukocyte–endothelial cell interactions during the inflammatory response (9, 10). To migrate into the target regions, the circulating leukocytes are activated by inflammatory cytokines and chemokines secreted locally by inflammatory cells, endothelial cells and

histocytes, to express integrins on their surface, such as very late antigen 4 (VLA-4, α4/β1, CD49d/CD29) and lymphocyte function-associated antigen 1 (CD11a/CD18), which enable firmer adhesion to other endothelial CAMs (9). The interaction between leukocytes and the endothelium is a major contributor in the inflammatory process (11, 12). However, the role of CAMs in myofasciitis has not been explored. To further understand the physiopathology mechanism of myofasciitis, an analysis of the expression analysis of CAMs may be of vital importance. We investigated the expression of ICAM-1 and its receptor (CD11a/18), VCAM-1 and its receptor (VLA-4), PECAM-1, and CD146 in muscle biopsies from patients with myofasciitis.

Materials and methods

Patient selection

Five patients who fulfilled diagnosis criteria for myofasciitis at Department of Neurology, Tongji Hospital were included. Biopsy specimens of muscle and fascia, as well as clinical and laboratory data obtained from these patients were retrospectively analyzed. The diagnosis of myofasciitis was determined based on suggestive clinical and laboratory findings, as well as muscle biopsy or magnetic resonance imaging (MRI) abnormalities [Table 1; (1)]. Other pathological entities, such as scleroderma, autoimmune myopathy, malignancies, and infection were excluded. There was no family history of neuromuscular disorders and no skin rashes were detected in the included patients. No vaccination was performed 1 year before the symptoms occurred. The fascia and muscle biopsy sites were determined by MRI. Muscle and fascia tissue from five patients without neuromuscular disorders served as controls. The study was approved by the Ethics Committee of Tongji Hospital and written informed consent was obtained from all included patients.

Serologic testing

All patients underwent myositis-specific autoantibody (MAA) and myositis-associated antibody (MSA) screening using a commercial semiquantitative line blot assay (Wuhan Kindstar Diagnostics Co., Ltd., Wuhan, China). MSAs and MAAs included anti-Mi2α and β, anti-TIF1γ, anti-MDA5, anti-NXP2, anti-SAE1, anti-Jo1, anti-SRP, anti-HMGCR, anti-PL7, anti-PL12, anti-EJ, anti-OJ, anti-Ku, anti-PM/Scl-100, anti-PM/Scl-75, and anti-Ro52 antibodies. The anti-nuclear, anti-SSA/Ro60, anti-SSB/La, anti-Sm, anti-RNP, anti-mitochondrial, anti-dsDNA antibodies, and rheumatoid factors (RF) were also evaluated. Serum cytokines were assayed by electro chemiluminescence immunoassay, including interleukin-6 (IL-6) (Roche, 05109442190), tumor necrosis factor-α (TNF-α) (SIMENS, LKNF1), interleukin-2 receptor (IL-2R) (SIMENS, LKIP1), interleukin-8 (IL-8) (SIMENS, LK8P1), and interleukin-10 (IL-10) (SIMENS, LKXP1). The assessment of inflammatory indexes was performed, including erythrocyte sedimentation rate (ESR) and C-reactive protein (CRP).

Histological, enzyme histochemical, and immunohistochemical studies

All biopsy specimens were rapidly cryopreserved in liquid nitrogen, and then stored at −80°C. The frozen sections (7 μm) were stained with hematoxylin and eosin, acid phosphatase, modified Gömöri trichrome, PAS, NADH tetrazolium reductase, cytochrome C oxidase, and ATPase at pH 4.3, 4.5, and 10.4. Eosinophils were detected by Wright-Giemsa staining. The immunohistochemical (IHC) analysis of cells expressing CD3 (1:200, MAC1477, Bio-Rad), CD4 (1:50, ab133616, Abcam), CD8 (1:50, ab93278, Abcam), CD68 (1:50, ab201340, Abcam), VCAM-1 (1:200, 11,444-1-AP, Proteintech), ICAM-1 (1:200, 10,831-1-AP, Proteintech), VLA-4 (1:200, 19,676-1-AP, Proteintech), CD11a/CD18 (1:1000, ab52895, Abcam), CD31/PECAM-1 (1:2000, ab9498, Abcam), and CD146 (1:200, Ab75769, Abcam) were performed using a 3, 3′-diaminobenzidine Detection Kit; the sections were then counterstained with hematoxylin. For immunofluorescence staining, expression of major histocompatibility complex class I (MHC-I) (1:100, ab23755, Abcam) and deposition of membrane attack complex (MAC) (1:50, Sc-58,935, Santa Cruz Biotechnology) on the fascia and sarcolemma were used with Alexa Fluor conjugated secondary antibody (1:400, Invitrogen) for 1 h. Images were obtained using a microscope (Olympus) or Confocal scanning (Olympus).

A modified semiquantitative scale previously defined by Corinna Preusse was used for analysis (2). Each sample was evaluated on 20 high-power fields (HPF; one HPF as 200×). The average number of cells in 6 randomly selected HPFs per sample was calculated and scored as follows: <5 positive cells, almost no staining (−); 5–20 positive cells, sparse staining (+); 21–50 positive cells, scatter staining (++); and >50 positive cells, abundant staining (+++). The up-regulation of MHC-I on non-necrotic myofibers and MAC

TABLE 1 Diagnostic criteria of myofasciitis.

Items
Major criteria:
Myalgia, swelling pain or symmetrical subcutaneous sclerotic induration on limbs
Minor criteria 1:
Fascial thickening with infiltration of lymphocytes and macrophages with or without eosinophils
Minor criteria 2:
Hyperintense fascia on MR fat suppression T2-weighted images
Exclusion criteria: system sclerosis, idiopathic inflammatory myopathy, infection, and malignancy

A diagnosis with myofasciitis will be made if a patient has the major criterion and one or two of the minor criteria.
MR, magnetic resonance.

deposition on sarcolemma were assessed as follows: no fibers stained (−); 0–10% of fibers stained (+); 11–30% of fibers stained (++); 31–60% of fibers stained (+++); and 61–100% of fibers stained (++++). For the positive staining on endothelium within the perimysium, the quantity and intensity were estimated separately and subjectively evaluated on a scale of -: absent, +: weak, ++: definite, +++: strong staining) (3). All biopsied sections were assessed by two independent experimenters.

Western blot

Muscle and fascia tissues from controls or patients with myofasciitis were homogenized in cell lysis buffer (Beyotime, China) supplemented with protease inhibitors (MCE, China) and phosphatase inhibitors (Promoter, China). Tissue lysates were centrifuged at 15000 × g for 15 min. The supernatant was collected and protein concentration was determined using the bicinchoninic acid assay. Total protein (20–50 μg) from each sample was resolved on 8% sodium dodecyl sulfate-polyacrylamide gels and transferred to 0.45 μM nitrocellulose filter membranes (Boster, China). The membranes were blocked with 5% skim milk for 1 h at room temperature to prevent non-specific binding of antibodies and were subsequently incubated over night with the primary antibodies. Primary antibodies include those against: glyceraldehyde-3-phosphate dehydrogenase (GAPDH) (1:5000, 60,004-I-Ig, Proteintech), VCAM-1 (1:1000, Ab134047, Abcam), ICAM-1 (1:1000, 10,831-1-AP, Proteintech), VLA-4 (1:1000, ab81280, Abcam), CD11a/CD18 (1:2000, ab52895, Abcam), CD31/PECAM-1 (1:2000, ab9498, Abcam), and CD146 (1:1000, Ab75769, Abcam). Membranes were washed with Tris-buffered saline with 0.05% Tween-20 and incubated for 1 h at room temperature with horseradish peroxidase-labeled anti-rabbit or anti-mouse secondary antibody (1:5000, Cell Signaling Technology). Blots were developed using enhanced chemiluminescence reagents (Servicebio, China) and evaluated using a charged-coupled device camera (Tanon 4,600). Quantification of immunoreactivity was performed by densitometric analysis using Fiji (NIH) software.

Statistical analysis

The data are presented as mean ± standard deviation (SD). Mann–Whitney U test was used for two groups. The statistical significance of the differences was evaluated using GraphPad Prism (Version 8.0.1). $p < 0.05$ was considered statistically significant.

Results

Case presentations

Five patients with myofasciitis were enrolled. The detailed clinical data of patients are presented in Table 2. Basic information of controls is displayed in Supplementary Table S1.

Patient 1

A 45 year-old man was admitted with fever (37.5–39.5°C) and myalgia for 25 days. No muscle weakness and paresthesia were reported. Normal muscle strength was indicated by Medical Research Council (MRC) grading. Muscle atrophy, hypertrophy, and abnormal pathological reflexes were absent. The level of serum creatinine kinase (CK) was normal (normal range: ≤ 190 U/L). An increased level of IL-6 was noted (8.21 pg./mL, normal range: < 5 pg./mL). Serum ESR was 55 mm/h (Normal range: 0–20 mm/h). The patient was negative for MAA and MSA. The level of rheumatoid factors (RF) was increased (36 IU/mL, normal range: < 20 IU/mL). Patient 1 was responsive to glucocorticoid monotherapy and had a favorable outcome.

Patient 2

A 28 year-old man presented with increasing induration of the upper limbs and tight feeling of the extremities for 5 months. Limb muscle strength was normal. The patients experienced difficulty in performing wrist extension and wrist flexion. There was no muscle atrophy, hypertrophy, or abnormal pathological reflexes. The serum CK level was normal. The patient exhibited increased levels of IL-6 (18.86 pg./mL), TNF-α (17.8 pg./mL, normal range: < 8.1 pg./mL), and IL-2R (1762 U/mL, normal range: 223–710 U/mL). MAA and MSA were negative. The patient was responsive to glucocorticoid monotherapy.

Patient 3

A 55-year-old man had experienced skin induration involving both forearms and legs with joint mobility disorder for 5 months. Physical examination revealed that the patient had difficulty performing the wrist flexion/extension task, forearm pronation/supination, hip flexion, and knee flexion. Limb muscle strength was normal. Blood eosinophilia (defined as $\geq 0.5 \times 10^9$/mL or 7% of total leukocytes) was evident. The patient was positive for anti-PM/Scl-75 antibodies. The level of serum CK was normal. CRP was elevated (14.5 mg/L, normal range: < 1 mg/L). Increased levels of IL-6 (24.96 pg./mL), TNF-α (13.0 pg./mL), and IL-2R (1,605 U/mL) were observed. The patient fulfilled the diagnostic criteria for EF (1). However, the possibility of CTD-related myofasciitis cannot be entirely excluded. Patient 3 was initially treated with glucocorticoid monotherapy but experienced no improvement. Addition of tacrolimus enabled achievement of clinical remission. The disorder of radioulnar and wrist joint function at the onset and recovery of joint movement are, respectively, displayed in Additional File 1 and 2.

Patient 4

A 30-year-old man was admitted with myalgia for 5 months. No joint movement disorder or limb muscle weakness was detected. Serum CK at onset was 3,169 U/L. The patient was positive for anti-Jo-1 and Ro-52 antibodies. The level of ESR was normal. The patient was diagnosed as CTD-related myofasciitis. The patient was administrated glucocorticoid and cyclophosphamide therapies and the serum CK declined to 214 U/L after 6 months.

Patient 5

A 32-year-old woman presented with myalgia and fever (37.5–39°C) for 12 months. The patient exhibited decreased limb muscle strength (4/5 MCR grade). No joint movement disorder was observed. The patient had been diagnosed with primary Sjogren's syndrome by rheumatologists 1 year previously. The serum CK level was normal and the serum anti-nuclear antibody titer was 1:3200. The patient was positive for Ro-52/SSA autoantibodies. The ESR was elevated (46 mm/h). The cytokine test revealed elevated levels of IL-2R, IL-6,

TABLE 2 Clinical finding of patients with myofasciitis.

Gender	Patient 1	Patient 2	Patient 3	Patient 4	Patient 5
	M	M	M	M	F
Age (years) at onset	45	28	55	30	32
Time (months), onset to admission	0.8	5	5	6	15
Clinical presentation	Myalgia and fever	Full-circumference swelling and induration of the distal limbs	Hardness of the proximal and distal extremities, and swelling pain	Myalgia and muscle weakness	Myalgia and fever
Fever	Yes	No	No	No	Yes
MRC	5	5	5	5	4
Joint movement disorder	No	Wrist joint	Radio-ulnar joint; wrist joint; hip joint; knee joint	No	No
ESR/CRP	ESR 55 mm/h	ESR 4 mm/h	CRP 14.5 mg/L	ESR 13 mg/L	ESR 46 mm/h
Eosinophilia	No	No	Yes	No	No
CK level at onset (U/L)	32	28	48	3,169	63
Cytokine	IL-6 8.21 pg./mL; TNF-α, IL-8, IL-10, IL-2R normal	IL-6 18.86 pg./mL; TNF-α 17.8 pg./mL; IL-2R 1762 U/mL; IL-8, IL-10 normal	IL-6 24.96 pg./ml; TNF-α 13.0 pg./mL; IL-2R 1,605 U/mL; IL-8, IL-10 normal	IL-6, TNF-α, IL-2R, IL-8, and IL-10 normal	IL-2R 1,042 U/mL; IL-6 19.94 pg./mL; TNF-α 44.3 pg./mL
Anti-nuclear antibody	Negative	Negative	1:100	Negative	1:3200; SS-A
MAAs and MSAs	Negative	Negative	PM/Scl-75	Jo-1, Ro-52	RO-52
Rheumatoid factor	36	Normal	Normal	Normal	27.5 IU/mL (< 20)
Diagnosis	Myofasciitis	Myofasciitis	Eosinophilic fasciitis	Myofasciitis	myofasciitis
Treatment	GC	GC	GC + FK506	GC+ cyclophosphamide	GC
Outcome	Improved	Improved	Improved	Improved	Improved

CK, creatine kinase; CRP, C reactive protein; ESR, erythrocyte sedimentation rate; GC, glucocorticoids; F, female; FK506, tacrolimus; M, male; MAAs, myositis-specific autoantibody; MSAs, myositis-associated antibody; MRC, Medical Research Council; No., number; IL-6, interleukin-6; IL-2R, interleukin-2 receptor; IL-8, interleukin-8; IL-10, interleukin-10; TNF-α, tumor necrosis factor-α;

and TNF-α (1,042 U/mL, 19.94 pg./mL, and 44.3 pg./mL, respectively). Rheumatoid factor was 27.5 IU/mL. The patient was administered glucocorticoid therapy and the clinical symptoms quickly resolved.

Upper and lower extremities MRI

Limbs MRI on fat suppression T2-weighted images indicated striking abnormalities. Thigh images of Patient 1 indicated the hyperintense signal of bilateral fascia of vastus medialis muscle and semimembranosus (Figure 1A). Patchy hyperintensity was distributed in upper arm muscle groups of Patient 1. Thickness and edema of subcutaneous superficial and deep muscular fasciae on lower extremity MRI images of Patient 2 were evident (Figure 1B). Upper arms images of Patient 2 showed slight signal hyperintensity in subcutaneous fatty and perifascicular tissues. Patient 3 demonstrated that marked hyperintense signals in a perimysial and perifascicular distribution in all thigh, calf (Figure 1C), and upper limb muscle groups. Muscular edema and thickening of the fascia of the posterior thigh muscles on fat suppression T2-weighted MRI images were observed in Patient 4 (Figure 1D). Thigh (Figure 1E) and forearm images (Figure 1F) of Patient 5 showed high signal intensity of the thickened deep and superficial fascia. These manifestations were in consistent with myofasciitis in these patients.

Pathological findings

Immunophenotype of inflammatory infiltration, up-regulation of MHC-1, and MAC deposition in biopsied specimens of patients with myofasciitis are presented in Figure 2, Table 3. Numerous inflammatory cells in the thickened fascia and perivascular inflammation were evident in biopsied specimens of patients with myofasciitis (Figures 2A-E). A few eosinophils were detected in the fascial tissues of Patient 3 but not of other four patients (Figures 2F-J). Macrophages and T lymphocytes constituted the predominant mononuclear cellular infiltrate and were dominantly distributed within the collagen tissues (Figures 2K-Y). Scatter B lymphocytes were detected in samples of all five patients (Figures 2Z-Dd). The expression of MHC-1 on the fibroblasts was particularly strong in five patients (Figures 2Ee-Ii). The intensity of MHC-I on the sarcolemma close to the immune cells was up-regulated in Patient 1 and 3. MAC was deposited on blood vessels in the fascia of the five patients (Figures 2Jj-Nn). No positive staining of CD4, CD8, CD68, and CD20 was observed in sections from controls (Supplementary Figure S1). Staining for MHC-I and MAC was detected on blood vessels in fascial tissues of control samples (Supplementary Figure S1).

The expression of CAMs in patients with myofasciitis is summarized in Table 4. Weak positive staining of VCAM-1 in the controls was noted (Figure 3A). However, there was the strong expression of VCAM-1 on

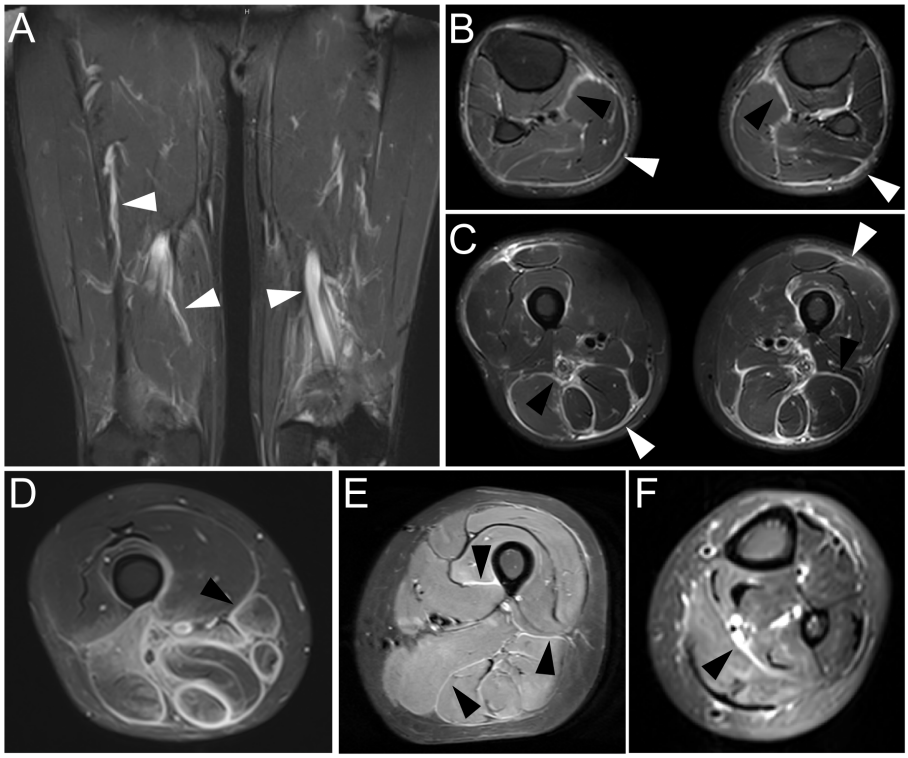

FIGURE 1
MRI findings at time of diagnosis in five patients with myofasciitis **(A)** Increased signal abnormalities were noted in deep fascia of bilateral fascia of vastus medialis muscle and semimembranosus (white arrowheads) on fat suppression T2-weighted thigh MRI in Patient 1. **(B)** MRI of the lower extremities displayed hyperintensity in superficial fasciae (bright arrowheads) and deep fasciae (black arrowheads) on fat suppression T2-weighted images in Patient 2. **(C)** Fat suppression T2-weighted thigh MRI in Patient 3 showed thickening and increased signal in superficial (bright arrowheads) and deep (black arrowheads) facias of posterior thigh muscles. **(D)** Muscular edema and thickening fascia (black arrowhead) of posterior thigh muscles on fat suppression T2-weighted MRI images were obvious in Patient 4. **(E)** Thickening deep fascia (black arrowheads) had high signal intensity on fat suppression T2-weighted MRI of thigh in Patient 5. **(F)** MRI of forearm in Patient 5 showed hyperintensity in deep fasciae (black arrowhead).

vascular endothelial cells within the connective tissue and a few inflammatory cells in patients with myofasciitis (Figure 3B). No positive staining of VLA-4 was observed in the controls (Figure 3C), but there was positive staining of VLA-4 on scatter inflammatory cells in patients with myofasciitis (Figure 3D). There was low-level expression of ICAM-1 on the tissues of controls (Figure 3E) but this was up-regulated in myofasciitis (Figure 3F). CD11a/CD18 was positive on inflammatory cells (Figure 3H), whereas no positive signal was observed in controls (Figure 3G). PECAM-1 was expressed on the vascular endothelium in both controls and myofasciitis (Figures 3I,J). Light expression of CD146 on blood vessels within connective tissue in controls (Figure 3K), whereas CD146 was strongly positive in myofasciitis (Figure 3L). Western blot results were consistent with those of the immunostaining study, and showed that ICAM-1, CD11a/18, VCAM-1, VLA-4, CD31, and CD146 at the protein levels in myofasciitis were significantly increased (Figures 4A,B).

Discussion

We identified immunopathological changes and the expression of cells adhesion molecules in five patients with myofasciitis, including one patient with EF, two patients with CTD-related myofasciitis, and two patients with unknown triggers, indicating the dysregulated immune response and the elevated expression of CAMs in myofasciitis.

The relationship between eosinophils and myofasciitis remained unclear. A previous study demonstrated elevated levels of serum eosinophilic cationic protein in EF (4). An increased capacity for eosinophilic migration in EF did not correlate with disease activity (5), suggesting that eosinophils may not be involved in the mechanism underlying the onset of this condition. Anti-PM/Scl-IgG-positive patients frequently exhibited extensive extramuscular features, pathologically manifested by perivascular inflammation (6). Perivasculitis was detected in the biopsied specimen of Patient 3 with anti-PM/Scl-75 antibodies. Therefore, the etiology of Patient 3 with EF may be associated with anti-PM/Scl-75 antibodies. Perivasculitis was also identified in other patients, which could be a trigger (1). Patient 4 was positive for anti-Jo-1 autoantibodies. Anti-Jo-1 autoantibodies are the first antibodies to aminoacyl histidyl transfer RNA synthetases to be detected in 15–25% patients with idiopathic inflammatory myopathy (7). Patients with anti-Jo-1 antibodies had unique histological features characterized by perimysial connective tissue fragmentation and inflammation (8). It was previously reported that a patient with positive anti-Jo-1 autoantibodies exhibited pulmonary vasculitis (9). Myofasciitis in Patient 4 may be associated with an anti-Jo-1-mediated disorder of the connective tissue. Patient 5 has been diagnosed with Sjögren syndrome, which may be related to myofasciitis (1). Although the risk factors of Patient 1 and 2 remain unknown, it is important to investigate them.

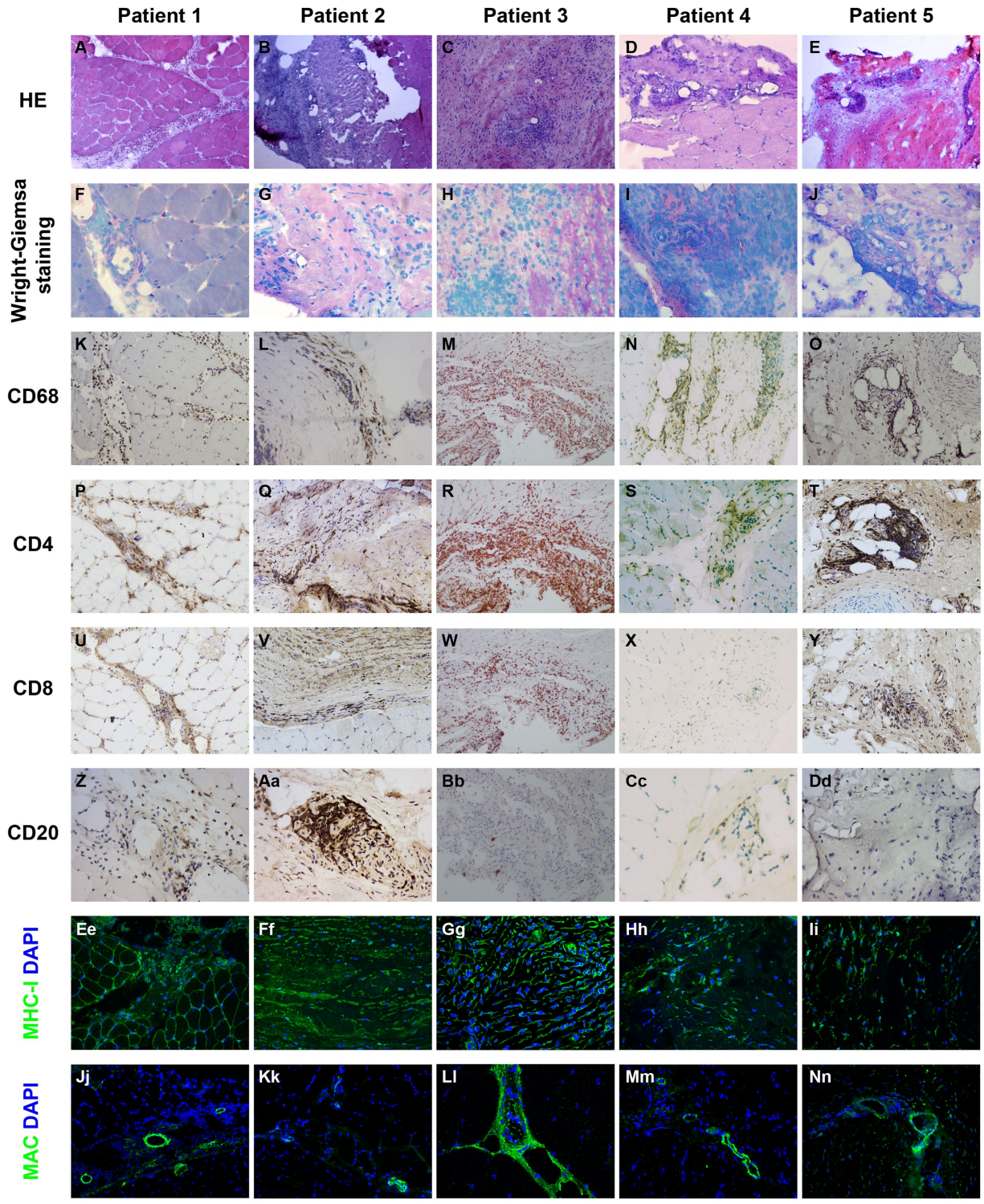

FIGURE 2
Immunohistochemical illustration of inflammatory infiltrate and immune-mediated factors in biopsied specimen of patients with myofasciitis. **(A–E)** Hematoxylin and eosin staining showed the numerous inflammatory cells in fascia and perivascular collections of inflammatory cells with minimal muscle damage in these patients. Original magnification: ×200. **(F–J)** A few eosinophils (black arrows) were observed in Patient 3. Original magnification: ×400. **(K–O)** A substantial infiltration of $CD68^+$ macrophages were noted in the affected fascia in these patients with myofasciitis. Original magnification: ×200. **(P–T)** Abundant $CD4^+$ T lymphocytes infiltrated into the fascia in these patients. Scale bar, 200μm. Original magnification: ×200. **(U–Y)** Scatter $CD8^+$ T lymphocytes were found in these patients. Original magnification: ×200. **(Z–Dd)** Scatter staining of $CD20^+$ B lymphocytes was noted in fascia of Patient 2. Rare B lymphocytes were detected in Patient 1, Patient 3, Patient 4, and Patient 5. Original magnification: ×400. **(Ee–Ii)** The MHC-I on the sarcolemma close to thickened fascia and inflammatory cells was up-regulated in these patients. Original magnification: ×400. **(Ji–Nn)** MAC was positive with a vascular strong staining pattern in these patients. Original magnification: ×400.

TABLE 3 Immunophenotype of inflammatory infiltration, up-regulation of MHC-1, and MAC deposition in patients with myofasciitis.

	Patient 1	Patient 2	Patient 3	Patient 4	Patient 5
$CD68^+$ macrophages	++	+	+++	+++	++
$CD3^+$ T lymphocytes	+++	+++	+++	+++	++
M/T	<1	<1	≈1	≈1	≈1
$CD4^+$ T lymphocytes	++	++	+++	++	+
$CD8^+$ T lymphocytes	–	+	++	++	+
CD4/CD8	>1	>1	>1	≈1	≈1
$CD20^+$ B lymphocytes	+	++	+	+	–
Eosinophils	–	–	+	–	–
Upregulation of MHC-1	+ (myofibers); ++ (blood vessels); ++ (fibroblasts)	- (myofibers); +++ (blood vessels); ++ (fibroblasts)	+ (myofibers); +++ (blood vessels); +++ (fibroblasts)	- (myofibers); ++++ (blood vessels); +++ (fibroblasts)	+ (myofibers); ++ (blood vessels); + (fibroblasts)
MAC deposition	+ (myofibers); +++ (blood vessels)	- (myofibers); +++ (blood vessels)	- (myofibers); ++ (blood vessels)	- (myofibers); +++ (blood vessels)	- (myofibers); +++ (blood vessels)

CD4/CD8, $CD4^+/CD8^+$ T lymphocyte ratio; M/T, macrophage/$CD3^+$ T lymphocyte ratio; MHC-I, major histocompatibility complex class I; MAC, membrane attack complex.

TABLE 4 Intensity of immunohistochemistry staining of cell adhesion molecules and their receptors expression in myofasciitis and HC.

		Patient 1	Patient 2	Patient 3	Patient 4	Patient 5	HC 1	HC 2	HC 3	HC 4	HC 5
VCAM-1	Vascular endothelium	+++	+++	+++	+++	+++	+	+	+	+	++
	Inflammatory cells	+	++	+++	+++	++	–	–	–	–	–
VLA-4	Vascular endothelium	–	–	–	–	–	–	–	–	–	–
	Inflammatory cells	++	++	+++	++	++	–	–	–	–	–
ICAM-1	Vascular endothelium	+++	+++	+++	+++	+++	++	++	++	++	++
	Inflammatory cells	++	++	+	++	+++	–	–	–	–	–
CD11a/CD18	Vascular endothelium	–	–	–	–	–	–	–	–	–	–
	Inflammatory cells	++	++	+++	++	+	–	–	–	–	–
PECAM-1	Vascular endothelium	+++	+++	+++	+++	+++	+++	+++	+++	+++	+++
	Inflammatory cells	+	+	++	+	+	–	–	–	–	–
CD146	Vascular endothelium	++	++	++	+	+	+	+	+	–	+
	Inflammatory cells	+	++	+++	++	++	–	–	–	–	–

VCAM-1, vascular cell adhesion molecule 1; VLA-4, integrin alpha 4/CD49D; ICAM-1, intercellular adhesion molecule 1; PECAM-1, platelet-endothelial cell adhesion molecule

The up-regulation of CAMs has been demonstrated in inflammatory or autoimmune diseases, such as idiopathic inflammatory myopathies (10–12), multiple sclerosis (13), asthma (14), rhinitis (15), and inflammatory bowel disease (16, 17). Previous research indicated that the CAMs on endothelial cells can be induced by several triggers, including pro-inflammatory cytokines, autoantibodies (18), lipopolysaccharide (19), proteinase 3 (20), reactive oxygen species, and antioxidants (21). Previous study reported increased serum IL-5 (4), hypergammaglobulinemia (22), elevated serum superoxide dismutase levels (23), and circulating overexpression of CD40 ligands (24), were detected in a few patients with EF. Elevated secretion of interferon-γ, IL-2, and leukemia inhibitory factor by peripheral blood mononuclear

10.3389/fneur.2023.1113404

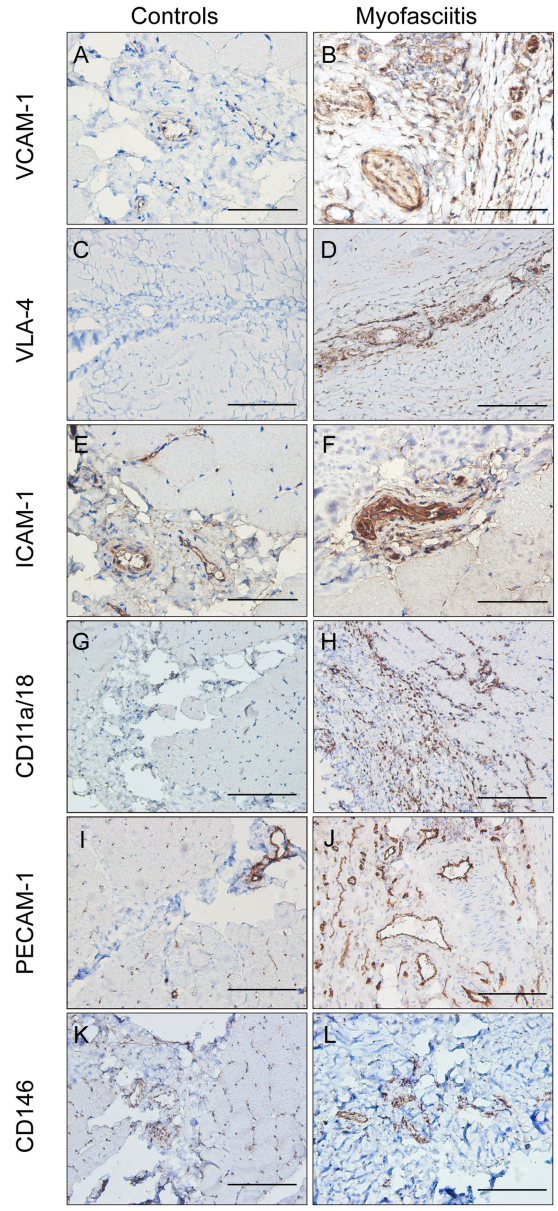

FIGURE 3
The expression of cell adhesion molecules in controls and patients with myofasciitis. **(A,B)** The weak expression of VCAM-1 in controls and up-regulated VCAM-1 on blood vessels and a few inflammatory cells in Patient 3. A and B, scale bar, 50μm. **(C,D)** No positive staining of VLA-4 in controls and the expression of VLA-4 on scattered inflammatory cells in Patient 2. C and D, scale bar, 100μm. **(E,F)** The low-level expression of ICAM-1 on vascular endothelium cells in controls and overexpressed ICAM-1 on vascular endothelial cells and a few inflammatory cells in Patient 2. E and F, scale bar, 50μm. **(G,H)** No positive staining of CD11a/CD18 in controls and the expression of CD11a/CD18 on scatter inflammatory cells in Patient 3. G and H, scale bar, 100μm. **(I,J)** The expression of PECAM-1 on blood vessels in controls and up-regulated PECAM-1 on blood vessels in Patient 3, especially in actively involved areas. **(I,G)**, scale bar, 100μm. (**K,L)** Very weak positive staining of CD146 on vascular endothelium cells in controls and strong intensity of CD146 on blood vessels in Patient 2. **(K,L)**, scale bar, 100μm.

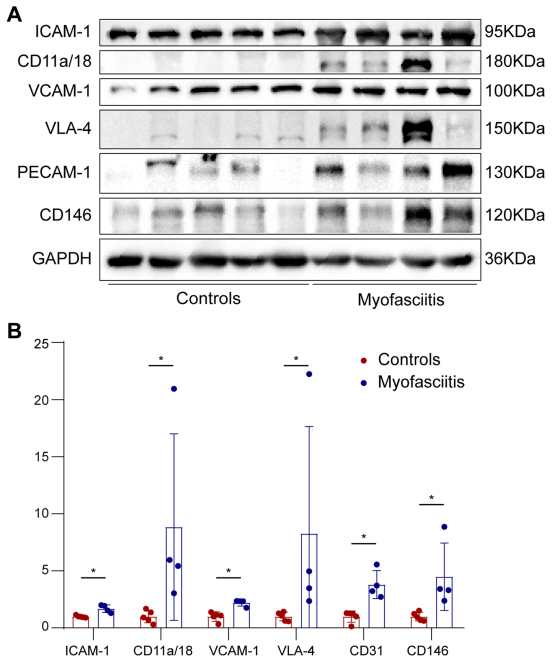

FIGURE 4
Western blot of cells adhesion molecules in muscle biopsies from controls and patients with myofasciitis. **(A)** Representative Western blot of ICAM-1, CD11a/CD18, VCAM-1, VLA-4, PECAM-1, and CD146 in muscle biopsies for five controls and four patients, including Patient 1, Patient 2, Patient 3, and Patient 5. **(B)** Quantitative analysis of ICAM-1, CD11a/CD18, VCAM-1, VLA-4, PECAM-1, and CD146 relative expression. n=5 for controls, n=4 for myofasciitis. *p<0.05. Statistical analyses were performed by Mann–Whitney U test.

cells was identified in four cases with EF (25). In this study, elevated serum cytokines in patients with myofasciitis was observed. Therefore, it is reasonable to presume that these inflammatory mediators may be responsible for the endothelial activation. It is supposed that receptors on leukocytes, such as VLA-4 binding to VCAM-1 and CD11a/CD18 binding to ICAM-1 on the surface of activated endothelium cells, may weaken gap formation or junctional endothelial cell–cell interactions that facilitate leukocyte transendothelial migration into the fascia in the pathological process of perivasculitis in myofasciitis.

Blockade of ICAM-1 was a well-established and highly effective treatment in vasculitis (26). The use of monoclonal antibodies and pharmacotherapy against these CAMs reduced the expression of CAMs and ameliorated vasospasm in animal experiment studies of treatment of vasospasm after subarachnoid hemorrhage (27). Therefore, endothelial activation in myofasciitis may be a potential treatment target for myofasciitis.

The limited sample size and the retrospective design from a single medical center were the main limitations of the study. Therefore, paucity of information and selection bias might exist. Studies with larger cohorts from multiple medical centers will further clarify the clinicopathological features of patients with myofasciitis. Another limitation is that all patients were Chinese; our results may therefore not be generalizable to other races.

Conclusion

To explore the precise therapeutic approaches of myofasciitis, it is of utmost importance to identify the underlying pathogenic

mechanisms. The endothelial activation in myofasciitis could potentially be therapeutic targets.

Data availability statement

The original contributions presented in the study are included in the article/Supplementary material, further inquiries can be directed to the corresponding author.

Ethics statement

The studies involving human participants were reviewed and approved by the Ethics Committee of Tongji Hospital. The patients/participants provided their written informed consent to participate in this study. Written informed consent was obtained from the individuals, for the publication of any potentially identifiable images or data included in this article.

Author contributions

BB and SJ contributed to the conceptualization of the study and funding acquisition. XM, HG, ZB, and LX performed the histological staining, western blot and statistical analysis. XM was a major contributor in writing the manuscript. BB has full access to all the data in the study and takes responsibility for the integrity of the data and the accuracy of the data analysis, contributed to critical revision of the manuscript for important intellectual content, and contributed to the supervision. All authors contributed to the article and approved the submitted version.

Funding

This study was supported by the National Natural Science Foundation of China (Grant number: 81873758 to BB).

Acknowledgments

We appreciate that the patients provided their medical data.

Conflict of interest

The authors declare that the research was conducted in the absence of any commercial or financial relationships that could be made as a potential conflict of interest.

Publisher's note

All claims expressed in this article are solely those of the authors and do not necessarily represent those of their affiliated organizations, or those of the publisher, the editors and the reviewers. Any product that may be evaluated in this article, or claim that may be made by its manufacturer, is not guaranteed or endorsed by the publisher.

Supplementary material

The Supplementary material for this article can be found online at: https://www.frontiersin.org/articles/10.3389/fneur.2023.1113404/full#supplementary-material

References

1. Pinal-Fernandez I, Selva-O' Callaghan A, Grau JM. Diagnosis and classification of eosinophilic fasciitis. *Autoimmun Rev*. (2014) 13:379–82. doi: 10.1016/j.autrev.2014.01.019

2. Preuße C, Goebel HH, Held J, Wengert O, Scheibe F, Irlbacher K, et al. Immune-mediated necrotizing myopathy is characterized by a specific Th1-M1 polarized immune profile. *Am J Pathol*. (2012) 181:2161–71. doi: 10.1016/j.ajpath.2012.08.033

3. Turkcapar N, Sak SD, Saatci M, Duman M, Olmez U. Vasculitis and expression of vascular cell adhesion molecule-1, intercellular adhesion molecule-1, and E-selectin in salivary glands of patients with Sjögren's syndrome. *J Rheumatol*. (2005) 32:1063–70.

4. Nishiya K, Tanimoto N, Hashimoto K, Hashizume M, Tominaga A. Serum and synovial fluid levels of interleukin-5 in a patient with eosinophilic fasciitis. *Ann Rheum Dis*. (1996) 55:935–6. doi: 10.1136/ard.55.12.935

5. Wasserman SI, Seibold JR, Medsger TA Jr, Rodnan GP. Serum eosinophilotactic activity in eosinophilic fasciitis. *Arthritis Rheum*. (1982) 25:1352–6. doi: 10.1002/art.1780251111

6. De Lorenzo R, Pinal-Fernandez I, Huang W, Albayda J, Tiniakou E, Johnson C, et al. Muscular and extramuscular clinical features of patients with anti-PM/Scl autoantibodies. *Neurology*. (2018) 90:e2068–76. doi: 10.1212/WNL.0000000000005638

7. Satoh M, Tanaka S, Ceribelli A, Calise SJ, Chan EKL. A comprehensive overview on myositis-specific antibodies: new and old biomarkers in idiopathic inflammatory myopathy. *Clin Rev Allergy Immunol*. (2017) 52:1–19. doi: 10.1007/s12016-015-8510-y

8. Mozaffar T, Pestronk A. Myopathy with anti-Jo-1 antibodies: pathology in perimysium and neighbouring muscle fibres. *J Neurol Neurosurg Psychiatry*. (2000) 68:472–8. doi: 10.1136/jnnp.68.4.472

9. Brown I, Joyce C, Hogan PG, Armstrong J, Steele R, Bansal AS. Pulmonary vasculitis associated with anti-Jo-1 antibodies. *Respir Med*. (1998) 92:986–8. doi: 10.1016/S0954-6111(98)90206-2

10. Figarella-Branger D, Schleinitz N, Boutière-Albanèse B, Camoin L, Bardin N, Guis S, et al. Platelet-endothelial cell adhesion molecule-1 and CD146: soluble levels and in situ expression of cellular adhesion molecules implicated in the cohesion of endothelial cells in idiopathic inflammatory myopathies. *J Rheumatol*. (2006) 33:1623–30.

11. Tews DS, Goebel HH. Expression of cell adhesion molecules in inflammatory myopathies. *J Neuroimmunol*. (1995) 59:185–94. doi: 10.1016/0165-5728(95)00045-4

12. De Bleecker JL, Engel AG. Expression of cell adhesion molecules in inflammatory myopathies and Duchenne dystrophy. *J Neuropathol Exp Neurol*. (1994) 53:369–76. doi: 10.1097/00005072-199407000-00008

13. Petersen ER, Ammitzbøll C, Søndergaard HB, Oturai AB, Sørensen PS, Nilsson AC, et al. Expression of melanoma cell adhesion molecule-1 (MCAM-1) in natalizumab-treated multiple sclerosis. *J Neuroimmunol*. (2019) 337:577085. doi: 10.1016/j.jneuroim.2019.577085

14. Håkansson L, Björnsson E, Janson C, Schmekel B. Increased adhesion to vascular cell adhesion molecule-1 and intercellular adhesion molecule-1 of eosinophils from patients with asthma. *J Allergy Clin Immunol*. (1995) 96:941–50. doi: 10.1016/S0091-6749(95)70232-6

15. Mukhopadhyay S, Malik P, Arora SK, Mukherjee TK. Intercellular adhesion molecule-1 as a drug target in asthma and rhinitis. *Respirology*. (2014) 19:508–13. doi: 10.1111/resp.12285

16. Stefanelli T, Malesci A, de la Rue SA, Danese S. Anti-adhesion molecule therapies in inflammatory bowel disease: touch and go. *Autoimmun Rev*. (2008) 7:364–9. doi: 10.1016/j.autrev.2008.01.002

17. Bardin N, Reumaux D, Geboes K, Colombel JF, Blot-Chabaud M, Sampol J, et al. Increased expression of CD146, a new marker of the endothelial junction in active inflammatory bowel disease. *Inflamm Bowel Dis*. (2006) 12:16–21. doi: 10.1097/01.MIB.0000194181.46930.88

18. Johnson PA, Alexander HD, McMillan S, Maxwell AP. Up-regulation of the endothelial cell adhesion molecule intercellular adhesion molecule-1 (ICAM-1) by autoantibodies in autoimmune vasculitis. *Clin Exp Immunol*. (1997) 108:234–42. doi: 10.1046/j.1365-2249.1997.3741271.x

19. Tseng TL, Chen MF, Hsu YH, Lee TJF. OroxylinA reverses lipopolysaccharide-induced adhesion molecule expression and endothelial barrier disruption in the rat aorta. *Toxicol Appl Pharmacol*. (2020) 400:115070. doi: 10.1016/j.taap.2020.115070

20. Taekema-Roelvink ME, VAN KOOTEN CEES, Van Der Kooij SANDRA, Heemskerk E, Daha MR. Proteinase 3 enhances endothelial monocyte chemoattractant protein-1 production and induces increased adhesion of neutrophils to endothelial cells by upregulating intercellular cell adhesion molecule-1. *J Am Soc Nephrol*. (2001) 12:932–40. doi: 10.1681/ASN.V125932

21. Cook-Mills JM, Marchese ME, Abdala-Valencia H. Vascular cell adhesion molecule-1 expression and signaling during disease: regulation by reactive oxygen species and antioxidants. *Antioxid Redox Signal*. (2011) 15:1607–38. doi: 10.1089/ars.2010.3522

22. Lakhanpal S, Ginsburg WW, Michet CJ, Doyle JA, Moore SB. Eosinophilic fasciitis: clinical spectrum and therapeutic response in 52 cases. *Semin Arthritis Rheum*. (1988) 17:221–31. doi: 10.1016/0049-0172(88)90008-X

23. Jinnin M, Ihn H, Yazawa N, Asano Y, Yamane K, Tamaki K. Elevated serum levels of manganese superoxide dismutase in patients with eosinophilic fasciitis. *Clin Rheumatol*. (2003) 22:505. doi: 10.1007/s10067-003-0781-7

24. Jinnin M, Ihn H, Yazawa N, Asano Y, Yamane K, Tamaki K. Circulating soluble CD40 ligand in patients with eosinophilic fasciitis. *Ann Rheum Dis*. (2003) 62:190–1. doi: 10.1136/ard.62.2.190

25. Viallard JF, Taupin JL, Ranchin V, Leng B, Pellegrin JL, Moreau JF. Analysis of leukemia inhibitory factor, type 1 and type 2 cytokine production in patients with eosinophilic fasciitis. *J Rheumatol*. (2001) 28:75–80.

26. Xu Y, Li S. Blockade of ICAM-1: a novel way of vasculitis treatment. *Biochem Biophys Res Commun*. (2009) 381:459–61. doi: 10.1016/j.bbrc.2009.02.111

27. Chaichana KL, Pradilla G, Huang J, Tamargo RJ. Role of inflammation (leukocyte-endothelial cell interactions) in vasospasm after subarachnoid hemorrhage. *World Neurosurg*. (2010) 73:22–41. doi: 10.1016/j.surneu.2009.05.027

frontiers | Frontiers in Neurology

TYPE Original Research
PUBLISHED 29 June 2023
DOI 10.3389/fneur.2023.1191520

Check for updates

OPEN ACCESS

EDITED BY
Giovanni Meola,
University of Milan, Italy

REVIEWED BY
Nakul Katyal,
Stanford Healthcare, United States
Aleksandra S. Kacar,
University of Belgrade, Serbia

*CORRESPONDENCE
Wilfor Aguirre-Quispe
✉ wilfor.aguirre.q@upch.pe

RECEIVED 22 March 2023
ACCEPTED 19 June 2023
PUBLISHED 29 June 2023

CITATION
Sanchez-Boluarte SS, Aguirre-Quispe W, Tacunan-Cuellar J, Sanchez-Boluarte AN and Segura-Chavez D (2023) Disability evaluation in patients with Guillain-Barre syndrome and SARS-CoV-2 infection.
Front. Neurol. 14:1191520.
doi: 10.3389/fneur.2023.1191520

COPYRIGHT
© 2023 Sanchez-Boluarte, Aguirre-Quispe, Tacunan-Cuellar, Sanchez-Boluarte and Segura-Chavez. This is an open-access article distributed under the terms of the Creative Commons Attribution License (CC BY). The use, distribution or reproduction in other forums is permitted, provided the original author(s) and the copyright owner(s) are credited and that the original publication in this journal is cited, in accordance with accepted academic practice. No use, distribution or reproduction is permitted which does not comply with these terms.

Disability evaluation in patients with Guillain-Barre syndrome and SARS-CoV-2 infection

Sofía S. Sanchez-Boluarte[1], Wilfor Aguirre-Quispe[2]*, Jhon Tacunan-Cuellar[3], Arantxa N. Sanchez-Boluarte[4] and Darwin Segura-Chavez[3]

[1]School of Medicine, Universidad Cesar Vallejo, Trujillo, Peru, [2]Neurosciences, Clinical Effectiveness and Public Health Research Group, Universidad Científica del Sur, Lima, Peru, [3]Department of Neurophysiology, Instituto Nacional de Ciencias Neurológicas, Lima, Peru, [4]School of Public Health, University of Washington, Seattle, WA, United States

Objective: Several cases of Guillain-Barre syndrome (GBS) associated with SARS-CoV-2 infection have been described. This study illustrated the demographic, clinical, and neurophysiological characteristics of patients with GBS and COVID-19, as well as associated factors with disability at discharge.

Materials and methods: A retrospective analytical observational study was conducted. It included patients diagnosed with GBS admitted in a national reference center in Peru between 2019 and 2021. Epidemiological, clinical, neurophysiological, and cerebrospinal fluid data were analyzed. A multivariate analysis, using the generalized linear model, was performed, considering the presence of disability at discharge as the dependent variable.

Results: Eight-one subjects diagnosed with GBS were included. The mean age was 46.8years (SD: 15.2), with a predominance of males (61.73%). The most frequent clinical presentation was the classic sensory-motor form in 74 cases (91.36%) with AIDP (82.35%) as the most frequent neurophysiological pattern in the group with COVID-19, while AMAN pattern predominated (59.26%) in those without COVID-19 (p=<0.000). The disability prevalence ratio at discharge between subjects with COVID-19 and those without COVID-19 was 1.89 (CI 1.06–3.34), p=0.030, adjusted for age, sex, and neurophysiological subtype.

Conclusion: The neurophysiologic subtype AIDP, and a higher disability were associated with the presence of COVID-19.

KEYWORDS

COVID-19, SARS-CoV-2, disability evaluation, Guillain-Barre syndrome, polyneuropathy

Highlights

- The AIDP neurophysiological pattern was the most frequent in patients with COVID-19.
- SARS-CoV-2 infection was associated with increased disability at hospital discharge.
- The cases of GBS and COVID-19 had a higher level of proteins in CSF.

Introduction

Coronavirus disease that first appeared in China in December 2019 is currently a pandemic with over two hundred million cases and over four million deaths (1). SARS-CoV-2 infection is a multi-systemic disorder that manifests primarily at the respiratory level causing respiratory failure in severe cases and triggering aa multisystem response (2–4). Currently, many neurological manifestations associated with SARS-CoV-2 infection have been reported, including Guillain-Barre syndrome (GBS) (4–6).

GBS is an immune mediated acute inflammatory polyneuropathy, preceded by a respiratory or gastrointestinal infection in 70% of cases which typically manifests as a progressive, areflexic, ascending quadriparesis. However, other variants have also been described. Based on electrophysiological and pathological characteristics, GBS has been classified as acute inflammatory demyelinating polyradiculoneuropathy (AIDP), acute motor axonal neuropathy (AMAN) and acute sensory motor axonal neuropathy (AMSAN) (7–10).

Previous epidemics have been associated with outbreaks of GBS, describing its association with several agents such as *Campylobacter jejuni*, *Haemophilus influenzae*, *Epstein–barr*, *Cytomegalovirus*, *Zika*, among others (11, 12). GBS is one of the most frequently associated diseases of the peripheral nervous system with SARS-CoV-2 infection (13). This study described demographic characteristics, clinical and neurophysiological manifestations of patients with GBS and SARS-CoV-2, and factors associated with disability at hospital discharge.

Materials and methods

We performed a retrospective analytical observational study approved by the Institutional Review Board of the National Institute of Neurological Sciences (INCN), Lima, Peru. We included patients with the diagnosis of GBS, admitted at the INCN, between 2019 and 2021. The INCN is the national reference center for neurological diseases in Peru where only moderate to severe cases of GBS are hospitalized.

During the COVID-19 pandemic, patients with GBS continued to be admitted to our center. However, those with severe respiratory symptoms were referred to general hospitals where COVID-19 cases were treated. The study included patients above 18 years of age, diagnosed with GBS according to the Brighton criteria. COVID-19 was diagnosed using the polymerase chain reaction (PCR) test for SARS-CoV-2 based on nasopharyngeal swab detection or by detecting the anti-SARS-CoV-2 antibodies.

Conditions that mimic GBS such as acute muscle or peripheral nerve diseases were excluded from the study. Medical records were used to collect epidemiological, clinical, and laboratory data including age, sex, duration of the disease, cerebrospinal fluid (CSF) characteristics, electromyography, medical history and management.

The patients underwent one electromyography after the first week of symptoms, and the neurophysiological diagnosis was obtained according to the Uncini's criteria (14).

Disability was measured using the Hughes functional grading scale as follows: 0, healthy; 1, minor symptoms, able to run; 2, able to walk 10 meters to more without support, unable to run; 3, able to walk 10 meters with help; 4, bedridden or wheelchair; 5, requires assisted ventilation; 6: dead (15). Disability was measured at admission, nadir (the day the highest score was reached) and at discharge, defined as a score ≥ 3 on the Hughes Scale. Also, the treatment response was defined as the decrease by at least one point on the Hughes Discharge Scale. Sample size was not considered in the study since all patients diagnosed with GBS during the reported period were included.

The mean or median, standard deviation, interquartile range (IQR) were used for continuous variables, and the categorical variables were expressed with frequencies and percentages. Normal assessment was performed using Shapiro Wilk test and the analysis between the groups was performed using a *t*-test in cases of quantitative variables with normal distribution or using Mann–Whitney U test. Additionally, chi-2 test, and Fisher's exact test were used for categorical variables. The statistical significance was set at 0.05. The groups were compared based on COVID-19 diagnosis, pre- and post-pandemic periods, and disability at discharge. Likewise, a generalized linear regression model was constructed, with the presence of disability at discharge as a dependent variable. The analysis was performed using STATA (v.17.0, Texas, USA). Approval for this study was granted by the Institutional Research Ethics Committee of the INCN, Lima, Peru.

Results

Characteristics of participants

We included 81 patients diagnosed with GBS between January 2019 and April 2021. The mean age of the patients was 46.8 years (SD: 15.2), with a predominance of the male sex (61.73%). Forty-four (54.32%) cases met level 1 of diagnostic certainty, 26 (32.10%) cases met level 2 and 11 (13.58%) met level 3. The median duration of disease at admission was 5 days (IQR: 3.0–8.0). The mean of the Hughes scale at both admission and nadir was 3.5 (SD:0.9), with the time at nadir of 7 days (IQR: 4.0–10.0). The most frequent clinical presentation was the classic motor sensory form in 74 cases (91.36%), 4 (4.94%) presented with Miller-Fisher syndrome, 2 (2.47%) with Bickerstaff encephalitis, and 1 (1.23%) patient with facial diparesis (Table 1).

Thirty-two (50.79%) subjects had a history of gastrointestinal infection and 17 (26.98%) with a history of respiratory infection. The CSF analysis showed albumin cytological dissociation in 49 (63.64%) patients. Electromyography was performed on 71 participants, of whom 39 (48.15%) underwent EMG after the 4th week of symptoms, with a median time from symptoms onset and the EMG of 14 days (IQR: 9–28). Thirty-three (46.48%) patients had AMAN, 29 (40.85%) AIDP, 4 (5.63%) AMSAN and 5 (7.05%) presented with no alterations in the study. The median hospitalization time was 14 days (IQR:9.0–21.0). The median for Hughes at discharge was 3 days (IQR: 2.0–3.0). Nine (14.06%) required mechanical ventilation. The results of treatment are as follows, 67 (83.75%) received intravenous

Abbreviations: CSF, Cerebrospinal fluid; AMAN, Acute axonal motor neuropathy; AMSAN, Acute sensory-motor axonal neuropathy; AIDP, Acute idiopathic demyelinating polyneuropathy; EMG, Electromyography.

10.3389/fneur.2023.1191520

TABLE 1 Demographic, clinical, and neurophysiological characteristics of participants in relation to SARS-CoV-2 infection.

Characteristics	Total	COVID-19	No COVID-19	*p* value
	n =81 (100%)	*n* =18 (22.22%)	*n* =63 (77.78%)	
Age (years), mean (SD)	46.8 (15.2)	43.9 (13.6)	47.6 (15.6)	0.370
Sex, *n* (%)				
Male	50 (61.73)	13 (72.22)	37 (58.73)	0.299
Female	31 (38.27)	5 (27.78)	26 (41.27)	
Duration illness (days)*	4 (3–8)	9.5 (7–18)	4 (2–6)	<0.000
Hughes score at admission, mean (SD)	3.5 (0.9)	3.6 (0.9)	3.4 (0.9)	0.519
Time to nadir (days)*	7 (4–10)	10 (7–19)	6 (4–9)	0.002
Hughes score at nadir*	4 (3–4)	4 (4–4)	4 (3–4)	0.930
Clinical diagnosis, *n* (%)				
Classic motor-sensory	74 (91.36)	18 (100.0)	56 (88.89)	0.799
Miller-Fisher syndrome	4 (4.94)	0 (0)	4 (6.35)	
Bickerstaff encephalitis	2 (2.47)	0 (0)	2 (3.17)	
Facial diparesis	1 (1.23)	0 (0)	1 (1.59)	
Progression type, *n* (%)				
Ascendent	31 (40.79)	0 (0)	31 (53.45)	<0.000
Descendent	45 (59.21)	18 (100.0)	27 (46.55)	
Previous infection history, *n* (%)				
Gastrointestinal	32 (50.79)	13 (72.22)	19 (42.22)	0.168
Respiratory	17 (26.98)	3 (16.67)	14 (31.11)	
No previous infection	11 (17.46)	2 (11.11)	9 (20.0)	
Duration of symptoms onset to the CSF sample (days)*	8 (4–15)	10.5 (8–21)	7 (4–14)	0.034
CSF Characteristics				
Glicemia (mg/dL)	61 (57–67)	66 (59–72)	59 (56–66)	0.046
Proteins (mg)	64 (41–124)	133.1 (72.9–188)	53 (38–86)	0.005
Cells	2 (1–4)	1 (1–2)	2 (1–6)	0.006
Albuminocytological dissociation, *n* (%)	49 (63.64)	15 (83.33)	34 (57.63)	0.180
Time of symptoms onset to the EMG*	14 (9–28)	28 (19.5–47.5)	11 (8–23)	0.003
Neurophysiological pattern**, *n* (%)				
AMAN	33 (46.48)	1 (5.88)	32 (59.26)	<0.000
AIDP	29 (40.85)	14 (82.35)	15 (27.78)	
AMSAN	4 (5.63)	1 (5.88)	3 (5.56)	
Normal	5 (7.05)	1 (5.88)	4 (7.41)	
Brighton criteria, *n* (%)				
1	44 (54.32)	15 (83.33)	29 (46.03)	0.020
2	26 (32.10)	2 (11.11)	24 (38.10)	
3	11 (13.58)	1 (5.56)	10 (15.87)	
Length of admission (days)*	14 (9–21)	11.5 (7–18)	15 (9–22)	0.157
Hughes score at discharge*	3 (2–3)	3 (3–4)	2.5 (2–3)	0.016
Mechanical ventilation, *n* (%)	9 (14.06)	1 (5.55)	8 (12.70)	0.013
Treatment, *n* (%)				
Immunoglobulines	67 (83.75)	17 (100)	50 (79.37)	0.123
Plasmatic exchange	6 (7.50)	0 (0)	6 (9.52)	
None	7 (8.75)	0 (0)	7 (11.11)	

(Continued)

TABLE 1 (Continued)

Characteristics	Total	COVID-19	No COVID-19	*p* value
	n =81 (100%)	*n* =18 (22.22%)	*n* =63 (77.78%)	
Disability at discharge, n (%)	46 (57.50)	15 (83.33)	31 (50.0)	0.012
Treatment response, n (%)	41 (50.62)	7 (38.89)	34 (53.97)	0.389

SD, standard deviation; IQR, interquartile range; CSF, Cerebrospinal fluid; AMAN, Acute axonal motor neuropathy; AMSAN, Acute sensory-motor axonal neuropathy; AIDP, Acute idiopathic demyelinating polyneuropathy; EMG, Electromyography. (*) median (IQR) (**) 10 patients did not have electromyography.

immunoglobulin, 6 (7.50%) received plasma replacement, 41 (50.62%) had response to treatment (Table 1).

Pre-pandemic versus pandemic period

From the period of March 2020 to April 2021, 31 subjects (38.3%) were diagnosed as GBS, of which 18 (58.0%) had a diagnosis of COVID-19, while in the period before the pandemic, from January 2019 to February 2020, 50 subjects (61.7%) received the diagnosis of GBS (Table 2). Patients during the pandemic period had longer duration of illness when compared to the groups treated before the pandemic (2019-february 2020), 7 (IQR 4.0–10.0) vs. 4 (IQR 2.0–6.0), $p = 0.006$; and a longer time at nadir, 9.0 (IQR 5.0–15.0) vs. 5.5 (IQR 3.0–8.0), $p = 0.002$; and a shorter hospitalization time, 12 days (IQR 7.0–18.0) vs. 16 days (IQR 9.0–26.0), $p = 0.033$ (Table 2). Twenty-nine (83.8%) received intravenous immunoglobulin during the pandemic, whereas only 38 (76.0%), $p = 0.046$ before the pandemic. There was neither a difference in Hughes' score at admission, nor in the response rate to the treatment comparing both periods (Table 3). In the period March 2020–April 2021, 18 cases (38.3%) were detected with both COVID-19 and GBS. COVID-19 was diagnosed using PCR in 7 cases and by rapid antibody testing in 11 participants. Of the 11 cases, 6 were positive for both IgM and IgG, 1 for IgM and 2 for IgG only. Fourteen (77.8%) had respiratory symptoms. The median time between onset of respiratory symptoms and neurological symptoms was 9 days (IQR:6.0–13.0). None of the patients with COVID-19 had GBS associated with the vaccine status.

COVID-19 versus non COVID-19

The COVID-19 group had thirteen (72.2%) males whereas 37 (58.73%) males were present in the group without COVID-19, $p = 0.299$. Mean age was similar in both groups, as was the median of the Hughes scale at admission and nadir. Compared with the group without COVID-19, participants with COVID-19 had a longer time of disease at admission, 9.5 (IQR: 7.0–18.0) vs. 4 (IQR: 2.0–6.0), $p < 0.000$; and at nadir, 10 (IQR:7.0–19.0) vs. 6 (IQR:4.0–9.0), $p = 0.002$ (Table 1). The classic sensory-motor clinical presentation was seen frequently in both groups, 13 (72.22%) patients in the COVID-19 group had a history of gastrointestinal infection, and nineteen had a respiratory infection (42.2%) in the group without COVID-19. The CSF characteristics, of the patients with COVID-19 had higher protein elevation, 133.1 (IQR: 72.9–188.0) when compared to those without COVID-19, 53.0 (IQR 38–86), $p = 0.005$. Albumin cytological dissociation was observed in 15 (83.3%) patients with COVID-19 vs. 34 (57.63%) patients in the other group, $p = 0.0.180$ (Table 1).

There were no differences in the disease duration at the time of sampling the CSF. The most frequent neurophysiological pattern in the group with COVID-19 was AIDP (82.4%), whereas AMAN predominated (59.26%), $p = <0.000$ in those without COVID-19. Hospitalization time was greater for those without COVID-19, 15 (IQR 9.0–22.0) vs. 11.5 (IQR 7.0–18.0), $p = 0.157$. Patients with COVID-19 had slightly higher score of Hughes 3 (IQR:3–4) comparing with those without COVID-19 2.5 (2–3) ($p = 0.016$). Patients with COVID-19 had with less frequency mechanical ventilation versus those without COVID-19 [1 (5.55%) versus 8 (12.70%), $p = 0.013$] (Table 1).

There was no significant difference between the Hughes at discharge, and mechanical ventilation requirement. All patients with COVID-19 received intravenous immunoglobulin at a dose of 0.4 g/kg, when compared to 50 (79.37%) patients in the group without COVID-19, 6(9.52%) received plasma replacement and 7 (11.11%) did not receive treatment. Fifteen patients (83.33%) of the group with COVID-19 had disability at discharge, comparing with 31 (50.0%) on the group without COVID-19. The response rate to treatment was similar in both groups (Table 1).

Disability versus non-disability groups

Patients who had a disability at discharge had a higher Hughes score upon admission [4 (IQR:3–4) compared to 3 (IQR:2–4), $p = 0.003$]. Additionally, they were more frequently diagnosed with the classic motor-sensory clinical diagnosis [44 (95.7%) versus 29 (85.3%), $p = 0.009$], and experienced a lower treatment response in comparison to those who were not disabled [16 (34.78%) versus 25 (73.53%), $p = 0.003$]. However, it is worth noting that the sex, age, length of admission, rate of mechanical ventilation, and neurophysiological diagnosis were comparable between both groups (Table 3). The prevalence ratio of disability at discharge in patients with and without COVID-19 was 1.89 (CI 1.06–3.34), $p = 0.030$, adjusted for age, sex, and neurophysiological subtype (Table 4).

Discussion

We found that there were no differences in the age, according to COVID-19 infection, which was unique when compared to the previously reported studies which had described a higher mean age for the group of patients with COVID-19 (3). Our patients were predominantly males, with a higher proportion in the COVID-19 group, possibly due to male predominance in patients with COVID-19 (16), which could predispose them to an increased risk of developing GBS.

TABLE 2 Demographic, clinical, and neurophysiological characteristics of GBS cases according to pre- and pandemic period.

Characteristics	January 2019–February 2020	March 2020–April 2021	*p* value
	n =50 (61.73%)	*n* =31 (38.27%)	
Age (years), mean (SD)	48 (16.3)	44.8 (13.1)	0.365
Sex, *n* (%)			
Male	19 (38.0)	12 (38.7)	0.949
Female	31 (62.0)	19 (61.3)	
Duration illness (days)*	4 (2–6)	7 (4–10)	0.006
Hughes score at admission, mean (SD)	4 (3–4)	4 (3–4)	0.4257
Time to nadir (days)*	5.5 (3–8)	9 (5–15)	0.002
Hughes score at nadir*	4 (3–4)	4 (3–4)	0.474
Clinical diagnosis, *n* (%)			
Classic motor-sensory	45 (90.0)	29 (93.6)	0.79
Miller-Fisher syndrome	2 (4.0)	2 (6.5)	
Bickerstaff encephalitis	2 (4.0)	0	
Pharyngocervicobraquial	0	0	
Facial diparesis	1 (2.0)	0	
Progression type, *n* (%)			
Ascendent	23 (48.9)	8 (27.6)	0.066
Descendent	24 (51.1)	21 (72.4)	
Previous infection history, *n* (%)			
Gastrointestinal	16 (43.2)	16 (61.5)	0.243
Respiratory	12 (32.4)	5 (19.2)	
No previous infection	6 (16.22)	5 (19.2)	
Time of symptoms onset to the CSF sample*	9 (4–15)	8 (5–13)	0.497
CSF Characteristics*			
Glicemia (mg/dL)	59 (55–64)	64.5 (59–72)	0.006
Proteins (mg)	54 (39–86)	83 (42–153)	0.152
Cells	2.5 (1–8)	1 (1–2)	0.001
Albuminocytological dissociation, *n* (%)	26 (56.5)	23 (74.2)	0.036
Time of symptoms onset to the EMG*	11 (8–17)	22 (14–33)	0.009
Neurophysiological pattern *, *n* (%)			
AMAN	27 (61.4)	6 (22.2)	0.007
AIDP	11 (25.0)	18 (66.7)	
AMSAN	2 (4.6)	2 (7.4)	
Normal	2 (4.6)	1 (3.7)	
Brighton criteria, *n* (%)			
1	22 (44.0)	22 (71.0)	0.059
2	20 (40.0)	6 (19.4)	
3	8 (16.0)	3 (9.7)	
Length of admission (days)*	16 (9–26)	12 (7–18)	0.033
Hughes score at discharge, *n* (%)	3 (2–3)	3 (2–4)	0.212
Mechanical ventilation, *n* (%)	7 (14.0)	2 (14.3)	0.978
Time to the treatment onset (days)*	6 (4–9)	5 (5–10)	0.582
Treatment, *n* (%)			

(Continued)

TABLE 2 (Continued)

Characteristics	January 2019–February 2020	March 2020–April 2021	*p* value
	n =50 (61.73%)	*n* =31 (38.27%)	
Immunoglobulines	38 (76.0)	29 (83.8)	0.046
Plasmatic exchange	6 (12.0)	1 (3.3)	
None	6 (12.0)	0	
Disability at discharge, *n* (%)	26 (53.1)	20 (64.5)	0.313
Treatment response, *n* (%)	27 (55.1)	15 (50.0)	0.659

SD, standard deviation; IQR: interquartile range; CSF: Cerebrospinal fluid; AMAN: Acute axonal motor neuropathy; AMSAN: Acute sensory-motor axonal neuropathy; AIDP: Acute idiopathic demyelinating polyneuropathy; EMG: Electromyography. (*) median (IQR) (**) 10 patients did not have electromyography.

TABLE 3 Characteristics of patients according to their state of disability at hospital discharge.

Characteristics	Disability	No disability	*p* value
	n =46 (57.50%)	*n* =34 (42.50%)	
Age (years), mean (SD)	48.4 (15.4)	44.2 (14.7)	0.225
Sex, *n* (%)			
Male	28 (60.87)	22 (64.71)	0.726
Female	18 (39.13)	12 (35.29)	
Duration illness (days)*	5 (2–9)	4 (3–7)	0.477
Hughes score at admission, median (IQR)	4 (3–4)	3 (2–4)	0.003
Time to nadir (days)*	7 (4–11)	5 (4–9)	0.131
Hughes score at nadir*	4 (4–4)	3.5 (2–4)	<0.000
Clinical diagnosis, *n* (%)			
Classic motor-sensory	44 (95.65)	29 (85.29)	0.009
Miller-Fisher syndrome	0 (0)	4 (11.76)	
Bickerstaff encephalitis	2 (4.35)	0 (0)	
Facial diparesis	0 (0)	1 (2.94)	
Progression type, *n* (%)			
Ascendent	16 (34.78)	14 (48.28)	0.245
Descendent	30 (65.22)	15 (51.72)	
Previous infection history, *n* (%)			
Gastrointestinal	19 (50.0)	13 (54.17)	0.663
Respiratory	9 (23.68)	7 (29.17)	
No previous infection	7 (18.42)	4 (16.67)	
CSF Characteristics*			
Glicemia (mg/dl)	61 (58–67)	59.5 (56–70)	0.464
Proteins (mg)	64 (39–112)	67 (41–133)	0.627
Cells	2 (1–3)	2 (1–8)	0.122
Albuminocytological dissociation, *n* (%)	27 (67.50)	22 (78.57)	0.317
Neurophysiological pattern *, *n* (%)			
AMAN	17 (41.46)	16 (53.33)	0.429
AIDP	20 (48.78)	9 (30.0)	
AMSAN	2 (4.88)	2 (6.67)	
Normal	2 (4.88)	3 (10.0)	
Brighton criteria, *n* (%)			

(Continued)

TABLE 3 (Continued)

Characteristics	Disability	No disability	*p* value
	n =46 (57.50%)	*n* =34 (42.50%)	
1	27 (58.70)	17 (50.0)	0.640
2	13 (28.26)	13 (38.24)	
3	6 (13.04)	4 (11.76)	
Length of admission (days)*	15.5 (10–23)	13 (8–17)	0.116
Mechanical ventilation, *n* (%)	7 (15.22)	1 (2.94)	0.070
Time to the treatment onset (days)*	6 (3–9)	6 (5–11.5)	0.289
Treatment, *n* (%)			
Immunoglobulines	40 (88.89)	26 (76.47)	0.249
Plasmatic exchange	2 (4.44)	3 (8.82)	
None	3 (6.67)	5 (14.71)	
Treatment response, *n* (%)	16 (34.78)	25 (73.53)	0.003

SD, standard deviation; IQR, interquartile range; CSF, Cerebrospinal fluid; AMAN, Acute axonal motor neuropathy; AMSAN, Acute sensory-motor axonal neuropathy; AIDP, Acute idiopathic demyelinating polyneuropathy; EMG, Electromyography. (*) 10 patients did not have electromyography.

TABLE 4 Associated factors for disability on the multiple regression analysis.

Variables	Bivariate analysis			Mutiple regression*		
	OR	IC 95%	*p*	OR	IC 95%	*p*
Sex						
Male	0.93	0.64–1.37	0.725	0.74	0.42–1.29	0.286
Female	Ref.			Ref.		
Age						
	1.01	0.99–1.02	0.210	1.01	0.99–1.02	0.117
Neurophysiological diagnosis						
Axonal	Ref.			Ref.		
Demielinizating	1.34	0.89–2.00	0.149	1.11	0.63–1.94	0.717
COVID-9						
No	Ref.			Ref.		
Yes	1.67	1.20–2.31	0.002	1.89	1.06–3.34	0.030

*Adjusted by age, sex, and neurophysiological diagnosis.

Unlike other studies, we did not observe a significant increase in the frequency of GBS cases during the pandemic (17), due to the measures established by the Ministry of Health of Peru that led to a decrease in the flow of patients in all health facilities in the country.

Patients with GBS and COVID-19 had longer admission durations when compared to those without COVID-19, this delay in care may have been related to the longer time of isolation of patients with respiratory symptoms by COVID-19. Likewise, the time between SARS-CoV-2 infection and the onset of GBS symptoms was 9 days, which is consistent with the hypothesis of a postinfectious mechanism associated with COVID-19, rather than direct neuronal damage or a para-infectious mechanism (10). The average duration has previously been reported to be 2 weeks, like other infections associated with GBS (3, 10, 18).

According to the results of our study in patients with COVID-19, the clinical manifestations and distribution of clinical variants were like those of classical GBS, characterized by sensory-motor predominance and a neurophysiological AIDP pattern, similar to previous reports (18–20). Likewise, cerebrospinal fluid protein levels were higher in patients with COVID-19, as described previously (19, 21) which attributes more to an immune response than to an inflammatory or infectious (19).

Independent of the concomitant infection with COVID-19, participants with GBS had a disease of similar severity both at admission and nadir; this differs from the studies reported previously, where differences have been found in the severity evaluated at admission (22), during hospitalization and at hospital discharge (18, 23). However, in the multivariate analysis that resulted in disability at hospital discharge, it was determined that infection with SARS-CoV-2 is associated with greater disability, although patients admitted to our center presented with COVID-19 of mild to moderate severity. The progression of disability was found to be slower in patients with

COVID-19 compared to patients without COVID-19. One reason attributed for this difference could be that most patients with COVID-19 had an electromyographic pattern corresponding to AIDP, a pattern associated with slower progression (16, 24).

Although patients admitted to our center had moderate to severe GBS, none had a fatal outcome, as reported in other countries, in which no changes in mortality associated with COVID-19 were evidenced (25).

The limitations of our study included selection bias as patients with severe respiratory symptoms from COVID-19 were referred to the general hospitals for multidisciplinary management, which can influence disability-related outcomes and severity. This situation, however, was due to the restrictions on health care and hospital admission introduced during the start of the pandemic. Despite having a significant number of cases, there was no balanced ratio between the groups with and without COVID-19. The uniformity in the diagnostic criteria for SARS-CoV-2 infection was also affected because of its modification by the Peruvian Ministry of Health in the very beginning of the pandemic. Other limitation is that on our resource limited settings, we were not able to perform serial EMGs and this could introduce wrong classifications, however, we followed Uncini criteria for the diagnosis.

It was concluded that patients with COVID-19 presented more frequently with the neurophysiological subtype AIDP, an increase in the concentration of proteins in CSF. Greater disability at discharge was associated with SARS-CoV-2 infection, despite evidence of slower progression in this group. We believe that these findings can not only be useful in the diagnostic approach aimed toward patients with a recent history of COVID-19, but also as a guide to the immediate prognosis of patients in this group.

Data availability statement

The raw data supporting the conclusions of this article will be made available by the authors, without undue reservation.

Ethics statement

The studies involving human participants were reviewed and approved by Instituto Nacional de Ciencias Neurologicas. Written informed consent for participation was not required for this study in accordance with the national legislation and the institutional requirements.

Author contributions

SS-B and DS-C contributed to conception and design of the study. SS-B and JT-C organized the database. SS-B, AS-B, and WA-Q performed the statistical analysis and wrote the first draft of the manuscript. All authors contributed to manuscript revision, read, and approved the submitted version.

Acknowledgments

The authors thank Aafreen Khan for English language support.

Conflict of interest

The authors declare that the research was conducted in the absence of any commercial or financial relationships that could be construed as a potential conflict of interest.

Publisher's note

All claims expressed in this article are solely those of the authors and do not necessarily represent those of their affiliated organizations, or those of the publisher, the editors and the reviewers. Any product that may be evaluated in this article, or claim that may be made by its manufacturer, is not guaranteed or endorsed by the publisher.

References

1. Zhou F, Yu T, Du R, Fan G, Liu Y, Liu Z, et al. Clinical course and risk factors for mortality of adult inpatients with COVID-19 in Wuhan, China: a retrospective cohort study. *Lancet*. (2020) 395:1054–62. doi: 10.1016/S0140-6736(20)30566-3

2. Rashid ZZ, Othman SN, Samat MNA, Kalsom U, Ken WK. Diagnostic performance of COVID-19 serology assays. *Malays J Pathol*. (2020) 42:13–21.

3. Trujillo Gittermann LM, Valenzuela Feris SN, von Oetinger Giacoman A. Relación entre COVID-19 y síndrome de Guillain-Barré en adultos. *Revisión Sistemática Neurología*. (2020) 35:646–54. doi: 10.1016/j.nrl.2020.07.004

4. Deng SQ, Peng HJ. Characteristics of and public health responses to the coronavirus disease 2019 outbreak in China. *J Clin Med*. (2020) 9:575. doi: 10.3390/jcm9020575

5. Akin L, Gözel MG. Understanding dynamics of pandemics. *Turk J Med Sci*. (2020) 5, 50:515–9. doi: 10.3906/sag-2004-133

6. Carod Artal FJ. Complicaciones neurológicas por coronavirus y COVID-19. *Rev Neurol*. (2020) 70:311–22. doi: 10.33588/rn.7009.2020179

7. van den Berg B, Walgaard C, Drenthen J, Fokke C, Jacobs BC, van Doorn PA. Guillain–Barré syndrome: pathogenesis, diagnosis, treatment and prognosis. *Nat Rev Neurol*. (2014) 10:469–82. doi: 10.1038/nrneurol.2014.121

8. Lehmann HC, Hartung HP, Kieseier BC, Hughes RA. Guillain-Barré syndrome after exposure to influenza virus. *Lancet Infect Dis*. (2010) 10:643–51. doi: 10.1016/S1473-3099(10)70140-7

9. Orlikowski D, Porcher R, Sivadon-Tardy V, Quincampoix JC, Raphael JC, Durand MC, et al. Guillain-Barre syndrome following primary cytomegalovirus infection: a prospective cohort study. *Clin Infect Dis*. (2011) 52:837–44. doi: 10.1093/cid/cir074

10. Uncini A, Vallat JM, Jacobs BC. Guillain-Barré syndrome in SARS-CoV-2 infection: an instant systematic review of the first six months of pandemic. *J Neurol Neurosurg Psychiatry*. (2020) 91:1105–10. doi: 10.1136/jnnp-2020-324491

11. Sedaghat Z, Karimi N. Guillain Barre syndrome associated with COVID-19 infection: a case report. *Case Rep*. (2020) 76:233–5. doi: 10.1016/j.jocn.2020.04.062

12. Wijdicks EFM, Klein CJ. Guillain-Barré syndrome. *Mayo Clin Proc*. (2017) 92:467–79. doi: 10.1016/j.mayocp.2016.12.002

13. Beghi E, Giussani G, Westenberg E, Allegri R, Garcia-Azorin D, Guekht A, et al. Acute and post-acute neurological manifestations of COVID-19: present findings, critical appraisal, and future directions. *J Neurol*. (2022) 269:2265–74. doi: 10.1007/s00415-021-10848-4

14. Uncini A, Ippoliti L, Shahrizaila N, Sekiguchi Y, Kuwabara S. Optimizing the electrodiagnostic accuracy in Guillain-Barré syndrome subtypes: criteria sets and sparse linear discriminant analysis. *Clin Neurophysiol*. (2017) 128:1176–83. doi: 10.1016/j.clinph.2017.03.048

15. van Koningsveld R, Steyerberg EW, Hughes RA, Swan AV, van Doorn PA, Jacobs BC. A clinical prognostic scoring system for Guillain-Barré syndrome. *Lancet Neurol*. (2007) 6:589–94. doi: 10.1016/S1474-4422(07)70130-8

16. Jin JM, Bai P, He W, Wu F, Liu XF, Han DM, et al. Gender differences in patients with COVID-19: focus on severity and mortality. *Front Public Health*. (2020) 8:152. doi: 10.3389/fpubh.2020.00152

17. Filosto M, Cotti Piccinelli S, Gazzina S, Foresti C, Frigeni B, Servalli MC, et al. Guillain-Barré syndrome and COVID-19: an observational multicentre study from two Italian hotspot regions. *J Neurol Neurosurg Psychiatry*. (2021) 92:751–6. doi: 10.1136/jnnp-2020-324837

18. Aladawi M, Elfil M, Abu-Esheh B, Abu Jazar D, Armouti A, Bayoumi A, et al. Guillain Barre syndrome as a complication of COVID-19: a systematic review. *Can J Neurol Sci J Can Sci Neurol*. (2022) 49:38–48. doi: 10.1017/cjn.2021.102

19. Sheikh AB, Chourasia PK, Javed N, Chourasia MK, Suriya SS, Upadhyay S, et al. Association of Guillain-Barre syndrome with COVID-19 infection: an updated systematic review. *J Neuroimmunol*. (2021) 355:577577. doi: 10.1016/j.jneuroim.2021.577577

20. Sriwastava S, Kataria S, Tandon M, Patel J, Patel R, Jowkar A, et al. Guillain Barré syndrome and its variants as a manifestation of COVID-19: a systematic review of case reports and case series. *J Neurol Sci*. (2021) 420:117263. doi: 10.1016/j.jns.2020.117263

21. Carrillo-Larco RM, Altez-Fernandez C, Ravaglia S, Vizcarra JA. COVID-19 and Guillain-Barre syndrome: a systematic review of case reports. *Wellcome Open Res*. (2020) 5:107. doi: 10.12688/wellcomeopenres.15987.2

22. Ahmad L, Businaro P, Regalbuto S, Gastaldi M, Zardini E, Panzeri M, et al. COVID-19 and Guillain-Barré syndrome: a single-center prospective case series with a 1-year follow-up. *Medicine (Baltimore)*. (2022) 101:e29704. doi: 10.1097/MD.0000000000029704

23. Filosto M, Cotti Piccinelli S, Gazzina S, Foresti C, Frigeni B, Servalli MC, et al. Guillain-Barré syndrome and COVID-19: a 1-year observational multicenter study. *Eur J Neurol*. (2022) 29:3358–67. doi: 10.1111/ene.15497

24. Palaiodimou L, Stefanou M, Katsanos AH, Fragkou PC, Papadopoulou M, Moschovos C, et al. Prevalence, clinical characteristics and outcomes of Guillain–Barré syndrome spectrum associated with COVID-19: a systematic review and meta-analysis. *Eur J Neurol*. (2021) 28:3517–29. doi: 10.1111/ene.14860

25. Arsenijević M, Berisavac I, Mladenović B, Stanarčević P, Jovanović D, Lavrnić D, et al. Rate of progression of Guillain-Barré syndrome is not associated with the short-term outcome of the disease. *Ir J Med Sci*. (2021) 190:357–61. doi: 10.1007/s11845-020-02310-7

frontiers | Frontiers in Neurology

TYPE Case Report
PUBLISHED 30 June 2023
DOI 10.3389/fneur.2023.1170693

Check for updates

OPEN ACCESS

EDITED BY
Giovanni Meola,
University of Milan, Italy

REVIEWED BY
Alvaro Macias,
Spanish National Centre for Cardiovascular Research, Spain
Roope Mannikko,
University College London, United Kingdom

*CORRESPONDENCE
Kai Yao
✉ jsyyyao6@126.com

RECEIVED 21 February 2023
ACCEPTED 02 June 2023
PUBLISHED 30 June 2023

CITATION
Zhao X, Zu H and Yao K (2023) A case report of Andersen-Tawil syndrome misdiagnosed with myodystrophy.
Front. Neurol. 14:1170693.
doi: 10.3389/fneur.2023.1170693

COPYRIGHT
© 2023 Zhao, Zu and Yao. This is an open-access article distributed under the terms of the Creative Commons Attribution License (CC BY). The use, distribution or reproduction in other forums is permitted, provided the original author(s) and the copyright owner(s) are credited and that the original publication in this journal is cited, in accordance with accepted academic practice. No use, distribution or reproduction is permitted which does not comply with these terms.

A case report of Andersen-Tawil syndrome misdiagnosed with myodystrophy

Xiuqin Zhao, Hengbing Zu and Kai Yao*

Department of Neurology, Jinshan Hospital Affiliated to Fudan University, Shanghai, China

Andersen-Tawil syndrome (ATS) is a rare periodic paralysis caused by the KCNJ2 gene mutation. Here, we report on an ATS patient misdiagnosed with myodystrophy. A 66-year-old man presented with a 60-year history of episodic weakness in the proximal muscles of the upper and lower limbs. The man has been diagnosed with muscle pathology and has undergone genetic examinations in many hospitals since childhood. We conducted a correct diagnosis in combination with the patient's history, electrical physiology, and genetic analysis and identified a heterozygous KCNJ2 gene variant (c.220A>G; p.T74A). Patients with ATS can develop permanent myasthenia characterized by chronic progressive myopathy. ATS patients should also pay special attention to the risks of anesthesia in surgery, including malignant hyperthermia (MH), muscle spasms affecting tracheal intubation or ventilation, and ventilator weakness. Early diagnosis and therapy could help delay the onset of myasthenia and prevent risks associated with anesthesia accidents.

KEYWORDS

Andersen-Tawil syndrome, KCNJ2, malignant hyperthermia, anesthetic considerations, long-term exercise test

Introduction

ATS is a rare form of periodic paralysis and accounts for less than 10% of all periodic paralysis (1,500,000) (1, 2). This disease is caused by a KCNJ2 gene mutation, which encodes the inward-rectifying potassium channel known as kir2.1 (3, 4). The incorrect folding of the kir2.1 protein and the abnormal function of the channel results in a dominant negative effect on the potassium channel current, leading to decreased inward rectifying potassium current (5), impairing the repolarization process of the resting action potential of muscle fibers, affecting the excitability of skeletal and cardiac muscles, and subsequently causing periodic paralysis and arrhythmia (skeletal muscle and heart symptoms) (6). Subtle characteristic facial and skeletal abnormalities are often indicative signs used to diagnose ATS. The expression of Variant KCNJ2 leads to malfunctions in the potassium channel, affecting the spatial distribution Vmem (resting potential) and disrupting the normal pattern of membrane voltage potential regionalization, which, in turn, leads to misexpression of the craniofacial patterning genes during embryonal development in mice (7). Many studies have observed that the craniofacial features of ATS represent a spectrum of phenotypic manifestations, which include a broad forehead, low-set ears, broad nose, and maxillary and mandibular hypoplasia. Skeletal anomalies included short stature, small hands and feet, scoliosis, and clinodactyly of the fifth finger and toe (8). ATS patients also commonly exhibit symptoms such as periodic paralysis, cardiac abnormalities (including ventricular arrhythmia, prolonged Q-T interval, and inverted U wave), and myopathy (4, 9). To clinically diagnose ATS, the presence of at least two out of the following three cardinal

features is typically required: periodic paralysis of skeletal muscles, characteristic dysmorphic features, or typical cardiac findings (6, 9).

Case report

A 66-year-old man presented with episodic limb weakness beginning at 2 years of age, sometimes in both lower extremities and sometimes in both the upper and lower limbs. Prolonged walking was often the predisposing factor, with seizure frequency occurring once or twice a month. With age, he appeared to have permanent muscle weakness, manifested by difficulty in running, squatting, standing up, and lifting the upper limbs. During this period, he visited many hospitals to check his creatine kinase (CK) levels, which ranged from approximately 600–1,000 U/L. Muscle biopsies of his calf, shoulder, and back were performed at the ages of 13, 20, and 26 at two hospitals. The examination results showed no abnormalities, leading to a suspicion of muscular dystrophy as a possible cause. He underwent genetic testing at the age of 26, but the diagnosis was still inconclusive. Twenty-five years ago, an electrophysiologic concentric needle examination of the iliopsoas muscle, the gluteus maximus, and the lumbar paraspinal muscles indicated the presence of myopathy in the patient. There was a suspicion of limb-type muscle malnutrition, but treatment with coenzyme Q10 was found to be ineffective. It is worth noting that he had all his teeth extracted due to difficulties during intubation during vocal cord polyp surgery and was found quadriplegic after general anesthesia 10 years ago. The doctor conducted a cervical spine magnetic resonance imaging (MRI) on the patient, but the results showed no abnormalities. The patient complained of limb weakness, which progressively worsened in the morning before admission. He fell to the ground, could not stand up, and was brought to the emergency department of our hospital. Physical examination of the patient's proximal part of the extremities presented amyotrophy (Medical Research Council Grade 4) and decreased tendon reflexes, and negative bilateral pathological signs. The electrocardiogram of our patient showed a U-wave inversion (Figure 1), and the 24-h dynamic electrocardiogram showed 245 premature ventricular contractions (PVCs) in a total of 91,847 heartbeats. The EMG examination revealed narrow and irregular waves during the needle examination, with no pronouncement of the fibrillation. A long-term exercise test indicated a significant decrease in the compound muscle action potential (CMAP) amplitude of the right little finger abductor muscle, measuring 74.4% lower than the baseline and a 66% reduction in the area (Figure 2).

The blood test results showed a potassium level of 2.9 mmol/L (normal value: 3.5–5.5 mmol/L). Additionally, the CK (creatine kinase) level was measured at 1,600 U/L, lactic acid level at 2.8, and lactate dehydrogenase (LDH) at 224 U/L. We considered the possibility of ATS given the patient's characteristic physical features, including short stature, small hands and feet, clinodactyly of the fifth toe, hypoplastic mandible, and low-set ears (Figure 3). An electrocardiogram revealed slightly inverted U waves. Further genetic analysis using the sequencing system (Amplicon Gene, Inc.) identified a heterozygous c.220A > G mutation in the exon 2 region of chromosome 17 of the KCNJ2 gene. This mutation resulted in the substitution of alanine with threonine at amino acid 74 (p.T74A) (Figure 1), which was reported to be a pathogenic mutation for ATS (10). Our patient had special physical characteristics. Based on the positive results of the long-term exercise test, muscle symptoms, and the genetic testing outcome, it was determined that he was not affected by the myopathic condition but rather ATS.

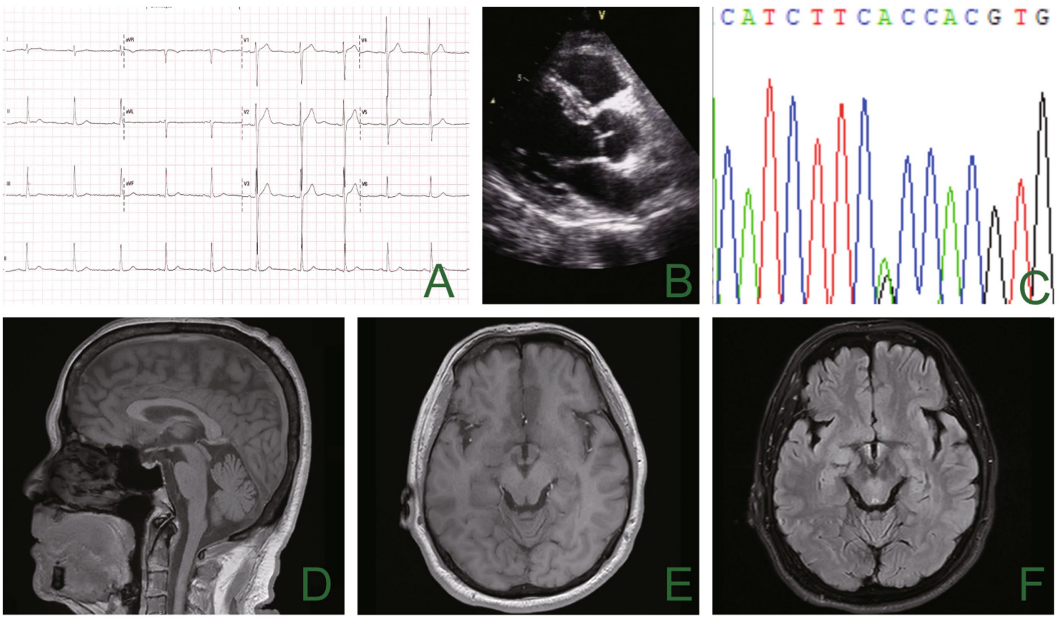

FIGURE 1
The electrocardiogram showed inverted U waves **(A)**, and the echocardiogram showed no apparent abnormality **(B)**. Genetic analysis using sequencing chromatograms identified a heterozygous KCNJ2 gene variant (c.220A>G; p.T74A) **(C)**. There was no noticeable abnormality in cranial magnetic resonance imaging **(D–F)**.

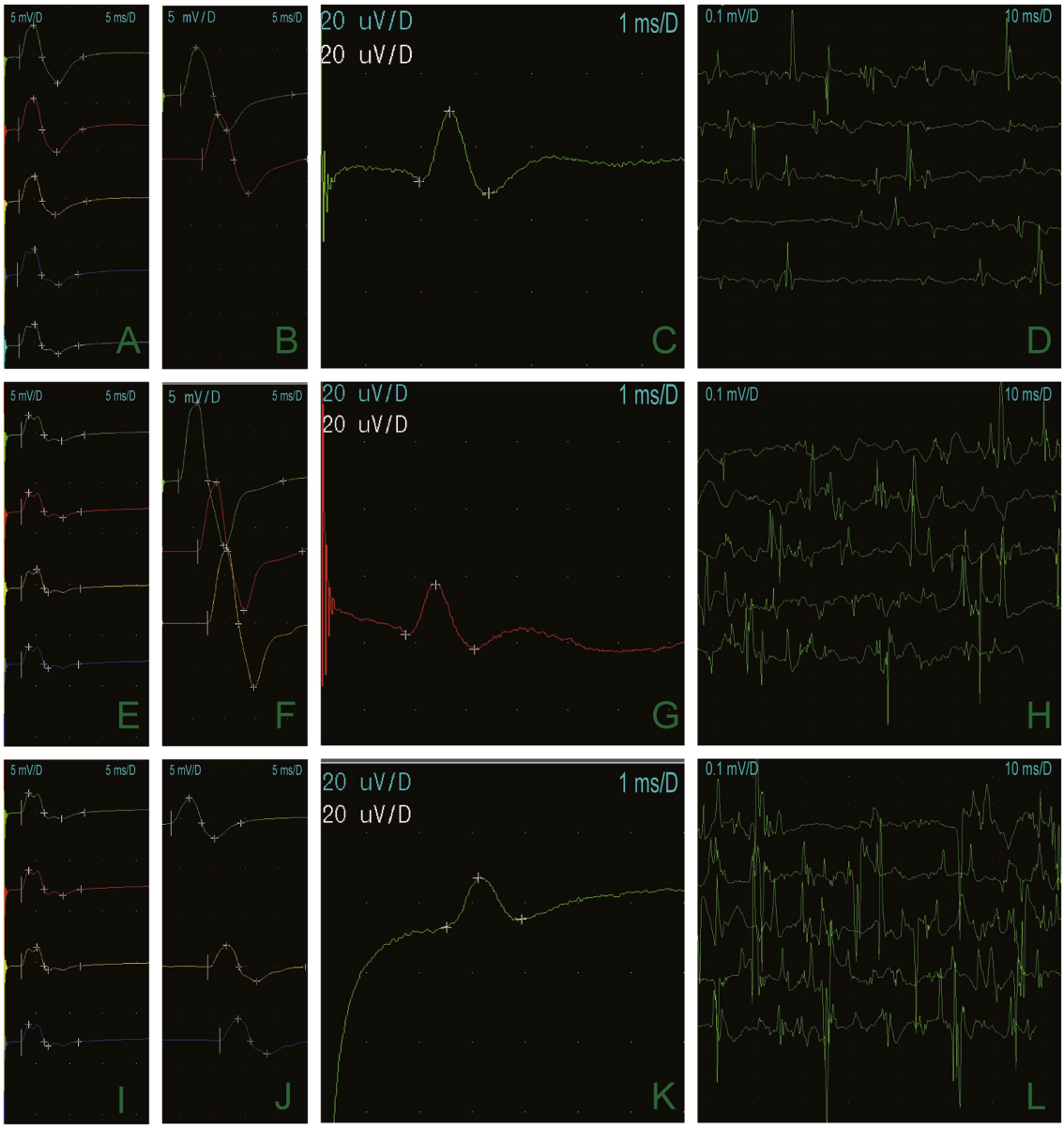

FIGURE 2
Long-term exercise test results demonstrated that the CMAP amplitude of the right little finger abductor muscle was 74.4% lower than it was at baseline, and the area was reduced by 66% **(A,E,I)**. The median nerve **(B)**, the ulnar nerve **(F)**, and the peroneal nerve **(J),** and motor conduction were normal. Sensory conduction of the median nerve **(C)**, the ulnar nerve **(G)**, and the superficial peroneal nerve **(K)** was normal. Electrophysiologic concentric needle examination fibrillation and a sharp positive wave at resting potentials **(D)**. Light contraction showed a narrow waveform **(H,L)**.

Discussion

The misdiagnosis of ATS as a muscle disease has rarely been reported before. Muscular dystrophy or other muscle disorders are often characterized by muscle weakness, muscle atrophy, and increased CK, and electromyography showed myogenic damage. These similarities in symptoms and test results can often lead to confusion and misdiagnosis in cases similar to our patients. Periodic paralysis can cause episodic and permanent weakness caused by fibrotic and fatty replacement, and the incidence of permanent weakness is 68% (11). Studies have found that the biopsy of the left rectus femoris muscle revealed the characteristic vacuolar myopathy caused by the dilation of the T-tube, accompanied by occasional degeneration and regeneration of muscle fibers in periodic paralysis (12). A morphological follow-up of a muscle biopsy showed mild vacuolar changes at the age of 12. After 17 years, a subsequent examination showed that 15% of the muscle fibers exhibited tubular aggregates and medium-grade myopathy (13). The reports above describe the relationship between muscle pathology and permanent weakness. Our case showed permanent weakness at approximately 28 years, which is consistent with the above description.

Jeong et al. conducted a whole-body muscle MRI analysis on periodic paralysis patients and found that muscle fatty infiltration and atrophy are present in primary periodic paralysis, especially in older individuals, which are suggestive of chronic progressive myopathy (14). The whole-body muscle MRI demonstrates a selective pattern of muscle involvement affecting the posterior compartment of the lower leg and the anterior thigh muscles. Moreover, fatty muscle infiltration

FIGURE 3
Short stature, facial features (AP and lateral), low-set ears, hypoplastic mandible, small hands and feet, clinodactyly of the fifth toe, and skeletal anomalies of the patient with ATS (permission was granted by the patient).

in these areas is more frequent and increases with age (15). Horga et al. reported that a man who presented with progressive proximal muscle weakness and mildly elevated CK was diagnosed with Becker muscular dystrophy (BMD) after a muscle biopsy showed abnormal myopathy in childhood. However, it was confirmed to be ATS by electromyography and genetic testing afterward (16). This case is similar to our case, where the patient also presented chronic and persistent limb muscle weakness, muscle atrophy, and a significant manifestation of myopathy in electromyography (EMG) examination, combined with previously normal blood K values and an abnormally increased blood CK value, which led to confusion with muscular dystrophy. The history of recovering muscle weakness during childhood could distinguish ATS from muscular dystrophy. Besides, ATS patients may have special appearance characteristics and experience a decrease in CMAP amplitude after a long exercise experiment. Permanent muscle weakness significantly impacts the patient's quality of life, underscoring the importance of improving diagnostic approaches to reduce the time between the onset of the disease and the age of diagnosis.

As a special type of periodic paralysis, ATS patients with periodic paralysis are susceptible to various anesthesia-related complications, including malignant hyperthermia (MH), muscle spasms, tracheal intubation, and extubation failure (17–19). MH is a rare pharmacogenetic disorder of the skeletal muscle, triggered by sensitivity to volatile inhalation anesthetic gasses (e.g., sevoflurane, isoflurane, and so on) and depolarizing muscle relaxants (e.g., succinylcholine), which leads to a rise in core body temperature, tachycardia, hypermetabolism, pH value (pH) imbalance (hypoxemia, hypercapnia, and metabolic acidosis), liver and kidney damage, and hypermetabolism in the skeletal muscle (20, 21). It had an estimated mortality rate of 70–80% (22). Hypokalemic periodic paralysis was easy to trigger MH during general anesthesia (23–27). In addition, the use of depolarizing neuromuscular blocking drugs in ion channelopathies patients may lead to uncontrollable skeletal muscle hypermetabolism and sustained muscle contraction (28), such as generalized muscle spasms and masseter spasms, which can thus affect tracheal intubation or ventilation. In serious cases, it may cause respiratory muscle weakness and require prolonged mechanical ventilation (29–34). In an assessment of 109 patients with genetically confirmed skeletal muscle channelopathy, 17% (10 out of 59) reported worsening symptoms after general anesthesia independent of the duration of surgery, with high potassium periodic paralysis (29%) being the most common. A few patients experienced episodes of weakness after anesthesia, and nine of these patients also experienced prolonged recovery time after general anesthesia, independent of the duration of the procedure. There were no reports of laryngospasm during anesthesia (35).

In conclusion, it can be explained why our patient experienced difficulty with tracheal intubation in anesthesia surgery and paralysis when he woke up after surgery. According to the literature, patients with periodic anesthesia are susceptible to various anesthesia-related complications. Given the presence of craniofacial malformation and the potential cardiac risks associated with ATS, it is crucial to give significant attention to the possibility of difficult airways and an increased risk of severe arrhythmia during anesthesia (36). Therefore, the administration of neuromuscular blocking agents to ATS patients is a contentious issue. In patients with ATS or related family history, we believe that the use of strong inhalation anesthetics or suxamethonium should be used with utmost caution to prevent the occurrence of MH or other severe complications (37).

Conclusion

The number of confirmed skeletal muscle channelopathy cases is increasing with the use of next-genetic sequencing, but its diagnosis remains challenging. We diagnosed an ATS patient who had been misdiagnosed with myopathy for a long time. Arrhythmias, typical craniofacial features, and a decrease in CMAP amplitude after a long exercise experiment are the key points for diagnosis. In addition, we described the anesthetic risks of ATS patients for the first time, including MH, muscle spasms, failure of tracheal intubation and extubation, and so on. More studies are needed to confirm how to diagnose ATS early, manage it, and prevent the risk of anesthesia accidents in the future.

Data availability statement

The datasets presented in this study can be found in online repositories. The names of the repository/repositories and accession number(s) can be found in the article/supplementary material.

Ethics statement

Written informed consent was obtained from the individual(s) for the publication of any potentially identifiable images or data included in this article.

Author contributions

XZ enrolled the clinical data and wrote the draft. KY and HZ revised the manuscript and supported the project. All authors contributed to the article and approved the submitted version.

Acknowledgments

The authors would like to thank the data provider from the Amplicon Gene of Shanghai.

Conflict of interest

The authors declare that the research was conducted in the absence of any commercial or financial relationships that could be construed as a potential conflict of interest.

Publisher's note

All claims expressed in this article are solely those of the authors and do not necessarily represent those of their affiliated organizations, or those of the publisher, the editors and the reviewers. Any product that may be evaluated in this article, or claim that may be made by its manufacturer, is not guaranteed or endorsed by the publisher.

References

1. Tawil R, Ptacek LJ, Pavlakis SG, DeVivo DC, Penn AS, Özdemir C, et al. Andersen's syndrome: potassium-sensitive periodic paralysis, ventricular ectopy, and dysmorphic features. *Ann Neurol.* (1994) 35:326–30. doi: 10.1002/ana.410350313

2. Sansone V, Griggs RC, Meola G, Ptácek LJ, Barohn R, Iannaccone S, et al. Andersen's syndrome: a distinct periodic paralysis. *Ann Neurol.* (1997) 42:305–12. doi: 10.1002/ana.410420306

3. Plaster NM, Tawil R, Tristani-Firouzi M, Canún S, Bendahhou S¨, Tsunoda A, et al. Mutations in Kir2.1 cause the developmental and episodic electrical phenotypes of Andersen's syndrome. *Cells.* (2001) 105:511–9. doi: 10.1016/s0092-8674(01)00342-7

4. Tristani-Firouzi M, Jensen JL, Donaldson MR, Sansone V, Meola G, Hahn A, et al. Functional and clinical characterization of KCNJ2 mutations associated with LQT7 (Andersen syndrome). *J Clin Invest.* (2002) 110:381–8. doi: 10.1172/JCI15183

5. Cannon SC. An expanding view for the molecular basis of familial periodic paralysis. *Neuromuscul Disord.* (2002) 12:533–43. doi: 10.1016/s0960-8966(02)00007-x

6. Veerapandiyan A, Statland JM. Tawil R. Andersen-Tawil Syndrome In: MP Adam, GM Mirzaa, RA Pagon, SE Wallace, LJH Bean and KW Gripp, editors. *GeneReviews®*. Seattle (WA): University of Washington, Seattle (2004)

7. Adams DS, Uzel SG, Akagi J, Wlodkowic D, Andreeva V, Yelick PC, et al. Bioelectric signaling via potassium channels: a mechanism for craniofacial dysmorphogenesis in KCNJ2-associated Andersen-Tawil Syndrome. *J Physiol.* (2016) 594:3245–70. doi: 10.1113/JP271930

8. Yoon G, Oberoi S, Tristani-Firouzi M, Etheridge SP, Quitania L, Kramer JH, et al. Andersen-Tawil syndrome: prospective cohort analysis and expansion of the phenotype. *Am J Med Genet A.* (2006) 140:312–21. doi: 10.1002/ajmg.a.31092

9. Donaldson MR, Jensen JL, Tristani-Firouzi M, Tawil R, Bendahhou S, Suarez WA, et al. PIP2 binding residues of Kir2.1 are common targets of mutations causing Andersen syndrome. *Neurology.* (2003) 60:1811–6. doi: 10.1212/01.wnl.0000072261.14060.47

10. Ballester LY, Benson DW, Wong B, Law IH, Mathews KD, Vanoye CG, et al. Trafficking-competent and trafficking-defective KCNJ2 mutations in Andersen syndrome. *Hum Mutat.* (2006) 27:388. doi: 10.1002/humu.9418

11. Cavel-Greant D, Lehmann-Horn F, Jurkat-Rott K. The impact of permanent muscle weakness on quality of life in periodic paralysis: a survey of 66 patients. *Acta Myol.* (2012) 31:126–33.

12. Basali D, Prayson RA. Episodic weakness and vacuolar myopathy in hypokalemic periodic paralysis. *J Clin Neurosci.* (2015) 22:1846–7. doi: 10.1016/j.jocn.2015.06.006

13. Gold R, Reichmann H. Muscle pathology correlates with permanent weakness in hypokalemic periodic paralysis: a case report. *Acta Neuropathol.* (1992) 84:202–6. doi: 10.1007/BF00311396

14. Jeong HN, Yi JS, Lee YH, Lee JH, Shin HY, Choi YC, et al. Lower-extremity magnetic resonance imaging in patients with hyperkalemic periodic paralysis carrying the SCN4A mutation T704M: 30-month follow-up of seven patients. *Neuromuscul Disord.* (2018) 28:837–45. doi: 10.1016/j.nmd.2018.06.008

15. Lee YH, Lee HS, Lee HE, Hahn S, Nam TS, Shin HY, et al. Whole-body muscle MRI in patients with hyperkalemic periodic paralysis carrying the SCN4A mutation T704M: evidence for chronic progressive myopathy with selective muscle involvement. *J Clin Neurol.* (2015) 11:331–8. doi: 10.3988/jcn.2015.11.4.331

16. Horga A, Raja Rayan DL, Matthews E, Sud R, Fialho D, Durran SCM, et al. Prevalence study of genetically defined skeletal muscle channelopathies in England. *Neurology.* (2013) 80:1472–5. doi: 10.1212/WNL.0b013e31828cf8d0

17. Urman RD, Rajan N, Belani K, Gayer S, Joshi GP. Malignant hyperthermia-susceptible adult patient and ambulatory surgery center: Society for Ambulatory Anesthesia and ambulatory surgical Care Committee of the American Society of anesthesiologists position statement. *Anesth Analg.* (2019) 129:347–9. doi: 10.1213/ANE.0000000000004257

18. Hopkins PM, Rüffert H, Snoeck MM, Girard T, Glahn KP, Ellis FR, et al. European malignant hyperthermia group guidelines for investigation of malignant hyperthermia susceptibility. *Br J Anaesth.* (2015) 115:531–9. doi: 10.1093/bja/aev225

19. Litman RS, Griggs SM, Dowling JJ, Riazi S. Malignant hyperthermia susceptibility and related diseases. *Anesthesiology.* (2018) 128:159–67. doi: 10.1097/ALN.0000000000001877

20. Torpy JM, Lynm C, Glass RM. JAMA patient page. Malignant hyperthermia. *JAMA.* (2005) 293:2958. doi: 10.1001/jama.293.23.2958

21. Lu Z, Rosenberg H, Li G. Prevalence of malignant hyperthermia diagnosis in hospital discharge records in California, Florida, New York, and Wisconsin. *J Clin Anesth.* (2017) 39:10–4. doi: 10.1016/j.jclinane.2017.03.016

22. Britt BA, Kalow W. Malignant hyperthermia: a statistical review. *Can Anaesth Soc J.* (1970) 17:293–315. doi: 10.1007/BF03004694

23. Lambert C, Blanloeil Y, Horber RK, Bérard L, Reyford H, Pinaud M. Malignant hyperthermia in a patient with hypokalemic periodic paralysis. *Anesth Analg.* (1994) 79:1012–4. doi: 10.1213/00000539-199411000-00034

24. Brownell AK. Malignant hyperthermia: relationship to other diseases. *Br J Anaesth*. (1988) 60:303–8. doi: 10.1093/bja/60.3.303

25. Parness J, Bandschapp O, Girard T. The myotonias and susceptibility to malignant hyperthermia. *Anesth Analg*. (2009) 109:1054–64. doi: 10.1213/ane.0b013e3181a7c8e5

26. Haberer JP, Fabre F, Rose E. Malignant hyperthermia and myotonia congenita (Thomsen's disease). *Anaesthesia*. (1989) 44:166. doi: 10.1111/j.1365-2044.1989.tb11182.x

27. King JO, Denborough MA, Zapf PW. Inheritance of malignant hyperpyrexia. *Lancet*. (1972) 299:365–70. doi: 10.1016/s0140-6736(72)92854-1

28. Jurkat-Rott K, Lerche H, Lehmann-Horn F. Skeletal muscle channelopathies. *J Neurol*. (2002) 249:1493–502. doi: 10.1007/s00415-002-0871-5

29. Azar I. The response of patients with neuromuscular disorders to muscle relaxants: a review. *Anesthesiology*. (1984) 61:173–87. doi: 10.1097/00000542-198408000-00011

30. Heiman-Patterson T, Martino C, Rosenberg H, Fletcher J, Tahmoush A. Malignant hyperthermia in myotonia congenita. *Neurology*. (1988) 38:810–2. doi: 10.1212/wnl.38.5.810

31. Mitchell MM, Ali HH, Savarese JJ. Myotonia and neuromuscular blocking agents. *Anesthesiology*. (1978) 49:44–7. doi: 10.1097/00000542-197807000-00014

32. Paterson IS. Generalized myotonia following suxamethonium. A case report. *Br J Anaesth*. (1962) 34:340–2. doi: 10.1093/bja/34.5.340

33. Thiel RE. The myotonic response to suxamethonium. *Br J Anaesth*. (1967) 39:815–21. doi: 10.1093/bja/39.10.815

34. Thomas A, Leopold U, Winkler H. Maligne Hyperthermie bei Paramyotonia congenita [malignant hyperthermia in paramyotonia congenita]. *Anaesthesiol Reanim*. (1988) 13:295–300. doi: 10.1212/wnl.38.5.810

35. Raja Rayan DL, Hanna MG. Managing pregnancy and anaesthetics in patients with skeletal muscle channelopathies. *Neuromuscul Disord*. (2020) 30:539–45. doi: 10.1016/j.nmd.2020.05.007

36. Park S, Heo W, Shin SW, Kim HJ, Yoo YM, Kim HY. General anesthesia using propofol infusion for implantation of an implantable cardioverter defibrillator in a pediatric patient with Andersen-Tawil syndrome: a case report. *J Dent Anesth Pain Med*. (2023) 23:45–51. doi: 10.17245/jdapm.2023.23.1.45

37. Hopkins PM, Girard T, Dalay S, Jenkins B, Thacker A, Patteril M, et al. Malignant hyperthermia 2020: guideline from the Association of Anaesthetists. *Anaesthesia*. (2021) 76:655–64. doi: 10.1111/anae.15317

frontiers | Frontiers in Neurology

TYPE Case Report
PUBLISHED 27 July 2023
DOI 10.3389/fneur.2023.1179992

Check for updates

OPEN ACCESS

EDITED BY
Giovanni Meola,
University of Milan, Italy

REVIEWED BY
Jae Eun Sim,
University of California, Irvine, United States
Corrado Italo Angelini,
University of Padua, Italy

*CORRESPONDENCE
Hai-shan Jiang
✉ jianghs@smu.edu.cn
Chao Yuan
✉ yuanchao613@163.com

RECEIVED 05 March 2023
ACCEPTED 10 July 2023
PUBLISHED 27 July 2023

CITATION
Chen D-h, Li W, Jiang H-s and Yuan C (2023) Case report: MELAS and T3271C mitochondrial mutation in an adult woman.
Front. Neurol. 14:1179992.
doi: 10.3389/fneur.2023.1179992

COPYRIGHT
© 2023 Chen, Li, Jiang and Yuan. This is an open-access article distributed under the terms of the Creative Commons Attribution License (CC BY). The use, distribution or reproduction in other forums is permitted, provided the original author(s) and the copyright owner(s) are credited and that the original publication in this journal is cited, in accordance with accepted academic practice. No use, distribution or reproduction is permitted which does not comply with these terms.

Case report: MELAS and T3271C mitochondrial mutation in an adult woman

Dong-hua Chen, Wei Li, Hai-shan Jiang* and Chao Yuan*

Department of Neurology, Nanfang Hospital, Southern Medical University, Guangzhou, Guangdong, China

Introduction: Patients with mitochondrial disorders always show neurological deficits. However, the diversity of clinical manifestations, genetic heterogeneity and threshold effect caused by maternal heredity make its diagnosis very challenging.

Case presentation: A 30-year-old female presented to our neurology department with a recurrence of symmetrical weakness proximally in the lower extremities. Seven years ago, the patient had a sudden onset of persistent weakness in bilateral proximal lower extremities, along with elevated creatinine kinase (CK) and CK-MB. Given the diagnosis of Guillain-Barre syndrome, she was treated with high-dose glucocorticoid (GC) therapy at the local hospital and recovered. After admission to our hospital, laboratory analysis revealed elevated CK and alpha-hydroxybutyrate dehydrogenase in serum. Electrocardiography showed sinus tachycardia and left high ventricular voltage. Electromyography (EMG) and evoked potential (EP) suggested peripheral neurogenic damage of the upper and lower extremities with myogenic wear. Chronic inflammatory demyelinating polyneuropathy (CIDP) was initially considered, but neurological symptoms were not significantly improved with glucocorticoid shock therapy. An elevated level of lactate was found. The short-tau inversion recovery (STIR) axial magnetic resonance image (MRI) revealed mild hyperintensities, indicating muscle edema. Meanwhile, muscle biopsies suggested pathological changes in mitochondrial disorders (MIDs) and neuronal damage. Further mitochondrial genome analysis revealed a heteroplasmic m3271 T>C mutation in the mitochondrial tRNA-Leu gene (UUR). Collectively, the patient was finally diagnosed with mitochondrial disorder and apparently improved after the corresponding treatment to regulate energy metabolism.

Conclusions: To our knowledge, it's the first report about MELAS with 3271 mutation that have only shown peripheral nerve motion impairment. Proximal weakness is also common in CIDP. In the context of this patient's experience, mitochondrial genome analysis provides an auxiliary criterion for differential diagnosis between MIDs and CIDP. In the meantime, we discussed the clinical effect of GCs on MIDs.

KEYWORDS

MELAS, T3271C mutation, peripheral nerve dysfunction, glucocorticoid therapy, case report

Introduction

Mitochondrial diseases are caused by mutations in nuclear or mitochondrial genes, characterized by defects in oxidative phosphorylation (1). Mitochondrial diseases have diverse clinical manifestations, of which neurological deficits are the most common symptoms and probably make the greatest contribution to morbidity and mortality (2). However, the diversity of clinical manifestations, genetic heterogeneity and threshold effect caused by maternal heredity make its diagnosis very challenging. Mitochondrial encephalopathy with lactic acid and stroke-like episodes is one of the most common maternal mitochondrial diseases. Herein, we report the first patient of MELAS with T3271C mitochondrial mutation who presented only as impaired movement.

Patient information

A 30-year-old female presented to our neurology department with **a** recurrence of symmetric**al** weakness proximally in the lower extremities. Seven years ago, the patient had a sudden onset of persistent weakness in the bilateral proximal lower extremities. At the time, she was able to stand with assistance and walk on her own. She then visited the local medical clinic for the first time at the age of 23. The only positive finding was the elevation of creatinine kinase (CK) (236 U/L) and CK-MB (29 U/L). She was then diagnosed with Guillain-Barre syndrome and largely recovered after high-dose glucocorticoid therapy.

TABLE 1 Timeline of this case report.

Times	Events
First hospital admission in 2012.	First appearance of muscle weakness in the lower extremities. Diagnosed with Guillain-Barre syndrome and treated with glucocorticoid therapy. Symptoms were largely recovered.
Second hospital admission in 2019 (Figure 1).	Recurrence of muscle weakness in the lower extremities. Misdiagnosed with Guillain-Barre syndrome and treated with glucocorticoid therapy. Diagnosed with mitochondrial disorder and treated with corresponding therapy to regulate energy metabolism. Symptoms were gradually recovered.

Clinical findings

Now the patient has been admitted to our hospital with a recurrence of neurological symptoms in the past 1 month. Neurological examination of the patient showed not only muscle weakness and hypotonia of extremities, but also muscle weakness of neck flexion [Medical Research Council (MRC) grade 4], elbow flexion (MRC grade 3) and knee extension (MRC grade 4). In addition, no tendon reflexes of the biceps brachii and triceps were found. No significant abnormalities were observed in cranial nerve examination, sensory system, autonomic nervous system, and meningeal irritation sign.

Timeline

The timeline of this case report was shown below (Table 1; Figure 1).

Diagnostic assessment

Laboratory analysis revealed elevated CK (246 U/L) and alpha-hydroxybutyrate dehydrogenase (alpha-HBDH) (232 U/L) levels in the patient. Results of other routine serologic investigations, cerebrospinal fluid (CSF) analysis, and autoimmune antibody titers, including peripheral neuropathy antibody spectrum in both serum and cerebrospinal fluid, were within normal limits. Electrocardiography revealed sinus tachycardia and left ventricular high voltage. Electromyography (EMG) and evoked potential (EP) suggested peripheral neurogenic damage of upper and lower extremities with myogenic damage. At the moment, the diagnosis of myopathy could not be ruled out, so we completed myositis autoantibody analysis and muscle magnetic resonance imaging (MRI). No myositis autoantibody was found. Under MRI

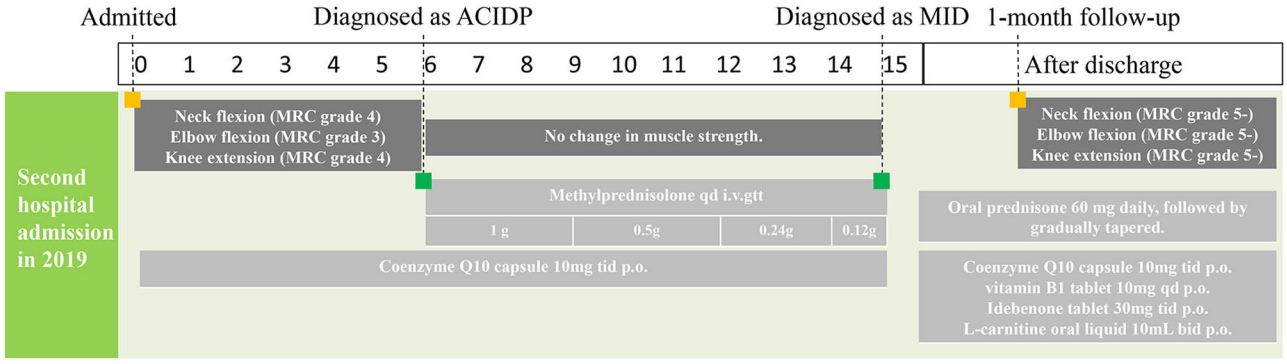

FIGURE 1
Timeline of this case report.

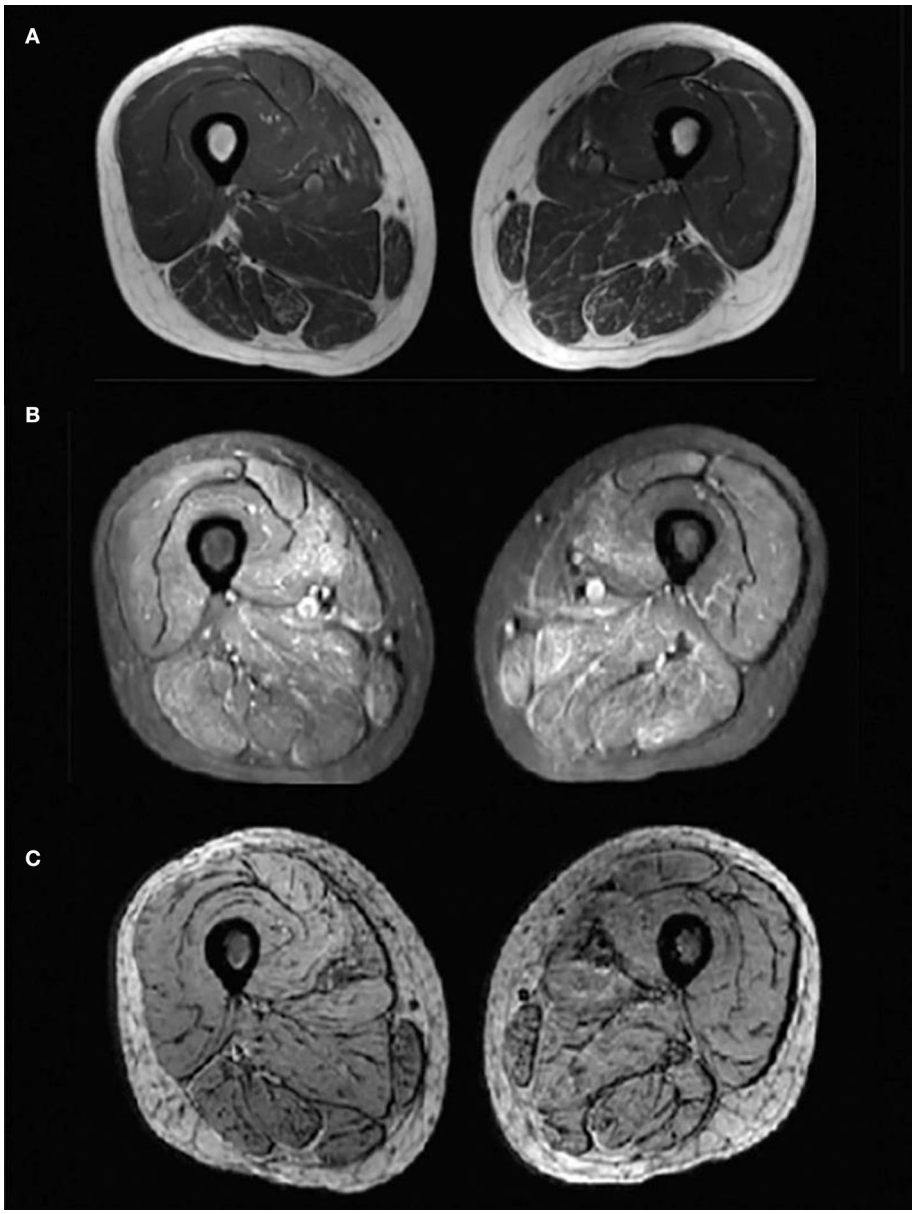

FIGURE 2
Magnetic resonance imaging (MRI) changes of bilateral thigh. Axial-T1-weighted MRI **(A)** showed hypointensity indicating no obvious fatty infiltration of the muscles and axial STIR MRI **(B)** showed slightly hyperintensities indicating mild muscle oedema. No hypointense structure was observed on axial SWI MRI **(C)**, indicating no angiogenesis.

scans (Figure 2), the characteristics of muscle lesions were not remarkable, and no obvious specific change in muscle group was found. However, there was edema in short-tau inversion recovery (STIR) sequences. Just then, a slight increase of blood lactic acid (8.7 mmol/L) was found in resting state, raising the suspicion of hereditary metabolic myopathy. Based on MRI finding, the tissue involved was then subjected to a muscle biopsy. The results (Figure 3) suggested pathological changes in MIDs and neuronal damage. So we thought MID might be the final diagnosis. In order to further clarify the diagnosis, mitochondrial DNA was carried out on the muscles involved and the results showed that there was a heteroplasmic m3271 T>C mutation in the mitochondrial tRNA-Leu gene (UUR), and the proportion of mutant mtDNA reached 87.4%.

Therapeutic intervention

According to MID diagnostic criteria in 2002, the patient met two main diagnostic indexes and could be diagnosed as MID with MELAS (3). After the diagnosis was confirmed, coenzyme Q10, vitamin B1, idebenone, and L-carnitine oral liquid were given to improve the function of the oxidative respiratory chain and regulate energy metabolism (Figure 1).

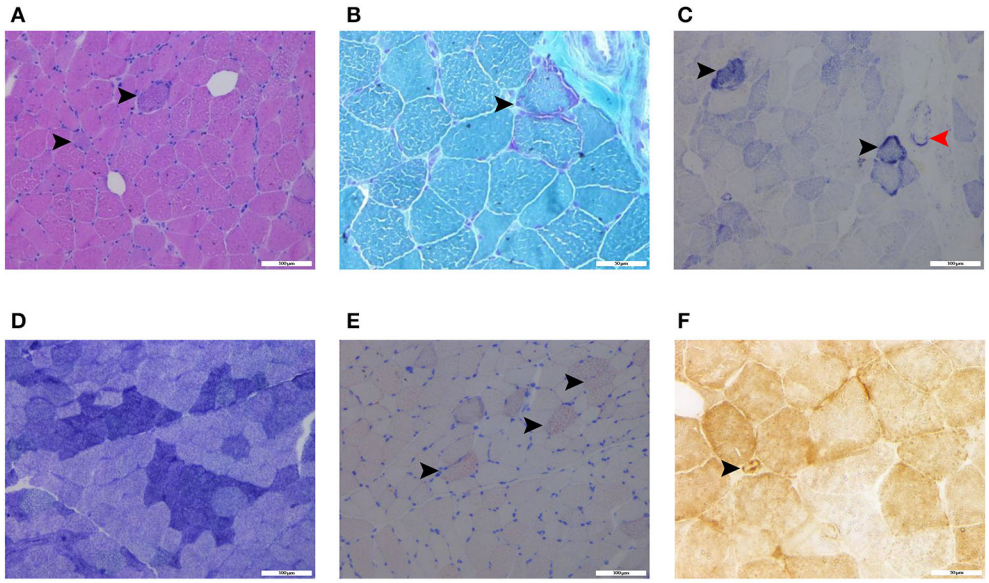

FIGURE 3
Histochemical stains of the thigh muscle biopsy specimens showed basophilic muscle fibers [**(A)**, haematoxylin and eosin stain, black arrows, scalebar: 100 μm], ragged-red fibers [**(B)**, modified Gomori trichrome stain, black arrow, scalebar: 50 μm], ragged-blue fibers [**(C)**, succinate dehydrogenase stain, black arrows, scalebar: 100 μm] and increased SDH activity in the vessels [**(C)**, succinate dehydrogenase stain, red arrow, scalebar: 100 μm], few grouping fibers [**(D)**, NADH-tetrazolium reductase, scalebar: 100 μm], increased fat droplets in some muscle fibers [**(E)**, Oil Red O stain, black arrows, scalebar: 100 μm], and COX-positive vessels [**(F)**, cytochrome c oxidase, black arrow, scalebar: 50 μm].

Follow-up and outcomes

After the treatment, the patient's symptoms had obviously improved and she could gradually stand and walk on her own. At 1-month follow-up, the muscle strength of neck flexion, elbow flexion and knee extension had recovered to MRC grade 5-/5.

Discussion

MELAS is one of the most common maternal MIDs. Approximately 80% of MELAS patients harbor m3243A>G mutation, while ~7 to 15% of MELAS patients carry m3271T>C mutation (4–6). Peripheral nerve dysfunction alone was extremely rare for MELAS patients. To the best of our knowledge, this is the first report of patient with MELAS with T3271C mitochondrial mutation who presented only as motor impairment movement. We believe that this case is meaningful for further understanding of MELAs with m3271T>C mutation in clinical settings.

The treatment of MELAS aims to improve mitochondrial function and regulate energy metabolism. In addition, drugs that affect mitochondrial function should be used with caution. Meanwhile, the guidelines for the diagnosis and treatment of MIDs do not recommend the use of glucocorticoid (GC), but in fact, MELAS patients appear to benefit from the use of GCs (7). In line with them, the MELAS patient in our case showed an improvement in muscle strength after GC therapy in the early stages of the disease. One possible explanation for this is that GCs are involved in mitochondrial regulation by acting directly on mitochondrial DNA through the mitochondrially localized glucocorticoid receptor (GR) or indirectly through interaction with nuclear genes (8, 9). Worth mentioning, MELAS associated with pure motor CIDP, a type of atypical CIDP, couldn't be ruled out in our case (10), which may explain the effectiveness of GCs. If necessary, a nerve biopsy may be performed to confirm the diagnosis of CIDP. Close metabolic monitoring of the patient is crucial when the patient has worsening symptoms or new symptoms of other organs. Further, first-degree relatives of the patient were recommended for lactic acid detection and genetic testing.

In conclusion, MELAS is sometimes misdiagnosed as CIDP because of similar clinical manifestations, which may lead to the delayed treatment and missed diagnosis of the patient's family. If necessary, muscle biopsy and mitochondrial DNA analyses should be performed for differential diagnosis.

Data availability statement

The original contributions presented in the study are included in the article/supplementary material, further inquiries can be directed to the corresponding authors.

Ethics statement

Written informed consent was obtained from the individual(s) for the publication of any potentially identifiable images or data included in this article.

Author contributions

D-hC, WL, H-sJ, and CY contributed to conception, design, acquisition of data, and analysis and interpretation of data. D-hC wrote the first draft of the manuscript. CY and H-sJ were responsible for revising manuscript. All authors contributed to read the manuscript and approved the submitted version.

Funding

This study was supported by the National Natural Science Foundation of China (Grant No. 82001315), Science and Technology Planning Project of Guangzhou (Grant No. 202102020832), and Medical Scientific Research Foundation of Guangdong Province (Grant No. C2023066).

Conflict of interest

The authors declare that the research was conducted in the absence of any commercial or financial relationships that could be construed as a potential conflict of interest.

Publisher's note

All claims expressed in this article are solely those of the authors and do not necessarily represent those of their affiliated organizations, or those of the publisher, the editors and the reviewers. Any product that may be evaluated in this article, or claim that may be made by its manufacturer, is not guaranteed or endorsed by the publisher.

References

1. Arena IG, Pugliese A, Volta S, Toscano A, Musumeci O. Molecular genetics overview of primary mitochondrial myopathies. *J Clin Med.* (2022) 11:632. doi: 10.3390/jcm11030632

2. Lax NZ, Gorman GS, Turnbull DM. Review: central nervous system involvement in mitochondrial disease. *Neuropathol Appl Neurobiol.* (2017) 43:102–18. doi: 10.1111/nan.12333

3. Bernier FP, Boneh A, Dennett X, Chow CW, Cleary MA, Thorburn DR. Diagnostic criteria for respiratory chain disorders in adults and children. *Neurology.* (2002) 59:1406–11. doi: 10.1212/01.WNL.0000033795.17156.00

4. Goto Y, Nonaka I, Horai S. A mutation in the Trna(Leu)(Uur) gene associated with the melas subgroup of mitochondrial encephalomyopathies. *Nature.* (1990) 348:651–3. doi: 10.1038/348651a0

5. Goto Y, Nonaka I, Horai S, A. New Mtdna mutation associated with mitochondrial myopathy, encephalopathy, lactic acidosis and stroke-like episodes (melas). *Biochim Biophys Acta.* (1991) 1097:238–40. doi: 10.1016/0925-4439(91)90042-8

6. Sakuta R, Goto Y, Horai S, Nonaka I. Mitochondrial dna mutations at nucleotide positions 3243 and 3271 in mitochondrial myopathy, encephalopathy, lactic acidosis, and stroke-like episodes: a comparative study. *J Neurol Sci.* (1993) 115:158–60. doi: 10.1016/0022-510X(93)90219-O

7. Finsterer J, Frank M. Glucocorticoids for mitochondrial disorders. *Singapore Med J.* (2015) 56:122–3. doi: 10.11622/smedj.2015026

8. Lee SR, Kim HK, Song IS, Youm J, Dizon LA, Jeong SH, et al. Glucocorticoids and their receptors: insights into specific roles in mitochondria. *Prog Biophys Mol Biol.* (2013) 112:44–54. doi: 10.1016/j.pbiomolbio.2013.04.001

9. Psarra AM, Sekeris CE. Glucocorticoids induce mitochondrial gene transcription in Hepg2 cells: role of the mitochondrial glucocorticoid receptor. *Biochim Biophys Acta.* (2011) 1813:1814–21. doi: 10.1016/j.bbamcr.2011.05.014

10. Lehmann HC, Burke D, Kuwabara S. Chronic inflammatory demyelinating polyneuropathy: update on diagnosis, immunopathogenesis and treatment. *J Neurol Neurosurg Psychiatry.* (2019) 90:981–7. doi: 10.1136/jnnp-2019-320314

Frontiers in Neurology

Explores neurological illness to improve patient care

The third most-cited clinical neurology journal explores the diagnosis, causes, treatment, and public health aspects of neurological illnesses. Its ultimate aim is to inform improvements in patient care.

Discover the latest Research Topics

See more →

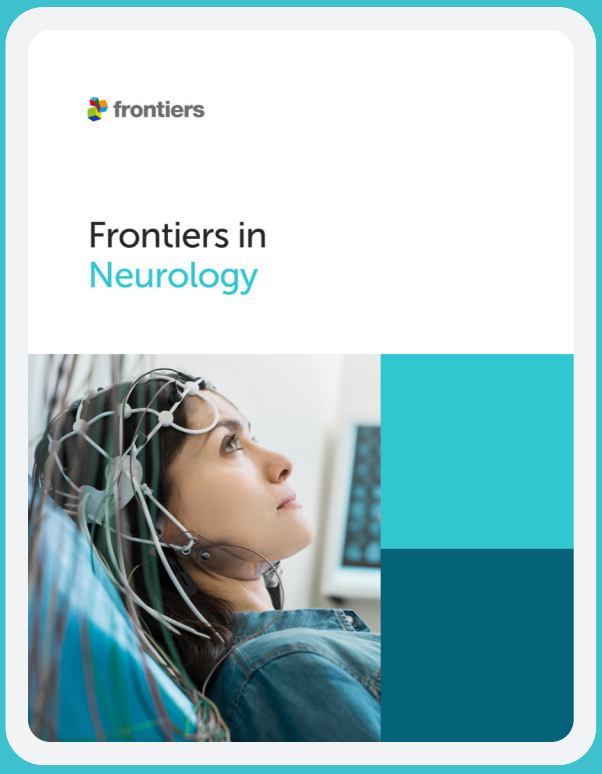

Frontiers

Avenue du Tribunal-Fédéral 34
1005 Lausanne, Switzerland
frontiersin.org

Contact us

+41 (0)21 510 17 00
frontiersin.org/about/contact